INTERNATIONAL
MINERALOGICAL ASSOCIATION

Fourth General Meeting

Papers and Proceedings

I. M. A. Volume

Mineralogical Society of India

INTERNATIONAL MINERALOGICAL ASSOCIATION

Fourth General Meeting

Papers and Proceedings

I. M. A. Volume

Mineralogical Society of India

Mineralogical Society of India

I. M. A. Volume

International Mineralogical Association

Papers and Proceedings

of the

Fourth General Meeting

New Delhi, December 15 & 22, 1964

Editor
P. R. J. NAIDU

Co-ordinating Editor
M. N. VISWANATHIAH

Published by the Society . 1966

PRINTED BY
H. NARASANNA, DEPUTY DIRECTOR
MYSORE UNIVERSITY PRINTING PRESS, MYSORE

INTERNATIONAL MINERALOGICAL ASSOCIATION

An Association of 23 National Mineralogical Societies

1960–1964

President	Prof. D. Jerome Fisher
First Vice-President	Prof. C. E. Tilley
Second Vice-President	Prof. G. P. Barsanov
Secretary	Prof. Jose L. Amorōs
Treasurer	Prof. L. G. Berry
Councilors:	Prof. P. R. J. Naidu
	Prof. Th. G. Sahama
	Prof. H. G. F. Winkler
Past President	Prof. Robert L. Parker

1964–1968

President	Prof. C. E. Tilley
First Vice-President	Prof. H. Strunz
Second Vice-President	Acad. D. S. Korzhinski
Secretary	Prof. A. Preisinger
Treasurer	Prof. L. G. Berry
Councilors:	Prof. T. F. W. Barth
	Prof. Doz. J. Kutina
	Prof. T. Watanabe
Past President	Prof. D. Jerome Fisher

FOREWORD

At the invitation of the Mineralogical Society of India, the International Mineralogical Association was pleased to hold their IV Session at Delhi in December 1964. 103 foreign and local delegates registered for the Session. This was also a very important Session for the International Mineralogical Association because the new office-bearers were elected for the period 1964–1968. Two Symposia and a general session were held for which, Abstracts of papers : nine for Zeolite symposium, eighteen for Carbonatite-Kimberlite Symposium, twenty four for the General Session, were received. Of these, only twenty eight full papers were received from the Chairman for publication in this Special Issue namely IMA volume of Mineralogical Society of India.

There has been a considerable delay in the publication of these articles for which the Editor offers his apologies to the authors.

The printing of these papers was undertaken by the Mysore University Press and the proof-reading, general editing and administrative supervision were done entirely by Dr. M. N. Viswanathiah, Professor and Head of the Department of Geology of the University of Mysore and who is also the Editor and Secretary of ' The Indian Mineralogist' assisted by his colleagues in the Department, Dr. B. V. Govinda Rajulu, Dr. A. S. Janardhanan, Sri M. N. Malur, Sri Asadulla Shariff and Sri T. V. Shivarudrappa. The official permission to have this work printed at the University Press was graciously accorded by Dr. K. L. Shrimali, Vice-Chancellor of the University of Mysore. The printing and processing of the magazine were very carefully carried out by Sri H. Narasanna, Deputy Director, of the Mysore University Press. The Editor records here his most sincere thanks and appreciation to all the above gentlemen.

This volume has been graciously released for distribution on 4–4–1967 by Sri S. Nijalingappa, Chief Minister of Mysore. The Mineralogical Society of India records here the deep sense of gratitude to the Chief Minister.

Editor.

TABLE OF CONTENTS

FOREWORD v

SYMPOSIUM ON KIMBERLITE–CARBONATITES

The kimberlite-carbonatite relationship *J. B. Dawson* 1

Potash feldspar and phlogopite as indices of temperature and partial pressure of CO_2 in carbonatite and kimberlite *D. K. Bailey* 5

Carbonatite in the alkaline complex of the Ice river area, Southern Canadian Rocky Mountains *June E. Rapson* 9

The composition of some garnets from African kimberlites *P. E. Grattan-Bellew* 23

Abundance and significance of some minor elements in carbonatitic calcites and dolomites *Shi H. Quon and E. Wm. Heinrich* 29

Carbonatites and alkalic rocks of the Arkansas river area, Fremont County, Colorado *E. Wm. Heinrich and D. H. Dahlem* 37

Intrusive carbonate rock near Ottawa, Canada *D. D. Hogarth* 45

Carbonatites of the Kaiserstuhl (W. Germany) and their magmatic environment *W. Wimmenauer* 54

Isotopic composition of strontium in carbonatites and kimberlites *J. L. Powell* 58

Experimental data bearing on the petrogenetic links between kimberlites and carbonatites *Peter J. Wyllie* 67

The average and typical chemical composition of carbonatites *D. P. Gold* 83

Fractional crystallization in the "carbonatite systems" $CaO–MgO–CO_2–H_2O$ and $CaO–CaF_2–P_2O_5–CO_2–H_2O$ *P. J. Wyllie and G. M. Biggar* 92

The strontium and barium contents of the Alnö carbonatites *Harry von Eckermann* 106

The minerals of the Oka carbonatite and alkaline complex, Oka, Quebec *D. P. Gold* 109

The pyroxenes of the Alnö carbonatite (Sövite) and of the surrounding fenites *Harry von Eckermann* 126

Carbonatites, their fabric, chemistry and their genesis *P. Paulitsch and H. Ambs* 140

Mineralogical and geochemical evolution of the carbonatites of the Kaiserstuhl, Germany (abs.) *L. van Wambeke* 148

A study of the pyrochlores, the columbite and the fermesite from the Lueshe carbonatite deposit (Republic of Congo) (abs.) *L. van Wambeke* 148

SYMPOSIUM ON ZEOLITES

Zeolites from North Mountains, Nova Scotia *F. Aumento and C. Friedlaender* 149

The effects of exchanged cations on the thermal behaviour of heulandite and clinoptilolite *Anna O. Shepard and Harry C. Starkey* 155

The dehydration and chemical composition of laumontite *Fredrik Pipping* 159

Hydrothermal synthesis of pollucite and its iron analogue (abs.) *Shoichi Kume and Mitsue Koizumi* 167

Two zeolites in zeolitic rocks in Japan (potassium clinoptilolite and powdery mordenite) (abs.) *Hideo Minato* 167

The chemical composition of analcime from the low-grade metamorphic rocks in Japan (abs.) *Waitsu Nakajima and Mitsue Koizumi* 167

Synthesis and stability of zeolites in the system (Na_2, Ca)O.Al_2O_3.7SiO_2–H_2O (abs.) *Waitsu Nakajima and Mitsue Koizumi* 168

Structural changes in zeolites caused by cation exchange at room temperature and dehydration under controlled pH_2O. (abs.) *Rustum Roy, A. M. Taylor, and W. Balgord* 168

Analcime from sedimentary and burial metamorphic rocks (abs.) *J. T. Whetten and D. S. Coombs* 169

GENERAL PAPERS

Melanterite from the Makum coal basin, Assam *D. N. D. Goswami* 170

Study of the temperature of crystallization of some Spanish fluorites by decrepitation method *M. Font-Altaba, J. Montoriol-Pous and J. M. Amigo* 172

Phase relations in the system $NaAlSi_3O_8$ (albite)–$NaAlSiO_4$ (nepheline)–$NaFeSi_2O_6$ (acmite)–$CaMgSi_2O_6$ (diopside)–H_2O and its importance in the genesis of alkaline undersaturated rocks *A. D. Edgar and J. Nolan* 176

Hydrogen-bonding site distribution on layer silicate surfaces *W. D. Johns and P. K. Sen Gupta* 182

Cleavage features in a Domain (twin) crystal *J. L. Amoros* 189

Ore microscopy and electron probe microanalysis of some manganese minerals with vredenburgite-type intergrowth *Takeo Watanabe and Akira Kato* 197

Nouvelles donnees sur la localisation des elements en traces dans les mineraux et dans les roches *J. Goni et C. Guillemin* 203

Illustrations of heterogeneity in phlogopite, feldspar, euxenite and associated minerals *J. Rimsaite and G. R. Lachance* 209

Observations on hydrothermal growth of quartz (abs.) *Tarun Bandopadhyaya and P. Saha* 230

Unit cell and space group of artificial cobaltomenite (abs.) *William G. R. de Camargo* 230

Metamorphic eclogites from Co. Donegal, Eire (abs.) *W. R. Church* 231

Phase transformations in a natural beryl (abs.) *Dibyendu Ganguly and Prasenjit Saha* 231

The application of nuclear magnetic resonance technique in the study of cation order-disorder and phase transitions in solids (abs.) *Subrata Ghose* 231

Crystal chemistry of basic copper phosphate and arsenate minerals (abs.) *Subrata Ghose* 232

A chemical study of some amphiboles from alkaline igneous rocks (abs.) *R. A. Howie* 233

A system of nomenclature for rare-earth minerals (abs.) *A. A. Levinson* 233

Influence of gases on the formation and destruction of "colour centres' in quartz by electrolysis (abs.) *Joachim Leitz and Benod Mehrotra* 233

The distribution of trace elements and silicates in Mediterranean marbles (abs.) *H. U. Nissen* 284

Calcium silicate and hydrogarnet formation in the system CaO–Al_2O_3–SiO_2–H_2O. (abs.) *Della M. Roy* 234

Application of variations in crystal field splitting of energy levels of 3d ions to indicate structural changes in various minerals including dehydrating zeolites and clays (abs.) *Rustum Roy* 235

Pressure-temperature relations for the dehydration of metastable serpentine at pressures from 15 to 20,000 psi. (abs.) *Rustum Roy and Jon N. Weber* 235

High-pressure autoclave for hydrothermal crystal growth (abs.) *Prasenjit Saha* 236

Polygonal texture in beryl (abs.) *Th. G. Sahama* 236

Structural changes in synthetic and natural al-hydroxides (bauxite from France) (abs.) *I. Valeton and B. B. Mehrotra* 237

PROCEEDINGS OF THE INTERNATIONAL MINERALOGICAL ASSOCIATION 238

INDEX 247

MINERALOGICAL SOCIETY OF INDIA, IMA VOLUME. 1966
INTERNATIONAL MINERALOGICAL ASSOCIATION, PAPERS, FOURTH GENERAL MEETING

SYMPOSIUM ON KIMBERLITE-CARBONATITES

THE KIMBERLITE–CARBONATITE RELATIONSHIP

J. B. DAWSON
Dalhousie University, Halifax, Canada

ABSTRACT

A survey of the world occurrences of kimberlite has shown that they are closely associated both in space and time with carbonatites or with rock-types that are often found within carbonatite complexes, *e.g.*, alnöite, olivine melilitite, nephelinite and monchiquite. Good examples of this relationship are found in Africa, North America, Russia and Sweden. A review of the geochemistry of kimberlites has established that although kimberlites contain high amounts of magnesia and iron, they also contain unusually high amounts of K_2O, TiO_2, CaO, CO_2, P_2O_5 and H_2O but their SiO_2 content is often low; these features combined with a high K/Na ratio and a comparatively low Mg/Fe ratio serve to distinguish the kimberlites from most peridotites and serpentinites. Chemically the kimberlites are most similar to alnöites, and there is every gradation from kimberlites and alnöites to carbonatites. More-over, the high concentration of Li, Rb, Sr, Ba, Y, La, Zr, and Nb found in kimberlites is most similar to that found in carbonatites and their associated alkaline rocks.

The intimate spatial, time and chemical relationships between kimberlites and rocks of the carbonatite suite cannot be fortuitous, and it must be concluded that these rock-types are genetically related. Since we have evidence of only very small volumes of kimberlite within the crust, on the basis of volume relationships it is difficult to envisage how comparatively large masses of carbonatite can be derived from kimberlite, as suggested by several workers, and it is suggested that some thought should be given to the possibility that kimberlite may originate by assimilation of crustal granite into the hydrous, magnesia-rock fraction of a carbonatite magma.

INTRODUCTION

During a review of the world occurrences of kimberlites and diamond deposits (Dawson, 1960), one of the features which came to light was the intimate relationship of kimberlites with other rare undersaturated rock types. Good examples of this close relationship are in Arkansas, where kimberlites occur with carbonatite, nepheline syenites, monchiquites, and ouachitite; in New York State, where alnöite dykes grade into kimberlite along their length (Martens, 1924); in Brazil (Rimann, 1915); in the U.S.S.R., where they are part of a petrographic suite embracing dunites, ijolites, urtites, nepheline syenites, alnöites and carbonatite; and in Bushmanland, South Africa, where kimberlite, nephelinite, and olivine melilitite occupies small diatremes and sills. Carbonatite dykes cut the kimberlite of the Premier Mine (Daly, 1925) and recently garnet peridotite nodules resembling the cognate xenoliths in kimberlite have been found in a carbonatitic tuff ring in northern Tanganyika (Dawson, 1964). The kimberlites are not only closely associated in space with the other rocks, but were also intruded at approximately the same time.

GENERAL DESCRIPTION OF THE KIMBERLITES

Mineralogically the kimberlites most closely resemble olivine melilitites and alnöites and, although melilite is absent in kimberlites (which is not surprising in view of the high H_2O content) the rock does contain calcium zeolites, and anorthite (the saturated equivalent of gehlenite) invariably appears in the kimberlite norm. Another strong link between kimberlite and carbonatite is the fact that they are the only two rocks in which moissanite has been found.

Chemically, the kimberlites contain high amounts of magnesia and iron, and also high amounts of potash, titania, lime, carbon dioxide, phosphorus and water; the silica content is sufficiently low for olivine always to appear in the norm, and occasionally nepheline, leucite, kaliophylite and calcium olivine. Within the general terms referred to above, however, the

chemical composition is very variable and with changes in the Ca/Mg ratio and/or an increase in the carbon dioxide content the kimberlites grade into alnöites and carbonatites (see Fig. 1).

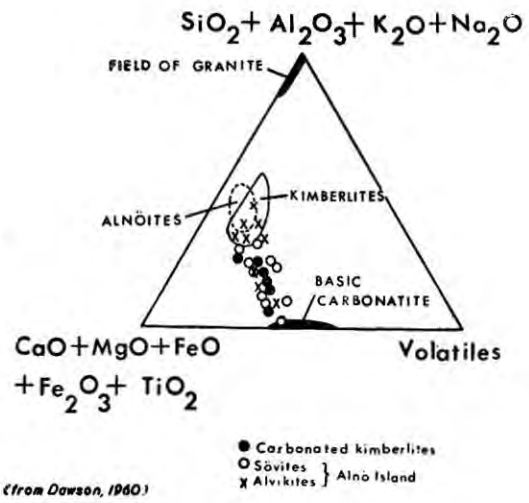

Fig. 1

The high K/Na ratio and the comparatively low Mg/Fe ratio of kimberlite serve to distinguish them from dunites, peridotites and serpentinites, and the K/Rb, Ga/Al and Mg/Fe/Mn ratios are quite unlike those of other ultrabasic rocks, being most similar to those for syenites and granitic rocks. In addition, the high concentrations of Li, Ba, Sr, Y, La, Zr and Nb (Dawson, 1962) are much higher than would be expected in rocks originating in the mantle, and are most similar to those found in carbonatites and their associated alkaline rocks.

Quite apart from the fact that the typical kimberlite mineral assemblage of diamond-pyrope-picroilmenite-phlogopite has never been found in rocks believed to originate in the mantle (Ross et al., 1954) we have sufficient chemical evidence to set kimberlites apart from the mantle-type ultrabasic igneous rocks. On the other hand there is abundant evidence of intimate spatial, time, chemical and mineralogical relationships between kimberlites and rocks of the carbonatite suite. These relationships are too persistent to be fortuitous, and it must be concluded that kimberlite is genetically related to the other rock types. This fact has also been recognised by Saether (1957) and von Eckermann (1961). Saether believes that carbonatite is derived by differentiation from a kimberlite parent, whilst von Eckermann has proposed that kimberlite results from a process whereby percolating carbon dioxide extracts calcium, iron and magnesium from melilite basalt (olivine melilitite), the leached cations combining with the carbon dioxide to form carbonatite. An objection to the theory that kimberlite is the parent of carbonatite is the volume relationships ; from observation of their intrusive bodies within the crust, it is known that kimberlite is much less abundant than carbonatite. Unless one is prepared to postulate that within the sima or mantle there are considerably larger bodies of kimberlite than we know in the crust, kimberlite would not seem to be sufficiently abundant to be regarded as parental material. von Eckermann's hypothesis, whilst explaining the intimate relationships between the kimberlites and the olivine melilitites, does not account for the high potash content of the kimberlites, the fact that in kimberlites K>Na whilst in the melilitites Na>K, and the high water content of the kimberlite. Moreover, extraction of various actions might be expected to produce a rock richer in SiO_2 than the original melilitite.

THE GENESIS OF KIMBERLITE

The main problem in the explanation of the genesis of kimberlite is to reconcile their high potash content with their extreme basicity. It is suggested that this may be achieved by a process in which crustal " granite " is in the first place incorporated into the water-rich ankeritic fraction of a carbonatite magma to give ultrabasic silicate rocks and a fluid rich in volatiles. During the intrusive phase, the ultrabasic rock mass may be disrupted and, whilst some larger masses become entrained and smoothed off in the fluidised rock mass during its ascent into the diatremes, many crystals from the disrupted

mass will react with the residual fluid to form kimberlite. The process, is envisaged as in Fig. 2.

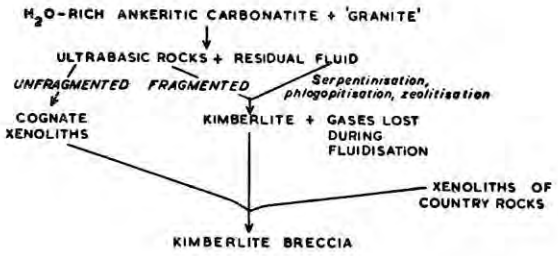

Fig. 2

This proposal, whilst somewhat radical, can give a reasonable explanation for the following kimberlite features.

1. The wide range of composition of kimberlites.
2. The high potash content of kimberlite and the high K/Rb and Ga/Al ratios.
3. The high amounts of the carbonatite-type trace elements.
4. The intimate association between kimberlites and rocks of the carbonatite suite.
5. The extremely small amounts of kimberlite, which points to their being the extreme end point of a magmatic cycle.

It may be pointed out that olivine-pyroxene-garnet-phlogopite assemblages are known at granite/dolomite contacts, and the process envisaged above is merely turning inside out the limestone assimilation hypothesis. This is very similar to the process proposed by Holmes (1950) for the formation of the ultrabasic potassic rocks of Uganda.

In conclusion, it is interesting to speculate that if the assimilation of granitic material is an important feature in the genesis of potassic basic rocks, as many petrologists believe, then to end up with a rock as undersaturated as kimberlite, the silica content of the original assimilating 'magma' must have been virtually nil. The only magmatic rock fulfilling this requirement would be carbonatite.

REFERENCES

DALY, R. A. (1925) Carbonate dykes of the Premier Mine. Transvaal : *Jour. Geol.* Vol. 33, pp. 659–684.

DAWSON, J. B. (1960) A comparative study of the petrography and geology of the kimberlites of the Basutoland province : *Ph.D. thesis*, University of Leeds.

—— (1962) Basutoland kimberlites : *Bull. Geol. Soc. Amer.* Vol. 73, pp. 545–560.

—— (1964) Carbonate tuff cones in northern Tanganyika : *Geol. Mag.*, Vol. 101, pp. 129–137.

ECKERMANN, H. VON. (1961) The petrogenesis of the Alnö alkaline rocks : *Bull. Geol. Inst. Univ. Uppsala.* Vol. 40, pp. 25-36.

HOLMES, A. (1950) Petrogenesis of katungite and its associates : *Am. Mineral.*, Vol. 35, pp. 772–792.

MARTENS, J. H. C. (1924) Igneous rocks of Ithaca, New York, and vicinity : *Bull. Geol. Soc. Amer.* Vol. 35, pp. 305–320.

RIMANN, E. (1915) Uber kimberlit und alnoit in Brasilien : *Tscher. Min. Petr. Mitt.*, Vol. 33, pp. 244–262.

ROSS, C. S., MYERS, A. T., AND FOSTER, M. D. (1954) Origin of dunites and olivine-rich inclusions in basaltic rocks : *Am. Mineral.*, Vol. 39, pp. 693–738.

SAETHER, E. (1957) The alkaline rock province of the Fen area in southern Norway : *Norsk. Vidensk. Selsk. Skrift.*, No. 1, p. 50.

DISCUSSION

James L. Powell (Oberlin College, Oberlin, U.S.A.) : Dr. Dawson has certainly made a very strong case for a closer examination of a possible genetic link between kimberlite and carbonatite. As he has pointed out, kimberlites are highly enriched in magnesium. Carbonatites, on the other hand, contain on the average much more calcium than magnesium. One difficulty in Dr. Dawson's hypothesis is that of explaining how a magnesium-rich rock, kimberlite, can form by an assimilative reaction between calcium-rich carbonatite magma and granite, a rock depleted

in both calcium and magnesium. The hydrous, magnesium-rich fractions of carbonatite magmas to which Dr. Dawson refers must, in view of the relatively small amount of dolomitic carbonatite, be rather scarce. Why should only magnesium-rich fractions of carbonatite magma, and not the more abundant calcium-rich ones, have assimiliated granite to form kimberlite ?

Author's reply : In reply to Dr. Powell's welcome comments, it is worthy of comment that, whilst the dolomitic carbonatite is rarer than calcitic, kimberlite itself is also volumetrically very insignificant, even compared with the carbonatites, within a particular igneous province *e.g.* the Arkansas igneous province. In reply to Dr. Powell's second question, the preferred reaction of the magnesium carbonate with assimilated granite is felt to be due to the fact that the dissociation temperature of magnesium carbonate is some 300°C lower than that of calcium carbonate (at 1 atmosphere). The contention that the magnesium within a mixed carbonate will react preferentially with silica introduced into the system is borne out by observations on metamorphic assemblages in which dolomite and quartz have reacted in the first instance to give forsterite and calcite ; only at higher temperatures are calcium-bearing silicates formed. In this connection, it is interesting to speculate as to whether the dunites, peridotites and pyroxenites found in carbonatite complexes may, in fact, be metasomatic in origin.

MINERALOGICAL SOCIETY OF INDIA, IMA VOLUME, 1966
INTERNATIONAL MINERALOGICAL ASSOCIATION, PAPERS, FOURTH GENERAL MEETING

POTASH FELDSPAR AND PHLOGOPITE AS INDICES OF TEMPERATURE AND PARTIAL PRESSURE OF CO_2 IN CARBONATITE AND KIMBERLITE

D. K. BAILEY
Department of Geology, Trinity College, Dublin

ABSTRACT

Initial studies of orthoclase+dolomite+H_2O⇌phlogopite+calcite+CO_2, at 1 kilobar total pressure, show that the temperature of reaction is strongly dependent on the partial pressures of H_2O and CO_2. With excess H_2O and deficient CO_2, phlogopite+calcite is the stable assemblage above 340°C, below which orthoclase+dolomite is stable: under conditions of excess CO_2, however, orthoclase+dolomite is stable up to 640°C. In the Rufunsa province, Northern Rhodesia some orthoclase in the carbonatite intrusions is rimmed by phlogopite, and the carbonatite pyroclastics contain both feldspathic fragments and phlogopite. Initially orthoclase was stable, setting an upper temperature limit of approximately 600°C to this near-surface activity; subsequently, with rising temperature or, more likely, declining partial pressure of CO_2, phlogopite became the stable potash silicate, setting a lower limit around 300°C. These inferences accord with earlier deductions based on the field relations and petrography (Bailey, 1960). In older and deeper complexes such as Nkumbwa Hill, Northern Rhodesia, phlogopite rock constitutes the inner metasomatic aureole, instead of the orthoclase rock of higher exposure levels such as Rufunsa. This presumbly reflects higher temperature with increasing depth, whereby potash feldspar would eventually become unstable in the presence of dolomite, regardless of CO_2 pressure.

Where dolomitic carbonates are present in kimberlite similar limits are imposed. The initial formation of phlogopite would be above 600°, assuming high P_{CO_2}, but the presence of xenoliths containing unaltered potash feldspar implies temperatures below the range 600°—300°C for the final emplacement of most kimberlite breccia.

PROCEDURE AND RESULTS

Potash feldspar and phlogopite are the common potash minerals in carbonatites, but they show a variable distribution pattern in these rocks. In some provinces phlogopite is the predominant potassic phase, almost to the exclusion of the feldspar, in other provinces either the reverse applies or there is development of both phases. An example of the last type is the Rufunsa volcanic province in Zambia (Bailey, 1960) in which some of the carbonatites contain fragments of orthoclase rimmed with phlogopite. It follows from this reaction relationship that if the relative stabilities of these two potash minerals in a carbonate assemblage can be established they should prescribe the conditions of formation of these rocks. Similar considerations apply, of course, to the relative stabilities of the two minerals in carbonatic kimberlite and the conditions of kimberlite emplacement.

The reaction* is the simplest expression of the possible relationships that might exist between these minerals. Reactions of this type, decarbonation⇌dehydration, though they must be common in nature, have not previously been studied systematically, but an initial study of the above reaction has been made at a total pressure of 1 kilobar (3–4 km depth) and the following is a brief preliminary account of the results. A full account will be given when the systematic investigation of the effect of total pressure is completed.

$$*K_2O.Al_2O_3.6SiO_2 + 6(CaO.MgO.2CO_2) + 2H_2O \rightleftharpoons K_2O.6MgO.Al_2O_3.6SiO_2.2H_2O + 6(CaO.CO_2) + 6CO_2$$

Orthoclase — Dolomite — Water — Phlogopite — Calcite — Carbon dioxide

In this investigation, pure natural orthoclase (Fianarantsoa, Madagascar) and dolomite (Oberdorf, Austria), finely ground and mixed in the proportions 1:6, are sealed with water in platinum capsules, and heated in cold-seal pressure vessels. Control of the vapor composition has been imposed by weighing in known amounts of water to the charge. The position of the reaction curve is then located by finding the temperature at which complete reaction to phlogopite+calcite takes place for a specific ratio of dry charge to water. If reaction is complete the experiment was above the equilibrium curve and the amount of water consumed and the amount of carbon dioxide generated can be calculated, giving the resultant vapor composition (open squares in Fig. 1). The results to date, plotted as temperature against

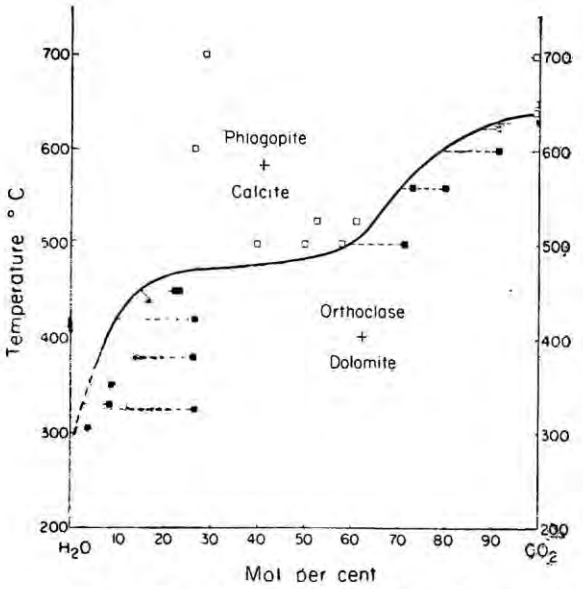

Fig. 1. Equilibrium diagram for the reaction orthoclase + dolomite+water $\rightleftharpoons$ phlogopite + calcite + carbon dioxide at 1 kb total pressure. Broken lines intersecting curve depict runs in which all four solid phases are present. Where water was sufficient for complete reaction the maximum content of CO_2 that might have been generated is shown by a solid square.

vapor composition, are shown in figure 1, and the probable limits of error are indicated. It will be noted that in runs in which all four solid phases persist the reaction was at the equilibrium curve but only an upper limit for the mole fraction of CO_2 can be fixed (solid squares) although with experience some estimate of the extent of reaction can be made from the relative proportions of the four phases. At the higher temperatures reaction is rapid, being complete in a few hours; at lower temperatures, although breakdown of dolomite is still rapid, the formation of phlogopite is sluggish and the curve in Fig. 1 may not be limited by the vapor composition as it approaches pure H_2O, so much as by the lower temperature limit for the formation phlogopite. The temperature of reaction in a CO_2–rich atmosphere rises slightly with increasing pressure and will presumably be limited by eventual intersections with other breakdown curves for dolomite.

APPLICATIONS

In the dissected carbonatite volcanoes of the Rufunsa province in Northern Rhodesia there has been extensive potash metasomatism with the formation of orthoclase rock from a variety of country rocks. Some of the orthoclase incorporated in the intrusions is rimmed by phlogopite, and the carbonatite volcanics variously contain either feldspathic fragments or are rich in phlogopite. It is clear from this that orthoclase initially was stable, setting an upper temperature limit of approximately 600°C to this near-surface activity. Subsequently, with rising temperature or, more likely, declining partial pressure of CO_2, phlogopite became the stable potash silicate in equilibrium with the carbonates, setting a lower limit of temperature around 300°C. Reaction of early-formed orthoclase to produce phlogopite is shown schematically in Fig. 2, from which it is readily seen that a variety of changes could give similar results, within the temperature span of the reaction. In the example cited a change such as that labelled (3) in Fig. 2, would appear the most reasonable because the formation of phlogopite rims on the orthoclase is plainly a late reaction, which would coincide with cooling, and with diminishing CO_2 content in the vapor, following precipitation of carbonates from the

late-stage fluids. This temperature range and the inferences about the sequence of activity with diminishing CO_2 pressure, accords with earlier deductions based on the field relations and petrography (Bailey, 1960, 1965). A survey

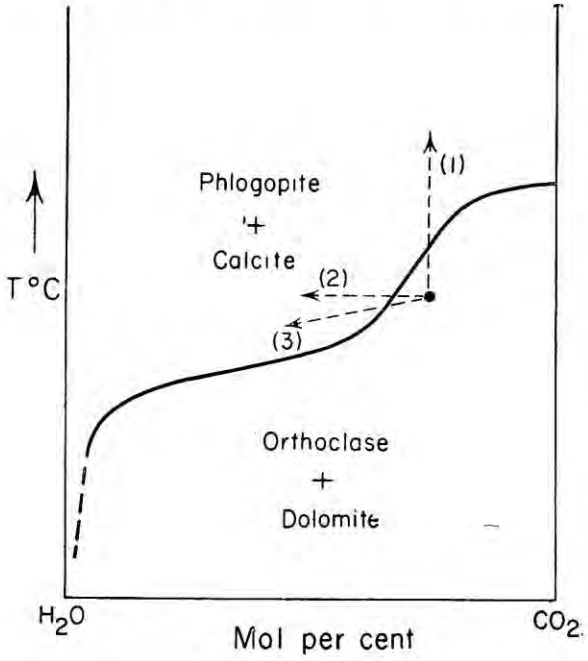

Fig. 2. Schematic diagram showing possible paths by which orthoclase could react to yield phlogopite: (1) with increasing temperature and constant vapor composition, (2) with diminishing CO_2 content in vapor at constant temperature, and (3) with decreasing CO_2 and cooling.

of the literature reveals that potash feldspar rimmed with phlogopite has been recorded in similar subvolcanic complexes in Malawi, Tanzania and elsewhere, and in other complexes the assemblage potash feldspar + dolomite frequently occurs in late-stage veins, emphasizing the possible applications of this reaction. In older and deeper complexes such as Nkumbwa Hill, Zambia, and Phalabora in the Transvaal there are zones of phlogopite rock in the country rocks adjacent to the carbonatite stem, in contrast to the orthoclase rock of higher exposure levels such as Rufunsa. This is probably a reflection of the expected higher temperature with greater depth in a complex, whereby a temperature would eventually be reached at which potash feldspar would be unstable in the presence of dolomite, regardless of CO_2 pressure (path 1 in Fig. 2). Similar considerations probably apply to the marked contrasts between the activity in the Rufunsa and Chilwa complexes and in the Tertiary volcanic complexes of Kenya and Uganda. In the latter the associated nephelinite volcanics bespeak a much higher temperature in the vents, and in the exposed carbonatite cores the characteristic potash mineral is phlogopite. In Rufunsa and Chilwa there is the marked development of potassic feldspars, strikingly displayed in the feldspathic breccias which have no counterpart in the Tertiary East African complexes.

Dolomitic carbonates are common in kimberlite, and this association together with the ubiquitous phlogopite of this rock imposes similar limits to those outlined for carbonatites. The initial formation of phlogopite would be above 600°C, assuming high P_{CO_2}, but the presence of xenoliths of feldspathic granulite, granite or arkose, containing unaltered potash feldspar implies temperatures below the range 600°-300°C for the final emplacement of kimberlite breccia. Such temperatures would be consistent with the conspicuous lack of thermal metamorphism of the wall rocks and xenoliths of most kimberlites.

The presence of potash feldspars and phlogopite in carbonatitic assemblages may therefore be an index of the conditions of formation, and should provide new limits for, and hence better understanding of, the high-level emplacement of carbonatite and kimberlite.

REFERENCES

BAILEY, D. K. (1960) Carbonatites of the Rufunsa valley, Feira District. *Bull. Geol. Surv. N. Rhodesia*, Vol. 5, pp. 1-92.

—— (1965) Carbonatite volcanoes and shallow intrusions in Zambia, in *The Carbonatites*, John Wiley and Sons, New York.

DISCUSSION

P. J. Wyllie (The Pennsylvania State University): 1. The described experimental procedure of weighing initial orthoclase, dolomite, and water into a capsule gives the ratio of CO_2/H_2O in the system as a whole. How did the author estimate the CO_2/H_2O ratio in the vapor phase itself, both above and below the isobaric univariant reaction curve plotted?

2. In the isobaric section through the petrogenetic model on which the reaction is plotted, the representation of the reaction by a single curve means that the reaction is divariant (isobaric univariant). Five phases participate in the reaction, and the phase rule requires that these are made up from five components. What are these five components? There are seven "oxide components", and if these cannot be reduced to five components, it appears that the reaction should proceed through a temperature interval, even under isobaric conditions. Presumably the answer lies in the chemical equation for the reaction.

Author's reply: The position of the reaction curve is located by the temperature at which there is complete reaction for a specific ratio of dry charge to water (in a sealed capsule) because if reaction is complete the amounts of water consumed and CO_2 generated can be calculated giving the resultant vapour composition. In runs in which all four solid phases persist the same calculation indicates only the possible limit of CO_2 generation but with some experience the extent of reaction can be gauged from the relative proportions of the four solid phases.

The answer to Dr. Wyllie's second question lies, as he infers, in the treatment of the reaction equation, which was not shown in the slides. The simplest explanation is that the orthoclase molecule can be treated as a component, which together with MgO, CaO, CO_2, and H_2O gives expression to the reaction in terms of five components.

J. Gittins (Toronto): What is the effect of decreased pressure on the reaction curve? Unless the curve is relatively insensitive to pressure changes it seems doubtful whether the results can be applied equally to Nkumbwa where the pressure may well have been 1 kb at the depth represented by the present erosional level, and to Mwambuto where the pressure must have been very considerably lower.

Author's reply: It is intended to study the variation of the reaction with total pressure but so for only a very few results are available. These indicate a slight increase of reaction temperature with increasing pressure and consequently it may be supposed that orthoclase would be stable to higher temperatures in deeper complexes. Until the variation has been studied systematically, however, it is not possible to be more explicit. The pressure in the Mwambuto complex may not have been as low as suggested by Dr. Gittins because the original height of the volcanic cone (mostly removed by erosion) is unknown. A more likely alternative is that pressures at the Nkumbwa level were in excess of 1 kb.

The author would like to thank Dr. Wyllie and Dr. Gittins for their contributions to the discussion, and to express his appreciation of Dr. Gittins' kindness in presenting the paper on the author's behalf.

MINERALOGICAL SOCIETY OF INDIA, IMA VOLUME, 1966
INTERNATIONAL MINERALOGICAL ASSOCIATION, PAPERS, FOURTH GENERAL MEETING

CARBONATITE IN THE ALKALINE COMPLEX OF THE ICE RIVER AREA, SOUTHERN CANADIAN ROCKY MOUNTAINS

JUNE E. RAPSON
University of Alberta, Calgary, Canada

ABSTRACT

The Ice River valley is situated among the westerly ranges of the southern Canadian Rocky Mountains, British Columbia. The region is the site of a nepheline syenite-ijolite-pyroxenite complex intruded into Cambro-Ordovician limestones and shales, and is dated by the potassium-argon method (with biotite) as Devonian in age.

Within the complex is a mass of carbonatite, at least two miles long and nine hundred feet across, associated with the basic and ultrabasic differentiates. The dominant carbonate is ankeritic in composition but calcite is invariably present and there is apparently an increase in the iron/magnesium content towards the centre of the mass. Sideritic concentrations occur in the form of later veins or dikes. Feldspar, sodic pyroxenes and pyrochlore are important accessory minerals.

Contact of the syenite and ijolite with the Palaeozoic limestones and shales is marked either by a narrow zone of fenitized rocks and contorted marble, or by a few, to many hundreds of feet of multicoloured hornfels and skarn.

Contact of the carbonatite with the ijolites and pyroxenites is marked by an intensely fractured and brecciated ferrugenous zone which merges into foliated and carbonatized aegerine-feldspar fenites which in turn merge into, and alternate with, the interveining pyroxenite-ijolite complex.

The following order of emplacement is suggested: (1) basic and ultrabasic differentiates (with veins cutting sedimentary rocks); (2) carbonatite (which fenitizes and contains xenoliths of (1); (3) nepheline syenite (which brecciates and veins ijolites and sedimentary rocks) and finally (4) various lamprophyres (which cut both syenite and sedimentary rocks).

INTRODUCTION

The Ice River valley is situated in Yoho National Park, British Columbia, in the westerly ranges of the southern Canadian Rocky Mountains (Fig. 1). The region, occupying approximately sixteen square miles, is the site of a nepheline syenite-ijolite-pyroxenite complex which is intruded into Cambrian and Ordovician sedimentary rocks. Associated with the basic and ultrabasic differentiates is a mass of ankeritic carbonatite.

This paper is a field and petrographic account firstly, of the contacts of the leucocratic and mesocratic alkaline rocks with the surrounding Ottertail limestone and secondly, of the nature of the carbonatite and its relationship to the ijolite-pyroxenite differentiates.

The area under consideration (Fig. 2) lies just north of the Garnet Mountain-Butwell Peak ridge and extends south to Shining Beauty Creek. It is bounded by Clawson Ridge on the southwest and on the east by the south flowing Ice River.

The field work was accomplished during the Fall in 1960, 1962 and 1963. A preliminary report on the field work of 1960 and 1962 was published previously (Rapson, 1963). The 1963 field work was financed jointly by the Geological Departments of the Universities of British Columbia and Alberta, Calgary. The cost of laboratory work, thin sections, drafting and photography was financed by the University of Alberta, Calgary.

The author is indebted to Mr. R. Bray (now at McMaster University), Mr. A. Gorveatt, University of Alberta, Calgary and Mr. M. Schau, University of British Columbia, for their assistance in the field. Dr. P. S. Simony, University of Alberta, Calgary kindly read the manuscript of this paper and offered suggestions for its improvement.

HISTORY OF PREVIOUS RESEARCH

At the close of the nineteenth century, G. M. Dawson noticed sodalite syenite pebbles in the vicinity of the Ice River thus indicating the whereabouts of the alkaline intrusion. Later Dawson visited the Ice River valley and collected a suite of representative rocks, these were reported (1885) and described petrographically by Barlow (1902). Meanwhile Whymper had collected sodalite syenite pebbles from the Beaverfoot river gravels and sent the material to Bonney for descriptions which were also published in 1902.

Between 1900 and 1914 prospectors entered the area and worked various opencasts, the most productive of which was in Shining Beauty Creek. Here, pyrite, galena, chalcopyrite and arsenopyrite were extracted from veins and pockets yielding economic returns for silver and zinc.

J. A. Allen then mapped the area during 1910, 1911 and 1912; the results were published in a memoir of the Geological Survey of Canada (1914).

No further work appears until 1955 when Jones noted the occurrence of aegerine-augite, acmite and pyrochlore in association with the central carbonate mass which had been mapped and described by Allan as a " stoped block ". Subsequently Pecora (1956) and Agard (1957) deduced that the mineral association indicated the presence of a carbonatite. This was confirmed (Rapson, 1964) by field and petrographic evidence.

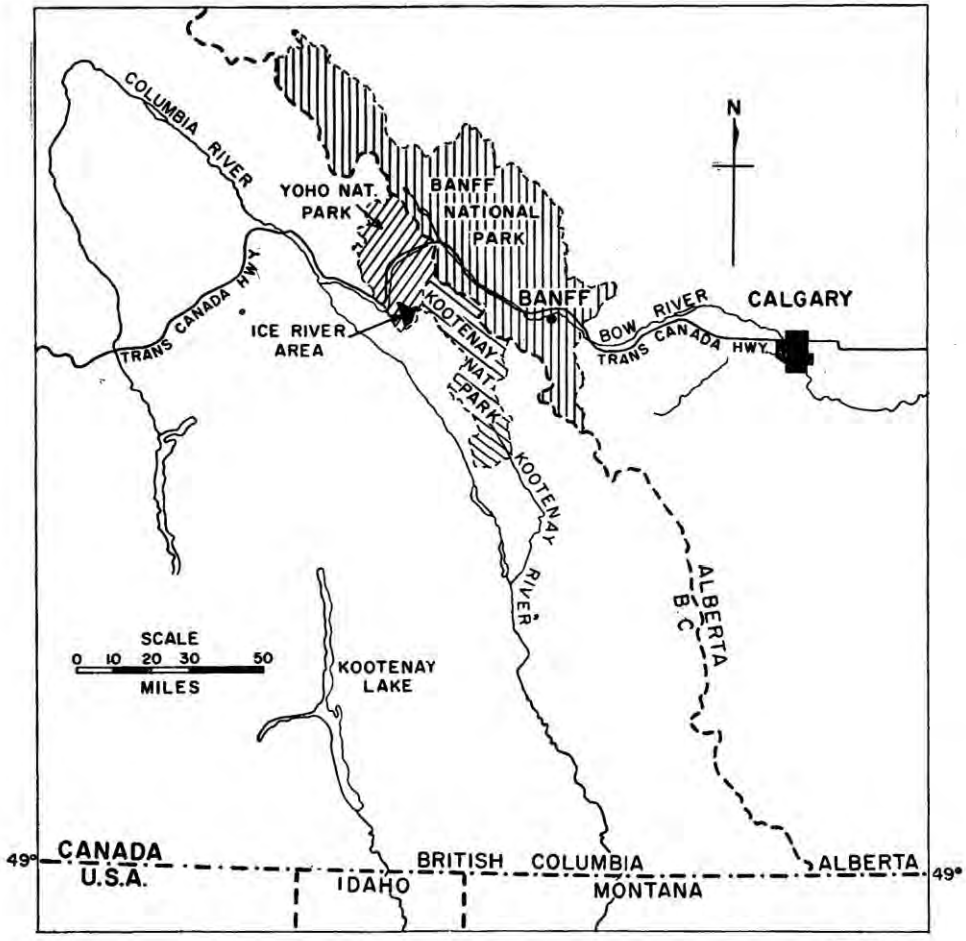

Figure 1.

Gussow and Hunt (1959) suggested that the complex could be eroded basement and therefore pre-Cambrian in age. The author, in 1960 went into the area to ascertain whether or not the contact with the surrounding sediment was a metamorphic one, and to collect material for absolute age determinations. These results were published in 1963.

GENERAL GEOLOGY

The alkaline complex cuts through and metamorphoses the surrounding sedimentary rocks. These are the Chancellor sandstones and shales and the Ottertail limestone presumably of Cambrian age, and the Goodsir shale of Ordovician age.

Absolute age determinations (by the potas-

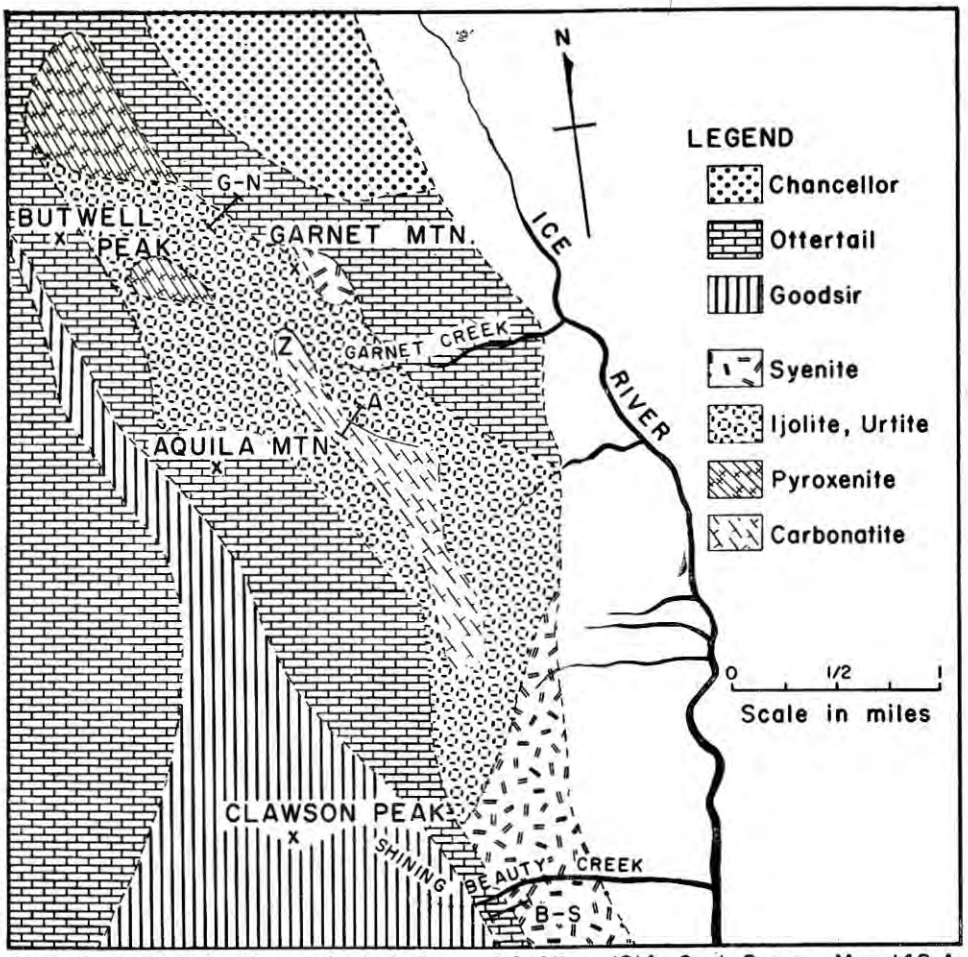

Geological Sketch Map adapted from J.A. Allan 1914 Geol. Survey. Map 142 A.

Figure 2.

Campbell (1961) discussed probable differentiation trends in the complex from the first formed melanocratic jacupirangite to the leucocratic nepheline syenite; he deduced that the sodalite syenite was a hybrid rock.

Absolute age determinations were made by Lowden (1960), Baadsgaard *et al.* (1961) and Edwards (in Rapson, 1963), indicating in each case a Devonian age for the complex.

sium-argon method with biotites) have been obtained from three independent sources, Lowdon (1960) Baadsgaard *et al.* (1961) and Edwards (in Rapson, 1963). Their results give a spread of 65×10^6 years, from 392×10^6 years to 327×10^6 years thus placing the intrusion in the Lower Palaeozoic era, no earlier than the Silurian and most probably during the Devonian period. The author (1963) suggested that the age spread may

be an indication of the total time of emplacement or differentiation of the complex.

The alkaline complex consists of leucocratic, mesocratic and melanocratic differentiates.

The leucocratic differentiates include such rock types as syenite, sodalite syenite, nepheline syenite, ditroite and foyaite. In the area under consideration these rocks occupy the southern end of the valley and a small area to the west of the peak of Garnet Mountain (Fig. 2). They are seen in contact with the Ottertail limestone, also veining and brecciating earlier leucocratic and mesocratic material (Plate I, Fig. 1), as well as the metamorphosed limestone. Contacts with the limestone may be examined at many localities along Clawson Ridge (Allan, 1914; Rapson, 1963) and on Garnet Mountain (Allan, 1914; Jones, 1956; Schau, 1964).

The melanocratic differentiate of the complex is a jacupirangite pyroxenite with magnetite, ilmenite, sphene and schorlamite as essential components.

The mesocratic differentiates include ijolite, urtite and malignite and grade in composition between the syenitic and pyroxenitic rock types.

In the area under consideration the mesocratic differentiates occupy the central part of the region from Butwell Peak to Shining Beauty Creek. They are seen in contact with the Ottertail limestone up Shining Beauty Creek and on the north side of the Garnet Mountain-Butwell Peak Ridge (Allan, 1914; Rapson, 1963). Contact with the syenite at Shining Beauty Creek and on Garnet Mountain is described as covered (Allan, 1914) or faulted (Schau, 1964).

The melanocratic rocks were mapped by Allan in a large mass north of Butwell Peak and in a smaller area southeast of Butwell Peak. The author observed them associated with mesocratic rocks to form a complex of interveining rock types in a zone on the flanks of Aquila Ridge. It is apparent that this zone surrounds the carbonatite on all sides. Schau (1964) notes the occurrence of a zone of ultramafic rocks west of the zone of basic rocks on Garnet Ridge with the two zones apparently merging into one another.

The carbonatite occupies an area of approximately two miles in length and nine hundred feet in width. It forms the eastern part of Aquila Ridge, the floor of the east and north sides of Garnet Cirque and apparently continues beneath the screes of Garnet Mountain Ridge. The carbonatite appears to fenitize the surrounding interveining melanocratic-mesocratic zone. The carbonatite contains ferrugenous concentrations and is in turn cut by veins or dykes of marble pegmatite and siderite. Rocks of similar composition are seen cutting the ijolite pegmatite zone along Garnet Ridge (Schau, 1964) in a position in line with the main mass of carbonatite in Aquila Ridge. The carbonatite has not been seen in contact with the syenite.

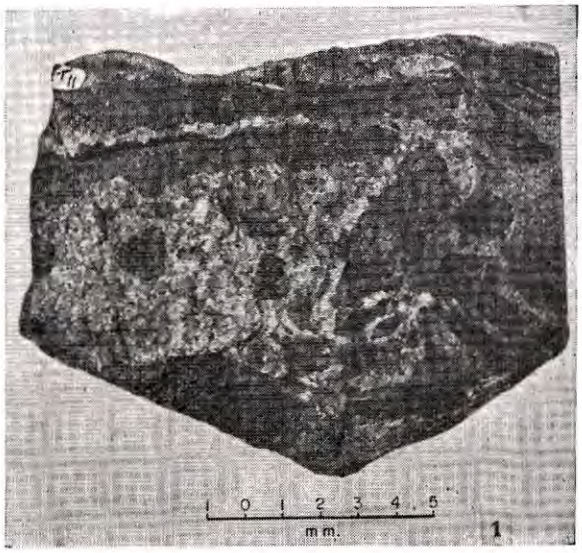

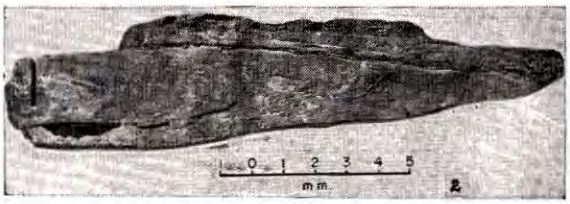

PLATE I

Fig. 1. Breccia of hornfels in syenite.
Fig. 2. Folded marble at the contact with syenite.

FIELD TRAVERSES AND SAMPLE DESCRIPTIONS

Nine sections or traverses across the various contacts have been examined and collected

systematically in the field, some of these have been described briefly (Rapson, 1963), four of them are described in this paper.

The sections are (Fig. 2) Shining Beauty Creek-south (B–S), Garnet Mountain Ridge-north side (G–N), Aquila Ridge Gully (A) and a traverse across a xenolith of ijolite pegmatite (Z) within the carbonatite on the north side of Garnet Cirque.

1. Shining Beauty Creek-south (B–S).

Contact of the Ottertail limestone with syenite.[1]

The limestones, at one thousand feet from the contact, are bedded, buff and grey coloured and sparsely laminated. Occasional sedimentary breccias are seen. There is some recrystallization of the calcite with a tendency to the alignment of micaceous material parallel to the bedding. Approaching the contact there is noticeable recrystallization and granulitization (Plate IV, Fig. 1) with pronounced alignment of flaky material. The original bedding and sedimentary structures are still clearly visible.

Two feet from the contact the limestones are intensely folded, contorted and completely recrystallized, showing a granular or even a schistose texture (Plate I, Fig. 2). Diopside and tremolite are developed in increasing amounts towards the contact.

A two inch band of multicoloured skarn and marble occurs, associated with medium grained hornfels, a few inches from the contact. The skarn is composed of diopside and tremolite in a recrystallized ground mass of calcite and containing patches of acmite and scapolite. The hornfels consists of a mosaic of scapolite with scattered clots of phlogopite and sericite A little feldspar and garnet are present.

At the contact the scapolite hornfels is brecciated and granulitized, then cemented or veined with natrolite.

The syenite from this locality is composed of 90 to 95 percent leucocratic material with 5 to 10 percent ferromagnesian minerals. The latter consist of patches of aegerine-augite in part altered to acmite and associated with magnetite or ilmenite. The leucocratic components consist of almost equal quantities of perthite and nepheline, both altered peripherally to cancrinite. Sodalite, sphene and a little plagioclase occur interstitially in varying proportions.

2. Garnet Mountain Ridge-north side (G–N).

Contact of the Ottertail limestone with ijolite (Fig. 3).[2]

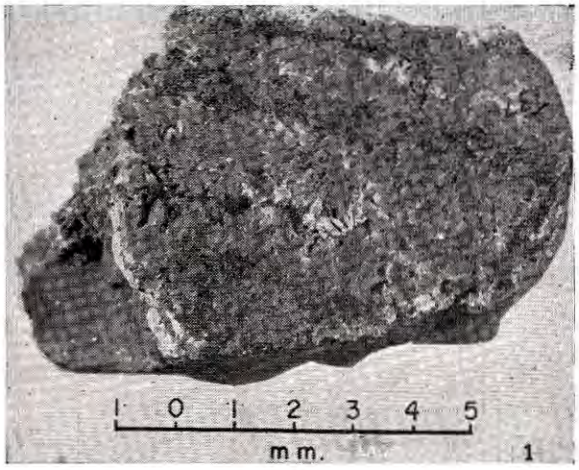

PLATE II

Fig. 1. Banded carbonatite.
Fig. 2. Brecciated carbonatite.

[1] References: Allan, 1914, p. 111; Rapson, 1963, p. 120.

[2] References: Allan, 1914, p. 113; Rapson, 1963, p. 121.

The Ottertail limestone, two thousand feet from the contact, consists of finely bedded calcareous mudstone with phyllitic partings. Some quartz sericite granulites with idocrase appear cutting or inter-bedded with the calcareous beds.

Approaching the contact the beds dip with increasing steepness until at thirty feet they are overturned; the calcareous beds become progressively recrystallized with the metamorphic minerals diopside and tremolite developed.

Calcite marble with tremolite (Plate IV, Fig. 2) is found at thirty feet with tremolite marble at twenty-five feet and chondrodite marble occurring twenty feet from the contact.

Approximately ten feet from the contact occurs a rock with a banded and foliated appearance. It is a marble with clots and stringers of well developed phlogopite and tremolite. This rock is succeeded by a mottled melanocratic breccia associated with coarse grained syenitic rock which is apparently invaded by the breccia (Plate IV, Fig. 3). The breccia consists of finely crystallized orthoclase, nepheline and aegerine which have been granulitized and disassociated then cemented by a feldspathic and chloritic matrix.

At the contact foliated leucocratic rock occurs veining a medium grained amphibolite. The leucocratic rock is composed of perthitic feldspar with some nepheline and zoned prisms of pyroxene; alternating foliae of the same

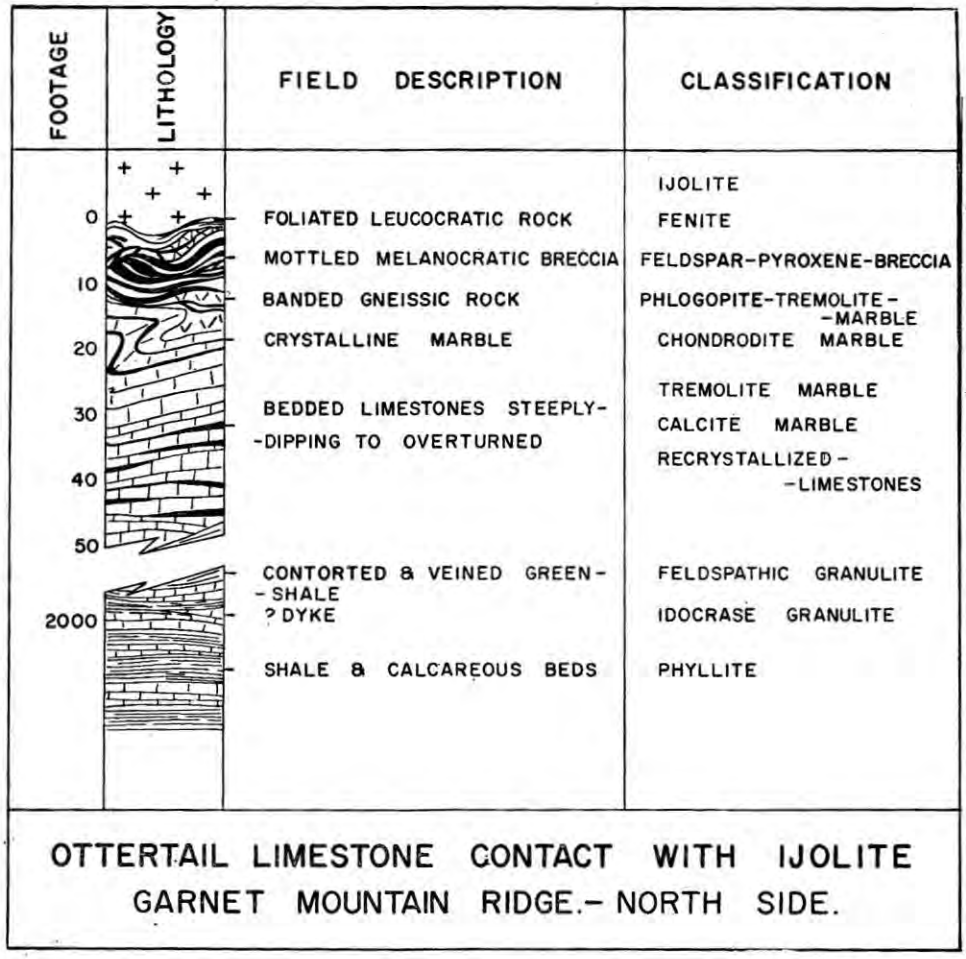

Figure 3.

composition are extensively granulitized; the rock may be classified as a fenite.[1]

The ijolite is composed of 65 percent leucocratic material and 35 percent melanocratic material. The leucocratic material consists of thoroughly calcitized anhedral nepheline prisms and subhedral orthoclase feldspar; the feldspar

3. *Aquila Ridge Gully (A)*

Contact of the carbonatite with the mesocratic-melanocratic zone (Fig. 4).

The traverse starts in the carbonate rock which may be banded or brecciated (Plate II, Figs. 1 and 2) and is dominantly ankeritic in composition but with some calcite also present.

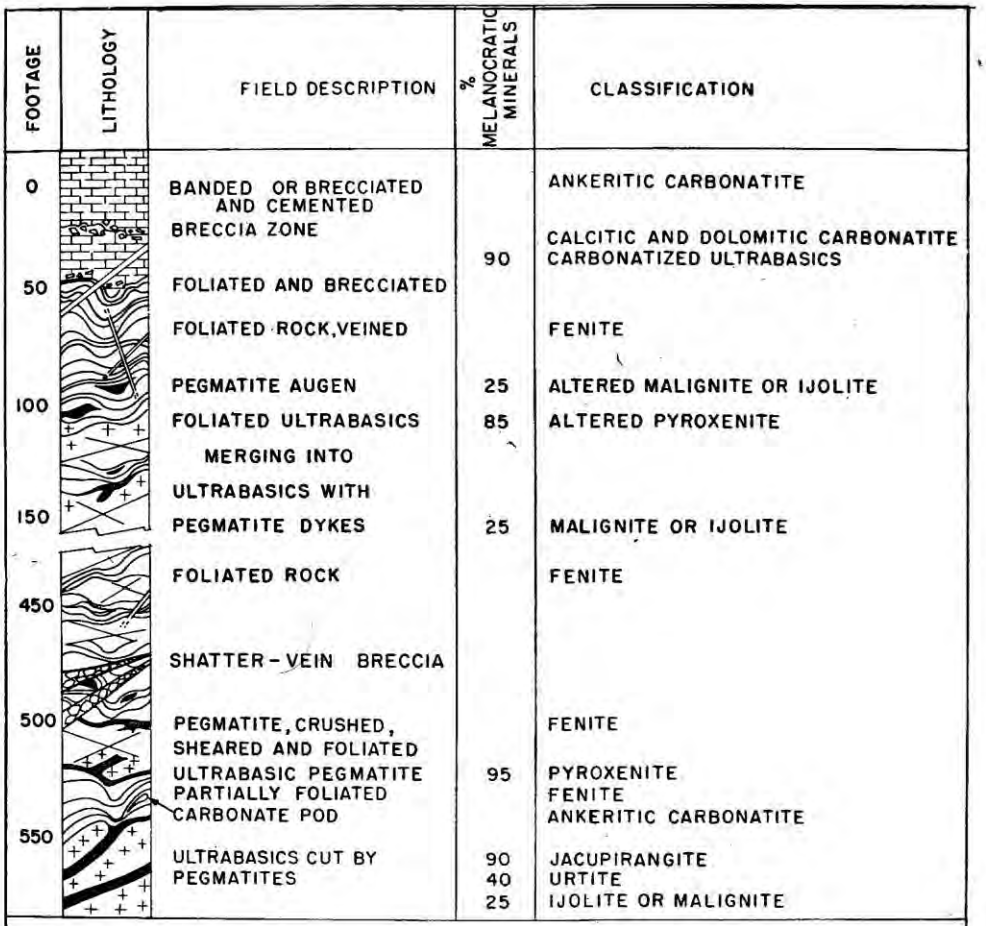

CARBONATITE AND ADJACENT ROCKS
GULLEY TRAVERSE - AQUILA RIDGE Figure 4.

is relatively fresh. The melanocratic material consists of very dark green aegerine-augite. Approaching the contact with the fenite the feldspars are replaced by cancrinite and all constituents brecciated and granulitized.

An intensely brecciated zone follows, then another twenty feet of iron stained carbonate containing dark coloured streaks and patches. The darker coloured material is granulitized and carbonatized pyroxene, visible as relict crystals.

1 " By fenites, accordingly, is meant " in situ " metasomatically altered (with or without substantial material exchanges) older contacting rocks irrespective of composition ". von Eckermann, 1948.

This part of the section is cut by some large dikes, one in particular is composed of coarsely crystalline white calcite with biotite and schorlamite. This particular dike cuts both the iron-stained carbonate and the succeeding foliated and brecciated contact rock.

The carbonate proper ends in another breccia zone adjacent to a complex of foliated rocks that are composed of at least 90 percent melanocratic material. These rocks may be described as carbonatized ultra-basics composed essentially of brecciated, sheared and recrystallized dark-green pyroxene (Plate V, Fig. 1). Dark-brown biotite has developed and the small amount of feldspathoid or feldspar formerly present is replaced by micaceous material and some sodalite, with the whole rock extensively veined by calcite. This foliated rock may be termed a fenite.

About eighty feet from the beginning of the traverse, pegmatite augen may be discerned within the foliated and fenitized mass. These pegmatite bodies merge into the foliated rock at their edges but at the centre preserve their original textures (Plate III, Fig. 1); they are more leucocratic than the ultra-basics within which they are foliated. Composed essentially of only 25 percent melanocratic material, they may be classified as either altered malignites or ijolites (Plate V, Fig. 3); the nature of the original feldspathoid or feldspar cannot be determined.

One hundred feet from the beginning of the traverse foliated rocks are composed of approximately 85 percent melanocratic material and may be identified as altered pyroxenite, possibly jacupirangite. Some parts of the section are covered but where exposed, foliated ultra-basics merge into unfoliated ultra-basics which in turn are cut by pegmatite dikes. These dikes are composed of 25 percent melanocratic material and thus classified as malignite or ijolite.

From one hundred and fifty feet to four hundred and twenty feet the section is much the same as that just described and is omitted from the figure in order to facilitate drafting.

From four hundred feet distinct basic and ultra-basic rocks are cut by pegmatite dikes and merge at intervals into intensely foliated zones. The foliated rocks have a more banded appearance than those previously noted (Plate III, Fig. 2). They are composed of alternating leucocratic and melanocratic foliae. The leucocratic foliae consist of a mosaic of granulitized

PLATE III

Fig. 1. Ijolite pegmatite foliated into fenite.

Fig. 2. Banded fenite-weathered surface.

feldspar and feldspathoid with melilite, some scapolite and carbonate. The alternating melanocratic foliae consist of brecciated and altered pyroxene and well developed biotite with scapolite and abundant muscovite or phlogopite. In addition calcite and scapolite may vein the whole rock and a narrow zone of sodalite may separate the foliae (Plate V, Fig. 2). These foliated rocks may be termed fenites.

Approximately four hundred and seventy feet and four hundred and ninety feet from the beginning of the traverse there are numerous shatter veins with unconsolidated breccia.

From five hundred and twenty feet to five hundred and forty feet fewer foliated bands occur and the original nature of the basic rocks cut by the pegmatite is discernible.

Between five hundred and forty feet and five hundred and eighty feet, a complex of pegmatite dikes and veins (Plate V, Fig. 4) of intermediate composition (that is with 15 percent to 40 percent melanocratic material) cut distinctly melanocratic rocks which are either melteigite or jacupirangite with 80 percent to 95 percent melanocratic material.

4. *Garnet Cirque-north side (Z)*

Xenolith in carbonatite (Fig. 5).

This traverse is across a xenolith which occurs within the main carbonatite mass before it is covered by the screes of Garnet Ridge.

The xenolith is ten feet across in the region of the traverse and approximately twenty feet in length. It is a pegmatite of ijolitic composition with 65 percent leucocratic material and about 35 percent melanocratic material. The leucocratic material is largely nepheline, with reaction rims of cancrinite and biotite. The melanocratic minerals are aegerine-augite with patches of aegerine and biotite. Calcite is present and appears to be primary.

The xenolith is cut by a small dike of finer grained basic rock veined with calcite. The dike rock is composed of approximately 95 percent

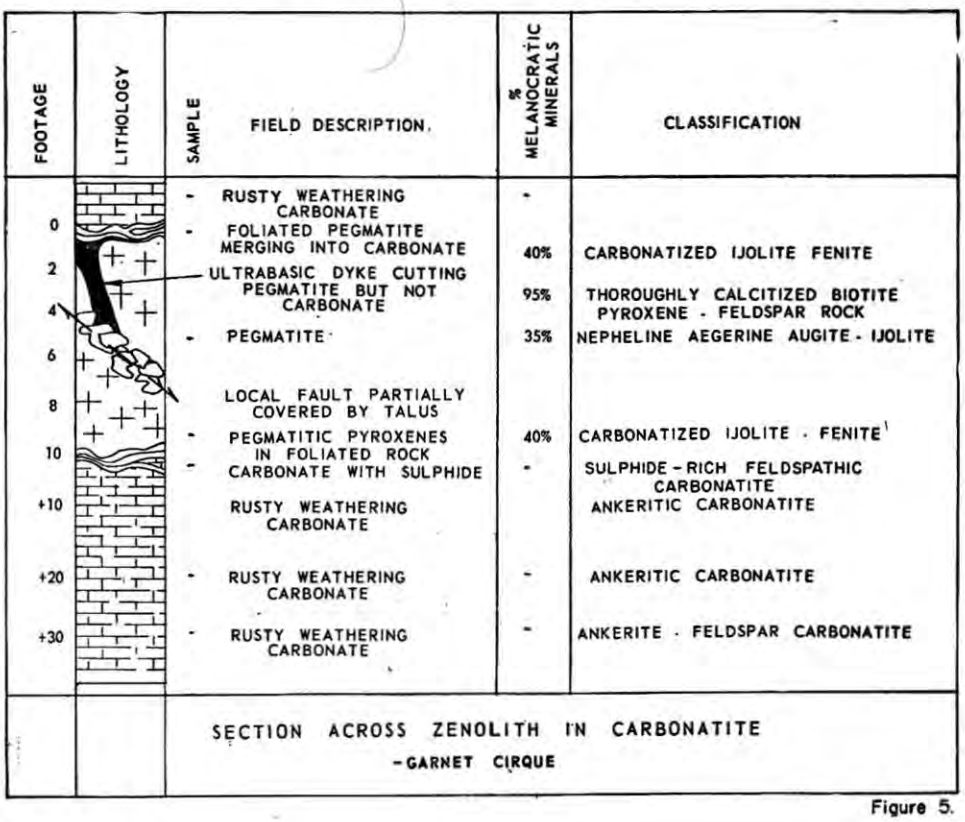

Figure 5.

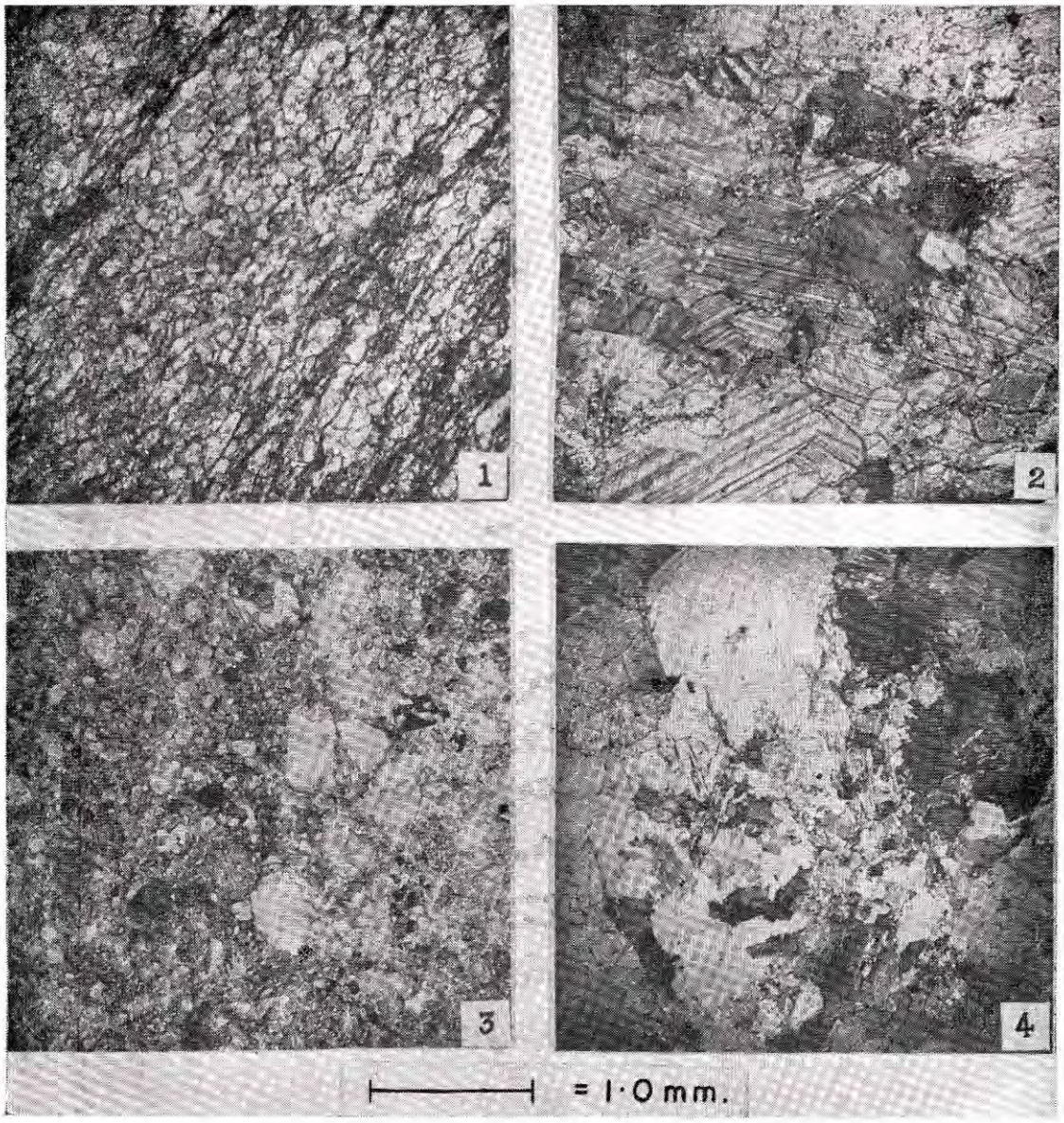

PLATE IV

Fig. 1. Recrystallized limestone with elongate minerals aligned parallel.

Fig. 2. Calcite marble with acicular tremolite developed.

Fig. 3. Feldspar pyroxene breccia at the contact with the ijolite.

Fig. 4. Feldspathic carbonatite. (double polarized light).

melanocratic material, now thoroughly carbonatized and with a considerable growth of secondary biotite. Toward the periphery of the xenolith the ijolite becomes carbonatized with the feldspar and feldspathoid recrystallized or completely replaced by muscovite and sodalite. At the periphery of the xenolith both ijolite pegmatite and the dike become foliated and merge into the surrounding carbonate rock.

THE CARBONATITE

The carbonatite is a white and buff or green coloured rock when fresh ; the colouration may give a banded (Plate II, Fig. 1) or mottled appearance to the rock. The carbonatite weathers to a red-brown colour due to abundant iron oxide occurring in patches and along cleavage cracks. Occasionally the rock is brecciated and then cemented (Plate II, Fig. 2). All samples are coarsely crystalline, averaging 2.0 to 2.5 mm. crystal size, but the crystals may range from 1.0 to 3.0 mm. in diameter. The texture is typically that of a marble.

Nearly all samples examined give an immediate reaction to dilute hydrochloric acid indicating the presence of some calcite, although the majority of the carbonate rock is insoluble.

In thin section the carbonate rock is seen as an interlocking crystal mosaic showing extensive granulitization, either throughout the whole section or localised into laminae.

Examination of the carbonate in a crush and with oils indicates a dominant ankeritic composion ($n_E = 1.5$ to 1.52 and $n_W = 1.69$ to 1.72), some siderite ($n_E = 1.63$) and calcite ($n_E = 1.485$ and $n_W = 1.655$) are present in varying proportions. The rock contains the highest proportion of calcite near the edge, with the ferromagnesian content of the carbonate increasing towards the centre of the mass.

Interstitial to the carbonate crystals, or occluded within them is fresh feldspar, either plagioclase (albite) (Plate V, Fig. 4) or orthoclase ; occasionally the plagioclase prisms have grown round an altered perthitic core. When the rock is granultized the feldspar crystals show distortion in the form of bending and ultimately fracturing.

Vermiform chlorite may also occur interstitially with hematite (altering to limonite), colourless garnet, diopside and phlogopite. In the zone adjacent to the contact with the mesocratic/melanocratic rocks (Aquila Ridge Gully) relict dark green pyroxene is visible occurring in stringers or foliae. Jones (1955) reports the presence of small crystals of pyrochlore. An ankeritic pod of carbonatite (occurring within the foliated ijolites) over five hundred feet from the contact in the traverse in the Aquila Ridge gully, is studded with small octohedra (0.3 mm. in size) of magnetite.

Samples of carbonatite were sent to Dr. J. Powell of Oberlin College Ohio, U.S.A. and to Dr. T. Deans of the Overseas Geological Survey, London, England for strontian isotope analysis. Additional examples of the skarns and unmetamorphosed limestone were also sent to Dr. Deans for comparative analysis. Preliminary results appear to compare favourably with results from carbonatites in other parts of the world.

The carbonatite only occurs in association with the mesocratic-melanocratic differentiates of the complex. These rocks are extensively foliated and fenitized in a zone or zones extending at least five hundred feet from their contact with the carbonatite.

Four facts tend to support the view that the carbonatite is the fenitizing agent :

1. The foliated and fenitized horizons increase in number and intensity of alteration as one approaches the carbonatite mass.

2. Replaced pyroxenes (visible as relict crystals) occur in a zone separating the carbonatite proper from the fenites and altered mesocratics ; this appears to indicate assimilation of the host rock at the edge of the carbonatite mass.

3. Ankeritic carbonatite pods occur in the foliated ijolite over five hundred feet from the contact with the carbonatite.

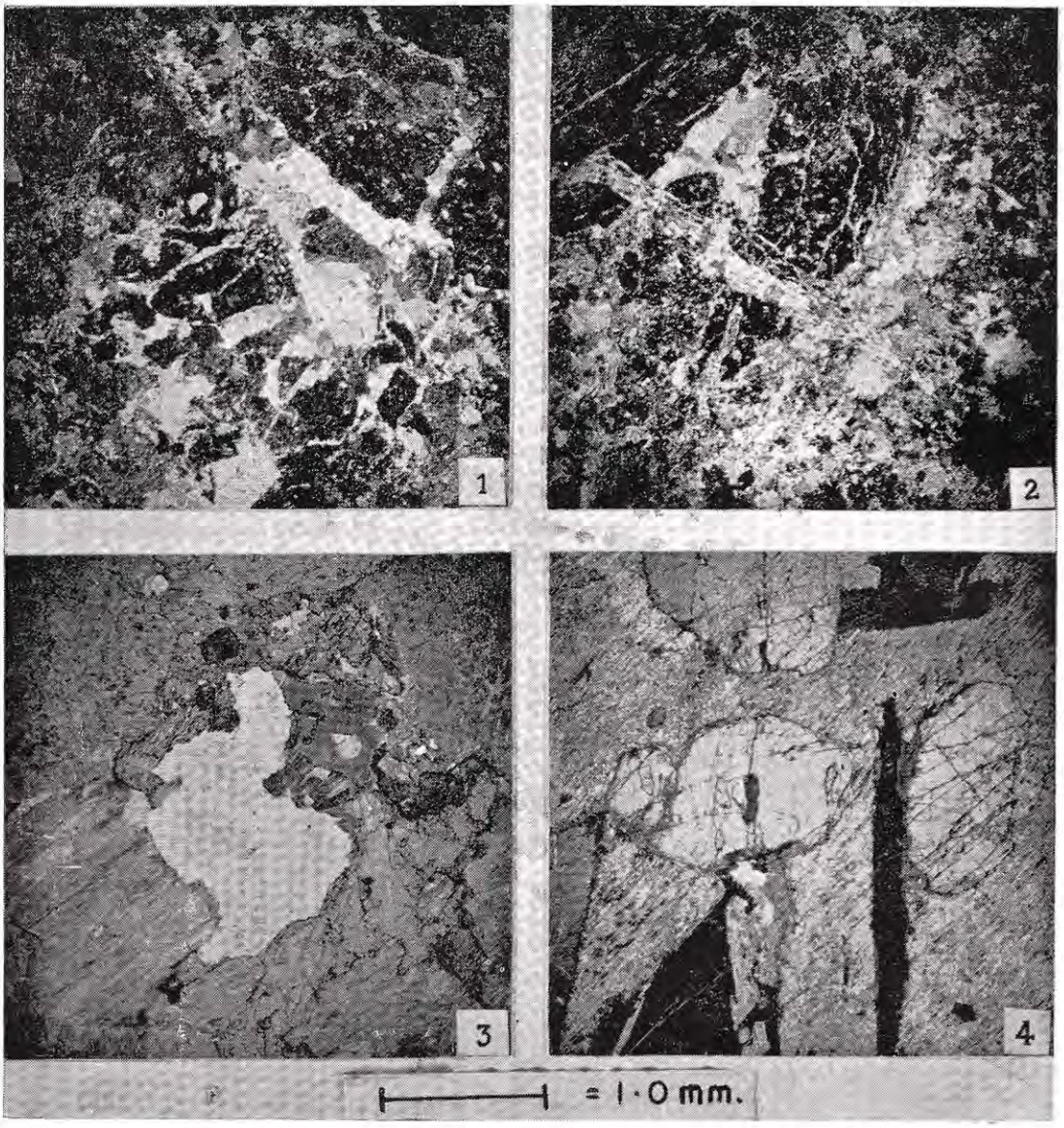

PLATE V

Fig. 1. Fenitized pyroxenite in a matrix of calcite and muscovite.

Fig. 2. Fenite with leucocratic and melanocratic foliae, veined with calcite and scapolite.

Fig. 3. Altered malignite or ijolite.

Fig. 4. Ijolite pegmatite with sericitized feldspar, aegerine-augite and apatite. (double polarized light).

4. At least one xenolith, ten feet wide, of ijolite pegmatite occurs well within the main mass of the carbonatite, and this xenolith exhibits granulitization and fenitization of its periphery.

ORDER OF EMPLACEMENT

The order of differentiation, and the order of emplacement of the components of an alkaline rock mass in general, and that of the Ice River area in particular, is considered to be from the most basic to the least basic differentiates (Allan, 1914; Campbell, 1961). It is possible that this order is substantiated by the results of absolute age determinations (Rapson, 1963) on different rocks of the complex.

Field evidence shows that the most basic rocks occur in zones merging into the mesocratic differentiates. In the zone adjacent to the carbonatite both melanocratic and mesocratic rocks intervein, with apparently no overall order in their emplacement (Fig. 4).

In this interveining zone both mesocratic and melanocratic differentiates are foliated and fenitized by the carbonatite. On Garnet Ridge, late ferrugenous differentiates of the carbonatite apparently cut the ijolite pegmatite zone (Schau, 1964) but not the adjacent syenite.

The mapped contact between the mesocratic differentiates and the syenite is not satisfactorily explained since it is either covered (Allan, 1914) or possibly faulted (Schau, 1964). In Shining Beauty Creek lateral apophyses and tongues of syenitic material brecciate and vein the ijolitic rocks, indicating a post ijolite age for the syenite.

The syenite is also seen brecciating and veining other rocks of leucocratic composition indicating two or more phases in the emplacement of the leucocratic differentiates. This is suggested by Campbell (1961) who considers, for example, that the sodalite syenite is a hybrid rock evolved separately from the nepheline syenite.

Fenites are present at the contacts of both the carbonatite with the mesocratic-melanocratic differentiates, and the syenitic or ijolitic differentiates with the surrounding sedimentary rocks. The fenites associated with the carbonatite contact are foliated gneissic rocks of alternating mesocratic and leucocratic composition (Plate V, Figs. 1 and 2). The fenites associated with the syenite or ijolite contacts are the pink or red coloured syenitic gneiss (Allan, 1914) and foliated microbreccias of an original mesocratic composition, cemented by a leucocratic matrix (Plate IV, Fig. 3).

The presence of a brecciated mesocratic rock may either indicate a more extensive mesocratic zone which was present before the emplacement of the syenite, or be indicative of a 'front' formed during feldspathisation or nephelinitisation prior to emplacement of either syenite or ijolite.

Since the syenite and carbonatite have not been observed in contact the priority of one over the other remains in doubt. However the close association of the carbonatite only with the mesocratic melanocratic differentiates, and the absence of late stage ferrugenous differentiates of the carbonatite cutting the syenite, could indicate that the emplacement of the carbonatite occurred before the emplacement of the syenite.

Therefore the following order of emplacement is suggested :

1. Basic and ultrabasic differentiates (with veins cutting sedimentary rocks).

2. Carbonatite which fenitizes and contains xenoliths of 1.

3. Nepheline syenite, which brecciates and veins both ijolites and sedimentary rocks; and finally

4. Various lamprophyres, which cut both the syenite and the sedimentary rocks.

REFERENCES

AGARD, J. (1956) Les gites mineraux associes aux roches alcalines et aux carbonatites: *Science de la Terre*, Tome 4, Nos. 1-2, pp. 103-151.

ALLAN, J. A. (1914) Geology of the Field Map Area, B.C. and Alberta. Memoir No. 55: *Geol. Surv. Canada*, pp. 1-312.

BAADSGAARD, H., FOLINSBEE, R. E. & LIPSON, J. (1961) Potassium-argon dates of biotites from Cordilleran Granites: *Bull. Geol. Soc. Amer.*, Vol. 72, No. 5, p. 62.

BARLOW, A. E. (1902) On the nepheline rocks of the Ice River, B. C.: *Ottawa Naturalist*. Vol. 16, p. 70.

BONNEY, T. G. (1902) On a sodalite syenite (ditroite) Junction Ice River Valley, Canadian Rocky Mountains: *Geol. Mag.* Vol. 9, p. 199.

CAMPBELL, F. A. (1961) Differentiation trends in the Ice River Complex, B.C.: *Amer. Jour. Sci.* Vol. 259, No. 3, pp. 173-180.

DAWSON, G. M. (1885) Physical and geological features of that portion of the Rocky Mountains between latitude 49° and 51° 30′: *Ann. Rpt. Geol. Surv. Canada*, Vol. 1, p. 120B.

von ECKERMANN, H. (1948) The alkaline district of Alnö Island. Sveriges: *Geol. Unders., Ser. Ca*, No. 36, p. 176.

GUSSOW, W. C. & HUNT, C. W. (1959) Age of the Ice River Complex Yoho National Park, B. C.: *Jour. Alta. Soc. Petrol. Geol.*, Vol. 7, No. 3, p. 62

JONES, W. C. (1955) Geology of the Garnet Mountain-Aquila Ridge Area. Ice River B. C. Unpublished M.Sc. thesis, University of British Columbia.

LOWDON, J. A. (1960) Geological Survey of Canada Age Determinations: *Geol. Surv. Can.* Paper 60-17. p. 51.

PECORA, W. T. (1956) Carbonatites: a Review. *Bull. Geol. Soc. Amer.*, Vol. 67, pp. 1537-1556.

RAPSON, J. E. (1963) Age and aspects of metamorphism associated with the Ice River Complex, British Columbia: *Bull. Can. Petrol. Geol.*, Vol. II, No. 2, pp. 116-124.

——— (1964) Intrusive Carbonate in the Ice River Complex, British Columbia: *Bull. Amer. Assoc. Petrol. Geol.*, Vol. 48, No. 4, p. 543 (abstract).

SCHAU, M. P. (1964) A Petrologic Study of Garnet Ridge, Ice River Complex, British Columbia. Univ. British Columbia (unpublished B.Sc. thesis).

DISCUSSION

E. Wm. Heinrich (Ann Arbor, U. S. A.): Would you please cite the evidence for placing the syenite younger than the carbonatite. You stated that both the carbonatite and the syenite intrude the mafic-ultramafic rocks, but which is the first to do so?

Author's reply: Since there is no contact of the syenite with the carbonatite, strictly speaking, the question remains debatable. I think the answer will lie in the nature of the feldspar breccias (with attendant feldspathization) at the fenitized zone in contact with the limestone. This zone may or may not be present when the syenite is in contact with the sediments (Rapson 1963. Bull. Can. Petrol. Geol. Vol. 2, p. 116).

MINERALOGICAL SOCIETY OF INDIA, IMA VOLUME, 1966
INTERNATIONAL MINERALOGICAL ASSOCIATION, PAPERS, FOURTH GENERAL MEETING

THE COMPOSITION OF SOME GARNETS FROM AFRICAN KIMBERLITES

P. E. GRATTAN-BELLEW
Department of Geological Sciences, McGill University, Montreal

ABSTRACT

The compositions of 46 very small specimens of garnet were determined from refractive indices, specific gravities and lattice constants and the known correlation of these properties with chemical composition. Sufficient material for wet chemical analysis was available for only two of these specimens. Most garnets were separated from kimberlites and some from eclogite nodules in kimberlites.

The composition of garnet as deduced from physical properties is not as accurate nor as complete as that found by chemical analysis. In the case, however, where sufficient material for chemical analysis is not available, determination of the composition from physical properties provides a satisfactory substitute, at least for some practical purposes as in diamond exploration work.

INTRODUCTION

The compositions of 46 small garnet specimens from African kimberlites were determined by measurement of the refractive indices, lattice constants and specific gravities, and the correlation of these physical properties with chemical composition after Winchell (1958, pp. 595–600). The normal percentages of spessartite and uvarovite were determined by calculation from the percentages of Mn and Cr found by spectroscopic analysis.

The use of chemical analysis for the determination of most of the compositions was precluded by the small size of the specimens available to the author. Sufficient material was available for wet chemical analysis of two garnet samples only (numbers 1 and 34; see tables 3 and 4).

Shortcomings inherent in the determination of the composition of garnet by correlation of physical properties with chemical composition:

1. The inability to show the skiagite component: this could result in an increase of a few percent in the amount of almandite calculated.

2. Due to the common occurrence of small cracks or microscopic inclusions in the crystals, it is difficult to obtain accurate measurements of the specific gravities of garnets. A low specific gravity measurement would be reflected mainly by the absence, or a deficiency in the percentage of grossularite.

In table 5, the compositions of the garnets derived by the author are compared with the compositions of the kimberlite garnet groups XIV, XV and with the eclogite group XVI of Tröger (1962, table 5, p. 669), and also with the compositions of garnets from the Siberian kimberlites after Smirnov (1959, table 7, p. 28).

RESULTS OF GARNET ANALYSES

Thirty eight garnets out of the 46 analysed by the author fall in group XIV of Tröger (1962, p. 669). Only 10 of these are shown in Table 2, as in the remainder grossularite was not found. The absence of grossularite in the analytical results is probably due to the measured specific gravity being lower than the graphically determined value. With the possible exception of garnet number 5, the 28 analysed garnets not shown in Table 2 probably fall in group XIV, as the calculated percentages of uvarovite are too high for the other groups.

In Table 5, the average compositions of the author's garnets falling in Tröger's groups XIV, XV and XVI are plotted: they correspond quite well with the average compositions calculated by Tröger (1962, p. 669). In groups XV and XVI the correspondence of the averages of the author's garnets with those of Tröger, is not as good as in group XIV. The analytical results used in calculating the average compositions of the author's groups XV and XVI are not as good as those used for group XIV. This probably

TABLE 1

Physical Properties of Garnets

Number of specimen	Name of pipe or locality	Tröger's group	color	a*	b*	G*
KIMBERLY REGION						
1	Kimberly Pool	XIV	orange	11.518	1.750	3.70 ±.02
2	Olifants Kop	XIV	orange	11.520	1.746	3.69 ±.02
3	Olifants Kop	XIV	violet	11.529	1.7415	3.68 ±.02
4	Frank Smith	XIV	orange	11.537	1.753	3.739±.02
5	Bellsbank	XIV	orange	11.532	1.757	3.77 ±.02
6	Jagersfontein	XIV	orange	11.532	1.747	3.70 ±.02
7	Kamfersdam	XIV	orange	11.534	1.747	3.70 ±.02
8	Kamfersdam	XIV	violet	11.522	1.7375	3.66 ±.02
9	Klipfontein	XIV	orange	11.536	1.7435	3.71 ±.02
SOUTH WEST AFRICA						
10	Berseba Reserve	XIV	orange	11.533	1.751	3.73 ±.02
11	Berseba Reserve	XIV	violet	11.528	1.749	3.72 ±.02
12	Lichtenfels	XIV	orange	11.539	1.748	3.70 ±.02
13	Lichtenfels	XIV	violet	11.557	1.750	3.68 ±.02
14	Lichtenfels	XIV	orange	11.542	1.7455	3.71 ±.02
15	Lichtenfels	XIV	orange	11.524	1.7415	3.67 ±.02
SOUTHERN RHODESIA						
16	Colossus	XIV	orange	11.544	1.755	3.73 ±.02
GUINEA						
17	Banonkoro	XV	orange	11.546	1.763	3.82 ±.02
SIERRA LEONE						
18	Yengema	XIV	orange	11.541	1.7515	3.72 ±.02
TANGANYIKA						
19	Mwadui	XIV	orange	11.539	1.7485	3.71 ±.02
20	Mamungo pipe	XIV	orange	11.539	1.752	3.67 ±.03
21	Mamungo pipe	XIV	violet	11.540	1.744	3.70 ±.02
22	Mpuru pipe No. 1	XIV	orange	11.603	1.7675	3.85 ±.02
23	Mpuru pipe No. 1	XV	orange	11.567	1.7635	3.80 ±.02
24	Mpuru pipe No. 1	XIV	orange	11.641	1.764	3.83 ±.02
25	Itagata pipes	XIV	orange	11.554	1.7605	3.82 ±.03
26	Itagata pipes	XIV	orange	11.545	1.754	3.71 ±.03
27	Itagata pipes	XIV	orange	11.542	1.7505	3.67 ±.02
28	Itagata pipes	XIV	orange	11.542	1.748	3.70 ±.02
29	Tambola pipe	XIV	orange	11.602	1.767	3.70 ±.03
30	Tambola pipe	XV	orange	11.562	1.7415	3.70 ±.02
31	Tambola pipe	XIV	orange	11.556	1.758	3.73 ±.02
32	Kimbelekese	XIV	orange	11.545	1.7515	3.74 ±.02
33	Kimbelekese	XIV	violet	11.515	1.7380	3.70 ±.02
34	Mingui	XIV	orange	11.532	1.755	3.80 ±.02
35	Gonambogo	XIV	orange	11.535	1.753	3.70 ±.02
36	Magoba	XIV	orange	11.542	1.745	3.67 ±.02
37	Daraja	XIV	violet	11.541	1.7465	3.72 ±.02
38	Daraja	XIV	orange	11.516	1.745	3.76 ±.03
39	Kitura	XIV	orange	11.541	1.751	3.70 ±.02
40	Mayaha	XIV	orange	11.538	1.7535	3.75 ±.02
41	Mvelevele	XIV	orange	11.548	1.7515	3.68 ±.02
42	Mvelevele	XV	orange	11.537	1.7475	3.78 ±.01
43	Makilawa	XIV	orange	11.537	1.746	3.69 ±.02
44	Munu	XIV	orange	11.533	1.749	3.72 ±.01
45	Kolongo	XV	violet	11.533	1.743	3.78 ±.02
46	Kolongo	XIV	orange	11.531	1.745	3.68 ±.02

* (*a*) lattice constants expressed in Ångstrom units
(*n*) refractive indices
(*G*) specific gravities.

TABLE 2—Part A

Results of analyses of garnets falling into Tröger's group XIV, expressed as end-members of the garnet series

End Members	Sample numbers 3	8	9	10	14
Pyrope	78.04	74.40	68.47	69.70	66.13
Almandite	8.93	6.62	14.18	16.66	12.48
Spessartite	0.50	0.43	0.68	0.89	0.56
Grossularite	2.03	1.68	7.64	1.68	6.06
Andradite	9.52	7.87	6.03	9.50	7.76
Uvarovite	1.00	9.00	3.00	1.60	7.00

End members	Sample numbers 19	21	37	38	44
Pyrope	67.43	62.88	60.71	66.09	70.47
Almandite	12.23	11.93	13.97	22.93	14.40
Spessartite	0.64	2.07	0.80	1.10	0.69
Grossularite	1.82	6.61	6.47	8.54	1.57
Andradite	9.88	6.52	6.56	1.36	10.90
Uvarovite	8.00	10.00	11.50	tr.	2.00

TABLE 2—Part B

Results of analyses of garnets falling in Tröger's groups XV and XVI, expressed as end-members of the garnet series

End members	Sample numbers 17	22	23	24
Pyrope	58.72	36.61	49.91	30.54
Almandite	27.64	32.38	22.98	30.47
Spessartite	0.70	0.87	1.26	no anal.
Grossularite	3.85	21.54	6.63	34.42
Andradite	9.11	5.62	9.23	4.56
Uvarovite	no anal.	3.00	10.00	no anal.

End members	Sample numbers 25	30	42	45
Pyrope	53.77	58.78	56.29	63.37
Almandite	29.86	13.73	25.54	22.40
Spessartite	no anal.	1.13	0.89	no anal.
Grossularite	10.75	16.73	15.70	15.23
Andradite	5.62	3.62	no anal.	?
Uvarovite	no anal.	6.00	1.60	no anal.

TABLE 3

Results of wet chemical analyses of garnet samples

	Sample No. 1	Sample No. 34
SiO_2	41.51	41.02
Al_2O_3	22.93	22.75
Fe_2O_3	1.00	1.05
FeO	10.84	10.19
CaO	3.62	4.51
MgO	19.31	18.80
Na_2O	0.09	0.08
K_2O	0.01	0.01
P_2O_5	0.20	0.19
TiO_2	0.48	0.78
MnO	0.38	0.38
Cr_2O_3	tr.	tr.
TOTALS	100.37	99.76

Sample No. 1: refractive index varies from 1.743—1.755 Analyst: H. Ulk, McGill University.
Sample No. 2: refractive index varies from 1.747—1.755

TABLE 4

Results of wet chemical analyses of two garnets, expressed as end members of the garnet series. The compositions derived from the measured physical properties are shown for comparison.

End members of garnet series	By chemical analysis		By correlation with physical properties	
	1	34	1	34
Pyrope	64.54	62.78	72.18	60.66
Almandite	23.89	23.23	19.32	27.56
Spessartite	0.83	0.83	0.70	no anal.
Grossularite	7.06	9.15	?	7.40
Andradite	0.17	3.22	7.80	4.38
Uvarovite	tr.	tr.	tr.	no anal.
Skiagite	3.15	3.72	no anal.	no anal.

TABLE 5

Part 1

	Author's garnets		
	Group XIV	Group XV	Group XVI
Pyrope	67.6±11	57.4±8	40.3±13
Almandite	15.1±12	22.5±8	30.9±2
Spessartite	0.8±1.2	1.0±0.3	0.9
Grossularite	5.0±4	11.6±7	22.2±12
Andradite	6.6±5	7.3±4	5.3±0.7
Uvarovite	5.9±5.5	5.9±4	3.0
Skiagite	*3.4	no anal.	no anal.

* Average of 2 garnets analysed chemically.

Part 2

	Tröger's groups			Simrnov
	Group XIV	Group XV	Group XVI	
Pyrope	67.5±8	49.5±12	43.5±7	72.8±4
Almandite	16.5±10	24.5±9	38±7	15.4±3
Spessartite	0.5±0.5	0.5±0.5	1±1	0.1±0.2
Grossularite	2±3	22±4	14±6	4.2±1.2
Andradite	4.5±4	3±3	3.5±4	4.2±2
Uvarovite	6±3	0.5±0.5	0	2.6±2.6
Skiagite	3±4	0	0	0

Subscript for tables—

Table 1 : Precision of measurements :

1. Lattice constants. Several duplicate runs gave a maximum variation of 0.002, but as measurements were made over a period of several months, the variation is probably somewhat larger.

2. Refractive indices. A maximum variation of 0.002 was found.

Table 2, Part A : Only the garnets that were found to contain end-members Pyrope, Almandite, Spessartite, Grossularite, Andradite, and with one exception, Uvarovite are shown.

Table 2, Part B : All garnet analyses falling in groups XV and XVI are shown, with the exception of sample 29 in which grossularite was not found.

Table 5 : Showing the groups into which the author's garnet fall, the compositions of Tröger's groups XIV, XV and XVI and the average of selected garnets from Siberian kimberlites after Smirnov.

Only the garnet samples shown in Table 2 were used in computing the averages shown in Part I of the above table.

accounts for the discrepancy between the compositions of the author's and Tröger's groups XV and XVI.

Most of the African ' kimberlite provinces '* are represented by the garnets analysed by the author. The author's samples together with those of Tröger (1962, p. 669) and Smirnov (1959, p. 28) provide analysed garnets from most of the known ' kimberlite provinces ', with the exception of those in South America, Australia and Asia. Eighty six percent of the garnets analysed, excluding those derived from eclogite nodules, fall in Tröger's group XIV, which thus appears to be the dominant garnet group in kimberlites.

ACKNOWLEDGEMENTS

The writer is indebted to Dr. E. Gerryts and Dr. G. Mannard who donated the samples used in this investigation.

Thanks are also due to Dr. A Frueh for his aid with the X-ray work, to K. Schryver for his careful reading of the manuscript and for several suggestions for its improvement, to Dr. J. S. Stevenson and other members of the staff at McGill University, who assisted the author in various ways.

The work on which this paper is based was carried out as an M.Sc. thesis at McGill University.

GRAPH OF REFRACTIVE INDICES (n) VERSUS LATTICE CONSTANTS (a) OF 46 ANALYSED GARNETS

FIGURE 1

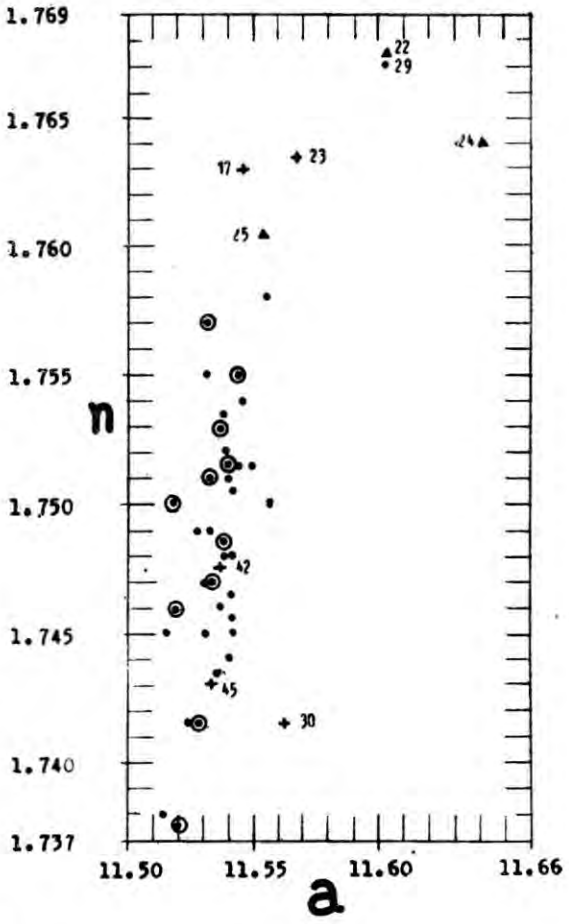

⊙ Garnets falling in Tröger's group XIV

▼ Garnets falling in Tröger's group XV

\+ Garnets falling in Tröger's group XVI

• Garnets from kimberlites known to be diamond bearing.

23 Sample numbers (see Table 1)

* The term ' kimberlite province ' is used loosely, to refer to groups of kimberlite pipes; it does not have any petrologic significance.

REFERENCES

SMIRNOV, G. I. (1959) Mineralogy of Siberian Kimberlites: *Int. Geol. Rev.* Vol. 1, No. 12, pp. 21–39.

TRÖGER, E. (1962) The Garnet group, relation between mineral, chemistry and rock type: *Int. Geol. Rev.* Vol. 4, No. 6, pp. 663–719.

WINCHELL, H. (1958) The composition and physical properties of garnet: *Am. Mineral.* Vol. 43, Nos. 5–6, pp. 595–600.

MINERALOGICAL SOCIETY OF INDIA, IMA VOLUME, 1966
INTERNATIONAL MINERALOGICAL ASSOCIATION, PAPERS, FOURTH GENERAL MEETING

ABUNDANCE AND SIGNIFICANCE OF SOME MINOR ELEMENTS IN CARBONATITIC CALCITES AND DOLOMITES [1]

SHI H. QUON[2] AND E. Wm. HEINRICH
Department of Geology and Mineralogy, The University of Michigan, Ann Arbor, Michigan, U.S.A.

ABSTRACT

Some 154 samples of carbonates (calcite, dolomite and ankerite) from 17 different carbonatite deposits in the United States, Canada, Europe and Africa have been analyzed by quantitative spectrographic methods for Ba, Sr, Mg, Fe, Al and Si. All calcites from geologically unquestionable carbonatites are notably enriched in barium and strontium by a factor 8-800x for barium and 26-170x for strontium over sedimentary calcites. Strontium always exceeds barium by a factor ranging from 6.5–55x. Among the three carbonate species, early calcite always contains the most barium and strontium; dolomite, the least; ankerite has intermediate amounts. Both elements decrease in amount with decreasing relative age of the carbonate species in a paragenetic sequence.

Early carbonatitic calcites, shown to be homogeneous, contain an average of 0.68% Mg, with six samples containing over 2% Mg. Higher Magnesium contents previously attributed to carbonatitic calcites stem in part from exsolved dolomite. Manganese is selectively and markedly enriched in ankerites. Iron usually exceeds manganese in calcites and dolomites.

Aluminum and silicon are present in all samples. In a few cases the amounts are of a magnitude that suggests the possible presence of submicroscopic impurities. Their constant presence in demonstrably homogeneous material, however, is difficult to explain.

High barium and strontium contents thus serve to identify carbonatitic calcites. No systematic variation in these two elements was found to distinguish carbonatites of one province from those of another.

INTRODUCTION

It has long been known that Ba and Sr are two elements strongly concentrated in carbonatites, igneous rocks that are characterized geochemically not only by Ba and Sr but also by the assemblage P, Ti, Nb, cerian RE, Th and F. Rhombohedral carbonate species, mainly calcite, dolomite and ankerite are the most abundant and widespread essential minerals of carbonatite; siderite, rhodochrosite, and RE carbonates such as bastnasite are only locally abundant in a few deposits. Because not all carbonatites are sufficiently well exposed for an unequivocal determination of their geological relations and because, indeed, there exists a variety of carbonate rocks whose geology and mineralogy are not sufficiently diagnostic to permit a decision as to their magmatic or hydrothermal origin and further because the source of the material for carbonatites proved intrusive remains speculative, investigators have been searching for means to separate, readily and *sans doute*, carbonatitic carbonates from those carbonate rocks that have passed through the sedimentary-metamorphic cycle. Of the characteristic minor elements listed above, rhombohedral carbonates are capable of containing RE, Ba and Sr. Most previous determinations of these elements have been made on the entire carbonatite rock, without regard to the phases present. The purposes of this investigation have been:

1. To determine the contents of Ba, Sr, Mn, Fe, Al, and Si of samples of pure carbonatitic calcite, dolomites and ankerites.

[1] Contribution No. 269, The Mineralogical Laboratory, Department of Geology and Mineralogy, The University of Michigan.

[2] Present Address: Northern Electric Company Limited, Research and Development Laboratories, Ottawa, Canada.

2. To relate any variation in these elements to paragenesis.
3. To determine if indeed carbonatitic carbonates can be identified, as such, by their minor element content and thus separated from carbonates of limestones and marble.

SAMPLES

A total of 154 samples of carbonatitic calcites, dolomites and ankerites was analyzed. These came from the following carbonatites and nearly all were collected personally by Heinrich so that their exact geology is well known.

U.S.A.

Magnet Cove, Arkansas
McClure Mountain, Colorado (several dikes)
(Iron Mountain, Gem Park, Amethyst, McCoy Gulch)
Iron Hill, Colorado
Bearpaw Mountains, Montana
Ravalli County, Montana
(several dikes and sills)

Canada

Oka, Quebec
Bancroft, Ontario (several bodies)
Lake Nipissing, Ontario

Europe

Alnö, Sweden
Fen, Norway
Kaiserstuhl, Germany

Africa

Sukulu Hills, Uganda
Tororo, Uganda
Mbeya (Panda Hill), Tanganyika
Ngualla, Tanganyika
Sangu Complex, Tanganyika (Ikomba)
Shawa, Southern Rhodesia
Chilwa Island, Nyasaland
Tundulu, Nyasaland

All of the samples were studied petrographically by means of thin sections; the identities of the carbonates were established by means of staining (alizarine-red), index of refraction measurements, and x-ray diffraction techniques. The purity of the samples was checked also by x-ray diffraction methods. Special care was exercised in searching for dolomite blebs exsolved from calcite and vice versa but only one additional example of this was discovered (Iron Hill, Colorado).

The complete paragenesis of the sample also was studied in thin section. These results will be the subject of another paper.

ANALYTICAL TECHNIQUE

A 170 centimeter Hilgar prism spectrograph with a d. c. arc was used for the quantitative determination of the minor elements. The general steps of procedure for the method of analysis followed that of the conventional d.c. arc analysis of powdered material where carbon electrodes are used have been adequately described by Ahrens (1954).

Throughout the investigation, a 220–volt d.c. power source was used. The current can be adjusted to 5.7 amps when the electrodes were closed. The sample electrode was made positive and the arc gap kept at 4 mm during the exposure. All electrodes were made from the National Carbon Company grade No. L4306 spectrographic carbon rod. The upper and lower electrodes were 1.25″ and 1.5″ in length respectively. The sample electrode cup was 2 mm deep and had a 3.5 mm diameter. The counter electrode was a piece of rod pointed with a pencil sharpener.

Kodak S. A. No. 2 spectrum plates were used and covered the range from 2400 to 5000 Å. After exposure, the plates were developed in Kodak D-19 developer for 3 minutes at 68°F, then rinsed in Kodak SB–1 stop bath, and fixed 5 minutes in Kodak F–6 fixer. Final washing was completed by rinsing first in tap water and then in distilled water; the plate was then air dried.

Two-line method was employed for plate calibration. Details of this method have been discussed by Churchill (1944). The spectral lines chosen were the carbon lines 2836.6 Å and 2837.6 Å.

The carbonates to be analyzed were hand picked under binocular and petrographic microscope from small crushed fragments of carbonatite samples. The pure carbonate was carefully ground with an agate mortar or mix mills to pass 150 mesh screen. The sample preparation was as follows: a one hundred milligram sample of ground carbonate was weighed out in precision balance, and a five hundred milligram mixture of Li_2CO_3 and CuO in the ratio of 10 : 1 was then added to the carbonate sample. A homogeneous sample was produced by thoroughly mixing both fractions in a Spex Mixer for fifteen minutes.

A series of standard samples were prepared for the analysis by mixing desirable proportion of pure oxides of Al, Si, Fe, Mg and carbonates of Mn, Ba, Sr with $CaCO_3$. Both CuO and Li_2CO_3 were used as internal standards and were added to each standard sample in the same manner as that of the test samples. All prepared standard and test samples were firmly packed individually in a electrode with a glass rod prior to the arcing.

The working curve for each element was constructed from the spectral lines obtained from the standard samples. The concentration is plotted against the log intensity ratio of the analytic line to the internal standard line.

The precision of the method is ± 5 percent with the exception of a few cases which are ± 8 percent of the amount present for all of the analyzed elements. As a check to insure against errors, twenty samples of the United States Bureau of Standards Limestone la, were analyzed. The results are found in good agreement. Additional errors in the analyzed samples were further reduced by determining every sample twice and the resultant average was regarded as a single obtained from the sample.

GENERAL RESULTS

The quantitative analytical results for Ba, Sr, Mg, Mn, Fe, Al and Si in carbonatitic calcite, dolomites and ankerites are summarized in Table 1.

As can be seen from Table 1, there is a large spread in the values for the minor elements contained in these calcites, dolomites and ankerites. Nevertheless, the average values show a preferential enrichment of certain carbonate species with respect to these elements. Calcite is preferentially enrichment of certain strontium. Dolomite contains the least barium and strontium, and ankerite has an intermediate amount. In addition, the strontium content always exceeds that of barium in all three carbonates.

Ankerite is preferentially enriched in manganese. Dolomite contains the least manganese, and calcite has an intermediate amount.

TABLE 1

Averages and ranges of minor elements in calcite, dolomite and ankerite samples analyzed.

Carbonate	Calcite		Dolomite		Ankerite	
% of all samples	47		28		18	
	Range	Average	Range	Average	Range	Average
Ba	0.004–0.4	0.106	Trace–0.14	0.032	0.04–0.23	0.107
Sr	0.22–2.55	0.85	0.03–0.67	0.31	0.41–1.03	0.61
Mg	0.068–2.52	0.68	-	11.17	2.66–6.44	5.29
Mn	0.015–1.12	0.19	0.017–0.34	0.20	0.009–3.0	0.58
Fe	0.015–1.20	0.29	0.06–0.79	0.47	1.5–4.0	—
Al	0.002–0.58	0.06	0.018–0.26	0.03	0.003–0.18	0.42
Si	0.03–0.85	0.20	0.029–0.18	0.18	0.05–1.1	0.35

Iron was present in minor amounts in all samples of both calcite and dolomite. The iron content of dolomite exceeds that of calcite by a factor of 1.5.

Aluminum and silicon are present in all the samples. In a few cases the amounts are of such a magnitude as to suggest the presence of submicroscopic impurities.

In many deposits the calcite contains relatively large amounts of barium and strontium. Whenever the calcite is enriched in these two elements, the dolomite or ankerite from the same deposit is also enriched in them.

COMPARISON WITH SEDIMENTARY AND METAMORPHIC CARBONATE ROCKS

A comparison of our analytical results with those obtained on marble and sedimentary limestones is presented in Table 2. Although an absolute comparsion of our results (col. 7) with those previously obtained is not possible, since whole rock samples were previously used, our results support the older data in every respect.

Other minerals in carbonatites beside the carbonates that contain Ba in notable amounts are phlogopite, alkali feldspar, apatite and barite. Sr may be contributed also by apatite and barite. All of the calcites from geologically authenticated carbonatites are notably enriched in Ba and Sr by a factor of 8-800x for Ba and 26–170x for Sr over sedimentary-metamorphic carbonates. Notably in carbonatitic calcites Sr always exceeds Ba by a factor ranging from 6.5–55x.

Carbonatitic calcites also are enriched in Mn and Mg over their sedimentary metamorphic counterparts. Early carbonatitic calcites, demonstrated to be homogeneous, contain an average of 0.68% Mg, with six samples containing over 2% Mg. Higher Mg contents previously attributed to calcites of carbonatites are due, at least in part to the presenceof dolomite either as small interstitial grains or, more likely to dolomite blebs within calcite, resulting from exsolution.

Thus it can be concluded that homogeneous carbonatitic calcites are characterized by relatively large and diagnostic amounts of Ba, Sr, Mg and Mn and that the presence of these concentrations serve to identify the calcite as carbonatitic in origin. To this list should be added also the Ce rare-earth elements. These too are notably enriched in carbonatitic calcites (see, for example, Higazy, 1954 and Rub, 1960).

It has been stated by Bailey (1961) that there is no distinct separation in the Ba and Sr contents of carbonatitic calcite from those of sedimentary calcite. This conclusion stems from his work on the Mkwisi-Keshya "intrusive limestones" of Northern Rhodesia, the calcite

TABLE 2

Comparison of minor elements in carbonatites and carbonatitic calcite with those of marble and limestone

	1	2	3	4	5	6	7
Ba	0.009	0.004	0.0005	0.0042	0.24	0.198	0.106
Sr	0.06	0.031	0.015	0.03	0.34	0.77	0.855
Mg	4.69	0.763		3.40	3.33		0.684
Mn	0.118	0.015		0.019	0.46		0.197
Fe	0.38	0.097		0.168	5.06		0.297
Al	0.21	0.074		0.039	1.86		0.066
Si	2.40	0.345		0.341	5.60		0.204

1. Limestone (Gold, 1963)
2. Paleozoic limestone (Shaw *et al.*, 1964)
3. Limestone (Higazy, 1954)
4. Grenville Marble (Shaw *et al.*, 1964)
5. Carbonatite averages (Gold, 1963)
6. Carbonatites (Higazy, 1954)
7. Carbonatitic calcites, averages (this study)

of which contains but 0.001–0.005% Ba and only 0.03–0.04% Sr. More recently, however, a new geological study of these "intrusive limestones" by Cairney (1964) has indicated that they are of metamorphic rather than magmatic origin. This conclusion is supported by data on the Sr isotope ratios determined by Powell and Hurley (1963) who found that the Sr^{87}/Sr^{86} ratio of the "intrusive limestone" is distinctly higher than those of carbonatites and resembles those of limestone: "this result suggests that the intrusive limestone is not carbonatite" (p. 51).

BANCROFT, ONTARIO, CALCITES

Of unusual interest are the results obtained on 10 calcites from the Bancroft district, Ontario, some of which occur in the peculiar calcite-fluorite-apatite "vein dykes" whose origin remains in dispute (see Heinrich, 1958). Others are from carbonate bodies whose geological relations are so complex that a simple and an immediate genetic designation are not possible. Recently Shaw *et al.* (1964) have ascribed a very complex origin to similar carbonate bodies in an area near Ottawa, calling them skarns. It is interesting to compare their results with our's (Table 3).

TABLE 3

Comparison of minor elements in carbonates from Bancroft and Ottawa areas, Ontario

	1	2
Ba	0.0053	nil–0.003
Sr	0.235	0.02–0.32 (av.0.15)
Mg	0.68	0.65 (av.)
Mn	0.149	0.18 (av.)
Fe	0.39	0.20 (av.)
Al	0.04	0.02 (av.)
Si	0.24	nil–0.002

1. Shaw *et al.* (1964) 2. This paper

This type of carbonate has Ba contents like those of sedimentary carbonate rocks; yet a notable enrichment in Sr persists. The remaining trace element assemblage is like that of typical carbonatitic calcites except for Si which is very low in Bancroft calcites.

Thus the minor element assemblage is genetically non-diagnostic, as of the present state of our knowledge.

PARAGENESIS AND MINOR ELEMENTS

Variations within single complexes

Systematic sampling and analysis of carbonates from individual carbonatitic deposits have not been attempted by other investigators. On the basis of a few analyzed carbonatite samples from Sukulu and Tororo, Uganda, Davies (1956) concluded that the carbonate fraction varies in its minor element content from place to place in individual carbonatites. He also noted the presence of finer grained, high-magnesium carbonate in some parts of the carbonatite and concluded that there is no systematic variation of minor elements in the calcite with respect to its position within the carbonatite.

A number of carbonates from the Dorowa and Shawa carbonatites in Southern Rhodesia were spectrochemically analyzed for trace and minor elements by Johnson (1961). He indicated that there is a similarity in minor element contents of both carbonatites, but that many of the elements vary erratically within individual carbonatite masses, with the result that there is a considerable difference in minor element composition of the carbonates in samples collected only a few feet apart.

Samples of carbonates from the Shawa carbonatite were available for the present investigation. These samples were collected in a systematic manner. There are two large ring dikes in the center of the Shawa carbonatitic alkalic complex. These two ring dikes are approximately 6000 feet in length, the one with a maximum width of about 1000 feet being situated to the northwest and the one with a width of about 500 feet being to the east. These dikes transect a serpentinized dunite plug. A systematic analysis of dolomite samples from the larger (north-western) ring dike shows significant variation in Ba, Sr and Mn. For Some 20 samples Sr ranged from 0.1–0.9, with notably higher concentrations in the inner part of the ring dike arc. Similarly, Ba generally decreased outward.

Variation among closely related carbonatites

The carbonatites of Sukulu Hills and Tororo, Uganda are nearby and genetically related (William, 1952). The former is lower in both Ba and Sr:

	Ba	Sr
Sukulu Hills	0.007	0.28
Tororo	0.05	0.47

Noteworthy variations in calcites from various carbonatites in south central Colorado also occur:

	Ba	Sr	Mg-Fe-Mn
Gem Park	0.22	1.1	Mg>Fe>Mn
Iron Mountain	0.03	0.92	Fe>Mg>Mn
Amethyst	0.2	0.47	Fe>Mn>Mg
McCoy Gulch	0.011	0.37	Fe>Mn>Mg
June No. 2	0.04	0.56	Mg>Mn>Fe
Iron Hill Gunnison Co.	0.06	0.4	Mg>Fe>Mn

Calcites from the Chilwa Island and Tundulu (Nyasaland) carbonatites, which belong to the comagmatic Chilwa series contain:

	Ba	Sr	Mg-Fe-Mn
Chilwa Island	0.40	0.42	Fe>Mg>Mn
Tundulu	0.031	1.48	Mn>Fe>Mg

In southwestern Tanganyika are three major carbonatites:

	Ba	Sr	Mg-Fe-Mn
Mbeya	0.043	1.35	Mg>Fe>Mn
Ngualla	0.23	1.23	Fe>Mg>Mn
Sangu	0.004	0.22	Fe>Mg>Mn

Thus it appears that among closely related carbonatites wide variations in minor element contents may be present, and no systematic variation by province is present.

MINOR-ELEMENT VARIATION IN A PORPHYRITIC CARBONATITE

A dolomitic carbonatite at Dorowa consists of corroded rhombohedra of dolomite as much as 4 cm across separated from a finegrained dolomitic matrix by a reaction rim of fibrous dolomite, several millimeters across (Johnson, 1961). Analyses were made of all three types of dolomite (Table 4).

TABLE 4

Variation in minor-element content in the Dorowa porphyritic carbonatite

	Ba	Sr	Mn	Fe	Al	Si
Phenocryst	0.09	0.34	0.046	0.94	0.043	tr
Fibrous rim	0.01	0.60	0.099	1.70	0.045	0.26
Matrix	0.01	0.26	0.08	1.40	0.040	tr

From textural relations it appears that the age sequence has been: 1. Phenocrysts, 2. Fibrous rim, 3. Matrix. The phenocrysts are not only corroded by the rims but the fibers are in comb-structure arrangement against the phenocryst contacts. The rims themselves are penetrated and traversed by minute veinlets of matrix material. Noteworthy enrichment of Ba characterizes the phenocrysts; the fibrous rims are enriched in Sr, and the rims and matrix dolomite are enriched in Fe and Mn.

MINOR ELEMENT VARIATION AND GENERAL SEQUENCE OF CRYSTALLIZATION

Wherever possible we have analyzed calcites in pairs from a single deposit, *i.e.*, both an earlier type and a younger type which veins or replaces the older. The results of these paired analyses are shown in Table 5. The data show

TABLE 5

Ba and Sr contents of calcites of different relative ages

Locality	Older calcite		Younger calcite	
	Ba	Sr	Ba	Sr
Kaiserstuhl, Germany	0.13	2.80	0.08	1.26
Fen, Norway	0.03	1.14	0.007	0.171
Tundulu, Nyasaland	0.03	2.75	0.03	0.19
Ngualla, Tanganyika	0.02	1.50	0.45	1.00
Mbeya, Tanganyika	0.035	1.72	0.05	0.85
Sukulu Hills, Uganda	0.501	0.63	0.0016	0.018
Tororo, Uganda	0.60	1.45	0.016	0.49
Ravalli County, Montana *	0.40	1.1	0.37	0.07

* Heinrich and Levinson, 1961

that, with one exception (Ngualla), early calcite is enriched or equal in Ba content with respect

to its junior partner. Sr is invariably markedly enriched in the senior calcite.

In addition, it is well established that in most complex carbonatite bodies, *i.e.*, those consisting of multi-phase intrusions, the *general* sequence of formation of the carbonate species is :

1. Calcite, 2. Dolomite, 3. Ankerite, 4. Siderite and Mn-carbonate, 5. RE carbonates (Garson and Smith, 1958 ; Pozharitskaya, 1962 ; Ginzburg, 1963 ; Heinrich, 1965).

From the data presented in Tables 1, 4 and 5 and from additional information reported in the literature the following trends are established for carbonatitic carbonate species :

Ba and Sr : Enriched in early calcite, decreased with decreasing age.

Mn and Fe : Enriched in the later species (ankeritic, sideritic).

Mg : Considerable amounts in early calcite, some of which may be exsolved as dolomite blebs ; a maximum during the intermediate (dolomite) stage, decreasing thereafter.

Al : A marked increase in the ankeritic stage.

Si : An apparent slight increase in the ankeritic stage.

RE : Noteworthy concentrations in early calcite, lesser amounts in intermediate stages, maximum concentration in the final stage.

Finally, it should be noted that when carbonatitic calcites rich in Ba and Sr, are subject to solution and redeposition as supergene travertines or " onyx " veins, they lose their Ba and Sr, once more demonstrating the correlation between decreasing temperature of formation and decreasing Ba-Sr contents in the rhombohedral carbonates.

ACKNOWLEDGEMENTS

We are indebted for financial support for several aspects of these studies to the University of Michigan, Horace H. Rackham - National Science Foundation Institutional Grant No. 39 and National Science Foundation Grant GP-3449. The contribution by Mrs. P. Chill for the typing of this manuscript is greatly appreciated.

REFERENCES

AHRENS, L. H. (1954) *Quantitative Spectrochemical Analysis of Silicates.* Pergamon Press, London.

BAILEY, D. K. (1961) Intrusive limestones in Keshya and Mkiwsi valleys, Northern Rhodesia : *Quart. Jour. Geol. Soc. London*, Vol. 117, pp. 419-446.

CAIRNEY, THOMAS (1964) A re-assessment of the origin of the Mkiwsi intrusive limestone : *Univ. Leeds. Res. Inst. African Geol.* 8th Ann. Rpt. 1962-63, pp. 25-26.

CHURCHILL, J. R. (1944) Techniques of Quantitative Spectrographic Analysis : *Ind. and Eng. Chem.*, Anal. Ed. 16, pp. 653-675.

DAVIES, K. A. (1956) The geology of part of southeast Uganda : *Geol. Survey Uganda, Mem.* No. 8.

GARSON, M. S. AND CAMPBELL SMITH, W. (1958) Chilwa Island : *Nyasaland Geol. Survey, Mem.* No. 1.

GINZBURG, A. I. (1963) New data on rare-element mineralogy : In *New Data on Rare-Element Mineralogy*, Consultants Bureau, N. Y., pp. 1-15.

GOLD, D. P. (1963) Average chemical composition of carbonatites : *Econ. Geol.* Vol. 58, pp. 988-996.

HEINRICH, E. Wm. (1958) *Mineralogy and Geology of Radioactive Raw Materials.* McGraw-Hill Book Co., Inc., New York.

——AND LEVINSON A. A. (1961) Carbonatic niobium-rare earth deposits, Ravalli County, Montana : *Am. Mineral.* Vol. 46, pp. 1424-1447.

————(1965) *Carbonatites* : Rand McNally and Co., Chicago, III, (in press).

HIGAZY, R. A. (1954) Trace elements of volcanic ultrabasic potassic rocks of southwestern Uganda and adjoining part of the Belgian Congo : *Geol. Soc. Am. Bull.* Vol. 65, pp. 39-70.

JOHNSON, R. L. (1961) The geology of the Dorowa and Shawa carbonatite complexes, Southern Rhodesia : *Geol. Soc. South Africa Trans.* Vol. 64, pp. 102-144.

POWELL, J. L. AND HURLEY, P. M. (1963) Isotopic composition of strontium in some carbonatites and carbonate rocks of uncertain classification, 10th Ann. Progr. Rpt. *U.S. Atom. Energy Comm.* NYO-10,517, Mass. Inst. Tech. pp. 51-52.

POZHARITZKAYA, L. K. (1962) Mineralogical-petrographic characteristics of carbonatites : In *Geology of Rare-Element Deposits*, 17, Gosgeoltekhizat, Moscow.

RUB, M. G. (1960) Alkalic intrusives in the Maritime Province : *Geochemistry*, Vol. 12, pp. 56–71.

SHAW, D. M., MOXHAM, R. I., FILBY, R. M. AND LAPKOWSKY, W. W. (1964) The petrology of some Grenville skarns, Part II, geochemistry : *Canadian Mineral.* Vol. 7, pp. 578–617.

WILLIAMS, C. E. (1952) Carbonatite structure, Tororo Hills, eastern Uganda: *Geol. Mag.* Vol. 89, pp. 286-292.

MINERALOGICAL SOCIETY OF INDIA, IMA VOLUME, 1966
INTERNATIONAL MINERALOGICAL ASSOCIATION, PAPERS, FOURTH GENERAL MEETING

CARBONATITES AND ALKALIC ROCKS OF THE ARKANSAS RIVER AREA, FREMONT COUNTY, COLORADO

E. Wm. HEINRICH AND D. H. DAHLEM
Department of Geology and Mineralogy, The University of Michigan, Ann Arbor, Michigan

ABSTRACT

Carbonatite dikes occur in an alkalic igneous province in south-central Colorado. The province covers an area of approximately 400 square miles and contains three alkalic intrusive masses with associated dike swarms, all intruding chiefly Precambrian meta-sediments of the Idaho Springs formation. Geological relations and a single age determination suggest a very late Precambrian age for the alkalic rocks.

The three intrusives are: (1) the Democrat Creek syenite-gabbro stock, (2) the Gem Park gabbroic stock, and (3) the McClure Mountain—Iron Mountain complex in which the intrusive sequence has been (a) gabbro, peridotite with titano-magnetite lenses, (b) hornblende syenite, (c) ijolite and nepheline syenite, (d) alkalic dikes and lamprophyres, and (e) carbonatites.

Carbonatite dikes and sills occur in the marginal parts of the Gem Park and McClure Mountain intrusives, in the fenitic halo of both, and in unaltered metamorphic rocks as far as 15 miles from the margins of the McClure Mountain body. The carbonatites range in thickness from less than one foot to about 10 feet; some have been traced for about 2000 feet. Those in Idaho Springs gneisses have fenitized their walls.

Three major petrologic types of carbonatites are distinguishable: (1) Feldspathic carbonatites, usually with feldspathic wall zones and carbonatitic cores: (2) Unzoned calcitic or dolomitic carbonatites containing accessory apatite, magnetite, ilmenite, feldspar, vermiculite, and sodic amphibole: (3) Ba-F-rich carbonatites characterized by barite and fluorite and in one deposit by the extraordinary assemblage cryolite, weberite, ralstonite, prosopite and pachnolite.

INTRODUCTION

A major new area of alkalic igneous rocks has been found in Fremont and Custer Counties, Colorado lying in a triangle whose apexes are Canon City on the east, Cotopaxi at the western end and Westcliffe at the southern tip. The area includes part of the thorium province of the Wet Mountains, most of which lies east of this triangle (Heinrich, 1958; Christman *et al.*, 1959). The senior author and his students began systematic mapping of the Precambrian areas on both sides of the Arkansas River between Canon City and Coaldale about 20 years ago (Heinrich, 1948; Bever, 1954: Salotti, 1960; Shappirio, 1962; Vian, 1965; Dahlem, 1965). Carbonatites were first found in the northernmost part of this area in 1959 by Heinrich and Shappirio. It now appears that these are possibly the only major carbonatites that occur on the north side of the Arkansas River Canyon, although a few lamprophyric dikes also have been found on the north side of the river. All major occurrences of alkalic rocks are south of the Arkansas.

Detailed mapping by Heinrich in the summers of 1961 and 1962 resulted in the discovery of numerous lamprophyric dikes and several carbonatites in the Arkansas Canyon between Parkdale and Cotopaxi and as far south as Indian Springs Park. One of these carbonatites, by far the most unusual, contains cryolite and several other rare fluoride minerals (Heinrich and Quon, 1963).

In the meantime the U. S. Geological Survey has continued mapping westward from the thorium province (Christman *et al.*, 1959) and has published preliminary descriptions of the McClure Mountain and Gem Park alkalic intrusives (Parker *et al.*, 1962; Parker and Hildebrand, 1963).

During the summer of 1964 the authors mapped and studied a previously unreported alkalic breccia pipe near Pinon Peak. The

purpose of this paper, the first of a series on the alkalic rocks, lamprophyres and carbonatites of the area, is to present the regional geological setting.

GENERAL GEOLOGY

Three alkalic intrusive complexes are known:

Democrat Creek Complex

This complex is in the McKinley Mountain Area (Christman *et al.*, 1959) (105° 22′ W., 38° 15′ N.) (Fig. 1, no. 3). The sequence of main units apears to be: (1) gabbro, (2) breccia, (3) albite syenite. (4) alkalic dikes, and (5) Th veins and carbonatites. The gabbro, a lensoid mass nearly 2,500 feet long, has been lumped with pre-complex " metamorphosed gabbroic and ultramafic rocks " by Christman *et al*, (1959, pp. 504–505), but actually it shows little or no metamorphism and resembles the gabbros of the McClure Mountain and Gem Park complexes. The main irregularly shaped breccia body, 2,500 feet long and as much as 1,500 feet

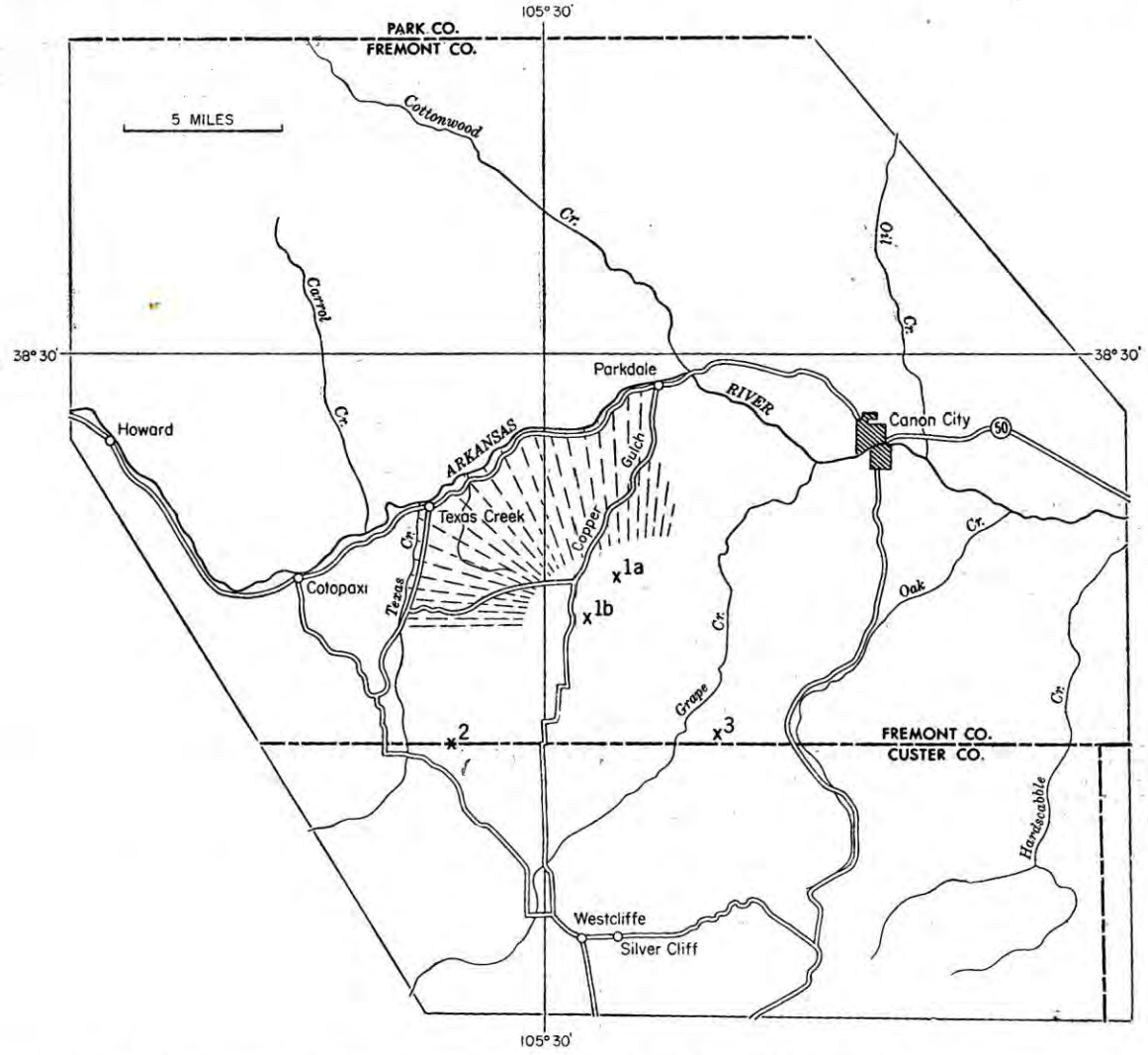

Fig. 1. Index map of the alkalic province of Fremont and Custer Counties, Colorado.
1a Iron Mtn. 1b McClure Mtn. 2. Gem Park 3. Democrat Creek.
Part covered by radiating dashed lines represents area around the McClure Mtn.—Iron Mtn. complex in which alkalic dikes and carbonatites are numerous.

wide, adjoins the southeast side of the syenite stock. It is older than the main syenite stock but younger than a small outlier. Five other small nearby breccia pipes have been found. The albite syenite stock underlies about 3 square miles, elongated slightly northwestward. Of several outliers that occur near its margins, three are older than the breccia body. Five groups of dikes are distinguishable : syenite ; melasyenite ; lamprophyre ; andesite and basalt gabbro. Two major feldspathized-fenitized zones occur along major fault zones, and Th veins are numerous and widespread. The age of the syenite by the zircon-alpha particle method is late Precambrian (595 m.y.) (Christsman *et al.*, 1959).

McClure Mountain-Iron Mountain Complex

The McClure Mountain–Iron Mountain complex (105° 30′ W., 38°20′ N.) (Fig. 1, no's 1b–1a) is an irregularly ovoid body measuring about 5 miles (NE.) by 4 miles (NW.) (Parker and Hildebrand, 1963). The largest of the three, it contains these main units in sequence ; (1) gabbro (Fig. 2), peridotite, Ti-magnetite

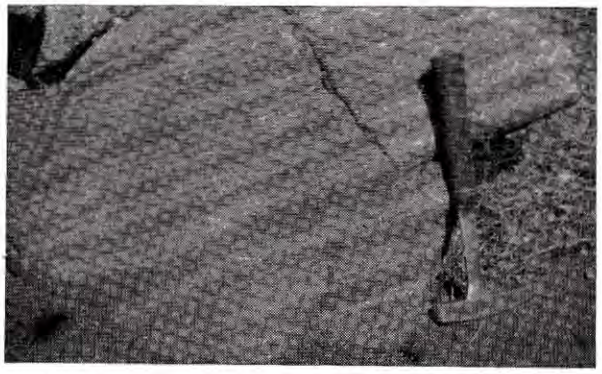

Fig. 2. Banded gabbro, Iron Mtn., Fremont Co., Colorado.

ore (Singewald, 1913 ; Becker *et al.*, 1961) ; (2) hornblende syenite (Fig. 3) ; (3) ijolite and nepheline syenite (Fig. 4) ; (4) alkalic dikes and lamprophyres, (5) carbonatites. Ring structures are not present in the complex (see Parker and Hildebrand, 1963, Fig. 181). The alkalic dikes are varied and numerous ; within the complex light colored syenitic and foidal syenitic types prevail, where as outside the complex more mafic syenitic varieties and lamprophyres dominate (Fig. 5).

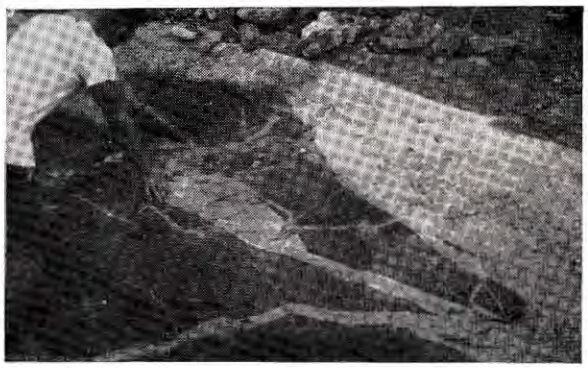

Fig. 3. Gabbro invaded by syenite. McClure Gulch, Fremont Co., Colorado.

A few carbonatite dikes cut rocks of the complex itself ; most, however, occur commonly with lamprophyres closely associated, either in the fenitic halo of the complex or most abundantly beyond the halo. Thus around the northern and northwestern sides of this complex there extends an irregular belt, about 6 miles wide, in which lamprophyres, other alkalic dikes and carbonatites are common (Heinrich *et al.*, 1964) (Fig. 1). The most distant known carbonatite (Amethyst group) occurs about 15 miles from the center of the complex. It is this belt that the writers have mapped and studied in detail and in which the newly discovered Pinon Peak breccia pipes also occur.

Gem Park Stock

The Gem Park Stock, the smallest of the three, is 5 miles southwest of the McClure Mountain complex (105° 32′ W., 38° 16′ N.) (Fig. 1, no. 2). It consists chiefly of alkalic gabbro, has a fenite halo, and is cut by numerous carbonatite dikes (Parkar *et al.*, 1962; Parker and Hildebrand, 1963).

All three complexes as well as their outlying satellitic dikes cut Precambrian metamorphic rocks which have been fenitized marginally to various degrees. Tertiary rhyolite overlies part of the Gem Park Stock. The age of the alkalic

rocks relative to that of the Pikes Peak granite the major intrusive rock of the region, is not known with certainty, but a lamprophyre has been found which cuts the metasomatic muscovitized zone around a pegmatite of Pikes Peak affinity. Thus they are probably post-Pikes Peak, and, of course, if all three complexes are indeed consanguineous, which appears to be very likely, then, on the basis of the age determination for the Democrat Creek syenite, they are the youngest Precambrian rocks of the region.

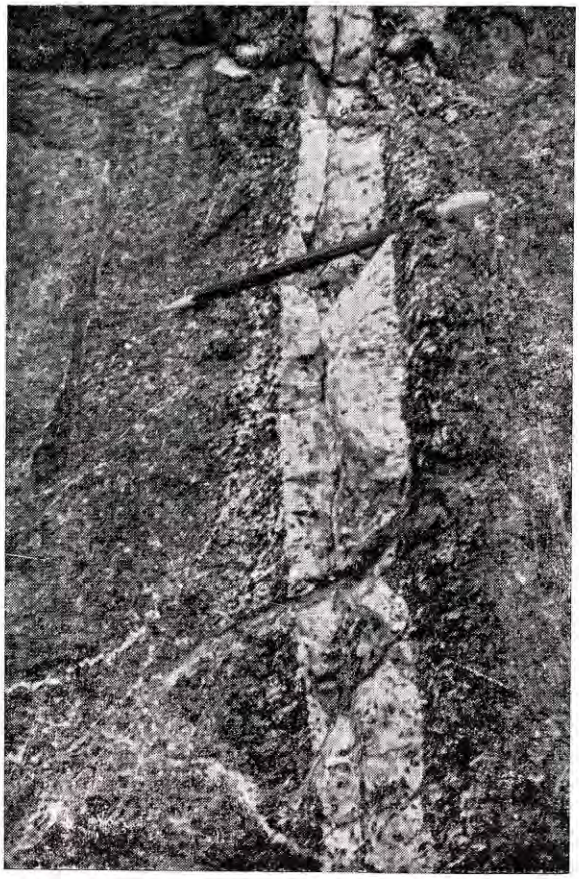

Fig. 4. Nepheline syenite dike cutting gabbro, McClure Gulch, Fremont Co., Colorado

At Texas Creek a carbonatite has been caught in a major north south fault zone and severely crushed. The fault is post-Laramide in age (Dahlem, 1965 ; Vian, 1965).

LAMPROPHYRES

In the " halo area " north and northwest of the McClure Mountain–Iron Mountain complex (Fig. 1), the authors have discovered about 150 lamprophyres. Most of these are dikes; a few are sills. Evidence for two distinct ages of lamprophyres was found in Baker Gulch just south of the Arkansas River in which a lamprophyre sill transects a faulted dike of lamprophyre.

Fig. 5. Zig-zag lamprophyre dike in sillimanite gneiss, head of Indian Spring gulch, Fremont Co.

Several general types of lamprophyres may be distinguished megascopically :

1. Very fine-grained to aphanitic (Fig. 5.)
2. Porphyritic
   (*a*) Phenocrysts of plagioclase
   (*b*) Phenocrysts of augite
   (*c*) Phenocrysts of olivine

Several of the dikes display bizarre textural features. A lamprophyre that is exposed near the mouth of Goldie Gulch close to its junction with Five Point Gulch, is normally porphyritic, with plagioclase phenocrysts as much as $\frac{1}{2}$ inch long in a dark gray aphanitic base. Locally, narrow marginal parts of the dike are spectacularly marked by concentrically zoned ovoids of lighter aphanitic material, as much as 2 inches long.

Another, which crops out in a small gulch ½ mile south of the Cabin Group of carbonatites, contains phenocrysts of augite, ½ to 4 inches across, some in glomeroporphyritic groups! Also included are xenoliths of granite gneiss in various stages of transformation to a pyroxene-bearing rock.

The lamprophyres are highly diverse in composition and in microscopic textures. All are mafic to ultramafic and alkalic. Carbonate is a ubiquitous constituent, occurring as anhedral interstitial matrix patches, replacement of matrix minerals and of phenocrysts, as vesicle fillings and as veinlets. Many lamprophyres can be seen cut by veins of carbonate in the outcrop.

The close relationship of the lamprophyres and the carbonatites is further shown by:

1. Their distribution. In many cases the presence of lamprophyre has indicated the nearby presence of one or more carbonatites, usually parallel.
2. Co-occupation of the same planar channelway by both lamprophyre and carbonatite (Goldie, McCoy Gulch, Klondyke). In these examples the carbonatite is invariably younger and the lamprophyre is carbonatized.

A complete study of the geology and petrology of the lamprophyres is now in progress.

BRECCIA PIPES

The Pinon Peak breccia pipes are about 10 miles south of Parkdale, ¾ mile north of Pinon Peak. They consist of two small closely adjacent lenticular bodies (35 × 50 feet and 250 × 20–60 feet) that have been punched through a granitic gneiss. The breccia pieces, some as much as several feet long, are mainly granitic gneiss with local concentrations of lamprophyre fragments; these are set in a subordinate, fine grained, light colored matrix. The breccia pieces are commonly outlined by a thin feldspathic reaction rim.

The northern smaller pipe has been strongly hematitized, and locally the larger contains disseminated crocidolite and veinlets of aegirine. Close to the two pipes and parallel with their axis of elongation a lamprophyre dike, 150 feet long, has been intruded into the gneiss.

Two other occurrences of breccia north of the Pinon Peak bodies may be similar. All of these breccias are currently the subject of detailed studies.

CARBONATITES

Core-type carbonatites are not present*; most of the carbonatites are dikes; a few are sills. They range in thickness from a few inches to about 10 feet; some have been traced for about ½ mile. Even the very thin dikes are extraordinarily persistent; some 4–6 inches thick extend for several hundred feet. Adjacent lamprophyres are carbonatized; adjacent granite or gneiss is partly fenitized, with aegirine veinlets extending as much as 10 feet away from a carbonatite that is but several inches thick in some examples!

Fig. 6. Feldspathic carbonatite, Klondyke deposit. Upper carbonate zone, lower feldspathic zone. Indian Spring Park, Fremont, Co., Colorado.

* This is one of the major differences between this group of carbonatites and those of the alkalic complex at Iron Hill, Gunnison County, Colorado, which is the only other known carbonatitic complex in Colorado and which is marked by a core carbonatite and ring structures.

The several types of carbonatites are :

1. Feldspathic carbonatite. Some of these have wall zones of hematitic potash feldspar with cores of carbonate (June No. 2), whereas in others the dike is dominantly feldspathic and carbonatite occurs only locally, usually marginally (Klondyke) (Fig. 6).
2. Relatively homogeneous calcitic or dolomitic carbonatites with accessory magnetite, ilmenite, apatite, feldspar, biotite, or vermiculite and sodic amphibole (Figs. 7 & 8) Most of the dikes are sövite, a few are rauhaugites; several contain both essential calcite and dolomite. Rare-earth carbonate minerals occur locally as do various niobium species.*
3. Carbonatites rich in Ba and F. In some of these the barite is irregularly distributed as replacement masses (Goldie, Dreamer's Hope); in others it forms a discrete lateral unit (Amethyst). The fluorite is usually purple and radioactive and replaces carbonate. Other minerals in this type of carbonatite include pyrite, galena, sphalerite, chalcopyrite, apatite, and various silicates.

Mineralogically the most complex of the carbonatites is the Goldie, which must certainly rank as one of the world's unique mineral deposits. A dike, 1–1½ feet wide and about 750 feet long, is sandwiched between an aplite and a lamprophyre. In addition to barite and fluorite it contains replacement nodules of fine-grained aluminofluoride minerals. So far cryolite, weberite, ralstonite, pachnolite, prosopite and possibly gearksutite have been identified (Heinrich and Quon, 1963).

The carbonatites are closely related to the thorium veins of the Wet Mountains (Heinrich, 1958; Christman *et al.*, 1959) and indeed, through the feldspathic type of carbonatite grade into this type of deposit. The brick-red thorium veins contain hematitic potash feldspar, quartz, barite and Fe-bearing carbonate with lesser amounts of sulfides, fluorite, alkalic amphibole, xenotime, thorite, thorogummite and brockite (Fisher and Meyrowitz, 1962). Many of the veins contain a fetid gas that escapes as the rock is broken. This gas also occurs in aplite and peg-

Fig. 7. Carbonatite dike cutting gabbro, Iron Mtn., Colo. Dike contacts dug out.

Fig. 8. Small carbonatite sill in biotite gneiss, Indian Spring Park, Fremont Co., Colorado. Note chilled margins in carbonatite.

* Ancylite, bastnäsite (?), an unidentified Ce mineral, lueshite, pyrochlore, fersmite, fergusonite, columbite, thorianite, monazite. The lueshite is in a vermiculite rock in the Gem Park Stock (Parker and Hildebrand, 1963 ; see also Nolan, 1964, p. A 15). So far, niobium minerals have been found associated only with the Gem Park Stock.

matite at the Goldie cryolite carbonatite (Heinrich and Quon, 1963).

The idea advanced by Phair and Fisher (1961) that the thorium veins represent a type of lateral secretion deposit related "...to potastic feldspathization of granite along weathered, oxidized fractures beneath an impervious cap of volcanic rocks" (p. D–1), is not in accord with the geology of the deposits and of the alkalic province.

TRAVERTINES

Small travertine deposits are widely distributed in the area; about 20 have been mapped by Dahlem (1965). Many are localized along faults of Laramide or post-Laramide age. Carbonate-rich metamorphic rocks are absent in the Idaho Springs formation nor are there available any Paleozoic or Mesozoic sediments from which $CaCO_3$ might have been obtained by circulating ground waters. It is considered at least not impossible that some of the carbonate was leached from larger concealed carbonatite bodies at depth. All but one of the occurrences consist of thin flat-lying beds copiously admixed with angular rock fragments locally derived. The exception is a "travertine vein" of pure comb-structure calcite localized in a granite breccia zone several miles south of Cotopaxi.

ACKNOWLEDGEMENTS

We are pleased to acknowledge that financial support for these investigations has been received through the following grants: The University of Michigan, Horace H. Rackham School of Graduate Studies—National Science Foundation Institutional Grant No. 39; and National Science Foundation Grant GP–3449.

REFERENCES

BECKER, R. M., SHANNON, S. S., Jr. AND ROSE, C. K. (1961) Iron Mountain titaniferous magnetite deposits, Fremont County, Colorado: *U.S. Bur. Mines Rept. Invest.* 5864.

BEVER, JAMES E. (1954) Geology of the Guffey area, Colorado: *Ph.D. Thesis*, Univ. of Mich.

CHRISTMAN, R. A., BROCK, M. R., PEARSON, R. C. AND SINGEWALD, Q. D. (1959) Geology and thorium deposits of the Wet Mountains, Colorado: *U.S. Geol. Survey Bull.* 1072-H.

DAHLEM, DAVID, H. (1965) Geology of the Texas Creek-Spike Buck Gulch Area, Fremont County, Colorado: *Ph.D. Thesis*, Univ. of Mich.

FISHER, FRANCIS G. AND ROBERT MEYROWITZ (1962) Brockite, a new calcium thorium phosphate from the Wet Mountains, Colorado: *Am. Mineral.* Vol. 47, pp. 1346-1355.

HEINRICH, E. Wm. (1948) Pegmatites of Eight Mile Park, Fremont County, Colorado: *Am. Mineral.* Vol. 33, pp. 420–448, 550–588.

———(1958) *Mineralogy and Geology of Radioactive Raw Materials*. McGraw-Hill Book Co., Inc., New York, pp. 353–355.

———AND QUON, S. H. (1963) New type of deposit of aluminofluoride minerals from Fremont County, Colorado (abs.): *Geol. Soc. Am. Spec. paper* 73, p. 169.

———DAHLEM D. H. & QUON, S. H. (1964) Carbonatites of the Arkansas River Valley area, Fremont County, Colorado (abs.): *Program 4th Meet. Intl. Mineral. Assoc.*, New Delhi.

NOLAN, THOMAS, B. (1964) Geological survey research, 1964: *U.S. Geol. Survey Prof. Paper* 501, A15.

PARKER, R. L., ADAMS, J. W. & HILDEBRAND, F. A. (1962) A rare sodium niobate mineral from Colorado: *U.S. Geol. Survey Prof. Paper* 450-C, C4-C6.

———AND HILDEBRAND, F.A. (1963) Preliminary report on alkalic intrusive rocks in the northern Wet Mountains, Colorado: *U.S. Geol. Survey Prof. Paper* 450-E, E8-E10.

PHAIR, GEORGE & FISHER, FRANCES G. (1961) Potassic feldspathization and thorium deposition in the Wet Mountains, Colorado: *U.S. Geol. Survey Prof. Paper* 424-D, D-1-D-2.

SALOTTI, CHARLES A. (1960) Geology and petrology of the Cotopaxi-Howard area, Fremont County, Colorado: *Ph.D. Thesis*, Univ. of Mich.

SHAPPIRIO, JOEL R. (1962) Geology and petrology of the Tallahassee Creek area, Fremont County, Colorado: *Ph.D. Thesis*, Univ. of Mich.

SINGEWALD, JOSEPH T., Jr. (1913) The titaniferous iron ores in the United States : *U.S. Bur. Mines. Bull.* 64, pp. 128-135.

VIAN, RICHARD W. (1965) Geology of the Devil's Hole area, Fremont County, Colorado : *Ph.D. Thesis*, Univ. of Mich.

MINERALOGICAL SOCIETY OF INDIA, IMA VOLUME, 1966
INTERNATIONAL MINERALOGICAL ASSOCIATION, PAPERS, FOURTH GENERAL MEETING

INTRUSIVE CARBONATE ROCK NEAR OTTAWA, CANADA

D. D. HOGARTH
University of Ottawa, Ottawa, Canada

ABSTRACT

Numerous small bodies of coarse-grained carbonate occur about 15 miles north of Ottawa. Major types are dolomite-calcite bodies, calcite veins, and breccias with phlogopite-apatite-carbonate matrix. Lenses of dolomite-calcite lie within a large circular mass of aplite; calcite veins and breccias are found both within the aplite and in surrounding syenite. Variants of the calcite veins include barite-calcite and eckermannite veins. Widespread fenitization developed soda amphiboles and albite; local fenitization, accompanying emplacement of the carbonate rocks, developed soda amphiboles and phlogopite (some with a reverse absorption formula). Calcite is rich in strontium. Apatite is common in each type of rock. Phlogopite is sparsely distributed in dolomite, is common in calcite veins, and is usually dominant in the breccia matrix. Magnetite is almost entirely restricted to dolomite, and betafite is found only in apatite-rich breccias, calcite veins or in calcitic portions of dolomite rocks.

Textural evidence suggests the carbonates formed, at least in part, through filling of fractures by a high temperature, carbonate-rich fluid. Some plastic flow took place after the formation of the selvage amphiboles. Ar^{40}/K^{40} ages on phlogopite from the fenite gave 930 m.y (dolomitic bodies) and 910 m.y. (calcite veins).

INTRODUCTION

Masses of intrusive carbonate are found near Meach Lake, about 15 miles north of the city of Ottawa. In many respects the carbonate rock resembles mobilized marble yet it shows mineralogical and geochemical similarities to rock now generally regarded to have solidified from a carbonate melt.

In recent years intrusive carbonate rocks have been the subject of many papers. Occurrences and theories of origin have been reviewed by Agard (1956), Leonardos (1956), Pecora (1956), and Smith (1956). Proponents of the igneous or carbonatite theory must account for carbonate melts at elevated temperatures and pressures. In the past this has been a stumbling block but recent work summarized by Wyllie and Tuttle (1960 and 1962) indicates that this hurdle is not insurmountable provided sufficient quantities of volatiles are maintained in the melt. In addition, carbonatitic lavas extruded from volcanos have been described from Uganda by Knorring and Dubois (1961) and from Tanganyika by Dawson (1962).

The intrusive carbonate rocks near Meach Lake are well exposed, some in three dimensions. They were examined in detail in order to yield evidence on their mode of formation and throw light on the formation of intrusive carbonate rocks in general. The following note is a preliminary account which summarizes results of work which has been in progress for the last two years.

GENERAL GEOLOGY

The Meach Lake area lies within " favourable belt " for intrusive carbonate rocks which extends 600 miles from Mt. St. Hilaire on the east to Marathon on the west (Fig. 1). Most of the occurrences north of Ottawa are on a ridge 2 miles wide, which fronts Meach Lake on the north and the Ottawa Valley plain on the south (Fig. 2).

Meach Lake lies near the southern part of a batholith which crops out over an area of about 100 square miles. The batholithic rocks are commonly weakly gneissoid and range in composition from diorite, through monzonite into alkalic syenite. Syenite with an average plagioclase content of about An_{15}, is the most common rock near Meach Lake. Quartz is usually present in small amounts and hornblende is ubiquitous. Within the batholith are large roof pendants of recrystallized limestone appearing

as attenuated antiformal folds plunging gently north-east.

A distinctive feature of the geology of the Meach Lake area is the prevalence of aplite and granite pegmatite. The largest body of aplite is roughly circular with an area 8/10 square mile. The composition alaskite with an average plagioclase composition of about An_8. Pegmatites are usually concordant and show very little internal zoning. They grade into aplite although a less common type of granite pegmatite is much coarser, shows some mineral zoning and is definitely later than the aplite.

Provisionally the intrusive carbonates can be grouped into three main types : dolomite-calcite bodies, calcite veins, and breccias with phlogopite-apatite-calcite matrix. This division is rather artificial as there is a continuous transition from one type to the other. The carbonate is coarse ; grains 3 mm. across are not uncommon.

INTRUSIVE DOLOMITE-CALCITE ROCK

A striking feature of the dolomite-calcite bodies is their location relative to the large aplite mass shown near the centre of Fig. 2. They are found, with two known exceptions, within

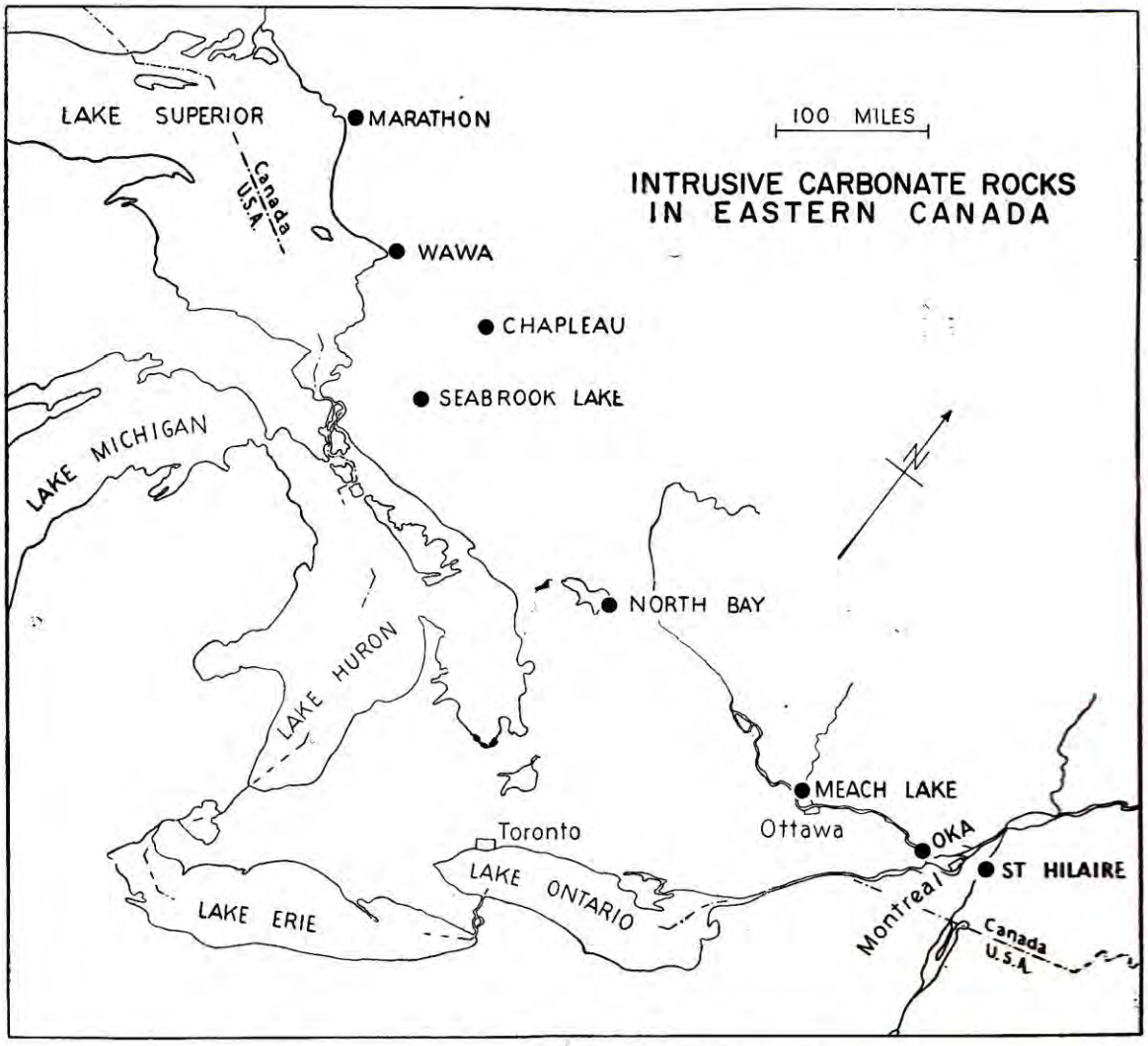

Fig. 1. Location of intrusive carbonate rocks in Eastern Canada.

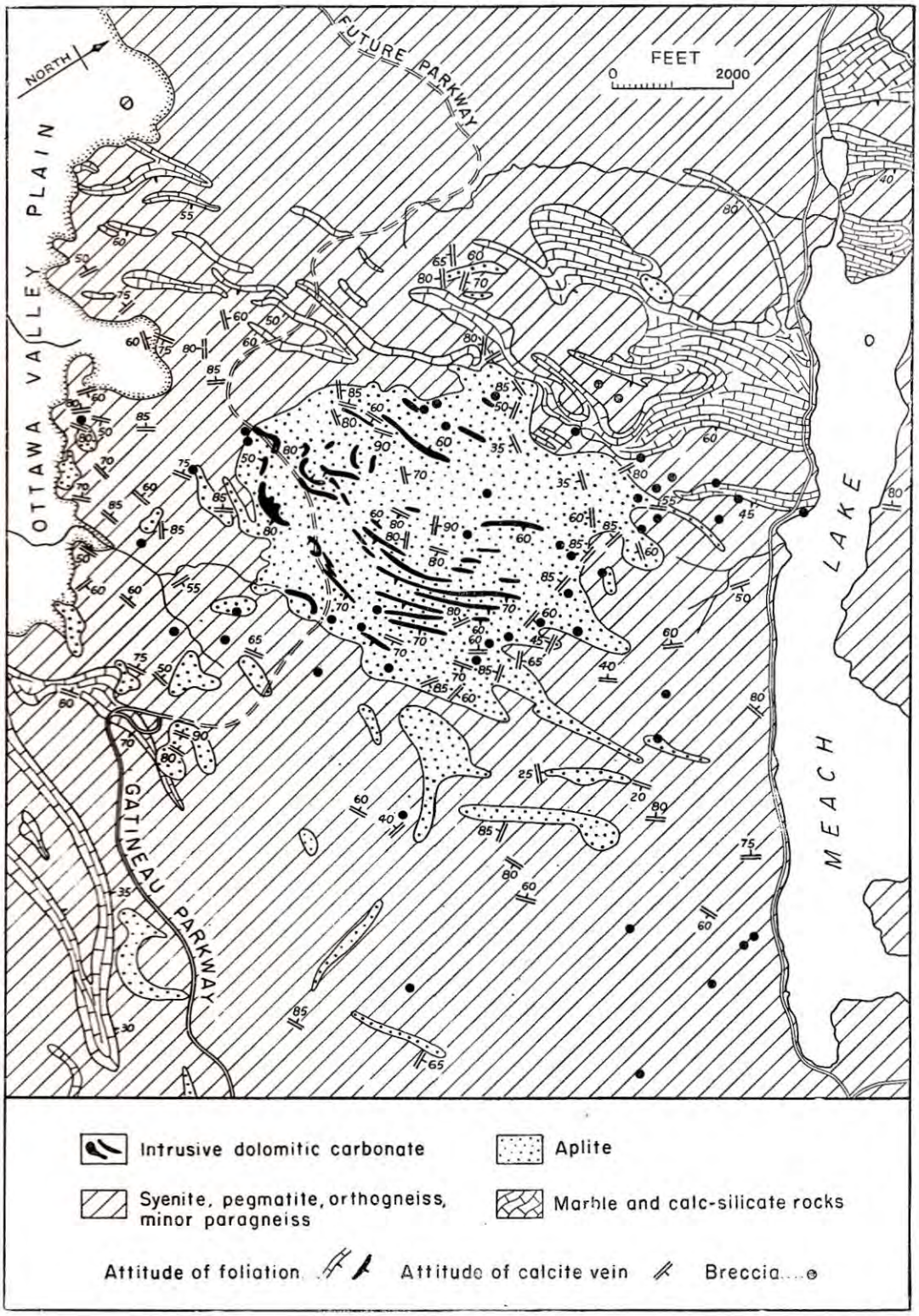

Fig. 2. Geological Map of the region southwest of Meach Lake, Quebec.

the aplite. These exceptions are small occurrences only 600 feet beyond the aplite margin.

In overall outline the occurrences appear arcuate but in detail they are discontinuous lenses. This feature has been illustrated but not discussed in an earlier publication (Hogarth, 1962, Fig. 13).

Dolomite-calcite rock is often distinctly foliated. The foliation is, in part, caused by alternating layers of dolomite and calcite and, in part, by a dimensional orientation of inequant grains of dolomite. The foliation is usually steeply dipping.

margin of the lenses. Other horizons, in which the carbonate is exclusively dolomite, are rich in crystals of magnetite and sometimes these horizons can be traced for several hundred feet. An unusual texture consists of coarse, rounded rhombohedra of dolomite in a finer-grained matrix of calcite (Fig. 3). Apatite is present in amounts ranging from 100% to 0% in short distances. Elongated crystals lie in the foliation planes and commonly show pronounced lineation. Sharp prisms of amphibole and plates of phlogopite-vermiculite are found near the

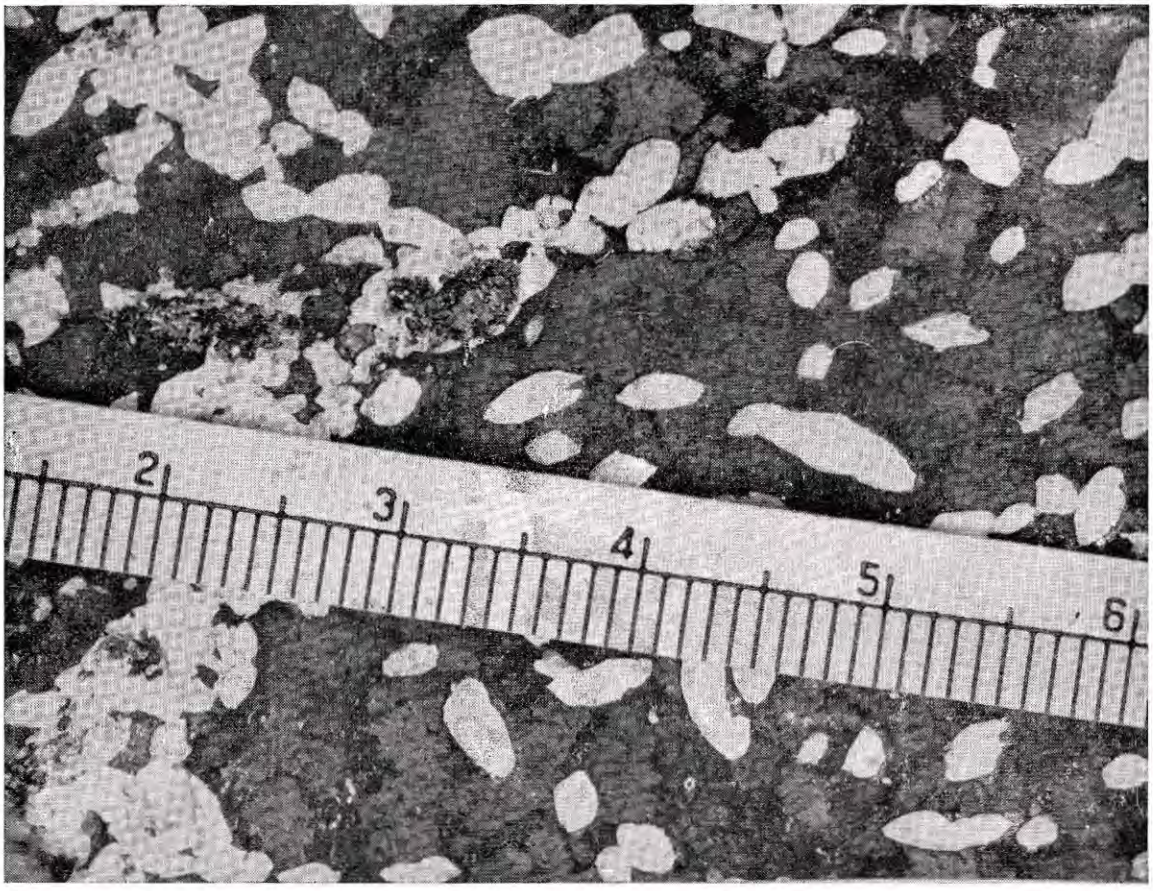

Fig. 3. Crystals of dolomite (light) in calcite (dark). Calcite has been stained by alizarin-red dye.

The mineralogy is simple. Dolomite and calcite make up the bulk of the rock which varies from pure dolomite to pure calcite. The most calcitic portions are normally at the margins of some of the bodies. Pyrite and pyrrhotite are ubiquitous, betafite occurs sparingly in calcitic portions, and barite, fluorite and quartz are rare.

CALCITE VEINS

Calcite-rich bodies are more sinuous or vein-like in form. The word "vein" is used in the morphological sense only. These occurrences rarely attain the size of their dolomitic counterparts; the largest seen was 6 feet wide and 500 feet long. Dips are usually steep.

The veins occur both within and outside the aplite and are often grouped in series, such as the three groups evident in Fig. 2. Commonly veins lie at the contact of syenite and small intrusions of aplite.

The calcite veins contain more minerals than the dolomite bodies. Phlogopite and amphibole are always present and, in some places, very coarse amphibole makes up the major portion of the rock. Fine-grained apatite is common and pyrite is a ubiquitous accessory mineral. Barite is locally abundant. Layered barite-calcite veins occur in the westernmost of the three groups. Betafite is often found near the borders of veins. Fluorite, soda pyroxene, quartz, magnetite, zircon, pyrrhotite and galena have been noted.

BRECCIAS

Veins rich in phlogopites pass imperceptibly into breccias with a matrix of phlogopite, apatite and calcite, and enclosing fragments of aplite and syenite. The distribution of these breccias is irregular, their outline roughly circular or oval. The largest occurrence is 410 feet long.

Macroscopic features of these rocks have been described by Béland (1951) and will only be noted here. Fragments tend to be angular although small pieces are rounded (Fig. 4). The neighbouring fragments may be of different rock type. There is no sorting. Outwardly these breccias pass transitionally through a fractured zone and into unbroken country rock.

Magnesian mica (interlayered phlogopite and vermiculite) is a major constituent of the matrix but the relative amount of each of the three major matrix minerals (phlogopite, apatite, and

Fig. 4. Breccia containing fragments of aplite and syenite and with a matrix of phlogopite, apatite and calcite.

calcite) may vary considerably even within short distances. The breccias south of Meach Lake usually hold very little calcite. It is of interest that a large breccia body in the upper part of Fig. 2 has been largely leached of carbonate resulting in collapse and formation of a water-filled sink.

The accessory minerals are similar to those of the calcite veins. The breccias usually contain small quantities of betafite in apatite-rich portions of the matrix. Around the crystals of betafite phlogopite is usually bent and apatite is fractured and iron-stained. In addition, the following minor minerals have been noted: pyrite, magnetite, pyrrhotite, microcline, soda actinolite, clinopyroxene, barite, zircon and fluorite.

FENITIZED ROCKS

The effects of fenitization are pronounced in the Meach Lake region. Within a few hundred feet of the carbonate bodies the country rock takes on an alkalic character and becomes pink due to tiny veinlets of red hematite. Plagioclase becomes rarer but more albitic, approaching An_7 in syenite and An_4 in aplite. Soda amphiboles appear in radiating clusters. Apatite and calcite become common. Acmite, betafite and specularite are rare but distinctive accessory constituents.

Closer to the dolomitic and calcitic rocks local fenitization effects are evident. Around dolomite aplite is almost entirely replaced, sometimes to several feet from the contact, by phlogopite and subsidiary richterite. The wall-rock of the calcite veins has, in some instances been replaced for several inches by eckermannite with subsidiary phlogopite (Fig. 5). In each case quartz is first attacked, being replaced by

Fig. 5. Aplite fenitized with phlogopite and eckermannite around a calcite vein.

soda amphibole. At several occurrences graphic granite has been partially changed to a graphic microcline-eckermannite rock. The formation of amphibole is closely followed by replacement of feldspars with phlogopite.

Metasomatism around the breccias is usually less apparent. Contacts of fragments with the matrix are usually sharp and often no alteration rim can be seen in the hand specimen. However thin sections of fragment margins show some phlogopite, eckermannite, aegirine-augite, apatite and calcite within an inch of the matrix; these minerals become very rare further out. Béland (1951, p. 364) notes syenite blocks with borders a centimeter thick partially replaced by carbonate.

To summarize, the stages of fenitization may be represented as follows:

1. Widespread fenitization
   (*a*) formation of eckermannite or richterite, albite, apatite and red hematite.
   (*b*) formation of specularite and acmite at an advanced stage (rare).
2. Localized fenitization accompanying the emplacement of carbonate bodies.
   (*a*) replacement of the available quartz by soda amphiboles.
   (*b*) soda pyroxenes appear (rare).
   (*c*) feldspars are replaced by phlogopite and minor amphibole.

Breccias are apparently formed at lower temperature than calcitic and dolomitic bodies and stage 2(a) is poorly developed around their included fragments.

MINERALOGICAL COMPARISONS

The mineral suites of the carbonate rocks north of Ottawa are, in many respects, similar to those from carbonatites, Thus Smith (1956) lists magnetite, apatite, biotite, pyroxene and amphibole as "essential" minerals of carbonatites but adds "they are not always present and hardly ever are all found in the same rock". It is noteworthy that all five minerals occur with the carbonates at Meach Lake.

The magnesian micas at Meach Lake resemble those from carbonatites and differ from micas from other geologic environments in the surrounding region. Vermiculite, which occurs in the breccias and dolomite-calcite bodies, is an abundant mineral in some African carbonatites (Smith, 1956). Compared with the mica from the well known mica-apatite deposits of the surrounding area (de Schmid, 1912), phlogopite at Meach Lake is fine grained and does not show abundant rutile inclusions.

Several types of pleochroism have been observed in phlogopite-biotite from fenites. The most interesting is one with a reverse absorption scheme(Hogarth, 1964). This type of pleochroism is characteristic of phlogopite and biotite from carbonatites and peridotites (Rimskaya-Korsakova and Sokolova, 1964).

It is well known that soda-rich silicates are important minerals in carbonatites and the associated igneous rocks. Generally pyroxenes occur in considerable quantity and amphiboles are very minor constituents but in some carbonatites such as Mbeya and Chilwa (Van der Veen, 1963, pp. 149–154) soda amphiboles are common. At Meach Lake soda amphiboles occur in fenite and the carbonate bodies. In general, amphiboles within the carbonate are somewhat less sodic than those in the surrounding fenite; those within the dolomite are less sodic than those within the calcite veins. Some crystals of richterite-actinolite in dolomitic carbonate bodies have rims of eckermannite.

Betafite is identical in structure (Hogarth, 1961) and similar in many other respects to pyrochlore, a mineral typical of carbonatites. Betafite from the Meach Lake region contains up to at least 4.04% Na_2O, 2.01% SrO, and 3.06% F, amounts characteristic of pyrochlore. Another fact suggestive of a link with pyrochlore from carbonatites if the $Nb_2O_5 : Ta_2O_5$ ratio which in betafite from this district varies from 24 : 1 to greater than 100 : 1 and lies in the range of pyrochlore from carbonatites and alkalic rocks. It is well above the crustal average of 11.4 : 1 (Van der Veen, 1963, pp. 164–175).

A remarkable feature of carbonatites is their high tenor of strontium. Pecora (1956, Table 3) gives the abundance of SrO in carbonatites as 0.5 to 2%. This is distinctly higher than the average for igneous rocks (0.05%) or the range for sedimentary limestone (0.05 to 0.09%; Noll, 1934).

In the Ottawa area sedimentary limestones and metamorphic carbonate rocks have contents of SrO similar to the values quoted from Noll. Seven limestone specimens average 0.07%. Three marble specimens also average 0.07%. The intrusive carbonates however contain much more strontia and fall within Pecora's range for carbonatites. Calcite isolated from a single breccia has 0.8%. Three dolomitic carbonate specimens average 1.1% and three vein calcite specimens average 1.9%.

GENESIS

The fragmental rocks near Meach Lake were first described as conglomerates by Mawdsley (1930) and later as explosive breccias by Béland (1951). Béland attributed rounding of the smaller fragments to corrosion by magmatic fluids which later deposited the minerals of the matrix. Béland's observation of the structure of these rocks has been repeated for new occurrences and all evidence would tend to support a non-sedimentary origin. In addition the presence of apatite and betafite, often as sharply formed crystals, would necessitate unusual sedimentary conditions of deposition and concentration.

Rafted blocks in carbonate-biotite rock would indicate the matrix was either emplaced as a liquid or intruded plastically. The "porphyritic" texture of the dolomitic carbonates is similar to that of carbonates crystallized from melts of similar composition (J. Gittins, personal communication). However, some of the calcite and dolomite crystals are noticeably bent and streaming of small crystals around large "phenocrysts" might indicate shear. Certainly there has been some plastic flow after the formation of vein amphiboles because crystals of eckermannite have been forcibly buckled and sometimes broken by the intruding calcite.

The spatial relationship of carbonate bodies to aplite is undeniable and this suggests a genetic connection. Any theory of the origin of the carbonate bodies should also account for the origin of the aplite but conclusions would be premature at this time. Detailed work on this subject is planned for the future. It is here postulated that the aplite was intruded into syenite near the close of Grenville igneous activity. Field relationships indicate this episode was closely followed by emplacement of dolomite-calcite bodies, then calcite veins. The position of breccias in the sequence is uncertain. K^{40}/Ar^{40} dates for phlogopite separated from fenite gave 930 ± 25 m.y. for dolomite-calcite bodies and 910 m.y. for calcite veins.

ACKNOWLEDGEMENTS

The writer gratefully acknowledges a grant from the Geological Society of America which defrayed the cost of field work and laboratory studies. Dr. M. G. Best of the University of Ottawa kindly read the manuscript and made helpful suggestions.

REFERENCES

AGARD, J. (1956) Les gites minéraux associés aux roches alkalines et aux carbonatites: *Sci. de la Terre*, Univ. Nancy, Vol. 4, pp. 103–151.

BELAND, R. (1951) Le pseudo-conglomerat du Lac Meach.: *Le Nat. Canad.* Vol. 78, pp. 361–366.

DAWSON, J. B. (1962) Sodium carbonate lavas from Oldoinyo Lengai, Tanganyika: *Nature*, Vol. 195, pp. 1075–1076.

HOGARTH, D. D. (1961) A study of pyrochlore and betafite: *Can. Mineral.* Vol. 6, pp. 610–633.

———(1962) A guide to the geology of the Gatineau-Lièvre district: *Can. Field Naturalist*, Vol. 76, pp. 1–55.

———(1964) Normal and reverse pleochroism in biotite: *Can. Mineral.* Vol. 8, p. 136 [Abstract].

von KNORRING, O. & DUBOIS, C. G. (1961) Carbonatitic lava from Fort Portal area in Western Uganda: *Nature*, Vol. 192, pp. 1064–1065.

LEONARDOS, O. H. (1956) Carbonatites com apatita e pirocloro: *Divisao de Fomento da Producao Mineral do Brasil*, Avulso No. 80.

MAWDSLEY, J. B. (1930) The Meach Lake conglomerate: *Trans. Roy. Soc. Can.* Vol. 24, Sect. 4, pp. 99–118.

NOLL, W. (1934) Geochemie des Strontiums mit Bemerkungen zur Geochemie des Bariums: *Chemie der Frde*, Vol. 8, pp. 507–600.

PECORA, W. T. (1956) Carbonatites: a review: *Bull. Geol. Soc. Amer.* Vol. 67, pp. 1537–1556.

RIMSKAYA-KORSAKOVA, O. M. & SOKOLOVA, E. P. (1964) On ferromagnesian micas with a reverse absorption formula: *Notes All Union Mineral. Soc.* Vol. 93, pp. 411–424 [in Russian].

de SCHMID, H. S. (1912) Mica: its occurrence, exploitation, and uses: *Can. Mines Branch*, Pub. No. 118. Sec. Edn.

SMITH, W. C. (1956) A review of some problems of African Carbonatites: *Quart. Jour. Geol. Soc. Lond.* Vol. 112, pt. 2, pp. 189–219.

VAN DER VEEN, A. H. (1963) A Study of pyrochlore: *Verh. ned. geol. mijnb. genoot.* Geol. Ser. No. 22.

WYLLIE, P. J. & TUTTLE, O. F. (1960) Experimental verification for the magmatic origin of carbonatites: *Int. Geol. Cong.* 21st Session. Part 13, pp. 310–318.

——(1962) Carbonatitic lavas: *Nature*, Vol. 194, p. 1269.

MINERALOGICAL SOCIETY OF INDIA, IMA VOLUME, 1966
INTERNATIONAL MINERALOGICAL ASSOCIATION, PAPERS, FOURTH GENERAL MEETING

CARBONATITES OF THE KAISERSTUHL (W-GERMANY) AND THEIR MAGMATIC ENVIRONMENT

W. WIMMENAUER
Schauinslandstr 14, Freiburg, West Germany

ABSTRACT

The Kaiserstuhl is a group of miocene volcanic hills approximately 15 km in diameter. Subvolcanic and volcanic rocks intrude into and cover the oligocene filling of the Upper Rhine graben. The Kaiserstuhl volcano s.str. consists mainly of leucite tephrite lavas, agglomerates and tuffs. There occur in the periphery younger flows of basanite, limburgite and olivine nephelinite with interstratified phonolitic tuffs. The subvolcanic core is uncovered in the centre of the hills. It is composed of minor intrusions of essexite, theralite and phonolite, these in turn being intersected by very numerous dikes of related composition (essexite and theralite porphyrites, monchiquites, mondhaldeites, dike phonolites, tinguaites, hauynophyres, bergalites). Dome-shaped phonolite bodies and dikes of the rocks mentioned above in brackets also invade the volcanic edifice and the underlying tertiary sediments.

In the subvolcanic centre, *carbonatite* intrusions cover a surface of about 1 km^2. There are some major thick plate-or dome-shaped bodies (formerly regarded as contact-metamorphic limestones) and many dykes, the width of which varies from a few cm to > 10 m. Sövites with calcite, micas, magnetite, apatite, forsterite and pyrochlore greatly prevail over later dolomitic-ankeritic carbonatites with barite. Immediately adjacent country rocks of the carbonatites are partly those of the essexitic family and phonolites, partly subvolcanic breccias. These consist of fragments of the above named rocks ; they were seemingly formed in close relation with the intrusion of the major carbonatite bodies. Geochemical analyses of the breccia by van Wambeke *et al.* yielded rather high contents of those elements, which are characteristic for ultrabasic rocks.

For the variety of the Kaiserstuhl rocks, an olivine nephelinitic parent magma is assumed. An essexitic and a foyaitic daughter magma developed by interaction of the assimilation of granitic material and crystallisation-differentiation. In the approximate and further surroundings of the Kaiserstuhl there occur olivine nephelinite and melilite ankaratrite in numerous pipes and dikes. The igneous constituents of the pipe breccias show obvious petrographic relations with kimberlites, although they do not attain the typical characteristics of the latter.

INTRODUCTION

The Upper Rhein Graben is one of the most prominent geological features in Central Europe. It extends from Basel (Switzerland) to Frankfurt over a length of 350 km. The maximum vertical dislocation is more than 4 km. The Kaiserstuhl volcano is situated near the southern end of the graben; it is a group of moderate hills of 6 to 9 miles in diameter. Leucite tephrite lavas and pyroclastics are the dominant rocks of the volcano proper; in the later stages of the volcanic activity, basanites, limburgites and olivine nephelinites also appeared. A core of subvolcanic intrusive rocks is exposed in the centre of the volcano; essexites and theralites with their dike equivalents are the most important constituents of this unit. Intrusive phonolites occur as members of the centre as well as in separate stocks in the tephrites and the tertiary sediments, which form the base of the volcanic edifice.

THE CARBONATITES

Carbonatites cover about one square kilometer in the centre of the Kaiserstuhl. They are intrusive into the essexites and phonolites, but locally cut in turn by the youngest dike rocks of the siliceous sequence. In the eastern half, the carbonatite intrusions are preceded by subvolcanic breccias. These consist of fragments of the earlier country rocks present in their neighbourhood, mostly essexites and phonolites. The largest carbonatite unit is the Badberg sövite body, a calcite rock, rather poor in silicates. Among the latter, biotite and hydrobiotite are the most common minerals;

magnetite and melilite in greater amounts are encountered locally. The sövites of Schelingen contain forsterite, magnetite and apatite. Pyrochlore and niobian perowskite are the most important additional components.

There are some observations, which might be significant for the composition of the original carbonatite magma. The immediately neighbouring country rocks and xenoliths of those in the carbonatites have undergone a more or less intensive carbonatization, but also a remarkable alkali metasomatism. Pyroxenes are converted into biotite, plagioclase into calcite and alkali feldspar. The apatites of the carbonatite itself are rich in liquid and gaseous inclusions, which contain crystals of halite, sylvite and calcite. All these phenomena indicate an important role of the alkalies in the carbonatitic medium.

The sövites are followed by a subordinate suite of alvikite dikes and dolomitic-ankeritic carbonatites.

ORIGIN

Relations with siliceous rocks

There are no intermediate members between the carbonatites and the siliceous alkaline rocks of the Kaiserstuhl. The question now arises, to which branch of the wide variety of rocks of the region the carbonatites might most likely be related. The bergalite, a carbonate-bearing hauynite-melilite-biotite rock, could be taken for the next of kin to the carbonatites, but its carbonates are mainly secondary. On the other hand, an isolated phonolite stock (Kirchberg) in the western Kaiserstuhl is accompanied by a small suite of alvikitic dikes of his own, but no general conclusion should be drawn from this single observation. Kimberlites *sensu stricto* are not present in Kaiserstuhl nor in its surroundings, but the two hundred volcanic pipes of the Urach region have often been compared with the South African kimberlite pipes. Similar pipes are also found at the eastern margin of the Upper Rhein Graben, near to the Kaiserstuhl. Melilite ankaratrites are their magmatic constituents. Related igneous rocks, mostly olivine nephelinites, of approximately the same age are very widespread around the Kaiserstuhl from eastern France over southern Germany to Bohemia. They prefer the more isolated and small occurences (as compared with the more voluminous alkali olivine-basalts of the Vogelsberg and other tertiary volcanos in Central Europe). Their appearance is obviously independent from the other kinds of basalts.

A magma of that type, that is a strongly undersaturated "nepheline basalt" or also "nepheline melilite-basalt magma" is assumed to be the parent magma for the variety of the Kaiserstuhl igneous rocks. It may closely correspond to the magma of the C group basalts of Kushiro and Kuno (1963).

TABLE 1

Niggli numbers of the main rock types mentioned in this paper

	si	*al*	*fm*	*c*	*alk*	*k*	*mg*
35 melilite ankaratrites of Central Europe	67.3	10.4	58.0	25.2	6.8	0.28	0.73
52 olivine nephelinites of Central Europe	75.1	15.8	51.2	25.8	7.6	0.21	0.58
Bergalite*, Oberbergen (K.)	76.0	17.5	33.5	31.5	17.5	0.26	0.41
4 limburgites, Sasbach (K.)	86.2	16.5	47.7	28.2	8.0	0.27	0.53
Average alkali olivine basalt of Hawaii	100.0	17.5	52.1	23.7	6.7	0.14	0.60
13 Tephrites and related lavas (K.)	104.4	19.0	40.7	31.1	9.2	0.31	0.44
6 essexites, theralites and dike equivalents (K.)	105.6	20.6	41.2	27.1	10.6	0.35	0.46
5 dike phonolites and tinguaites (K.)	136.0	31.3	22.8	23.4	20.4	0.37	0.39
Trachytoid phonolite, Kirchberg (K.)	192.5	41.2	15.5	12.5	30.8	0.35	0.38

* with 26.4 CO_2 corresponding to 8.42% CO_2.

Comprehensively, a simple crystallization-differentiation of such a magma would not yield the large amount of plagioclase rich leucite tephrites and essexites nor the highly feldspathic phonolites. An assimilation of sialic rocks has therefore, to be supposed, which produced, on interaction with differentiation, the actual diversity of the Kaiserstuhl silicatic sequence. This hypothesis is supported by numerous fenitized gneiss and granite xenoliths, namely in the phonolites. An alternative hypothesis would be the derivation of the tephrites, essexites and limbergites from a primary alkali olivine-basalt magma. But this assumption is rendered difficult by the fact, that typical basaltic rocks, representing that magma, are practically absent. Additional hypotheses to account for the mineralogical and chemical differences from basalts, the higher alkali content and the more potassic character of the Kaiserstuhl rocks could also not be avoided.

Genesis of the carbonatites

Rather little information can be drawn from the petrographic observations in the Kaiserstuhl concerning the origin of the carbonatites. But some of the olivine nephelinites in the region, mentioned before, give perhaps important indications for that problem. In a particular rock of the Feldberg (Black Forest), the carbonates attain up to 30% of the whole rock. They are concentrated in numerous vugs of a few millimeters in size. The filling of those vugs begins by the formation of nepheline (in very uncommon skeleton-like forms), pyroxene and biotite. The carbonate is mostly dolomite ; in later stages calcite, a serpentine mineral and quartz follow. These minerals represent certainly a wide range of temperature, going down to typical hydrothermal formations. Therefore the vugs cannot be regarded simply as carbonatitic differentiations. But they show, in any case, the ability of the olivine nephelinite magma to generate rather large amounts of carbonatic matter. It is furthermore remarkable, that those portions of the rock, which contain many carbonatic segregations, are also enriched in strontium and niobium, elements particularly significant for the carbonatites. Similar phenomena of nephelinitic and carbonatic differentiation have recently been described by Saggerson & Williams (1964) in the case of the ngurumanite from Tanganyika.

So it may be concluded, that the observations in the Kaiserstuhl and its environment favour the hypothesis of a close connection of the carbonatites with a strongly undersaturated magma, represented by the olivine nephelinites and melilite ankaratrites of the region. This statement would be well in line with the opinion expressed for instance by King & Sutherland (1960) in a more general way. These authors found the assemblage of olivine nephelinites, carbonatites and phonolites to be a very common one with the carbonatites of South and East Africa. Experimental studies of P. J. Wyllie (1964 a) showed the probability of carbonatite generation from very basic alkaline magmas (e.g. alkaline peridotite magma ; cf also von Eckermann 1948). The author emphasizes the wide distribution of melilite in the systems investigated. The sequence of older sövite and younger dolomitic-ankeritic carbonatite, observed in the Kaiserstuhl and elsewhere, is now also explained by experiments (Wyllie 1964b) as the regular consequence of fractional crystallization of a carbonatite magma.

CONCLUSION

The alkaline silicatic rocks of the Kaiserstuhl (Germany) are hypothetically derived from a deep-seated undersaturated magma, which is represented by the olivine nephelinites and melilite ankaratrites of the region. Field and petrographic relations and experimental studies (P. J. Wyllie) point at the same source also for the carbonatites.

REFERENCES

von Eckermann, H. (1948) The alkaline district of Alnö Island : *Sveriges Geol. Unders.* Ser. Ca, No. 36, pp. 1-176.

King, B. C. and Sutherland, D. S. (1960) Alkaline rocks of Eastern and South Africa. *Sci. Progress* Vol. 48, pp. 298-321, 504-523, 709-720.

KUSHIRO, I. AND KUNO, H. (1963) Origin of primary basalt magmas and classification of basaltic rocks. *Jour. Petr.* Vol. 4, pp. 75–89.

SUGGERSON, E. P. AND WILLIAMS, L. A. J. (1964) Ngurumanite from southern Kenya and its bearing on the origin of rocks in the northern Tanganyika alkaline district: *Jour. Petr.* Vol. 5, pp. 40–81.

WIMMENAUER, W. (1963) Beiträge zur Petrographie des Kaiserstuhls I–VII. *Neus Jb. Miner. Abh. 91*, 131–150, 1957, 93, 133–173, 1959, 98, 367–415, 1962 und 99, 231–276.

———(1963) Die Bedeutung der Olivinnephelinite und Melilithankaratrite im tertiaren Vulkanisums Mitteleuropas: *Neues Jb. Miner., Mh.* pp. 278–282.

WYLLIE, P. J. (1966) Experimental data bearing on the petrogenetic links between kimberlites and carbonatites. *Min. Soc. India.*, I.M.A. Volume.

———(1966) Fractional crystallization in synthetic carbonatite magmas. *Min. Soc. India.*, I.M.A. Volume.

MINERALOGICAL SOCIETY OF INDIA, IMA VOLUME, 1966
INTERNATIONAL MINERALOGICAL ASSOCIATION, PAPERS, FOURTH GENERAL MEETING

ISOTOPIC COMPOSITION OF STRONTIUM IN CARBONATITES AND KIMBERLITES

J. L. POWELL
Oberlin College, Oberlin, Ohio, U.S.A.

ABSTRACT

The average Sr^{87}/Sr^{86} ratio of specimens from 32 carbonatites is 0.7032 ± 0.0010 (σ). The Sr^{87}/Sr^{86} ratios of carbonatites are distinctly lower than those of most limestones and are similar to those of mafic igneous rocks. Study of the Sr^{87}/Sr^{86} ratios of carbonatites, associated alkalic rocks, and some sedimentary carbonate rocks has indicated that: (1) carbonatites are not limestone xenoliths, (2) carbonatites are comagmatic with their associated alkalic rocks, and (3) carbonatites are derived from a sub-sialic source, probably from the mantle. The Sr^{87}/Sr^{86} ratio, when used in conjunction with field evidence, seems to provide a reliable empirical criterion for recognition of carbonatites.

Granites, and particularly older ones, have very high Sr^{87}/Sr^{86} ratios. If kimberlites are formed as a result of an assimilative reaction between carbonatite magma and granite ;they should have higher Sr^{87}/Sr^{86} ratios than carbonatites. Sr^{87}/Sr^{86} analyses of 11 whole-rock kimberlite specimens give values ranging from 0.705 to 0.721. This result is consistent with the kimberlite=carbonatite magma+granite hypothesis, but the higher Sr^{87}/Sr^{86} ratios of the kimberlites may have been caused instead by microscopic inclusions of foreign rock in the specimens analyzed. Measurement of the Sr^{87}/Sr^{86} ratios of primary minerals separated from kimberlite specimens would resolve this problem.

INTRODUCTION

Strontium possesses 4 naturally occurring stable isotopes of mass 88, 87, 86, and 84. Sr^{87} is also formed by the radioactive decay of Rb^{87}. The abundance of Sr^{87} in any system, commonly expressed by the Sr^{87}/Sr^{86} ratio, increases with time as an almost linear function of the Rb/Sr ratio of the system. Since the Rb/Sr ratios of geologic environments vary, so do Sr^{87}/Sr^{86} ratios. In certain instances Sr^{87} may be used as a geological tracer to provide petrogenetic information.

Faure and Hurley (1963) found the Sr^{87}/Sr^{86} ratios of basalts to vary between 0.702 and 0.707. They estimate the average Sr^{87}/Sr^{86} ratio of the sialic portion of the continental crust as 0.722± 0.005. The Sr^{87}/Sr^{86} ratios reported by Faure and Hurley (1963) must be corrected by –0.0030 to account for a systematic bias in their analytical procedure. If a rock is derived from the same source regions as basalt magmas its Sr^{87}/Sr^{86} ratio, like those of basalts, should be low. If a rock is derived by a process involving significant amounts of sialic crustal rocks its Sr^{87}/Sr^{86} ratio should be substantially higher than those of basalts. Faure and Hurley also emphasize that rocks derived from the same parent magma would have had identical Sr^{87}/Sr^{86} ratios at the time they crystallized.

This paper is a summary of the application of the Sr^{87} tracer technique to the problems of origin of carbonatite and kimberlite. Details of analytical procedures and more complete discussions of the principles and results are given by Powell *et al.* (1962, 1965a) and Powell (1965a, 1965b, 1965c).

SR^{87}/SR^{86} RATIOS OF CARBONATITES

The Sr^{87}/Sr^{86} ratios of most of the carbonatites which have been analyzed are listed in Table 1. The results of Hamilton and Deans (1963) are excluded because interlaboratory discrepancies prohibit direct comparison of their data with those of the M. I. T. Isotope Geology Laboratory where all of the other measurements listed in Table 1 were performed. The Sr^{87}/Sr^{86} ratios of these carbonatites vary from 0.702 to 0.705.

The Sr^{87}/Sr^{86} ratios of the sedimentary carbonate rocks and marbles that have been analyzed are listed in Table 2. With the exception of the very old Bulawayan limestone their Sr^{87}/Sr^{86} ratios vary from 0.706 to 0.713.

TABLE 1

Sr^{87}/Sr^{86} Ratios of Carbonatites*

Locality	(Sr^{87}/Sr^{86})†	(Sr^{86}/Sr^{88})
United States		
Magnet Cove, Arkansas	0.7046	0.1191
Iron Hill, Colorado	0.7046	0.1193
Mountain Pass, California	0.7044	0.1189
Canada		
Oka, Quebec	0.7032	0.1195
Lake Nipissing, Ontario	0.7031	0.1192
Nemegosenda Lake, Ontario	0.7035	0.1189
Lackner Lake, Ontario	0.7032	0.1197
Firesand River, Ontario	0.7024	0.1188
Seabrook Lake, Ontario	0.7037	0.1192
Cargill Twp., Ontario	0.7019	0.1196
Clay Twp., Ontario	0.7032	0.1190
Prairie Lake, Ontario	0.7028	0.1187
Chipman Lake, Ontario	0.7022	0.1195
Twp. 107, Sudbury Dist., Ontario	0.7021	0.1187
Europe		
Alnö, Sweden	0.7022	0.1193
Fen, Norway	0.7021	0.1202
Stjernoy, Norway	0.7028	0.1187
Africa		
Spitzkop, South Africa	0.7028	0.1194
Loolekop, South Africa	0.7051	0.1194
Glenover, South Africa	0.7038	0.1202
Premier Mine, South Africa	0.7028	0.1189
Shawa, Southern Rhodesia	0.7034	0.1183
Kaluwe, Northern Rhodesia	0.7021	0.1193
Kangankunde, Nyasaland	0.7016	0.1193
Chilwa Island, Nyasaland	0.7041	0.1191
Chigwakwalu, Nyasaland	0.7050	0.1190
Busumbu, Uganda	0.7032	0.1184
Tóroro, Uganda	0.7025	0.1188
Sukulu, Uganda	0.7026	0.1196
Mrima, Kenya	0.7044	0.1194
Rangwa, Kenya	0.7042	0.1101
Oldoinyo Lengai, Tanganyika	0.7033	0.1287
Average for 32 carbonatites	$=0.7032 \pm 0.0010\ (\sigma)$	

* Data from Powell *et al.* (1965a), from Powell (1965c), and from unpublished work.

† All Sr^{87}/Sr^{86} ratios are normalized to $Sr^{86}/Sr^{88}=0.1194$ and expressed relative to a value of about 0.708 for the Sr^{87}/Sr^{86} ratio of the Eimer and Amend $SrCO_3$ interlaboratory standard.

TABLE 2

Sr^{87}/Sr^{86} Ratios of Sedimentary Carbonate Rocks and Marbles

Rock Type and Locality	(Sr^{87}/Sr^{86})*	Reference
Limestone, Bulawayan, S. Rhodesia	0.702†	Gast (1960) ; Hamilton and Deans (1963) ; Hedge and Walthall (1963)
Marble, pre-Grenville, New York	0.7062	Hedge and Walthall (1963)
Marble, Grenville, Canada	0.707†	Gast (1960) ; Krogh (1964) ; Pinson *et al.* (1958) ; Powell *et al.* (1965a)
Limestone, Newland, Belt series	0.707	Gast (1960)
Limestone, Ottertail, British Columbia	0.7083	Powell *et al.* (1965a)
Limestone, Eocene, Haiti	0.7086	Hedge and Walthall (1963)
Limestone, L. Ordovician, Texas	0.7087	Hedge and Walthall (1963)
Limestone, Madison, Montana	0.7087	Powell *et al.* (1965a)
Limestone, Trenton, Montreal, Quebec	0.7090	Powell *et al.* (1955a)
Limestone, Ordovician, Iswos, U.S.S.R.	0.7097	Herzog *et al.* (1958)
Dolomite, Transvaal, nr. Olifantsfontein	0.7099	Powell *et al.* (1965a)
Limestone, Ordovician, Texas	0.711	Gast (1960)
Dolomite, Mlindi Ring, Nyasaland	0.7129	Hamilton and Deans (1963)

* Normalized to $Sr^{88}/Sr^{88}=0.1194$ and corrected so that all values are expressed relative to a value of about 0.708 for the Eimer and Amend $SrCO_3$ standard.

† Average of the values reported in each reference.

Fig. 1 is a histogram plot showing the frequency distribution of the Sr^{87}/Sr^{86} ratios of carbonatites (data from Table 1), carbonate vein-dikes (data from Powell, 1965a), sedimentary carbonate rocks (data from Table 2), and continental mafic rocks (data from Faure, 1963 ; Faure and Hurley, 1963 ; and Hedge and Walthall, 1963).

It is apparent from Fig. 1 that the Sr^{87}/Sr^{86} ratios of carbonatites are distinctly lower than those of most sedimentary carbonate rocks and are similar to those of continental mafic rocks. Powell et al. (1965a) showed that the Sr^{87}/Sr^{86} ratios of the carbonatites at Oka, Quebec ; Magnet Cove, Arkansas ; and Iron Hill, Colorado, were in each case identical to those of their associated alkalic rocks. These results indicate that carbonatites are either comagmatic with their associated alkalic rocks, or they are mobilized limestone xenoliths whose Sr^{87}/Sr^{86} ratios have been changed by diffusion of Sr^{87} to those of the alkalic magmas which engulfed them. The latter alternative can be rejected as a general explanation on purely geologic grounds. In addition, Powell *et al.* (1965a) showed that no appreciable diffusion of Sr^{87} had occurred in a very small xenolith of Trenton limestone that had been enclosed in an alkalic magma at Mount Royal, Montreal. Both the geologic evidence and the strontium isotopic evidence strongly support the conclusion that carbonatites are not limestone xenoliths but have been derived by crystallization from the same magma as their associated alkalic rocks.

The difference between the Sr^{87}/Sr^{86} ratios of accepted carbonatites and those of most sedimentary carbonate rocks suggests the use of the Sr^{87}/Sr^{86} ratio as an empirical criterion for determining whether carbonate rocks of uncertain origin are carbonatites. An example of the application of this criterion to the carbonate rocks at Keshya and Mkwisi, Northern Rhodesia, is given by Hamilton and Deans (1963) and Powell (1965b).

The spread in the Sr^{87}/Sr^{86} ratios of carbonatites is small compared to the spread in the ratios of the continental mafic rocks shown in Fig. 1. This indicates that the source regions of the carbonatite-alkalic rock suite are quite homogeneous with respect to the Sr^{87}/Sr^{86} ratio, and that carbonatites in general have not been significantly contaminated with more radiogenic

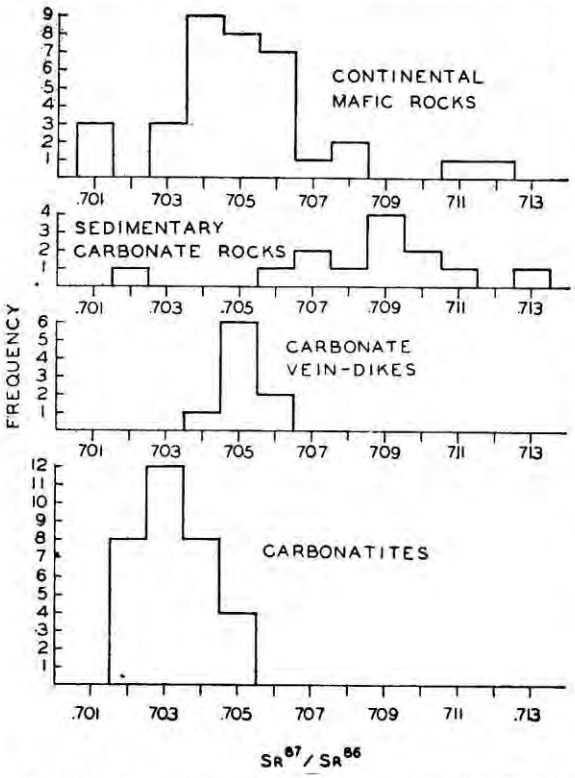

Fig. 1. Histogram plot of the frequency distribution of the Sr^{87}/Sr^{86} ratios of continental mafic rocks, sedimentary carbonate rocks, carbonate vein-dikes, and carbonatites.

Sr^{87} from the sialic crust. These conclusions are consistent with the hypothesis that carbonatites are derived from the simatic part of the crust or from the mantle, and with the fact that they have such high strontium concentrations that their inherently low Sr^{87}/Sr^{86} ratios are relatively unaffected by contamination with crustal rocks.

The Sr^{87}/Sr^{86} ratios of carbonatites are at least as low as the initial Sr^{87}/Sr^{86} ratios of all except the very oldest continental mafic rocks, and they are identical to those of the oceanic basalts analyzed by Gast *et al.* (1964) and Powell *et al.* (1965b). This indicates that carbonatites and their related alkalic rocks are not derived by processes involving significant amounts of rocks from the sialic crust. Therefore the strontium isotopic evidence offers strong quantitative support to the hypothesis that the parent magmas of the carbonatite-alkalic rock association are derived from beneath the sial and probably from the upper mantle.

Although the low Sr^{87}/Sr^{86} ratios of carbonatites indicate that they are not mobilized limestone xenoliths and that they contain juvenile strontium, it does not necessarily follow from this evidence that the carbon dioxide in carbonatites is also juvenile. For example, carbonatites could conceivably be formed as residual products of the differentiation of a basaltic or granitic magma which had assimilated a relatively small amount of limestone. The Sr^{87}/Sr^{86} ratio of such a carbonatite might be only slightly higher than that of the original basaltic or granitic magma. A carbonatite formed in this way would contain strontium that was mainly juvenile but carbon dioxide that was resurgent.

SR^{87}/SR^{86} RATIOS OF CARBONATE VEIN-DIKES

Fig. 1 also shows the frequency distribution of the Sr^{87}/Sr^{86} ratios of 9 specimens from the carbonate veins or vein-dikes at Ravalli Co., Montana; the Rocky Boy Stock, Montana; Lemhi Co., Idaho; and the Cardiff Uranium Mines, Haliburton Co., Ontario. These data and their interpretation are discussed in detail by Powell (1965a). The average Sr^{87}/Sr^{86} ratio of the 9 specimens is significantly higher than that of the carbonatites listed in Table 1. This fact cannot be explained by fractionation of the strontium isotopes, since such effects, whether natural or experimental, are compensated for by normalizing all measured Sr^{87}/Sr^{86} ratios to a constant value of Sr^{86}/Sr^{88}. The exceptionally high concentrations of strontium in some of the vein-dikes would appear to rule out the possibility that their higher Sr^{87}/Sr^{86} ratios are caused

by contamination of carbonatite magmas with sialic crustal rocks. Powell (1965a) states that the strontium isotopic evidence suggests that the carbonate vein-dikes that have been analyzed are genetically unrelated to the type of magma or fluid which gives rise to the typical massive carbonatites.

SR^{87}/SR^{86} RATIOS OF KIMBERLITES

Holmes (1950) proposed that the rock katungite, a potash-rich, augite-free, olivine melilitite chemically similar to kimberlite, was formed by the assimilation of granitic basement rocks by a carbonatite magma. Elsewhere in this volume J. B. Dawson proposes that kimberlites themselves are formed by such a process.

It has been shown that carbonatites have very low Sr^{87}/Sr^{86} ratios which average 0.7032. While no figure for the average Sr^{87}/Sr^{86} ratio of granitic rocks is available, an approximate value may be calculated. Faure and Hurley (1963) estimate the average Rb/Sr ratio of granites as 1.00. The Sr^{87}/Sr^{86} ratio of a rock with Rb/Sr = 1.00, an age of one billion years, and initial $Sr^{87}/Sr^{86} = 0.704$, using equation 2 of Faure and Hurley (1963, p. 39), would be about 0.745. This is probably a reasonable rough estimate of the average Sr^{87}/Sr^{86} ratio of one billion year-old granites. Gast (1961) lists analyses of 9 granites ranging in age from 1100 million years to 2900 million years; they have Sr^{87}/Sr^{86} ratios varying between 0.740 and 1.003. It is clear that granites, and especially the older granites of the continental basements, have relatively high Sr^{87}/Sr^{86} ratios.

If Dawson's hypothesis is correct, kimberlites should have Sr^{87}/Sr^{86} ratios intermediate between those of carbonatites and those of granites. The much higher concentrations of strontium in carbonatites might tend to swamp out the less abundant strontium from the granites, however, with the result that the Sr^{87}/Sr^{86} ratios of kimberlites might be only very slightly higher than those of carbonatites. A simple approximate calculation can be made to determine the effect of assimilation of granite with 350 ppm strontium and $Sr^{87}/Sr^{86} = 0.745$ upon the Sr^{87}/Sr^{86} ratio of an average carbonatite magma with 3500 ppm strontium and $Sr^{87}/Sr^{86} = 0.7032$. Holmes (1950) calculates that in order to produce katungite a carbonatite magma must assimilate an amount of granite approximately equal to its own mass. It will be assumed for the purpose of this calculation that the masses of carbonatite magma and granite which are mixed to produce kimberlite are equal. Since the ratio of strontium in carbonatite to that in granite in this example is $3500/350 = 10$, a kimberlite formed by Dawson's hypothesis with the starting materials specified above would contain approximately 90 per cent carbonatitic strontium and approximately 10 per cent granitic strontium. The Sr^{87}/Sr^{86} ratio of such a carbonatite would be $0.7032\ (0.90) + 0.745\ (0.10) = 0.7074$. This figure is distinguishable with the present analytical precision from the Sr^{87}/Sr^{86} ratios of carbonatites and oceanic basalts. Since many granitic basement rocks have considerably higher Sr^{87}/Sr^{86} ratios than 0.745, at least some kimberlites would be expected to have Sr^{87}/Sr^{86} ratios higher than 0.7074.

As a first step in applying the Sr^{87} tracer method to the kimberlite problem, a number of whole-rock kimberlite specimens have been analyzed for Sr^{87}/Sr^{86} and Rb/Sr. The results are shown in Table 3. The Sr^{87}/Sr^{86} ratios of the kimberlites analyzed are variable, are higher than those of carbonatites, and in most cases are higher than those of basalts. The Rb/Sr ratios of these kimberlites are so low that there has been no significant increase in their Sr^{87}/Sr^{86} ratios since the Cretaceous period. It can be concluded that at least some kimberlites contain significant amounts of strontium which must have come from the sialic part of the crust.

The data reported in Table 3 are consistent with Dawson's hypothesis that kimberlite forms by a reaction between carbonatite magma and granite. On the other hand, it is well known that kimberlites contain numerous inclusions of foreign rock of all sizes from microscopic to very large. Although kimberlite specimens with

obvious macroscopic inclusions were avoided in this work, it is quite possible that most or perhaps all of the specimens analyzed contained inclusions of foreign rock of microscopic size. The presence of such inclusions could easily account for the higher Sr^{87}/Sr^{86} ratios observed in some of the specimens.

the time of their crystallization the same relatively high Sr^{87}/Sr^{86} ratio as the magma itself.

I believe that further study of the abundance of Sr^{87} in primary minerals from kimberlites would permit the hypothesis that kimberlite is formed by an assimilative reaction between carbonatite magma and older granitic rocks to

TABLE 3

Sr^{87}/Sr^{86} and Rb/Sr Ratios of Kimberlites

Sp. No.	Locality and Description	(Sr^{87}/Sr^{86})*	(Rb/Sr)†
R4831	Premier Mine, whole rock	0.721	0.2
R4831	Premier Mine, fraction soluble in acetic acid	0.718	
R4831	Premier Mine, fraction insoluble in acetic acid	0.729	
R40	Premier Mine, whole rock	0.711	0.1
R41	Premier Mine, whole rock	0.711	0.1
R42	Premier Mine, whole rock	0.717	0.15
R5015	Kimberley Mine, whole rock	0.706	0.2
R5015	Kimberley Mine, fraction soluble in acetic acid	0.707	
R4829	Kimberely Mine, whole rock	0.707	0.1
R4830	Monastery Mine, whole rock	0.718	0.3
R4832	Murfreesboro, Ark., whole rock	0.708	0.2
R17	Marakabei, Bastuoland, whole rock	0.705	0.02
R32	Koidu, Sierra Leone, whole rock	0.707	0.1
R35	Koidu, Sierra Leone, whole rock	0.706	0.2

* Normalized to $Sr^{86}/Sr^{88}=0.1194$.

† Approximate-determined by x-ray fluorescene. If Rb/Sr=0.3, the increase in Sr^{87}/Sr^{86} per 100 m.y. is about 0.0013.

It is apparent from these remarks that the Sr^{87} tracer technique cannot be successfully applied to the kimberlite problem if whole-rock kimberlite specimens are to be used, because it is probably impossible to obtain specimens of kimberlite that can be demonstrated to be completely free of all foreign inclusions regardless of size. It may still be possible, however, to apply this technique to the problem of the origin of kimberlite if primary minerals from kimberlites, and not whole-rock specimens, are analyzed. If Dawson is correct, such minerals as primary olivine in kimberlite, for example, will have crystallized from contaminated carbonatite-kimberlite magma and will have had at be tested. The major difficulty in such a study is that of obtaining large enough specimens of fresh kimberlite to permit mineral separations to be made. The author would be pleased to hear from persons who might be able to contribute such specimens.

ACKNOWLEDGEMENTS

I would like to thank Professor P. M. Hurley in whose laboratory at the Massachusetts Institute of Technology all of my analyses were made. Professor Hurley's laboratory receives support from the U. S. Atomic Energy Commission under Contract AT (30–1)–1381. I thank all of those individuals and organizations who contributed specimens to this work.

REFERENCES

FAURE, G. (1963) The isotopic composition of strontium in mafic rocks : In P. M. Hurley et al. *NYO*-10,517. *Eleventh Ann. Prog. Rep. (M.I.T.)*, pp. 125-126

FAURE, G. AND HURLEY, P. M. (1963) The isotopic composition of strontium in oceanic and continental basalts : Application to the origin of igneous rocks. *Jour. Petr.* Vol. 4, pp. 31-50.

GAST, P. W. (1960) Limitations on the composition of the upper mantle : *Jour. Geophys. Res.*, Vol. 65, pp. 1287-1297.

——— (1961) The rubidium-strontium method : *Ann. N. Y. Acad. Sci.* Vol. 91, pp. 181-184.

GAST, P. W., TILTON, G. R. AND CARL HEDGE (1964) Isotopic composition of lead and strontium from Ascension and Gough Islands : *Science*, Vol. 145. pp. 1181-1185.

HAMILTON, E. I. AND DEANS, T. (1963) Isotopic composition of strontium in some African carbonatites and limestones and in strontium minerals : *Nature*, Vol. 198, pp. 776-777.

HEDGE, C. E. AND WALTHALL, F. G. (1963) Radiogenic strontium-87 as an index of geologic processes : *Science*, Vol. 140, pp. 1214-1217.

HERZOG, L. F., PINSON, W. H. AND CORMIER, R. F. (1958) Sediment age determination by Rb/Sr analysis of glauconite : *Bull. Amer. Ass. Petrol. Geol.*, Vol. 42, pp. 717-733.

HOLMES, A. (1950) Petrogenesis of katungite and its associates : *Am. Mineral.*, Vol. 35, pp. 772-792.

KROGH, T. (1964) Strontium isotopic variation and whole rock isochron studies in the Grenville province of Ontario : *Ph.D. Thesis*, Massachusetts Institute of Technology, Cambridge, Mass.

PINSON, W. H., HERZOG, L. F., FAIRBAIRN, H. W. AND CORMIER, R. F. (1958) Sr/Rb age study of tektites : *Geochim. et Cosmochim. Acta*, Vol. 14, pp. 331-339.

POWELL, J. L., HURLEY, P. M. AND FAIRBAIRN, H. W. (1962) Isotopic composition of strontium in carbonatites : *Nature*, Vol. 196, pp. 1085-1086.

POWELL, J. L., HURLEY, P. M. AND FAIRBAIRN, H. W. (1965a) The strontium isotopic composition and origin of carbonatites : In *The Carbonatites*, O. F. Tuttle and J. Gittins, editors. Wiley-Interscience, New York (in press).

POWELL, J. L., FAURE, G. AND HURLEY, P. M. (1965b) Strontium 87 abundance in a suite of Hawaiian volcanic rocks of varying silica content : *J. Geophys. Res.* Vol. 70.

POWELL, J. L. (1965a) Isotopic composition of strontium in four carbonate vein-dikes. *Am. Mineral.*, Vol. 50, pp. 1921-1928.

——— (1965b) Isotopic composition of strontium in carbonate rocks from Keshya and Mkwisi, N. Rhodesia : *Nature* (in press).

——— (1965c) Low abundance of Sr^{87} in Ontario carbonatites : *Am. Mineral.*, Vol. 50, pp. 1075-1079.

DISCUSSION

J. Gittins (University of Toronto, Canada) : The Sr isotope method of distinguishing carbonatites from sedimentary limestones depends on the assumption that a limestone if melted under magmatic conditions would not equilibrate with the surrounding magma. The attempt made to prove this assumption by studying a limestone xenolith from the Mount Royal essexite has certain weaknesses : the xenolith was only mildly recrystallized and must have remained essentially solid during its immersion in the magma.

An attempt has been made at Toronto to study the effect on sedimentary limestone of extreme metamorphism and metasomatism of the type that might be expected when limestone is melted by incorporation in magma. Three results follow :

1. White, medium-grained Grenville marble with minor phlogopite and graphite : 0.707
2. Calcite from very coarse-grained calcite-fluorite-apatite-pyroxene rock in Grenville marble sequence : 0.705
3. Calcite from calcite-potash-feldspar-biotite-rock at contact between syenite and Grenville marble : 0.703

It does appear that when limestone is extensively metasomatized by a magma the Sr isotope composition of the calcite equilibrates with that of the magma.

I do not believe that carbonatites are remelted limestones but it seems doubtful if this can be proved by the Sr isotope composition.

Author's Reply: Dr. Gittins' comments and new analyses are welcome additions to this discussion. His statement that the limestone xenolith from Mt. Royal was " . . . only mildly recrystallized and must have remained essentially solid . . . " contradicts the conclusions of Clark (1952),* who states that in the Corporation quarry, Montreal, where the xenolith in question was collected, the Trenton limestone has been recrystallized and whitened due to the volatilization of hydrocarbons, and has been intensely crumpled and thoroughly plasticized. I contend that the fact that this small 18 x 24 inch xenolith, even though thoroughly heated, plasticized, and engulfed in a relatively strontium-rich magma, preserved the Sr^{87} abundance of its parent limestone, is evidence that migration of Sr^{87} in bodies of carbonate rocks the size of most carbonatites is negligible.

Dr. Gittins' statement that his group has made an attempt to " . . . study the effect on sedimentary limestone of extreme metamorphism and metasomatism . . . " and the description of the three specimens analyzed would seem to imply that these specimens all started with the same Sr^{87}/Sr^{86} ratios and that their ratios have subsequently been altered by metamorphism and/or metasomatism. There is, however, no evidence to support the view that these three specimens ever had identical Sr^{87}/Sr^{86} ratios. The authors referred to in Table 2 above have already reported values for the Sr^{87}/Sr^{86} ratio of Grenville marble which vary between 0.705 and 0.708. Gittins' new data for the two samples of Grenville marble merely confirm this variation. It is of interest to note that all the Sr^{87}/Sr^{86} ratios which have been reported for specimens of bonafide Grenville marble are distinctly higher than the ratios of all of the analyzed carbonatites from Ontario and Quebec.

It is difficult to interpret the third analysis listed by Gittins. The figure of $Sr^{87}/Sr^{86} = 0.703$ is almost exactly the mean value which I have obtained for carbonatites and related alkalic rocks. It seems possible that this calcite might be a primary part of the calcite-potash feldspar-biotite rock. Even if it is metasomatically altered Grenville marble, a minor amount of such calcite at the contact between an alkalic rock and a marble can hardly be compared with the much, much larger relative volumes of calcite in most carbonatite complexes.

Dr. Gittins does not describe the mechanism by which the Sr^{87} abundances of limestone xenoliths might be made equal to those of the surrounding magmas. In general, such a change might be caused either by isotopic fractionation or by diffusion or migration of one or more isotopes. Fractionation of the strontium isotopes could not be the mechanism of equilibration, however, since the effects of fractionation have been compensated for by normalizing all observed Sr^{87}/Sr^{86} ratios to a constant value of Sr^{86}/Sr^{88}.

The xenolith experiment referred to above provides evidence which indicates that migration of Sr^{87} in heated carbonate rocks is negligible. It should be kept in mind that the Sr^{87} in carbonate rocks is non-radiogenic and occupies calcium or strontium lattice positions. Therefore the only driving force which could cause Sr^{87} to preferentially migrate from a limestone xenolith into an adjacent magma would be its slightly higher concentration in the limestone. The difference between the Sr^{87}/Sr^{86} ratios of limestones, which might average around 0.708, and those of alkalic rocks, which might average around 0.703, is only 0.7 per cent. It remains to be shown that diffusion driven by such a small concentration difference could cause the Sr^{87}/Sr^{86} ratios of bodies of carbonate rocks the size of most carbonatites to become equal to those of the surrounding alkalic rocks.

Another important fact is that the Sr^{87}/Sr^{86} ratios of the 32 carbonatites listed in Table 1 are identical to each other within the precision of the analytical technique employed. To put this another way, none of the values listed in

* CLARK, T. H. (1952) Montreal area, Laval and Lachine map-areas. *Quebec Dept. Mines Geol. Rep.*, Vol. 46, pp. 108–109.

Table 1 differ significantly from the mean value. If these carbonatites are limestone xenoliths, in each case diffusion of Sr^{87} must have been so thorough as to make the difference between the Sr^{87}/Sr^{86} ratios of the xenolith and the alkalic magma below the limit of detection. Such complete equilibration seems highly unlikely.

In the light of this discussion, it seems fair to say that both the geologic evidence and the strontium isotopic evidence strongly support the conclusion that carbonatites are not mobilized limestone xenoliths. The strontium isotopic evidence in this case merely offers quantitative support to the already overwhelming geologic field evidence. It has never been stated that the strontium isotopic evidence "proved" this point.

MINERALOGICAL SOCIETY OF INDIA. IMA VOLUME, 1966
INTERNATIONAL MINERALOGICAL ASSOCIATION, PAPERS, FOURTH GENERAL MEETING

EXPERIMENTAL DATA BEARING ON THE PETROGENETIC LINKS BETWEEN KIMBERLITES AND CARBONATITES[1]

PETER J. WYLLIE[2]
Department of Geochemistry and Mineralogy, The Pennsylvania State University
University Park, Pennsylvania, U.S.A.

ABSTRACT

The genetic relationships among kimberlites, carbonatites, and associated alkaline igneous rocks are being investigated by phase equilibrium studies in a number of silicate-carbonate systems, with special emphasis on liquidus studies. The precipitation of calcite from melts in the system CaO-CO_2-H_2O at temperatures near 650°, through a wide pressure range, was regarded by Wyllie and Tuttle as experimental verification for the magmatic origin of carbonatites. Addition of silicates has yielded signicant results in the systems: CaO-SiO_2-CO_2-H_2O (J. L. Haas), CaO-MgO-SiO_2-CO_2-H_2O (G. W. Franz), albite-nepheline-$CaCO_3$-$Ca(OH)_2$-H_2O (D. H. Watkinson), and anorthite-albite-Na_2CO_3-H_2O (A. F. Koster van Groos). The heterogeneous phase relationships in these systems indicate that a variety of petrogenetic processes may be effective. There is a persistent thermal barrier on the liquidus of several systems which suggests that normal peridotite magmas are incapable of yielding a residual lime-rich carbonatite magma by fractional crystallization. However, there is evidence in other systems that crystallization of an alkaline magma may yield a residual carbonatite magma. Liquid immiscibility has been discovered between some silicate melts and sodium carbonate melts, adding support to the suggestion that carbonatite magmas may be derived as immiscible fractions from parent alkali peridotite magmas. This fact also provides support for the hypothesis that a primary alkali carbonatite magma could form and persist without significant contamination by silicates until conditions (pressure, temperature, or composition) were reached where the immiscibility relationship ceased to exist. Mineral assemblages in the systems studied are closely comparable with those in many carbonatite complexes. The wide distribution of melilite is notable.

INTRODUCTION

The field evidence that many carbonatites are intrusive and possibly magmatic was incompatible with available experimental data until Wyllie and Tuttle (1960) demonstrated that liquids in the system CaO-CO_2-H_2O precipitate calcite at temperatures down to 640°C through a wide pressure range. Liquids in this system were described as "synthetic carbonatite magmas". Neither the experimental data nor the field and petrographic studies provide reliable estimates of the compositions of natural carbonatite magmas at their time of intrusion. This is clear from the variety of hypotheses to be found in the geological literature. The composition and physical characteristics of a carbonatite magma must depend upon the processes involved in its formation. Systems more complex than CaO-CO_2-H_2O have been investigated in efforts to elucidate two problems: the physical and chemical nature of carbonatite magmas, and the origin of carbonatite magmas. The first problem has been discussed by Wyllie and Biggar (1965), and the present paper deals with the second problem. It outlines an experimental program that is designed to test the various hypotheses of origin which have been proposed on the basis of petrological studies and inferences. Although the experiments are concerned with melts, it is recognized that even if some carbonatites are emplaced as magmas, it does not follow that all carbonatites are magmatic.

Hypotheses for the origin of carbonatite magmas

The origin of carbonatites has been discussed in some detail in several reviews (Pecora, 1956; Smith, 1956; King and Sutherland, 1960; Tomkeieff, 1961; Kukharenko and Dontsova, 1964; King, 1965). The experimental results reviewed in this paper have bearing on three of the hypo-

[1] Contribution number 64-71 from the College of Mineral Industries.
[2] Present address: Department of Geophysical Sciences, The University of Chicago, Chicago 37, Illinois.

theses of origin that have been proposed for magmatic carbonatites on the basis of field and petrological investigations:

(1) Carbonatite magmas are residual melts derived by fractional crystallization of a "carbonated alkali peridotite magma". King and Sutherland (1960) have discussed the evidence for this view.

(2) Carbonatite magmas are primary, possibly extremely rich in alkali carbonates. Such a magma was proposed by von Eckermann (1948) as the parent magma for the alkalic rocks of the Alnö complex. Attention has been focussed on this hypothesis by the recent eruption in Tanganyika which produced a lava *flow* composed almost entirely of carbonates of sodium and calcium (Dawson, 1962).

(3) Carbonatite magmas are derived as immiscible liquid fractions from a kimberlite or melilite-basalt parent magma (von Eckermann, 1961). There has been an increasing awareness in recent years of possible genetic connections between kimberlites and carbonatites (von Eckermann, 1948, 1958; Dawson, 1960, 1962, 1964; Garson, 1961; Davidson, 1964).

Experimental approaches

Three approaches have been adopted in the investigation of the phase relationships in systems more complex than CaO-CO_2-H_2O. The first is to study the phase relationships in a series of quaternary systems where one component has been added to the ternary system. Results obtained in systems with MgO and P_2O_5, respectively, as the fourth component provide some insight into differentiation processes in carbonatite magmas (Biggar, 1962; Wyllie, 1965; Wyllie and Biggar, 1965). The system with SiO_2 as the fourth component is the simplest system combining silicate minerals and carbonates (Haas and Wyllie 1963; Wyllie and Haas, 1965).

The second approach is to add to the ternary system silicate minerals such as feldspars, nepheline, pyroxenes, and olivine. These systems contain five or six components and it is therefore impossible to follow paths of crystallization even under isothermal isobaric conditions. However, useful information can be determined directly from the phase fields intersected by selected composition joins through the systems.

The third approach is to start with silicate "mineral components" and to add to these an excess of alkalis in the form of carbonates. Experimental determination of the phase fields intersected by joins through the tetrahedron $CaAl_2Si_2O_8$–$NaAlSi_3O_8$–Na_2CO_3–H_2O provides information about the relationships between a silicate magma and a hypothetical alkali carbonate magma.

Abbreviations used for the phases encountered in the various systems discussed are summarized in Table 1.

TABLE 1

Abbreviations used for phases in figures and text

V	Vapor	C_2S	Ca_2SiO_4	En	Enstatite
L	Liquid	C_3S	Ca_3SiO_5	Fo	Forsterite
CC	Calcite	Sp	Spurrite	Ab	Albite
CH	Portlandite	Ch	Calciochondrodite	An	Anorthite
MH	Brucite	Di	Diopside	Ne	Nepheline
P	Periclase	Ak	Akermanite	NC	Na_2CO_3
QZ (Q)	Quartz	Me	Melilite	No	Noselite
Wo	Wollastonite	Mo	Monticellite	Can	Cancrinite
Ra	Rankinite	T	Tridymite	Co	Corundum
Carng	Carnegeite	Cr	Cristobalite	Mu	Mullite

THE SYSTEM CaO-SiO_2-CO_2-H_2O

This is the simplest system combining the "synthetic carbonatite magmas" and silicate melts, and the phase relationships provide a basis for interpretation of the more complex systems. Phase relationships at liquidus temperatures in the presence of excess vapor have been determined at a pressure of 1 kilobar (Haas and Wyllie, 1963; Wyllie and Haas, 1965).

The Vapor-Saturated Liquidus Surface

Fig. 1 is a schematic diagram showing the position of the vapor-saturated liquidus surface, ABCD, which gives the compositions of liquids coexisting with a crystalline phase and with a vapor phase on the vaporus surface extending

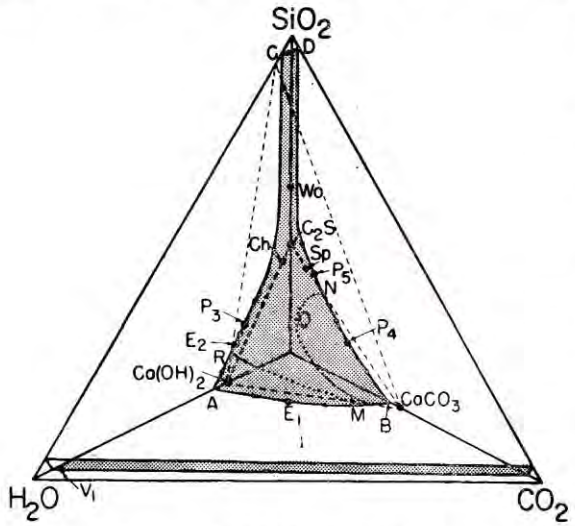

Fig. 1. The system CaO-SiO_2-CO_2-H_2O. For abbreviations see Table 1. A schematic isobaric tetrahedran for 1 kilobar pressure. The large shaded area represents the vapor-saturated liquidus surface, and the small area represents the vaporous surface.

between CO_2 and H_2O. The vaporus surface will be treated as the line CO_2–H_2O in subsequent discussions, because the vapor phase at 1 kilobar pressure contains only a small proportion of dissolved solids. The vapor-saturated liquidus surface lies close to the composition plane Ca_2SiO_4–$CaCo_3$–$Ca(OH)_2$, and intersects it along the line MON. Crystalline phases encountered in the portion of the system studied all lie on this composition plane; they are dicalcium silicate, spurrite, calciochondrodite, calcite, and portlandite. Phase relationships on the lower part of the liquidus surface are therefore almost ternary, and it is convenient to project the liquidus surface on to the composition plane. The results are shown in Fig. 2. Hydrous phases other than portlandite and calciochondrodite were not encountered in this study, but from the available data (Roy, 1958) it seems possible that phase Y (Dellaite) in the system CaO-SiO_2-H_2O might have a stability field as a primary phase on the liquidus at 1 kilobar pressure.

Extending from the ternary eutectics and peritectics E_1, E_2, P_3, P_4, and P_5, whose positions are shown schematically in Fig. 1 and in projection in Fig. 2, there are quaternary liquidus field boundaries giving the compositions of liquids coexisting with two crystalline phases and a vapor phase. These meet in the quaternary peritectics and eutectic P_8, P_7, and E_6, represented in projection in Fig. 2. The ternary eutectic liquid E_1 coexists with the vapor V_1 (Fig. 1), which contains only a very small proportion of CO_2. It can be shown on theoretical grounds, although it was not proven experimentally, that the vapors coexisting with the quaternary peritectic and eutectic liquids also have compositions close to V_1.

From the results shown in Fig. 2, and from what is known of the bounding binary and ternary systems, it is possible to deduce the phase relationships for the whole system. The result is shown in Fig. 3, which is somewhat distorted in order to show the isobaric liquidus field boundaries at 1 kilobar pressure. Fig. 2 is a key to the primary phase volumes in the lower part of Fig. 3. The phase relationships above the composition Ca_2SiO_4 are reasonable estimates based on known experimental data for the systems CaO-SiO_2 and SiO_2-H_2O. It is assumed that the two-liquid field does not reach the vapor-saturated liquidus surface. This is probably true for the system CaO-SiO_2-H_2O, but possibly not for the system CaO-SiO_2-CO_2.

The small liquidus fields for rankinite and for tricalcium silicate are omitted for simplicity.

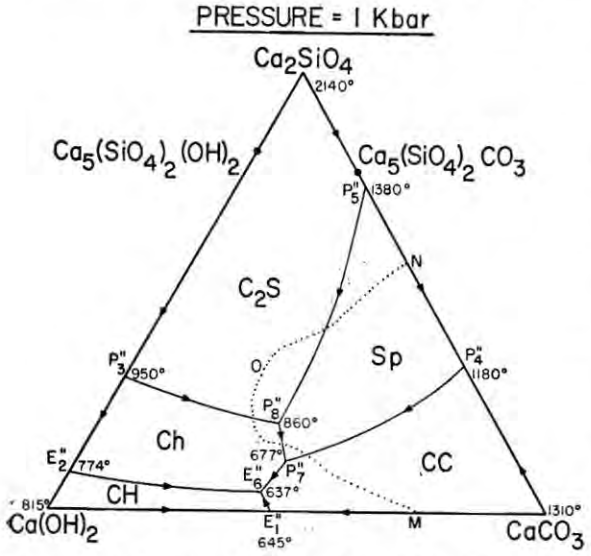

Fig. 2. The system CaO-SiO_2-CO_2-H_2O. For abbreviations see Table 1. Liquidus field boundaries and primary phase fields for 1 kilobar pressure projected from the vapor-saturated liquidus surface (Figure 1) on to the plane Ca_2SiO_4-$CaCO_3$-$Ca(OH)_2$.

The plane Ca_2SiO_4-CO_2-H_2O intersects the vapor-saturated liquidus surface in the line XY, which is a temperature maximum corresponding to the melting of Ca_2SiO_4 in the presence of a vapor phase. Silicate liquids with compositions above this thermal divide yield on crystallization only silicate minerals and vapors, whereas liquids with compositions below this line yield a residual melt corresponding to the synthetic carbonatite magma. At temperatures below 860°C at 1 kilobar pressure the residual liquid precipitates spurrite, calciochondrodite, calcite, and portlandite, as illustrated in Fig. 2.

It is of interest to note that although there is a large field for spurrite on the liquidus, extending down to temperatures of 677°C at 1 kilobar pressure, wollastonite has no stability field on the liquidus below the thermal divide XY in Fig. 3, despite the fact that wollastonite is normally regarded as a low temperature mineral compared to spurrite in carbonate dissociation sequences. However, it can be shown that at higher pressures wollastonite does appear on the low temperature liquidus between the fields for spurrite and calcite. In order to illustrate how dissociation reactions become involved with liquidus reactions it is necessary to use a diagram showing the vapor phase compositions. The petrogenetic model (Wyllie, 1962) has proved useful for this purpose.

Composition of Vapors: The Petrogenetic Model

Fig. 4 is an isobaric section through the petrogenetic model for the system at 1 kilobar pressure, showing divariant curves for one liquidus and for one sub-solidus reaction. The upper curve extending to the ternary eutectic E_1 was measured experimentally by Wyllie and Tuttle (1960, Fig. 10B), and it gives the compositions of the vapor phase in equilibrium with liquids on the field boundary BE_1 in Fig. 3. The lower curve was calculated using the available data for the formation of spurrite from calcite and wollastonite in the presence of Co_2 (Harker and Tuttle, 1957). Greenwood (1962) discussed similar curves in thermodynamic

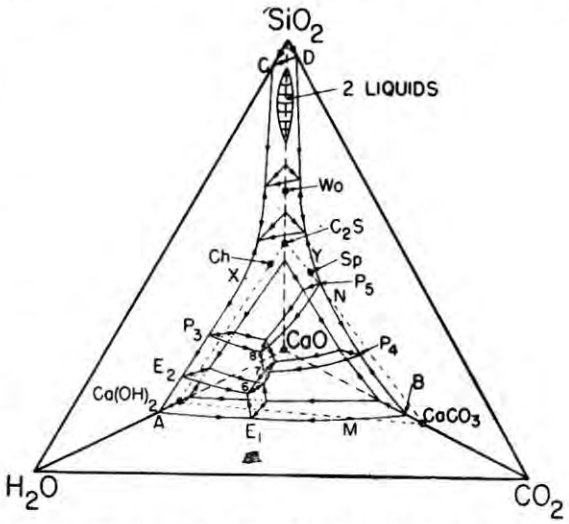

Fig. 3. The system CaO-SiO_2-CO_2-H_2O. For abbreviations see Table 1. Schematic liquidus field boundaries and primary phase volumes at 1 kilabar pressure. Compare Figure 2. The dotted line XY represents the intersection of the vapor-saturated liquidus surface with the plane C_2S-CO_2-H_2O. This is a thermal barrier on the liquidus.

terms. The possible intervention of a narrow stability zone for tilleyite has been ignored in the present discussion (Harker, 1959). This diagram shows that although wollastonite is stable in the presence of CO_2 to temperatures well above the eutectic E_1, its upper stability temperature limit lies below E_1 when the assemblage involves an aqueous vapor phase. Thus,

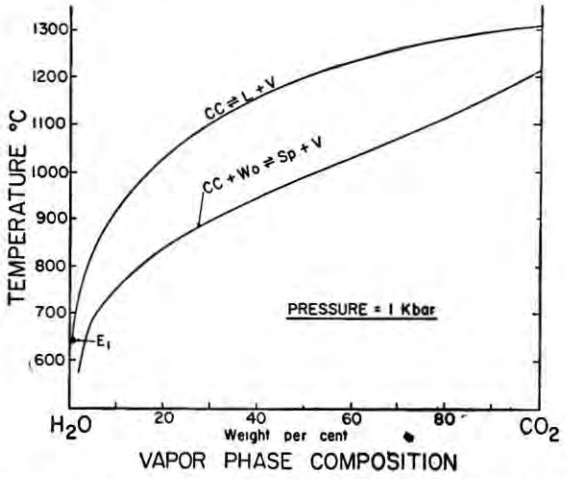

Fig. 4. The system CaO–SiO_2–CO_2–H_2O. For abbreviations see Table 1. Isobaric section through the petrogenetic model at 1 kilobar pressure. The upper reaction curve gives the experimentally located position of the ternary field boundary BE_1 in Figure 3. The lower reaction curve shows the calculated position of a quaternary subsolidus reaction. This figure shows the proper scale for the schematic Figures 5 and 6 which follow.

the low temperature assemblage is not stable on the liquidus of the system at this pressure, whereas the high temperature assemblage, spurrite + vapor, is stable with the liquids. With increasing pressure, however, the dissociation reaction moves upwards through the section until it intersects the liquidus curves producing a stability field for wollastonite on the liquidus.

Details of the liquidus and sub-solidus relationships in the petrogenetic model are shown in Figs. 5 (liquidus) and 6 (sub-solidus). These figures are schematic, being distorted near the H_2O composition in order to show the various reaction curves. The true scale is indicated by the curves in Fig. 4. The lettering of the peritectics and eutectics corresponds to the lettering in Figs. 1, 2, and 3. The sub-solidus assemblages in Fig. 6 are of two types. From each peritectic or eutectic on the vapor-saturated liquidus surface, one sub-solidus assemblage (including a vapor phase) extends to lower temperatures, and these are intersected by the curves for dissocia-

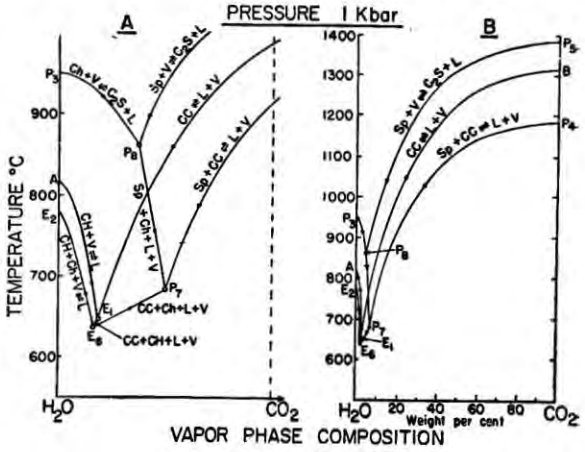

Fig. 5. The system CaO–SiO_2–CO_2–H_2O. For abbreviations see Table 1. Schematic isobaric section through the petrogenetic model at 1 kilobar pressure showing liquidus relationships. Lettering corresponds to that in Figure 2. For correct scale see Figure 4. *A* is an enlarged version of the relationships near H_2O in *B*.

tion reactions: decarbonation reaction curves extending from the CO_2 axis, and dehydration reaction curves extending from the H_2O axis. The more important of these dissociation reactions are shown schematically, and the points of intersection, S_1 and S_2, represent univariant assemblages. The temperatures of S_1 and S_2 are not known.

The effect of increasing pressure on these reactions has been discussed by Wyllie and Haas (1966). With increasing pressure the temperatures of the liquidus reactions decrease slightly, whereas the temperatures of dissociation reactions increase appreciably. The univariant reactions S_1 and S_2 in Fig. 6 therefore move upwards towards P_8 and P_7. At the pressure where S_2 reaches P_7, an invariant point is formed marking the coexistence of six phases Wo + CC + Sp

+ Ch + L + V. Wyllie and Haas (1966) illustrated the univariant reaction curves extending from this point, and these include univariant reaction curves P_9, P_{10}, and P_{11} extending to pressures above the invariant point which include wollastonite and liquid among the

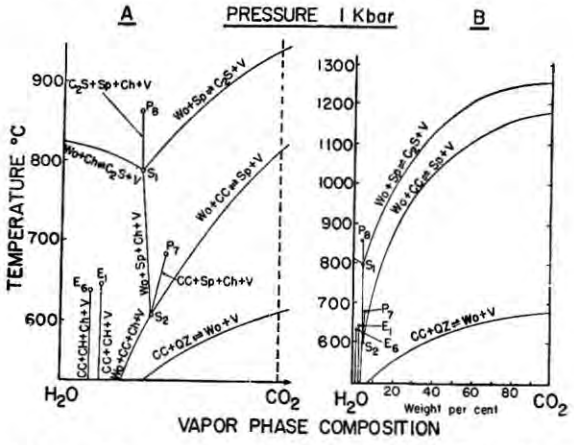

Fig. 6. The system CaO-SiO_2-CO_2-H_2O. For abbreviations see Table 1. Schematic isobaric section through the petrogenetic model at 1 kilobar pressure showing subsolidus relationships. Lettering and scale corresponds to that in Figure 5.

equilibrium assemblage. Wollastonite thus has a stability field on the low temperature liquidus at pressures above this invariant point. This is illustrated in Fig. 7, which is a projection of the vapor-saturated liquidus surface similar to that of Fig. 2, only at a higher pressure.

Fig. 16 does not include all of the possible decarbonation reactions that may occur in this system at 1 kilobar pressure. For example, if tilleyite had been included in this diagram, a field for primary tilleyite should appear on the liquidus in Fig. 7, in the region of P_{11}, if tilleyite remained stable at the unknown higher pressure of Fig. 2.

Conclusions

The SiO_2 content of the eutectic liquid E_6 is about 1% by weight, and the Ca_2SiO_4 content is about 3%. Thus, it appears that silicate components are not very soluble in the low temperature "synthetic carbonatite magmas" with compositions near the join $CaCO_3$-$Ca(OH)_2$. Solution of 1% SiO_2 in the eutectic liquid E_1 depresses the melting temperature by 8° C (Figs. 2 and 3), and when more SiO_2 is added to the system, liquidus temperatures rise rapidly from E_6, with calciochondrodite and spurrite appea-

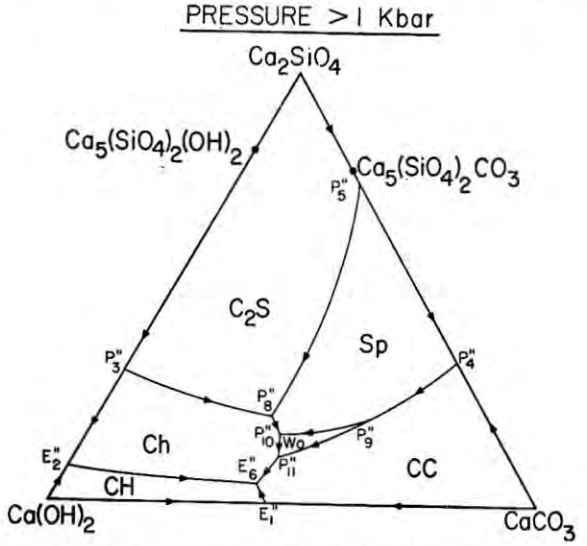

Fig. 7. The system CaO-SiO_2-CO_2-H_2O. For abbreviations see Table 1. Schematic liquidus field boundaries and primary phase fields for a high pressure projected from the vapor-saturated liquidus surface (Figure 1) on to the plane Ca_2SiO_4-$CaCO_3$-$Ca(OH)_2$. Compare Figure 2; an area for primary wollastonite has replaced the peritectic P_7.

ring as primary crystalline phases. These minerals have not been reported in carbonatites. The intervention of a wollastonite field between spurrite and calcite at higher pressures (Fig. 7) is therefore of interest, because many carbonatites do contain a pyroxene, and the occurrence of wollastonite in a simple synthetic system may indicate the occurrence of pyroxene in a similar position in a more complex system (cf. King, 1965, p. 78).

This system is too simple to provide a useful model illustrating possible relationships between alkalic igneous rocks and carbonatites, but one feature of the phase relationships is significant. Liquids with compositions above the plane XY-Ca_2SiO_4 (Fig. 3) can yield only

silicate phases and vapors on crystallization, whereas liquids below this plane follow crystallization paths leading to the low temperature liquids precipitating hydrated and carbonated phases. With fractional crystallization, these liquids would reach the eutectic E_6 or its vapor-absent equivalent next to the CaO volume. If this relationship persists in more complex systems, and the magnitude of the temperature maximum along XY suggests that it would, then it may be concluded that residual carbonatite magmas could be produced only from silica-undersaturated magmas, with the minimum level of silica-undersaturation required being given by the ratio $SiO_2/CaO = 1/2$.

The high temperature silicate melts are separated from the low temperature "carbonatite" melts by a pronounced thermal barrier (XY). According to Fig. 3, the silicate minerals precipitated from the high temperature melts do not coexist with the carbonated and hydrated crystalline phases. However, Fig. 7 shows that under appropriate conditions, wollastonite, a "high temperature" silicate mineral, can be precipitated from a low temperature melt alongside calcite.

THE SYSTEM CaO–MgO–SiO_2–CO_2–H_2O

Addition of MgO to the system just described introduces several other silicate minerals that are found in carbonatites and associated igneous rocks, as well as providing liquids with composition approaching those of the ultrabasic magmas that have been proposed as the parents of these rocks. The system also contains several minerals occurring in kimberlites. Franz (1965) has recently completed a doctoral thesis dealing with the melting relationships in this system; only a brief account of his results is given following the preliminary account of results in the system CaO-MgO-SiO_2-H_2O.

CaO–MgO–SiO_2–H_2O

Fig. 8 shows the compositions of the minerals occurring in this system, and the positions of the two compositions joins investigated (the heavy lines) at 1 kilobar pressure by Franz and Wyllie (1963). Fig. 9 shows schematically the positions of the liquidus field boundaries in the ternary systems which include H_2O as a component. The field boundaries for CaO-SiO_2-H_2O are taken from Fig. 3 and the field for rankinite has been included. Those for the system CaO-

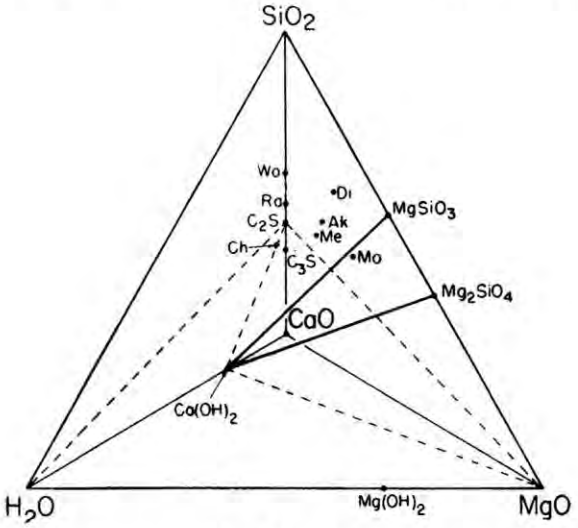

Fig. 8. The system CaO–MgO–SiO_2–H_2O. For abbreviations see Table 1. The two heavy lines are the composition joins studied. They intersect the dashed compatibility tetrahedron C_2S–MgO–$Ca(OH)_2$–H_2O.

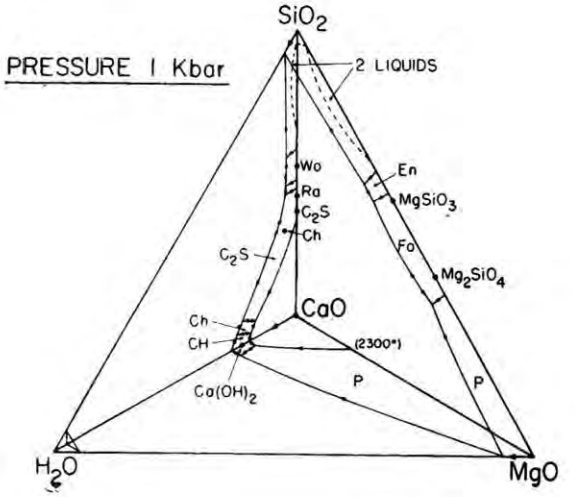

Fig.9. The system CaO–MgO–SiO_2–H_2O. For abbreviations see Table 1. Schematic liquidus field boundaries at 1 kilobar pressure for the ternary systems CaO-MgO-H_2O, CaO-SiO_2-H_2O (Figure 3), and MgO-SiO_2-H_2O.

MgO-H_2O are taken from Wyllie (1965). Those for MgO-SiO_2-H_2O are schematic, based on the reasonable assumption that H_2O under pressure dissolves in the liquids of the binary system MgO-SiO_2, depressing the liquidus temperatures but not affecting the phase relationships significantly. It is assumed that the two-liquid field disappears before the H_2O-saturated liquidus field boundary is reached. The H_2O-saturated liquidus field boundaries in Fig. 9 form the three edges of the H_2O-saturated vaporus surface for the quaternary system.

The primary phases and liquidus field boundaries on the H_2O-saturated liquidus surface are shown schematically in Fig. 10. The general arrangement of the phase fields on this

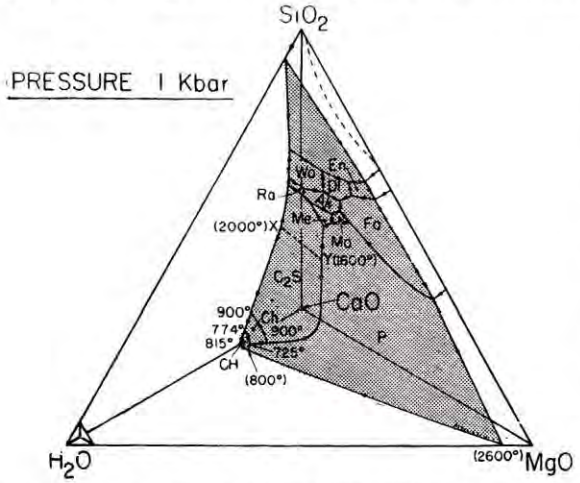

Fig. 10. The system CaO-MgO-SiO_2-H_2O. For abbreviations see Table 1. Schematic field boundaries and primary phase fields on the vapor-saturated liquidus surface (shaded : compare Figure 9) at 1 kilobar pressure. The phase relationships on the lower left part of the surface are distorted. Temperatures in parentheses are estimated. XY is part of a temperature maximum on the vapor-saturated liquidus surface corresponding to the line of intersection of the surface with the plane Ca_2SiO_4-MgO-H_2O.

surface is similar to that for the dry system CaO-MgO-SiO_2. A small percentage of H_2O dissolves in the liquids of the dry system, depressing the liquidus temperatures but probably causing few significant changes in the phase relationships except towards the portlandite corner of the surface. It can be seen in Fig. 9 that the primary phase volume for CaO is screened from the H_2O-saturated surface by primary phase volumes for periclase, portlandite, calciochondrodite, and dicalcium silicate. The temperatures of the peritectic at 900°C and the eutectic at 725°C in Fig. 10 were measured by Franz and Wyllie (1963). The temperatures in parentheses are estimated. Franz (1965) has revised these temperatures to 875°C and 725°C, and estimated the compositions of the peritectic liquid as 62.1% $Ca(OH)_2$, 25.6% Ca_2SiO_4, 11.3% MgO, and 1% H_2O by weight, and of the eutectic liquid as 92.7% $Ca(OH)_2$, 4.3% Ca_2SiO_4, 2.5% MgO, and 0.5% H_2O.

The plane MgO–C_2S–H_2O forms one side of the dashed compatibility tetrahedron in Fig. 8, and this plane intersects the H_2O-saturated surface along a line, part of which is the dashed line XY in Fig. 10. This line is a temperature maximum on the liquidus, corresponding to the temperature maximum along C_2S–MgO in the dry system, and it acts as a thermal barrier. Liquids with original compositions above XY (extended towards MgO) cannot yield low temperature residual liquids precipitating the hydrated phases.

CaO–MgO–SiO_2–CO_2

From what is known of the systems CaO–SiO_2–CO_2–H_2O (Figs. 2 and 3), and CaO–MgO–CO_2 (Wyllie, 1965) it can be concluded that the CO_2-saturated liquidus surface for the system CaO–MgO–SiO_2–CO_2 would be similar to that for the hydrous system in Fig. 10, with less vapor dissolved in the liquids, possibly with part or all of the two-liquid field extending to the CO_2-saturated surface, with higher liquidus temperatures, and, most important, with a primary phase field for calcite replacing the portlandite field, and with a more extensive primary phase field for spurrite replacing the calciochondrodite field. Additional phase fields may also be involved. A compatibility tetrahedron corresponding to that illustrated in Fig. 7 would still be present, and the temperature maximum

corresponding to XY (extended towards MgO) would also persist as a thermal barrier. Liquids with original compositions above XY would therefore be unable to produce residual liquids capable of precipitating the carbonated phases.

CaO–MgO–SiO_2–CO_2–H_2O

Fig. 10 can also serve as a model for the five-component system CaO–MgO–SiO_2–CO_2–H_2O at 1 kilobar pressure, with the two volatiles CO_2 and H_2O represented by the same corner of the tetrahedron. The general arrangement of the silicate phase fields on the vapor-saturated liquidus surface (surface similar to the shaded surface above XY in Fig. 10, with the liquids containing dissolved CO_2 and H_2O, and coexisting with a vapor phase whose composition varies between H_2O and CO_2) would be similar to that shown in Fig. 10. However, the situation becomes more complex for liquids below XY, because the compositions of the primary phases change as the vapor composition changes from H_2O towards CO_2. The low temperature liquids correspond to synthetic carbonatite magmas. Near the compositions portlandite and calcite on the CaO–volatile join, the liquids would persist to lower temperatures than those indicated in Fig. 10, precipitating spurrite, calciochondrodite, calcite, and portlandite, as indicated in Fig. 2, with these phases coexisting with periclase, as indicated in Fig. 10. Brucite would appear instead of periclase when the liquidus temperature becomes less than about 630°C. Other phases would appear as a result of the additional decarbonation reactions occurring in this system.

In the system CaO–MgO–SiO_2–CO_2 there are several decarbonation reactions involving "high temperature" silicate minerals and the carbonated minerals spurrite and calcite. Consideration of the petrogenetic model indicates that the presence of H_2O in the vapor phase will cause the divariant dissociation reactions to become involved with the low temperature liquidus reactions, giving rise to the appearance of " high temperature " minerals such as forsterite, monticellite, pyroxenes, and akermanite on the low temperature liquidus equivalent to that below XY in Fig. 10, as well as on the high temperature liquidus above the thermal barrier (XY in Fig. 10). Franz (1965) has confirmed that at 1 kilobar pressure, melting begins in this system at 605°C as a result of the univariant reaction:

Calcite + brucite + portlandite + monticellite + vapor $\rightleftharpoons$ liquid. Forsterite becomes stable in equilibrium with the liquid at a reaction occurring at 895°C.

A temperature maximum equivalent to XY (extended towards MgO) would persist in the 5-component system (see Fig. 3 for CaO–SiO_2–CO_2–H_2O, Fig. 10 for CaO–MgO–SiO_2-H_2O and for CaO–MgO–SiO_2–CO_2, with the differences noted above). This temperature maximum would act as a barrier separating the high temperature silicate liquids, corresponding to ultrabasic magmas, from the low temperature synthetic carbonatite magmas. At 1 kilobar pressure, original liquids in this system precipitating minerals such as olivine, pyroxene, monticellite and melilite (akermanite) could not yield residual liquids precipitating the carbonated and hydrated phases. However, some of these "high temperature" minerals may be precipitated alongside calcite from the low temperature synthetic carbonatite magma.

Effect of Pressure

The temperature maximum across the dicalcium silicate liquidus, corresponding to XY in Fig. 10, is a very prominent feature. It is unlikely that even very high pressures, in the presence of volatile components, could be effective in destroying this thermal barrier. It has been shown that at higher pressures in the system CaO–MgO–CO_2–H_2O dolomite should appear as an additional mineral stable on the synthetic carbonatite liquidus (Wyllie, 1965). Similarly, at higher pressures in the system CaO–SiO_2–CO_2–H_2O, wollastonite becomes stable on the synthetic carbonatite liquidus (Fig. 7). Thus, at higher pressures, dolomite and wollastonite could appear on the low temperature

liquidus in the five-component system. Other silicate minerals could appear in similar positions as a result of changes in the relative positions of decarbonation reactions and liquidus reactions in the petrogenetic model, as previously shown for wollastonite. The possibilities even in this five-component system are many. The results obtained by Franz (1965) indicate that at quite low pressures (2 to 3 kilobars) forsterite should replace monticellite in the equation given above for the beginning of melting in the system.

Conclusions

The above considerations lead to the conclusion that at 1 kilobar pressure and, indeed, through a wide range of pressures, high temperature silicate melts precipitating originally minerals such as olivine, pyroxene, melilite, and monticellite are incapable of yielding low temperature residual melts which precipitate carbonated and hydrated phases. On the basis of this evidence, therefore, it appears to be unlikely that a carbonated peridotite magma could yield a carbonatite magma by crystallization differentiation. However, the parent magma envisaged by proponents of this hypothesis is a carbonated alkali peridotite magma, and as shown in the next section, the addition of mineral components such as nepheline *may* provide alternative crystallization paths which by-pass the thermal barrier and lead to low temperature liquids.

The presence of calcite in many ultramafic igneous rocks has been generally attributed to late stage alteration. However, it now appears possible for mineral assemblages involving olivine, pyroxene, monticellite, melilite, and calcite to be precipitated simultaneously from magmas at low to moderate temperatures (in the range 600°C to 800°C). These results suggest that some carbonate minerals in ultramafic rocks may be primary rather than secondary, and this suggestion may be particularly applicable to some kimberlites.

ALBITE–NEPHELINE–$CaCO_3$–$Ca(OH)_2$–H_2O

Fig. 11 is a composition tetrahedron for the system CaO–Na_2O–Al_2O_3–SiO_2, which contains a representative of the basic oxides (CaO) and the alkalis (Na_2O). In order to bring the system into reasonable conformity with carbonatite compositions it is necessary to add CO_2 and H_2O as components, and a six-component system is difficult to handle, both theoretically and experimentally. One way to tackle such a system is to consider the phase relationships in the four-component system illustrated " in the presence of CO_2 and H_2O under pressure ". Another way is to plot empirically the phase fields intersected by the composition joins selected for study; usually, the compositions of vapors, liquids, and many of the crystalline phases encountered do not lie on this join at all.

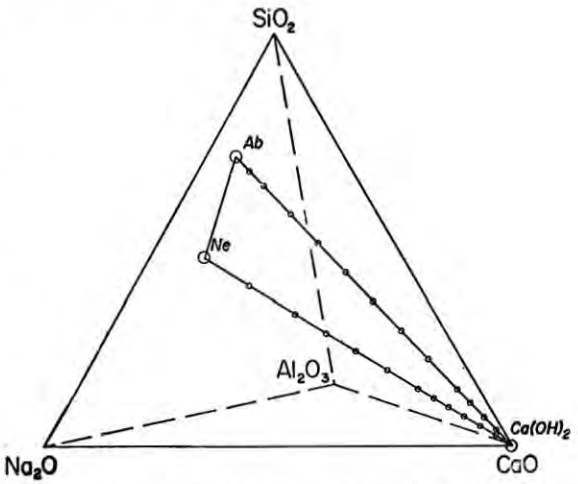

Fig. 11. The system CaO–Na_2O–Al_2O_3–SiO_2–H_2O. For abbreviations see Table 1. The composition joins Ab-$Ca(OH)_2$ and Ne-$Ca(OH)_2$.

Results obtained in two joins in Fig. 11 ($NaAlSi_3O_8$(Ab)–$Ca(OH)_2$–H_2O and $NaAlSiO_4$ (Ne)–$Ca(OH)_2$–H_2O) have been presented orally (Watkinson and Wyllie, 1963), and Watkinson (1965) recently completed a detailed experimental study of these joins with calcite added for his doctoral thesis.

From Watkinson's results it appears that original liquids precipitating plagioclase feldspar cannot yield residual synthetic carbonatite magmas because there is a thermal barrier extending across the field for the primary crystalliza-

tion of dicalcium silicate similar to those described for simpler systems (Figs. 3 and 10). However, the phase fields intersected by the composition join nepheline–$CaCO_3$–$Ca(OH)_2$–H_2O indicate that a nepheline–rich melt can yield a residual synthetic carbonatite magma precipitating calcite. During fractional crystallization in this system, there is evidence that soda is displaced from the residual melt into the coexisting vapor phase. This vapor phase in nature would be a most effective fenitizing agent. There is also evidence from the experiments indicating that fractional crystallization of a nepheline–rich melt with coexisting vapor would eventually lead to a stage where the remaining melt and vapor phases exhibited continuous solubility (or critical phenomena), becoming a single, homogeneous fluid phase. If this is confirmed, it suggests that fractional crystallization of a nephelinitic magma could yield a carbonatite magma which after further crystallization would be transformed continuously into a soda–rich hydrothermal or "carbothermal" solution.

The melilite occurring in this system is soda-rich, as indicated by refractive index measurements. The melilite is stable only above a univariant reaction curve which passes through 625°C at 1 kilobar pressure, and higher temperatures with increasing pressure. The reaction is a complex one, involving the breakdown of melilite and the formation of a hydrogarnet. The equivalent reaction in nature would involve the formation of a garnet from melilite.

The sequence of minerals precipitated during fractional crystallization of nepheline-rich melts in the nepheline composition join is similar to the parageneses occurring at some carbonatite complexes. The very wide range of compositions where melilite coexists with liquid and other crystalline phases is notable, and the similarity is most striking for those carbonatite complexes where melilite is developed. Watkinson (1965) considered the fractional crystallization of a liquid with the composition 90% nepheline and 10% calcite, saturated with H_2O vapor (with 25% H_2O added to the charge) at 1 kilobar pressure. From his experimental results, the sequence of mineral assemblages that would develop are: nepheline (1105-1070°C), nepheline + melilite (1070–950°C), melilite + noselite (950–875°C), melilite + cancrinite (875–800°C), and calcite + melilite + cancrinite (800 to less than 650°C). He compared these mineral assemblages with some of the parageneses at the Oka carbonatite complex (Gold, 1963): the nepheline-pyroxene rocks (jacupirangite, ijolite, urtite), nepheline okaite (nepheline and melilite), okaite (hauyne and melilite), and finally the calc-silicate carbonatite with melilite and calcite.

THE SYSTEM CaO–Na_2O–Al_2O_3–SiO_2–CO_2–H_2O

The effect of excess alkalis on the phase relationships in silicate-carbonate systems is being investigated by studying the phase fields intersected by composition joins through the system CaO–Na_2O–Al_2O_3–SiO_2 (Fig. 11) in the presence of CO_2 and H_2O under pressure. The CO_2 has been added as the "mineral component" Na_2CO_3, and various percentages of H_2O have been added to mixtures on the join NaAlSi_3O_8(Ab)–$CaAl_2Si_2O_8$(An)–Na_2CO_3. Preliminary results have been presented orally (Koster van Groos and Wyllie, 1963A), and a brief note has been published (Koster van Groos and Wyllie, 1963B). A wide miscibility gap was recognized in this system between the silicate liquid and the carbonate liquid. Because of the complexity of the system, the initial exploratory work was followed by investigation of the anhydrous system Na_2O–Al_2O_3–SiO_2–CO_2.

Albite–Na_2CO_3–CO_2–H_2O

Fig. 12 shows the results obtained in the anhydrous join at 1 kilobar pressure, in the presence of excess CO_2. A trace of a mineral with the noselite structure (No) was present in most runs, but this is regarded as a non-equilibrium phase. Under these conditions, it is not expected that much excess CO_2 dissolves in the liquid phases, and the compositions of each of the immiscible liquids is believed to be repre-

sented approximately by the horizontal axis. This agrees reasonably well with results published for the join albite-Na_2CO_3 in the presence of excess H_2O. The temperature of the solidus could not be ascertained because without the coexistence of the carbonate melt (L_2), the silicate glass starting material refused to crystallize.

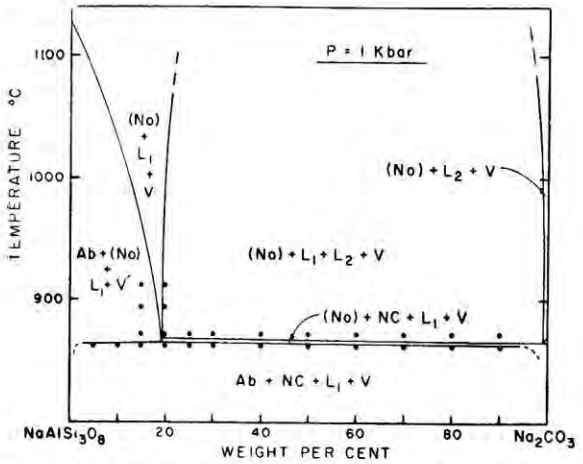

Fig. 12. The system Na_2O-Al_2O_3-SiO_2-CO_2. For abbreviations see Table 1. Phase fields intersected by the composition join $NaAlSi_3O_8$-Na_2CO_3 in the presence of excess CO_2 at 1 kilobar pressure. The join is shown in Figure 15. Compare the miscibility gaps in Figures 12 and 15.

In the composition join albite-Na_2CO_3-H_2O at 1 kilobar pressure, a similar miscibility gap occurs (Koster van Groos and Wyllie, 1963B) at temperatures above 750°C (Fig. 13). Charges quenched from the two-liquid field consist of mixtures of the silicate glass (L_1), and aggregates of sodium carbonate which crystallized from the carbonate liquid (L_2) during the quench. Partial separation of the two liquids on a gross scale is observed in most runs, and Fig. 14 illustrates the separation of the two liquids on a finer scale. This is a photomicrograph of crushed fragments in immersion oil, with the nicols crossed. The silicate glass is isotropic, but a large glassy fragment is outlined approximately by the distribution of birefringent specks which represent the original globules of carbonate-rich liquid in the silicate liquid. These have crystallized to fine-grained aggregates of sodium carbonate during the quench. Their spherical shape can be seen where their density is least, towards the thin edges of the glass fragment.

It is worth emphasizing the fact that the two liquids L_1 and L_2 in Fig. 13 are true melts. They coexist with a third fluid phase called here a

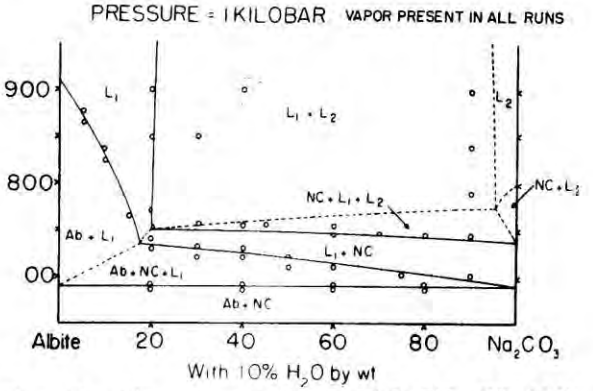

Fig. 13. The system Na_2O-Al_2O_3-SiO_2-CO_2-H_2O. For abbreviations see Table 1. Preliminary diagram showing the phase fields intersected at 1 kilobar pressure by the join Ab-Na_2CO_3 in the presence of 10 weight percent H_2O (see Figure 26). Cancrinite and noselite are also present in parts of the diagram.

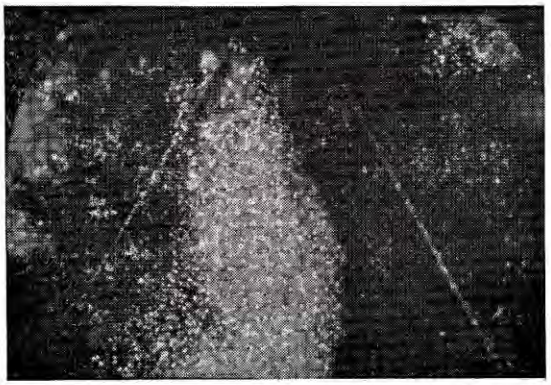

Fig. 14. The system Na_2O-Al_2O_3-SiO_2-CO_2-H_2O. Photomicrograph of immersion oil mount of a crushed charge from the field L_1+L_2 in Figure 13 (nicols crossed). The isotropic silicate glass is crowded with small spheres composed of sodium carbonate crystal aggregates.

vapor, which is a dense aqueous solution containing some CO_2, a small proportion of dissolved silicate and an unknown proportion of

dissolved sodium carbonate. In some parts of the system there may be continuous solubility relationships between a soda-rich liquid and the vapor phase, but in the pressure, temperature and composition range of the present investigation the existence of two liquid phases and a vapor phase appears to be well established. This points to the complexities of the phase relationships in natural carbonatite systems, where alkalis may play an important role.

The phase relationships intersected by the join illustrated in Fig. 13 are more complex than indicated, because a mineral with the cancrinite structure has a considerable range of stability across the diagram ; this is not significant in connection with the liquid immiscibility, however.

Plagioclase Feldspar–Na_2CO_3–H_2O

The phase fields intersected by joins of this type are very complex. With $Ab_{80}An_{20}$ in the presence of 10 weight % H_2O the two-liquid field is still intersected, although it is somewhat narrower, and the fields for the silicate liquid and the carbonate liquid are correspondingly wider. The solidus temperature at the silicate end of the diagram is hardly changed. Other phases which appear are a mineral with the noselite structure and wollastonite.

In their reference to preliminary data from this plagioclase join, Koster van Groos and Wyllie (1963B) reported that nepheline was one of the new phases produced. This has not been confirmed, but there is now evidence from the join $Ab_{50}An_{50}$–Na_2CO_3–H_2O that nepheline may have a stability field below the solidus.

Na_2O–Al_2O_3–SiO_2–CO_2

Fig. 15 shows schematically the position of the vapor-saturated liquidus surface in this system at a fairly high pressure. The composition joins albite–Na_2CO_3 and nepheline–Na_2CO_3 are shown. The shaded area on the vapor-saturated liquidus surface represents the quaternary volume of liquid immiscibility intersected here by the vapor-saturated liquidus surface. According to unpublished work on the composition join albite–Na_2CO_3 by Koster van Groos and Wyllie (see Fig. 12) this miscibility gap is intersected through a wide range of pressures. If the pressure is decreased, however, reactions occur in the system Na_2O–SiO_2–CO_2 causing the compatibility join Na_2CO_3–SiO_2 to be replaced by a series of joins connecting Na_2CO_3 with

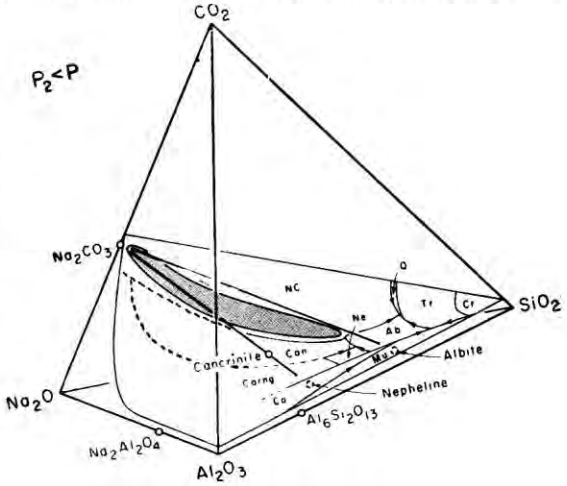

Fig. 15. The system Na_2O-Al_2O_3–SiO_2–CO_2. For abbreviations see Table 1. Schematic diagram for a pressure of about 1 kilobar showing the intersection of a liquid miscibility gap (shaded) by the vapor-saturated liquidus surface.

sodium silicates. This has the effect of lowering the position of the vapor-saturated liquidus surface in Fig. 15 in a series of steps, each step corresponding to one of the reactions, and the size of the miscibility gap intersected by the surface also decreases. At a fairly low total pressure, less than approximately 30 bars, the miscibility gap is not encountered at all by compositions on the join albite–Na_2CO_3. These reconnaissance results indicate that an originally homogeneous liquid in the system can be made to split into two immiscible liquid phases by increasing the pressure. In a more complex system, it is possible that the same effect may be achieved by increasing the partial pressure of CO_2.

Conclusions

Although much experimental work remains to be completed in this complex system, the

results obtained do draw attention to the possible role of liquid immiscibility in the genesis of carbonatites and associated igneous rocks. It is difficult to understand how a deep-seated primary magma composed largely of alkali carbonates could be generated in the mantle of the earth, and it is difficult to understand how such a magma could persist until it reached a high level in the earth's crust without the occurrence of almost complete reaction with the silicates of the crust. The lava flows composed essentially of carbonates of sodium and calcium erupted recently from Oldonyo Lengai in Tanganyika, whatever their origin, managed to reach the surface without becoming contaminated by silicates (Dawson, 1962). An immiscibility relationship between an alkali carbonate magma and the silicates is a possible explanation. Further experimental studies are required to test von Eckermann's (1961) proposal that carbonatite magmas represent an immiscible fraction from a melilite-basalt or kimberlite magma, but at least it has been established that liquid immiscibility does exist between silicate and carbonate melts.

The miscibility gap may be encountered as a result of changes in temperature, bulk composition (albite and plagioclase joins), partial pressure of H_2O (Figs. 12 and 13), total pressure in the anhydrous system(as discussed for Fig. 15), and possibly the partial pressure of CO_2. With this degree of variability, there are many processes which could lead to the intersection of a two-liquid field, or to the coalescence of two liquid phases.

SUMMARY AND CONCLUSIONS

Many of these conclusions are based on preliminary experimental data, and they serve only as working hypotheses. The experimental results will be extrapolated directly to natural occurrences by using the terms "silicate magmas" and "carbonatite magmas" instead of the correct terms "silicate liquids with compositions approaching those of silicate magmas", and "liquids with compositions approaching possible carbonatite magmas".

There is a persistent thermal barrier on the liquidus of the systems studied which suggests that only undersilicated liquids are capable of yielding a residual lime-rich carbonatite magma. Even peridotite magmas of the tholeiitic type would be too rich in silica to yield a residual carbonatite. However, a nepheline-rich silicate magma can produce a residual carbonatite magma by a process of fractional crystallization. An alkali peridotite magma may therefore be capable of yielding the same product. It is not known how much nepheline or alkali would need to be added to a system such as $CaO–MgO–SiO_2–CO_2–H_2O$ in order that it could yield a residual carbonatite magma, and therefore it is not known whether a kimberlite magma could yield a residual carbonatite magma. However, it has been established that two of the important "high temperature" minerals of a kimberlite, forsterite and monticellite, can coexist in equilibrium with a carbonatite magma at temperatures as low as 605°C. This suggests that the carbonates which occur in abundance in many kimberlites cannot safely be relegated to the role of secondary minerals, the product of late stage alteration. Immiscibility between silicate liquids and carbonate liquids has been established. The compositions of the liquids involved are not closely related to normal concepts of silicate magmas and carbonatite magmas, but the results do indicate that the separation of a derivative carbonatite magma as an immiscible liquid fraction from a parent peridotite or kimberlite magma is a possibility. It also provides some support for the hypothesis that a primary alkali carbonate magma could form and persist without significant contamination by silicates until conditions (composition, temperature, or pressure) were reached where the immiscibility relationship ceased to exist.

The conclusions thus provide support for each of the three hypotheses outlined in the Introduction: (1) Carbonatite magmas can be residual melts derived from a carbonated alkali peridotite magma, or from a nephelinite magma (King, 1965); (2) A primary alkali carbonate

magma could form and persist; (3) An immiscible carbonatite magma fraction could separate from a parent silicate magma under appropriate conditions.

One possible link between kimberlites and carbonatites is the confirmation that the carbonate minerals occurring in abundance in many kimberlites need not represent alteration products. Even if the carbonates do not represent precipitates from a carbonatite magma derivative from the kimberlite, they could represent precipitates from a carbonatite magma in equilibrium with the crystalline components of a kimberlite. If kimberlites are emplaced by a process of fluidization, these experiments suggest that the gases or "fluids" invoked by advocates of this hypothesis could be replaced by carbonatite magma. This would probably satisfy the physical requirements of the process, and it would provide a source for the carbonates occurring in kimberlites. The experimental demonstration that minerals such as monticellite and forsterite can be precipitated alongside calcite from a synthetic carbonatite magma confirms that the association is possible. These results support Daly's (1925) conclusion, based on field and petrographic studies, that the carbonate dikes in the kimberlite at the Premier diamond mine were magmatic in origin.

There is no reason to suppose that all carbonatites are formed by the same process, nor that all are magmatic. The experimental results obtained so far confirm that a variety of processes are possible, and that carbonatites could be developed in several ways.

ACKNOWLEDGEMENTS

This research was supported by the National Science Foundation, Grants G 19588 and GP-1870.

REFERENCES

BIGGAR, G. M. (1962) High pressure-high temperature phase equilibrium studies in the system CaO-CaF_2-P_2O_5-H_2O-CO_2 with special reference to the apatites: *Ph.D. thesis*, University of Leeds.

DALY, R. A. (1925) Carbonate dikes of the Premier Diamond Mine, Transvaal: *Jour. Geol.*, Vol. 33, pp. 659–84.

DAVIDSON, C. F. (1964) On diamantiferous diatremes: *Econ. Geol.*, Vol. 59, pp. 1368–1380.

DAWSON, J. B. (1960) A comparative study of the geology and petrography of the kimberlites of the Basutoland province: *Ph.D. thesis*, University of Leeds.

———(1962a) The geology of Oldoinyo Lengai: *Bull. Volcan.*, Vol. 24, pp. 349–387.

———(1962b) Basutoland kimberlites: *Bull. Geol. Soc. Amer.*, Vol. 73, pp. 545–560.

———(1964) Carbonate tuff cones in northern Tanganyika: *Geol. Mag.*, Vol. 101, pp. 129–137.

ECKERMANN, H. von (1948) The alkaline district of Alnö Island: *Sverig. Geol. Unders.* Ser. Ca, No. 36.

———(1958) The alkaline and carbonatitic dykes of the Alnö formation on the mainland northwest of Alnö Island: *Kungl. Svensk. Vetenskap., Handl.*, Fj. ser., Bd. 7, p. 61.

———(1961) The petrogenesis of the Alnö alkaline rocks: *Bull. Geol. Instit. Univ. Uppsala*, Vol. 40, pp. 25–36.

FRANZ, G. W. (1965) Melting relationships in the system CaO-MgO-SiO_2-CO_2-H_2O: a study of synthetic kimberlites: *Ph.D. thesis*, The Pennsylvania State University.

FRANZ, G. W. AND WYLLIE, P. J. (1963) Phase relationships in portions of the joins $MgSiO_4$-$Ca(OH)_2$ and $MgSiO_3$-$Ca(OH)_2$ at 1 kilobar pressure (abstract): *Geol. Soc. Amer.*, Spec. Paper, Vol. 76, pp. 62–53.

GARSON, M. S. (1961) The Tundulu carbonatite ring complex in southern Nyasaland: *Ph.D. thesis*, University of Leeds.

GOLD, D. P. (1963) The relationship between the limestone and the alkaline igneous rocks of Oka and St. Hilaire, Quebec: *Ph.D. thesis*, McGill University, Montreal.

GREENWOOD, H. J. (1962) Metamorphic reactions involving two volatile components: *Carnegie Inst. Washington Year Book*, Vol. 61, pp. 82–85.

HAAS, J. L. AND WYLLIE, P. J. (1963) The system CaO-SiO_2-CO_2-H_2O. 1. Melting relationships in the presence of excess vapor (abstract): *Trans. Amer. Geophys. Union*, Vol. 44, p. 117.

HARKER, R. I. (1959) The synthesis and stability of tilleyite, $Ca_5Si_2O_7(CO_3)_2$: *Amer. Jour. Sci.*, Vol. 257, pp. 656–567.

HARKER, R. I. AND TUTTLE, O. F. (1957) Synthesis of spurrite and the reaction wollastonite + calcite $\rightleftharpoons$ spurrite + carbon dioxide: *Amer. Jour. Sci.*, Vol. 255, pp. 226-234.

KING, B. C. (1965) Petrogenesis of the alkaline igneous rock suites of the volcanic and intrusive centres of Eastern Uganda: *Jour. Petr.*, Vol. 6, pp. 67-100.

KING, B. C. AND SUTHERLAND, D. S. (1960) Alkaline rocks of eastern and southern Africa, Parts I, II, and III: *Sci. Progress*, Vol. 48, pp. 298-321, 504-524, 709-720.

KOSTER van GROOS, A. F. AND WYLLIE, P. J. (1963a) The system $CaO-Na_2O-Al_2O_3-SiO_2-CO_2-H_2O$. II. The join $NaAlSi_3O_8-Na_2CO_3-H_2O$ (10 weight %) (Abstract): *Trans. Amer. Geophys. Union*, Vol. 44, pp. 117-118.

———(1963b) Experimental data bearing on the role of liquid immiscibility in the genesis of carbonatites: *Nature*, Vol. 199, pp. 801-802.

KUKHARENKO, A. A. AND DONTSOVA, E. I. (1964). A contribution to the problem of the genesis of carbonatites: *Econ. Geol.*, USSR, Vol. 1, pp. 31-46 (English translation).

PECORA, W. T. (1956) Carbonatites. a review: *Bull. Geol. Soc. Amer.*, Vol. 67, pp. 1537-1556.

ROY, D. M. (1958) Studies in the system $CaO-Al_2O_3-SiO_2-H_2O$, IV; phase equilibria in the high-lime portion of the system $CaO-SiO_2-H_2O$: *Am. Mineral.*, Vol. 43, pp. 1009-1028.

SMITH, W. CAMPBELL (1956) A review of some problems of African carbonatites: *Quart. Jour. Geol. Soc. Lond.*, Vol. 112, pp. 189-219.

TOMKEIEFF, S. I. (1961) Alkalic ultrabasic rocks and carbonatites in the U.S.S.R.: *Internat. Geol. Rev.*, Vol. 3, pp. 739-758.

WATKINSON, D. H. (1965) Melting relations in parts of the system $Na_2O-K_2O-CaO-Al_2O_3-SiO_2-CO_2-H_2O$ with applications to carbonate and alkalic rocks: *Ph.D. thesis*, The Pennsylvania State University.

WATKINSON, D. H. AND WYLLIE, P. J. (1963) The system $CaO-Na_2O-Al_2O_3-SiO_2-CO_2-H_2O$. I. The joins $NaAlSi_3O_8-Ca(OH)_2-H_2O$ and $NaAlSiO_4-Ca(OH)_2-H_2O$. (Abstract): *Trans. Amer. Geophys. Union*, Vol. 44, pp. 117-118.

WYLLIE, P. J. (1962) The petrogenetic model, an extension of Bowen's petrogenetic grid: *Geol. Mag.*, Vol. 99, pp. 558-569.

———(1965) Melting relationships in the system $CaO-MgO-CO_2-H_2O$, with petrological applications: *Jour. Petr.*, Vol. 6, pp. 101-123.

——— AND BIGGAR, G. M. (1966) Fractional crystallization in the "carbonatite systems" $CaO-MgO-CO_2-H_2O$ and $CaO-CaF_2-P_2O_5-CO_2-H_2O$: *Min. Soc. India.*, I.M.A. Volume.

——— AND HASS, J. L. (1965) The system $CaO-SiO_2-CO_2-H_2O$: I. Melting relationships with excess vapor at 1 kilobar pressure: *Geochim. Cosmochim. Acta*, (in press.)

——— AND HASS, J. L. (1966) The system $CaO-SiO_2-CO_2-HO_2$: II. The petrogenetic model: *Geochim. Cosmochim. Acta.*, (Manuscript to be submitted).

——— AND TUTTLE, O. F. (1960) The system $Cao-CO_2-H_2O$ and the origin of carbonatites: *Jour. Petr.*, Vol. 1, pp. 1-46.

MINERALOGICAL SOCIETY OF INDIA, IMA VOLUME, 1966
INTERNATIONAL MINERALOGICAL ASSOCIATION, PAPERS, FOURTH GENERAL MEETING

THE AVERAGE AND TYPICAL CHEMICAL COMPOSITION OF CARBONATITES

D. P. GOLD
Department of Geochemistry and Mineralogy, The Pennsylvania State University
University Park, Pennsylvania, U.S.A.

ABSTRACT

Some 200 odd analyses for major and minor constituents and a lesser number of trace element analyses, representing 55 carbonatite occurrences from 15 countries and 3 continents, are averaged to give " The average chemical composition of carbonatites." A weighted average, designated " The typical composition ", is derived by summing the average values of the individual carbonatite occurrences and dividing by the number of occurrences. The " typical " abundance figures, which are probably the more meaningful values, are as follows (in weight per cent) : SiO_2, 5.67 ; CO_2, 32.16 ; TiO_2, 0.50 ; Al_2O_3, 1.77 ; Fe_2O_3, 3.88 ; FeO, 3.71 ; MnO, 0.78 ; MgO, 6.10 ; CaO, 37.06 ; BaO, 0.45 ; SrO, 0.89 ; Na_2O, 1.09 ; K_2O, 0.87 ; P_2O_5, 1.73 ; F, 0.38 ; Cl, 0.31 ; S, 0.18 ; SO_3, 0.46 ; ΣRare-earth oxides, 0.59 ; H_2O+, 1.42 ; with trace amounts in parts per million as : Sc, 10 ; Co, 18.8 ; Ni, 32.4 ; Cr, 102 ; V, 105 ; Mo, 64 ; W, 5.9 ; Cu, 88 ; Pb, 27 ; Zn, 160 ; Sn, 2.5 ; Ga, 2.4 ; Y, 113.7 ; Zr, 461 ; Nb+Ta, 560 ; Ge, 3.3 ; Tl, 0 ; Li, 15 ; Cs, 0 ; Rb, 52 ; Th, 649 ; U, 57 ; Be, 5 ; B, tr ; Ag, 3.9 ; In, 0. These figures indicate a general impoverishment in sialic, and an enrichment in ' deep-seated ' constituents.

The available data on carbon, oxygen, strontium and magnesium isotopic composition of carbonatites and carbonate rocks of sedimentary origin are reviewed, and it is concluded that carbonatites could not be derived from sedimentary carbonate rocks.

INTRODUCTION

A scan of the literature yielded a total of some 200 complete and partial analyses for major and minor constituents, between 2 and 156 analyses of selected trace elements, of carbonate rocks and carbonated (or carbonatitized) kimberlitic rocks from carbonatite complexes and dikes, carbonatitic kimberlite and kimberlite dikes and pipes. These analyses represent some of the constituents of carbonate-rich rocks from 55 occurrences with carbonatitic affinities. Some complexes have been well sampled for selected elements, whereas for others only a few, or even only one partial analysis are available. That chemical analytical data (no matter how incomplete) are available from only 55 of some 150 carbonatitic occurrences recorded in the literature, shows how limited and selective is our knowledge of the geochemistry of carbonatites.

A strong geographic bias exists in the sampling data, with 41 of the 55 sampled carbonatite occurrences being located in East and Southern Africa. Generally, this group represents about one half of the total number of samples ; about 70 per cent of the remainder came from Scandinavia. A geographic bias is unavoidable as carbonatites tend to occur, singly or in clusters, along major lineaments ; their distribution apparently controlled by deep-seated fault zones.

SOURCES OF SAMPLES

The distribution, by country, of the occurrences referred to in this paper are :

Africa

Kivu–Lueshe.

Ruanda–Kibuye.

Uganda–Bukusu. Busumbu, Katwe, Kalyango, Lolekek, Lokupoi and Napak, Sukulu Hill, Tororo.

Kenya–Homo Bay, Mrima Hill, Rangwa, North Ruri, South Ruri, Tuige, Sokolo Point.

Tanzania (Tanganyika)–Igwisi Crater, Kerimasi, Mbeya (Panda), Oldoinyo L'engai, Oldoinyo Dili, Rukuku (Kiwurungi area), Sangu, Sangwe scarp, Ukisi, Wigu Hill.

TABLE 1

Average and typical abundances of major and minor constituents and some trace elements of carbonatites

	I	II	III	IV	V	VI	VII
Major and minor constituents in weight per cent							
SiO_2	9.58/206	9.14	5.82/42	5.67	5.14	63.16	49.65
CO_2	29.29/203	27.96	33.04/39	32.16	41.74	0.10	0.61
TiO_2	0.65/205	0.62	0.51/43	0.50	0.07	0.74	1.46
Al_2O_3	2.90/196	2.77	1.82/42	1.77	0.40	15.58	17.08
Fe_2O_3	4.33/176	4.13	3.99/36	3.88	as FeO	2.34	3.80
FeO	4.37/148	4.17	3.81/28	3.71	0.49	3.53	4.11
MnO	0.72/250	0.69	0.80/45	0.78	0.14	0.11	0.11
MgO	6.69/243	6.39	6.27/44	6.10	7.79	2.76	4.68
CaO	34.06/213	32.52	38.07/39	37.06	42.30	4.59	7.00
BaO	0.40/241	0.38	0.46/37	0.45	0.001	0.03	0.1–1.0
SrO	0.81/203	0.77	0.91/30	0.89	0.07	0.03	0.1–1.0
Na_2O	1.02/182	0.97	1.12/35	1.09	0.03	3.27	6.13
K_2O	1.47/182	1.40	0.89/31	0.87	0.16	3.17	3.69
P_2O_5	1.86/197	1.77	1.78/36	1.73	0.045	0.22	0.2–2.0
F	0.73/122	0.69	0.39/18	0.38	0.033	0.066	0.12*
Cl	0.28/45	0.27	0.32/10	0.31	0.015	0.023	0.05*
S	0.48/110	0.46	0.19/16	0.18	0.12		0.03*
SO_3	0.50/85	0.48	0.47/21	0.46			
ΣREO×	3.20/232	3.05	0.61/29	0.59	0.003	0.016	0.044*
H_2O+	1.40/172	1.37	1.46/36	1.42	1.63		
	104.74	100.00	102.73	100.00			
Trace amounts in parts per million							*Syenite*
Sc	11.0/39	11.0	10.0/10	10.0	1.0	13.0	3.0
Co	21.5/57	21.5	18.8/14	18.8	0.1	18.0	1.0
Ni	17.5/55	17.5	32.4/14	32.4	20.0	100.0	4.0
Cr	66.0/68	66.0	102.0/16	102.0	11.0	117.0	2.0
Mo	59.0/27	59.0	64.0/8	64.0	0.4	1.7	0.6
V	94.0/40	94.0	105.0/7	105.0	20.0	90.0	30.0
W	5.2/6	5.2	5.9/5	5.9	0.6	2.0 ?	1.3
Cu	30.3/78	30.3	88.0/10	88.0	4.0	70.0	5.0
Pb	54.0/87	54.0	27.0/11	27.0	9.0	16.0	12.0
Zn	153.0/39	153.0	160.0/2	160.0	20.0	80.0	130.0
Sn	1.1/9	1.1	2.5/4	2.5	<1.0	32.0	>1.0
Ga	2.6/50	2.6	2.4/13	2.4	4.0	26.0	30.0
Y	137.8/61	137.8	113.7/20	113.7	30.0	20.0	20.0
Zr	925.0/108	925.0	461.0/17	461.0	19.0	170.0	500.0
Nb	1198.0/156	1198.0	560.0/28	560.0	0.3	20.0	35.0
Ta					<0.1	2.7	2.1
Ge	7.1/7	7.1	3.3/5	3.3	0.2	2.0	1.0
Tl	0.0/4	0.0	0.0/4	0.0	<0.1	1.7	1.4
Li	10.0/46	10.0	15.0/11	15.0	5.0	50.0	28.0
Cs	0.00/5	0.0	0.0/1	0.0	<1.0	10.0	0.6
Rb	48.7/32	48.7	52.0/9	52.0	3.0	280.0	110.0
Th	1626.0/108	1626.0	649.0/5	649.0	1.7	13.0	13.0
U	50.0/75	50.0	57.0/5	57.0	2.2	2.6	3.0
Be	4.4/23	4.4	5.0/7	5.0	<1.0	4.2	1.0
Ag	2.7/9	2.7	3.9/4	3.9	<0.1	0.2	<0.1
B	0.0/2	0.0	0.0/1	0.0	20.0	13.0	9.0
In	0.0/4	0.0	0.0/4	0.0	<0.1	0.1	<0.1

Malawi (Nyasaland)–Chilwa Island, Kangankunde, Songwe vent, Tundulu.

Zambia (Northern Rhodesia)–Nkambwa Hill.

Southern Rhodesia-Chishanya, Dorowa, Shawa.

Mozambique–Monte Muambe.

South Africa–Elands and Crocodile river, Loolekop (Palabora), Magnet Heights, Premier Diamond Mine, Spitzkop.

Eurasia

Norway–Fen area, Stjernoy.

Sweden–Alnö area.

U.S.S.R.–Saizha carbonatite, Sallanlatvinsk massif (Karelia), East Sayan Mts.

North America

Canada–Cargill, Clay. Firesand, Lackner Lake (Nemegos), Oka, Seabrook Lake.

United States-Magnet Cove, Mountain Pass.

CALCULATION OF 'THE AVERAGE' AND 'THE TYPICAL' COMPOSITION

The average chemical composition was derived by averaging the analyses of the carbonate-rich and silicate-carbonate rocks obtained from the following sources: Bassett, 1956; Bloomfield and Garson, 1963; Bowden, 1962; Brogger, 1921; Brown, 1964; Coetzee and Edwards, 1959; Daly, 1925; Davies, 1956; Dawson, 1962; Dias, 1961; Du Bois *et al.*, 1963; von Eckerman, 1948, 1951, 1958, 1960, 1960, 1962, 1963, 1963; Erickson and Blade, 1963; Fawley and James, 1955; Fick and Van Der Heyde, 1959; Fockema, 1952; Garson and Campbell Smith, 1958; Garson, 1962; Gevers, 1948: Gold 1963; Harpum, 1959; Heier, 1961, 1962; Higazy, 1954; Holmes, 1956; Jeffery, 1959, 1962; Johnson, 1961; King, 1948; von Knorring and Du Bois, 1961; Konev, 1962; McCall, 1958; Meyer, 1957, 1958; Olson *et al.*, 1954; Parsons, 1961; Reeve and Deans, 1954; Russel *et al.*, 1954; Saggerson, 1952; Schofield and Haskin, 1964; Serba, 1962, 1963; Strauss and Truter,1950, 1950; Swift, 1952; Vainshtein *et al.*, 1961.

Unfortunately, there is a wide variation (see Table 2) in the abundance of any one element within a particular complex, and also between different complexes (*e.g.* rare-earth oxides at Mountain Pass average 6.27% for 107 samples; SiO_2 at Alnö averages 18.88% for 65 samples). Because high or low values for a large number of samples from a single occurrence, largely the result of either over or inadequate sampling, tend to unbalnce the 'average' values, a weighted average was computed and designated the 'typical composition.' This was derived by averaging the average composition for each carbonatite occurrence, thus reducing the influence of each occurrence to one sample. Where averages and limits were all that was available in the literature, they were summed as of equal weight.

The average amount, together with the number of analyses are listed in column I. In column II these average amounts are reduced to 100% (– ~0.50%). The average of the individual averages, together with the number of complexes sampled, are listed in column III. The 'typical' composition, reduced to 100% (– ~0.30%), is given in column IV. For comparison the average chemical composition of sedimentary carbonate rocks, igneous rocks, and alkalic rocks (and syenites) are given in columns V, VI, and VII respectively.

The values for the major and minor constituents of igneous rocks were calculated from the

---

← *Note:* O~F=0.16, O~Cl=0.07, O~S=0.09 in column IV.
O~F=0.29, O~Cl=0.06, O~S=0.23 in column II.

Columns:
I Average of 'carbonatites'/number of analyses.
II Average of 'carbonatites'/reduced to 100 per cent.
III Average of 'Individual carbonatite complexes/number of complexes. (Typical abundance).
IV Typical abundance reduced to 100 per cent.
V Average of sedimentary carbonate rocks.
VI Average of igneous rocks.
VII Average of alkaline rocks: trace amounts for syenites; * for syenites.

figures given by Wickman (1954); the trace amounts are quoted from Green (1959). The major and minor constituents of alkaline rocks are an average of the constituents for fifteen alkaline rock groups listed by Daly (1933). Because the trace element content for these rocks is not listed, the recent values for the syenites are included (Turekian and Wedepohl, 1961). The chemical content of sedimentary carbonate rocks is quoted from Turekian and Wedepohl (1961).

(2) melteigites, ijolotes, urtites, and nepheline (cancrinite) syenites." The constant association of similar, specific rock types in most carbonatite complexes from different geologic setting and from different parts of the world, the distinctive mineralogy and geochemistry (Pecora, 1956; Gold, 1963) of the carbonate rocks, the similarities of certain isotope ratios (Baertschi, 1957; Holmes, 1958; von Eckermann *et al.*, 1951; Powell *et al.*, 1962; Hamilton and Deans, 1963; Kukharenko and Dontsova, 1964) between

TABLE 2

Range in values for individual constituents

Major and minor constituents in weight per cent			Trace elements in parts per million		
	For total sample	For individual complexes		For total sample	For individual complexes
SiO_2	49.65 - tr.	31.06 - tr.	Sc	50 - 0	50 - 0
CO_2	48.02 - 3.12	44.21 - 12.29	Co	130 - 0	99 - 0
TiO_2	5.20 - tr.	2.50 - tr.	Ni	280 - 0	200 - 0
Al_2O_3	18.19 - tr.	10.34 - tr.	Cr	1360 - 0	748 - 0
Fe_2O_3	38.88 - tr.	8.19 - tr.	V	425 - 0	250 - 16
FeO	44.60 - tr.	24.13 - tr.	Mo	800 - 0	403 - 1
MnO	8.60 - tr.	8.60 - 0.09	W	17.7 - 0.6	17.7 - 0.6
MgO	42.68 - tr.	19.34 - tr.	Cu	1461 - 0	732 - 0
CaO	64.04 - 0.83	53.37 - 15.54	Pb	700 - 0	94 - 0
BaO	8.40 - tr.	2.66 - tr.	Zn	1120 - 0	168 - 152
SrO	18.24 - tr.	6.13 - tr.	Sn	5 - 0	5 - 0
Na_2O	30.00 - tr.	29.56 - tr.	Ga	20 - 0	13 - 0
K_2O	12.75 - tr.	7.84 - tr.	Y	1000 - 0	350 - 0
P_2O_5	11.56 - tr.	7.19 - tr.	Zr	8400 - 0	3685 - 0
F	39.72 - tr.	2.26 - tr.	Nb, Ta	52000 - 0	2985 - 0
Cl	3.86 - tr.	2.90 - tr.	Ge	50 - 0	17 - 0
S	20.30 - tr.	0.69 - tr.	Tl	0 - 0	0 - 0
SO_3	4.40 - tr.	2.46 - tr.	Li	100 - 0	100 - 0
ΣREOX	38.92 - tr.	6.27 - 0.01	Cs	0 - 0	0 - 0
H_2O+	9.61 - tr.	5.38 - tr.	Rb	400 - 0	300 - 0
			Th	20090 - 0	2375 - 0
			U	3320 - 0	54.6 - 0.55
			Be	29 - 0	15 - 0
			B	tr.	tr.
			Ag	10 - 0	8 - 1.7
			In	0 - 0	0 - 0

ISOTOPIC COMPOSITION

From a survey of carbonatites, Kukharenko and Dontsova (1964) noted that "...carbonatites are associated with a perfectly definite complex of rocks belonging to two series: (1) olivinites and nepheline pyroxenites (jacupirangites) and

complexes and with ultrabasic igneous rocks, suggest that carbonatites are derived from a similar parent material and emplaced by a somewhat similar process.

The available carbon and oxygen isotope data for carbonatites are summarized and compared

schematically in Fig. 1. All values are recalculated in terms of the Chicago PDB standard and reported as δ0‰+δC‰, where these represent respectively

$$\frac{O^{18}/O^{16} \text{ sample} - O^{18}/O^{16} \text{ Std}}{O^{18}/O^{16} \text{ Std}} \times 1000,$$

and $$\frac{C^{13}/C^{12} \text{ sample} - C^{13}/C^{12} \text{ Std}}{C^{13}/C^{12} \text{ Std}} \times 1000$$

Keith and Weber (1964) report median δ0‰, δC‰ values of −11.39±4.95 and −0.26±3.09 for 24 Precambrian limestones and marbles; −5.58±3.60 and −0.13±2.61 for 321 marine limestones; −8.56±4.11 and −0.41±3.33 for 180 fresh water limestones. Working in the classical Kola Peninsula area, Kukharenko and Dontsova (1964) compared the carbon and oxygen isotope gated the carbon isotopic composition of some Scandinavian alkaline intrusions, and found the ratio to vary with rock type. At Alnö δC‰ varied from +5.5 in a beforsite dike, to −4.6 in an alvikite dike, with a mean for 12 samples of +0.36. The variation in the Fen area is from +3.4 for rodbergite to −2.5 for rauhaugite, with a mean for 8 samples of +0.6. Two samples from Stjernoy average −1.9, whereas one sample of albite-sövite from Seiland ran −3.1.

Another important isotope ratio is that of strontium. Powell *et al.* 1962 reports a mean Sr^{87}/Sr^{86} ratio of 0.7065 ± .0003 for 21 carbonatites; a ratio greater than 0.709 (range 0.709 to 0.714) for limestones and marbles; a ratio of approx. 0.708 for continental basalts and 0.707 for oceanic basalts. Hamilton and Deans (1963)

FIGURE 1 CARBON AND OXYGEN ISOTOPIC COMPOSITION OF SOME CARBONATITES AND LIMESTONES OF SEDIMENTARY ORIGIN.

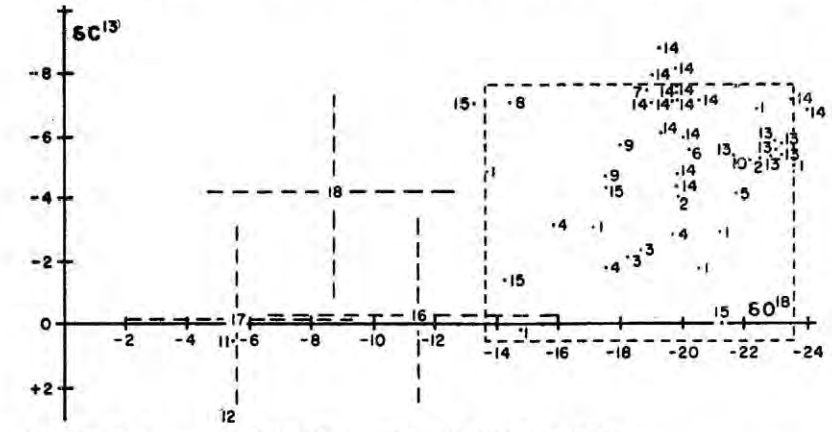

1 ALNÖ, SWEDEN	(BAERTSCHI, 1957)	10 SPITZKOP, S AFRICA	"
2 IRON HILL, COLORADO	"	11 TRANSVAAL dolomite, S. AFRICA	(Holmes, 1958)
3 CHILWA ISLAND, NYASALAND	"	12 KASEDIA limestone, UGANDA	"
4 TUNDULU, NYASALAND	"	13 OKA, QUEBEC, CANADA	(Keith, unpub.)
5 SUKULU HILL, UGANDA	"	14 KOLA PENINSULA, carbonatites	(Kukharenko, and
6 KATWE CRATER, UGANDA	"	15 IMANDRA-VURZUGA sediments, KOLA	Dontsova, 1964)
7 KALYANO VOLCANO, UGANDA	"	16 PRECAMBRIAN limestones & marbles	(Keith, and
8 MBUGA CRATER, UGANDA	"	17 MARINE limestone	Weber, 1964)
9 PREMIER MINE, S. AFRICA	"	18 FRESH-WATER limestones	"

RANGE FOR CARBONATITES (Holmes, 1958)

ratios of the carbonatites with those of Proterozoic sedimentary rock of the Imandra-Varzuga formation. The average of 15 samples from 8 carbonatites is δ0‰ −20.2, δC‰ −7.0; whereas the 6 sedimentary rocks averaged δ0‰ −15.1, δC‰ −2.7. von Eckermann *et al.*, 1951, investi- confirmed the validity of this ratio by finding a mean ratio of 0.7060 for 9 carbonatites from widely separate areas ranging in age from Precambrian to modern. This ratio which is lower than that found in sialic rocks, was found to be constant for the carbonatite as well as the

associated silicate rocks–a fact which led Powell *et al.* (1962) to conclude ' that the source material for these rocks is located beneath the sial '.

Kirillov and Rylov (1963) compared the distribution of magnesium isotopes in rocks from the Kola Peninsula. The distribution of Mg^{24}, Mg^{25}, Mg^{26} and concentration ratio C^{24}/C^{26} for Proterozoic dolomitic sediments is 78.58, 10.11, 11.31 and 6.95; for carbonatites 78.45, 10.15, 11.40 and 6.88; for olivine 78.45, 10.15, 11.40 and 6.88; and ultrabasic rocks 78.40, 10.16, 11.44 and 6.85 respectively. They note the affiliation of carbonatites with olivine and ultrabasic rocks, and concludes that they could not have formed from the dolomitic sediments.

SUMMARY AND CONCLUSIONS

1) The results summarize the available chemical and isotopic data pertinent to carbonatites. Because of over sampling (at this stage) in certain cases, inadequate sampling in most cases, the ' typical composition ' values are more meaningful than those of the ' average composition.'

2) Generally, in carbonatites there is an accumulation of C, Ca, Mg, Ba, Sr, Fe, Mn, Ti, Zr, P, Nb, Ta, Rare-earths, Th, U, F, Cl, Y, Cu, S with respect to crustal rocks *i.e.* an impoverishment in sialic constituents. The index or distinguishing elements are: Ba, Sr, Zr, Nb, Y, Rare-earth, Mn, P, and F.

3) The $\delta 0\%$ and $\delta C\%$ values for carbonatites range between −13.0 and −24.0 for oxygen, and 5.5 and −9.0 for carbon. Detailed data are needed regarding the variation and distribution of the carbon and oxygen isotopes within a complex.

4) The strontium isotope work is the most important recent advance to the problem of the genesis of carbonatites.

5) The distribution of magnesium isotopes deserves further testing.

6) More chemical data from carbonatite complexes are needed. The optimum is a large number (at least 20 at this stage) of analyses for major and minor constituents and a broad spectrum of trace elements (at present only the data from Tundulu complex, Malawi, approaches this objective). All too few ' broad spectral ' analyses are available. This is due mainly to the difficulty and cost of analyzing 'carbonatites' and to the lack of a suitable standard.

7) I propose that a standard ' carbonatite ' similar to G. 1, and W. 1 be prepared and distributed, and that the members of the symposium discuss the requirements of such a standard and the means of preparing and distributing the sample. The standard should be prepared from fresh carbonate rocks, which are readily available in a quarry or trenches, from a well-known, readily accessible carbonatite complex. Also, the composition of the sample should conform fairly closely to the ' typical ' composition presented in this paper.

REFERENCES

BAERTSCHI, P. (1951) Relative abundances of oxygen and carbon isotopes in carbonate rocks: *Nature*, Vol. 168, pp. 288–289.

———(1957) Messung und Deutung Relativer Häufigkeits-variationen von O^{18} und C^{13} in Karbonatgesteinen und Mineralien: *Schweiz. Min. Petr. Mitt.*, Vol. 37, pp. 73–152.

BASSET, H. (1956) The Igwisi craters and lavas; *Rec. Geol. Surv. Tanganyika*, Vol. 4, (1954), pp. 96–102.

BLOOMFIELD, K. AND GARSON, M. S. (1963) Complete analyses of rocks carried out in 1960: *Rec. Geol. Surv. Nyasaland*, Vol. 2, pp. 111–118.

BOWDEN, P. (1962) Trace elements in Tanganyika carbonatites: *Nature*, Vol. 196, p. 570.

BROGGER, W. C. (1921) Die Eruptivegesteine des Kristianiagebietes; IV. Das Fengebiet in Telemark, Norwegen: *Videnskr. Selsk. Skr. 1. Mat Naturo Kristiania*, No. 9.

BROWN, P. E. (1964) The Songwe scarp carbonatite and associated feldspathization in the Mbeya Range, Tanganyika: *Quart. Jour. Geol. Soc. Lond.*, Vol. 120, pp. 223–240.

COETZEE, C. L. AND EDWARDS, C. B. (1959) The Mirma Hill carbonatite, Coast Province, Kenya: *Trans. Geol. Soc. South Africa*, Vol. LXII, pp. 373–395.

DALY, R. A. (1933) *Igneous rocks and the depths of the earth:* McGraw Hill, New York and London.

——(1925) Carbonate dikes of the Premier Diamond Mine, Transvaal: *Jour. Geol.*, Vol., 33, No. 7, pp. 659-684.

DAVIS, K. A. (1952) The building of Mount Elgon (East Africa): *Geol. Surv. Uganda*, Mem. 7.

——(1956) The geology of part of South-East Uganda: *Geol. Surv. Uganda*, Mem. 8.

DAWSON, J. B. (1962) Sodium carbonate lavas from Oldoinyo L'engai, Tanganyika: *Nature*, Vol. 195, No. 4846, pp. 1075-1076.

DIAS, M. BETTENCOURT (1961) Geology of Monte Muambe: *Prov. Mocambique, Serv. Geol. e Minas, Estudos, notas e trabalhos*, No. 27, pp. 39-64.

DUBOIS, C.G.B., FURST, J., GUEST, N.J. AND JENNINGS, D. J. (1963) Fresh natro carbonatite lava from Oldoinyo L'engai: *Nature*, Vol. 197, No. 4866, pp. 445-446.

ECKERMANN, H. von., UBISCH, H. von., AND WICKMAN, F. E. (1952) A preliminary investigation into the isotopic composition of carbon from some alkaline intrusions: *Geochem. et Cosmochim. Acta*, Vol. 2, pp. 207-210.

ECKERMANN, H. von., (1948) The alkaline district of Alnö Island: *Sverig. Geol. Unders.* Ser. Ca. No. 36, Stockholm.

——(1951) The distribution of barium and strontium in the rocks and minerals of the syenite and alkaline rocks of Alnö Island: *Arkiv. Min. Geol.*, Vol. No. 13.

——(1958) The alkaline and carbonatitic dikes of the Alnö formation on the mainland north-west of Alnö Island: *Kgl. Vet. Akad. Handl.*, Ser. 4, Bd. 7, No. 2, Stockholm.

——(1960) Boulders of volcanic breccia at the Sälskär shoals north of Alnö Island: *Arkiv. Min. Geol.*, Bd. 2, Pt. 6, No. 40, pp. 529-537.

——Contributions to the knowledge of the alkaline dikes of the Alnö region:

(1) Kimberlite dike from the right-hand inspection tunnel at Bergeforsen:

(2) Ouachite dike from the right-hand inspection tunnel at Bergeforsen:

(3) Radioactive beforsitic carbonatite dike: *Arkiv Min. Geol.*, Bd. 2, Pt. 6, No. 41, 1960, pp. 539-550.

(4) Beforsite dike rich in BaO and CO_2 in the Fagervik soft water tunnel: *Arkiv. Min. Geol.* Bd. 3, Pt. 1, No. 2, 1962, pp. 65-68.

(5) Carbonatized Jotnian diabase dike in the Fagervik soft water tunnel:

(6) Kimberlite dike from the Fagervik soft water tunnel rich in phlogopite:

(7) Carbonatite rich in fluorite from the Fagervik soft water tunnel:

(8) Carbonatitic kimberlite from Sundsvall: *Arkiv. Min. Geol.*, Bd. 3, Pt. 3, No. 12, 1963, pp. 259-275.

(9) Carbonatitic kimberlite from Sundsvall: *Arkiv. Min. Geol.*, Bd. 3, Pt. 5, No. 19, 1963, pp. 397-402.

(10) Carbonatite rich in apatite and quartz from Vintjärns Varv at Sundsvall: *Arkiv. Min. Geol.*, Bd. 3, Pt. 5, No. 20, 1963, pp. 403-406.

ERICKSON, R. L. AND BLADE, L. V. (1963) Geochemistry and petrology of the alkaline igneous complex at Magnet Cove, Arkansas: *U.S. Geol. Surv.* Prof. Paper 425.

FAWLEY, A. P. AND JAMES, T. C. (1955) A pyrochlore (columbium) Carbonatite, Southern Tanganyika: *Econ. Geol.*, Vol. 50, pp. 571-585.

FICK, L. J. AND van der HEYDE, C. (1959) Additional data on the geology of the Mbeya carbonatite: *Econ. Geol.*, Vol. 54, pp. 842-872.

FOCKEMA, R. A. P. (1952) The geology of the area around the confluence of the Elands and Crocodile Rivers: *Trans. Geol. Soc. South Africa*, Vol. 55, pp. 155-171.

GARSON, M. S. AND SMITH, W. CAMPBELL (1958) Chilwa Island: *Geol. Surv. Nyasaland*, Mem. No. 1.

GARSON, M. S. (1962) The Tundulu carbonatite ring-complex in Southern Nyasaland: *Geol. Surv. Nyasaland*, Mem. No. 2.

GEVERS, T. W. (1948) Vermiculite at Loolekop, Palabora, North East Transvaal: *Trans. Geol. Soc. South Africa*, Vol. 51, pp. 133-178.

GOLD, D. P. (1963) The relationship between the limestones and the alkaline igneous rocks of Oka and St. Hilaire, Quebec: *Unpub. Ph.D. thesis*, McGill Univ., Montreal, Canada.

——(1963) Average chemical composition of carbonatites: *Econ. Geol.*, Vol. 58, pp. 988-991.

GREEN, J. (1959) Geochemical table of elements for 1959: *Bull. Geol. Soc. Amer.*, Vol. 70, pp. 1127–1184.

HAMILTON, E. J. AND DEANS, T. (1963) Isotopic composition of strontium in some African carbonatites and limestones and in strontium minerals: *Nature*, Vol. 198, No. 4882, pp. 776–777.

HARPUM, J. R. (1959) Complete analyses of rocks carried out in 1957: *Rec. Geol. Surv. Tanganyika*, Vol. 7, pp. 96–104.

HEIER, K. S. (1961) Layered gabbro, hornblendite, carbonatite and nepheline syenite on Stjernoy, North Norway: *Norsk Geol. Tidskr.*, Vol. 41, pp. 109–135.

———(1962) A note on the U, Th and K content of the nepheline syenite and carbonatite on Stjernoy, North Norway: *Norsk Geol. Tidskr.*, Vol. 42, pp. 287–292.

HIGAZY, R. A. (1954) Trace elements of volcanic ultrabasic potassic rocks of southwestern Uganda and adjoining part of the Belgium Congo: *Bull. Geol. Soc. Amer.*, Vol. 65, pp. 39–70.

HOLMES, A. (1956) The ejectamenta of Katwe Crater, South-west Uganda: *Verk. Konink. Nederland Geol. Mijnbo Genootschap, Geol. Ser.*, Deel 16, pp. 139–166.

———(1958) Spitzkop carbonatite, Eastern Transvaal: (Abst.) *Bull. Geol. Soc. Amer.*, Vol. 69, pp. 1525–1526.

JEFFERY, P. G. (1959) The geochemistry of tungsten, with special reference to the rocks of the Uganda Protectorate: *Geochim. et Cosmochim. Acta*, Vol. 16, pp. 278–295.

———(1962) The flourine content of some standard samples: *Geochim. et Cosmochim. Acta*, Vol. 26, pp. 1355–1356.

JOHNSON, R. L. (1961) The Geology of the Dorowa and Shawa carbonatite complexes, Southern Rhodesia: *Trans. Geol. Soc. South Africa*, Vol. LXIV, pp. 101–145.

KEITH, M. L. AND WEBER, J. N. (1964) Carbon and oxygen isotopic composition of selected limestones and fossils: *Geochim. et Cosmochim. Acta*, Vol. 28, pp. 1787–1816.

KING, B. C. (1948) The Napak area of Southern Karamoja, Uganda: *Geol. Surv. Uganda*, Mem. No. V.

KIRILLOV, A. S. AND RYLOV, V. S. (1963) Origin of magnesium in carbonatites: *Zap. Vses. Mineralog. Obshchestva*, Vol. 92, pp. 228–231. (Quoted from Chem. Abst. Vol. 59, 1963, 3662c).

KNORRING, O. von. AND DU BOIS, C. G. B. (1961) Carbonatitic lava from Fort Portal area in western Uganda: *Nature*, Vol. 192, pp. 1064–1065.

KONEV, A. A. (1962) Carbonatites of the Saizhinsk alkalic-ultrabasic complex: *Zap. Vses. Mineralog. Obshchestva*, Vol. 91, pp. 165–169.

KUKHARENKO, A. A. AND DONTSOVA, E. I. (1964) A contribution to the problem of the genesis of carbonatites: *Econ. Geol. U.S.S.R.*, (English translation) Vol. 1, Nos. 3 & 4, pp. 31–46.

MCCALL, C. J. H. (1958) Geology of the Gwasi area: *Geol. Surv. Kenya*, Rept. No. 45.

MEYER, A. (1957) Un type particulier de roche carbonatèe au Ruanda (Afrique centrale): *Comp. Rendus Acad. Sci. Paris*, Vol. 245, pp. 976–978.

———(1958) La carbonatite Lueshe (Kivu): *Congo Belge Serv. Geol. Bull.*, No. 8, Fasc 5, pp. 1–19.

OLSON, J. C. (1954) Rare-earth mineral deposits of the Mountain Pass District, San Bernardino County, California: *U. S. Geol. Surv.*, Prof. Paper 261.

PARSONS, C. E. (1961) Niobium-bearing complexes east of Lake Superior: *Ontario Dept. of Mines*, Geol. Rept. No. 3.

PECORA, W. T. (1956) Carbonatites: a review: *Bull. Geol. Soc. Amer.*, Vol. 67, pp. 1537–1556.

POWELL, J. M., HURLEY, P. M. AND FAIRBAIRN, H. W. (1962) Isotopic compositions of strontium in carbonatites: *Nature*, Vol. 196, No. 4859, pp. 1085–1086.

REEVE, W. H. AND DEANS, T. (1954) An occurrence of carbonatite in the Isoka district of Northern Rhodesia: *Col. Geol. and Min. Resources*, Vol. 4, No. 3, p. 279.

RUSSEL, H. D., HIEMSTRA, S. A. AND GROENEVELD, D. (1954) The mineralogy and petrology of the carbonatite at Loolekop, Eastern Transvaal: *Trans. Geol. Soc. South Africa*, Vol. 57, pp. 197–208.

SAGGERSON, E. P. (1952) Geology of the Kisumu district: *Geol. Surv. Kenya*, Geol. Rept. No. 21.

SCHOFIELD, A. AND HASKIN, L. (1964) Rare-earth element distribution in eight terrestrial materials: *Geochim. et Cosmochim. Acta*, Vol. 28, No. 4. pp. 437–446.

SERBA, B. I. (1962) Cobalt content in carbonatites: *Geochemistry*, (English translation) No. 9, pp. 967–968.

———(1963) Carbonatites in the Sallanlatvinsk massiff: *Sov. Geol.*, (English translation) Vol. 6, pp. 125–131.

STRAUSS, C. A. AND TRUTER, F. C. (1950) The alkali complex at Spitzkop, Sekukuniland, Eastern Transvaal: *Trans. Geol. Soc. South Africa*, Vol. 53, pp. 81-123.

———(1950) Post-Bushveld ultrabasic, alkali and carbonatitic eruptives at Magnet Heights, Sekukuniland, Eastern Transvaal: *Trans. Geol. Soc. South Africa*, Vol. 53, pp. 169–190.

SWIFT, W. H. (1952) The geology of Chishanya, Buhera District, Southern Rhodesia: *Trans. Edin. Geol. Soc.*, Vol. XV, pp. 346–359.

TUREKIAN, K. K. AND WEDEPOHL, K. H. (1961) Distribution of the elements in some major units of the earth's crust: *Bull. Geol. Soc. Amer.*, Vol. 72, pp. 175–192.

VAINSHTEIN, E. E., POZHARITSKAYA, L. K. AND TURANSKAYA, H. V. (1961) Behavior of the rare earths in the process of formation of carbonatites: *Geochemistry*, (English Translation) No. 11, p. 1151–1154.

WICKMAN, F. E. (1954) The "total" amount of sediments and the composition of the 'average igneous rock': *Geochim. et Cosmochim. Acta*, Vol. 5, pp. 97–110.

MINERALOGICAL SOCIETY OF INDIA, IMA VOLUME, 1966
INTERNATIONAL MINERALOGICAL ASSOCIATION, PAPERS, FOURTH GENERAL MEETING

FRACTIONAL CRYSTALLIZATION IN THE "CARBONATITE SYSTEMS" $CaO-MgO-CO_2-H_2O$ and $CaO-CaF_2-P_2O_5-CO_2-H_2O$*

P. J. WYLLIE† AND G. M. BIGGAR
Department of Geochemistry and Mineralogy, The Pennsylvania State University University Park, Pennsylvania, U.S.A. and School of Chemistry, The University of Leeds, Leeds, England

ABSTRACT

Many carbonatite masses exhibit inhomogeneities on both large and small scales. Evidence for large scale differentiation is offered by the successive intrusion of sövite, ankeritic sövite, and finally siderite carbonatites at complexes such as Chilwa Island. On a smaller scale, the segregation of minerals is illustrated by the development of apatite-rich bands and lenses in the carbonatite. In the system $CaO-MgO-FeO-H_2O$, the minerals calcite, portlandite, periclase, and iron oxide are stable on the vapor-saturated liquidus above 600°C at pressures below about 900 bars, with brucite, dolomite (or ankerite), and siderite appearing on this liquidus only at successively higher pressures. In the system $CaO-CaF_2-P_2O_5-CO_2-H_2O$, apatite and calcite may crystallize simultaneously through a wide range of pressures and temperatures (as low as 575°C). However, any liquid containing initially more than a small percentage of P_2O_5 precipitates apatite before calcite. The synthetic carbonatite magmas are very fluid, and crystal settling occurs within a few minutes. Paths of crystallization and the sequence of minerals precipitated are dependent upon several variables, including changes in temperature, in pressure, and in the composition of the vapor phase (CO_2-H_2O) in equilibrium with liquid and crystals. It can be shown from the phase relationships in these systems that fractional crystallization of synthetic carbonatite magmas is capable of producing differentiation sequences similar to those occurring at Chilwa Island and elsewhere.

INTRODUCTION

The recognition of reasonably low temperature melts in the system $CaO-CO_2-H_2O$ which can precipitate calcite was regarded by Wyllie and Tuttle (1960a, 1960b) as verification for the magmatic origin of carbonatites when the field relationships were consistent with this interpretation. The "synthetic carbonatite magmas" in the ternary system are extremely fluid, and crystal settling occurs within a few minutes. The possibility of fractional crystallization and differentiation in more complex systems was discussed briefly in the earlier papers.

Accounts of the varied field relationships of carbonatites and associated igneous rocks have been provided in reviews by Pecora (1956), Smith (1956), and by King and Sutherland (1960). There is good field evidence that some carbonatites, at least, are magmatic in origin, and the available experimental data now supports this conclusion. Many carbonatite masses exhibit inhomogeneities on both large and small scales suggesting the operation of differentiation processes. Evidence for large-scale differentiation is offered (but not proven) by the successive emplacement of calcitic sövite, ankeritic sövite, and finally sideritic carbonatites (Garson and Smith, 1958). Similar sequences are quite common, and five other examples were cited by Garson and Smith (1958, p. 110). Another effect which may be related to differentiation processes is provided by von Eckermann's conclusion (1948, p. 148) that in the magma column of the Alnö carbonatite complex, the sövite magma (calcite) formed at an upper level (estimated pressure 900 bars), whereas the beforsite magma (dolomite) formed at greater depth and at greater pressure (estimated 2,400 bars).

The Chilwa Island complex also provides examples of the segregation of minerals on a smaller scale, with the development of apatite-rich bands and lenses in the carbonatite. This is a common feature of many carbonatites.

* Contribution number 64-69 from the College of Mineral Industries, The Pennsylvania State University.
† Present address: Department of Geophysical Sciences, The University of Chicago, Chicago, Illinois.

The present contribution summarizes experimental data from synthetic systems in which dolomite and apatite can be precipitated alongside calcite in order to see whether crystallization differentiation in the "synthetic carbonatite magmas" is capable of reproducing the natural differentiation products occurring in the examples cited.

THE SYSTEM CaO-MgO-CO_2-H_2O

Wyllie and Tuttle began investigation of the quaternary system in 1958 with the intention of finding out whether liquids in the system could precipitate first calcite and then dolomite. However, problems of interpretation were encountered and the experimental study still awaits completion. The preliminary experimental data available, together with data from the bounding ternary systems, provided the basis for a theoretical analysis of the system (Wyllie, 1965). The key to the symbols used as abbreviations of phase names is given in Table 1.

Decarbonation Reactions and Liquidus Relationships

The upper temperature stability limits of brucite, magnesite, and dolomite in the systems bounding the quaternary system are given in Fig. 1, along with the melting relationships in the system CaO-CO_2-H_2O. The lower melting curve, E_1, corresponds to the ternary eutectic where melting begins in the system.

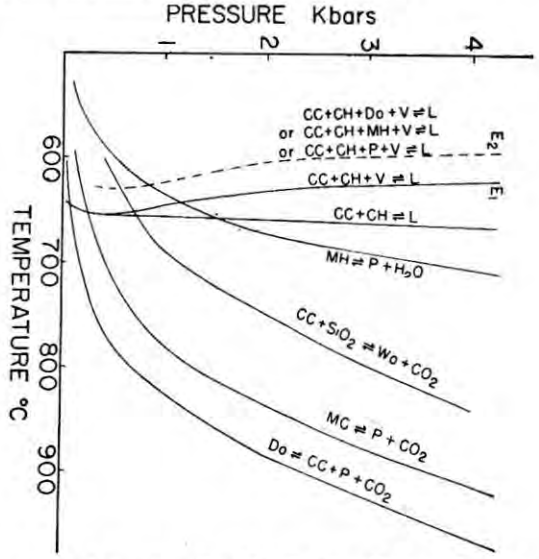

Fig. 1. The system CaO-MgO-CO_2-H_2O. For abbreviations see Table 1. Univariant reactions with one silicate reaction for comparison (calcite+quartz $\rightleftharpoons$ wollastonite+CO_2). E_1 is the minimum liquidus temperature in the system CaO-CO_2-H_2O, and E_2 is the same for quaternary system (see Fig. 2). In the reaction E_2, periclase is replaced by brucite and then dolomite at successively higher pressures (see Fig. 5). After Harker and Tuttle (1955, 1956), Goldsmith and Heard (1961), Roy and Roy (1957), Wyllie and Tuttle (1960a), and Raynor and Wyllie (unpublished).

TABLE 1

The system CaO-MgO-CO_2-H_2O

Key to invariant and univariant assemblages in Fig. 5. There are eight phases involved: calcite (CC), portlandite (CH), dolomite (Do), magnesite (MC), brucite (MH), periclase (P), liquid (L), and vapour (V).

Q_1	–	CC	+	CH	+	MH	+	P	+	L	+	V.	E_4	–	CC	+	MH	+	P	+	L	+	V.
Q_2	–	CC	+	CH	+	Do	+	MH	+	L	+	V.	E_5	–	CC	+	CH	+	MH	+	L	+	V.
Q_3	–	CC	+	Do	+	MH	+	P	+	L	+	V.	E_6	–	CC	+	CH	+	MH	+	P	+	V.
R_1	–	CC	+	CH	+	MH	+	P	+	V.			E_7	–	CC	+	Do	+	MH	+	L	+	V.
R_2	–	CC	+	Do	+	MH	+	P	+	V.			E_8	–	CH	+	Do	+	MH	+	L	+	V.
R_3	–	CC	+	CH	+	Do	+	MH	+	V.			E_9	–	CC	+	CH	+	Do	+	L	+	V.
S_3	–	Do	+	MC	+	MH	+	P	+	V.			E_{10}	–	CC	+	CH	+	Do	+	MH	+	L.
E_1	–	CC	+	CH	+	L	+	V.					E_{11}	–	Do	+	MH	+	P	+	L	+	V.
E_2	–	CC	+	CH	+	P	+	L	+	V.			E_{12}	–	CC	+	Do	+	P	+	L	+	V.
E_3	–	CH	+	MH	+	P	+	L	+	V.			E_{13}	–	CC	+	Do	+	MH	+	P	+	L.

Additional abbreviations used for phases are: hydroxylapatite-HAp, fluorapatite-FAp, the hypothetical carbonatapatite - CAp.

Wyllie and Tuttle (1960b) found in their preliminary work at 1 kilobar pressure that the quaternary eutectic, E_2, where melting begins, occurred at 620°C, 25°C lower than in the ternary system. The dashed curve E_2 in Fig 1. is an estimate for the quaternary reaction, located 25°C below the ternary eutectic reaction E_1. Marcello Carapezza, a visitor to the Pennsylvania State University from the University of Bologna, has recently confirmed that the reaction curve lies between 590°C and 610°C at 4 kilobars pressure.

It will be shown in the following discussion that the magnesian phase involved in the eutectic reaction E_2 may be periclase, or brucite, or dolomite, depending upon the pressure. The change from periclase to brucite occurs at a pressure very close to 1 kilobar, and at 500 bars pressure, periclase is certainly stable rather than brucite.

Fig. 2 shows schematically the liquidus phase

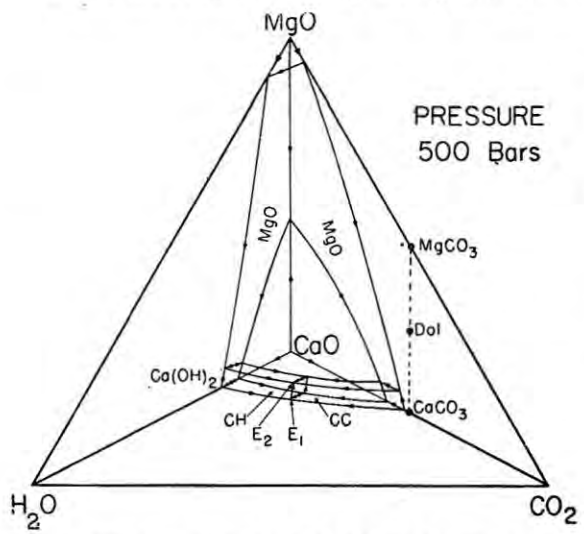

Fig. 2. The system CaO-MgO-CO_2-H_2O. For abbreviations see Table 1. Schematic liquidus field boundaries and primary phase volumes at 500 bars pressure.

relationships in the quaternary system at 500 bars pressure. The ternary field boundaries and phase fields for the primary crystallization of lime, of periclase, of calcite, and of portlandite, extend into the quaternary system as surfaces and phase volumes, respectively, separated by quaternary field boundaries. The preliminary results of Wyllie and Tuttle (1960b, and unpublished) confirm that only a small amount of MgO (probably less than 5 weight percent) is soluble in the ternary eutectic liquid E_1, and that this depresses the minimum liquidus temperature in the quaternary system by about 25°C, at E_2. From the quaternary field boundaries limiting the primary phase volumes for calcite and portlandite there rise two isobaric divariant surfaces, one giving compositions of liquids saturated with both periclase and lime, and the other of liquids saturated with periclase and a vapor phase.

The four ternary field boundaries which are saturated with vapors from the edges of the quaternary vapor-saturated surface which gives the compositions of liquids coexisting with a crystalline phase or phases, and with a vapor phase on the vaporus surface, which is effectively coincident with the join CO_2–H_2O. The vapor-saturated liquidus surface includes fields for the primary crystallization of periclase, calcite, and portlandite, these fields meeting at the quaternary eutectic E_2. As the liquids on this surface change composition from the carbonate to the hydrate side of the tetrahedron, so does the vapor phase change composition from CO_2 to H_2O. The vapor phases in equilibrium with the eutectic liquids E_1 and E_2 are very rich in H_2O. This is why neither magnesite nor dolomite appear on the liquidus at this pressure, despite the fact that the eutectic reaction curve E_2 lies well within the stability fields for these minerals in the presence of CO_2 (Fig. 1). In order to appreciate the effect of vapor phase composition on the stability fields of dolomite and magnesite, and to compare these stability fields with the liquidus relationships, it is necessary to use a diagram in which the vapor phase composition is represented. The petrogenetic model (Wyllie, 1962) has proved useful for this purpose.

Composition of Vapors: The Petrogenetic Model

Fig. 3 illustrates schematically an isobaric section through the petrogenetic model for the

quaternary system at a pressure of 500 bars. Only reactions or assemblages involving a vapor phase are shown on the diagram, and the horizontal axis gives the composition of the vapor phase in each assemblage at various temperatures. Univariant reactions are represented by points, and the lines represent the intersections of divariant reaction surfaces with the isobaric section. Fig. 3A is drawn approximately to scale, with some distortion near the H_2O composition so that the relationships may be seen, and Figs. 3B and 3C are enlarged to illustrate two ways in which the sub-solidus reaction curves could intersect. In subsequent discussions, only the arrangement in Fig. 3B will be considered.

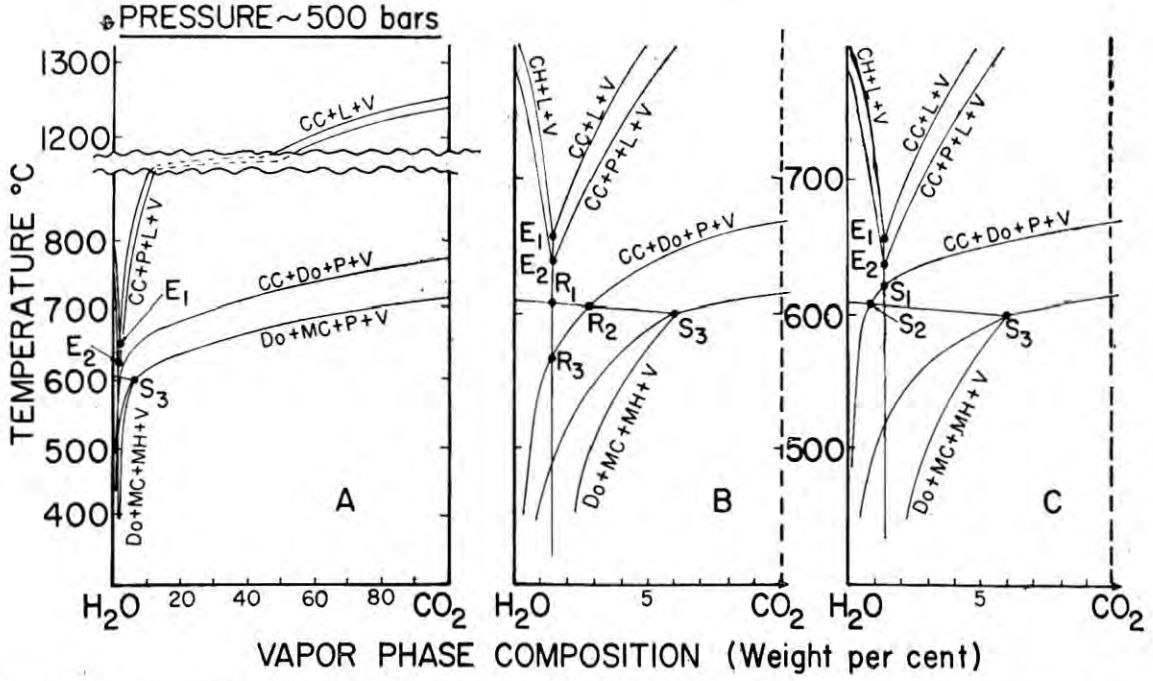

Fig. 3. The system CaO-MgO-CO_2-H_2O. For abbreviations see Table 1. Schematic isobaric section through the petrogenetic model at 500 bars pressure. A. Approximately to scale; relationships near the H_2O axis are not distinguishable. B and C. Alternative arrangements for reactions near the H_2O axis.

The arrangement of the two ternary liquidus reactions (isobaric field boundaries) meeting at the ternary eutectic E_1 is based on experimental data (Wyllie and Tuttle, 1960a; Fig. 10B for 1 kilobar pressure). In the presence of CO_2 at 500 bars pressure, calcite melts at about 1,240°C (Wyllie and Tuttle, 1960a, Fig. 14). When the vapor phase is diluted with H_2O the melting temperature is lowered, and when the vapor phase contains more than about 80 weight per cent of H_2O the melting temperature decreases markedly for each slight increase in H_2O content. This reaction curve meets the portlandite melting curve (isobaric field boundary) at E_1, at 655°C, where the vapor phase composition is very rich in H_2O. The liquidus field boundaries on the vapor-saturated liquidus surface for the quaternary system (Fig. 2) involve the additonal phase periclase. These boundaries are represented by the curves located approximately 25°C below the ternary curves in Fig. 3, and they meet at the quaternary eutectic E_2. Below E_2 there extends a curve for the sub-solidus assemblage, CC + CH + P + V.

The arrangment of the sub-solidus reaction curves meeting at S_3 is based on results from the system MgO-CO_2-H_2O (Walter, Wyllie and Tuttle, 1962, Fig. 6). The three reactions which

involve the dissociation of magnesite, the dissociation of brucite, and the conversion of magnesite to brucite have been illustrated in a 1 kilobar isobaric section through the petrogenetic model by Wyllie (1962, Fig. 3). Their positions within the petrogenetic model are changed only slightly by the presence of dolomite as an additional phase. The assemblage Do+MC+P+V represents the dissociation of magnesite, in the presence of dolomite, and the reaction curve therefore extends from the point for the dissociation of magnesite in the presence of pure CO_2, to lower temperatures as the vapor phase is diluted with H_2O. This meets the similar curve for the dissociation of brucite at S_3, and extending to lower temperatures from this point is a curve for the conversion of brucite to magnesite, in the presence of dolomite. The fourth curve extending to lower temperatures from S_3 is necessitated by the presence of dolomite, but this need not concern us in the present discussion. The temperature and the vapor phase composition for S_3 have been determined experimentally by Walter, Wyllie and Tuttle (1962) at presures of 1 and 4 kilobars. Greenwood (1962) has discussed similar reaction curves in thermodynamic terms.

In the presence of CO_2 at 500 bars pressure, dolomite dissociates at a temperature about 60°C higher than magnesite (Fig. 1), and in Fig. 3 the reaction curve for the dissociation of dolomite in the quaternary system has therefore been placed about 60°C higher than that for the dissociation of magnesite (in the presence of dolomite). This curve meets that for the dissociation of brucite at the univariant point R_2. Other univariant sub-solidus reactions are represented by the points R_1 and R_3, where the dissociation reaction curves intersect the subsolidus curve below the eutectic E_2.

Fig. 3 shows that although liquid, dolomite, and magnesite are simultaneously stable through a limited temperature range at 500 bars pressure, these phases cannot coexist because each phase assemblage is in equilibrium with a vapor phase of different composition. In the presence of an aqueous vapor phase with the composition of the vapor in equilibrium with liquidus near the eutectic E_2, dolomite and magnesite, as well as brucite, are stable only at temperatures lower than that of the eutectic E_2.

An isothermal line can be drawn through Fig. 3A in such a way that it intersects the curves for the reactions CH+P+L+V, CC+P+L+V, CC+Do+P+V, and Do+MC+P+V. The points of intersection give the compositions of the vapor phase in each assemblage at 500 bars pressure and at the temperature of the isothermal line. Since the compositions of the crystalline phases are known (neglecting solid solution) and the liquid composition is known approximately, a knowledge of the vapor phase composition provides sufficient information for the construction of an isobaric isothermal phase diagram for the quaternary system. Fig, 4 illustrates such a diagram for 1 kilobar pressure and 770°C; these conditions were selected because the vapor phase compositions are better known

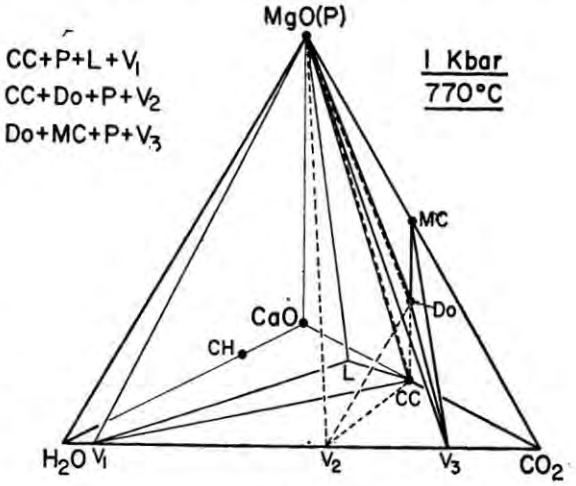

Fig. 4. The system CaO–MgO–CO_2–H_2O. For abbreviations see Table 1. Isobaric isothermal section at 1 kilobar pressure and 770°C showing three 4-phase tetrahedra.

experimentally at 1 kilobar pressure than the schematic values for 500 bars given in Fig. 3. The four-phase tetrahedron for CH+P+L+V has been omitted for simplicity.

Fig. 4 shows that the four-phase tetrahedron

involving liquid, CC+P+L+V_1, is separated from the four-phase tetrahedron involving dolomite, CC+Do+P+V_2, by the three-phase space CC+P+V_{1-2}. The plane CC–P–V_1 is a barrier separating the liquid from the large stability fields for dolomite and magnesite. With decreasing temperature, the vapor phases V_1, V_2 and V_3 all change composition towards H_2O. It can be seen from Fig. 3 that in a given temperature interval V_2 and V_3 change composition for more than does V_1, so that V_2 and V_3 approach V_1 in composition. At 500 bars pressure (Fig. 3) and at 1 kilobar pressure (Wyllie and Tuttle, preliminary results) the liquid is consumed in a eutectic reaction (E_2) before V_2 overtakes V_1 so that dolomite cannot reach the liquidus. However, at higher pressures, V_2 does overtake the vapor phase of a four-phase tetrahedron involving a liquid phase, and then dolomite does have a stability field on the liquidus.

The Effect of Pressure

Fig. 1 shows that the temperatures of the univariant melting reactions involving a vapor phase decrease slightly with increasing pressure. The temperatures of the univariant dissociation reactions, on the other hand, increase appreciably with increasing pressure. In isobaric sections through the petrogenetic model at increasing pressures, therefore, the divariant sub-solidus reaction curves will move upwards in the section until they intersect the liquidus reaction curves which simultaneously are moving downwards. It can be seen in Fig. 3B that as the pressure is increased above 500 bars, the divariant curve for the dissociation of brucite, $R_1R_2S_3$, will intersect the solidus at E_2, generating an invariant point (Q_1) where E_2 and R_1 become coincident, and then move to higher temperatures; brucite will then be stable on the liquidus. At a higher pressure, the divariant curve for the dissociation of dolomite, R_2R_3, will in turn intersect the solidus at an invariant point (Q_2), producing a stability field for dolomite on the liquidus. These changes are illustrated in detail in Figs. 5 and 6.

Fig. 5 is a schematic PT projection for the quaternary system which is based on the available experimental data, a qualitative consideration of the effect of pressure on the reactions in the petrogenetic model (Figs. 3 and 6), and the application of Schreinemakers' principles for the invariant points Q_1, Q_2, and Q_3. The univariant reaction curves labeled E refer to

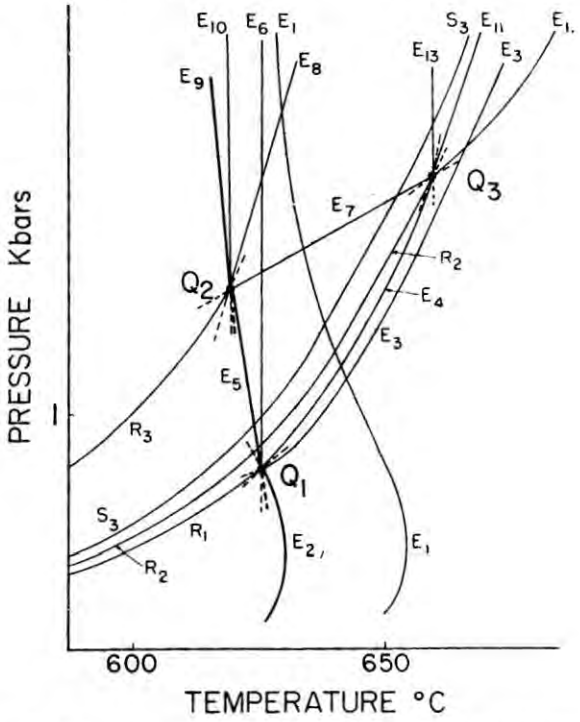

Fig. 5. The system CaO–MgO–CO_2–H_2O. For key to the reactions see Table 1. Schematic univariant reactions around invariant points Q. The reactions E involve a liquid phase, whereas R and S are sub-solidus. The heavy line through Q_1 and Q_2 gives the temperature of beginning of melting (equivalent to E_2 in Fig. 1).

reactions including a liquid phase, and the subsolidus reaction curves are labeled R or S. Table 1 lists the phase assemblages for each reaction.

The three reactions R_1, R_2, and S_3 lie at temperatures just below the dissociation curve for brucite (Figs. 1 and 3B). The reaction E_1 is the eutectic melting reaction in the ternary system CaO–CO_2–H_2O (Figs. 1 and 3B). The

heavy line corresponds to the dashed line E_2 in Fig. 1, representing the quaternary eutectic melting reaction. In Fig. 5, this is divided into three portions by the invariant points Q_1 and Q_2, each portion corresponding to one of the three assemblages listed in Fig. 1: E_2 represents the assemblage CC + CH + P + L + V, E_5 the assemblage CC+CH+MH+L+V, and E_9 the assemblage CC+CH+Do+L+V.

Fig. 6 provides a key to the reactions plotted in Fig. 5. Fig. 6A is reproduced from Fig. 3B, an isobaric section through the petrogenetic model at 500 bars pressure. The curve *mm* represents the upper stability limit of brucite, and *dd* represents the upper stability limit of dolomite. The invariant point Q_1 is generated at a pressure in the region of 1 kilobar when R_1 meets E_2, as shown in Fig. 5. Four reaction curves extend to higher pressures above Q_1, each including brucite and liquid in the phase assemblage. The vapor-absent reaction (E_6, Fig. 5) is not represented in the petrogenetic model, Fig. 6C.

At a higher pressure, the reaction R_3 meets the quaternary eutectic E_5 as shown in Fig. 5 (see also Fig. 6C). Above this pressure, dolomite becomes stable on the liquidus below the univariant reactions E_7 and E_8 (Fig. 6E). Recent studies by Carapezza suggest that the point Q_2 may occur in the region of 1.5 kilobars (personal communication). The third invariant point, Q_3, is generated when the reactions E_4, E_7, and R_2 become coincident (see Fig. 6E). Another invariant point may be generated at a very high pressure when the reactions S_3 and E_{11} become coincident. The composition of the vapor phase involved in the reaction S_3 becomes richer in H_2O with increasing pressure. It contains 94 weight percent of H_2O at 1 kilobar, and 96 weight percent of H_2O at 4 kilobars (Walter, Wyllie and Tuttle, 1962, Fig. 6), but since the vapor phase in the reaction E_{11} probably contains at least 98 or 99 weight percent of H_2O, considerably higher pressures would be required before the reaction curves would intersect. Above this hypothetical invariant point, magnesite would have a field of stability on the liquidus.

The right-hand diagrams in Fig. 6 illustrate schematically the primary crystalline phases on the vapour-saturated liquidus surface of the quaternary system at various pressures. Fig. 6B corresponds to the situation illustrated in Fig. 2, where periclase, portlandite, and calcite are the only crystalline phases stable in equilibrium with liquids and vapours. Fig. 6D illustrates the appearance of brucite on the vapor-saturated liquidus surface, and Fig. 6F shows the field for dolomite. With increasing pressure the dolomite field expands until it separates the field for brucite from the calcite field. The stability fields for brucite and dolomite in equilibrium with liquid extend towards CaO from the vapor-saturated liquidus surface, just as the fields for portlandite and calcite do in Fig. 2. If magnesite does become stable on the liquidus at very high pressure, its stability field would replace and extend from the peritectic E_{11} in Fig. 6H.

The phase assemblages at the univariant points and divariant curves in the petrogenetic model diagrams can be read directly from the diagrams showing the liquidus surface. For example, the univariant assemblage E_5 in Fig. 6C consists of L + V plus the three crystalline phases CC + CH + MH occurring around the point E_5 in Fig. 6D. The divariant assemblage between E_4 and E_5 in Fig. 6C consists of L + V plus the two crystalline phases CC + MH occurring on either side of the line E_4E_5 in Fig. 6D.

FeO as an Additional Component

Addition of iron to the system introduces the minerals siderite, ankerite, and iron oxides. It also introduces problems involving oxidation states and a vapor phase of more complex composition than $CO_2 + H_2O$, which makes both experimental and theoretical analysis of the system difficult. However, it is known that siderite dissociates at much lower temperatures than magnesite and dolomite. At 1 kilobar

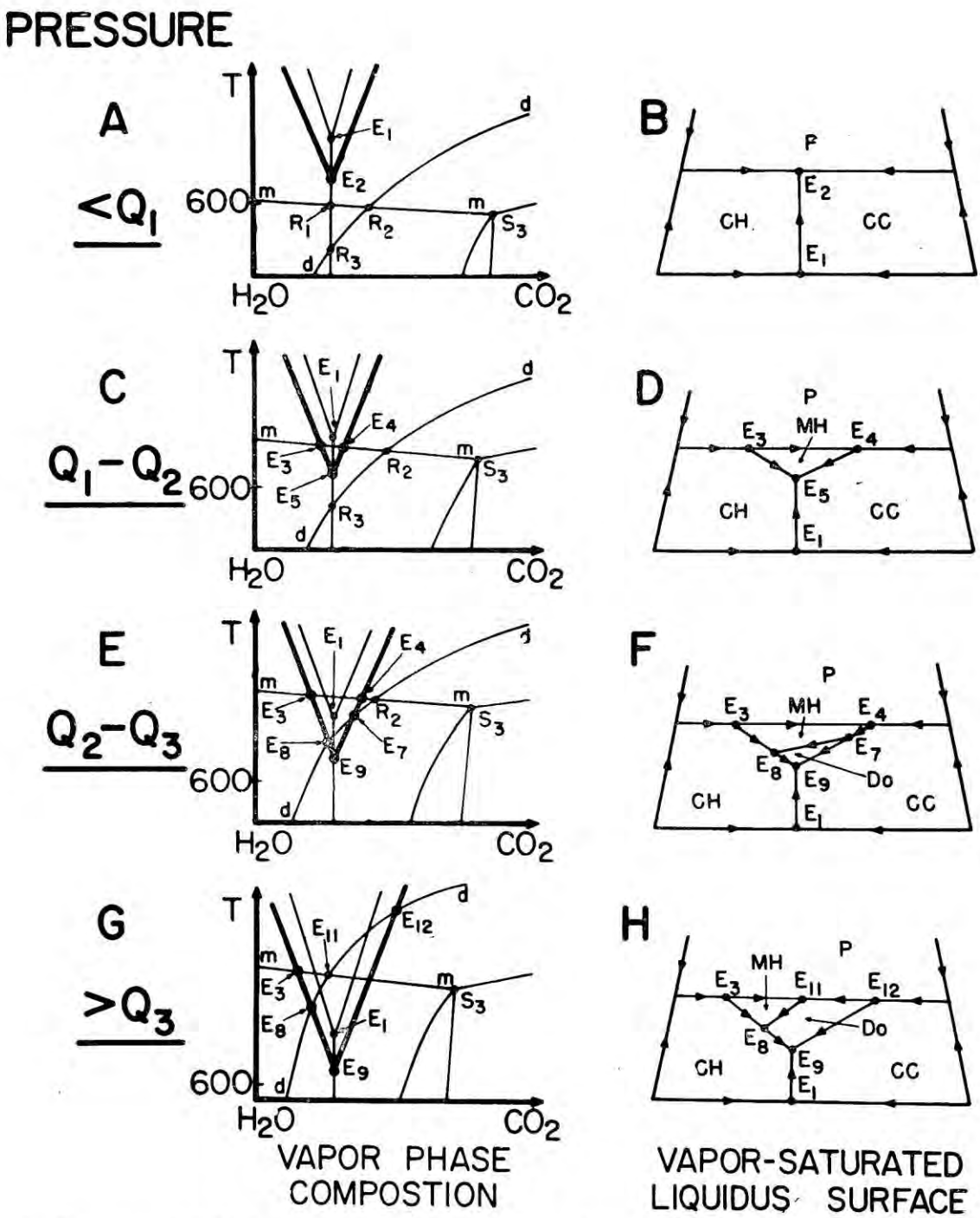

Fig. 6. The system CaO-MgO-CO_2-H_2O. For abbreviations see Table 1. *mm* is the upper temperature stability limit of brucite, and *dd* is the same for dolomite. The heavy lines give the temperature of beginning of melting in the presence of each vapor phase composition. Schematic diagrams illustrating the effect of increasing pressure on the phases stable on the vapor-saturated liquidus surface. Compare the right-hand diagrams with Fig. 2, and the left-hand diagrams (isobaric sections through the petrogenetic model) with Fig. 3. The univariant reactions E, R, and S are illustrated in Fig. 5 and tabulated in Table 1.

pressure, for example, magnesite dissociates at 820°C (Fig. 1), whereas siderite dissociates at a temperature near 450°C (preliminary results of Raynor and Wyllie). The dissociation temperature is very dependent upon the oxygen fugacity in the system (French and Eugster, 1963). The isobaric dissociation curve for siderite in the petrogentic model (with the vapor phase components other than CO_2 being plotted jointly as "H_2O") would thus be located well below the corresponding curves for magnesite and dolomite shown in Fig. 3. Therefore, much higher pressures would be required for the siderite dissociation curve to reach the solidus in the system, and only then could siderite become stable on the liquidus. A moderate amount of FeO in the system would probably lead to the precipitation of ankerite rather than dolomite. Any excess of iron above that soluble in ankerite would probably be precipitated as iron oxides through a wide pressure range, and only at very high pressures would the precipitation of siderite from the liquid be possible.

Processes of Crystallization

Crystallization may proceed in this system as a result of changes in temperature, changes in the pressure, and changes in the composition of the vapor phase in equilibrium with the liquid. The path of crystallization, and the sequence of minerals precipitated, is therfore dependent upon several variables. The effects of each of these must be considered in turn.

At sufficiently high, constant pressure, Fig. 6H shows that for a liquid coexisting with a vapor and precipitating initially calcite, the calcite would be joined at a lower temperature by one of the phases periclase, dolomite, or portlandite. With fractional crystallization the final liquid at E_9 would precipitate calcite, dolomite, and portlandite. Thus, under isobaric conditions, the sequence of crystallization for the carbonates is calcite, followed by calcite plus dolomite.

Consider a liquid on the primary field for calcite in Fig. 6H, near to the field boundary $E_{12}E_9$, coexisting with calcite and vapor. An increase of pressure causes the size of the dolomite field to increase, and the field boundary could therefore cross the liquid composition, placing the liquid in the primary phase field of dolomite. If equilibrium is maintained, the calcite crystals in the original liquid would be converted to dolomite. Thus, we could have the same liquid composition precipitating calcite at lower pressures, and dolomite at higher pressures, with no change in temperature or vapor phase composition. The detailed change in phase relationships are actually quite complex.

Now, consider a liquid on the field boundary $E_{12}E_9$ in Fig. 6H, coexisting with calcite, dolomite, and vapor. If the vapor phase composition is enriched in H_2O under isobaric isothermal conditions, and if equilibrium is maintained, Fig. 6G shows that the calcite would dissolve, and the liquid composition would move across the dolomite field, with the dolomite dissolving. Conversely, if the vapor phase were enriched in CO_2 under isobaric, isothermal conditions, the liquid would crystallize completely, leaving an assemblage of calcite and dolomite.

The final liquid produced by fractional crystallization of synthetic carbonatite magmas in this system, as in other related systems, always precipitates hydrous minerals such as portlandite. Portlandite has not been reported from carbonatites. It is possible that the extremely H_2O–rich composition of the vapor phase in equilibrium with the final liquids (e.g. E_9 in Fig. 6G) may rarely be attained in natural occurrences because of the restraints imposed by the regional controls. If there is a regional limit for the maximum H_2O–content of vapors, this could cause the carbonatite magmas to crystallize completely to carbonates, with all H_2O being given off to the vapor phase. For example, crystallization could be completed at some point on the field boundary $E_{12}E_9$ in Fig. 6H, before the vapor phase composition reached E_9 (see Fig. 6G). For this to occur, there would have to be rather sensitive regional control on the

vapor phase composition, because the temperature of the solidus in Fig. 6G is clearly very sensitive to small changes in vapor phase composition.

Comparison with Natural Carbonatites

There are so many ways in which liquids in the system $CaO–MgO–FeO–CO_2–H_2O$ could crystallize, that any detailed exposition of how differentiation might occur would not be meaningful. It has been demonstrated in a general way how the paths of crystallization and the nature of the crystalline phases being precipitated or resorbed are affected by changes in temperature, in pressure, and in the compositions of coexisting vapor phases. The effect of each variable was considered in turn, but it is unlikely in nature that only one of these variables would be changing during crystallization. All three may be included among the regional factors which exert independent, external controls on the behaviour of a carbonatite magma.

Crystallization would proceed in a carbonatite magma as a result of decreasing temperature. However, since explosive activity is an important feature in the history of carbonatite complexes, pressure variations may play at least as significant a role in their crystallization as does decrease in temperature. Furthermore, it is probable that the vapor phase composition during the crystallization of a carbonatite magma would not be governed entirely by the crystallizing magma, but in part, at least, by the regional conditions. The chemical potentials of H_2O and CO_2 and, in a general way, therefore, the compositions of the vapor phase may be determined by the regional chemical potential gradients. However, during periods of volcanic activity, significant deviations from the regional gradients may be anticipated, and it may well be that regional chemical potential gradients cease to have any local significance.

It has been shown that at a sufficiently high pressure, the sequence of precipitation of carbonates from the system $CaO–MgO–FeO–CO_2–H_2O$, with decreasing temperature, could be calcite, dolomite, and finally siderite. The intrusion of carbonatites at Chilwa Island (Garson and Smith, 1958) follows the same time sequence, with calcitic sövite being followed by the emplacement of ankeritic sövite, and finally by sideritic carbonatites. This intrusion sequence, then, could be explained by crystallization differentiation of a carbonatite magma.

The composition of the carbonate minerals being precipitated from a synthetic carbonatite magma is pressure dependent. At low pressures, a liquid can precipitate only calcite and not dolomite or siderite ; but at higher pressures the same liquid would precipitate dolomite or ankerite, with siderite being precipitated only at very high pressures. This pressure effect may provide an explanation for von Eckermann's demonstration (1948, p. 148) that the sövite magma (calcite) in the Alnö carbonatite magma formed at an upper level (estimated pressure 900 bars), whereas the beforsite magma (dolomite) formed at greater depth (estimated pressure 2,400 bars).

THE SYSTEM $CaO–CaF_2–P_2O_5–CO_2–H_2O$

Apatite is a ubiquitous accessory mineral in carbonatites, and it may become highly concentrated in bands and lenses. The behaviour of apatite in synthetic carbonatite magmas has been studied experimentally by G. M. Biggar, who determined the solid-liquid-vapor phase relationships in the systems $CaO–CaF_2–P_2O_5–H_2O$ and $CaO–P_2O_5–CO_2–H_2O$ (Fig. 7) for his Ph.D. degree at the University of Leed, (Biggar, 1962). The results were presented orally in 1962 (Biggar and Wyllie, 1962), and some possible applications of the work have been published (Wyllie, Cox, and Biggar, 1962). The main results of the study, extracted from manuscripts in preparation by Biggar and Wyllie, are outlined below.

Fig. 7 shows the two quaternary systems which were investigated, and the inner tetrahedra marked by the heavy lines show the composition range of starting mixtures which were used. The phase relationships at 1 kilobar

pressure are illustrated in these subtetrahedra in Fig. 8. The phase relationships do not change significantly within the pressure range 500 bars to 4 kilobars. Temperatures shown in Figs. 8 and 9 were measured experimentally, except for those enclosed in parentheses, which were estimated.

CaO-P_2O_5-CO_2-H_2O

Liquidus field boundaries within the composition join $CaCO_3$-$Ca(OH)_2$-$Ca_3(PO_4)_2$-H_2O at 1 kilobar pressure are illustrated in Fig. 8. This join is not a quaternary system because calcite melts incongruently, and the vapor phase coexisting with the liquids has compositions

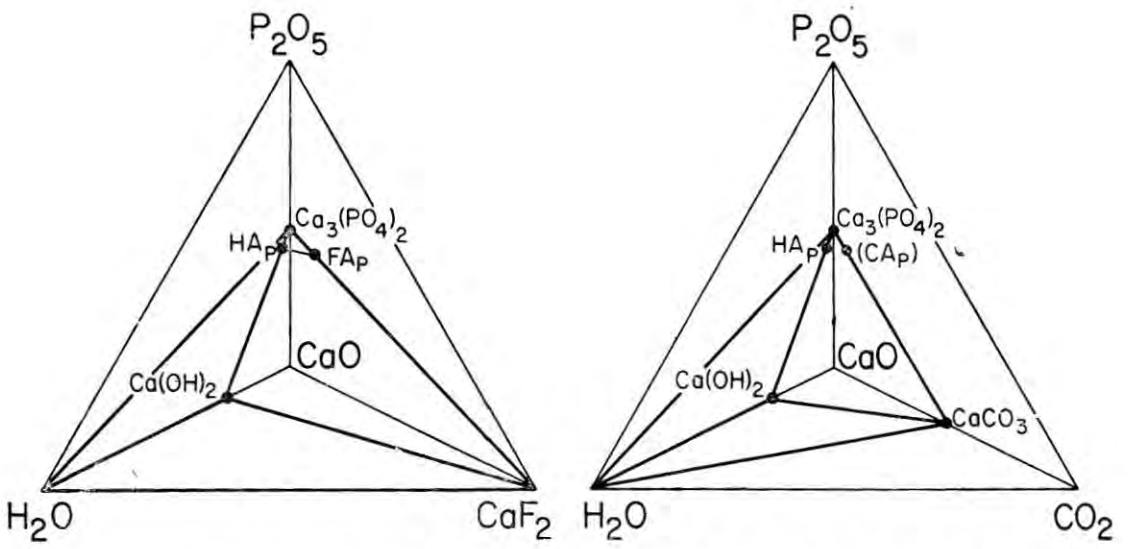

Fig. 7. The compositions investigated in the systems CaO-CaF_2-P_2O_5-H_2O and CaO-P_2O_5-CO_2-H_2O are indicated by the subsidiary tetrahedra marked by heavy lines.

CaO-CaF_2-P_2O_5-H_2O

Fig. 8 shows the liquidus field boundaries in the quaternary system $Ca(OH)_2$-CaF_2-$Ca_3(PO_4)_2$-H_2O at 1 kilobar pressure. The join $Ca(OH)_2$–CaF_2–$Ca_3(PO_4)_2$ is a ternary eutectic system at this pressure, with only a few weight percent of $Ca_3(PO_4)_2$ soluble in the low temperature liquid on the join $Ca(OH)_2$–CaF_2. The liquidus surface with apatite as a primary phase rises steeply from the ternary eutectic at 675°C. In the presence of H_2O the phase relationships are very similar. A few percent of H_2O dissolves in the ternary liquids, depressing the liquidus temperature by small amounts. The eutectic at 665°C is the minimum liquidus temperature in the system, and this liquid coexists with fluorite, portlandite, apatite (composition 55 hydroxylapatite, 45 fluorapatite, weight percent), and a vapor phase composed essentially of H_2O.

varying between H_2O and CO_2. The join $CaCO_3$-$Ca(OH)_2$ does not remain binary above about 950°C, which causes the liquidus field boundaries to leave this composition tetrahedron near $CaCO_3$. Hydroxylapatite occurs in the system, and no definite evidence for the formation of a carbonatapatite was obtained.

Despite these differences from the fluorite system, the general pattern of the phase relationships is very similar. Only a few weight percent of $Ca_3(PO_4)_2$ is soluble in the synthetic carbonatite magma near the join $CaCO_3$–$Ca(OH)_2$, and the primary field for apatite rises steeply from the quaternary eutectic at 639°C on the vapor-saturated liquidus surface. The liquid at the eutectic coexists with calcite, portlandite, apatite (mainly hydroxylapatite, with possibly some carbonatapatite in solid solution), and a vapor phase composed of $H_2O + CO_2$ which is very rich in H_2O.

$Ca_3(PO_4)_2$–CaF_2–$CaCO_3$–$Ca(OH)_2$

Fig. 9 illustrates schematically the liquidus phase relationships in this system at a pressure of 1 kilobar. It is based on results for the system $CaCO_3$–$Ca(OH)_2$–CaF_2 (Gittins and Tuttle, 1964) and the results shown in Fig. 8. No vapor phase is represented in the diagram, but because calcite melts incongruently at this pressure there is a vapor phase rich in CO_2 in part of the system. The quaternary eutectic liquid, at an estimated temperature of 575°C, coexists with calcite, fluorite, and portlandite. Addition of H_2O to the system would not change the relationships significantly; a few weight percent of H_2O would dissolve in the liquid causing liquidus temperatures to be depressed slightly (compare Fig. 8).

and Biggar (1962) has shown that these relationships persist through a wide pressure range.

Apatite crystals coexisting in equilibrium with liquid or vapor were small and equant, whereas those precipitated from a melt during a rapid quench formed acicular prisms exhibiting a variety of parallel and skeletal growths (Wyllie, Cox, and Biggar, 1962). Liquids in the system are extremely fluid. It was observed that even the long apatite needles precipitated from the liquid during a quench tended to settle towards the bottom of the capsule containing the charge.

Segregation of Apatite in Carbonatites

The experimental data establish the facts that a carbonatite magma containing initially

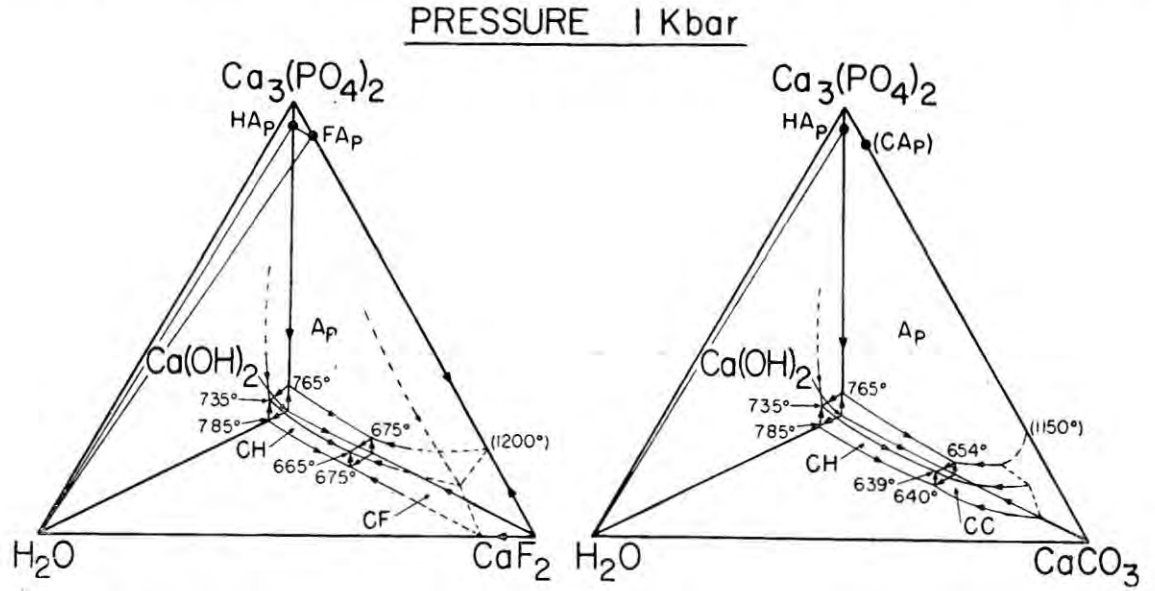

Fig. 8. Liquidus phase relationships encountered in the systems of Fig. 7 at 1 kilobar pressure. The phase relationships in the $CaCO_3$ tetrahedron are quaternary, but they cannot be represented in this tetrahedron; the complete tetrahedron in Fig. 7 is required for representation of the vapor phase composition, for example. Temperatures in parentheses were estimated.

Figs. 8 and 9 show that the presence of a small percentage of P_2O_5 in a synthetic carbonatite magma is sufficient to produce apatite as a crystalline phase on the liquidus. The diagrams also show that calcite and apatite can be precipitated simultaneously from a synthetic carbonatite magma through a wide temperature range, more than a few percent of P_2O_5 would begin to precipitate apatite before calcite, and that calcite and apatite could be co-precipitated through a wide temperature interval. The synthetic carbonatite magmas are very fluid, and crystal settling occurs with both calcite and apatite. Given a carbonatite magma precipita-

ting these minerals, there is a good chance that partial segregation of the minerals could occur as a result of crystal settling during quiet periods. With the onset of explosive activity, producing movement within the magma column, any accumulations of apatite-rich mixtures would become streaked out forming bands parallel to the flow structures in the crystallizing magma. There is little difficulty in accounting for the observed flow banding and segregation of apatite on the basis of a magmatic carbonatite intrusion.

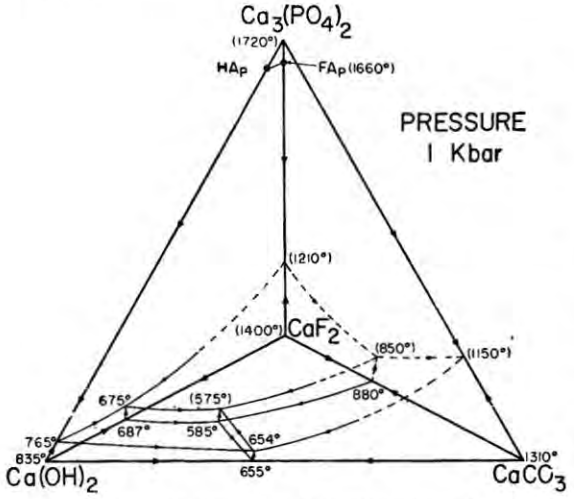

Fig. 9. Schematic diagram of the liquidus phase relationships in the system $Ca_3(PO_4)_2$–CaF_2–$CaCO_3$–$Ca(OH)_2$ at 1 kilobar pressure. Temperatures in parentheses were estimated.

Detailed examination of apatites in carbonatites might be worth while. For example, material enclosed by dendritic or skeletal apatites could provide information about the composition of the magma from which the apatites crystallized. This might be one of the most promising places to seek portlandite.

CONCLUSION

The geological history of a carbonatite complex is undoubtedly complicated, probably with different processes occurring simultaneously within the magma, as well as in succession. Repeated intrusions of fluid, reactive volatile-charged carbonatite magma may be followed by differentiation, the action of vapors and solutions given off by the crystallizing carbonatite or emanating from greater depths, metasomatism occurring within as well as around the complex, and the development of explosion breccias with concommitant changes in pressure on the magma at greater depth. Superimposed on the effects of these processes may be the effects of remobilization, plastic flow, later metamorphism, shearing and recrystallization. Reconstruction of the history of each carbonatite complex is the responsibility of the geologists studying them in the field, and the function of the experimental petrologist is to provide a foundation of reasonable possibilites for sound reconstruction. Conclusions reached from experimental and theoretical examination of the phase relationships in the systems CaO-MgO-FeO-CO_2-H_2O and CaO-CaF_2-P_2O_5-CO_2-H_2O indicate that the intrusion sequences recorded at some carbonatite complexes could be explained on the basis of differentiation processes occurring during the crystallization of a carbonatite magma. Changes in temperature, is pressure, and in vapor phase composition may all play an important role in crystallization processes. This adds support to the magmatic hypothesis when such an origin is proposed on the basis of field studies.

ACKNOWLEDGMENTS

We are grateful to O. F. Tuttle for his comments during preparation of the manuscript, to D. K. Bailey and H. J. Greenwood for their review of part of the manuscript. Research in the "dolomite" system was supported by National Science Foundation Grants G 19588 and GP-1870, and research in the "apatite" systems was supported by the Department of Scientific and Industrial Research.

REFERENCES

BIGGAR, G. M. (1962) High pressure high temperature phase equilibrium studies in the system CaO-CaF_2-P_2O_5-H_2O-CO_2 with special reference to the apatites : *Ph.D. dissertation*, University of Leeds, England.

BIGGAR, G. M. AND WYLLIE, P. J. (1962) Solid-liquid-vapor phase relationships at high pressures in parts of the system CaO-CaF_2-CO_2-H_2O-P_2O_5 (Abstr.) : *Jour. Geophys. Res.*, Vol. 67, pp. 3542-3543.

ECKERMANN, H. von, (1948) The alkaline district of Alnö Island : *Sverig Geol. Unders.* Ser. Ca, No. 36.

FRENCH, B. M. AND EUGSTER, H. P. (1963) Stability of siderite, $FeCO_3$ (Abstr.); *Geol. Soc. Amer.* Spec. Paper No. 73, pp. 155-156.

GARSON, M. S. AND SMITH, W. CAMPBELL, (1958) Chilwa Island : *Geol. Surv. Nyasaland* Memoir 1.

GITTINS, J. AND TUTTLE, O. F. (1964) The system CaF_2-$Ca(OH)_2$-$CaCO_3$: *Amer. Jour. Sci.*, Vol. 262, pp. 66-75.

GOLDSMITH, J. R. AND HEARD, H. C. (1961) Sub-solidus phase relationships in the system $CaCO_3$-$MgCO_3$: *Jour. Geol.*, Vol. 69, pp. 45-74.

GREENWOOD, H. J. (1962) Metamorphic reactions involving two volatile components : *Carnegie Inst. Washington Year Book*, Vol. 61, pp. 82-85.

HARKER, R. I. AND TUTTLE, O. F. (1955) Studies in the system CaO-MgO-CO_2. Part 1. The thermal dissociation of calcite, dolomite and magnesite : *Amer. Jour. Sci.*, Vol. 253, pp. 209-224.

———(1956) Experimental data on the P_{CO_2}-T curve for the reaction : calcite+quartz=wollastonite+carbon dioxide : *Amer. Jour. Sci.*, Vol. 254, pp. 239-256.

KING, B. C. AND Sutherland, D. S. (1960) Alkaline rocks of eastern and southern Africa, Parts I, II, and III. *Sci. Progress*, Vol. 48, pp. 298-321, 504-524, 709-720.

PECORA, W. T. (1956) Carbonatites : a review. *Bull. Geol. Soc. Amer.*, Vol. 67, pp. 1537-1556.

SMITH, W. CAMPBELL, (1956) A review of some problems of African carbonatites : *Quart. Jour. Geol. Soc. Lond.*, Vol. 112, pp. 189-219.

WALTER, L. S. WYLLIE, P. J. AND TUTTLE, O. F. (1962) The system MgO-CO_2-H_2O at high pressures and temperatures : *Jour. Petr.*, Vol. 3, pp. 49-64.

WYLLIE, P. J. (1962) The petrogenetic model, an extension of Bowen's petrogenetic grid : *Geol. Mag.*, Vol. 99, pp. 558-569.

———(1965) Melting relationships in the system CaO-MgO-CO_2-H_2O, with petrological applications : *Jour. Petr.*, Vol. 6, pp. 101-123.

WYLLIE, P. J. AND TUTTLE, O. F. (1960A) The system CaO-CO_2-H_2O and the origin of carbonatites : *Jour. Petr.*, Vol. 1, pp. 1-46.

———(1960B) Experimental verification for the magmatic origin of carbonatites : *Proc. 21st Int. Geol. Congress, Copenhagen*, Vol. 13, pp. 310-318.

WYLLIE, P. J., COX, K. G.. AND BIGGAR, G. M. (1962) The habit of apatite in synthetic and igneous systems : *Jour. Petr.*, Vol. 1, pp. 1-46.

DISCUSSION

A. D. Edgar (Dept. Geology, University of Western Ontario, London, Canada) : Have you considered the effect of the addition of alkalies to the systems discussed in this paper? Would the replacement of CaO by Na_2O and K_2O in the systems CaO-MgO-FeO-CO_2-H_2O and CaO-CaF_2-P_2O_5-CO_2-H_2O be expected to lower the final crystallization temperatures?

Author's reply: Addition of Na_2CO_3 and K_2CO_3 would definitely lower the final crystallization temperature in these systems. The effect of alkalis on the melting of $CaCO_3$ has been known for many years. For example, the liquidus for the system $CaCO_3$-Na_2CO_3-K_2CO_3 was described by P. Niggli in 1919 (*Z. anorg. u. allgem. Chem.*, Vol. 106, p. 131). More recently J. Gittins and O. Tuttle have studied the melting relationships in the systems CaO-Na_2O-CO_2-H_2O and CaO-K_2O-CO_2-H_2O at 1 kilobar pressure, and some of their results will be included in the forthcoming book on "*Carbonatites*" (editors J. Gittins and O. F. Tuttle ; John Wiley & Sons Inc.) The possible role of alkali carbonatite magma was mentioned briefly by P. J. Wyllie and O. F. Tuttle in a note on "Carbonatitic lavas" (*Nature*, Vol. 194, p. 1269, 1962).

MINERALOGICAL SOCIETY OF INDIA, IMA VOLUME, 1966
INTERNATIONAL MINERALOGICAL ASSOCIATION, PAPERS, FOURTH GENERAL MEETING

THE STRONTIUM AND BARIUM CONTENTS OF THE ALNÖ CARBONATITES

HARRY von ECKERMANN
Geological Research Laboratory, Ripsa, Sweden

ABSTRACT

A series of new analyses of alvikites and beforsites indicates that the earlier established distribution of barium and strontium in the carbonatites of the Alnö region (1952), is not generally applicable. The Sr:Ba-ratio has been found to vary from 0.02 to 14.00.

While the previous sövite analyses showed a Sr:Ba-ratio of 0.27 to <0.01, in the sövite boulders of a breccia, strontium exceeds barium, the ratio rising to 6.60.

INTRODUCTION

A paper on the distribution of strontium and barium in the rocks of the Alnö alkaline region on the Swedish east-coast was published by the present author in the year 1951. Since then a series of new analyses has been made of which several refer to carbonatites, either sövites or ankeritic dolomitic dike rocks (beforsites).

DISSCUSSION OF OLD AND NEW ANALYSES

As I pointed out in my previous paper *Rankama's* and *Sahama's* (1950, p. 457) statement

" That the behaviour of barium very much resembles that of strontium, and the rocks rich in one of the metals are usually rich in the other as well "

is only moderately true. The earlier analyses from Alnö, presented in Table 1, comprises sövites rich in both barium and strontium as well as sövites rich in barium and poor in strontium.

The new analyses, presented in Table 2, still more emphasize the discrepancy. While the Sr : Ba-ratio of the sövites of the first series of analyses did not rise above 0.27, one of the new series runs as high as 6.24, the lowest value being 2.19. There is a definite difference of level within the volcanic vent between these two series of sövites. The first one was sampled from sövites at the present erosion surface, while the second one represents sövites brought up from deeper levels, either as boulders or rather as rounded blocks and matrix of the volcanic breccia at Sälskär shoals (1960), or as boulders and fragments within the alnöite-breccia at Hovid (1948, p. 100). This seems to indicate a concentration of barium towards the upper part of the sövite body and a corresponding lowering of the Sa : Ba-ratio, while at lower levels, say about 1-2 km below the present erosion surface strontium is the dominant metal.

TABLE 1

	Gram/ton		Number of analyses		Average gram/ton		Ratio
	Ba	Sr	Ba	Sr	Ba	Sr	Sr : Ba
Leucocratic alkaline dikes	720–5.500	85–1.020	4	3	3.430	760	0.21
Sövites	450–2.610	25–0.120	5	5	1.300	360	<0.01–0.27
Alnöites	750–2.240	90–0.340	4	5	1.700	270	0.16
Kimberlites	2.330–2.420	45–0.540	3	2	2.390	270	0.11
Beforsites (dolomitic carbonatites)	<45–5.470	<45–2.540	7	14	2.320	660	0.29
Alvikites (calcitic carbonatites)	270–6.900	<25–2.115	8	12	2.390	400	0.17
Exception : Beforsite rich in Sr	990	6.260	1	1	990	6.260	6.31
Number of analyses			32	42			

As to the beforsites, the low average value of the earlier main series, 0.29, is both higher and lower than the individual values of the four new analyses, which vary between 0.002 and 13.00. The first named series include, however, one single dike of a ratio >1, which I previously believed to be an unusual exception, *viz.* the beforsite dike at Stavreviken with a Sr : Ba-ratio of 6.31 (1948). In the case of the beforesites no relation of the Sr : Ba-ratio to their depth within the volcanic vent has been discovered. The same may be said about the alvikitic and beforsitic kimberlites, where the lava column, where they accumulated, forming carbonatite bodies. The earlier analyzed beforsites as well as beforsitic kimberlites were all sampled at the erosion surface, while those analyzed more recently were derived from tunnels and drillholes up to 200 m below the surface. While the former generally contained very few discernible globules in thin slides, the latter contained considerably more. As an analysis of the globules proved impossible on account of the difficulty of their separation from the rock, the Sr : Ba-ratio of them remains unknown in both cases.

TABLE 2

	Gram/ton		Number of analyses		Average gram/ton		Ratio
	Ba	Sr	Ba	Sr	Ba	Sr	Sr : Ba
Borengite	1.170	90	1	1	1.170	90	0.08
Sövite boulders, volcanic breccia	1.340	8.360	1	1	1.340	8.360	6.34
Sövite-apatite-matrix of breccia	720	1.510	1	1	720	1.510	2.20
Sövite boulders, Alnöite breccia	1.340	2.930	1	1	1.340	2.930	2.19
Alnöite	1.040	920	1	1	1.040	920	0.89
Kimberlites	1.080- 2.690	1.340-2.840	3	3	2.090	1.780	0.44-1.24
Kimberbite-block, tuffitic breccia	270	750	1	1	270	750	2.76
Alvikitic kimberlite	<26	940	1	1	<26	940	>36.50
Beforsitic kimberlite Sr>Ba	180- 540	670-1.170	2	2	360	920	2.17-3.23
Beforsitic kimberlite Sr<Ba	1.970	1.150	1	1	1.970	1.150	0.56
Beforsites Sr>Ba	180- 540	2.340-2.930	2	2	360	1.690	5.42-13.00
Beforsites Sr<Ba	45.250-93.300	130-1.260	2	2	71.250	520	0.002-0.02
Number of analyses			18	18			

variation is even greater, from 0.56 to > 36.50. In the latter case, however, a certain relationship to the occurrence of mica, olivine (serpentine), apatite and carbonate-globules (1961, pp. 34-35) may be traced. According to previously published analyses of the Ba and Sr contents of the Alnö minerals the mica and apatite both contain a fairly high percentage of barium while the strontium is dominant in the serpentine (olivine).

The carbonate-globules, according to my previously advanced suggestion, are but bubbles of carbon fusibles, absorbing mainly Ca, Mg, Fe and Th, U and rare earths during their rise through the alnöite and kimberlite to the top of

Much more work has to be done on the Alnö carbonatites, of which hundreds of samples remain to be analyzed before a reasonable explanation of the variations of the Sr-Br-ratio may be found. Tentatively, I suggest variations in pressure, temperature, content of fusibles (especially flourine) and chemical composition of the mother rock supplying the contents of the globules, to be responsible for the wide range of variations.

So far, the investigation of Sr : Ba-ratios of the Alnö carbonatites do not confirm another statement made by *Quon* and *Heinrich* (1964) at this symposium. They claim, that

" In geologically unquestionable carbonatites strontium *always* exceeds barium by a factor ranging from 6.5 to 55 times (1964) ".

My analyses, quoted above, have all been checked chemically as well as spectroscopically. Consequently, strontium is not, always dominant over barium and I wonder if the Alnö carbonatites really constitute the only departure from this rule.

REFERENCES

von ECKERMANN, H. (1952) The distribution of barium and strontium in the rocks and minerals of the syenitic and alkaline rocks of Alnö Island: *Arkiv f. Min. och Geol. K.V.A.* Bd 1, pp. 367–375.

——(1960) Boulders of volcanic breccia at the Sälskär shoals north of Alnö Island: *Arkiv f. Min. och Geol. K.V.A.* Bd 2, pp. 529–537.

——(1948) The alkaline district of Alnö Island: *S.G.U.* Ser. Ca, No. 36.

——(1961) The petrogenesis of the Alnö Alkaline Rocks, *Bull. Geol. Inst.* University of Uppsala, Vol. XL.

RANKAMA, K. AND SAHAMA, TH. G. (1950) *Geochemistry*, University of Chicago Press.

QUON SHI H. AND HEINRICH E. WM. (1964) Abundance and significance of some minor elements in carbonatitic calcites and dolomites. (Abst.) I.M.A. Fourth general meeting Kimberlite-Carbonatite symposium, New Delhi.

DISCUSSION

E. Wm. Heinrich (Ann Arbor): Our determinations being made on carbonate crystals and not on carbonatite rocks may explain the different results obtained by von Eckermann.

MINERALOGICAL SOCIETY OF INDIA, IMA VOLUME, 1966
INTERNATIONAL MINERALOGICAL ASSOCIATION, PAPERS, FOURTH GENERAL MEETING

THE MINERALS OF THE OKA CARBONATITE AND ALKALINE COMPLEX, OKA, QUEBEC

D. P. GOLD
Department of Geology and Geophysics, The Pennsylvania State University
University Park, Pennsylvania, U.S.A.

ABSTRACT

Of the following minerals, which have been identified from the rocks within and associated with the Oka Complex, some 45 full and partial chemical analyses have been completed on the minerals: calcite, dolomite, siderite, magnesite, ancylite, parisite, strontianite, orthoclase, microcline, albite, labradorite, nepheline, hauynite, augite, titanaugite, sodian augite, diopside, aegerine-augite, aegerine, hornblende, lamprobolite, arfvedsonite, soda-amphibole (probably richterite), tremolite, forsterite, chrysolite, monticellite, serpentine, melilite (all approximately $NaM_{35}Ge_{10}Ak_{55}$), biotite (green and brown varieties), phlogopite, vermiculite, sericite, chlorite, melanite, andradite, grossularite, zirconium garnet, sphene, wollastonite, niocalite, cancrinite, vesuvianite, cebollite, quartz, kaolinite, analcite, natrolite, thompsonite, wairakite, fluorapatite, apatite, wilkeite, britholite, monazite, magnetite, maghemite, hercynite, hematite, ilmenite, rutile, pyrochlore, thorian pyrochlore, perovskite, niobium perovskite, latrappite, periclase, pyrite, chalcopyrite, pyrrhotite, galena, sphalerite, barite, flourite, jarosite.

The minerals in the carbonate rocks reflect the abnormal amounts of Zr, Nb, Ce, La, Nd, Sr, Ba, P, Mn, Ti, Na, K, F, S, Cu, Cr they contain, as do the minerals of the silicate rocks which generally are enriched in Ti, Fe^{2+}, Fe^{3+}, Mn, Mg, Ca, Sr, Ba, P, Zr, Nb, Ce, La, Nd, Cr, CO_2, and deficient in Si and K. Substitution is common, and may account for the anomalous optical properties of some minerals.

The Complex, currently the world's largest single producer of niobium, is a double ring structure $4\frac{1}{2}$ by $1\frac{1}{2}$ miles, and comprises various carbonate rock types, which are intruded by ring dykes, arcuate dykes and cone-sheets of okaite, jacupirangite, melteigite, ijolite, urtite, and juvite. Late dykes of carbonate, alkali lamprophyre, and ijolite rocks occur within and peripheral to the Complex, whereas late alnoite dykes and plugs are located along conjugate planes about the long axis of the Complex which coincides with the crest of the regional Beauharnois arch. Pleistocene and Recent sediments cover much of the Complex, which was emplaced, during Lower Cretaceous times, into Precambrian anorthosite and gneiss, and Palaeozoic sedimentary 'cover' rocks since removed by erosion.

GENERAL STATEMENT

The Oka Complex is located about 20 miles west of Montreal on the north shore of the Lake of Two Mountains, and forms a shallow depression $4\frac{1}{2}$ miles ($6\frac{1}{4}$ km) long by $1\frac{1}{2}$ miles ($2\frac{1}{4}$ km) wide amongst the Oka hills. The Oka hills have a circular outline, which is about 10 miles (15 km) across, and rise to a height of 400 to 700 feet above the surrounding plane. The northwestern half of these hills is underlain mainly by anorthosites and gabbros of the Morin Series, and the southeastern half by paragneisses of the Grenville Series (both Proterozoic). The alkali and carbonate rocks, which constitute the Oka complex, occur in an oval-shaped double ring structure which transgresses the northeasterly trending regional structure almost at right angles; the trend of the long axis being N45°W.

The Oka Complex, together with dykes, sills and plutons of alkaline rocks, are exposed in a broad east-west belt across the St. Lawrence Lowlands, and constitute the Monteregian Petrographic Province. The plutons are exposed as 9 hills, separated by irregular intervals, in a slightly curved belt eastward of Montreal, and vary in composition from olivine perknite, through essexite and akerite to syenite. Locally, in the Montreal area and westward to Oka, a number of diatreme breccias, alnöite dykes and plugs, and alnöite breccia pipes are exposed. Some of the inclusions in the breccias indicate the presence, at the time of intrusion, of formations long since removed by erosion.

The age of the Oka Complex as well as the other Monteregian plutons is indicated as 100 ± 15 million years, *i.e.* Lower Cretaceous. Unlike the other Monteregian plutons, which stand out as prominent hills, the Oka Complex occupies a topographic depression, which is partially surrounded by the Oka hills, and is filled mainly by Pleistocene glacial and proglacial deposits. A Pre-Pleistocene 'crater' lake over the central core of the northern ring was filled with up to 300 feet of silt and clay deposited in the proglacial Champlain sea.

Two major suites of rocks make up the Oka Complex; ultramafic alkaline rocks and carbonate rocks. The silicate rocks are intruded as ring and arcuate dykes into the carbonate rock masses, and are located mainly in the rim zones of the two rings. Carbonate rocks of different types occur mainly in the central zone or core with lesser amounts in the rim zones. All rock types exhibit intrusive features, and are thought to represent differentiates and assimilated rocks derived from the monteregian parent magma. The gneisses in contact with the alkaline rocks have been metasomatically altered by the addition of Ca, Mg, Na and by the removal of Si and K, into fenites.

PETROLOGY

Country rocks

In the precints of the Complex, anorthosite, gabbroic anorthosite, gabbro and mangarite underlie a small sector in the north, whereas quartz-feldspar-biotite gneiss and quartz-feldspar-hornblende gneiss with subordinate amounts of quartzite and pegmatite constitute the bulk of the country rocks.

Fenites

The alteration aureole may be divided into the " in situ " fenites and the mobilized fenites. An 'outer shock' or 'fracture' zone is characterized by aegerine-augite and calcite veins, that appear to follow joints and fissures. Closer to the Complex these veins become more numerous, with the appearance of nepheline and clear orthoclase and the disappearance of quartz, and the conversion of the bulk composition to that of a syenite. The process is one of progressive aegerinization, in which aegerine-augite replaces quartz and soda feldspar with the formation of nepheline and, in places, orthoclase. Later solutions have introduced biotite, uralitized the aegerine and liberated magnetite. Adjacent to the complex and up to 200 feet from it are the structurally conformable rocks designated the the 'mobilized fenites'. These are sheared and show flow features.

Carbonate rocks

These underlie more than half surface area of the Complex, and are conveniently subdivided on a textural and/or mineralogical basis into 7 main groups. Except for the dolomitic varieties, the carbonate rocks are composed essentially of medium to coarse-grained grey to white calcite, and a host of minor and accessory minerals which include: apatite, magnetite, biotite, soda-pyroxene, diopside, olivine, monticellite, melilite, tremolite, melanite, nepheline, dolomite, pyrite, pyrrhotite, pyrochlore, niobium perovskite, latrappite, and niocalite. The most widespread and abundant of the latter are apatite, magnetite, biotite and soda-pyroxene.

Almost everywhere the carbonate rocks are banded; the minor and accessory minerals occurring mainly in thin layers, lenses, boudins or inconsistent bands within broader carbonate bands. Except for local involutions these bands are concentric to the margin of the Complex. Individual types of carbonate rocks occur as arcuate tabular bodies or boudins within other carbonate rocks, and do not have any distributional arrangement with respect to the intruded silicate rocks.

The main groups of carbonate rocks are:

(1) Coarse-grained banded calcite rock, with minor amounts of apatite, magnetite and biotite and accessory forsterite, soda-pyroxene and pyrochlore. This group constitutes the bulk of the carbonate rocks in the rim zone.

(2) Coarse-grained banded aegerine-apatite-biotite-magnetite calcite rock, occurs locally in

bands and lenses within the coarse-grained calcite rocks. Red-brown pyrochlore (type 2) is the main accessory mineral.

(3) Medium-to coarse-grained monticellite-calcite rock forms the core of the northern ring and occurs as thick bands elsewhere in the Complex. The monticellite occurs as euhedral tabular prisms 0.1 mm to 5 cm long, rarely as shelled orbicubes, and may be completely or partially altered to a blue serpentine-like material. In the rock, monticellite constitutes from 20 to 50 per cent; biotite occurs in minor amounts; perovskite, magnetite, apatite and in places pyrochlore (type 4) in accessory amounts.

(4) Very coarse-grained calcite rock, consisting almost exclusively of calcite (up to 5 cm in length), with sparce accessory magnetite, pyrochlore, and tremolite occur mainly in a thick band in the southern ring and in a few scattered thin bands elsewhere. The rock contains more than 1.5 per cent strontium, which is apparently accommodated in the calcite. Some biaxial calcite was noted.

(5) Dolomitic rocks occur most abundantly in the northern sector of the Complex. Commonly, it is fine-grained grey banded rock with minor amounts of apatite, calcite and magnetite and accessory pyrochlore, but massive coarse-grained buff varieties are present. Thin dolomite-magnetite dykes and veins are present in and around the Complex.

(6) Melilite calcite rocks, consisting of from 30 to 50 per cent melilite with medium-grained calcite and accessory apatite, occur as thin bands or pods in a few places.

(7) Niocalite calcite rocks are found in two bands, respectively 60 feet and 15 feet thick, in the Bond Zone. Most of the niocalite occurs as yellow green prismatic grains between 0.5 and 4 mm in length, generally disseminated in coarse-grained calcite rock, though locally it may be concentrated into bands. Accessory minerals include apatite, melilite, magnetite, melanite and biotite.

(8) Other carbonate rocks include: thin sideritic band marginal to pyrite-pyrrhotite veins; veins consisting of fine-grained calcite and dolomite with accessory melanite and magnetite; and calcitic rocks rich in magnetite and apatite, and magnetite and melanite.

Okaite and Jacupirangite rock series

Rocks of this series vary in composition from melilite-magnetite rocks, through melilite-nepheline rocks (okaites), melilite-hauynite and melilite-nepheline-titanaugite rocks, to nepheline-titanaugite and titanaugite-rich rocks (Jacupirangites). Generally these rocks are coarse-grained, and contain minor amounts of calcite, magnetite and apatite and accessory perovskite. Alteration of melilite to cebollite, vesuvianite and dolomite; nepheline to zeolite minerals is well developed in places. The melilites from these rocks are unzoned and conform to the general formula $NaM_{35}Ge_{11}Al_{54}$, where NaM represents the soda-melilite molecule, Ge, gehlenite and Ak, akermanite. The titanaugite is one of the most basic ever recorded. Wairakite, the calcium analogue of analcite was found in one sample.

These rocks are exposed in a crescentric shaped body 4000 feet long by 1250 feet wide underlying Husereau Hill, and in 6 arcuate dykes to the southeast. No melilite-bearing rocks have been found in the southern ring.

Ijolite series

Rocks of the ijolite group are characterized by the presence of soda-pyroxene and nepheline. They constitute the bulk of the silicate rocks exposed in the Complex. Many types crop out in the Oka area including malignite, urtite, microurtite, melanite urtite, ijolite, microijolite, wollastonite-melanite ijolite, melteigite, and wollastonite-melanite melteigite as well as transitional varieties. The more silicic varieties are exposed as thick lenticular bodies near the margin and apparently grade into fenite. Arcuate dykes of ijolite are widespread, being particularly numerous in the 'rim zone'. There is commonly a reaction zone, containing much fine-grained biotite, between the ijolite and the carbonate rocks.

Biotite replacement rocks

In places, zones of hydrothermal alteration and intense biotitization are found within the silicate rocks. All stages may be seen from incipient alteration around the edges of joint blocks, to completely replaced rocks consisting of biotite and calcite with accessory magnetite, hornblende, pyrochlore, pyrite and pyrrhotite. The biotitized zones occur as inward dipping planar and arcuate bodies which transgress the litho-structure.

Alnöite, alnöite breccia, and breccia pipes

The alnöite consists of phenocrysts of augite, hornblende, olivine (in places rimmed by monticellite), biotite in a matrix of essentially fine-grained melilite with subordinate amounts of magnetite, calcite, apatite, ilmenite, nepheline and pyrite. They occur as irregular plugs and dykes with local dilations and intrude rocks both of the Complex and the surrounding country ; their distribution following a distinct geometrical pattern. Most of the alnöites contain a variety inclusions of foreign rocks, with which there is almost no reaction. In places inclusions are numerous, especially near the intrusive margins and alnöite grades into alnöite breccia, and in extreme cases into breccia which consists of rock fragments in a matrix of finer fragments and rock flour.

Fragmentation of some phenocrysts suggests a highly viscous magma. The presence of lapilli or globules of alnöite, and polished inclusions in the alnöite breccia, suggest a gas streaming or "fluidization process" as a mechanism of emplacement.

Later dykes

Dykes of kersantite, minette, ijolite, monchiquite, and fourchite and carbonate rocks crop out in the precints of the Complex. The preferred directions of strike are : east-west, north-south, northwest-southeast.

Sulphide and fluorite-bearing veins

These are exposed, and were intersected in drill cores, in various parts of the Complex. These are late features that appear to be emplaced along joint planes associated with minor faults.

A genetic sequence involving 5 main stages is suggested from field relations. These are :

(*a*) The emplacement of the carbonate rocks. Various stages are apparent within the carbonate rocks, with monticellite calcite rocks being the last of any volumetrically importance.

(*b*) The intrusion of the melilite-rich silicate rocks okaite and jacupirangite rock series.

(*c*) Intrusion of the ijolitic rocks.

(*d*) The introduction of hydrothermal solutions along cone sheet type fractures, biotitizing the silicate rocks and introducing a second niobium mineralization.

(*e*) The emplacement of the alnöite dykes and plugs, and breccia pipes. Late alkaline dykes are probably associated with this phase.

STRUCTURE

But few of the smaller dykes are continuous planar or curvi-planar bodies as indicated on the map. Most have been separated or rafted apart within the carbonate rocks, to produce boudins on all scales from inches to tens of feet in length, and in all stages of development. The amount of rafting apparently is not great, as the boudins lie in planar units which are generally oblique to the banding of the carbonate rocks.

Except for the central portion of the northern ring the foliation of the carbonate rocks dips outwards-shallow near the center, steeper near the margins (see Fig. 1), suggesting a ring dyke mechanism for emplacement. For the most part the silicate rocks in the southern ring and the melilite-bearing rocks in the northern ring conform to the ring dyke model. In contrast the ijolite dykes exposed in the northern ring dip inwards, suggesting a cone sheet type of emplacement.

The long axis of the Complex coincides with the axis of the regional Beauharnois arch. About this axis, vertical sets of conjugate planes

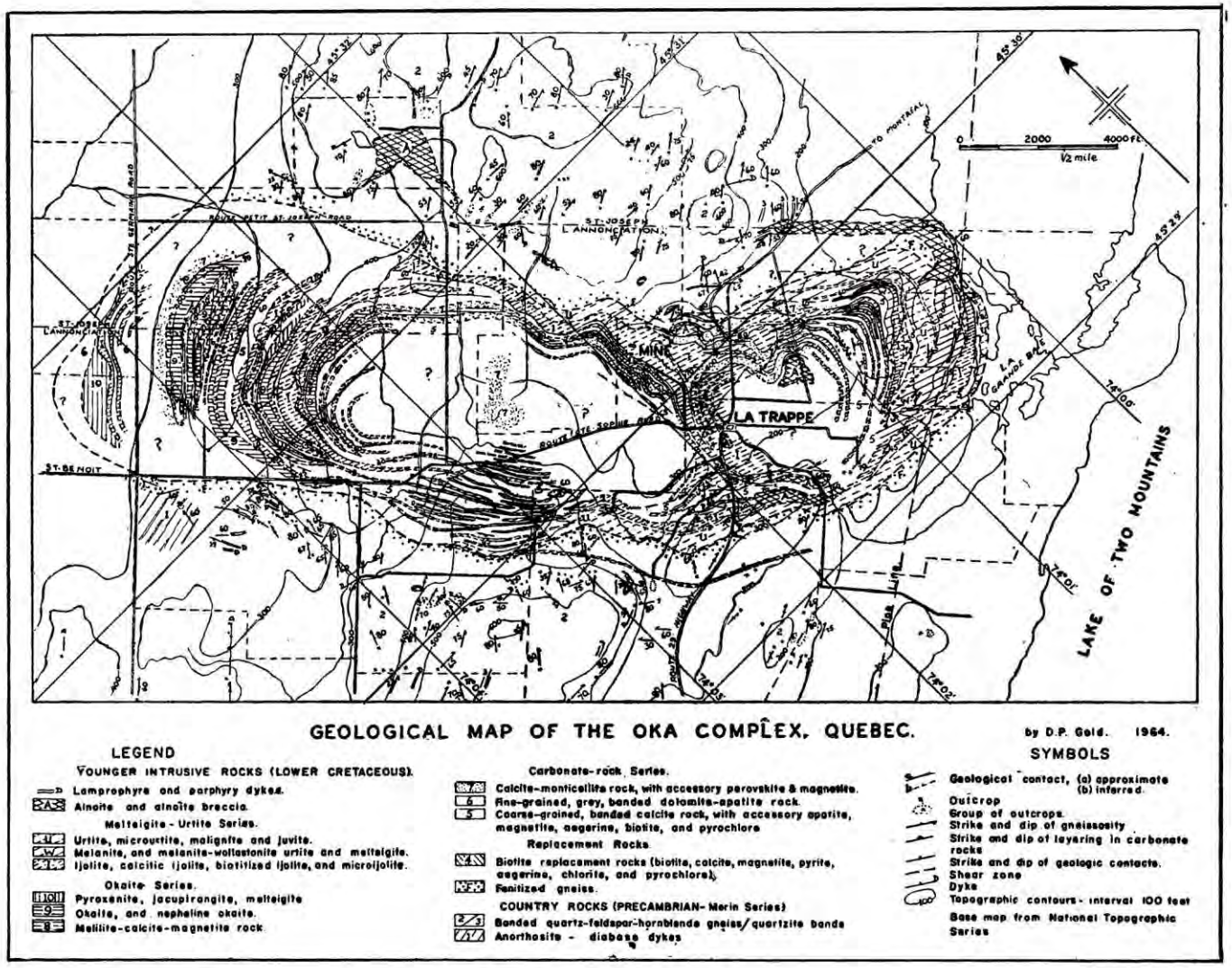

GEOLOGICAL MAP OF THE OKA COMPLEX, QUEBEC. by D.P. Gold. 1964.

LEGEND

YOUNGER INTRUSIVE ROCKS (LOWER CRETACEOUS).

- Lamprophyre and porphyry dykes.
- Ainoite and ainoite breccia.

Melteigite - Urtite Series.

- Urtite, microurtite, malignite and juvite.
- Melanite, and melanite-wollastonite urtite and melteigite.
- Ijolite, calcitic ijolite, biotitized ijolite, and microijolite.

Okaite Series.

- Pyroxenite, jacupirangite, melteigite
- Okaite, and nepheline okaite.
- Melilite-calcite-magnetite rock.

Carbonate-rock Series.

- Calcite-monticellite rock, with accessory perovskite & magnetite.
- Fine-grained, grey, banded dolomite-apatite rock.
- Coarse-grained, banded calcite rock, with accessory apatite, magnetite, aegerine, biotite, and pyrochlore

Replacement Rocks.

- Biotite replacement rocks (biotite, calcite, magnetite, pyrite, aegerine, chlorite, and pyrochlore).
- Fenitized gneiss.

COUNTRY ROCKS (PRECAMBRIAN- Morin Series)

- Banded quartz-feldspar-hornblende gneiss/quartzite bands
- Anorthosite - diabase dykes

SYMBOLS

- Geological contact, (a) approximate (b) inferred.
- Outcrop
- Group of outcrops.
- Strike and dip of gneissosity
- Strike and dip of layering in carbonate rocks
- Strike and dip of geologic contacts.
- Shear zone
- Dyke
- Topographic contours - interval 100 feet

Base map from National Topographic Series

at 095°–180°, and 115°–160° respectively, describe the attitude and location of alnoite dykes and pipes, and the margin of the Complex (see Fig. 2). Parallel lineaments on 075° describe the northwest and southeast boundaries. Other dykes are located along inward dipping planes whose strike parallels the long axis.

There is a remarkable coincidence between the geometry of the Complex and the local and regional geology (see Fig. 2); the conjugate planes conforming to the shear and tension joint plane attitudes over an arch. Moreover, the intersection of two major structural trends at Oka, *viz.*, the Beauharnois arch with the easterly striking 'lineament' along which the Monteregian Hills and various breccia pipes are aligned and which extends westward along the Ottawa valley into the Ottawa-Bonnchere graben, suggest a strong structural control for the location and emplacement of the Complex.

GEOCHEMISTRY

The geochemistry of the main rock types exposed in the precints of the Complex are summarized in Table 0. As could be predicted from the enrichment of Ti, Fe^{2+}, Fe^{3+}, Mn, Mg, Ca, Sr, Ba, P, Zr, Nb, Ce, La, Nd, Cr, CO_2 in the silicate rocks, and Zr, Nb, Ce, La, Nd, Sr, Ba, P, Mn, Ti, Na, K, F, S, Cu, Cr in the carbonate rocks, a host of rare and unusual minerals are present.

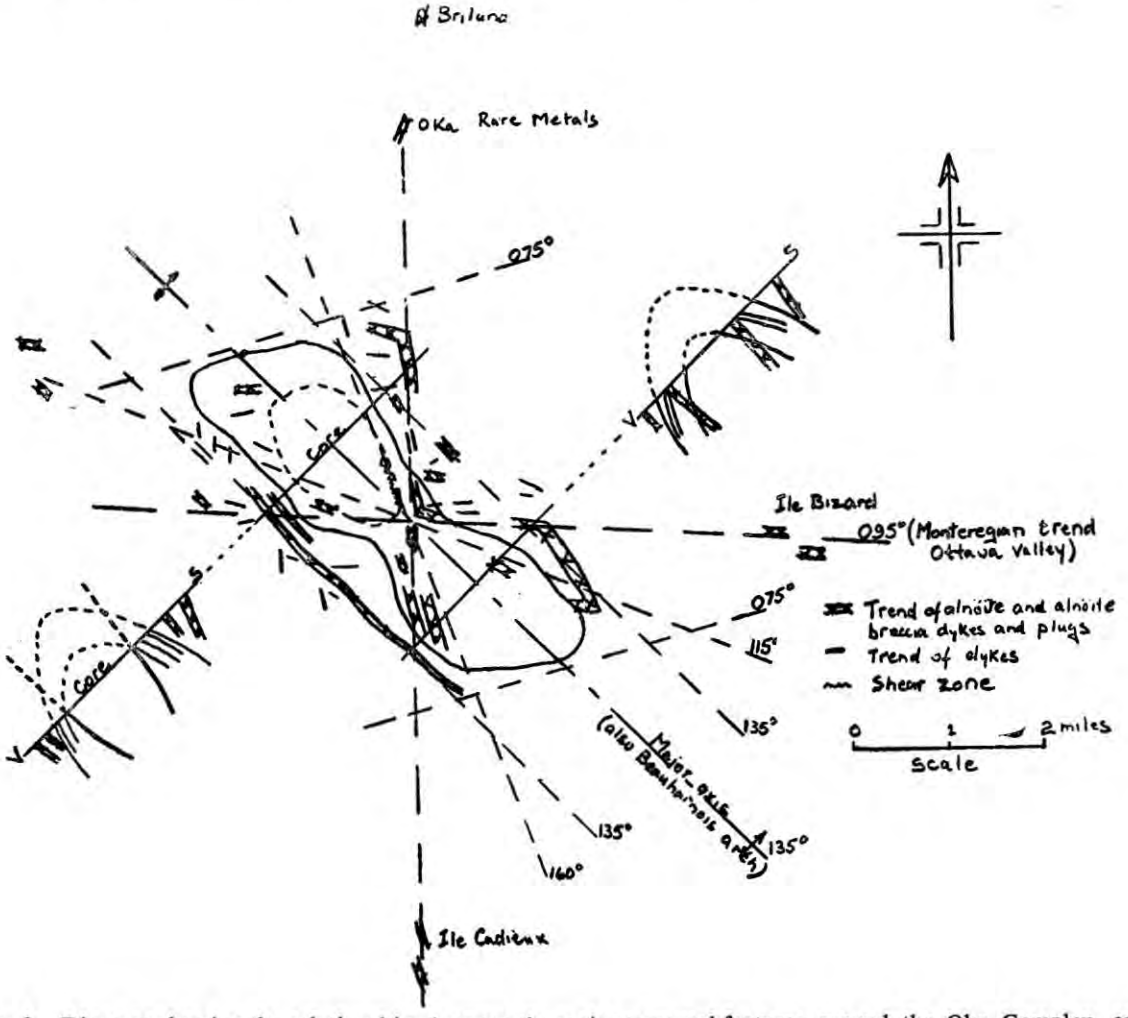

Fig. 2. Diagram showing the relationships between the main structural features around the Oka Complex, and vertical sections through the northwestern and southeastern rings respectively.

TABLE 0

Average abundance of major and minor constituents in different rock assemblages (weight %)

	Anortho-site	Fenite	Okaite	Jacupi-rangite	Urtite ijolite	Alnöite	Calcite rock	Dolomite calcite rock	v. c. g. calcite rock	Monticellite calcite rock
No. of analyses	4	1	4	2	6	4	5	7	5	9
SiO_2	54.61	59.53	30.87	33.52	39.05	31.03	4.66 (6)	1.73 (1)	0.07 (1)	14.68 (1)
TiO_2	0.12	0.75	2.39	3.70	0.66	2.40	0.28 (19)	0.05	0.07	0.30
Al_2O_3	25.18	16.21	14.11	12.25	15.54	7.84	2.89	0.89 (1)	0.00 (1)	2.37 (1)
Fe_2O_3	0.46	1.01	5.92	8.22	4.65	6.98	3.69	4.35 (1)	1.30	4.17
FeO	1.53	1.83	4.12	3.46	2.14	6.54	1.24	3.21 (1)		
MnO	0.03	0.23	0.51	0.32	0.75	0.24	0.71 (6)	1.06	0.67	0.70
MgO	1.40	2.31	4.99	8.52	3.07	13.21	2.31 (6)	15.67 (1)	1.09 (1)	9.64 (1)
CaO	9.00	5.57	24.45	20.87	17.14	22.75	47.04 (6)	29.68 (1)	51.22 (1)	37.84 (1)
SrO	0.06	0.04	0.42	0.25	0.18	0.19	1.37 (19)	1.64	1.90	0.89
BaO	0.01	0.09	0.47	0.51	0.22	0.35	0.17 (19)	0.13	0.10	0.18
Na_2O	4.41	7.21	4.51	2.17	7.74	2.07	0.48	0.30 (1)	0.14 (1)	0.46 (1)
K_2O	1.22	5.02	1.28	1.35	2.56	1.55	0.36	0.16 (1)	0.49 (1)	0.37 (1)
P_2O_5	0.07	0.24	1.59	2.35	1.40	1.92	3.86	7.16 (1)	1.81 (1)	5.50 (1)
CO_2	1.09	—	2.32	1.62	2.61	1.67	28.84	34.68 (1)	40.44 (1)	18.53 (1)
H_2O	—	0.51	1.04	1.36	2.08	1.06	0.28	0.15 (1)	0.03 (1)	0.52 (1)

Braketed figures indicate number of analyses for a particular component if different from the total indicated at the top of the column.

MINERALOGY

The existence of unusual rocks near Oka has long attracted the attention of geologists, but not until radioactive minerals were found near La Trappe in 1953, was any systematic work done on the mineralogy of the Complex. The potential 'ore' minerals were investigated by Nickel (1956, 1958, 1960, 1963), Perrault (1959, 1960, 1964), Hogarth (1959, 1960), Hughson and Sen Gupta (1964). Apart from work on an amphibole (Perrault, A.S.T.M. Card 9–434), and a pyroxene (Tanguay, 1963) the descriptive mineralogy of the 'guange' minerals has been left to the resources of the writer (Gold, 1963, 1964). All available data are compiled and presented.

To date some seventy minerals and mineral varieties have been identified from the rocks within and associated with the Oka Complex. These are as follows:

Carbonate minerals: Calcite, dolomite, siderite, magnesite, ancylite, parisite, strontianite.

Silicate minerals: Orthoclase, microcline, albite, labradorite, nepheline, hauynite, augite, titanaugite, diopside, aegerine-augite, aegerine, sodian augite, hornblende, lamprobolite, arfvedsonite, soda amphibole (probably richterite), tremolite, forsterite, chrysolite, monticellite, serpentine, melilite, biotite, phlogopite, vermiculite, sericite, chlorite, melanite, andradite, grossularite, zirconium garnet, sphene, wollastonite, niocalite, cancrinite, vesuviantie, cebollite, kaolinite, quartz, and the zeolite group minerals-analcite, natrolite, thompsonite and wairakite.

Phosphate minerals: Fluorapatite, apatite, britholite, wilkeite, monazite.

Oxide minerals: Magnetite, maghemite, hercynite, hematite, ilmenite, rutile, prochlore, thorian pyrochlore, perovskite, niobium perovskite, latrappite, periclase.

Sulphide minerals: Pyrite, chalcopyrite, pyrrhotite, galena, sphalerite.

Other minerals: Barite, fluorite, jarosite.

Undoubtedly, more minerals will be found during the course of routine identification of mill concentrates and systematic study of the various rock types.

The chemical composition and optical properties of some of these minerals are listed in Tables 1–6.

Comments

Olivines: Chrysolite occurs sparingly in bands in the carbonate rocks. Forsterite ($Nx = 1.660$, $Ny = 1.680$, $Nz = 1.698$) is the dominant olivine in alnoite. The monticellite is alumina-rich, and in places, is intergrown with melilite.

Melilites: The melilites are all soda-rich varieties, in spite of occuring in different rock types. The melilites (Nos. III and IV) from the silicate rocks, conform to the general formula $NaM_{35}Ge_{11}Ak_{54}$, whereas those from carbonate rocks (Nos. V and VI) are close to $NaM_{35}FeGe + Ge_{11}Ak_{54}$ (where $Ak = Ca_2MgSi_2O_7$, $Ge = Ca_2Al_2SiO_7$, $FeGe = Ca_2Fe^{2+}SiAlO_7$, $NaM = NaCaAlSiO_2$). All are uniaxial negative; some have nepheline intergrowths, others contain fine blebs of monticellite.

Wollastonite: The wollastonite occurs as silky green platy crystals up to 4 inches in length, in coarse-grained wollastonite ijolite (wollastonite, nepheline, sodian augite, melanite).

Garnet: The typical garnet is a dark brown to black andradite. Apart from the absence of alumina, a somewhat high zirconium and low titanium content, they conform chemically and optically to melanite. In places they are intergrown with sodian augite.

Pyroxenes: Sodian augite is the common pyroxene of the carbonate and ijolitic rock types. It may be easily mistaken for aegerine. Titanaugite occurs in the jacupirangite and the alnoite rock types, and exhibits brilliant interference colours which vary from berlin blue to dark brown, with different segments of the crystal changing at different angles. Hourglass extinction is common. The analysis indicates a 24.7% Al substitution in Z position, and a lower titanium content than is indicated by the optical properties. High alumina substitution may account for this.

Amphiboles: Hornblende is found in the border zone between ijolite and carbonate rocks,

TABLE 1

	OLIVINES		MELILITES			WOLLASTONITE		GARNETS	
	I	II	III	IV	V	VI	VII	VIII	IX
SiO_2	39.36	33.32	39.78	38.68	39.64	39.98	50.15	33.86	32.0
TiO_2	0.28	Nil	Nil	Nil	Nil	Nil	Nil	2.07	5.0
Al_2O_3	Nil	2.55	10.33	10.60	6.62	4.47	0.14	Nil	3.8
Fe_2O_3	0.81	0.92	2.02	0.45	1.47	1.89	0.04	20.93	14.0
FeO	2.84	6.25	1.44	1.81	2.01	2.59	0.60	1.72	
MnO	4.78	2.87	0.38	0.35	0.91	1.21	0.96	1.05	2.6
MgO	49.15	21.50	7.06	7.66	7.72	7.29	Nil	1.08	1.0
CaO	1.49	32.14	33.02	34.28	34.32	34.86	46.97	32.34	42.0
Na_2O	0.07	0.16	3.69	3.92	3.35	3.08	0.35	0.27	
K_2O	0.01	Nil	0.24	Nil	0.24	0.12	0.05	0.04	
P_2O_5	0.87	0.04	0.69	0.11	1.21	2.14	Nil	5.93	
H_2O+	0.47	0.09	0.38	0.36	0.88	0.86	0.38	0.41	
H_2O-	Nil	0.01	0.06	0.01	0.24	Nil	Nil	0.02	
CO_2	Nil	0.20	Nil	1.14	Nil	Nil	0.45	Nil	
SrO	0.03	0.02	0.88	0.44	1.00	1.59	-		
BaO	-	-	0.09	-	0.44	0.01	-	-	
ZrO_2	-	-	0.18	-	0.21	0.30	-	0.30	3.7
	100.16	100.07	100.24	99.81	100.26	100.39	100.09	100.02	104.1
N_x-N_e	1.653	1.650	1.627	1.625	1.628	1.629	1.618		
N_y-N	1.668	1.662					1.627	1.86	1.94
N_z-N_o	1.685	1.667	1.633	1.633	1.633	1.635	1.633		
$2V_z$	88°								
$2V_x$		69-70.5°					40°		
$C\hat{}Z$							13°		
S.G.	3.290	3.173	2.990	2.988	3.127	3.041	2.859	3.692	3.70

Number of ions per:

	4(0)	4(0)	14(0)	14(0)	14(0)	14(0)	18(0)	24(0)
Si	0.983	0.912 .994	3.687	3.636	3.801	3.925	5.940	6.446
Al	-	0.082	1.128	1.174	0.748	0.517	0.019	-
Zr	-	-	0.008	-	0.009	0.014 5.98	- 5.96	0.027 3.32
Ti	0.005	-	- 6.08	- 6.08	- 6.00	-	-	0.296
Fe^{3+}	0.015	0.019 1.105	0.141	0.031	0.106	0.139	0.004	2.996
Mg	1.828	0.876	0.975	1.072	1.103	1.066	-	0.306
Fe^{2+}	0.059 2.02	0.143	0.112	0.142	0.161	0.213	0.059	0.273
Mn	0.101	0.067	0.030	0.027	0.073	0.101	0.096 6.13	0.169
Na	0.003	0.008	0.663	0.714	0.622	0.586	0.081	0.101 6.02
Ca	0.009	0.933 .94	3.187 3.93	3.294 4.03	3.362 4.08	3.368 4.06	5.886	5.161
K	tr	-	0.029	-	0.030	0.015	0.008	0.009
Sr	tr	tr	0.047	0.023	0.055	0.090		
Ba	-	-	0.003	-	0.016	-		

I Chrysolite from coarse-grained olivine-magnetite-pyrochlore-calcite rock. Columbium Mining Products trench, Bond Zone. Analyst, H. Ulk, 1961.

II Monticellite from monticellite-calcite rock. DDH M14, 100 feet. Analyst, H. Ulk, 1961.

III Melilite from okaite. Sample Oka A463 (Dufresne Hill). Analyst, W. H. Herdsman, 1964. (a = 7.753 °A; c = 5.027 °A)

IV Melilite from nepheline okaite. Sample Oka A72 (Husereau Hill). Analyst, H. Ulk, 1961. (a = 7.761 °A; c = 5.033 °A;)

V Melilite from calcite-melilite rock. Sample Oka A52 (Bond Zone). Analyst, W. H. Herdsman, 1964. (a = 7.776 °A; c = 5.028 °A).

VI Melilite from niocalite-calcite rock. Sample Oka A434a (Trench 4, Bond Zone). Analyst, W. H. Herdsman, 1964. (a = 7.781 °A; c = 5.022 °A).

VII Wollastonite from wollastonite-melanite melteigite. DDH G15, 330 feet. Analyst, H. Ulk, 1961.

VIII Melanite from wollastonite-melanite melteigite. DDH G15, 330 feet. Analyst, W. H. Herdsman, 1964.

IX Zirconium garnet. Partial analysis, after Nickel, 1960.

TABLE 2

	PYROXENES			AMPHIBOLES			MICAS		
	X	XI	XII	XIII	XIV	XV	XVI	XVII	XVIII
SiO_2	39.89	48.71	47.16	53.60	36.94	38.70	39.44	37.65	36.60
Al_2O_3	14.94	2.04	1.49	0.00	17.93	14.52	8.56	18.25	18.25
TiO_2	2.30	0.66	0.24	0.07	-	1.33	0.15	3.73	1.41
Fe_2O_3	5.62	5.32	5.33	1.12	6.70	5.99	3.81	1.43	3.21
FeO	2.01	5.30	6.61	1.33	4.96	5.46	5.17	5.28	10.34
MnO	0.21	1.83	1.36	1.33	-	0.10	1.63	0.10	1.60
MgO	10.14	11.73	10.92	16.38	12.59	15.51	25.86	20.96	17.27
CaO	24.33	22.12	23.70	25.24	14.08	13.08	0.32	0.57	0.28
Na_2O	0.10	1.58	1.07	0.04	2.34	1.14	0.17	0.61	0.73
K_2O	0.03	0.04	0.04	0.01	2.11	2.42	11.94	9.30	9.32
P_2O_5	0.16	0.05	0.59	0.38	-	0.33	0.17	0.08	0.21
H_2O+	0.13	0.08	1.14	0.07	2.35	1.22	1.36	1.10	0.81
H_2O-	0.07	0.01	Nil	-	-	0.02	0.04	-	Nil
CO_2	Nil	Nil	Nil	-	-	Nil	Nil	Nil	Nil
F	-	-	-	0.06	-	-	1.83	0.18	0.03
SrO	-	-	-	0.067	-	-	-	-	-
BaO	-	-	-	0.019	-	-	-	-	-
	99.87	99.51	99.65	99.72	100.00	99.82	100.45	99.24	100.06
O-F				0.02			0.75	0.07	0.01
				99.70			99.70	99.17	100.05
N_x	1.725	1.700	1.703	1.6794	1.579	1.670			
N_y	1.732	1.707	1.711	1.6855	1.591	1.682	1.597	1.618	1.620
N_z	1.745	1.722	1.725	1.7099	1.650	1.690			
$2V_z$	58-64°	64°	66°	56°±4°	65°				
$2V_x$						77°	0° - 5°	0° -10°	0 -10°
$z \wedge c$	33-37°	44°		40°±3°		10°			
$x \wedge c$			22°						
S.G.	3.399	3.570	3.518	3.29		3.135	3.077		

Number of ions per:

	6(0)		6(0)		6(0)		6(0)		24(0)		24(0)		24(O, OH, F)			
Si	1.506	2.00	1.866	2.00	1.863	2.00	1.988	2.000	5.452	8.00	5.668	8.00	7.720	7.62	5.463	9.29
Al	0.494		0.092		0.069		-		2.548		2.332		1.463		3.120	
Al	0.171		-		-		-		0.570		0.173		-		-	
Ti	0.065		0.019		0.007		0.002		-		0.147		0.016		0.407	9.15
Fe^{3+}	0.159		0.153		0.158		0.031		0.744	4.69	0.659	5.04	0.416		0.157	
Mg	0.570	2.02	0.669	2.05	0.643	2.05	0.905	1.997	2.768		3.383		5.587	6.41	4.529	5.18
Fe^{2+}	0.063		0.169		0.218		0.041		0.611		0.668		0.627		0.640	
Mn	0.007		0.059		0.045		0.042		-		0.012		0.200		0.012	
Na	0.007		0.117		0.082		0.004		0.670	3.29	0.324	2.76	0.047	2.27	0.171	1.96
Ca+Ba+Sr	0.975		0.903		0.969		0.984		2.226		1.983		0.015		0.071	
K	0.001		0.002		0.002				0.397		0.452		2.208		1.720	
OH									2.312	2.31	1.191	1.19	1.315	2.15	1.065	1.15
F													0.838		0.083	

		2.01	5.39	9.29	0.83
					0.014

X — Titanaugite from nepheline jacupirangite. DDH S9, 370 feet. Analyst, H. Ulk, 1961.

XI — Sodian augite from coarse-grained calcite rock. DDH S6, 565-570 feet. Analyst, H. Ulk, 1961.

XII — Sodian augite from wollastonite-melanite melteigite. DDH G15, 330 feet. Analyst, W. H. Herdsman, 1964.

XIII — Diopside from carbonate rock. Analyst, O. Ingamells, 1964. (Reported by M. Tanguay, 1963, 1964). (Also includes $ZrO_2 < 0.03$, $CuO < 0.01$, $BeO < 0.005$.)

XIV — Hornblende from ijolite-calcite rock contact zone. DDH A14, 700 feet. G. Perrault, A.S.T.M. card 9-434.

XV — Lamprobolite from alnoite inclusion in breccia. DDH A16, 675 feet. Analyst, W. H. Herdsman, 1964.

XVI — Phlogopite from Mill circuit; pyroxene-pyrochlore-calcite rock, pit A 2. Analyst, W. H. Herdsman, 1964.

XVII — Biotite from alnoite. Sample Oka A. 368 (Bond Zone). Analyst, H. Ulk, 1962.

XVIII — Biotite from pyroxene-biotite-calcite rock. DDH S6, 560 feet Analyst, H. Ulk, 1962.

TABLE 3

	NEPHELINES		HAUYNITE		MAGNETITE		
	XIX	XX	XXI	XXII	XXIII	XXIV	XXV
SiO_2	37.88	41.60	40.86	42.12	7.45	2.21	0.83
TiO_2	Nil	Nil	Nil	Nil	3.18	3.85	3.71
Al_2O_3	31.57	34.11	33.64	29.13	5.17	7.25	0.15
Fe_2O_3	0.13	0.54	1.21	0.66	54.30	56.98	64.28
FeO	0.29	0.20	0.14	0.19	17.23	21.60	24.52
MnO	0.01	0.03	0.02	0.02	5.36	1.49	3.71
MgO	0.39	0.05	0.07	0.54	5.42	3.91	0.60
CaO	5.60	1.59	0.89	3.49	1.83	1.54	1.58
Na_2O	15.85	17.96	14.74	11.33	-	-	-
K_2O	7.47	1.61	6.78	0.46	-	-	-
P_2O_5	0.22	0.52	0.53		0.47	0.39	0.31
H_2O+	0.10	0.45	0.39				
H_2O-	0.01	0.14	Nil				
CO_2	Nil	0.65	0.56				
Sro	0.21	0.08					
$SO_3^=$				9.03			
	99.73	99.53	99.83	96.97	100.41	99.22	99.69
Ne	1.538	1.540	1.540				
N				1.490			
No	1.543	1.547	1.545				
S.G.	2.637	2.620	2.596				
	Number of ions per:						
	32(0)	32(0)	32(0)		32(0)	32(0)	32(0)
Si	7.650	8.133	8.135		2.010	0.623	0.251
Al	7.513	7.961	7.892		1.644	2.407	0.053
Zr							
Ti		-			0.645	0.816	0.843
Fe^{3+}	0.019	0.080	0.121		11.026	12.079	14.623
Mg	0.117	0.014			2.179	1.642	0.271
Fe^{2+}	0.048	0.033			3.888	5.089	6.199
Mn	0.001	0.005			1.195	0.355	0.950
Na	6.202	6.893	5.686			-	-
Ca	1.145	0.015			0.422	0.308	0.380
K	1.924	0.407	1.743				
Sr	0.024	0.009					

15.325 | 15.925 | 15.770

7.684 | 7.394 | 7.800

XIX Nepheline from nepheline okaite. Sample Oka A72 (Husereau Hill). Analyst, H. Ulk, 1961.

XX Nepheline from wollanstonite-melanite urtite. Analyst, H. Ulk, 1961.

XXI Nepheline from wollastonite-melanite melteigite. DDH G15, 330 feet. Analyst. W H. Herdsman, 1964.

XXII Hauynite from nepheline okaite. Sample Oka A72 (Husereau Hill). Partial analysis, H. Ulk, 1961.

XXIII Magnetite from monticellite calcite rock, 3000 feet southeast of mine. Analyst, H. Soutar, 1964. Sample Oka A278.

XXIV Magnetite from okaite, Dufresne Hill. Sample Oka A463. Analyst, H. Soutar, 1964.

XXV Magnetite from soda-pyroxene-magnetite-pyrochlore-calcite rock, pit A2, St. Lawrence Columbium and Metals Corp. Sample Oka A466. Analyst, H. Soutar, 1964.

TABLE 4

	NIOCALITE		BRITHOLITE
	XXVI	XXVII	XXVIII
CaO	47.50[1]	46.96[1]	28.84
SiO_2	29.70	29.90	12.28
Nb_2O_5	16.56	18.86	-
Al_2O_3	1.31[2]	0.16[2]	0.47
Re_2O_3	-	-	33.43[4]
Fe_2O_3	0.54[3]	0.54[3]	0.14[3]
FeO			
TiO_2	0.22	0.26	0.09
MnO	1.28	0.99	-
MgO	0.28	0.70	0.20
Na_2O	0.78	0.55	0.21
K_2O	0.02	0.00	-
P_2O_5	0.60	0.07	16.96
H_2O^+	0.16	0.18	0.54
F	1.70	1.73	2.10
ThO_2	-	-	5.62
	100.65	100.90	100.88
O~F	0.71	0.73	0.90
	99.94	100.17	99.98

	Number of ions per:		
	XXVI	XXVII	XXVIII
	36(0, OH, F)		26(0, OH, F)
Ca	12.852	12.754	6.474
Na	0.389	0.270	0.086
K	0.006	-	-
	13.247	13.024	
Nb	1.923	2.166	-
Th	-	-	0.268
Fe	0.105	0.104	0.023
Mg	0.106	0.266	0.063
Mn	0.279	0.214	-
Ti	0.043	0.504	0.014
ΣRE	-	-	2.564
	2.456	3.254	9.492
Al	0.397	0.047	0.106
Si	7.632	7.597	2.575
P	-	-	3.008
	8.029	7.644	5.689
OH	0.273	0.305	0.754
F	1.381	1.390	1.391
	1.654	1.695	2.145

[1]Includes SrO. [2]Includes rare earth oxides and ZrO_2. [3]Total iron as Fe_2O_3. [4]Rare earths comprise:
CeO_2 15.0, La_2O_3 5.6, Nd_2O_3 8.0, Pr_2O_3 1.9, Sm_2O_3 1.5, Gd_2O_3 0.9, Y_2O_3 0.4, $(Pr,Dy)_2O_3$ 0.1 total 33.4%.

N_x-N_e		1.701	
N_y		1.714	
N_z-N_o		1.720	1.72
$2V_x$		56°	
c^z		12°	
S.G.		3.32	3.86
	1	2	
a	10.83	10.42	9.48
b	10.42	20.39	
c	7.38	7.38	6.96
β	109° 40'		

(Note: 1 = for monoclinic cell: 2 = for pseudo-orthorhombic cell.)

XXVI Niocalite from diamond drill-core, Bond Zone (Nickel, et al. 1958). General formula $(Ca,Nb)_{16}Si_8(0,OH,F)_{36}$

XXVII Niocalite from trenches, Bond Zone (Nickel, et al, 1958).

XXVIII Britholite, from britholite vein, Dufresne Hill (Hughson and Sen Gupta, 1964). Probable formula $(Ca,Re,Th,Fe,Mg,Ti)_5[(P,Si,Al)O_4]_3(OH,F)$.

TABLE 5

PEROVSKITE, NIOBIUM PEROVSKITE AND LATRAPPITE

	1	2	3	4	5	6
TiO_2	51.20	51.79	38.63	25.00	15.50	10.05
CaO	38.20	33.88	33.16	28.70	27.96	25.95
Nb_2O_5	0.69	4.86	15.80	27.60	39.36	43.90
Ta_2O_5	0.07	0.39	1.32	2.79	-	-
Na_2O	0.31	0.67	1.22	3.75	4.50	4.03
K_2O	0.23	Nil	Nil	0.22	0.01	0.03
CeO_2	1.60			2.04		
Ce_2O_3	-	0.19*	0.26*	-	0.08*	2.03*
Nd_2O_3	0.23	-	-	0.30	-	-
La_2O_3	0.80	-	-	0.94	-	-
ZrO_2	0.13	Nil	Nil	0.95	-	-
SrO	0.35	-	-	0.65	-	-
MgO	0.12	Nil	Nil	-	1.19	2.20
Fe_2O_3	2.84+	5.85	7.45	6.38+	7.18+	8.74+
FeO		0.86	0.86			
MnO	Nil	Nil	Nil	0.10	0.18	0.77
SiO_2	Nil	0.48	0.48	Nil	Nil	0.45
ThO_2	0.17	-	-	0.04	-	-
S	-	-	-	-	-	0.90
H_2O+	1.44	0.40	0.32	0.90	-	0.36
L.o.I.	-	-	-	-	2.13	0.29
Al_2O_3	-	0.44	0.36	-	-	-
	98.22	99.81	99.86	100.36	98.08	99.70

* Rare earths calculated as Ce_2O_3.

\+ Total iron calculated as Fe_2O_3.

N						
SG		4.24	4.227			4.40
Number of ions per						
	24(0)	24(0)	24(0)	24(0)	24(0)	24(0)
Si	-	0.089	0.094	-	-	0.097
Al	-	0.096	0.083	-	-	
Fe^{3+}	0.412	0.813	1.093	1.008	1.157	1.239
Mg	0.034	-	-	-	0.379	0.709
Ti	7.411	7.203	5.656	3.941	2.494	1.634
Nb	0.060	0.407	1.391	2.616	3.806	4.291
Ta	0.003	0.020	0.070	0.159	-	-
Fe^{2+}	-	0.133	0.140	-	-	-
Mn	-	-	-	0.018	0.032	0.142
Na	0.116	0.240	0.461	1.524	1.866	1.689
Ca	7.878	6.713	6.917	6.446	6.409	6.011
Si	0.039	-	-	0.079	-	-
K	0.056	-	-	0.058	0.003	0.008
Th	0.007	-	-	0.003	-	-
Zr	0.013	-	-	0.097	-	-
Ce	0.108	-	-	0.003	-	-
Nd	0.016	0.013	0.019	0.023	0.006	0.161
La	0.057	-	-	0.073	-	-
	8.290	7.099	7.537	8.324	8.316	8.011
	7.920	8.628	8.487	7.724	7.836	7.970

1. Brown perovskite from alkaline dyke on the Oka Rare Metals property, 10,000 feet northeast of the Oka Complex. (G. Perrault, Ecole Polytechnique, Montreal. Personal Communication, 1960). Ao for pseudoisometric unit, 7.71°A.
2. Black niobium perovskite from okaite, Dufresne Hill. Sample Oka A463. Analyst, W.H. Herdsman, 1964.
3. Black niobium perovskite from monticellite calcite rock, 3,000 feet southeast of mine. Sample Oka A278. Analyst, W.H. Herdsman, 1964.
4. Black niobium perovskite from monticellite calcite rock, Columbium Mining Products property (Bond Zone). Ao for pseudoisometric unit, 7.73° A. (G. Perrault, Ecole Polytechnique, Montreal. Personal Communication, 1960).
5. Black latrappite. Mill concentrate, St. Lawrence Columbium and Metals Corporation. Trace elements (semi-quantitative) in per cent: Si 0.2, Mn 0.09, Sn, 0.02, Al 0.1, V 0.03, Cu 0.02, Ni 0.03, Zr 0.1, Sr 0.3, Ta 0.1. (Mines Branch Report MS-AC 64-534, 1964).
6. Black latrappite from monticellite calcite rock, Columbium Mining Products property (Bond Zone). Cell parameters: a = 5.448, b = 7.777, c = 5.553 ° A. Trace elements (semi-quantitative) in per cent: Ce 1.5, La 0.3, Zr 0.3, Sr 0.2, Y 0.1, Al 0.09, Ni 0.04, Gd 0.03, V 0.03, Dy 0.01, Yb 0.01. (Nickel and McAdam, 1963).

TABLE 6

PYROCHLORE

	1	2	3	4	5	6	7	8	9	10	11
Nb_2O_5	40.53	46.97	48.04	48.80	54.80	55.80	56.30	57.97	60.00	47.40	65.80
Ta_2O_5	3.08	2.18	2.77	2.10	0.75	0.50	0.25	0.26	0.50	3.54	0.04
TiO_2	10.42	7.49	8.64	7.20	5.80	6.52	5.20	5.36	4.50	6.38	2.59
Fe_2O_3	-	1.98	-	1.90	1.66	2.70	1.14	1.08	2.70	1.89	0.56
FeO	1.80	-	2.06	-	-	-	-	-	-	-	-
ZrO_2	1.45	0.99	1.99	0.95	0.66	1.00	2.03	2.09	1.00	4.10	0.60
Na_2O	2.88	2.39	1.46	2.30	5.10	4.50	5.10	5.25	3.50	2.05	6.20
K_2O	0.00	-	0.00	-	-	-	-	-	0.60	-	0.00
CaO	17.11	18.68	20.32	19.80	17.20	15.08	17.90	15.11	15.08	19.80	15.80
SrO	0.65	0.49	0.67	0.47	0.32	1.09	0.76	0.78	0.60	0.26	0.93
BaO	tr	-	tr	-	-	-	-	-	-	-	-
MgO	0.00	0.15	tr	0.42	-	-	0.68	0.56	1.00	-	0.00
MnO	1.17	0.08	0.09	0.08	0.06	0.07	0.05	0.06	0.37	0.28	0.00
Ce_2O_3	2.20	7.70	8.87	7.06	7.34	3.00	3.78	4.09	3.00	8.66	1.63
La_2O_3	-	1.45	-	1.39	1.09	0.70	0.68	0.70	0.70	1.22	0.37
Nd_2O_3	-	1.89	-	1.82	1.06	-	1.83	1.89	-	1.22	0.39
Y_2O_3	0.20	0.07	0.10	0.07	0.12	0.12	0.08	0.08	0.12	0.21	0.17
U_3O_8	1.83	0.72	0.59	0.69	0.02	0.45	0.08	0.08	0.10	0.56	0.03
ThO_2	7.23	1.15	1.08	1.10	0.02	0.63	1.47	1.51	0.23	0.03	0.20
Gd_2O_3	-	-	-	-	-	0.20	-	-	0.20	-	-
SnO_2	0.00	-	0.00	-	0.20	-	-	-	-	-	0.00
TlO_2	-	-	-	0.12	0.03	-	0.03	-	-	-	0.00
F	2.17	3.93	2.30	3.80	3.92	3.69	2.13	2.19	3.69	2.15	4.61
H_2O^+	7.50	-	0.87	0.12	0.18	1.24	0.35	-	1.24	0.36	0.59
P_2O_5	-	-	-	0.02	0.08	-	0.24	-	-	0.04	0.07
S	-	-	-	0.01	0.11	-	0.04	-	-	0.05	0.04
SiO_2	-	-	-	0.83	0.10	0.08	0.42	-	-	0.15	0.17
Al_2O_3	-	-	-	0.00	0.00	-	0.00	-	-	0.00	0.00
PbO	0.10	-	0.06	-	-	-	-	-	0.08	-	-
L on Ig	-	1.54	-	-	-	-	-	0.91	-	-	-
	100.30	98.82	99.90	101.05	100.62	97.37	100.54	99.97	99.21	100.35	100.79
O~F	0.90	1.65	1.00	1.60	1.65	1.55	1.00	0.92	1.55	0.91	1.94
	99.40	97.17	98.90	99.45	98.97	95.82	99.54	99.05	97.66	99.44	98.85
SG.			4.33		4.38						
a°A	10.36		10.38	10.43	10.393		10.428			10.395	10.4195

1. Thorian pyrochlore. Manny Zone. (Hogarth, 1961: sample No. H7. Ce_2O_3 = Σcerium earths, Y_2O_3 = Σyttrium earths).
2. Deep red pyrochlore (type 1), from St. Lawrence Columbium and Metals Corporation property. (G. Joncas, University of Sherbrooke, Quebec. Personal communication, 1962).
3. Reddish-brown pyrochlore (type 1), from Bond Zone. (Hogarth, 1961: sample No. H8a. Ce_2O_3 = Σcerium earths, Y_2O_3 = Σyttrium earths).
4. Deep-red pyrochlore (type 1) in ijolite, from pit A2, St. Lawrence Columbium and Metals Corporation property. (G. Perrault, Ecole Polytechnique, Montreal. Personal communication, 1964).
5. Chocolate-brown, cerian pyrochlore (type 2) from soda pyroxene-calcite rock, pit A1, St. Lawrence Columbium and Metals Corporation property. (Perrault, 1964, and personal communication).
6. Red pyrochlore (type 3), from St. Lawrence Columbium and Metals Corporation property. (Perrault, 1961).
7. Very fine-grained brownish-red pyrochlore (type 3) from biotitized ijolite, between pits A1 and A2, St. Lawrence Columbium and Metals Corporation property. (Perrault, 1964, and personal communication).
8. Red pyrochlore, (type 3) from St. Lawrence Columbium and Metals Corporation property. (G. Joncas, University of Sherbrooke, Quebec. Personal communication, 1962).
9. Red pyrochlore (type 3). Average chemical composition of mill concentrate. St. Lawrence Columbium and Metals Corporation, (Engineering and Mining Jour. Oct. 1961).
10. Black zirconium pyrochlore (type 4), from biotite-monticellite calcite rock, footwall of pit A2, St. Lawrence Columbium and Metals Corporation property. (Perrault, 1964, and personal communication).
11. Buff pyrochlore (type 5) from coarse-grained calcite rock, from pit A2, St. Lawrence Columbium and Metals Corporation property. (Perrault, 1964, and personal communication).

tremolite amongst the alteration products of monticellite, and richterite in fine acicular crystals within the carbonate rocks. Lamprobolite occurs as phenocrysts and in the groundmass of alnoite and alnoite breccia.

Micas: The micas are typically those of ultramafic suites. Two main stages of biotite are present, an earlier green variety (Fe-rich) and a late brown variety (Mg-rich).

Nepheline: Lime-rich nepheline (No. XIX) occurs in the okaite group of rocks, while nepheline from the ijolite group conforms closely to Burger's ideal nepheline ($Na_3KAl_4Si_4O_{16}$). A soda-rich variety, close to carnegieite in composition, was found in wollastonite urtite, suggesting a high temperature of formation.

Wairakite: This rare calcium analogue of analcite was identified, by its X-ray diffractometer pattern, from an aggregate of cream and pale coloured crystals in altered nepheline okaite. The alteration is ascribed to late hydrothermal activity which affected parts of the Complex.

Magnetite: Magnetite is the commonest of the opaque minerals and occurs most abundantly in the okaite jacupirangite rocks, and in selected bands within the carbonate rocks. Hercynite is commonly associated with magnetite in the silicate rocks, either as exsolved lamellae within, or as blebs within and/or about the crystals. Magnetite from the carbonate rocks commonly exhibit trapezohedral faces.

Niocalite: Niocalite is a yellow, prismatic, niobium silicate mineral with the general formula $(Ca,Nb)_{16}Si_8(O,OH,F)_{38}$. It is the only new mineral so far identified from the Complex.

Britholite: A 9-inch thick vein of massive 'britholite' with associated magnetite and pigeonite (?) is exposed on Dufresne Hill. The analysis shows it to be a thorium-bearing intermediate member of the britholite-apatite series, containing 33.43 per cent rare earth elements.

Perovskite: Perovskite occurs, as brown to black, cubic crystals, in all except the ijolitic rock types, being most abundant in the monticellite calcite rocks. The composition varies from niobium-poor (perovskite) in the silicate rocks, through niobium-bearing varieties to niobium-rich (latrappite-Nb>Ti) in the carbonate rocks.

Pyrochlore: Pyrochlore is a complex niobium oxide of variable composition. Six types, which vary in composition from 40.53 to 65.80 per cent Nb_2O_5, have so far been recognized at Oka. The composition apparently varies with rock type. According to Hogarth (1961) the general formula is $A_{16-x}B_{16}(O,OH)_{48}(F,OH)_{18}$ in which A is dominantly Na or Ca and less commonly U, Th and the rare earth elements: the B position is occupied by Nb, though Tc and Ta may substitute for it.

ORIGIN

The main hypotheses advanced for the origin of the Complex are:

1. Metamorphism of Palaeozoic limestone by alkaline igneous rocks.
2. Assimilation of Palaeozoic limestone by alkaline magma.
3. Metamorphism of Grenville marble by alkaline igneous rocks.
4. Assimilation of Grenville marble by alkaline magma.
5. Differentiated magmatic carbonate and silicate rocks.

The marked structural discordance; the location of the Complex within Precambrian rocks stratigraphically far below the Palaeozoic cover rocks; and the unusual and distinctive petrology, rule out the first three hypotheses. Moreover, metamorphic effects associated with the other Monteregian hills are restricted to narrow zones.

The hypothesis involving the assimilation of Grenville limestone is not consistent with the stable isotope data (Sr^{87}/Sr^{86}, O^{18}/O^{16}, C^{13}/C^{12}, and S^{34}/S^{32} ratios all indicate that both the carbonate and the silicate associated with the Complex are 'mantle' in type); the lack of any mineralogical zoning with respect to the intruded rocks; the lack of any skarn assemblages; the distinctive mineralogy and trace and major element geochemistry.

I conclude that Oka rocks are differentiates of a magma, with a parent whose composition was an alkali peridotite. I envisage a cylindrical magma chamber of great vertical extent (confirmed by gravity data) developing volatiles (CO_2, H_2O, Nb_2O_5, P_2O_5, F *etc.*) at the top and kimberlitic types (alnöite) near the base. A structural trap prevented the escape of the volatiles which are necessary for the formation of the carbonate rocks. The alnöite dykes and plugs represent a late stage intrusion of the residual magma (possibly recharged) during the closing phase of the intrusive cycle.

ACKNOWLEDGEMENTS

During the investigative work, support of one form or another was provided by one or more of the following agencies: Quebec Department of Mines, McGill University, National Research Council of Canada-grants Nos. A 1186 and A 1783 (part of the Upper Mantle project), and more recently, the National Science Foundation in Washington. This support is gratefully acknowledged. I thank the three Mining Companies operating in the Oka area for use of their drill-hole data and plans, and to the members of the Ecole Polytechnique for providing data on the ore minerals.

REFERENCES

ANON, (1961) St. Lawrence columbium project starts production in Quebec: *Eng. and Min. Jour.*, Vol. 162, No. 10, pp. 98–104.

CARBONNEAU, C. (1964) Mining fresh carbonatite rocks for production of pyrochlore concentrates: *A. M. I. E.* Annual Meeting, February 1964, New York. Symposium of high temperature refractory metals.

DAVIDSON, A. (1963) A study of okaite and related rocks near Oka, Quebec: *Unpub. M.Sc. thesis*, Univ. of British Columbia.

GOLD, D. P. (1962) The Oka Complex: *54th N.E.I.G.C. Guide Book*, Montreal Meeting, pp. 7–14.

———(1963) The relationship between the limestone and the alkaline igneous rocks of Oka and St.-Hilaire, Quebec: *Unpub. Ph.D. thesis*, McGill University, Montreal.

———(1964) On some minerals from the Oka alkaline complex. Oka, Quebec: Paper presented at Min. Assoc. Canada annual meeting, Toronto. (*Abst.*) *Can. Mineral*, Vol. 8, Pt. 1.

GRIMES-GRAEME, R. H. C. (1935) The origin of the intrusive igneous breccias in the vicinity of Montreal, Quebec: *Unpub. Ph.D. thesis*, McGill University, Montreal.

HARVIE, R. (1909) On the origin and relations of the Palaeozoic breccia of the vicinity of Montreal: *Roy. Soc. Canada, Trans.* Ser. 3, Vol. 3, Sec. 4, pp. 249–299.

HOGARTH, D. D. (1961) A study of pyrochlore and betafite: *Can. Mineral*, Vol. 6, Pt. 5, pp. 610–633.

HOWARD, W. V. (1922) Some outliers of the Monteregian Hils: *Roy. Soc. Canada, Trans.* Ser. 3, Vol. 16, Sec. 4, pp. 47–95.

HUGHSON, M. R. AND SEN GUPTA, J. G. (1964) A thorium intermediate member of the britholite-apatite series: *Am. Mineral*, Vol. 49, pp. 937–951.

MAURICE, O. D. (1957) Preliminary report on Oka Area: *Quebec Dept. Mines*, Prelim. Rept. No. 351.

NICKEL, E. H. (1956) Niocalite, a new calcium niobium silicate mineral: *Am. Mineral*, Vol. 41, pp. 785–786.

———ROWLAND, J. F. AND MAXWELL, J. A. (1958) The composition and crystallography of niocalite: *Can. Mineral*, Vol. 6, Pt. 2, pp. 264–272.

———(1960) A zirconium-bearing garnet from Oka, Quebec: *Can. Mineral*, Vol. 6, Pt. 4, pp. 549–556.

———AND MCADAM, R. C. (1963) Niobium perovskite from Oka, Quebec; a new classification for minerals of the perovskite group: *Can. Mineral*, Vol. 7, Pt. 5, pp. 683–697.

———(1964) Latrappite a proposed new name for the perovskite-type calcium niobate mineral from the Oka area of Quebec: *Can. Mineral*, Vol. 8, Pt. 1, pp. 121–122.

PERRAULT, G. (1959) Determination de la composition Chimique de pyrochlore d'Oka par spectrofluorescence des rayons X: L'Ingenier, summer 1959, pp. 40–46.

———(1960) Perovskite from Oka, Quebec: Paper presented at Min. Assoc. Canada annual meeting, Toronto.

———(1961) Pyrochlore from Oka: Paper presented at Can. Inst. Min. Metallurgy meeting, Quebec City.

———(1964) Pyrochlore from Oka, Province of Quebec, Canada: Paper presented at Min Assoc. Canada annual meeting, Toronto. (*Abst.*) *Can. Mineral*, Vol. 8, Pt. 1.

ROWE, R. B. (1956) Niobium (columbium) deposits of Canada : *Geol. Surv. Canada, Econ. Geol.* Ser. No. 18, pp. 65–88.

STANSFIELD, J. (1923) Extensions of the Monteregian Petrographic Province to the west and northwest ; *Geol. Mag.*, Vol. 60, pp. 433–453.

TANGUAY, M. G. (1963) (*Abst.*) *A. C. F. A. S. Convention*, Quebec City.

——(1964) Identification of clinopyroxenes by X-ray diffraction and optical methods : (*Abst.*) *Can. Mineral*, Vol. 8, Pt. 1.

MINERALOGICAL SOCIETY OF INDIA, IMA VOLUME, 1966
INTERNATIONAL MINERALOGICAL ASSOCIATION, PAPERS, FOURTH GENERAL MEETING

THE PYROXENES OF THE ALNÖ CARBONATITE (SÖVITE) AND OF THE SURROUNDING FENITES

HARRY von ECKERMANN
Geological Research Laboratory, Ripsa, Sweden

ABSTRACT

Chemical analyses and optical data are reported for the pyroxenes of 7 sövites and 7 adjoining fenites. The Mg and (Fe+Mn) atoms show an almost perfect replacement reciprocity, their total remaining practically constant throughout the series of analyses.

The oxidation ratio seems to have had a decisive effect on the composition of the pyroxenes. Plotted against the atomic $\frac{Fe}{Fe+Mg+Ca}$ ratio the specific gravity of pyroxenes with $Al > Fe'''$ are located on a curve different from the one of the pyroxenes with $Fe''' > Al$. Both curves are almost straight lines.

INTRODUCTION

My program of study of the rocks of the alkaline region includes a complete chemical and optical investigation of its minerals. I am making the pyroxenes the subject of this first preliminary paper.

For the analyses I am greatly indebted to the expert chemists, Miss Telma Bergren, the late Dr. G. K. Almström and the former head of the laboratory of the mineralogical department of the Museum of National History in Stockholm, Mr. R. Blix. Two of the analyses were made by myself (1939) before the closure of my private chemical laboratory in Stockholm. The speeific gravities have been determined by weighing in benzol. All optical determinations have been carried out on the universal stage, using Leitz equipment.

The minerals were separated from 15 different typical rocks within the main occurrence on Alnö Island. The brecciating sövite dikes were included but not the deep-seated carbonatitic dike rocks, which are still the subject of current research. To ensure cleanness the minerals were carefully handpicked under the microscope from the crushed rocks. On the advice of the late Professor G. Aminoff no chemicals,—neither acetic or chloritic acid, nor heavy liquids, were used to separate the pyroxenes from their generally carbonatitic base. Instead, magnetic and centrifugal methods were used to obtain a fairly small residue for the last manual microscopic treatment. It proved, however, in most cases impossible to pick out pyroxenes absolutely free from minute inclusions of carbonate and apatite. The remaining small amount had, therefore, to be deducted from the analyses. As the carbonate inclusions were proved by staining to be calcite the deduction could be calculated from the carbonic acid content of the original analyses.

The analyses comprise four pyroxenes from the sövite quarries south and north of the farm Smedsgarden, two pyroxenes from the centre of the sövite pegmatite north of Stolpas, one pyroxene from the very contact of the sövite-pegmatite towards a basic fenite, six pyroxenes from leucocratic and basic fenites, sampled in the immediate neighbourhood of the sövite contacts, and finally two pyroxenes from the rheomorphic melanocratic and basic fenites (ijolite and jacupirangite). A list of the analyses is given in Table 1 and the analyses in Tables 2 and 3.

THE CHEMICAL COMPOSITION

The pyroxenes are all monoclinic and more or less aegirine-augitic. The composition of the monoclinic pyroxenes was expressed by *Machatschki* by the general formula $XYZ_2(O,OH,F)_6$ where $X = Ca^{+2}, Na^{+1}, K^{+1}$, $Y = Mg^{+2}, Fe^{+2}, Fe^{+3}, Al^{+3}$ and $Z = Si^{+4}, Al^{+3}$. *Schiebold* combined the

two types $XYZO_6$ with Y-cations of eight-, respectively sixfold coordination, and YYZ_2O_6 with cations of sixfold coordination only, into a general formula $X_mY_{2-m}(Si,Al)_2(O,OH,F)_6$), where X = Ca,Na,K,Mn(n = 8) and Y = Mg,Fe, Al,Ti,Mn(n = 6). Finally, *Strunz* writes the general formula of augite $Ca_{6\cdot5}Na_{0\cdot5}Fe^{+2}Mg_6(Al,Fe^{+2}Ti)_2(Al_{1\cdot5-3\cdot5}Si_{14\cdot5-12\cdot5}O_{48})$,—in ægirine-augite Fe^{+3} replacing some Al,Fe^{+2} and Na some Ca.

When calculating the formulæ of the Alnö pyroxenes one finds that they generally agree very nicely with both the general formula of *Machatschki* and that of *Schiebold* if m = 1, and also with that of *Strunz*, except that the Mg : Fe^{+2}-ratio in several analyses exceeds its theoretical limit of 2 : 1.

Basing the calculation on the YZ-groups instead on the oxygen-groups one arrives at the formulae given in Table 4 and condensed in Tables 2 and 3. The reason for this method of calculation is the alteration of the original oxidation ratio of the iron which I have found to occur occasionally when grinding samples for analysis. This occurs especially if the grinding is carried too far, and mainly affects the oxygen groups of the formulae. As the analyses in this case have been carried out by four different chemists I do not know if the grinding has been properly watched. A slight error may, therefore occur in some of the analyses, and in fact 7 of them show a small excess of the oxygen-group.

The content of Al in the Y-group varies considerably and is lacking in analyses 4, 5 and 12. The variation in the Z-group is still more pronounced and reaches a maximum value in the somewhat titaniferous augite pyroxene of the jacupirangite, replacing Si to 21½%. This is an interesting figure, as *Strunz* (1957, p. 190) gives 25% as the theoretical, but still unproved, limit. If the analyses are plotted against the atomic ratios and in a series of decreasing percentages of Na + K in the X-group, we obtain the diagram of Fig. 1, which brings out some interesting features. To begin with it illustrates the almost perfect replacement reciprocity of the Mg on the one hand and the Ti + Al + Fe^{+2} + Mn + Fe^{+3} on the other within the Y-group, their total being practically a constant throughout the series of analyses, or in other words half their sum is represented in the diagram by a straight line. On the other hand, Al and Si of the Z-group, although generally reciprocal, show

TABLE 1

List of pyroxene analyses.

1. Aegirine-augitic pyroxene, rich in titanium, from the sövite quarry at Smedsgården. Chemist: T. Berggren.

2. Aegirine-augitic pyroxene, rich in titanium, from the sövite quarry at Åś jetty. Chemist: H. von Eckermann.

3. Aegirine-augitic pyroxene, fairly rich in titanium, from the sövite quarry at Smedsgården. Chemist: G. K. Almström.

4. Aegirine augite, fairly rich in titanium, from the sövite quarry at Smedsgården. Chemist: G. K. Almström.

5. Aegirine augite from sövite pegmatite at the Smedsgården farm. Chemist: T. Berggren.

6. Aegirine-augite from sövite pegmatite at Smedsgården farm. Chemist: T. Berggren.

7. Aegirine-augite from the contact of the sövite pegmatite east of Smedsgården. Chemist: T. Berggren.

8. Aegirine-augite, rich in titanium, from an ijolite quarry south-east of Hörningsholm manor house. Chemist: T. Berggren.

9. Aegirine-augite, rich in titanium, from nepheline-fenite contact towards sövite south of Hörningsholm manor house. Chemist: T. Berggren.

10. Aegirine-augite from a leucocratic fenite contact at Smedsgården farm. Chemist: R. Blix.

11. Aegirine-augite from a leucocratic nephelinitic fenite contact close to the Slada farm. Chemist: G. K. Almström.

12. Aegirine-augitic pyroxene from basic nephelinitic fenite close to sövite contact west of Hörningsholm Chemist: H. von Eckermann.

13. Aegirinitic diopsidic pyroxene, rich in titanium, from the melteigitic basic fenite east of Hörningsholm, close to a sövite contact. Chemist: T. Berggren.

14. Aegirinitic diopsidic pyroxene, rich in titanium, from the basic fenite quarry west of Åś jetty. Chemist: T. Berggren.

15. Aegirinitic augite, rich in titanium, from the jacupirangite quarry at the Släda farm. Chemist: T. Berggren.

TABLE 2

Analyses of pyroxenes of sövites and sövite-pegmatites.

	Sövites								Sövite-pegmatites					
	1		2		3		4		5		6		7	
	%w	M.P. x100	%w	M.P. x100	%w	M.P. x100	%w	M.P. x100	%w	M.P. x100	%w	M.P. x100	%w	M.P. x100
SiO_2	43.34	75.49	45.60	75.92	47.52	79.12	48.26	80.35	49.05	81.67	49.60	82.58	50.65	84.33
TiO_2	1.23	1.54	0.94	1.18	0.93	1.16	0.94	1.18	0.60	0.75	0.69	0.86	0.61	0.76
ZrO_2	0.00	—	—	—	0.01	0.01	—	—	0.00	—	—	—	0.00	—
Al_2O_3	9.36	9.18	8.01	7.86	5.01	4.92	4.23	4.15	2.22	2.18	2.69	2.64	2.18	2.14
Fe_2O_3	6.74	4.22	4.70	2.94	6.68	4.18	5.33	3.34	9.32	5.84	8.04	5.04	8.15	5.10
FeO	2.48	3.45	4.31	6.00	3.62	5.04	4.56	6.35	10.20	14.20	10.70	14.89	6.51	9.06
MnO	0.18	0.25	0.13	0.18	0.10	0.14	0.07	0.10	1.65	2.33	1.32	1.86	0.55	0.78
MgO	11.25	27.90	11.08	24.48	11.25	27.90	12.35	30.63	5.14	12.75	6.28	15.58	8.85	21.95
CaO	21.91	39.19	23.59	42.02	22.60	40.30	21.82	38.89	18.00	32.10	16.54	29.49	19.56	34.89
BaO	0.00	—	—	—	0.03	0.02	0.00	—	0.06	0.04	—	—	0.00	—
SrO	0.00	—	—	—	<0.01	—	—	—	—	—	—	—	0.00	—
Na_2O	0.64	1.03	0.92	1.48	0.91	1.47	1.19	1.92	3.10	5.00	2.25	3.63	1.83	2.95
K_2O	0.54	0.57	0.27	0.29	0.27	0.29	0.57	0.61	0.20	0.21	0.53	0.56	0.28	0.30
Cl	0.03	0.09	—	—	0.02	0.06	—	—	0.03	0.09	V_2O_5 0.10	V_2O_5 0.07	0.02	0.06
F	0.05	0.26	0.09	0.47	0.07	0.37	—	—	0.15	0.79	—	—	0.01	0.05
H_2O^+ 110°	0.28	1.55	0.16	0.84	0.22	1.22	0.68	3.78	0.21	1.17	0.49	2.72	0.15	0.83
H_2O^- 110°	0.09	—	0.12	—	0.68	—	0.34	—	0.20	—	0.63	—	0.27	—
Total	100.19		99.92		99.92		100.34		100.13		99.86		99.62	

1. $X_{0.94}\ Y_{1.00}\ Z_{2.00}\ (O,OH,Cl,F)_{6.00}$ 2. $X_{0.99}\ Y_{1.00}\ Z_{2.00}\ (O,OH,Cl,F)_{6.01}$ 3. $X_{1.00}\ Y_{1.00}\ Z_{2.00}\ (O,OH,Cl,F)_{6.01}$ 4. $X_{0.99}\ Y_{1.01}\ Z_{2.00}\ (O,OH,Cl,F)_{.04}$
5. $X_{1.00}\ Y_{1.00}\ Z_{2.00}\ (O,OH,Cl,F)_{6.05}$ 6. $X_{1.00}\ Y_{0.99}\ Z_{2.00}\ (O,OH,Cl,F)_{6.04}$ 7. $X_{0.95}\ Y_{1.00}\ Z_{2.00}\ (O,OH,Cl,F)_{6.00}$

$X = Ca + Ba + Sr + Na + K$ $Y = Ti + Al + Fe^{+2} + Fe^{+3} + Mn + Mg$ $Z = Si + Al$

TABLE 3

Analyses of the pyroxenes of fenites and rheomorphic fenites bordering on the carbonatites.

	Ijolite		Nepheline fenite		Fenites				Basic fenites						Jacupirangite	
	8		9		10		11		12		13		14		15	
	%w	M.P. x100	%w	M.P. x100	%w	M.P. x100	%w	M.P. x100	%w	M.P. x100	%w	M.P. x100	%w	M.P. x100	%w	M.P. x100
SiO_2	45.32	75.46	48.35	80.50	49.61	82.60	49.75	82.83	41.81	69.61	46.54	77.49	46.43	77.31	42.80	71.26
TiO_2	2.16	2.70	1.55	1.94	0.50	0.63	0.47	0.59	3.01	3.77	1.81	2.27	2.16	2.19	2.28	2.85
ZrO_2	—	—	V_2O_5 0.12	V_2O_5 0.08	0.00	—	—	—	—	—	0.15	0.12	—	—	0.00	—
Al_2O_3	7.27	7.13	3.27	3.21	2.75	2.70	3.07	3.01	7.99	7.84	6.31	6.19	6.27	6.15	9.86	9.67
Fe_2O_3	5.91	3.70	6.26	3.42	15.49	9.70	17.77	11.13	9.10	5.70	5.46	3.42	6.87	4.30	5.68	3.56
FeO	5.62	7.82	9.39	13.07	4.90	6.82	5.37	7.48	7.23	10.06	5.56	7.74	6.03	8.39	6.05	8.42
MnO	0.36	0.51	0.80	1.13	1.62	2.28	1.03	1.45	0.38	0.54	0.33	0.47	0.52	0.73	0.29	0.41
MgO	9.56	23.71	7.53	18.68	4.64	11.51	3.50	8.68	6.80	16.87	9.77	24.23	8.48	21.03	8.87	22.00
CaO	21.35	38.07	20.16	35.95	15.80	28.17	10.29	18.35	22.59	40.28	22.05	39.32	20.78	37.05	23.14	41.26
BaO	—	—	—	—	<0.005	—	—	—	<0.01	—	0.02	0.01	—	—	0.02	0.01
SrO	—	—	—	—	<0.005	—	—	—	<0.01	—	0.01	0.01	—	—	0.00	—
Na_2O	1.32	2.13	1.85	2.98	4.46	7.19	7.49	11.92	0.65	1.05	1.12	1.81	1.27	2.05	0.72	1.16
K_2O	0.68	0.72	0.42	0.45	0.21	0.22	0.39	9.41	0.11	0.11	0.53	0.56	0.92	0.98	0.13	0.14
Cl	0.05	0.14	—	—	0.02	0.06	—	—	—	—	0.04	0.11	0.05	0.14	0.03	0.09
F	0.06	0.32	—	—	0.01	0.05	—	—	—	—	0.02	0.11	0.04	0.21	0.07	0.37
$H_2O^{+110°}$	0.28	1.55	0.05	0.28	0.15	0.83	0.97	5.38	0.12	0.67	0.10	0.56	0.28	1.55	0.10	0.56
$H_2O^{-100°}$	0.08		0.00		(0.21)		0.17		0.17		0.02		0.06		0.20	
Total	100.03		99.75		100.16		100.17		99.96		99.92		100.19		100.24	

8. $X_{1.00}\,Y_{1.00}\,Z_{2.00}\,(O,OH,Cl,F)_{5.00}$ 9. $X_{0.99}\,Y_{1.00}\,Z_{2.00}\,(O,OH,Cl,F)_{5.99}$ 10. $X_{1.00}\,Y_{0.99}\,Z_{2.00}\,(O,OH,Cl,F)_{6.04}$ 11. $X_{1.00}\,Y_{1.00}\,Z_{2.00}\,(O,OH,Cl,F)_{6.09}$
12. $X_{1.00}\,Y_{1.00}\,Z_{2.00}\,(O,OH,Cl,F)_{6.02}$ 13. $X_{1.01}\,Y_{1.00}\,Z_{2.00}\,(O,OH,Cl,F)_{6.08}$ 14. $X_{0.99}\,Y_{1.00}\,Z_{2.00}\,(O,OH,Cl,F)_{6.07}$ 15. $X_{1.00}Y_{1.00}Z_{2.00}\,(O,OH,Cl,F)_{6.00}$

$X = Ca + Ba + Sr + Na + K$ $Y = Ti + Al + Fe^{+2} + Fe^{+3} + Mn + Mg$ $Z = Si + Al$

some very marked irregularities of the Al-curve, as for instance in the case of the sövite (no. 1), the sövite pegmatite (no. 6) and the jacupirangite (no. 15). Similar aberrations occur in the same pyroxenes in the "Na+K"-and "Ca+Ba+Sr"-curves of the X-group.

TABLE 4

Molecular percentages within each of the groups X,Y and Z

Anal. No.	X	Y	Z
1.	$((Na,K,)_8Ca_{92})$	$(Ti_3Al_8(Fe^{tot},Mn)_{27}Mg_{62})$	$(Al_{16}Si_{84})$
2.	$((Na,K,)_4Ca_{96})$	$(Ti_2Al_8(Fe^{tot},Mn)_{28}Mg_{32})$	$(Al_{14}Si_{86})$
3.	$((Na,K)_8Ca_{92})$	$(Ti_2Al_2(Fe^{tot},Mn)_{32}Mg_{64})$	$(Al_{10}Si_{90})$
4.	$((Na,K)_{11}Ca_{89})$	$(Ti_2Al_6(Fe^{tot},Mn)_{30}Mg_{64})$	(Al_9Si_{91})
5.	$((Na,K)_{25}Ca_{75})$	$(Ti_2Al_2(Fe^{tot},Mn)_{66}Mg_{30})$	(Al_4Si_{96})
6.	$((Na,K)_{22}Ca_{78})$	$(Ti_2Al_6(Fe^{tot},Mn)_{64}Mg_{36})$	(Al_6Si_{94})
7.	$((Na,K)_{16}Ca_{84})$	$(Ti_2Al_2(Fe^{tot},Mn)_{45}Mg_{51})$	(Al_4Si_{96})
8.	$((Na,K)_{13}Ca)_{87}$	$(Ti_6Al_4(Fe^{tot},Mn)_{36}Mg_{54})$	$(Al_{14}Si_{86})$
9.	$((Na,K)_{16}Ca_{84})$	$(Ti_4Al_2(Fe^{tot},Mn)_{50}Mg_{44})$	(Al_7Si_{93})
10.	$((Na,K)_{34}Ca_{66})$	$(Ti_2Al_1(Fe^{tot},Mn)_{36}Mg_{28})$	(Al_4Si_{96})
11.	$((Na,K)_{57}Ca_{43})$	$(Ti_2Al_6(Fe^{tot},Mn)_{72}Mg_{20})$	(Al_4Si_{96})
12.	$((Na,K)_6\ Ca_{94})$	$(Ti_8Al_0(Fe^{tot},Mn)_{52}Mg_{40})$	$(Al_{21}Si_{79})$
13.	$((Na,K)_{11}Ca_{89})$	$(Ti_6Al_6(Fe^{tot},Mn)_{34}Mg_{54})$	$(Al_{12}Si_{88})$
14.	$((Na,K)_{14}Ca_{86})$	$(Ti_0Al_6(Fe^{tot},Mn)_{40}Mg_{48})$	$(Al_{12}Si_{88})$
15.	$((Na,K)_8\ Ca_{92})$	$(Ti_0Al_8(Fe^{tot},Mn)_{36}Mg_{50})$	$(Al_{19}Si_{81})$

Plotting in Fig. 2 the weight percentages of the oxides against the weight percentage of the SiO_2-content a marked replacement reciprocity of total Fe, calculated as FeO, plus MnO on the one hand and MgO on the other is noticeable. It is almost perfect up to 45.7% SiO_2 but shows at higher values an irregularly increasing MgO-dominance. There is also a general reciprocity between the CaO and Na_2O+K_2O curves, but it is less pronounced and more irregular, the irregularities occuring in the previously mentioned pyroxenes of analyses 1, 6 and 15. Seeking an explanation for these aberrations I plotted the atomic oxidation ratios $Fe^{+3} : Fe^{+2}+Fe^{+3}$, which resulted in the rather irregular curve of Fig. 3. No connection between the irregularities and the oxidation rate can be traced from this diagram but it illustrates the great variation between pyroxenes of similar rocks. The ratios of pyroxenes from leucocratic fenites vary between 0.38 and 0.76, those from sövites between 0.50 and 0.62, from sövite pegmatites between 0.45 and 0.53, from basic fenites between 0.49 and 0.51 and from rheomorphic fenites between 0.49 and 0.59. Of these values, the highest ones, *i.e.* those for aegirine-augites from the sövite–leucocratic fenite-contacts, are of special interest. They suggest a maximum oxidation reaction at these contacts, which may, perhaps, be explained by a corresponding maximum concentration of high-tension carbon dioxide resulting from an addition of the free CO_2 within the carbonatitic magma to the CO_2 set free by the fenitization reaction: $CaCO_3+SiO_2=CaSiO_3+CO_2$. The lower oxidation ratios of the pyroxenes at the "sövite-basic fenite" contacts may be explained by the absence of any remaining silica as quartz or easily decomposed metasilicates to start a fenitization reaction. In consequence, the oxidation ratio of the pyroxenes within these rocks as well as in the sövites and the sövite pegmatites must have been mainly governed by the local concentration of free CO_2 and variation of CO_2-pressure. This is also confirmed by the approximately equal order of magnitude of the oxidation ratio. However, there is one exception. While the oxidation ratios of the rheomorphic fenites lie within the 0.45–0.62 limits of the lower values, there is an exception in the case of the above mentioned 0.38–ratio of one of the pyroxenes from a leucocratic fenite. It may perhaps be explained by the dominantly feldspathic composition of the fenite in question. This seems to have been originally an Archaeic schist fairly rich in feldspar and poor in quartz which was regionally fenitized and feldspathized by the action of the fairly remote central sövite magma. The alteration of the biotite of the original rock into pyroxene may, in consequence, have occurred at some distance from the present contact towards a brecciating sövite dike and at a comparatively low oxidation rate. This dike could, therefore, not have started any fenitization action or alteration of the earlier fixed oxidation ratio.

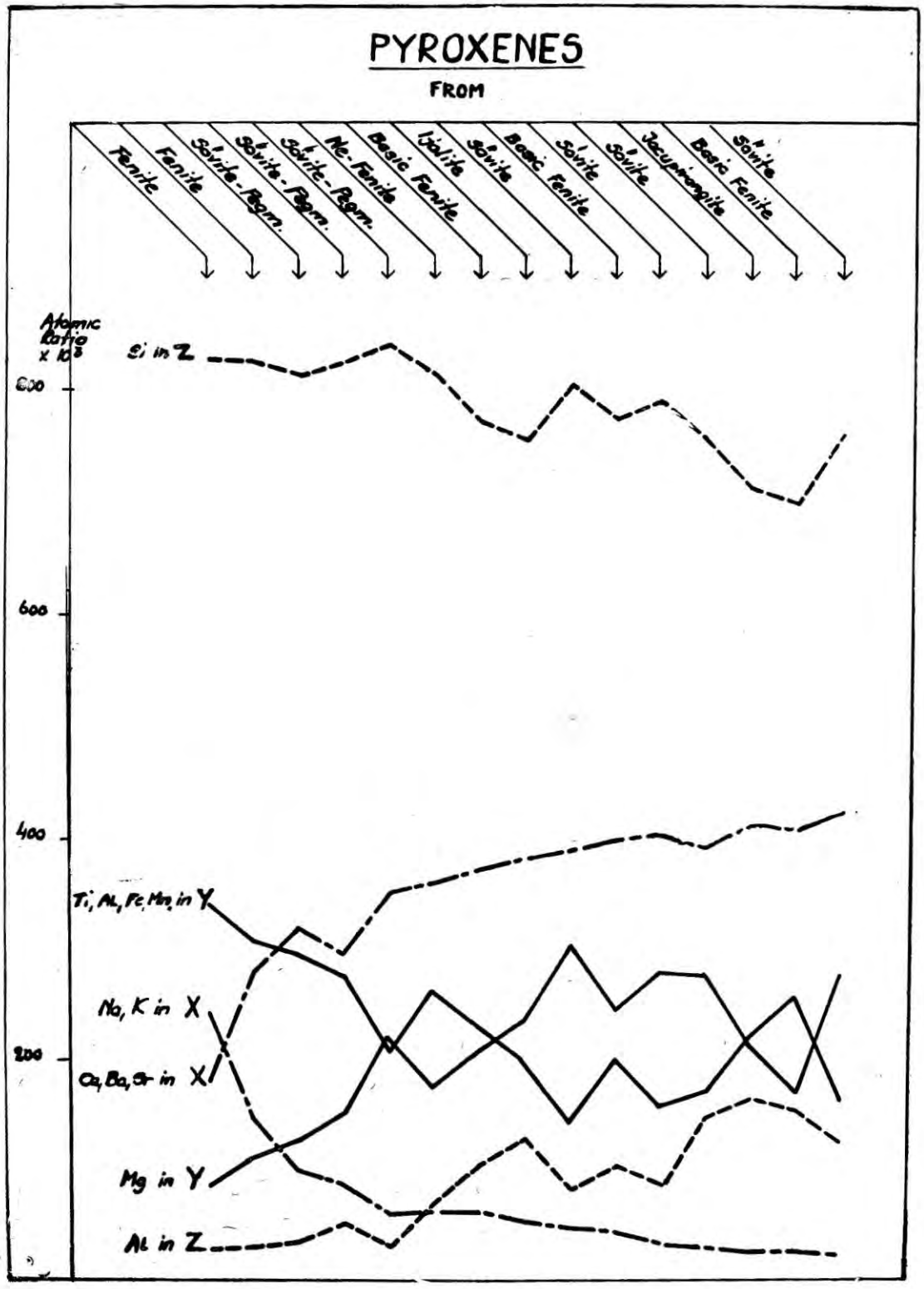
PYROXENES
FROM
Fenite
Fenite
Sövite-Pegm.
Sövite-Pegm.
Sövite-Pegm.
Ne-Fenite
Basic Fenite
Ijolite
Sövite
Basic Fenite
Sövite
Sövite
Jacupirangite
Basic Fenite
Sövite
Atomic Ratio x 10³
Si in Z
800
600
400
200
Ti, Al, Fe, Mn in Y
Na, K in X
Ca, Ba, Sr in X
Mg in Y
Al in Z

Fig. 1

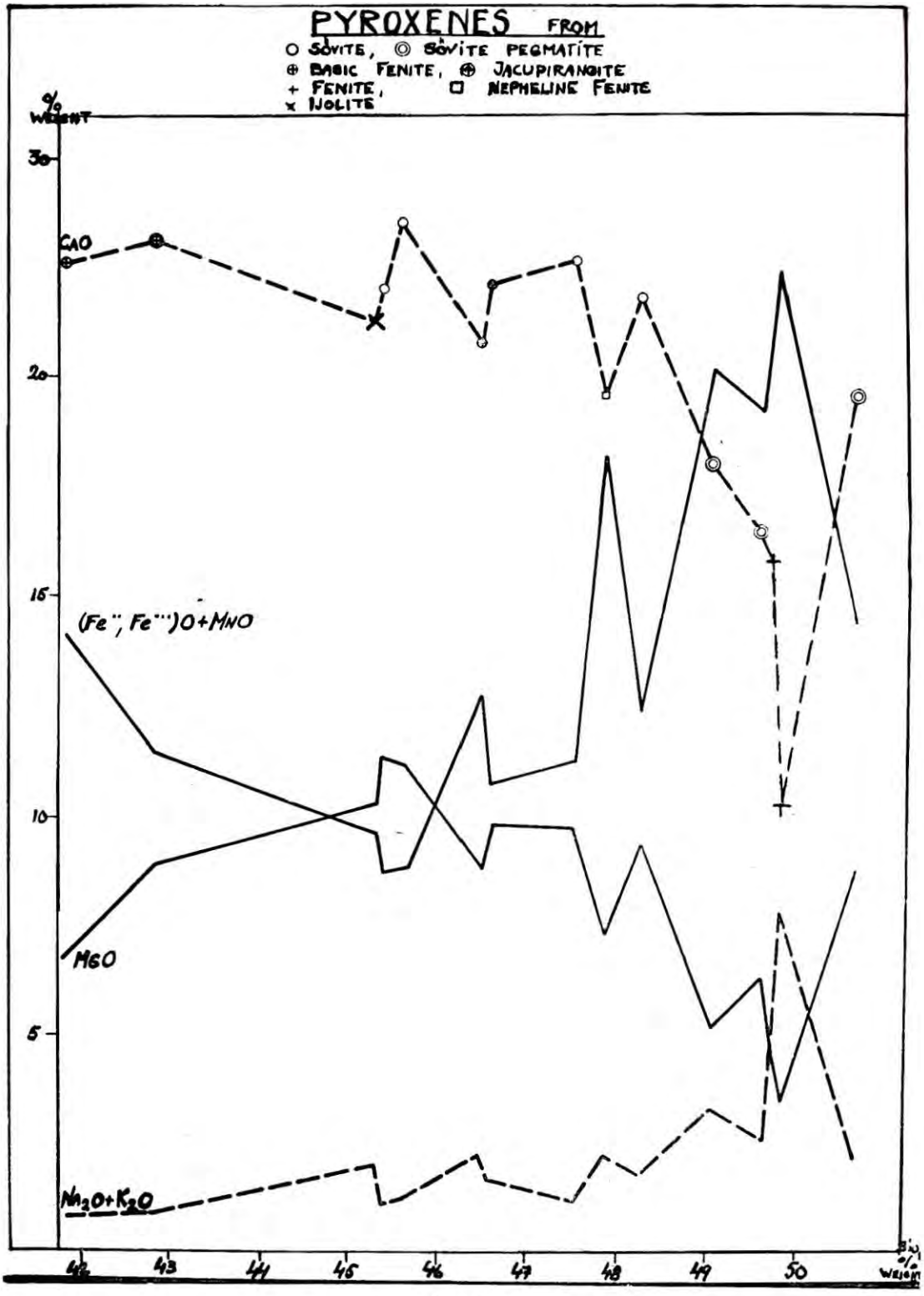
PYROXENES FROM
○ SÖVITE, ◎ SÖVITE PEGMATITE
⊕ BASIC FENITE, ⊕ JACUPIRANGITE
+ FENITE, □ NEPHELINE FENITE
× IJOLITE
% WEIGHT
30
20
15
10
5
CaO
(Fe", Fe"')O+MnO
MgO
Na2O+K2O
42
43
44
45
46
47
48
49
50

Fig. 2

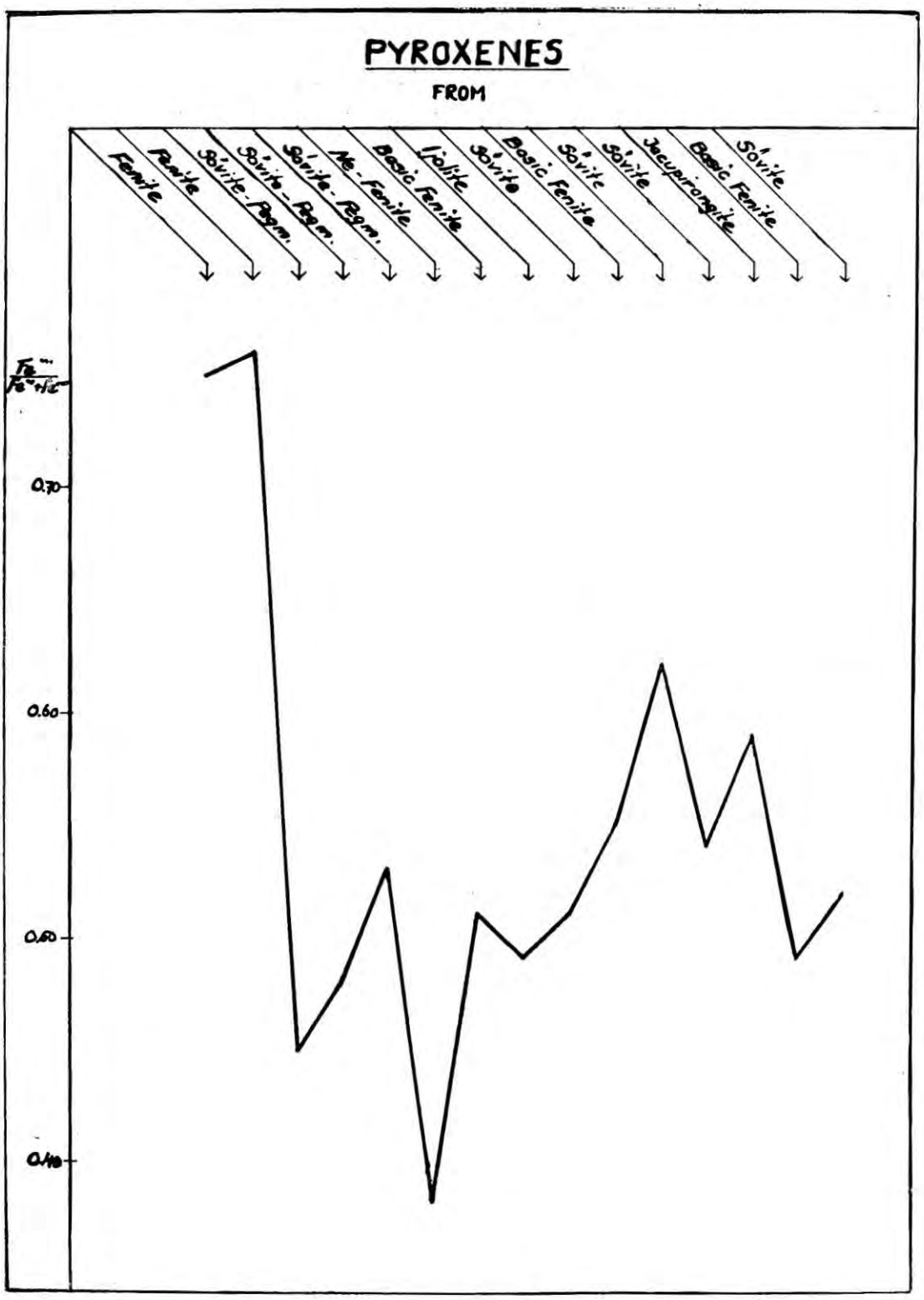
PYROXENES
FROM
Fenite
Fenite
Sövite-Pegm.
Sövite-Pegm.
Sövite-Pegm.
Me.-Fenite
Basic Fenite
Iolite
Sövite
Basic Fenite
Sövite
Sövite
Aegyprinite
Basic Fenite
Sövite
0.70
0.60
0.50
0.40

Fig. 3

Finally, plotting of the atomic percentages of the X and Y groups may give an indication of the quality and reliability of the analyses. Theoretically, all the analyses should fall along the straight line " 50–50 " of Fig. 4, the size of the X-group being the same at the sum of the

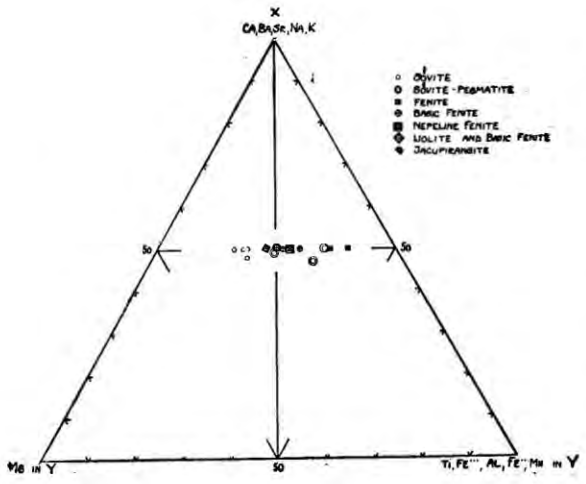

Fig. 4

two components " Mg " and " Ti,Fe^{+3},Al,Fe^{+2}, Mn " of the Y-group. Only three analyses show any deviation from the theoretical 50%: a very slight one in the case of sövite pegmatite (analysis 7), a small one in the case of a sövite (analysis 1) and a somewhat larger one in the case of another sövite pegmatite (analysis 6). These aberrations may be due to an excess of free carbonic acid entrapped as minute vesicles during the crystallization of the pyroxenes and that, in consequence, too much CaO was calculated as impurity in the original analysis. The diagram also illustrates the Mg-dominance in the pyroxenes of the sövites as compared with the sövite pegmatites, and the Fe(total)-dominance in the pyroxenes of the leucocratic fenite contacts.

THE SPECIFIC WEIGHTS

Measurement of the specific gravity of the pyroxenes included the carbonate and apatite inclusions which were deduced from the original analyses. In eight cases they amounted to 1.7—2.7%, while they were absent in the other seven. But in both cases minute, probably gas-filled vesicles, observable in thin slides at very high magnification may have reduced the specific gravity value. Further pulverizing of the sample by the chemist may also help to explain discrepancies as some of these vesicles may have been opened up and disappeared. In consequence, a series of determinations had to be carried out for each pyroxene. The maximum and minimum values of these determinations and the calculated average values are given in Table 5.

TABLE 5

Specific weights of pyroxenes

Anal. No.	Sp. Wt.	Average of	Determinations ranging from
Sovites			
1.	3.325	20	3.073 to 3.460
2.	3.328	10	3.326 to 3.331
3.	3.337	10	3.330 to 3.348
4.	3.338	10	3.335 to 3.340
Sovite-pegmatites			
5.	3.519	20	3.421 to 3.562
6.	3.507	10	3.489 to 3.517
7.	3.476	20	3.394 to 3.473
Ijolite			
8.	3.381	10	3.369 to 3.390
Nepheline-fenite			
9.	3.460	20	3.394 to 3.479
Leucocratic fenites			
10.	3.513	10	3.502 to 3.520
11.	3.599	10	3.586 to 3.606
Basic fenites			
12.	3.437	10	3.409 to 3.440
13.	3.371	10	3.368 to 3.380
14.	3.410	10	3.396 to 3.419
Jacupirangite			
15.	3.441	10	3.335 to 3.447

There seems to exist a definite relationship between the oxidation ratio and the average specific weight of the pyroxenes. Plotting the atom-percentage-ratio of total Fe : Fe+Mn+Mg+Ca (=XY-groups minus alkalies) the

pyroxenes of Al > Fe^{+3} and those of Fe^{+3}>Al fall on two different curves, apparently straight lines. As shown by Fig. 5 all pyroxenes from sövites, basic fenites and ijolite fall along one line, while those from sövite pegmatites, leucocratic fenites and jacupirangite fall along the other one. The projection of the first mentioned line points towards the most Fe^{+3}–dominant sövite-pegmatite pyroxenes of the other one. Unfortunately, as already stated above, the analyses and the specific gravities do not quite correspond to each other, although determined on the same sample. Furthermore, I have already drawn attention to errors in oxidation ratio due to a prolonged and too far-reaching pulverisation of the sample. In consequence, these sources of error may influence the above mentioned relationship between specific weight and Fe^{+3} : Al-ratio to such an extent that it may actually be nothing but a coincidence. Further analyses may give a definite answer.

THE OPTICAL DATA

Before the rocks were crushed and powdered in order to prepare samples for separation of the pyroxenes a representative set of thin slides was made from each rock. From these thin slides the axial angles and extinctions of the pyroxenes were determined on the universal stage and the average, obtained from values of each set of thin slides, was taken to represent the optical data of the pyroxene in question. Several of the pyroxenes proved to be of more or less zonal structure, the rims always being more aegiritic than the cores. Narrow rims were neglected and the determinations carried out on the cores only, though in the case of pronounced heterogeneous pyroxenes, such as those of analyses 1, 5, 7 and 9, the minimum and maximum values were recorded.

The refractive indices were determined by immersion liquids on the universal stage. In this case, too, only minimum and maximum values were established in the above mentioned four pyroxenes. Even a comparatively slight heterogeneity of the pyroxenes of analyses 2, 4, 6, and 8 made a reliable determination of n-values difficult, for which reason only $n\gamma$ and $n\alpha$ were recorded. The pyroxenes of analyses 3, 10, 11, 12, 13, 14 and 15 were apparently homogeneous. They allowed a determination of $n\beta$, which is believed to be fairly correct.

The optical data are given in Table 6 and the axial angles and the $n\gamma$ and $n\alpha$ refractive indices also in the diagram, Fig. 6. These data

TABLE 6

Optical data

Anal. No.	$n\gamma$	$n\beta$	$n\alpha$	$n\gamma - n\alpha$	c/α	$2V_{Na} \pm 1°$
1.	1.725-1.731		1.698-1.701	0.029-0.033	-33°- -41°	+53°-+70°
2.	1.738		1.706	0.032	-29°	+68°
3.	1.726	1.705	1.698	0.028	-39°	+58°
4.	1.730		1.699	0.031	-35°	+61°
5.	1.748-1.751		1.718-1.721	0.028-0.033	-26°- -36°	+55°-+72°
6.	1.743		1.710	0.033	-30°	+77°
7.	1.731-1.735		1.707-1.710	0.028-0.037	-28°- -32°	+74°-+77°
8.	1.745		1.715	0.030	-29°	+58°
9.	1.740-1.766		1.706-1.730	0.028-0.036	-20°- -38°	+64°-+82°
10.	1.768	1.748	1.731	0.037	-20°	±90°
11.	1.783	1.767	1.745	0.038	-12°	—82°
12.	1.742	1.720	1.710	0.032	-41°	+56°
13.	1.739	1.722	1.714	0.025	-29°	+59°
14.	1.735	1.713	1.704	0.031	-29°	+67°
15.	1.743	1.723	1.717	0.026	-48°	+60°

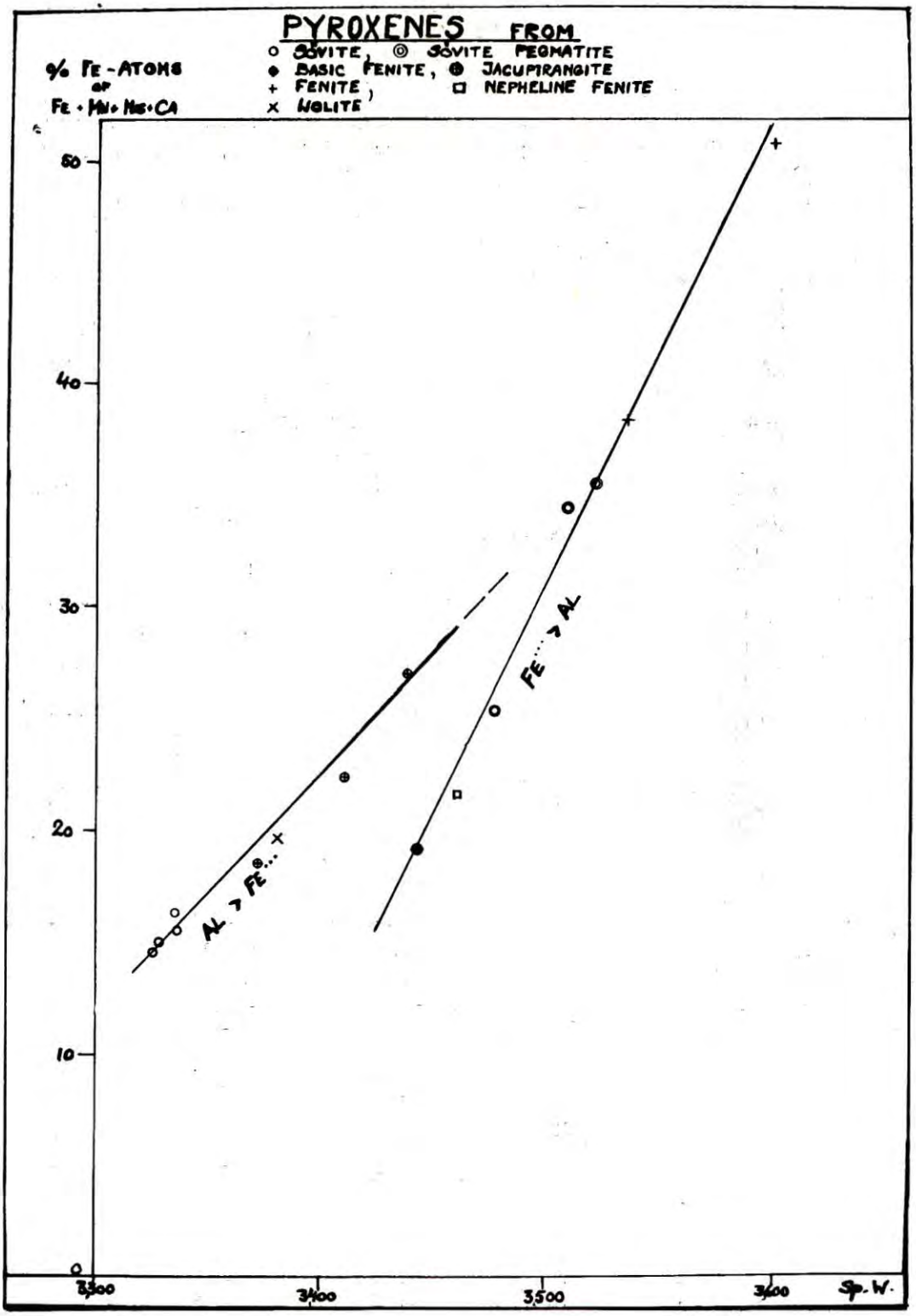
PYROXENES FROM
% Fe-ATOMS or Fe + Mn + Mg + Ca
○ JOVITE, ◎ JOVITE PEGMATITE
● BASIC FENITE, ⊕ JACUPIRANGITE
+ FENITE, □ NEPHELINE FENITE
× MOLITE
60
40
30
20
10
0
Al > Fe⁺⁺⁺
Fe⁺⁺⁺ > Al
3300
3400
3500
3600
Sp. W.

Fig. 5

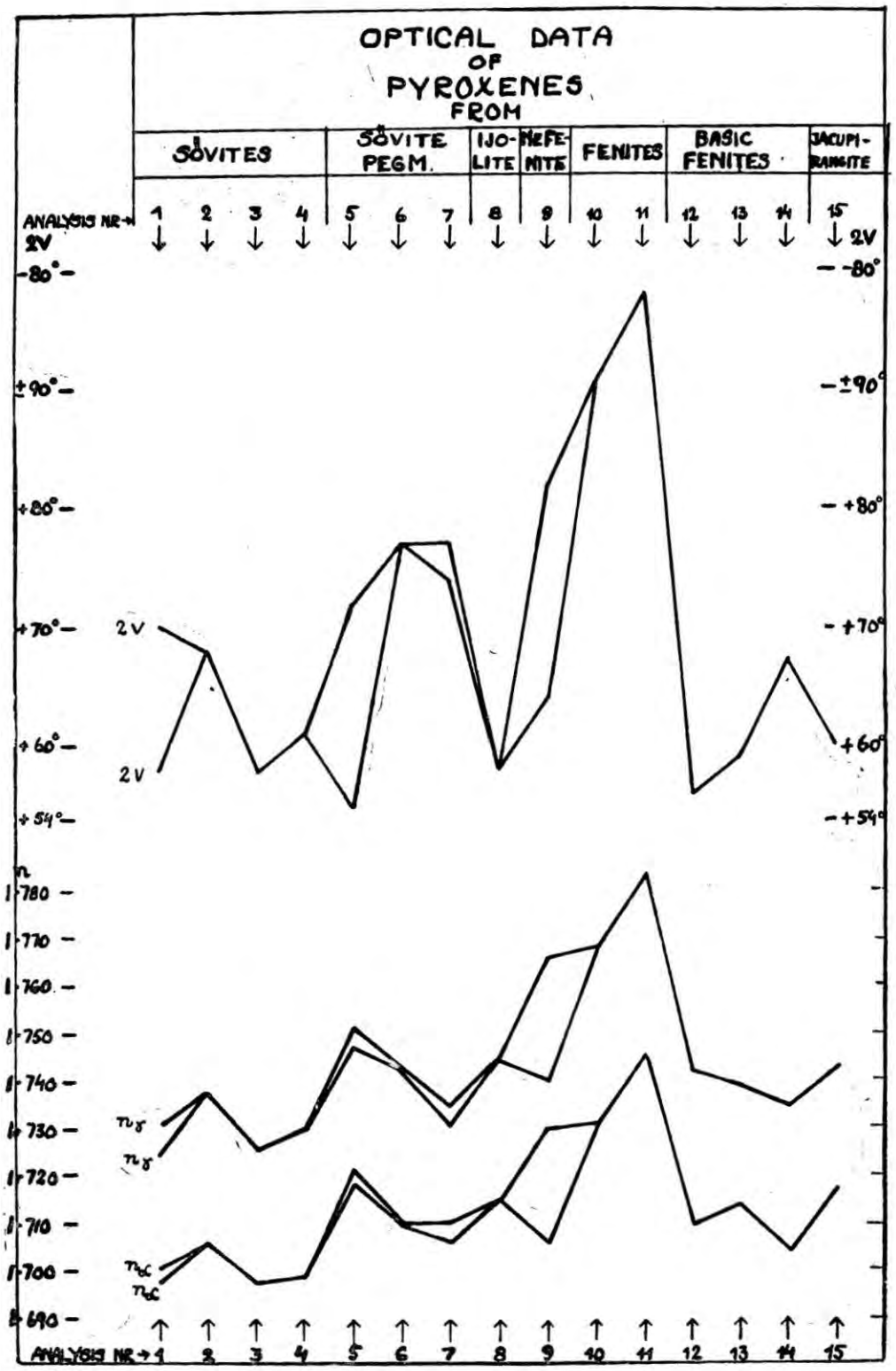
OPTICAL DATA
OF
PYROXENES
FROM
SÖVITES
SÖVITE PEGM.
IJO-LITE
MEFE-MITE
FENITES
BASIC FENITES
JACUPI-RANGITE
ANALYSIS NR→
2V
2V
2V
2V
ANALYSIS NR→

Fig. 6

do not agree very well with *Tröger's-Larsen's* diagram of "augites–aegirine-augites–aegirines". This is probably for several reasons, the most important being:

(1) the presence of inclusions of calcite and apatite in the pyroxenes of the thin slides and in the crystals or crystal fragments used in immersion determinations but deducted from the analyses,

(2) the occurrence of TiO_2 in the pyroxenes in amounts varying from 0.47% up to 3.01%,

(3) the occurrence of V_2O_5 in analyses 6 and 9, ZrO_2 in analyses 13 and various trace elements recorded in Table 7,

(4) the presence of various amounts of minute CO_2–filled vesicles, especially numerous in the pyroxenes from extremely carbonatitic rocks, and

(5) the more or less pronounced zonal structure of the majority of the pyroxenes.

(6) the presence of trace elements, of which, unfortunately, only a rather incomplete qualitative determination was made spectrographically (Table 7).

CONCLUSION

Even at one and the same locality thin slides of rock samples taken only a few centimeters apart show variations of up to several degrees in the axial angles of the pyroxenes. The optical as well as the physical and chemical data of the present investigation are, therefore, average values and the three sets of data are not necessarily in complete agreement with each other though deriving from the same mineral. But even if only approximate they give a general idea of the characteristics of the pyroxenes of the Alnö sövite and its adjoining fenites and their derivates.

The present research has brought to light the great variety of the Alnö pyroxenes, from diopsidic and titaniferous aegirine-augites to strongly aegirinic ones. This wide spread of compositions seems to be duplicated in the case of the pyroxenes of the Russian alkaline Siberian rocks, as illustrated by the works of Konova (1961), Jaschina (1962) and others. For other similar alkaline regions associated with carbonatites and kimberlites as in eastern and southern Africa only a few, mostly random analyses, have been published, and are insufficient for comparisons to be made.

TABLE 7

Qualitative spectrographic analyses of some of the pyroxenes.

Anal. No.	1	3	4	7	13	15
Al	++	++	++	+	++	++
As	*					
Ba	*			*	*	+
Be	—			+		
Bi	*	*		*		
Ca	+	+	+	+	++	+
Cd		*				
Co	*	*	*	+		
Cr	—		+	*		+
Cu	*	+	+	*	—	+
Fe	++	+	+	++	++	+
Ga	*	*	+		+	+
K	+		+	+	+	+
Mg	++	++	++	++	++	++
Mn	+	+	+	+	+	+
Na	+	+	+	+	+	+
P						
Pb	*	—	*	*		*
Si	+	+	++	+	++	++
Sn	*		*	+	—	
Ti	+	+	+	+	++	+
Ta			+			*
Tl				*		*
V	*	*	+	*	*	*
Zn	*	+		*	+	*
Zr		*			+	

++ Occur in comparatively large amounts.

\+ Occurs. Two of the strongest and last disappearing lines shown in the spectrum.

* Probably occurring, but uncertain. The strongests spectral line observed.

— Uncertain, but probably not occurring. The quantity, normally observable was about 0.01%.

REFERENCES

JASCHINA, R. M. (1962) The alkaline rocks of Siberia, pp. 7-38. Akademija Nauk SSSR, Instituta geologii, Wypusk 76.

KONOVA, A. V. (1961) Urtite-ijolitic intrusives of south-eastern Tuby and some questions about their genesis. Akademija Nauk SSSR, Instituta geologii, Wypusk 60.

STRUNZ, H. (1957) Mineralogische Tabellen, 3. Auflage, Leipzig.

DISCUSSION

Bibhuti Mukherjee (Geological Survey, Calcutta): The effect of grinding on oxidation led the professer to calculate the unit of pyroxene not on the basis of total available oxygen atoms (on total anions as the unit). It was also stated that the valency status of iron were changed by grinding for long time. Has this affect been proved from actual analysis of the mineral before and after grinding? Has the structural change been observed from X-ray study?

Author's reply: The increased oxidation ratio of the iron was discovered when part of an already ground sample was left by mistake in a moving grinder over week end. When taken out of grinder it was quite hot. The analysis gave 5.83% Fe_2O_3 and 3.49% FeO, indicating an aegirine content not quite in agreement with previously determined optical data. A second analysis of the original sample, listed as no. 2 in this paper, gave 4.70% Fe_2O_3 and 4.31% FeO. The almost identical total iron content of the two analysis, 6.63%, resp. 6.64% proves the homogeneity of the two samples. A repeated prolonged grinding test confirmed the oxidation effect. Unfortunately, I had at that time no means at my disposal for X-ray studies.

MINERALOGICAL SOCIETY OF INDIA, IMA VOLUME, 1966
INTERNATIONAL MINERALOGICAL ASSOCIATION, PAPERS, FOURTH GENERAL MEETING

CARBONATITES, THEIR FABRIC, CHEMISTRY AND THEIR GENESIS

P. PAULITSCH AND H. AMBS
Mineralogisch-Petrographisches Institut der Technische Hockschule, Darmstadt

ABSTRACT

Carbonatites from :Schelingen (Kaiserstuhl) and other localities were investigated with x-ray, optical and chemical methods. Comparing the *fabric*-diagrams of these carbonatites with such of Alnö (von Eckermann, 1948) and Sφve (Sæther, 1957, Ambs, 1962), we see in all three cases similar geometrical relations.

This observation leads us to the interpretation of geometrical two-fold phases of origin, namely *deformation and the new recrystallization.* During the new recrystallization a new typical *fabric*-habit was formed conformable with Wimmenauer (1962, 1963). Biaxial calcites in these carbonatites are orientated (compare Paulitsch, 1950). The content of Sr determined by Wambeke (1960) is relatively high; that gives for the Mg-content too.

The experiments of *Wyllie & Tuttle (1960)* in the system CaO-CO_2-H_2O with respect to the amount of pressure and the investigations about the isotopic composition of oxygen and carbon of Bærtschi (1957) and Paulitsch & Hahn-Weinheimer (1961) with respect to different types of paragenesis are corresponding very well with our *fabric*-results.

INTRODUCTION

Today carbonatites are recognized to be a special type or genesis: Because of

1) their *paragenesis* with basic rocks, rich in alkalis,
2) their *characteristic minerals*, which belong to the pyrochlor-group, and
3) their *trace-element-distribution* with a high Strontium-content.

DETERMINATION OF CALCITE GRAIN-FABRIC

The interesting question from the *petrofabric* point of view is:

Is a special *calcite grain-fabric* involved in the carbonatites or can it be compared with those already known from other rock formations?

Fig. 1 shows all the well-known types of calcite fabric. The first c-axes diagram, on the left, describes a calcite fabric, which would be expected in magmatic flow. The second diagram represents the recrystallized fabric with two maxima, according to Felkel (1929).

The fourth column shows a metamorphic fabric from Auerbach-marble, Odenwald; there is a maximum for *c* (top diagram), and from X-ray results (not shown here) prism *a* $(11\bar{2}0)$ often lies parallel to *B*. The sedimentary fabric of Carrara in the next diagram is poorly orientated, while new X-ray results show, that the Harnish Carrara in the last two diagrams has a good orientation of the prism *a* $(11\bar{2}0)$ (top diagram) and rhombohedron *r* $(10\bar{1}1)$ of calcite (bottom diagram). The main-axis of calcite lies parallel to the lineation and lies at the south pole in the two diagrams.

The purpose of our investigations is to fill the *gap* in the carbonatite study, to contribute diagrams for Kaiserstuhl-carbonatites and to compare those with the diagrams already available for Sφve (Saether, 1957) and Alnö (v. Eckermann, 1948).

Fig. 2 shows the investigated rock specimen from Kaiserstuhl/Schelingen with white coarse-grained and dark fine-grained layers; the colour is given by koppite, magnesioferrite and to a lesser extent apatite and mica. We obtained the oriented specimen by the courtesy of Prof. Wimmenauer.

At the last meeting (1960) we were able to collect the samples from Sφve (Ulefoss) for comparison. Fig. 3 shows the mixture of basic rocks with calcite.

Fig. 4 answers the first question, concerning the position of the 294 *c*-axes in Schelingen; this figure represents the *c*-axes orientation for

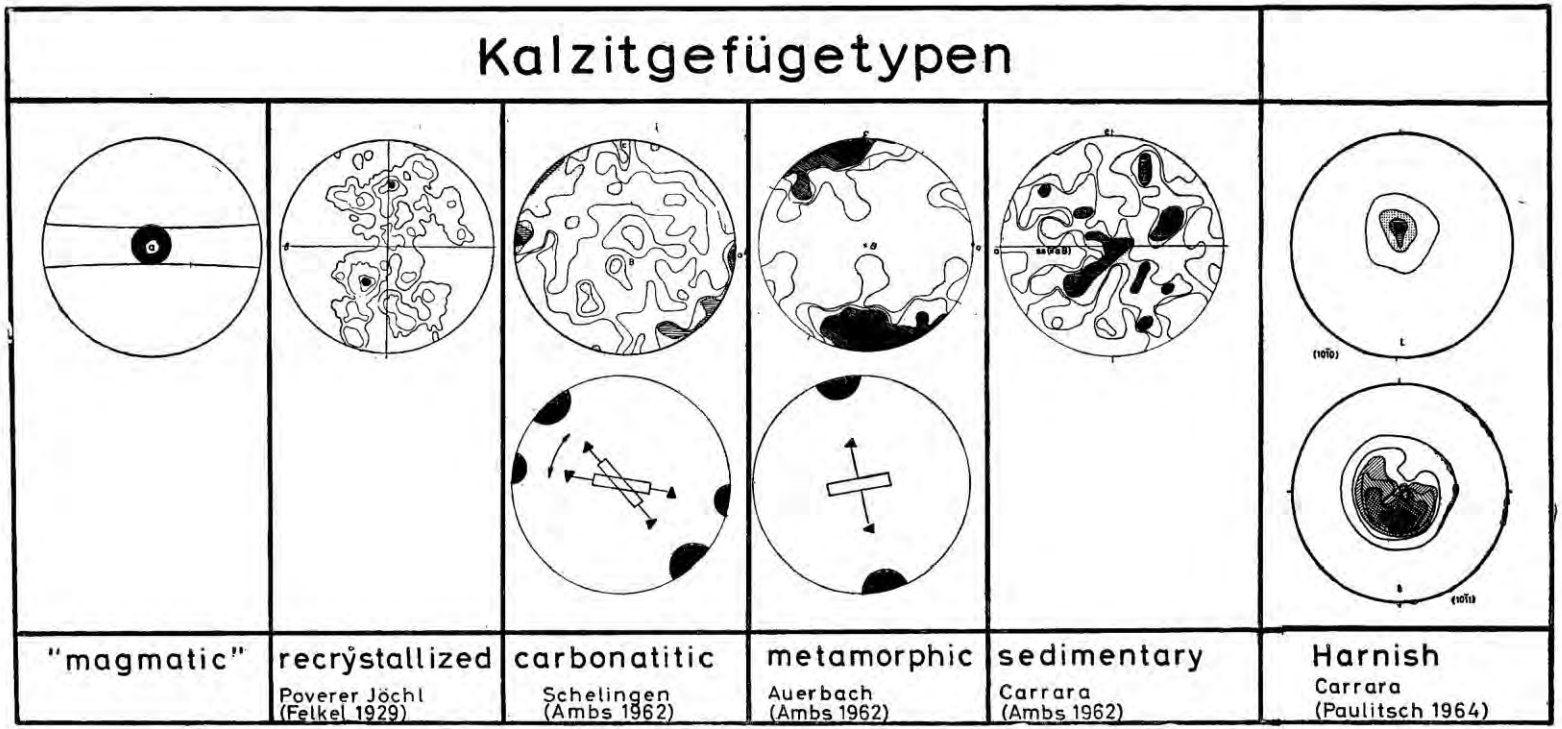

Fig. 1. Types of calcite fabric (from left to right)

(a) "*Magmatic*" *fabric*, expected.

(b) *Recrystallized fabric*: Poverer Jöchl, parallel b; 276 *c*-axes; (5-4)-3-2-1-0. After Felkel, 1929.

(c) *Carbonatite fabric:* Kaiserstuhl/Schelingen. subnormal b;
Top diagram: 294 *c*-axes;-5-3, 5-2, 5-0, 5-0; Schmidt. Maximum I and II.
Bottom diagram: the calcite-shape is parallel to c (0001) in carbonatitic rocks.

(d) *Metamorphic fabric*: Auerbach/Odenwald, normal b;
Top diagram: 100 *c*-axes;-5-3-2-1-0; Schmidt.
Bottom diagram: the calcite-shape is normal to c (0001) in metamorphic rocks.

(e) *Sedimentary fabric:* Carrara/Italy, normal b; 101 *c*-axes;-5-3-2-1-0; Schmidt.

(f) *Harnish fabric:* Carrara/Italy;
Top diagram: x-ray results from the determination of prism *m* $(10\bar{1}0)$.
Bottom diagram: x-ray results from the determination of rhombohedron *r* $(10\bar{1}1)$.

various regions in Schelingen samples. The two diagrams on the right describe the position of the *c*–axes in coarse-and fine-grained specimens respectively. The regions of large and fine grains together in the left diagram have the following features in *common*:

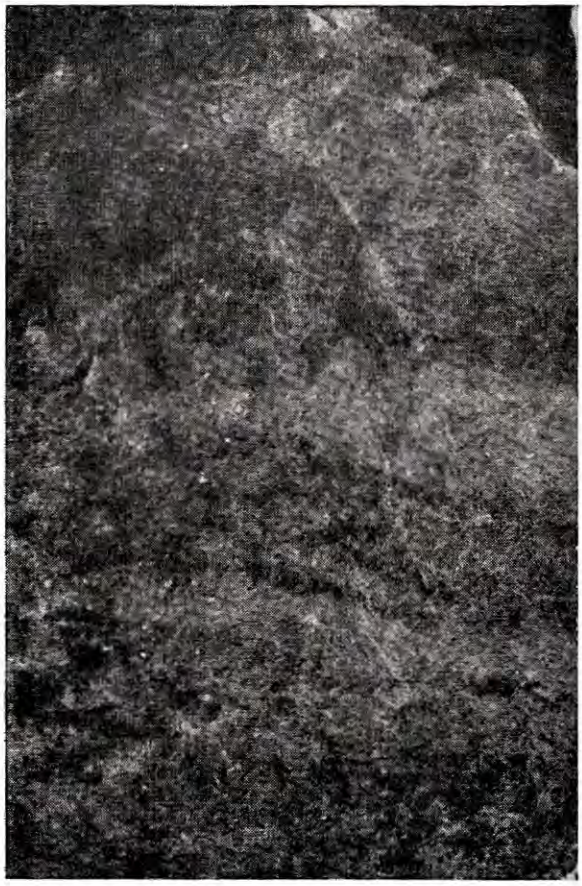

Fig. 2
Rock specimen from Kaiserstuhl/Schelingen, (x 2).

1. Maximum I in *a* of the fabric in the outer circle.

2. Maximum II on the ground circle at a distance of about 30°

3. The maximum I, particularly in the layers with large grains, is elongated in the (*ab*)–plane of the fabric.

4. These diagrams, which are compared, have all shown a small maximum about *c* of the fabric.

These first three features can be said to show *homogeneity*.

5. The pattern from the *e*–rhombohedron planes in Fig. 5 shows no distinct maximum. Only the diagram at bottom-right shows a concentration of *e*-planes near the maximum II of the *c*-axes; it belongs to the fine-grained layers.

We shall now compare the orientation of the calcite axes in Kaiserstuhl carbonatites with that in Sφve (Saether, 1957) and in Alnö (v. Eckermann, 1948).

In Fig. 6, the first 3 diagrams show the preferred orientation in *a* of the fabric, which continues as far as maximum II, and the corresponding concentration in *c* of the fabric, which is particularly apparent in the Alnö-diagram on the right.

The first three diagrams, Sφve and Schelingen show also a *double-girdle* of varying intensity; the angle between the girdles is about 52°-126° respectively. These are the observations.

Now we shall try to interpret the results and common features of the *carbonatite-fabric*.

In Fig. 7, we shall regard the double-girdle in the first row for Sφve, and in the last row for Schelingen as a *fabric twinned* in the rhombohedron *e* $(01\bar{1}2)$ or *f* $(02\bar{2}1)$ as described in the first diagram of the second row. Twinned planes could, in fact, be determined only in three cases for *e* $(01\bar{1}2)$, since the lamellae or cleavage planes necessary as confirmatory evidence, were generally *not always present in the twinned, recrystallised grains*.

Maximum I and the maximum II in the second and third diagrams of the second row will be regarded as showing *recrystallization texture* corresponding to the observations of Felkel (1929), Griggs and Turner et al. (1960) during experiments on syntectonic recrystallization.

Another characteristic is the *special shape* of the calcite-grains, as shown in the third diagram which are, in fact, elongated parallel to the limiting rhombohedral planes and subparallel to the *c*–axis.

The grain-elongation with the formation of subindividuals has already been experimentally observed by Griggs and Turner et al. (1960).

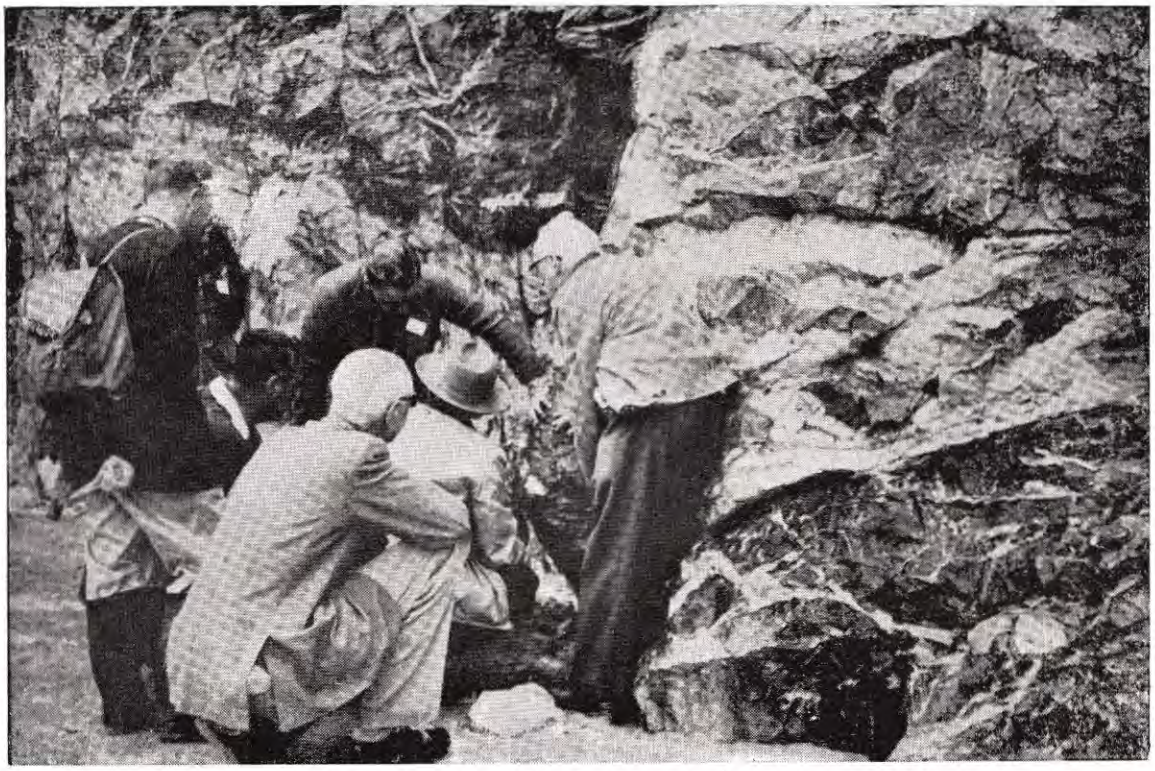

Fig. 3. The carbonatites from Sφve, South-Norway.

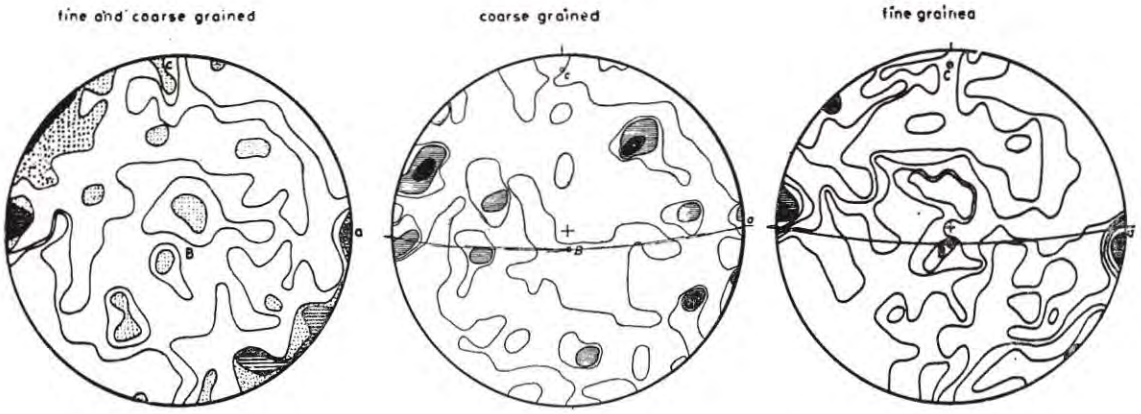

(a) (b) (c)

Fig. 4. Calcite-orientation in carbonatites from Kaiserstuhl/Schelingen (from left to right).

(a) Subnormal b ; optical axes of 294 calcite grains (*fine and coarse grained*); -5-3.5-2.5-0.5-0 ; Schmidt. Maximum I and maximum II near *a*.

(b) Subnormal b ; optical axes of 121 calcite grains (*coarse grained*); -4-3.5-3-1-0 ; Schmidt. maximum I and II near *a*.

(c) Subnormal b; optical axes of 173 calcite grains (*fine grained*); -7.5-6-3.5-2-1-0 ; Schmidt. Maximum I and maximum II near *a* in (*ac*).

All the fabrics show an interrupted (*ac*)—girdle with a maximum in *c* of the fabric, which would indicate *deformation*, as shown in the fourth diagram in the middle row.

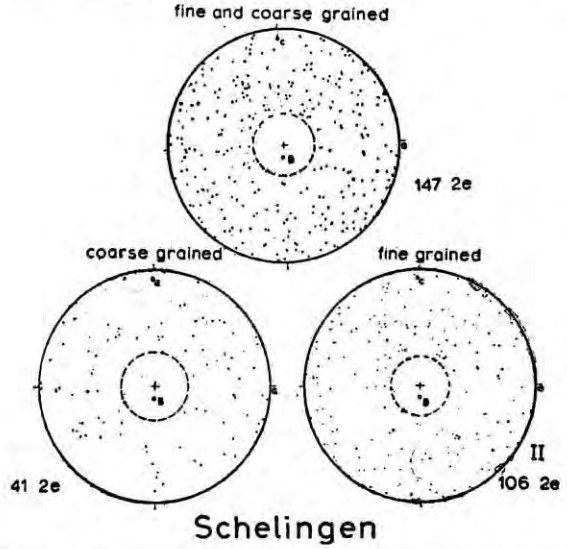

Fig. 5. Orientation of e (01$\bar{1}$2) calcite lamellæ (two per grain) for carbonatites from Kaiserstuhl/Schelingen.
Top diagram: Subnormal b; 147x2e-poles of (01$\bar{1}$2) lamellæ of the *fine coarse grained* calcites; Schmidt.
Bottom diagram, left: Subnormal b; 41x2e-poles of e (01$\bar{1}$2) lamellæ of the *coarse grained* calcites; Schmidt.
Bottom diagram, right: Subnormal b; 41x2e-poles of e (01$\bar{1}$2) lamellæ of the *fine grained* calcites; Schmidt.

To make this complete we should also mention another feature which indicates deformation: the *optically anomalous calcite-grains*.

In the carbonatites, biaxial calcite-grains appear, whereby the optically anomalous axial plane in the biaxial calcites lies mostly *parallel* to prism *a* (11$\bar{2}$0) of the *single crystal*, as shown in the first (upper) diagram of Fig. 8.

Therefore in the fabric there is a maximum parallel to the (*ac*)–plane, which appears in the case of the Schelingen sample. The symmetry of 69 single crystals causes another maximum for the deformation-planes at a distance of 60° (on the ground circle left); maximum *b* can be explained by the fact that the axial plane may also lie *normal* to the prism *a* (11$\bar{2}$0) of the single crystal as shown in the same figure, bottom left.

When the calcite orientation is homogeneous we are able to construct the *pressure-and-tension-vectors* for each grain by the method of Turner (1953) and Hansen (1962), top diagram right.

In the case of the crystals, which form a direction group and whose *c*-axes lie subnormal to the layering-in the center of the diagram-the corresponding maxima for the pressure-and-tension-vectors are represented in the diagram

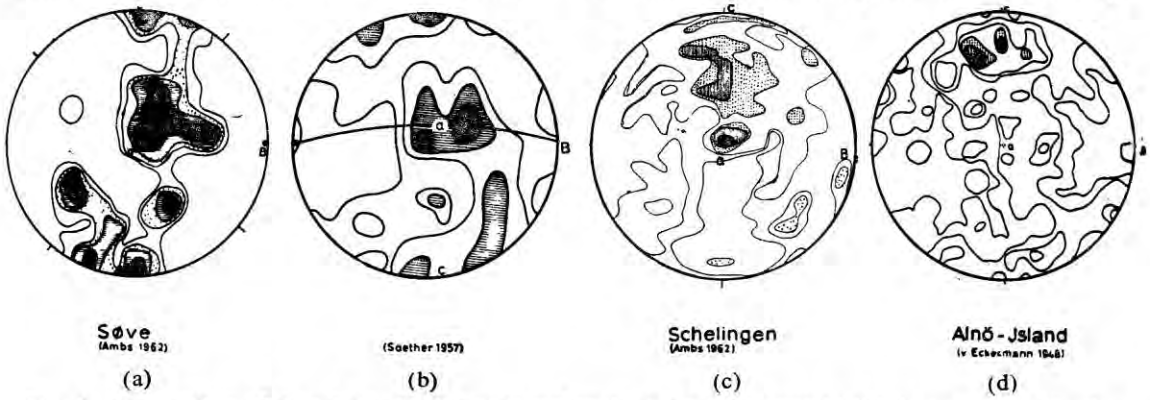

Fig. 6. Comparison of the calcite orientation in carbonatites from Kaiserstuhl/Schelingen, sφve (Saether 1957, Ambs 1962) and Alnö (v. Eckermann 1948) (from left to right).
(a) Sφve/Ulefoss/South-Norway, subnormal *a*; 101 *c*-axes;-5-3-2-1-0; Schmidt. maximum I and maximum II (Ambs 1962).
(b) Sφve/Ulefoss/South-Norway, subnormal *a*; 101 *c*-axes;-6-3-2-1-0, 5; Schmidt. Maximum I and maximum II (Sæther 1957).
(c) Kaiserstuhl/Schelingen, subnormal *a*; 294 *c*-axes;-5-3, 5-2-5-0, 5-0; Schmidt. Maximum I elongated in (*ab*) and maximum II in (*ac*) of the fabric (Ambs 1962).
(d) Alnö Island/Sverige, subnormal *a*; 300 *c*-axes, determined by J. Ladurner 1947;-6-5-4-3-2-1-0. (v. Eckermann 1948).

at bottom right. The vectors lie as determined by the symmetry in the (*ac*)–plane of the fabric.

We should also mention here as relevant to the complex carbonatite fabric in which we have evidence of *crystallization and deformation*, Baertschi's (1957) observations as to the *carbon isotope distribution.* His result corresponds to a point on the border between the metamorphic calcites and the recrystallized calcites found in alpine clefts.

The C^{13}/C^{12} determinations carried out by Taylor, Frechen and Degens (1964) on carbonatites from the Laacher See district also give similar values for the carbon isotope distribution.

Evalution of *Mg-content* showed that the values lie between 0% and 0.21%.

In Fig. 1 the gap in the carbonatite-column now has been filled in.

CONCLUSION

To summarize, we can say that the three features: *maximum I and maximum II* and the *grain-shape* indicate *recrystallization* and that the (*ac*)*-girdle, the maximum in c of the fabric and the biaxial calcites point to deformation.*

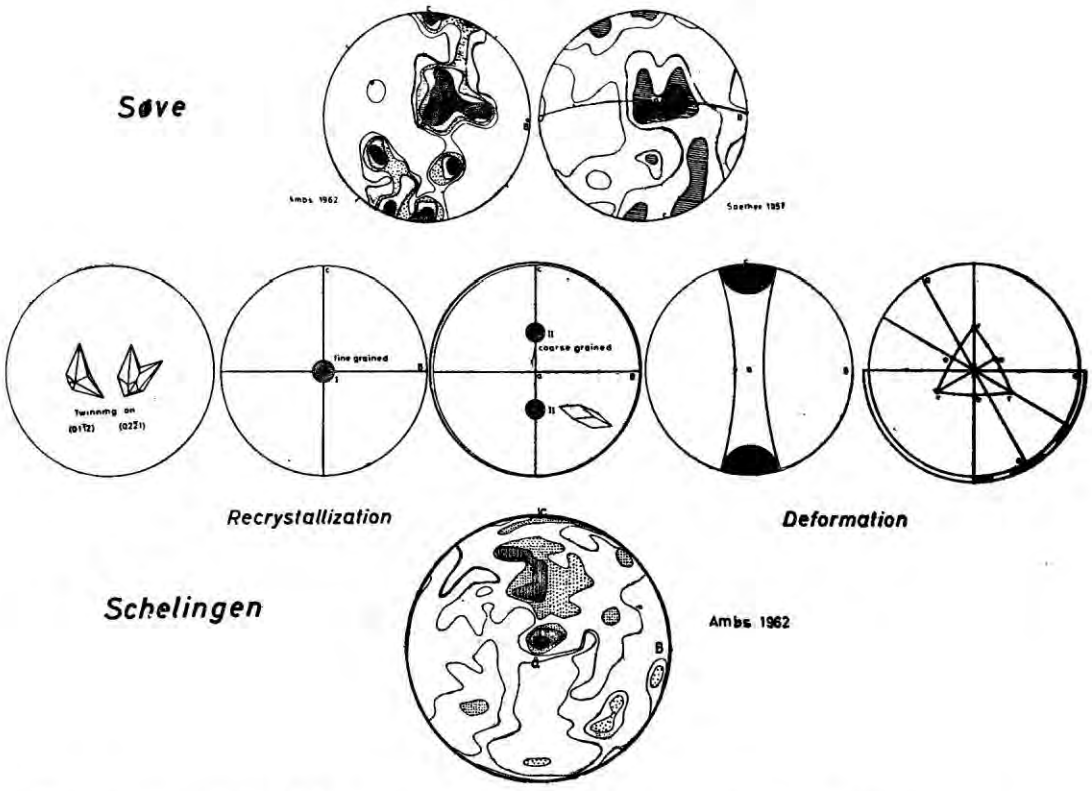

Fig. 7. Interpretation of the results and common features of the *carbonatite fabric*:
Maximum I and maximum II in the (*ac*)-plane of the fabric show *recrystallization*;
The maximum in *c* of the fabric, the (*ac*)-girdle and the biaxial calcites show *deformation.*

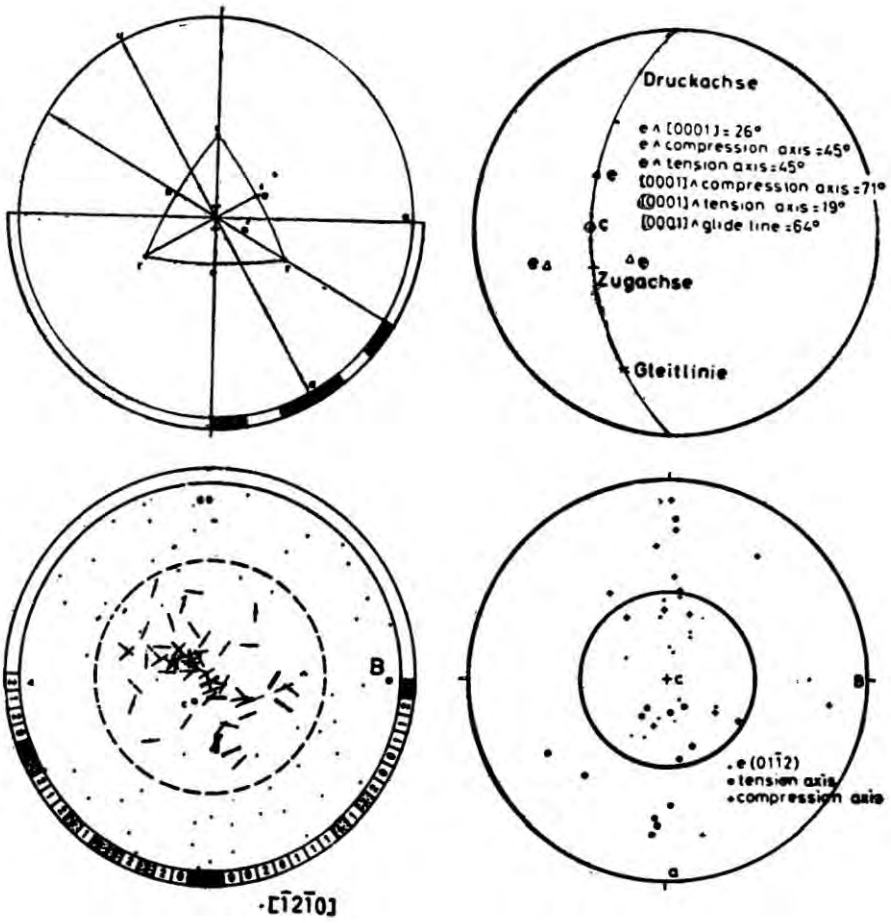

Fig. 8. Further features, which indicate *deformation* in carbonatites from Schelingen.

Top diagram, left: The optically anomalous axial plane in biaxial calcite-grains mainly lies parallel to prism *a* (11$\bar{2}$0) in the stereographic projection of a single crystal. 27 axial planes ; -52-29-10-0. Wulff-net.

Bottom diagram, left: The optically anomalous axial plane in biaxial calcite-grains gives a maximum parallel to the (*ac*)-plane in the fabric. 69 axial planes. Wulff-net.

Top diagram, right: Relation of deduced stress axes (tension and compression), to the twin plane *e* (01$\bar{1}$2), *c* axis and the glide line in calcite, shown in Wulff-net. After Turner (1953) and Hansen (1962).

Bottom diagram, right: The construction of the pressure-and-tension-vectors for 14 calcite-grains, which lie near *c* of the fabric, gives a distribution in the (*ac*)-plane.

REFERENCES

BAERTSCHI, P. (1957) Messung und Deutung relativer Häufigkeitsvariationen von ^{18}O und ^{13}C in Karbonatgesteinen und-mineralien: *Schweiz. min. petr. Mitt.* Vol. 37, pp. 73–152.

von ECKERMANN, H. (1948) The Alkaline district of Alnö island: *Sveriges geol. Undersökning Avhandl. och uppsatser, Ser. Ca.*, Vol. 36, pp. 1–176.

FELKEL, E. (1929) Gefügestudien an Kalktektoniten: *Jahrb. d. Geol. Bundesanstalt Wien.* Vol. 79.

GRIGGS, D. T., PATERSON, M. S., HEARD, H. C. AND TURNER, F. J. (1960) Annealing recrystallization in calcite crystals and aggregates: *Geol. Soc. Amer., Memoir.* No. 79, pp. 21–37.

HANSEN, E. AND BORG, J. Y. (1962) The dynamic significance of deformation lamellae in quartz of a calcite-cemented sandstone: *Amer. Jour. Sci.* Vol. 260, pp. 321–336.

PAULITSCH, P. (1950) Zweiachsige Kalzite und Gefügeregelung: *Tscherm. Min. Petr. Mitt.* Vol. 2, pp. 180–197.

——— (1956) Die optische Achsenebene als Ebene der Deformation im Einkorn und Gefüge von Kalzit. *Carinthia*, Angelfestband

PECORA, W. T. (1956) Carbonatites: A review. *Bull. Geol. Soc. Amer.* Vol. 67, pp. 1537–1566.

SAETHER, E. (1957) The Alkaline rock province of the Fen area in Southern Norway: *D.K.N.V.S. Skriften.* Vol. 1, p. 92.

TAYLOR, H. P., Jr., FRECHEN, J. AND DEGENS, E. T. (1964) Oxygen and carbon isotope studies of Carbonatites from Laacher See district, Germany. *Vortrag auf der Tagung der Geol. Soc. of Amer. Miami.*

WAMBEKE, L. v. (1960) Geochemical Prospecting and Appraisal of Niobium-bearing Carbonatites by X-ray Methods: *Econ. Geol.* Vol. 55, pp. 732–758.

WIMMENAUER, W. (1959) Karbonatite in Kaiserstuhl: *Fortschr. Min.* Vol. 37, pp. 67–69.

——— (1962) Zur Petrogenese der Eruptivgesteine und Karbonatite des Kaiserstuhls: *Neues Jb. Min., Mh.* pp. 1–11.

——— (1963) Beiträge zur Petrographie des Kaiserstuhls, Teile VI und VII: *Neues Jb. Min. Abh.* Vol. 99, pp. 231–276.

WYLLIE, P. J. AND TUTTLE, O. F. (1960) The system $CaO—CO_2—H_2O$ and the origin of carbonatites: *Jour. Petr.* Vol. 1. pp. 1–46.

MINERALOGICAL SOCIETY OF INDIA, IMA VOLUME, 1966
INTERNATIONAL MINERALOGICAL ASSOCIATION, PAPERS, FOURTH GENERAL MEETING

MINERALOGICAL AND GEOCHEMICAL EVOLUTION OF THE CARBONATITES OF THE KAISERSTUHL, GERMANY

L. van WAMBEKE

ABSTRACT

The carbonatites of the Kaiserstuhl were formed during the last magmatic stage of differentiation of the alkaline rocks. They are composed of several different carbonatitic phases : the sovites, the brown carbonatites and the dolomites. The sovites besides calcite I (generally more than 90% of the rocks) contain as accessory minerals apatite, magnetite, biotite and hydrobiotite, several types phlogopite (Ba and Mn phlogopites), pyrochlore and more rarely Nb-perovskite, olivine, forsterite, melilite, sulfides, mossite and columbite. Genetically associated with this phase are alvikites, veins cutting the essexitic and phonolitic rocks.

The brown carbonatites constitute an intermediary phase between the sovites and the dolomites. The most characteristic minerals of this phase are calcite II (more than 90%) and goethite associated with apatite, pyrochlore and more rarely magnetite.

The dolomitic phase is composed mainly of dolomite associated or not with calcite II, and by barite (5 to 35% of the rocks) with accessory minerals such as monazite, bastnaesite, goethite, manganophlogopite and more rarely apatite.

Data concerning the mineral geochemistry are given. Ba, Sr and the rare earths are largely distributed through the carbonates, the phosphates and the niobium-bearing minerals. Both generations of calcites and dolomites contain appreciable amounts of rare earths. The geochemical evolution of the different carbonatitic phases is described and the mean content for about 25 elements is given for the whole carbonatitic mass and for the different carbonatitic phases.

The geochemical data as well as the isotopic abundances of Ca^{13} and O^{18} are in agreement with a magmatic origin for the sovites, for the brown carbonatites and for the alvikites. The dolomitic phase is more likely hydrothermal.

The study outlines the importance of carbonatites as a possible source of Nb ; P and magnetite for the sovites and of Ba, rare earths, Mn, Fe, Zn, Pb and Th for the dolomitic phase.

A STUDY OF THE PYROCHLORES, THE COLUMBITE AND THE FERSMITE FROM THE LUESHE CARBONATITE DEPOSIT (REPUBLIC OF CONGO)

L. van WAMBEKE

ABSTRACT

The Lueshe carbonatitic deposit is one of the most important ore deposits for niobium in the world. Besides pyrochlore, columbite and fersmite, Nb is largely distributed in the Ti-bearing minerals such as ilmenite, aegyrite and also in the Zr-bearing minerals mainly zircon. Lueshite ($NaNbO_3$) also occurs in a fenitized vermiculite rich zone.

A mineralogical and geochemical study is made especially on the different pyrochlores, on columbite and on fersmite. Both last minerals appear mainly as pseudomorphs after pyrochlore. Fersmitization is frequently associated to columbitization. Two main types of pyrochlores are found. Besides normal pyrochlores characterizing carbonatite deposits, a new variety with high Sr and hydroxyl contents is described (parameter $a_o > 10.5$FÅ). Some pyrochlores of Leushe contain many inclusions of ilmenite, rutile, calcite, apatite, kaolinite, aegyrite and a mineral of the goyazite type.

Chemical analyses, formulas and parameters are given for the pyrochlores, the columbite and the fersmite.

MINERALOGICAL SOCIETY OF INDIA, IMA VOLUME, 1966
INTERNATIONAL MINERALOGICAL ASSOCIATION, PAPERS, FOURTH GENERAL MEETING

SYMPOSIUM ON ZEOLITES

ZEOLITES FROM NORTH MOUNTAINS, NOVA SCOTIA

F. AUMENTO AND C. FRIEDLAENDER
Department of Geology, Dalhousie University, Halifax N.S.

ABSTRACT

A number of zeolites from the Triassic basalts of Nova Scotia were re-examined optically and with X-ray techniques. Analcite, apophyllite, chabazite, heulandite, laumontite, natrolite, and stilbite were studied as well as various other minerals occurring as intergrowths or inclusions.

Cell parameters were first calculated from Buerger Precession photographs and then recalculated with greater precision from indexed diffractograms. Wide variations of cell parameters were detected. Examination of the available chemical data indicated that the water content plays an important part in controlling the cell parameters. This was supported by dehydration and high temperature diffractometry experiments.

A sequence of crystallization, which does not correspond to the geographic and stratigraphic distribution of the zeolites observed, is tentatively derived from field observations.

INTRODUCTION

The object of the present study was to use X-ray diffraction techniques to detect the variations in cell parameters of the Nova Scotia zeolites. Results were later used as comparative material in studies on the thermal transformations of zeolites and associated hydrated silicates (Aumento, 1965). Observations on chemical compositions, optical properties, and occurrence are included wherever possible to further characterize the specimens.

OCCURRENCE

The North Mountains (Digby, Annapolis, King's Counties, Nova Scotia) are formed by basaltic rocks of Triassic age, in which several varieties of zeolites have long been known to occur. The following species of zeolites were studied: analcite, apophyllite, chabazite (including the variety "acadialite"), gmelinite, heulandite, laumontite, mordenite, natrolite, stilbite and thomsonite. Some observations were also made on leonhardite, clinoptilolite and mesolite.

Material for the present study was collected in the field; additional reference material was obtained from the Royal Ontario Museum and from the Nova Scotia Museum of Science. The latter included some samples collected and labelled by T. L. Walker and described in his study on the zeolites of Nova Scotia (Walker and Parsons, 1922).

The sketch map (Fig. 1.) indicates the approximate western-most occurrence of a number of zeolites and associated minerals, as well as occurrences of high concentrations of zeolite pipes. It reveals a certain pattern which appears to be related to the difference in age of the basalts in the eastern and western part of the North Mountain, but does not correspond to the sequence of crystallization described below.

Many cavities contain two or more zeolites in close "association". It is thus possible to give a probable sequence of crystallization for the more common minerals. Quartz generally acted as the base onto which zeolites were deposited in the following order:

Chabazite and gmelinite first, followed by stilbite, heulandite, laumontite, apophyllite, analcite, thomsonite, and finally natrolite (with mesolite intergrowths).

A number of flows, which have been distinguished in the Triassic North Mountains Basalts, indicate that the basalts to the East (Colchester and Cumberland Counties) are possibly at a lower stratigraphic horizon than those of the West (Bay of Fundy shore). If the same basalts were to extend westwards along the North Mountains, one might expect to find something

similar to a stratigraphic distribution of the zeolites. In fact, the minerals which are first in the crystallization sequence appear to be limited to the eastern outcrops, together with the intermediate minerals, which are widespread. Thomsonite and natrolite, however, which are last in the sequence of crystallization, although absent from the eastern outcrops, are concentrated in the intermediate basalts, and are completely absent from the western basalts.

Stilbite, analcite and heulandite persist at a considerable distance to the west, but zeolitization is completely absent in the younger, westernmost outcrops.

Neither the order of crystallization nor the geographical distribution are in agreement with the work of Kostov (1957–1960), or with the observations by G. P. L. Walker (1960–1961) on the regional distribution of zeolites in Iceland and Ireland. It is suggested that the availability of free silica plays an important part in these discrepancies. Free silica is abundant in the North Mountains, whilst in eastern Iceland the basalts are known to be silica-poor.

OPTICAL OBSERVATIONS

Optical properties, determined with the aid of a Leitz four-axis universal stage and Waldmann Sphere, were found to be in accordance with published data. Some intergrowths were observed between a predominant phase and a minor constituent, as for instance between heulandite and stilbite. The constituent minerals were later identified in the diffractograms.

X-RAY DETERMINATIONS

Buerger Precession photographs provided cell parameters to an accuracy of ± 0.02 Å, together with unambiguously indexed reflections for space group determinations.

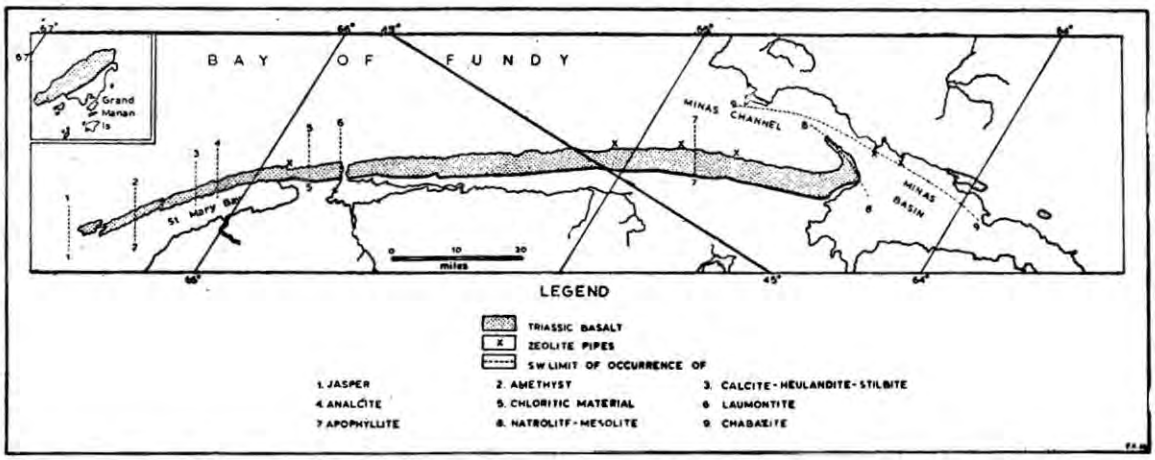

Fig. 1. Sketch map of the occurrence of the Triassic basalts on the North Mountains, Nova Scotia.

Previous experience has proved that some zeolites are so sensitive to heat treatment that even variations in the grinding and sample preparation could affect the diffractograms. Careful precautions were therefore taken in sample preparation, and the technique was standardized. Two sample mounts were prepared for each specimen, one for intensity measurements, where preferential orientations were successfully reduced (Aumento, 1965), the other for precise $2\theta^\circ$ determinations. In the latter, tungsten (after Swanson *et al.*, 1953-1964) or quartz (after Smith, 1956) were used as internal standards. Both were found to give similar correction factors.

The techniques and corrections discussed by Parrish (1962) were incorporated in diffractometry. Siemens instrumentation was used throughout. Diffractograms were taken with

Mn-filtered Fe radiation, and scans were repeated at higher 2 θ angles with Ni-filtered Cu radiation to provide more information in the lower "d" spacing range. Scanning speeds of 1/8 °2 θ/minute were used with 1° divergence slits, a 0.1 mm receiving slit, statistical error of 0.5%, and a chart speed of 8 cm/°2 θ. Corrected 2 θ values were obtained with an accuracy of better than ±0.01° 2 θ.

Cell parameters obtained from Buerger Precession photographs were processed by an I. B. M. 1620 computer to calculate all possible values of the "d" spacings for each mineral for the h, k, l, range −3 to +10. Answer cards with indices violating the space groups in question were eliminated; the remainder were automatically sorted in order of ascending values of "d". Calculated "d" values were then compared visually with observed "d" values.

The procedure was first carried out for the known pure minerals, and results were applied to doubtful intergrowths. In this way the different constituents were determined and indexed diffractograms were obtained for each phase.

Refined cell parameters were obtained by solving simultaneous equations using numerous pre-selected combinations of the indexed "d" spacings. Only "d" spacings with values of less than 2 Å were used in the calculations. This method of computation is generally not as satisfactory as one based on least-squares techniques. However, it is easier to program, and when used with small "d" spacings accurately determined, will provide cell parameters with accuracies in the order of ±0.005 to ±0.001 or better.

Numerous samples of North Mountains zeolites were studied in this way. Final values for the cell parameters are tabulated in Table I. Column I gives the mode of the cell parameter skew distribution for any one species. Column II gives the maximum total error, both for experimental observations and calculations. Column III gives the maximum range of cell parameter values obtained on either side of the mode of Column I. Parameters in Column IV were obtained mainly from the publication by Mikheev (1957) and from Powder Data File cards (A.S.T.M.) Those in Column V are as listed in Volume 4 of the book "Rock Forming Minerals" by Deer, Howie and Zussman. Where only one sample of the species was available for investigation, and no variation in cell parameters could therefore be determined, a dotted line is placed in the appropriate places in Column IV.

Analcite, apophyllite, gmelinite, and mordenite were always found as single crystals. Heulandite and stilbite were found only as single phases when they occurred as small clusters of minute euhedral crystals. As soon as larger heulandite crystals were examined, small amounts of stilbite, and in one case clinoptilolite (distinguished from heulandite according to the techniques of Mumpton, 1960) could be detected as intergrown phases. Larger stilbite crystals and clusters contained intergrown heulandite. Diffractograms of chabazite always contained a few extra lines, and these could be completely accounted for by assuming a second phase of gmelinite. Laumontite was never quite fresh, due to its rapid dehydration, so that leonhardite lines were always detected. Extra lines, which could be explained by a second phase of mesolite, were found in natrolite and thomsonite.

The total error in calculating the cell parameters was well below the amount of variation found in the values for different samples of the same species. Generally speaking, this variation is within the limits of values detected by various workers and listed in Table I.

In order to explain the variations in cell parameters, a number of complete chemical analyses were carried out on samples whose cell parameters were closest to the mode of the skew distribution. Both rapid wet chemical analyses and X-ray spectrographic techniques were employed. The investigations of Walker and Parsons (1922) provided additional chemical

data, which was used wherever their original material was available for X-ray studies. Chemical data and cell parameters are listed in Table II.

Analcite, apophyllite, stilbite and heulandite were further subjected to thorough dehydration and rehydration experiments, and were also studied with high temperature diffractometry techniques (Aumento, op. cit.).

These investigations have shown that changes in water content can contribute often to variations in cell parameters. In other specimens, however, the maximum variations attributable to changes in water content are not large enough to explain the variations observed in the natural minerals.

The variations found in analcite can be easily simulated by inducing slight hydration or rehydration on natural samples. In apophyllite, however, whereas the state of hydration causes greater variations in the "c" parameter (perpendicular to the platy habit) than in the "a" parameter, the maximum variation possible was found to be ten times smaller than the natural variation. Other causes, perhaps the substitution of water by fluorine in natural samples, will have to be found for apophyllite.

Natural stilbite and heulandite samples showed considerable variations in water content, which caused major changes of their "b" parameters. Further variations could be induced by dehydration and hydration. It is therefore

TABLE I

Cell parameter variations of the North Mountains Zeolites

Crystal Species	Corrected mean values of cell parameters	Maximum error	Maximum variation in cell parameters	Value of cell parameters from literature	
	I	II	III	IV	V
Analcite	a: 13.708 Å	± 0.005 Å	± 0.016 Å	13.684 Å—	13.7 Å
Apophyllite	a: 8.995	0.005	0.035	8.960	— 9.00
	c: 15.627	0.005	0.228	15.78	—15.84
Chabazite	a: 13.785	0.006	0.051	13.75	—13.80
	c: 14.890	0.007	0.080	14.94	—15.0
Mordenite	a: 18.092	0.004	— —	18.13	—18.13
	b: 20.479	0.004	— —	20.49	—20.49
	c: 7.522	0.004	— —	7.52	— 7.52
Natrolite	a: 18.281	0.005	— —	18.31	—18.30
	b: 18.619	0.005	— —	18.66	—18.63
	c: 6.592	0.005	— —	6.60	— 6.60
Thomsonite	a: 13.003	0.005	— —	13.04	—13.07
	b: 13.189	0.005	— —	13.06	—13.09
	c: 13.251	0.005	— —	2×6.63	—2×6.63
Mesolite	a: 18.925	0.005	0.038	3×18.9	—18.9
	b: 6.582	0.005	0.011	6.55	— 6.55
	c: 18.497	0.005	0.043	18.813	—18.48
	β: 90°10′	0°2′	0°3′	90°0′	—90°
Laumontite	a: 14.919	0.005	— —	14.90	—14.90
	b: 13.156	0.005	— —	13.17	—13.17
	c: 7.545	0.005	— —	7.55	— 7.55
	β: 68°30′	0°11′	— —	68°46′	—111°30′
Heulandite	a: 7.466	0.005	0.056	7.45	— 7.46
	b: 17.868	0.005	0.178	17.80	—17.84
	c: 15.831	0.005	0.076	15.85	—15.84
	β: 91°26′	0°7′	0°23′	91°25′	—91°26′
Stilbite	a: 13.681	0.005	0.061	13.60	—13.63
	b: 18.182	0.005	0.118	18.13	—18.17
	c: 11.300	0.005	0.031	11.29	—11.31
	β: 129° 8′	0°10′	0°12′	129°10′	—129°10′

	Mineral	Origin (N.S.)	Cell Parameters: Å a	b	c	β	CHEMICAL ANALYSES. SiO_2	TiO_2	Al_2O_3	Fe_2O_3	FeO	MnO	CaO	MgO	K_2O	Na_2O	SrO	P_2O_5	F	H_2O^+	H_2O^-	Total	Less O≡F	Final Total	Major Traces
A	Analcite	Cape Blomidon	13.717 ±0.003			-	54.84	0.12	23.32	0.04	0.00	0.06	0.06	0.00	0.35	13.20	0.00	0.13	n.d.	8.40	0.00	100.52 %	-	100.52 %	None
A	Apophyllite	Cape Blomidon	8.994 ±0.005		15.620 ±0.005	-	50.52	0.06	1.03	Tr.		0.03	24.69	0.69	5.60	0.38	0.00	0.07	1.17	16.40	0.00	100.64 %	-0.49	100.15 %	Y , Zn, Rb
W	Chabazite	Fasson's Bluff	13.780 ±0.006	-	14.900 ±0.007	-	49.46	n.d.	17.91	0.11		0.01	8.24	0.01	1.12	1.14	0.46	n.d.	n.d.	21.89		100.43 %	-	100.43 %	n.d.
W	Mordenite	Morden	18.092 ±0.004	20.479 ±0.004	7.552 ±0.004	-	67.08	n.d.	11.85	0.31		n.d.	1.56	0.00	2.08	4.74	n.d.	n.d.	n.d.	12.84		100.46 %	-	100.46 %	n.d.
W	Natrolite	Cape Blomidon	18.181 ±0.005	18.549 ±0.005	6.592 ±0.005	-	47.34	n.d.	27.17	0.01		n.d.	0.48	n.d.	0.28	15.42	n.d.	n.d.	n.d.	9.47		100.17 %	-	100.17 %	n.d.
W	Thomsonite	Cape Blomidon	13.003 ±0.005	13.189 ±0.005	13.251 ±0.005	-	39.96	n.d.	31.02	0.14		n.d.	11.98	n.d.	0.18	4.19	n.d.	n.d.	n.d.	12.85		100.32 %	-	100.32 %	n.d.
W	Mesolite	Cape d'Or	18.320 ±0.005	6.580 ±0.005	18.490 ±0.005	90°10' 0° 2'	46.01	n.d.	26.66	0.38		n.d.	9.88	n.d.	0.20	4.66	n.d.	n.d.	n.d.	12.69		100.48 %	-	100.48 %	n.d.
W	Laumontite	Margaretville	14.919 ±0.005	13.156 ±0.005	7.545 ±0.005	68°30' 0°11'	50.96	n.d.	21.60	0.03		n.d.	11.27	n.d.	0.18	0.32	n.d.	n.d.	n.d.	16.04		100.40 %	-	100.40 %	n.d.
W	Heulandite	Digby Neck	7.460 ±0.005	17.868 ±0.005	15.811 ±0.005	91°26' 0° 7'	57.26	n.d.	16.81	0.05		n.d.	6.58	n.d.	1.02	0.54	1.26	n.d.	n.d.	16.22		99.74 %	-	99.74 %	n.d.
A	Stilbite	Cape Blomidon	13.681 ±0.005	18.182 ±0.005	11.300 ±0.005	129° 8' 0°10'	55.08	0.00	16.54	Tr.	0.10	Tr.	7.63	0.20	0.53	0.93	Tr.	0.00	n.d.	14.65	4.22	99.88 %	-	99.88 %	Y.

Tr Trace only. n.d. Not Determined. TABLE II. Analysts: A : Aumento (1965) W : Walker and Parsons (1922)

Chemical analyses and cell parameters of the North Mountains Zeolites

concluded that changes in water content for the platy minerals stilbite and heulandite are sufficient to cause the variations detected in natural samples. This does not exclude, however, other causes which may also be playing an important role.

The samples of mordenite and natrolite used had suffered dehydration after prolonged exposure to the atmosphere, and therefore gave cell parameters a little smaller than those described in the literature. Large variations in parameters are not generally found for these two minerals. Variations in chabazite are probably of a more complex nature, considering the cation exchange properties of the mineral.

SUMMARY AND CONCLUSIONS

Wide variations have been found in the cell parameters of the natural zeolites from Nova Scotia. Preliminary investigations using dehydration and rehydration experiments in conjunction with chemical analyses and high temperature diffractometry have shown that the change of water content of the minerals exerts an important influence on the cell parameters. This is especially true for the platy zeolites and apophyllite, where the major variations are perpendicular to the platy habit. Although variable water content is not the sole cause of these variations, other factors could not be detected because of the lack of comprehensive chemical data for each of the specimens studied.

REFERENCES

AUMENTO, F. (1965) Thermal transformations of selected zeolites and related hydrated silicates. *Ph.D. Thesis*, Dalhousie University. pp. 1–281.

DEER, W. A., HOWIE, R. A. AND ZUSSMAN, J. (1963) *Rock Forming Minerals*. Vol. 4. pp. 338–428. Longmans, London.

KOSTOV, I. (1957–1959) The Zeolites in Bulgaria. Annuaire de l'Université de Sofia ; Faculté de Biologie, Géologie et Géographie. Vols. *LII & LIII*. Livre 2.

KOSTOV, I. (1960) Composition and paragenesis of zeolitic minerals. Report. 21st Int. Geol. Congress Norden. Part 17. pp. 122–127.

MIKHEEV, W. I. (1957) *Rentgenometritcheski apredelitel mineralov*. Gosgeoltekhizdat, Moscow.

MUMPTON, F. A. (1960) Clinoptilolite redefined. *Amer. Min.* Vol. 45. p. 368.

PARRISH, W. (1962) *Advances in X-ray Diffractometry and X-ray Spectrography*. Centrex Publishing Company, Eindhoven.

SMITH, J. V. (1956) The powder patterns and lattice parameters of plagioclase feldspars. I. The soda-rich plagioclases. *Min. Mag.* Vol. 31. pp. 47–68.

SWANSON, H. E., *et al.* (1953–1964) Standard X-ray Diffraction Powder Patterns. *N. B. S. Circular* No. 539.

WALKER, G. P. L. (1960) Zeolite zones and dike distribution in relation to the structure of the basalts of eastern Iceland. *Jour. Geol.* Vol. 68, pp. 515–528.

WALKER, G. P. L. (1961) The amygdale minerals in the Tertiary lavas of Ireland–III Regional Distribution. *Min. Mag.* Vol. 32, pp. 503–527.

WALKER, T. L., AND PARSONS, A. L. (1922) Zeolites of Nova Scotia. University of Toronto Studies, *Geological Series. N. 14*, pp. 13–73.

MINERALOGICAL SOCIETY OF INDIA, IMA VOLUME, 1966
INTERNATIONAL MINERALOGICAL ASSOCIATION, PAPERS, FOURTH GENERAL MEETING

THE EFFECTS OF EXCHANGED CATIONS ON THE THERMAL BEHAVIOUR OF HEULANDITE AND CLINOPTILOLITE

ANNA O. SHEPARD AND HARRY C. STARKEY
U. S. Geological Survey, Denver, Colorado

The effects of three cations, calcium, sodium, and potassium, on the thermal behavior of heulandite and clinoptilolite have been studied by means of exchange experiments and X-ray diffraction at temperatures up to 1050°C. The clearest indications of the effects of the cations were obtained with clinoptilolite treated with calcium chloride and heulandite treated with potassium chloride. The Ca-clinoptilolite inverted on heating like heulandite, whereas the thermal behavior of the K-heulandite was similar to that of clinoptilolite : it did not invert and was more stable than heulandite. These results differed from those of previously reported experiments (Mumpton, 1960, p. 360), possibly because of the method of exchange employed.

Particle size of samples was reduced to two microns and concentration of solutions was one normal for the exchange experiments. A pressure cooker was used to increase the rate of exchange, temperatures of 118° ± 2°C being maintained for 16 hours. Silica, alumina, the alkalies, the alkaline earths, and water were determined in the treated samples by standard methods of rock analysis, microchemical analysis, flame photometry, and colorimetric methods.

Although there was loss of silica and relative gain in alumina in all samples in which cations were exchanged, the silica : alumina ratio of all treated minerals was still within the range of values of its type mineral. The exchange of cations was nearly complete, as can be judged by the amounts of unexchanged cations (Tables 1 and 2). Analyses for the cations that were

TABLE 1. Natural and treated heulandites

Chemical composition			Composition of unit cell (0=72)					
Oxides	1	2	Element	1	3	4	2	5
SiO_2	59.76	57.12	Si	27.70	26.75	27.57	26.70	26.05
Al_2O_3	14.96	16.31	Al	8.17	9.18	8.53	8.98	10.47
Fe_2O_3	.23	.02	Ca	3.40	.53	.35	3.96	3.97
MgO	.33	.04	Mg	.23	—	.07	.03	.14
CaO	6.85	7.90	Na	.58	.03	7.27	1.93	.13
Na_2O	.65	2.13	K	.81	8.34	.01	.34	.02
K_2O	1.38	.57						
TiO_2	.02	.00						

1. Heulandite, Summit, N. J. Analyst : Dorothy F. Powers.
2. Heulandite, Paterson, N. J. Analyst : Dorothy F. Powers.
3. Summit, N. J., heulandite treated with KCl. Analyst : Ellen S. Daniels.
4. Summit, N. J., heulandite treated with NaCl. Analyst : Ellen S. Daniels.
5. Paterson, N. J., heulandite treated with $CaCl_2$. Analyst : Wayne Mountjoy.

introduced are less significant because minor amounts of impurities were formed during exchange, and because of possible contamination by adsorbed cations. Optical properties of the treated minerals indicated that K-clinoptilolite and Na-heulandite had recrystallized. The refractive indices of Ca-clinoptilolite were between those of clinoptilolite and heulandite. Replacement of Ca by K lowered the indices of heulandite.

TABLE 2.

Clinoptilolite from the Upper Cretaceous Pierre Shale

Chemical composition		Composition of unit cell (O=72)				
Oxides	1	Element	Atoms per unit cell			
			1	2	3	4
SiO_2	65.11	Si	29.77	29.35	29.44	28.85
Al_2O_3	11.64	Al	6.27	6.87	6.72	6.53
Fe_2O_3	.12	Ca	.71	2.53	.01	.05
FeO	.04	Mg	.57	.28	.03	.14
MgO	.84	Na	2.14	.06	5.85	.02
CaO	1.45	K	1.38	.29	.19	8.61
Na_2O	2.42					
K_2O	2.36					
H_2O+	7.57					
H_2O-	6.00					
TiO_2	.43					
P_2O_5	.04					
MnO	.02					
CO_2	.00					
Cl	.00					
F	.01					
SO_3	.65					
BaO	1.10					
Total	99.80					

1. Natural Clinoptilolite
   Analyst: Elaine L. Munson.
2. Clinoptilolite treated with $CaCl_2$
   Analyst: Ellen S. Daniels.
3. Clinoptilolite treated with NaCl
   Analyst: Ellen S. Daniels.
4. Clinoptilolite treated with KCl
   Analyst: Wayne Mountjoy.

Cell dimensions and volumes of the natural and treated minerals were determined by Dr. David B. Stewart, U. S. Geological Survey (Table 3). The cell size increases when K enters either structure. The volumes of the heulandite samples are always larger than those of the corresponding clinoptilolite samples.

Thermal behavior of the natural and treated minerals. Thermal behavior was tested by dynamic heating using a diffractometer heating stage (Skinner, Stewart, and Morgenstern, 1962). The heating rate was 3°C/minute, and oscillation scanning of the 020 peak was at the rate of 1/2°/min. When inversion was complete, the sample was scanned to 35° 2θ, after which the oscillation scanning was resumed while the sample was heated to destruction.

Minerals with the small divalent Ca cation inverted whereas those with the large univalent K cation did not invert. The d-spacings of the high-temperature phase of Ca-clinoptilolite corresponded with those of heulandite B, the high-temperature phase of heulandite; the stabilities also were correlated, but the thermal changes of Ca-clinoptilolite are sluggish: the temperature of inversion is raised approximately 75° and the temperature of destruction 150°. Potassium heulandite did not invert but the destruction of its structure occurred approximately 50° below that of natural clinoptilolite. K-clinoptilolite was more stable than natural clinoptilolite. In these tests higher thermal stability is correlated with higher percent of silica in the crystal framework.

The thermal behavior of the sodium-treated minerals cannot be explained in terms of cation size and silica : alumina ratio. Na-heulandite inverts like heulandite but the temperature of inversion is depressed 150° and the stability of the B phase is the same as that of heulandite. The thermal behavior of Na-clinoptilolite is distinctive. In the lower temperature range the crystal structure begins to contract like that of an inverting mineral, but at higher temperatures (above 350°) it begins to expand to the original spacings, which are maintained to the tempera-

ture of destruction. The mineral is more stable than natural clinoptilolite.

Relationship of water to the thermal behavior of heulandite and clinoptilolite. Water was determined in samples of heulandite and clinoptilolite and the products derived from them before and after heating by an infrared absorption technique (Dr. Irving A. Breger and Mr. John C. Chandler of the U.S. Geological Survey). Analyses were made on 2-mg samples dispersed in 300-mg pellets of potassium bromide. The pellets were maintained at 110°C, and absorption values at 2.96μ were determined using a Perkin-Elmer model 21 double beam infrared spectrophotometer. A 300-mg potassium bromide pellet, also heated to 110°C, was maintained in the reference beam.

Water-loss curves, determined by heating each sample to a known temperature for one-half hour and then analyzing it by infrared spectrophotometry, differed from the curve obtained during dynamic heating (Koizumi, 1953). The latter curve has been interpreted to suggest a continuous loss of loosely and tightly held water under nonequilibrium conditions. The infrared curves indicate that there is no water loss in heulandite at temperatures from 110° to nearly 350°C. Loss of water above 350° takes place rapidly. The water-loss curve of Ca-clinoptilolite parallels that of heulandite.

When heated above 110°C, clinoptilolite begins to lose water in the same temperature range as heulandite but the loss proceeds gradually rather than rapidly. At 800° clinoptilolite still contains 4.5 percent H_2O. K-heulandite is comparable to clinoptilolite in its gradual loss of water.

Anomalous zeolites of heulandite-clinoptilolite structure. Zeolites which behave thermally like a mixture of clinoptilolite and heulandite have been found in the Nevada Test Site, the Tertiary John Day Formation of Oregon, and at Nutriosa, east-central Arizona (Shepard, 1961 ; Shepard and Starkey, 1964). On heating, part of the mineral has a high-temperature phase like heulandite and part remians stable like clinoptilolite. The refractive indices of the mineral are more nearly those of clinoptilolite than those of heulandite, and the temperature of inversion is higher than for heulandite.

In both optical properties and thermal behavior these anomalous zeolites resemble clinoptilolite in which cation exchange is incomplete, that is, in which alkalies are only partially replaced by calcium. In the study of the genesis and relationship of heulandite-clinoptilolite minerals it is essential to recognize evidences of cation exchange in ground water, as well as to establish homogeneity and purity of the minerals. Thermal tests of the phase of the minerals supplement chemical, optical, and X-ray data.

TABLE 3. Cell dimensions and volumes of natural and treated minerals

	a±.02Å	b±.02Å	c±.01Å	β	Vol ±.04Å^3
Clinoptilolite, natural (Pierre Shale)	17.317	17.929	7.411	113° 53.5'	2103.9
Clinoptilolite + KCl	17.413	17.917	7.400	114 0.8	2109.0
Heulandite + KCl	17.393	17.995	7.419	113 53.3	2123.2
Clinoptilolite + NaCl	17.332	17.924	7.389	113 52.0	2099.2
Heulandite + NaCl	17.373	17.962	7.421	113 45.9	2119.3
Clinoptilolite + $CaCl_2$	17.194	17.808	7.375	113 43.2	2067.4
Heulandite, natural (Summit, N.J.)	17.281	17.890	7.410	113 38.6	2098.7

REFERENCES

KOIZUMI, M. (1953) The differential thermal curves and the dehydration curves of zeolites: *Mineral. Jour. Japan*, Vol. 1, No. 1, pp. 36–47.

MUMPTON, F. A. (1960) Clinoptilolite redefined: *Amer. Min.* Vol. 45, pp. 351–369.

SHEPARD, A. O. (1961) A heulandite-like mineral associated with clinoptilolite in tuffs of Oak Spring Formation, Nevada, Test Site, Nye County, Nevada, in short papers in the geologic and hydrologic sciences, *U.S. Geol. Survey Prof. Paper* 424–C, pp. C320–C323.

SHEPARD, A. O., AND STARKEY, H. C. (1964) Effect of cation exchange of the thermal behavior on heulandite and clinoptilolite, in short papers in geology and hydrology: *U.S. Geol. Survey Prof. Paper* 475–D, pp. D89–D92.

SKINNER, B. J., STEWART, D. B. AND MORGENSTERN, J. C. (1962) A new heating stage for the X-ray diffractometer: *Amer. Min.* Vol. 47, pp. 962–967.

MINERALOGICAL SOCIETY OF INDIA, IMA VOLUME 1966
INTERNATIONAL MINERALOGICAL ASSOCIATION, PAPERS, FOURTH GENERAL MEETING

THE DEHYDRATION AND CHEMICAL COMPOSITION OF LAUMONTITE

FREDRIK PIPPING
Geologiska Forskningsanstalten, Otnäs, Finland

ABSTRACT

X-ray data of the monoclinic unit cell, chemical analyses, DTA and TGA diagrams are presented for seven laumontites.

The first step of dehydration occurs at room temperature, is reversible and consists of the expulsion of 2 out of 16 H_2O from the unit cell. This dehydration is accompanied by shrinkage of all cell edges, a decrease of the β angle, and a decrease of the cell volume by about 50 Å^3. The product is traditionally called leonhardite.

Chemical analyses combined with DTA and TGA data show that the endogene reaction at 480°C for pure Ca-laumontite weakens with increasing alkali substitution. Instead a new endogene reaction appears at about 625°–630°C, and another at 780°C when about 40 per cent Ca is substituted.

It is concluded that the substitution of Ca by Na and/or K is purely a "zeolitic" substitution *i.e.*, 2Ca=Na+K. The constant ratio of Al : Si=0.50, even in laumontites with extreme substitution of Ca, is the main evidence. At 40 per cent substitution of Ca the space for H_2O molecules in the unit cell is considerably reduced and redisposed. The number of H_2O molecules diminishes from 16 to 14, as in the "primary leonhardite" described by Fersmann.

INTRODUCTION

Unit cell data of laumontites have been published by Coombs (1952), Heritsch (1956), Tennyson (1960) and Pipping (1961). Coombs found significant differences in the cell edges for laumontite proper and its partly dehydrated equivalent called leonhardite.

This dehydration at room temperature has, since the discovery of laumontite, excited much interest by mineralogists. Already in 1849 Rammelsberg noticed that the process is reversible, *i.e.* leonhardite regains the water in moist air or when submerged in water. Fersmann (1909) agreed with these views but introduced a new concept in the discussion, "primary leonhardite", a laumontite–like mineral with high content of alkalies, which neither dehydrates nor rehydrates at room temperature. The "primary leonhardite" has only 14 H_2O in the unit cell formula, compared with 16 H_2O for the laumontite proper, according to Fersmann (op. cit.).

A large number of chemical analyses of laumontites were listed by Doelter (1921) and Coombs (1952) has published a selection of new ones in his comprehensive study of laumontite and leonhardite. The chemical composition of laumontite is thus fairly well known, and the unit cell content is generally given as $Ca_4Al_8Si_{16}O_{48} + 16\ H_2O$. This is the pure Ca-laumontite, but it is known that both Na and K occur in the laumontite structure, usually referred to as substituting Ca. The mechanism of substitution has been thoroughly discussed by Coombs (1952), who concludes that the substituion is a mixture of the "feldspathic" and "zeolitic" types of substitution.

DTA and TGA data on laumontite have been published by Koizumi (1953), Pécsi-Donáth (1963) and Eskola and Hentola (1960).

MATERIAL AND METHODS

Material

The material included in the present study is listed according to decreasing Ca-content and the numbering I–VII found in tables and diagrams refers to the following short descriptions of the samples :

I. Laumontite from Huelgoat, (Bretagne), France. No. 3870 in the mineral collections of the University of Helsinki. Originally No. 9 in the collections of F. Steinheil (1767–1831), and so probably from the type locality of Gillet de

Laumont. Mostly a fine white powder, with only a few small crystal fragments.

II. Laumontite from Petersberg, Halle an der Saale, Germany. Chemical, optical and X-ray data (d-spacings) published by Koch (1959). Crystal fragments of 1-5 cm length ; white to cream coloured.

III. Laumontite from the " surroundings of Tblisi ", Kaukasus, USSR. From the A.E. Fersmann Mineralogical Museum, Moscow, USSR. Fissure filling in shale; white to bluish white in colour.

IV. Laumontite from Lammi, Southern Finland. Boulder in glacial gravel, source unknown, almost pure laumontite rock. Brick-red.

V. Laumontite from Tusby, Southern Finland. Boulder in glacial gravel, source unknown, almost pure laumontite rock; white to cream coloured.

VI. Laumontite from Kuhmoinen, Southern Finland. Laumontitized migmatitic rock at the margin of a large fault-line. A detailed petrographic and mineralogic description of the locality given by Eskola (Eskola and Hentola, 1960). White to cream coloured.

VII. " Primary leonhardite " from Kurtsy (nowadays Ukrainka) Crimea, USSR. From the A.E. Fersmann Mineralogical Museum, Moscow, USSR. Most probably the same material as described by Fersmann (1909). Fissure filling in quartz diabase (?) ; light reddish brown material.

X-ray Methods

The measurement and calculation of the monoclinic cell edges and the β-angle of the samples I–VI has been performed by the following method. Coombs (1952), Heritsch (1956) and Pipping (1961) agree completely on the indexing of reflections. The reflections (400), (040), (002) and (201) all lie in the range 20°.50 and 28°.00 2 θ and so does the reference reflection (1011) for quartz (2 θ = 26°.66 and d = 3.343 Å using the wavelength 1.54178 Å for Cu Kα radiation ; see e.g. Frondel, 1962). A suitable mixture of laumontite and quartz (85 and 15 weight-% respectively) was oscillated in the diffractometer scanning the afore-mentioned range. The sample was first soaked in water, and was allowed to dry during the diffractometer run. Previous experimentation had shown that the laumontite changed into leonhardite during drying, and the sudden change in the angles of the recorded reflections indicates that the dehydration process is abrupt. A detailed account of the methods is found in Pipping (1964).

Other Physical Constants

The optical constants for the leonhardite form have been determined on the U-stage by Mrs. Toini Mikkola.

The specific gravity was determined by the floating method, using a Westphal balance.

DTA and TGA

The DTA diagrams were obtained with a Leeds-Northrup apparatus with a temperature rise of 10°C/min.

The TGA diagrams were obtained with a Stanton apparatus with a temperature rise of 6.6°C/min.

Chemical Analyses

The chemical analyses (Table 2) are all new analyses made by Mrs. Irja Huhta (Nos. I–IV and VI–VII) formerly of the Geological Survey of Finland, and H. B. Wiik (No. V) of the Geological Survey of Finland. Although the author is aware of several analyses of No. I (probably good ones) and of analyses for No. II (Koch, 1959) and Nos. VI and VII (Eskola and Hentola, 1961 ; Fersmann, 1909), it was found advisable to have all analyses made in the same laboratory to permit better comparison. Special care was taken with the alkalies.

RESULTS

The X-ray investigation (Table 1) shows that there are differences in the cell sizes of laumontite and its partly dehydrated equivalent leonhardite, as already found by Coombs (1952).

TABLE 1

Unit cell dimensions of the laumontite and leonhardite forms of samples I-VI. The laumontite form=La, the leonhardite form=Le. For description of methods and samples see the text.

			Unit Cell Dimensions of Laumontite and Leonhardite					
			a_o	b_o	c_o	β_o	V_o	$\triangle V_o$
I	Huelgoat	La	15.041	13.180	7.710	113°.13	1405.57	55.41
	Bretagne, France	Le	14.770	13.056	7.595	112°.80	1350.16	
II	Petersberg	La	15.008	13.160	7.702	113°.22	1397.94	41.52
	Halle, Germany	Le	14.790	13.068	7.612	112°.68	1356.42	
III	Tblisi	La	15.027	13.180	7.707	113°.08	1404.18	60.28
	Kaukasus, USSR	Le	14.723	13.048	7.571	112°.48	1343.90	
IV	Lammi	La	15.029	13.180	7.695	113°.10	1402.07	50.80
	Finland	Le	14.747	13.068	7.594	112°.58	1351.27	
V	Tusby	La	15.030	13.172	7.716	113°.34	1402.53	40.49
	Finland	Le	14.812	13.104	7.605	112°.68	1362.04	
VI	Kuhmoinen	La	15.053	13.160	7.721	113°.43	1403.37	47.95
	Finland	Le	14.782	13.076	7.602	112°.71	1355.42	

The cell edges are given in Å-units. Each value for a_o, b_o, c_o and β_o is an average of eight (8) separate determinations from diffractometer recordings. The error of the average varies from ±0.0087 Å to ±0.0020 Å. The error of the β-angle varies from ±0.24° to ±0.08°. $\triangle V_o$ is the difference La V_o - Le V_o.

TABLE 2

Chemical analyses and unit cell content of samples I–VII. For description of the samples see the text.

Weight—%

	I	II	III	IV	V	VI	VII**
SiO_2	51.41	51.92	51.97	51.12	50.54	51.86	51.00
TiO_2	n.d.	n.d.	n.d.	0.04	0.02	0.02	n.d.
Al_2O_3	22.20	22.09	22.33	22.29	22.17	22.44	22.48
Fe_2O_3	0.05*	0.03*	0.01*	0.54	0.22	0.07	0.21*
FeO				0.37	0.00	0.14	
MnO	n.d.	n.d.	n.d.	n.d.	0.003	n.d.	0.03
MgO	n.d.	n.d.	n.d.	0.20	0.18	0.04	n.d.
CaO	12.01	11.75	11.68	11.29	10.58	10.47	6.96
Na_2O	0.07	0.13	0.21	0.26	0.54	0.74	2.58
K_2O	0.12	0.34	0.13	0.73	1.93	0.97	4.36
P_2O_5	0.01	n.d.	0.02	0.05	0.00	0.05	0.03
CO_2	n.d.	n.d.	n.d.	n.d.	0.00	n.d.	0.00
H_2O+	12.60	11.81	11.91	11.64	11.35	11.68	11.14
H_2O-	1.64	1.79	1.79	1.69	2.65	1.58	1.20
	100.11	99.86	100.05	100.22	100.18	100.06	100.00

I–IV and VI–VII, analyst Irja Huhta; V, analyst H.B. Wiik

* Total iron given as Fe_2O_3

** Analysis recalculated to 100.00, after subtraction of 2.18 Wt-% CO_2 and equivalent CaO, for calcite.

Unit cell content

	I	II	III	IV	V	VI	VII
Si	15.82	15.98	15.89	15.98	15.64	16.09	16.14
Ti	—	—	—	0.01	—	—	—
Al	8.05	8.01	8.05	8.07	8.09	8.21	8.38
Fe'''	0.01	0.01	—	0.13	0.05	0.02	0.06
Fe''	—	—	—	0.09	—	0.04	—
Mn	—	—	—	—	—	—	0.01
Mg	—	—	—	0.09	0.08	0.02	—
Ca	3.96	3.87	3.83	3.72	3.51	3.48	2.37
Na	0.04	0.08	0.12	0.16	0.32	0.44	1.58
K	0.05	0.13	0.05	0.29	0.76	0.38	1.76
P	—	—	—	—	—	0.01	0.01
H_2	14.61	13.96	13.97	13.66	14.44	13.71	13.02
O	62.35	61.93	61.75	62.08	62.07	62.22	62.00**

** The unit cell content calculated for O = 62.00, according to Fersmann's formula.

The unit cell volumes differ on the average by very nearly 50 Å^3 (the last column in Table 1). This corresponds very well to the effective volume taken by two oxygen atoms, or (neglecting the protons) water molecules, in silicate structures. This concept of "oxygen volume" has for instance been used by Belov (e.g. Mamedov and Belov, 1963) in his analyses of the crystal chemistry of Ca-silicate minerals. The numerical values for this "oxygen volume" given by Belov (op. cit.) lie around 23 Å^3. For other structures we find values up to 25 Å^3. The difference in cell size between laumontite and leonhardite found by the present author closely corresponds to two such "oxygen volumes". It must be concluded that the first step of dehydration of laumontite (at room temperature) to leonhardite, consists of the expulsion of two molecules of water from the laumontite structure. It is unfortunate that there are no reliable X-ray data available for the "primary leonhardite", No. VII in this study. Although the diffractometer pattern of this sample is like the patterns of the other samples it differs so much that the indexing of reflections could not be made by direct analogy. However, it has been ascertained that this "primary leonhardite" does not undergo any change in cell dimensions when treated like the other samples. This is in full agreement with the facts recorded by Fersmann (1909), who first presented and named this mineral or mineral variety.

From the chemical analyses in Table 2, the unit cell content for the samples I–VI has been calculated for the leonhardite form. This calculation was made using the unit cell volumes for leonhardite (Table 1) and the specific gravity values given in Table 3. The good agreement of X-ray, chemical and physical data for the samples I–VI may be seen from the fact that the number of oxygen atoms in the unit cell averages 62.07, when it theoretically should be 62.00. Another fact that may be read from Table 2 is that the ratio Al : Si is fairly constant, 0.5. Further the sum $Ca+\frac{Na+K}{2}$ will be found constant at about 4.

TABLE 3

Physical constants of leonhardite varieties of samples I–VII. Description of samples and methods in the text.

	I	II	III	IV	V	VI	VII
Sp. gr.	2.273	2.263	2.269	2.269	2.266	2.283	2.296
	±0.001	±0.001	±0.001	±0.001	±0.001	±0.001	±0.001
α	1.505	1.506	1.504	1.506	1.504	1.504	1.501
β	1.513	1.517	1.515	1.515	1.515	1.510	1.508
γ	1.518	1.520	1.518	1.518	1.518	1.513	1.512
2Vα	42°	42°	35°	41°	41°	82°	33°
$c\wedge\gamma$	32°	36°	39°	28°	34°	32°	30°
$\gamma-\alpha$	0.013	0.014	0.014	0.012	0.014	0.009	0.011

The optical constants determined by Toini Mikkola ; specific gravity by Fredrik Pipping.

Coombs (1952) discusses thoroughly the composition of laumontites and the alkali substitution. He concludes that the substitution of Ca by Na and/or K takes place in two ways simultaneously, *i.e.* by "feldspathic" and "zeolitic" substitution. In the former CaAl is replaced by NaSi and/or KSi, while in the latter Ca is replaced by 2 Na or 2 K. In the first-mentioned type of substitution the ratio Al : Si would be conspicuously lowered by increasing alkali introduction; *e.g.* substitution of 1/2 Ca gives theoretically Al : Si = 0.45.

The figures presented in the present study are thus in favour of the purely "zeolitic" type of substitution. Further scrutiny of the chemical analyses shows that the Na content steadily increases with decreasing Ca, whereas K is irregular. K may be greater or less than Na. This indicates that Na substitutes Ca in definite positions in the lattice. From comparison of ionic radii this seems very probable. Considering the ionic radius of K, about 1.40 Å, it is very like the radius of a water molecule. K therefore most probably will be found in positions normally occupied by water molecules, or it may be found to reduce the space normally disposed by water molecules in the lattice. In the case of No. VII it seems certain that K has taken sites which otherwise should be filled with H_2O.

The DTA and TGA diagrams in Figs. 1 and 2 have here been connected to the chemical composition of the samples. Previous DTA studies of laumontites (Koizumi, 1953; Pécsi-Donáth, 1963) have not recorded the chemical composition of the used samples. The present study reveals considerable differences in the thermal behaviour along with differences in chemical composition. The following features of the DTA diagrams may be pointed out:

1. The rather sharp endogene peak at 480°C in samples I–III almost disappears in the samples IV–VII.
2. In the samples V and VI appears a new peak at 625°–630°C, traceable even in sample IV.
3. In sample VII the first peak at about 300°C is strongly accentuated, and a quite new peak at 780°C appears.
4. In all TGA diagrams the stepwise expulsion of water can be seen.

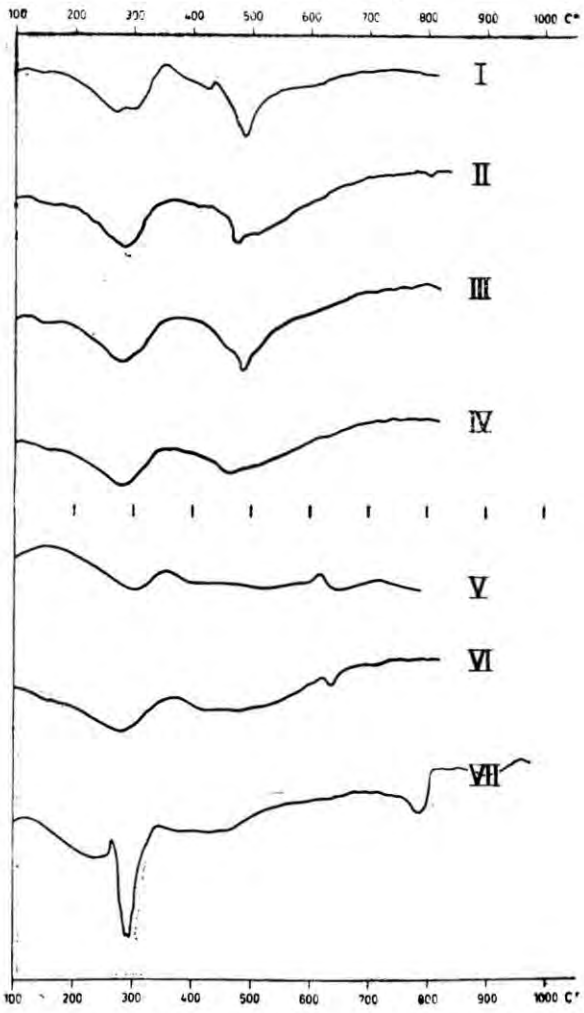

Fig. 1. DTA diagrams of samples I–VII.

These features indicate that increasing alkali substitution leads to barriers which postpone the expulsion of water to higher temperatures. When discussing the chemical composition of laumontites in the foregoing, it was suggested that K introduced into the lattice probably occupies water positions or otherwise considerably reduces the space normally occupied by water molecules. This hypothesis is well supported by the gradual change of thermal behaviour exposed in the DTA diagrams.

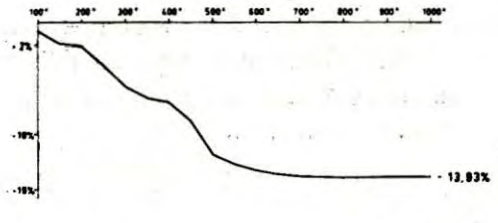

LAUMONTITE I
Bretagne, France
6,6°C/min.

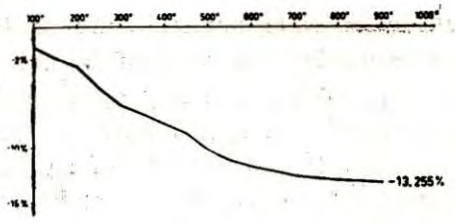

LAUMONTITE V
Tusby, Finland
6,6°C/min.

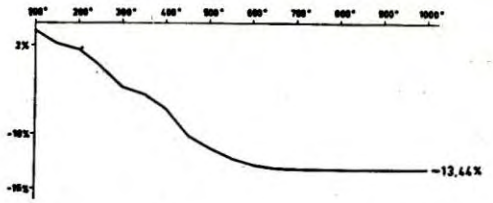

LAUMONTITE II
Halle, Germany
6,6°C/min.

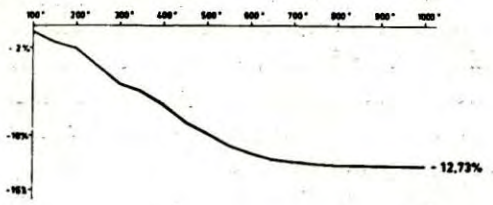

LAUMONTITE VI
Kuhmoinen, Finland
6,6°C/min.

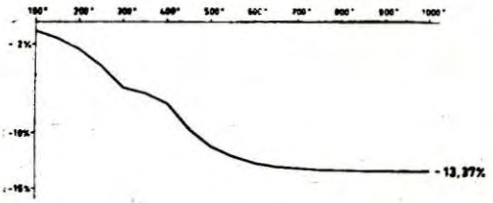

LAUMONTITE III
Kaukasus, Tbisi, USSR
6,6°C/min

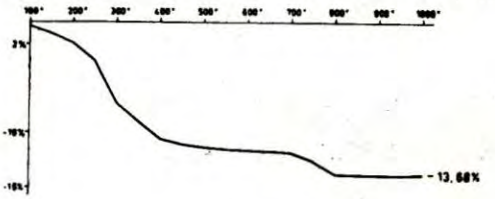

LAUMONTITE VII
Krim, Kurtsy, USSR
6,6°C/min

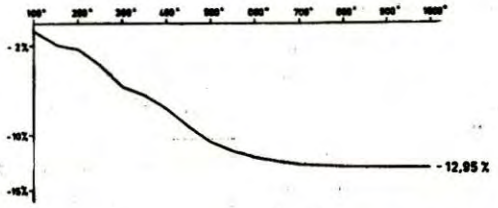

LAUMONTITE IV
Lomni, Finland
6,6° C/min

Fig. 2. TGA diagrams of samples I–VII.

CONCLUSIONS

The dehydration of laumontite at room temperature results in a decrease of the unit cell volume of about 50 Å^3, closely corresponding to the volume of two molecules of water. Laumontite has a water content of 16 H_2O in the unit cell, and the dehydration product leonhardite 14 H_2O.

The chemical analyses give evidence that Ca is substituted by Na and/or K so that $Ca = \frac{Na+K}{2}$, i.e. by "zeolitic" substitution. It is suggested that Na occupies definite Ca positions in the lattice, whereas K takes certain positions usually occupied by water molecules. This seems to hold good especially for the "primary leonhardite", with a high alkali content and not capable of rehydration at room temperature like other leonhardites.

The DTA investigation confirms that some of the water is differently bound or differently distributed in the lattice of alkali rich laumontites when compared with alkali free varieties.

ACKNOWLEDGEMENTS

The author expresses his thanks to the following persons and institutions providing him with laumontite samples for the present investigation: Prof. G. P. Barsanov, A. E. Fersmanns Mineralogical Museum, Akademii Nauk, Moscow, USSR; Prof. M. Saksela, The Institute of Geology and Mineralogy, University of Helsinki, Finland; Dr. R. A. Koch, Leipzig, Germany and Mr O. Näykki, M.A., University of Helsinki, Finland. It is with deep feelings of gratitude that my thoughts seek the memory of Prof. Pentti Eskola who provided me with material from Kuhmoinen in Southern Finland.

I forward my best thanks to Mrs. Irja Huhta and H. B. Wiik who made the chemical analyses, and to Mrs. Toini Mikkola who determined the optical constants of my samples.

Further thanks are due to J. Hyyppä and K Punakivi for their technical assistance in the DTA and TGA investigations.

The financial support of Leo and Regina Wainstein Foundation made it possible for me to present this paper at the IMA Session in New Delhi.

REFERENCES

Coombs, D. S. (1952) Cell size, optical properties and chemical composition of laumontite and leonhardite. *Am. Mineral.* Vol. 37, pp. 812–830.

Doelter, C. (1921) *Handbuch der Mineralchemie*, Steinkopf, Dresden u. Leipzig, T II, pp. 37–52.

Eskola, Pentti (with contributions by Yrjö Hentola), (1960) Laumontite in Finland. *Ind. Mineral*, Vol. 1, pp. 29–41.

Fersmann, A. E. (1909) Etudes sur les zeolithes de la Russie, I. *Trav. du Musée Géol. Pierre le Grand prés l Acad. Impér. des Sciences de St.—Petersbourg* Tom II. pp. 103–150.

Frondel, Clifford (1962) *Dana's System of Mineralogy, Vol. III. Silica minerals. (7th ed.)*. John Wiley and Sons Inc., New York and London.

Heritsch, Haymo (1956) Die Rontgenkristallographie von. Laumontite von Stainz (Steiermark). *Tschermaks mineral. Petr. Mitt. Folge* 3, Band 5, Heft 4, pp. 335–342.

Koch, R. A. (1959) über den Laumontit des Petersberges bei Halle a.d. Saale. *Neues Jahrb. Mineral., Jahrg.* 1958, pp. 58–67.

Koizumi, Mitsue (1953) The Differential Thermal Analysis Curves and the Dehydration Curves of Zeolites. *Mineral. Jour. Japan*, Vol. 1, pp. 36–47.

Mamedov, Kh.S. and Belov, N. V. (1958) Crystal structure of Mica-like hydrous Calcium silicates: okenite, nekoite, truscottite and gyrolite. New Silicate radical (Si_8O_{15}). *Dokl. Akad. Nauk, USSR*, 121, pp. 713–716. In English: Crystal Chemistry of Large-Cation Silicates, by Acad. N. V. Belov, Consultants Bureau, New York, 1963.

Pecsi-Donath, Éva (1963) A zeolitok termikus bomlásának vizsgálata DTA módszerrel, (French abstract). *Bulletin of the Hungarian Geological Society* 93, *Clay minerals volume*, pp. 32–39.

Pipping, Fredrik (1961) Laumontite from Viitasaari, Central Finland. *Bull. Com. Finland.*, Vol. 196, pp. 67–72.

——— (1964) Laumontit, dess dehydrering och kemiska sammansättning. Med bilaga rörande laumontitförekomster i Finland. *Unpublished thesis in the archives of Åbo Akademi*, Finland.

Tennyson, Christel (1960) Berylliummineralien und ihre pegmatitische Paragenese in den Graniten von Tittling/Bayerischer Wald. *Neues Jahrb. Mineral., Abh.*, Vol. 94, pp. 1253–1265.

MINERALOGICAL SOCIETY OF INDIA, IMA VOLUME, 1966
INTERNATIONAL MINERALOGICAL ASSOCIATION, PAPERS, FOURTH GENERAL MEETING

HYDROTHERMAL SYNTHESIS OF POLLUCITE AND ITS IRON ANALOGUE

SHOICHI KUME AND MITSUE KOIZUMI

ABSTRACT

Pollucite ($Cs_2O.Al_2O_3.4SiO_2.Aq$) is a Cs-containing zeolite rarely found in nature. Recently, Kopp* *et al.* (1963) reported the synthesis and some physical properties of the iron analog of pollucite ($Cs_2O.Fe_2O_3.4SiO_2.Aq$). In the same report, these authors briefly mentioned the weak magnetism of this iron analog.

To examine these experimental results in detail, 9 kinds of gels with the chemical compositions of $Cs_2O.(Al_2O_3)_{x/8}.(Fe_2O_3)_{1-x/8}.4SiO_2.Aq$ ($x=0, 1, \ldots, 8$) were prepared and hydrothermally treated at 450°C and 1 kb for 3 days. This treatment was sufficient to crystallize the gels and to form homogeneous isotropic powdery crystals. By means of microscopic observation and X-ray diffraction, it was proved that these crystals belonged to the system between pollucite and its iron analog and also that this system formed a continuous solid solution. Using the same crystals, the magnetic susceptibility was measured in the temperature range from 80° to 300°K. There was no trace of any kind of the ferro-or ferri-magnetism mentioned by Kopp *et al.*, and all specimens behaved paramagnetically in the above-mentioned temperature range.

TWO ZEOLITES IN ZEOLITIC ROCKS IN JAPAN (POTASSIUM CLINOPTILOLITE AND POWDERY MORDENITE)

HIDEO MINATO

ABSTRACT

A mineralogical investigation of some zeolitic rocks was made. One of them occurring in a white tuffaceous bed in Itaya, Yamagata prefecture, Japan consists mainly of potassium clinoptilolite. The X-ray powder method showed that the principal constituent was clinoptilolite, associated with small amounts of quartz and mordenite. Sometimes small prismatic crystals of clinoptilolite were found in small cavities under the microscope. The chemical composition is $(K_{2.4}Na_{0.4})\ (Ca_{0.9}Mg_{0.8})\ (Al_{5.9}Fe_{0.3})\ Si_{30}O_{72}.14.1H_2O+6.8H_2O$. The name potassium clinoptilolite is proposed because of the high potassium content. Another specimen from a white tuffaceous bed in Minase, Akita prefecture, Japan is composed of white powdery mordenite. The mordenite was investigated by means of the X-ray powder method and by chemical analysis. Some industrial uses of these materials were investigated also.

THE CHEMICAL COMPOSITION OF ANALCIME FROM THE LOW-GRADE METAMORPHIC ROCKS IN JAPAN

WAITSU NAKAJIMA AND MITSUE KOIZUMI

ABSTRACT

Recently, Saha (1959, 1961) reported that analcime exhibits solid solution through an extensive range of composition, and suggested the importance of determining the composition of natural analcime of varying modes of origin and the possibility of using analcime as a geothermometer for low-grade metamorphic rocks.

*KOPP, O. C., HARRIS, L. A., CLARK, G. W. AND YAKEL, H. L. (1963). A hydrothermally synthesized iron analog of pollucite–its structure and significance. *Am. Mineral.* Vol. 48, pp. 100–109.

Applying the linear relation between SiO_2 content and d-spacing, the chemical composition of analcime from several areas in Japan was determined. From the results and the data on chemical composition of analcimes collected from the literature, it is concluded that "igneous analcime" which fills amygdales of volcanic rocks has a composition close to the ideal composition of analcime. On the other hand, "metamorphic analcime" which replaces glassy matters in low-grade metamorphic rocks is within more broad range of composition $Na_2O.Al_2O_3$4.4-5.8 SiO_2.2.2-2.9H_2O.

On the chemical composition of analcimes from the low-grade metamorphic terrains in Japan, it is suggested that the composition range of analcime from the Miocene series, with a steep geothermal gradient, is narrower than that of analcime from the Cretaceous series most of which is considered to have a normal thermal gradient.

SYNTHESIS AND STABILITY OF ZEOLITES IN THE SYSTEM (Na_2, Ca)O.Al_2O_3.7SiO_2-H_2O

WAITSU NAKAJIMA AND MITSUE KOIZUMI

ABSTRACT

The silica-rich Na-Ca zeolites such as heulandite and mordenite are among the common zeolites of low-grade metamorphic rocks. In order to determine the stability of these zeolites and related minerals, the system (Na_2, Ca)O.Al_2O_3.7SiO_2-H_2O has been investigated in the temperature range 200-550°C at pressures of 0.5 to 3kb. Gel-mixtures were used as the starting materials.

Heulandite, mordenite, analcime, wairakite, plagioclase, quartz, and montmorillonite minerals were synthesized. Among the zeolites, minerals with the analcime structure appeared in the widest P-T range. The upper limit of their formation temperature scarcely changed with pressure and ascended linearly from 375°C to 500°C as the Ca end-member increased.

Mordenite and heulandite were obtained from gels with Na_2O : CaO ratios from 2 : 3 to 0 : 5. The P-T range of the above two zeolites was as follows. Mordenite : <450°C, 2-3kb. Heulandite : <400°C, 1-2 kb (appeared dominantly at 2kb). From these results, it is suggested that zeolites with higher SiO_2 content were rather stable under higher pressure of water vapor.

STRUCTURAL CHANGES IN ZEOLITES CAUSED BY CATION EXCHANGE AT ROOM TEMPERATURE AND DEHYDRATION UNDER CONTROLLED pH_2O

RUSTOM ROY, A. M. TAYLOR, AND W. BALGORD

ABSTRACT

Although zeolites are usually thought of as substances which undergo continuous water loss without structural change, there have been very few experiments to establish this fact.

The present report covers an extensive experimental study of the Na-P (phillipsite-harmotome) and analcite families. The influence of cation exchange (even at room temperature) of K, Ca, Ba, Ni, Co, etc. is shown to cause substantial changes in the powder X-ray pattern, reflecting changes of symmetry as well as unit cell parameters.

Using controlled partial pressures of H_2O in the range of about 10^{-3} to 10^{0} atm and recording thermogravimetric balances, the compositional changes with temperature have been recorded, and the kinetics of each step-wise change also studied. High temperature X-ray diffraction, under

the same pH_2O conditions, provides an indication of the structural changes corresponding to the compositional breaks. General conclusions which can be drawn from the results are :

I. Many zeolites, depending equally on the parent structure and exchangeable cation, undergo several steps in the dehydration process.

II. Structural changes correspond to first order dehydration reactions, continuous or second order dehydration reactions over a temperature range, and true polymorphic changes.

Finally, the results of hydrothermal experiments are used to indicate the enormous differences between the stable and several metastable dehydration reaction series.

ANALCIME FROM SEDIMENTARY AND BURIAL METAMORPHIC ROCKS

J. T. WHETTEN AND D. S. COOMBS

ABSTRACT

Analcime from sedimentary and burial metamorphic rocks ranging in age from Carboniferous to Quaternary from a dozen different areas has been analyzed by X-ray, optical, and in some cases by chemical means. The analcime lattice dimensions range from $a_o = 13.711$Å to 13.673 Å. Cell size, correlated by Saha (1959) with synthetic analcime composition (the principal substitution being Na and Al for Si) is considered a useful indicator of composition for natural analcime. The analcimes described in this report vary considerably in composition, from $(NaAl)_{15\cdot3}Si_{32\cdot7}O_{96}\cdot nH_2O$ to $(NaAl)_{12\cdot8}Si_{35\cdot2}O_{96}\cdot nH_2O$.

Analcime which has apparently formed either by precipitation or by reaction of clay minerals with highly saline water (e.g., Lockatong formation) is generally relatively silica-poor and free silica is sometimes lacking in the mineral assemblage. In contrast, analcime formed by reaction of saline water with acid volcanic glass (e.g., Yavapai playa lake beds) is silica-rich, probably because of the high activity of the silica contained in the glass. Analcime from rocks of burial metamorphic origin (e.g., Murihiku group and Currabubula formation) tends to be of intermediate composition, and may represent a closer approach to the quartz-analcime equilibrium.

Cell dimensions of analcime from individual rock suites are for the most part consistently the same, even in samples separated stratigraphically by as much as 15,000 feet. Thus it is not likely that the analcime silica content is solely a function of temperature, and the analcime composition is of doubtful significance as a geothermometer.

MINERALOGICAL SOCIETY OF INDIA, IMA VOLUME, 1966
INTERNATIONAL MINERALOGICAL ASSOCIATION, PAPERS, FOURTH GENERAL MEETING

GENERAL PAPERS

MELANTERITE FROM THE MAKUM COAL BASIN, ASSAM

D. N. D. GOSWAMI
Department of Geology, Gauhati University, Assam, India

ABSTRACT

An unusual mineral was observed in the coals of the Makum basin, Assam. The mineral is blue-green in colour inside the coal mine but becomes white when exposed to day light at the surface. It occurs both in crystal forms and also as concretions. The data obtained from optical, chemical and X-ray studies identify the mineral to be melanterite having a Fe : Cu : : 5 : 1. It is inferred that it was formed by the oxidation of pyrite which occurs in abundance in microscopic form in the coal.

OCCURRENCE

An unusual mineral was observed in the coal mines of the Makum basin (Lat. 27°15′N and 27°25′N : long. 95°40′E and 95°55′E), Upper Assam. Inside the mine the mineral is found hanging from the coal pillars, roofs and walls in the workings. It also grows on coal samples exposed to moist air in the laboratory. The mineral described in the present study was collected from the Baragolai mine (Lat. 27°16′N : Long. 95°43′E) in the Makum area.

PHYSICAL PROPERTIES

In proper humid environment, the mineral is blue green in colour, which fades away with the loss of humidity. The mineral dissolves easily in water when the temperature is raised. It becomes white outside the mine when exposed to dry air at the surface.

Crystals when developed are short, prismatic and delicate to handle. The mineral shows well developed cleavage and vitreous luster. The hardness is about 2 and the streak is colourless (Fig. 1).

It also occurs in the form of concretions and small stalactitic tufts from the roofs of the mine and also as fibrous mass and as encrustation.

From the above physical properties, mode of occurrence and association, this mineral has been identified as Melanterite belonging to the melanterite series (Palache *et al.* 1951).

OPTICAL PROPERTIES

The refractive index of the mineral was determined by the immersion method and the other optical properties studied on thin sections. The observed properties were correlated with the published results of the natural and artificial Melanterite (Table 1).

Fig. 1. Melanterite crystal resting upon shale. Fig. represents double the size of the natural crystals.

CHEMICAL PROPERTIES

An analysis shows the presence of FeO (24.52%), CuO (in trace) SO_3 (31.42%) and H_2O (44.06%). The mineral thus conforms well to the composition of mineral Melanterite.

X-RAY STUDY

Powder x-ray photograph of the mineral was taken with the filter Zr and Mo K. The x-ray photograph is prominent in low angle in comparision to the high angle (Fig. 2). A number of lines are developed, four of them

TABLE 1

Optical Properties of Melanterite

Optical Properties	A.S.T.M. Card	Winchell (1959)	Palache and Others (1951)	Observed (author)
α	1.4713	1.467	1.4713	1.465
β	1.4788	1.47–.48	1.4782	1.475
γ	1.4856	1.478–.489	1.4856	1.485
$\gamma-\alpha$	0.0143	0.011–0.022	—	0.020
2V	85.27	Large	85.27	+ve
Sign	+ve	+ve	+ve	Large 82°–86°
$Z \wedge C$	—	54–78	—	65–70

being prominent. The observed values are summarised and compared with the A. S. T. M. card (Table 2).

TABLE 2

ϕ	dÅ Observed	dÅ A.S.T.M. card
4.105	4.965	4.90
5.267	3.859	3.70
6.108	3.33	3.23
7.370	2.752	2.75

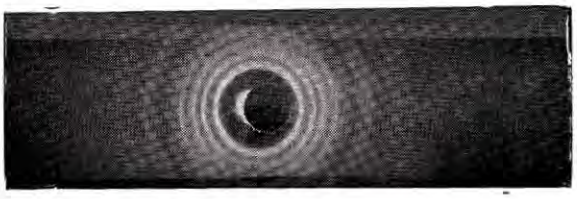

Fig. 2. Powder X-ray photograph of Melanterite.

CONCLUSION

The coal of the Makum basin is rich in sulphur, largely in the pyritic form. The study of a few polished blocks of coal under the reflected light shows the presence of pyrite in various forms like stringers, individual crystals and disseminated grains. Melanterite is obviously formed from the oxidation of pyrite present in the coal. This is the first reported occurrence of Melanterite in Indian coal and there are indications that other members of the series like pisanite and kerovite may be present.

ACKNOWLEDGEMENT

The author's thanks are due to Dr. J. M. Choudhury, Head of the Department of Geology, Gauhati University for guidance and help in this study, to the Department of Physics, Gauhati University, for facilities for X-ray study and to the A.R.T. Company for help in collecting the samples in the mine.

REFERENCES

AZAROFF, L.V. AND BUERGER, M. J. (1958) *The powder method in X-ray crystallography*. McGraw Hill Book Company. Inc., New York.

ECKEL, B. (1933) Stability relationship of Colorado Pisanite (Cuprian Melanterite): *Am. Mineral*, Vol. 18.

PALACHE, C., BERMAN, H. AND FRONDEL, C. (1951) *Dana's System of Mineralogy*, John Wiley and Sons., Inc. New York.

WINCHELL, W. (1959) *Elements of Optical Mineralogy*. Part II. John Wiley and Sons., Inc. New York.

MINERALOGICAL SOCIETY OF INDIA, IMA VOLUME, 1966
INTERNATIONAL MINERALOGICAL ASSOCIATION, PAPERS, FOURTH GENERAL MEETING

STUDY OF THE TEMPERATURE OF CRYSTALLIZATION OF SOME SPANISH FLUORITES BY DECREPITATION METHOD *

M. FONT-ALTABA, J. MONTORIOL-POUS AND J. M. AMIGO
Laboratorio de Cristalografía y Mineralogia, Universidad de Barcelona, Barcelona, Spain

ABSTRACT

By means of the application of decrepitometric technique we could study the formation temperature of different fluorite deposits in Spain. The inflexion points of decrepitometric curves of mineral samples from these deposits have been determinated. A study was carried out on the contents of trace elements by using optical and x-ray fluorescence spectrographic methods.

INTRODUCTION

When a mineral crystallizes from an aqueous phase, microinclusions of this aqueous phase remain in its interior in small cavities.

These small cavities are initially completely full of liquid, but as the temperature decreases, the liquid shrinks and a gaseous phase appears.

If the mineral is experimentally heated, when the crystallisation temperature is reached, the liquid phase again will fill the whole space of microcavities. Therefore, if we observe a thin section of the same through a microscope with heatable stage, we shall be able to find the temperature at which it takes place, (Twenhofel 1947, Ingerson 1947, Bailey, 1949).

Another method for observing this phenomenon is based on the acoustic detection of the breakage of crystals, that is the decrepitation of the mineral (Scott 1948, Peach 1949). This mineral breakage is produced by increasing the pressure inside the inclusions on raising the temperature.

Firstly, the most superficial cavities burst, producing a more or less constant number of noises per unit time.

At the moment the temperature reaches the crystallisation point, all the inclusions begin to burst, and the number of noises per unit time increases suddenly. The most important factor is the frequency and not the intensity of noises.

If the mineral has secondary inclusions, an increase of the frequency of the noises is produced before reaching the crystallisation temperature. It is quite easy to differenciate the primary and secondary inclusions because the increase of frequencies takes place at different temperature and therefore at different times.

TECHNIQUE USED

The samples were crushed, and by means of a series of sieves the fraction between 0.25–2.25 mm size was separated. This fraction was treated with dilute hydrochloric acid in order to eliminate the carbonates. It was washed with distilled water and dried at a low temperature (30°C). One cm^3 of the prepared sample was introduced into a furnace, the temperature of which was controlled by a timer switch. The temperature was taken by means of a Cr/Al thermocouple near the sample. The temperature was increased at 5°C/minute in the zone over 100°C. The frequency of the noises was detected by means of a stetoscope of the same diameter as the diameter of the furnace.

PRESSURE CORRECTION

The temperatures listed in the figures have not been corrected for the phenomenon of compression of the liquid in the inclusions caused by pressure at the time the inclusions were formed.

The temperature measured in the laboratory was somewhat lower than the real temperatures prevailing when the inclusions were formed (Ingerson, 1947).

The pressure on a crystal growing at depth, is a question that can only be guessed at in

* Work supported by the " Fomento de la Investigación en la Universidad " of Spanish Educational Ministry.

some cases, even supposing the depth was known exactly.

In the case of the fluorite studied herein, considering the geological history of the area of the deposits and the overlying rocks existing at the time of crystallisation of the fluorite, we obtain corrections of less than 10°C, according to the correction curves published by Kennedy (1950). These temperature corrections are too small to have much geological significance of the crystallisation temperatures of the fluorites.

LOCALITY OF THE SAMPLES

The samples studied came from the following deposits:

(a) Osor

Situated near Osor (Gerona) on the road Osor-Angles-Gerona. This is the most important deposit of Catalonia and one of the most important in Spain. Fluorite appears as well developed veins, of varying thickness reaching in some parts 15 m. The wall rocks are generally gneiss and metamorphic rocks (Van der Sijp, 1951).

(b) Matagalls

The deposit is situated on the NE slope of Matagalls hill(Montseny Mountains, Barcelona). The mineral appears as veins of about 2 m thickness or as discontinuous nests. The wall rock is pink granite.

(c) Berta

Situated between Papiol and Rubi, 15 Km from Barcelona (Montoriol-Pous, 1963). The fluorite (Montoriol-Pous & Font-Altaba, 1964) appears in discontinuous nests following the microtectonics of the area (Montoriol-Pous and Font-Altaba, 1965). The nests are found in veins of mylonite developed in a monzonitic granite.

(d) Americana

Situated near the village of Riaño (León). The fluorite appears in a highly disturbed zone; in some places it occurs as vertical veins, while in others it appears almost horizontal and sheeted. The wall rock is mountain limestones.

INTERPRETATION OF RESULTS

The experimental results obtained can be seen in the Figs. 1, 2 and 3.

(A) Crystallization temperatures

Even though some have noticed the formation of fluorite at a high temperature (Yates

		A	B
Osor	1	375	420
	2	360	420
	3	360	420
	4	350	410
	5	360	415
	6	350	405
	7	360	415
Matagalls	1	330	420
	2	320	410
Berta	1	280	290
	2	280	290
	3	285	295
	4	285	295
	5	295	300
	6	285	290
	7	285	290
Americana	1	280	350
	2	275	320

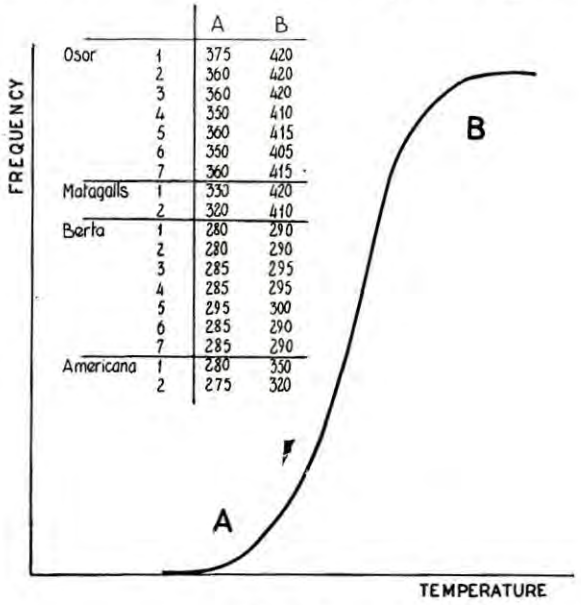

Fig. 1

and Thomson, 1959), in a number of cases relatively low temperatures are indicated (Freas, 1961 and Weller *et al.*, 1962). The values found by us are relatively high in the case of the deposits Berta and Americana, and very high in the deposits Osor and Matagalls.

		A	B	C	D
Americana	3	180	200	250	330
"	4	250	260	280	350
Matagalls	3	340	355	380	435

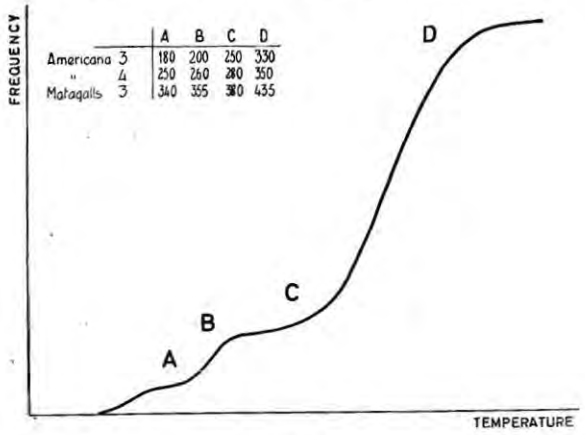

Fig. 2

(B) Interpretation of the form of the frequency/temperature curve

Most of the samples studied (18 of 22) belong to the type shown in Fig. 1. The fluorites here had a simple history: once the crystallisation was finished, no other processes have affected them.

Three of the samples (2 coming from Americana mine and 1 from Matagalls) have curves of the type in Fig. 2. The portion C–D of the curve corresponds to the first crystallisation of the mineral, whereas the portion A–B–C is the result of changes suffered by the fluorite later on. These may be the recrystallisation that took place at lower temperatures than the original ones, resulting in the fluorite being well crystallised.

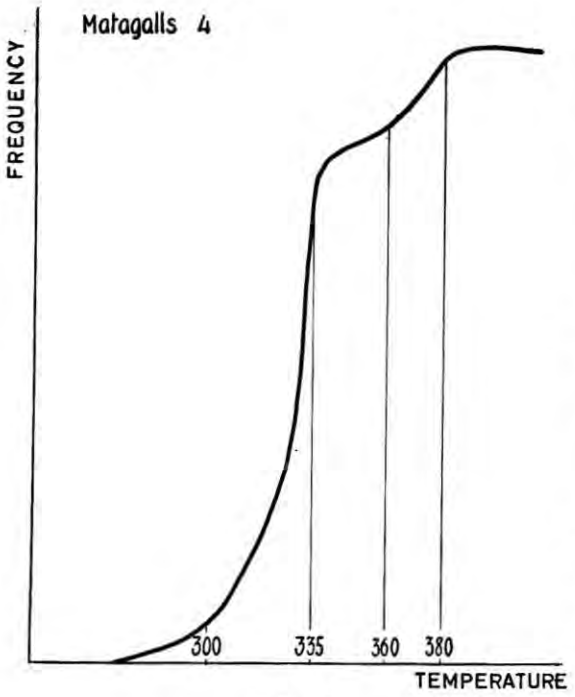

Fig. 3

Only one sample coming from Matagalls is depicted by the type of curve in Fig. 3. This shows that there has been a recrystallisation at high temperature almost reaching the temperature of mineral formation.

CONCLUSION

From the above, we think that, in general, the fluorites of the deposits under study crystallized at high temperature, and were not affected afterwards.

A few samples which were affected by later processes were recrystallized either at a low temperature, (*e.g.* Americana and Matagalls) or at a high temperature (*e.g.* Matagalls).

SPECTROGRAPHY

In the fluorites described here, no significant differences were formed in the contents of trace elements in relation to the formation temperature. We detected in almost all samples the presence of 10 elements.

Mg, Al, Si, Mn, Fe, Cu, Ag, Sn, Ba, Pb.

The spectrographic analysis was carried out by means of Bausch and Lomb grating spectrograph, model 11, of 1.5 m, working in the region of ultraviolet (1850–3700 Å). The optical spectrographic analysis agrees with the x-ray fluorescence analysis, carried out by means of a Phillips vacuum spectrograph.

REFERENCES

BAILEY, S. W. (1949) *Jour. Geol.*, Vol. 57, p. 304.

FREAS, D. H. (1961) Temperatures of mineralisation by liquid inclusions, Cave-in-rock flourspar district, Illinois : *Econ. Geol.*, Vol. 66, No. 3, pp. 542–556.

INGERSON, EARL, (1947) Liquid inclusions in geologic thermometry : *Am. Mineral*, Vol. 32, Nos. 7 & 8, pp. 375–388.

KENNEDY, G. C. (1950) Pneumatolysis and the liquid inclusion method of geologic thermometer : *Econ. Geol.*, Vol. 45, No. 6, pp. 533–547.

MONTORIOL-POUS, J. (1963) Estudio del yacimiento de fluorita Mina Berta de San Cugat del Valles (Barcelona) : *Tesis, Universidad de Barcelona.*

———J. Y. FONT-ALTABA, M. (1964) *Bol. R. Soc. Espanola de Hist. Nat. (G.)*, Vol. 62, p. 229.

———(1965) *Inst. Geol. y Min. de Espana*, p. 78.

PEACH, P. A. (1949) A decrepitation geothermometer : *Am. Mineral*, Vol. 34, Nos. 5 & 6, pp. 413–421.

SCOTT, H. S. (1948) *Econ. Geol.*, Vol. 43, p. 637.

TWENHOFEL, W. S. (1947) The temparature crystallization of a fluorite crystal from Luna Country, New Mexico : *Econ. Geol.*, Vol. 42, No. 1, pp. 78–82.

VAN DER SIJP, J. W. Ch. M. (1951) Petrography and Geology of Montseny-Guillerias : *Tesis Rijkuniversiteit Utrech.*

WELLER, J. M., GROGAN, R. M., AND TIPPIE, F. E. (1952) *Illinois State Geol. Surv.*, Vol. 76, p. 329.

YATES, R. G. AND THOMSON, G. A. (1959) *U. S. Geol. Surv.*, Prof. Paper. p. 312.

MINERALOGICAL SOCIETY OF INDIA, IMA VOLUME, 1966
INTERNATIONAL MINERALOGICAL ASSOCIATION, PAPERS, FOURTH GENERAL MEETING

PHASE RELATIONS IN THE SYSTEM $NaAlSi_3O_8$ (albite)–$NaAlSiO_4$ (nepheline)–$NaFeSi_2O_6$ (acmite)–$CaMgSi_2O_6$ (diposide)–H_2O AND ITS IMPORTANCE IN THE GENESIS OF ALKALINE UNDERSATURATED ROCKS

A. D. EDGAR AND J. NOLAN
Department of Geology, University of Western Ontario, London, Canada
and Department of Geology, Johns Hopkins University, Baltimore, U.S.A.

ABSTRACT

Phase relations have been determined within several planes contained in the system $NaAlSi_3O_8$ (albite)–$NaAlSiO_4$ (nepheline)–$NaFeSi_2O_6$ (acmite)–$CaMgSi_2O_6$ (diopside)–H_2O. The partial pressure of oxygen was controlled in all planes containing the alkali pyroxene end-member acmite, using the conventional solid buffer assemblages. The low melting point in the plane Ab–Ne–Di is located on the Ab–Ne join at $Ab_{73}Ne_{27}$ at a temperature of $835 \pm 5°C$ at 1 Kb P_{H_2O}; the low melting point in the plane Ab–Ne–Ac at $715 \pm 5°C$ and at 1 Kb P_{H_2O} is located at $Ab_{15}Ne_{30}Ac_{55}$. Melting relations have also been studied for portions of the following intermediate compositional planes: Ab–Ne–$Ac_{50}Di_{50}$, Ab–Ne–$Ac_{80}Di_{20}$, Ab–Ne–$Ac_{90}Di_{10}$, and Ab–Ne–$Ac_{95}Di_5$. The inferred low melting points in such planes show a close agreement with the normative plot for rocks of the nepheline syenite clan. The significance of the composition of the pyroxene and the effect of P_{H_2O} in the genesis of alkaline undersaturated rocks is discussed.

INTRODUCTION

Phase relations have been determined within certain compositional planes contained in the system $NaAlSi_3O_8$ (albite)-$NaAlSiO_4$ (nepheline) –$NaFeSi_2O_6$ (acmite)–$CaMgSi_2O_6$ (diopside)–H_2O at total pressures of 1,000 and 2,000 Kg/Cm². This system can be considered to represent the addition of the pyroxene end-members acmite and diopside to the silica and potash-poor portion of Petrogeny's Residua System (SiO_2-$NaAlSiO_4$-$KAlSiO_4$). Because many undersaturated alkaline rocks contain significant amounts of these pyroxene molecules, the present study should be important to the understanding of the genesis of these rocks; and, in view of this, the experimentally determined phase relations in the above system have been compared with the normative compositions of both peralkaline and alkaline undersaturated rocks.

This investigation shows that the composition of the pyroxene plays a dominant role in the genesis of these rocks with the total pressure (P Total) and fugacity of oxygen (fo_2) being of secondary importance. The close correspondance between the normative compositions of rocks of the nepheline syenite clan and the inferred low melting points of the various compositional planes in this system suggests that many of these rocks have formed by a process of crystal⇌liquid equilibria.

The initial part of this investigation was a study of the simpler systems $NaAlSi_3O_8$ (albite) $NaAlSiO_4$ (nepheline)–$NaFeSi_2O_6$ (acmite)–H_2O (Nolan, 1965,) and $NaAlSi_3O_8$ (albite)–$NaAlSiO_4$ (nepheline)–$CaMgSi_2O_6$ (diopside)–H_2O (Edgar, 1964). The second author of this paper has been responsible for the preliminary studies involving the determination of melting relations within certain pyroxene compositional planes in the combined system $NaAlSi_3O_8$–$NaAlSiO_4$-$NaFeSi_2O_6$-$CaMgSi_2O_6$-H_2O. Because data for all of these systems has been published elsewhere (Edgar, 1964; Nolan, 1965), results will be presented graphically and no tables of melting data will be given in this report.

EXPERIMENTAL METHODS

(*a*) *Preparation of Starting Materials:* The majority of starting materials used in this study were prepared as homogeneous gels using a modification of the method proposed by Roy

(1956). The materials used for these initial compositions have been listed in an earlier publication (Nolan and Edgar, 1963) together with the modifications required in the preparation of gels containing Fe_2O_3. A few compositions in the nepheline–albite join of this system were prepared as glasses and kindly loaned to one of the authors by Dr. J. W. Geig, formerly of the Geophysical Laboratory.

(*b*) *Apparatus:* All crystallization experiments were carried out in "cold-seal" pressure vessels (Tuttle, 1949) using the sealed gold capsule method described by Goranson (1931) for the non-iron bearing compositions; and the three-tube buffer technique, described by Eugster and Wones (1962) for iron bearing compositions. In the latter technique a Ni-NiO buffer assemblage was used to control partial oxygen pressures. Temperatures were recorded with chromel-alumel thermocouples calibrated at the melting points of Zn (419.5°C) and NaCl (801°C) and are believed to be accurate to within ±5°C. Total pressures were measured by a Bourdon-tube pressure guage and are believed accurate to within ±4% of the stated values.

The products of the runs were examined with the petrographic microscope and by X-ray powder diffraction methods.

RESULTS

(*a*) *The System $NaAlSi_3O_8$ (albite)–$NaAlSiO_4$ (nepheline)–$CaMgSi_2O_6$ (diopside)–H_2O:* Phase relations in this system have been described by Edgar (1964) at 1,000 Kg/cm² water vapour pressure, and by Schairer and Yoder (1960) at atmospheric pressure. Due to the high melting temperatures in this system only a small portion of the liquidus surface at 1,000 Kg/cm² water vapour pressure could be determined using conventional "Tuttle-type" pressure vessels. Fortunately this low melting area, close to albite-rich compositions, is the area of petrological interest.

A projection of the liquidus surface from the H_2O apex of the tetrahedron onto the anhydrous plane (Albite-Nepheline-Diopside) is shown in Fig. 1. This system is not ternary (even neglecting the water component) due to the operation of the "plagioclase effect"

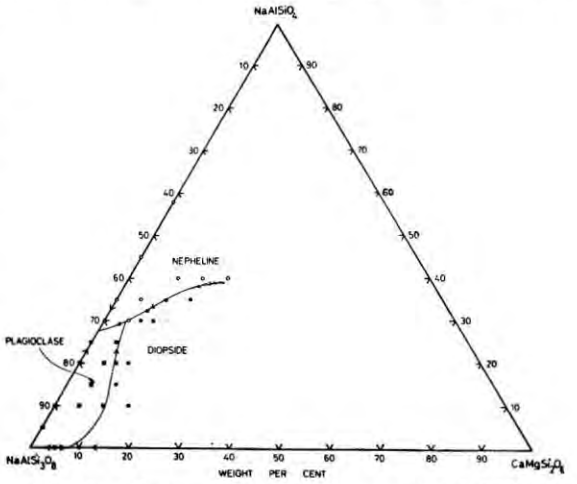

Fig. 1. Phase relations in the system $NaAlSi_3O_8$–$NaAlSiO_4$-$CaMgSi_2O_6$–H_2O at 1000 Kg/cm² water vapor pressure. Projection from the H_2O apex onto the anhydrous plane.

(Bowen, 1945). This effect results in the crystallization of plagioclase rather than pure albite from compositions containing diopside. The exact composition of the crystallizing plagioclase is not known but is not believed to be rich in the anorthite molecule (Edgar, 1964). The minimum melting temperature in this system is 835°±5°C located at $Ne_{27}Ab_{73}$.* The reaction point at which diopside, nepheline, plagioclase, liquid and vapour coexist is located at $Di_5Ne_{29}Ab_{66}$ at a temperature of 855°±5°C. The composition of this reaction point is considerably richer in the albite molecule than the corresponding reaction point at atmospheric pressure (Schairer and Yoder, 1960). The explanation for this enrichment of the albite molecule with increased water vapour pressure is not yet fully understood.

(*b*) *The System $NaAlSi_3O_8$ (albite)–$NaAlSiO_4$ (nepheline)-$NaFeSi_2O_6$ (acmite)–H_2O*: Phase relations in this system will shortly be published

* Throughout this paper, compositions are expressed in terms of weight percentages of standard mineral molecules *e.g.* Ne=nepheline, Ab=albite, Di=diposide, Ac=acmite.

elsewhere (Nolan, 1965,). The high melting temperatures of nepheline rich compositions has not permitted phase relations to be determined at compositions in excess of 50 weight per cent of the nepheline molecule. This system is complex due to the incongruent melting of acmite, producing under hydrothermal conditions and using a Ni–NiO buffer, a liquid plus magnetite. As a result, the system must be treated in terms of five components, namely Na_2O-Al_2O_3-Fe_2O_3-FeO-SiO_2 (excluding H_2O).

Phase relations in this system at 1,000 Kg/cm² and 2,000 Kg/cm² total pressure are given in Fig. 2. The areas labelled "Nepheline+Magnetite+Liquid, Albite+Magnetite+Liquid

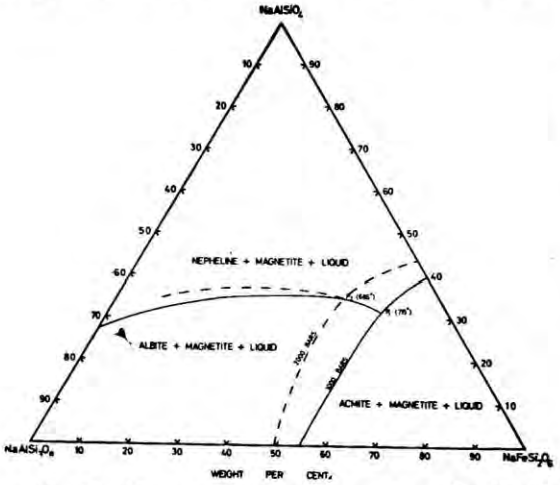

Fig. 2. Phase relations in the system $NaAlSi_3O_8$–$NaAlSiO_4$-$NaFeSi_2O_6$–H_2O at 1,000 and 2,000 Kg/cm² total pressure. Projection from the H_2O apex onto the anhydrous plane. For explanation of broken line and points P_1 and P_2 see text.

and Acmite+Magnetite+Liquid" are traces of phase volumes (which in a 3 dimensional model would have curved surfaces) within the five component system in the plane $NaAlSi_3O_8$–$NaAlSiO_4$–$NaFeSi_2O_6$. The lines separating these areas are not boundary curves but traces of curved boundary surfaces in the above plane.

The "low-melting" point in this system at 1,000 Kg/cm² total pressure, denoted P_1 in Fig. 2, is located very close to the composition $Ab_{15}Ne_{30}Ac_{55}$ at a temperature of 715°±5°C; at a total pressure of 2,000 Kg/cm², the "low melting" point is slightly richer in the albite and nepheline molecules and is located at $Ab_{20}Ne_{35}Ac_{45}$ at the temperature of 686°±5°C. This is labelled P_2 in Fig. 2 and indicates that an increased total pressure has a small but significant effect on both the "low-melting" compositions and temperatures in this system.

It should be emphasized that the points P_1 and P_2 on Fig. 2 are not ternary invariant points but piercing points (c.f. Muan, 1957) of univariant lines within the five component system piercing the plane $NaAlSi_3O_8$–$NaAlSiO_4$–$NaFeSi_2O_6$ at points P_1 (1,000 Kg/cm² total pressure) and at P_2 (2,000 Kg/cm² total pressure). At each of these points four crystalline phases, albite, nepheline, acmite, magnetite, as well as a liquid and vapor phase coexist in equilibrium.

(c) *The System $NaAlSi_3O_8$ (albite)–$NaAlSiO_4$ (nepheline) – $NaFeSi_2O_6$ (acmite) – $CaMgSi_2O_6$ (diopside)–H_2O at 1,000 Kg/cm² Total Pressure*: Phase relations in this system have been determined for compositions represented by four pyroxene compositional planes, namely Ab–Ne–$Ac_{95}Di_5$, Ab–Ne–$Ac_{90}Di_{10}$, Ab–Ne–$Ac_{80}Di_{20}$ and Ab–Ne–$Ac_{50}Di_{50}$. On Fig. 3 a projection of these four compositional planes onto the

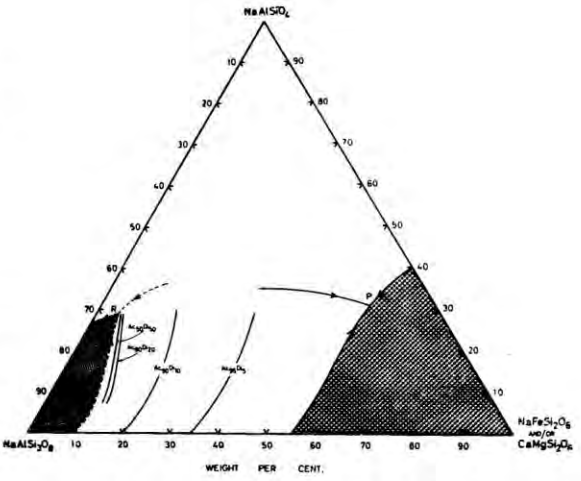

Fig. 3. Phase relations in the system $NaAlSi_3O_8$–$NaAlSiO_4$-$NaFeSi_2O_6$-$CaMgSi_2O_6$-H_2O at 1,000 Kg/cm² total pressure, showing the effects of addition of the diopside molecule to the albite-nepheline-acmite-H_2O system as represented by the compositional planes $Ac_{95}Di_5$, $Ac_{90}Di_{10}$, $Ac_{80}Di_{20}$ and $Ac_{50}Di_{50}$.

$NaAlSi_3O_8 - NaAlSiO_4 - NaFeSi_2O_6$ has been plotted. From this diagram it is obvious that a small amount of $CaMgSi_2O_6$ introduced into the system has a marked effect on the sizes of the phase volumes, particularly pyroxene. For example, the addition of 5 weight per cent $CaMgSi_2O_6$ represented by the $Ac_{95}Di_5$ plane, shifts the feldspar-pyroxene phase boundary approximately 20 weight per cent toward the $NaAlSiO_4$–$NaAlSi_3O_8$ join of the system. With subsequent increments of $CaMgSi_2O_6$ to the composition of the pyroxene in the $NaAlSi_3O_8$–$NaAlSiO_4$–$NaFeSi_2O_6$–H_2O system, movement of this boundary surface continues but by successively smaller amounts until in the Ab–Ne–$Ac_{50}Di_{50}$ plane the boundary curve separating the feldspar and pyroxene phase volumes is very close to that determined for the phase boundary in the $NaAlSi_3O_8$–$NaAlSiO_4$–$CaMgSi_2O_6$–H_2O system at the same pressure. This indicates that the composition of the pyroxene in this system has a profound effect in the size of the phase volumes produced at the liquidus surface. This system is discussed in greater detail by Nolan (1965).

PETROLOGICAL CONSIDERATIONS

In order to compare the experimental data obtained for this system with the compositions of alkaline and peralkaline undersaturated rocks, a procedure similar to that used by Tuttle and Bowen (1958) to compare rocks of the granite clan with phase relations in the saturated portion of Petrogeny's Residua System has been used. All rocks from Washington (1917), and some from more recent publications, containing 80 per cent or more of the normative constituents acmite + diopside, orthoclase + albite, and nepheline + kalsilite have been recalculated to 100 per cent and plotted as normative pyroxene, normative feldspar and normative feldspathoid. On Fig. 4, 142 plutonic rock compositions have been plotted and show two areas of concentration. The major concentration is located close to the alkali feldspar-feldspathoid join (at a composition close to the eutectic in the $NaAlSiO_4$–$NaAlSi_3O_8$–H_2O system) and extending into the ternary diagram as far as 15 weight per cent of the pyroxene component. The other concentration lies away from the major density of concentration at more pyroxene-rich compositions. Rocks constituting this second density area are the peralkaline undersaturated rocks, termed agpaites by Ussing (1912), who defined them as peralkaline nepheline syenites having a ratio of $\frac{Na_2O+K_2O}{Al_2O_3} > 1.2$ (expressed in molecular proportions). Fig. 5 shows a similar plot for 114 volcanic and hypabyssal alkaline undersaturated rocks. For these rocks, there is only one marked density of concentration again plotting close to the alkali feldspar-feldspathoid join.

A comparison of the normative compositions for plutonic, hypabyssal and volcanic undersaturated alkaline rocks (Figs. 4 and 5) with

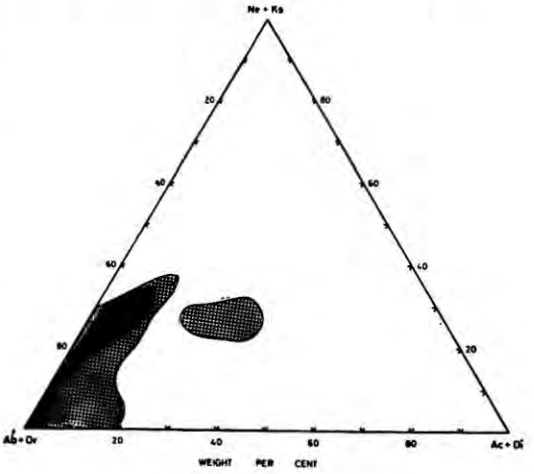

Fig. 4. Density distribution for 142 plutonic rocks containing 80 per cent or more normative Ne, Ks, Ab, Or, Ac, Di, recalculated to 100 per cent and plotted as Ne+Ks, Ab+Or, Ac+Di. The majority of the samples plot in the heavily shaded area.

the phase relations in the experimental system (Fig. 3) shows that the maximum density of rock compositions falls very close to the inferred low melting compositions in the $Ac_{50}Di_{50}$ and $Ac_{80}Di_{20}$ pyroxene compositional planes. Such planes more or less cover the average composition of alkali pyroxenes from rocks of the

nepheline syenite clan.* The data for pyroxene compositions used here has been very kindly provided by Miss Ruth Tyler, Kings' College, University of London. These relations suggest that many of these rocks have been formed by a process of crystal⇌liquid equilibria. The density distribution for the agpaitic rocks (Fig. 4) agrees very closely with the inferred low melting point in the $Ac_{95}Di_5$ pyroxene plane in the experimental system. This plane fulfils the average pyroxene compositional requirements for these rocks where the typical pyroxene is an aegirine. The formation of aegirine in these rocks is presumably a reflection of the high $\frac{Na_2O+K_2O}{Al_2O_3}$ ratio, causing the alkalies to combine with trivalent ions other than Al^{+3}.

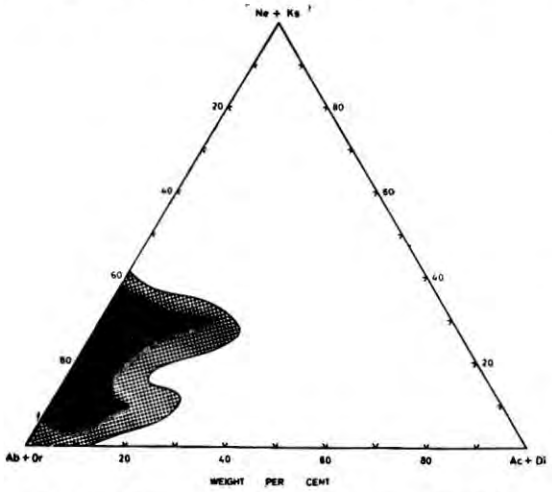

Fig. 5. Density distribution diagram for 144 hypabyssal and volcanic rocks containing 80 per cent or more normative Ne, Ks, Ab, Or, Ac, Di, recalculated to 100 per cent and plotted as Ne+Ks, Ab+Or, Ac+Di. The majority of the samples plot in the heavily shaded area.

The intensive parameters, fo_2 and P Total, have a similar effect as the pyroxene composition in making a closer approximation between the data of the synthetic systems and the natural assemblages. Examination of Fig. 2 indicates that there is a significant compositional change in the piercing point with increase in P Total from 1,000 Kg/cm² to 2,000 Kg/cm². The latter pressure represents a depth of approximately 8 Km, which probably conforms to the pressure-depth parameters usually associated with nepheline syenite intrusions. Increasing P Total even further would almost certainly give a closer approximation between the normative compositions and the data from the synthetic systems but this would not give a true picture for the natural occurence in regard to depth. It is likely that alkaline undersaturated rocks have formed at depths similar to those of granites. Luth, Jahns and Tuttle (1964) have shown that the most probable pressure conditions for the formation of granites is approximately 3 Kb (*i.e.* at 12 Km depth). It seems likely therefore that the pressures used in the present study are realistic insofar as the natural occurrence of rocks of this type are concerned.

Similarly an increase in the value of fo_2 would almost certainly increase the pyroxene phase volume, shifting the piercing point further towards the maximum density distribution of the normative compositions. However, since the mineral assemblages of most nepheline syenites indicate that they have crystallized within the magnetite stability field, an increse in fo_2 resulting from using a hematite-magnetite buffer assemblage (corresponding to the upper limit of the stability of magnetite) instead of a Ni-NiO assemblage would only extend the pyroxene phase volume by a small amount.

This study indicates that the composition of the pyroxene crystallizing is one of the dominent factors in the genesis of alkaline and peralkaline undersaturated rocks and that both P Total and fo_2 behave in a sympathetic manner but to a lesser extent.

ACKNOWLEDGEMENTS

Most of the early part of this work has been carried out at the University of Manchester

* To approximate more closely the composition of natural pyroxenes occurring in alkaline undersaturated rocks, the effect of adding the hedenbergite ($CaFeSi_2O_6$) in addition to dipside and acmite should be considered. This investigation is currently being undertaken by one of the authors (J. Nolan).

under the supervision of Professor W. S. MacKenzie. Some of the work has also been done by one of the authers (J. Nolan) in Professor Hans Eugster's laboratory at Johns Hopkins University, Baltimore. The authors gratefully acknowledge help and encouragement from both Professors MacKenzie and Eugster. Dr. Ruth Tyler, Kings College, University of London, kindly supplied us with unpublished chemical analyses of pyroxenes from alkaline rocks. Financial support for this work was provided in the form of Ontario Research Foundation Scholarships to A. D. Edgar and Department of Scientific and Industrial Research grants to J. Nolan for which grateful acknowledgement is here by made.

REFERENCES

BOWEN, N. L. (1945) Phase equilibria bearing on the origin and differentiation of alkaline rocks : *Amer. Jour. Sci.*, Daly Vol., p. 75.

EDGAR, A. D. (1964) Phase equilibrium relations in the system $CaMgSi_2O_6$ (diopside)-$NaAlSiO_4$ (nepheline)-$NaAlSi_3O_8$ (albite-H_2O at 1,000 Kg/cm^2 water vapor pressure : *Am. Mineral*, Vol. 49, p. 573.

EUGSTER, H. P. AND WONES, P. R. (1962) Stability relations of the ferruginous biotite, annite : *Jour. Petr.*, Vol. 3, p. 82.

GORANSON, R. W. (1931) The solubility of water in granite magmas : *Amer. Jour. Sci.*, Vol. 22, p. 481.

NOLAN, J. (1965) Melting relations in the system albite-nepheline-acmite-diopside-water and their bearing on the genesis of alkaline undersaturated rocks : *Trans. Roy. Soc. Edin.*, (in press).

———AND EDGAR, A. D. (1963) An X-ray investigation of synthetic pyroxenes in the system acmite-diopside-water at 1,000 Kg/cm^2 water vapour pressure : *Min. Mag.*, Vol. 33, p. 625.

MUAN, A. (1957) Phase equilibrium relationships at liquidus temperatures in the system FeO-Fe_2O_3-Al_2O_3-SiO_2 : *Jour. Amer. Ceram. Soc.*, Vol. 40, p. 420.

ROY, K. (1256) Aids in hydrothermal experimentation : II. methods of making mixtures for both " dry " and " wet " phase equilibrium studies : *Jour. Amer. Ceram. Soc.*, Vol. 39, p. 145.

SCHAIRER, J. F. AND YODER, H. S. (1960) The nature of residual liquids from crystallization, with data on the system nepheline-diopside-silica : *Amer. Jour. Sci.*, Vol. 258 A, p. 273.

TUTTLE, O. F. (1649) Two pressure vessels for silicate-water studies *Geol. Soc. Amer. Bull.*, Vol. 60, p. 1727.

———AND BOWEN, N. L. (1958) Origin of granite in the list of experimental studies in the system $NaAlSi_3O_8$-$KAlSi_3O_8$-SiO_2-H_2O : *Geol. Soc. Amer. Memoir.*, Vol. 74, p. 153.

USSING, N. V. (1912) Geology of the country around Julianehaab, Greenland : *Medd. ϕm Gronland*, Vol. 38, p. 143.

WASHINGTON, H. S. (1917) Chemical analyses of igneous rocks : *U.S. Geol. Surv.*, Prof. Paper, No. 99, p. 1201.

MINERALOGICAL SOCIETY OF INDIA, IMA VOLUME, 1966
INTERNATIONAL MINERALOGICAL ASSOCIATION, PAPERS, FOURTH GENERAL MEETING

HYDROGEN-BONDING SITE DISTRIBUTION ON LAYER SILICATE SURFACES

W. D. JOHNS AND P. K. SEN GUPTA
Department of Earth Sciences, Washington University, St. Louis, U. S. A.

ABSTRACT

Structural configurations based on ionic models have been used with considerable success to explain physical and chemical properties of silicates. Although it is known that Si–O bonds have considerable, and perhaps dominant covalent character, the full implications of this have not been fully explored. Fyfe has most recently emphasized the tetrahedral spatial distribution of bonding orbitals in oxygen, overlapping with hybridized sp^3 orbitals in silicon.

Examination of the resulting tetrahedral distribution of electrons in the Sl–O assemblage in layer silicates, shows that the lone pair oxygen orbitals are distribed with hexagonal symmetry about the hexagonal holes in the oxygen surface of the idealized layer silicate. These lone pair electrons are available for H-bonding in a manner analogous to H-bonding in water.

The adsorption of certain organic species on layer silicate surfaces takes place in a manner compatible with the spatial distribution of the oxygen sp^3 tetrahedral configuration. The adsorbed organic molecule will often assume an orientation on the silicate surface so that the R-H....O bond approaches linearity.

Silicate structural configurations based on ionic models have been used with considerable success to explain physical and chemical properties of silicates. An example has been the general applicability of the so-called Pauling (1929) rules, based exclusively on the notion of an ionic model of bonding. Although it is known that the silicon-oxygen bond has considerable, and probably dominant covalent character, the implications have not been fully explored. It was Coulson (1951), who suggested that covalent structures can be inferred whenever tetrahedral coordination is observed, and that although the more electronegative element may carry a small excess of elcctrons, and impart ionic character to the bond, directional valence forces determine the stereochemistry if the degree of covalency is sufficiently large. This results essentially from the tetrahedral hybridization of sp^3 orbitals. More recently Fyfe (1964) has stressed the importance and universality of hybridization in inogranic structures.

In a very important paper, Grim and Bradley (1955) have taken up this theme as regards the structure of the layer silicates. In particular they noted that the Si–O covalent bonding induces tetrahedral disposition of electron density maxima about each of the oxygen atoms constituting the external hexagonal oxygen layer of the Si–O network. Two of these maxima are directed toward the two neighboring silicon atoms, the other two induced maxima assume the other two tetrahedral positions. Another important aspect of their thesis involves extension to the oxygen atoms comprising octahedral coordination. Fig. 1 schematically summarizes this covalent model. In Fig. 1 (a) the tetrahedral distribution of electrons about each silicon

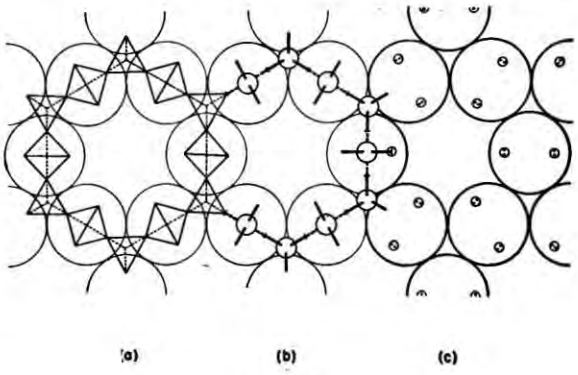

Fig. 1

a) Tetrahedral distribution of electrons about each oxygen and silicon atom in the surface layers of sheet silicates ;

(b) Spatial distribution of inferred sp^3 orbitals ;

(c) Resulting sites of maximum electron density and their distribution.

and oxygen atom is depicted; in Fig. 1 (b) the spatial disposition of inferred sp^3 orbitals is shown; in Fig. 1 (c) are indicated the resulting sites of maximum electron density and their distribution over the external oxygen surface. In the idealized layer silicate configuration these sites are disposed in a hexagonal array about the "holes" in the hexagonal oxygen layer. For a covalent model these sites would correspond to lone pair orbitals, each occupied by two electrons.

It could be anticipated, therefore, that these sites and their distribution would play an important role in the surface chemistry of layer silicates involving adsorption of polar groups or molecules brought into juxtaposition to the surface. It would be expected that hydrogen bridging between surface oxygens and electronegative atoms could take place, utilizing the lone pair electrons in a manner analogous to hydrogen bonding between water molecules. Demonstration of such hydrogen bonding, even more specifically, positive indication of hydrogen bonds directed so as to preserve the tetrahedral angle of the inferred oxygen sp^3 orbitals, would tend to further substantiate the covalent model described by Grim and Bradley (1955).

Several types of situations are known which provide the opportunity to examine this postulate. If a layer of (OH) ions were superimposed on the external oxygen layer of a silicate sheet, it could be expected that at least a portion of the (OH) groups would be oriented with the O-H bond inclined, directed toward the tetrahedral orbitals of the oxygen substrate. The minerals of the kaolinite group are illustrative of this situation. In all of the kaolin minerals, adjacent layers are superimposed so that oxygen atoms and (OH) groups of contiguous layers are paired (Brindley, 1951). It is significant that each (OH) group is superimposed on the oxygen substrate exactly at those sites indicated previously in Fig. 1 (c). Although OH.....O bonding between kaolinite layers has been postulated for some time, it is only recently that attempts have been made to ascertain the orientation of the (OH) bond relative to the contiguous oxygen substrate. Serratosa *et al.* (1963), Wolff (1963), and more recently Farmer (1964), utilizing infra-red adsorption spectroscopy, have attempted to do this. These studies have resulted in conflicting interpretations and thus are not definitive in this respect. A unique solution awaits application of a polarized infra-red source.

Another approach is to determine the orientation of polar molecules adsorbed on the oxygen substrate, directing attention to the directional orientation of potential hydrogen bonds formed between oxygen atoms of the substrate and electronegative atoms in the adsorbed molecule. In explaining the interlamellar imbibition of simple alcohols and neutral amines by montmorillonite, Emerson (1957) proposed that OH.....O bonds are formed between the organic molecules and oxygen atoms of the montmorillonite substrate. He assumed that the OH.....O must be linear, and more specifically, directed to form at the tetrahedral angle dictated by the oxygen sp^3 orbital. This imposed a specific orientation on the entire alcohol or amine molecule and enabled calculation of interlayer separations, which showed good agreement with observed values. More recently Brindley and Ray (1964) in studying adsorption of long chain primary alcohols by montmorillonite, accepted Emerson's model for OH.....O bonding and could thus infer molecular orientations consistent with their experimental data. In each of these instances a tetrahedrally disposed linear OH...O bond was assumed, a molecular orientation inferred, and then confirmed experimentally.

The authors wish to present some additional data derived by first determining the orientation of the intercalated organic molecule and then, indirectly, the pertinent hydrogen bond orientation. These data result from a recent study of the structures of alkyl-ammonium vermiculites. Butyl–, hexyl–, octyl–, decyl–, and dodecyl–ammonium vermiculites were prepared by

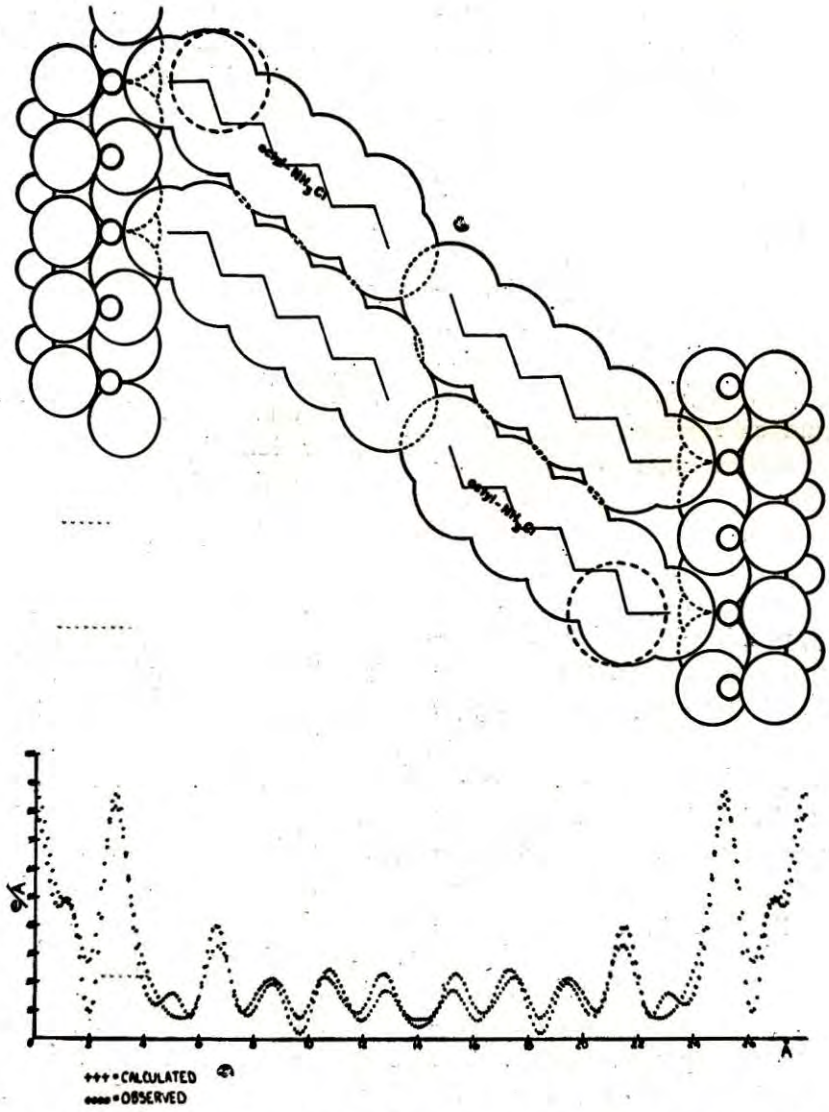

Fig. 2. Structure of octyl-ammonium vermiculite complex with composition $[Mg_6Al_2Si_6O_{20}(OH)_4]=[^+H_3N\text{-octyl}]_2$. 2 octyl-NH_3Cl

replacing the exchangeable interlayer inorganic cations by treatment with aqueous solutions of the appropriate alkyl–amine hydrochlorides. Although similar examples could be selected for illustration from any of the alkyl amines mentioned, octyl and hexyl systems will be referred to here. Three types of complexes were formed as exemplified by the following formulations:

(1) $[Mg_6Al_2Si_6O_{20}(OH)_4] = [^+H_3N\text{–octyl}]_2 \cdot 2\ \text{octyl–}NH_3Cl$

(2) $[Mg_6Al_2Si_6O_{20}(OH)_4] = [^+H_3N\text{–octyl}]_2 \cdot 1\ \text{alkyl–}NH_3Cl$

(3) $[Mg_6Al_2Si_6O_{20}(OH)_4] = [^+H_3N\text{–alkyl}]_2$

Complex (1) is formed when vermiculite crystals are immersed in an excess of octylamine hydrochloride. Stoichiometric exchange takes place between inorganic and organic cations, and in addition, two moles per formula unit of neutral octylamine hydrochloride are adsorbed. A 28.13Å (001) periodicity results. X-ray structural studies indicate the organic molecular orientation shown in Fig. 2. Electron density plots along [001], based on calculated and observed F's are also given and indicate the essential correctness of the proposed model. Of particular importance here is the orientation of the octyl-ammonium ions. The aliphatic chains are inclined at 54.7°. Thus the C–N bond is oriented perpendicular to the oxygen surface of the silicate sheet. The $-NH_3^+$ group penetrates somewhat into the hexagonal opening in the oxygen substrate.

When this complexed vermiculite crystal was washed with water to remove the adsorbed amine hydrochloride, a stage was reached when one-half of the hydrochloride was removed, and a collapsed phase with perfect 24.00Å (001) periodicity was produced, with a composition expressed by (2) above. Fig. 3 shows schematically the structure of this complex. Calculated and observed electron density plots are also included. It is important to note that the octyl-ammonium ions maintain their previous orientation, even though the remaining adsorbed neutral octyl-amine hydrochloride molecules have changed their orientation, lying with their aliphatic chains parallel to and in contact with the silicate substrate. The octyl-ammonium ions now interfinger a bit.

Further washing with water effectively removes all of the adsorbed neutral amine hydrochloride, allowing the alkyl ammonium ions to interpenetrate completely as shown in Fig. 4. The original chain orientation is still preserved, with the N–C bond again perpendicular to the (001) silicate surface. The complex depicted is actually the hexyl-ammonium complex, but identical orientations were obtained with all other species. Calculated and observed electron density plots along [001] are included as before. The details of these structural determinations are the subject of a paper to be published elsewhere.

The most significant point of comparison of these three complexes is the persistent orientation of the alkyl ammonium ions in spite of considerable variation in content and orientation of adsorbed neutral species. It is significant to inquire as to the factors controlling this orientation. The uniqueness of this orientation stems from maintenance of the perpendicular orientation of the C-N bond of the alkyl ammonium ion. It is further impressive that with this orientation, the three hydrogen atoms of the $-NH_3^+$ group are disposed tetrahedrally, constituting the corners of the base of the nitrogen coordination tetrahedron. In these positions they are capable of forming essentially linear bridges between the nitrogen of the organic molecule and the oxygen of the silicate surface. It appears feasible to conclude that triads of –N–H.....O bonds do indeed form at alternate sites in the hexagonal array of potential sites about the hexagonal "holes" in the oxygen surface, determining and stabilizing the observed organic molecular orientation.

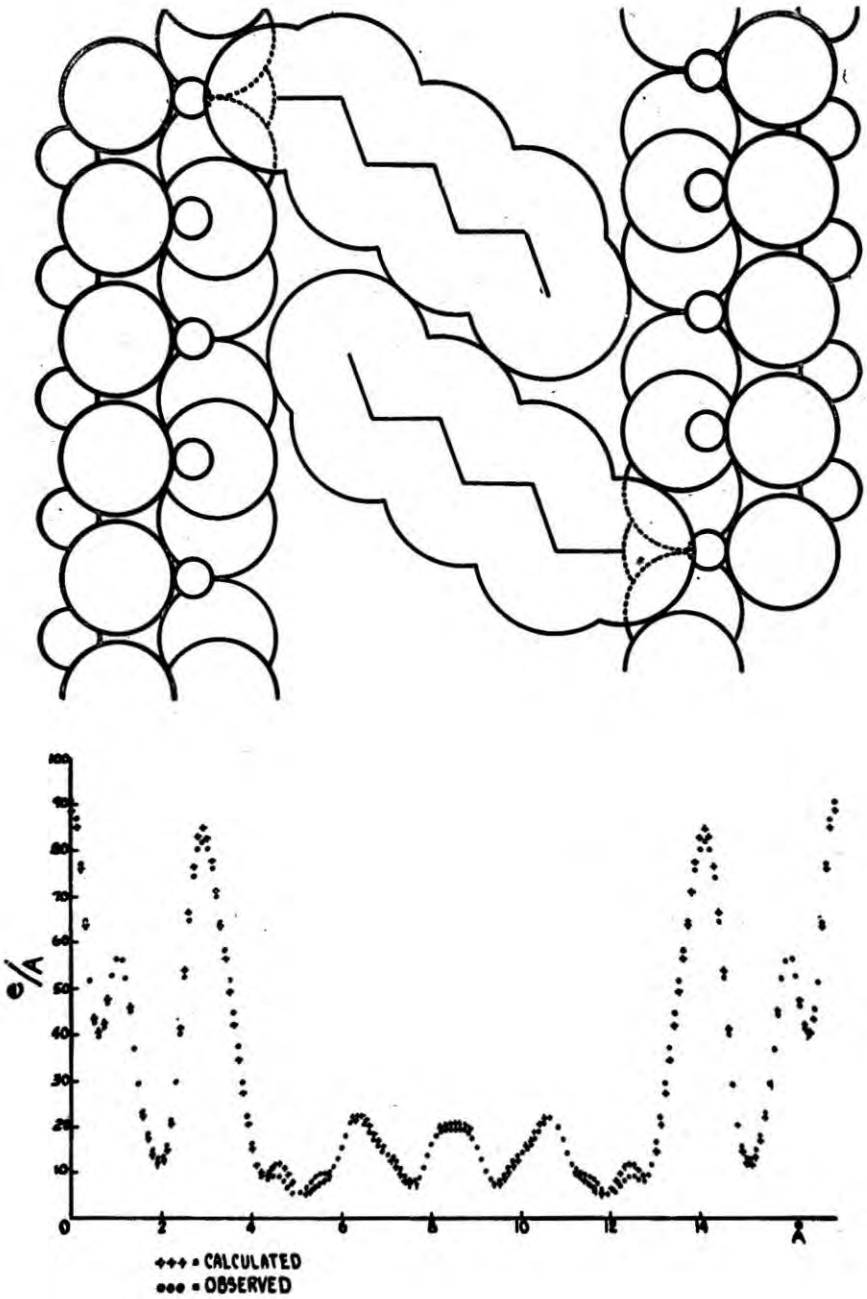

Fig. 3. Structure of octyl–ammonium vermiculite complex with composition $[Mg_6Al_2Si_6O_{20}(OH)_4]=[^+H_3N\text{-octyl}]_2 \cdot 1$ octyl-NH_3Cl

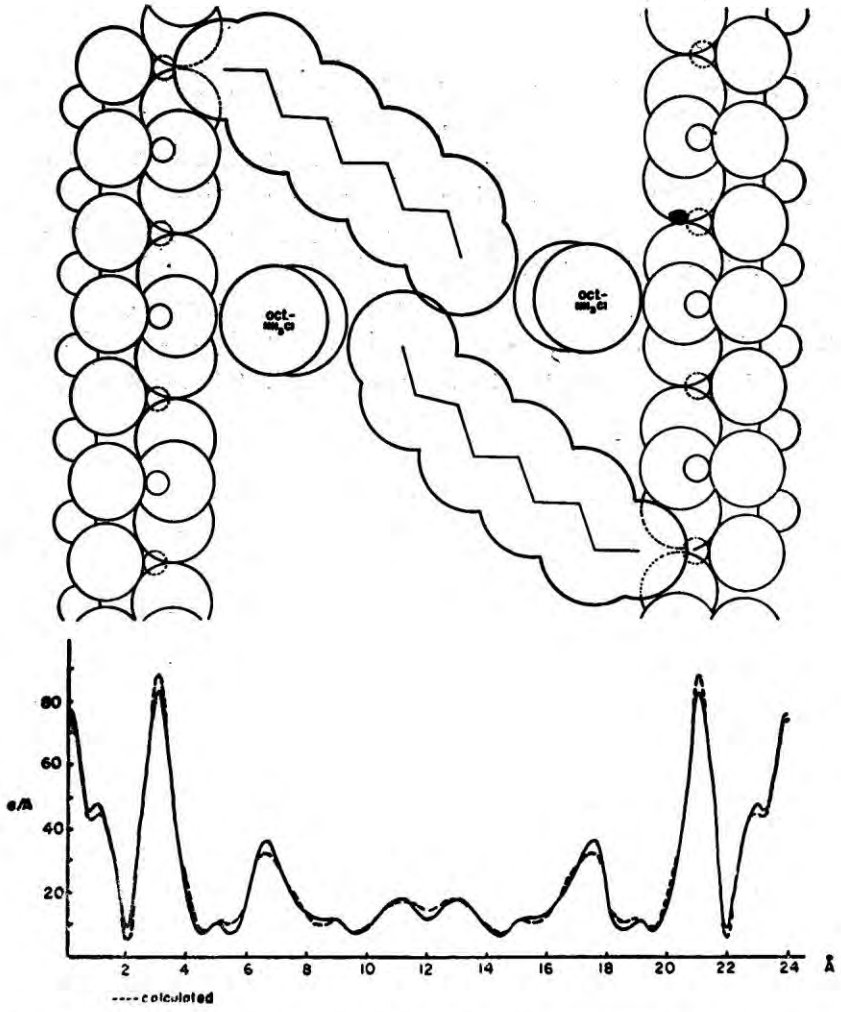

Fig. 4. Structure of hexyl-ammonium vermiculite complex with composition $[Mg_6Al_2Si_6O_{20}(OH)_4]=[^+H_3N\text{-hexyl}]_2$

This and evidence cited earlier lead us to conclude that the covalent model described by Grim and Bradley, and its relation to potential H-bonding site distribution, provide a generally useful structural principle, which may serve as a guide in studies of the surface chemistry of layer silicates in general.

ACKNOWLEDGEMENTS

This study was supported by National Science Foundation Grant No. GP 2719.

REFERENCES

BRINDLEY, G. W. (1951) *X-ray Identification and Crystal Structures of Clay Minerals*, Mineralogical Society, London.

——AND RAY, S. (1964) *Am. Mineral.* Vol. 49, pp. 106–115.

COULSON, C. A. (1951) *Valence*, Oxford Univ. Press, London.

EMERSON, W. W. (1957) *Nature*, Vol. 180, pp. 48–49.

FARMER, V. C. (1964) *Science*, Vol. 145, pp. 1189–1190.

FYFE, W. S. (1964) *Geochemistry of Solids*, McGraw-Hill, N. Y.

GRIM, R. E. & BRADLEY, W. F. (1955) *Geol. Rundschau*, Vol. 43. pp. 469–474.

PAULING, L. (1929) *Jour. Amer. Chem. Soc.*, Vol. 51. pp. 1010–1026.

SERRATOSA, J. M., HIDALGO, A. AND VINAS, J. M. (1963) *International Clay Conference*, Vol. 1, pp. 17–26.

WOLFF, R. G. (1963) *Am. Mineral*, Vol. 48, pp. 390–399.

MINERALOGICAL SOCIETY OF INDIA, IMA VOLUME, 1966
INTERNATIONAL MINERALOGICAL ASSOCIATION, PAPERS, FOURTH GENERAL MEETING

CLEAVAGE FEATURES IN A DOMAIN (TWIN) CRYSTAL*

J. L. AMOROS
School of Technology, Southern Illinois University, U.S.A.

ABSTRACT

The peculiarities of growth of TGS crystals are studied by the drop technique and the main growth velocities have been determined. By slow etching using as etching reactant alcohol-water, it is possible to delineate domains, and mosaic structures. The mechanism of solution proceeding layer by layer is demonstrated. Cleavage (fractographic) technique shows domain substructure in TGS single crystals grown above the Curie point. Microfractures are nucleated in relation to domain walls. Hackled structures are examined in (010) fresh cleavage surfaces. Dendritic formations are shown in the interior of TGS crystals.

In the course of a research on the growth of crystals, we have studied synthetic ferroelectric crystals. Some of the features observed are of general interest and therefore I take the opportunity to present some results at the IMA meeting; however, the substance is far from being a mineral. I shall refer in what follows to triglycine sulfate, a well-known ferroelectric crystal.

The crystals of the ferroelectric triglycine sulfate (TGS) belong to the space group $P2_1$, changing into $P2_1/m$ above the Curie point 47°C. Mathias *et al.* (1957), Wood and Holden (1957), Hoshino *et al.* (1957) and (1959). Crystals grown below the Curie point do not show morphological development denoting the lack of the plane of symmetry *m* perpendicular to the polar axis besides the non complete equivalence of the development of mirror symmetric faces. This effect is difficult to measure and it could also be explained by assuming influence of the method of growing the crystals.

Crystals grown by the Holden technique above the Curie point, namely 55°C, showed an overall velocity of growth much higher than the corresponding to crystals grown below the Curie point. These crystals show starvation surfaces formed by inclusions of different shape. They are irregular in shape when dissolution effect has been intense, but generally the starvation surface is formed by drop like inclusions alternating with negative crystals. Many times it is possible to observe starvation lines when dissolution has affected only the edges of the growing crystal. Crystals grown above the Curie point were without starvation surfaces and much clearer, and they persisted so at room temperature after a slow cooling in an oven. The only thing that differenciates both kinds of crystals is the easiness of the natural (010) cleavage of the crystals grown above the Curie point, in accordance with the dramatic change in bonding along (010) as detected from thermal expansion studies Enhkova *et al.* (1960).

VELOCITIES OF GROWTH

The velocities of growth of important faces of TGS crystals have been determined by the method of the drop Amoros *et al.* (1963). According to this method, a small drop of about 0.1–0.2 cc. of slightly undersaturated solution is allowed to evaporate on a microscope slide. The sequence of events is studied by taking photographs at constant intervals of time. We have used a Wild petrographic microscope, equipped with Leica photographic camera. In our experimental conditions, the photographs were taken at intervals of two minutes beginning after the first nuclei appeared. All photographs

* The research reported in this document has been sponsored in part by Air Force Office of Scientific Research, OAR under Grant No. AF EOAR 62–92 through the European Office, Aerospace Research, United States Air Force.

were enlarged to have a 400 magnification, copy over which the measurements were made. As it was not possible to use a reference point inside the growing crystals, we measured the distance between pairs of parallel faces. Sets of 20 crystals were measured.

Growth in a drop is a highly competitive phenomenon. Accordingly the growth velocity of a given face changes with time. The curves of Fig. 1 are typical. The upper part of the curve shows an anomaly due to the effect of the reduction of the volume of the drop in the last moments of the growth. In this moment the volume of the liquid drop is too small to allow a free diffusion and the growth of the crystals is accordingly slowed down. The measured velocities of growth (at room temperature) in the straight part of the curve are the following:

$$V_{001} = 0.002_4 \mu \text{seg}^{-1}$$

$$V_{110} = 0.067_6 \mu \text{seg}^{-1}$$

Most of the crystals are formed by nuclei that rest on (001). The result are diamond section platlets, limited by (110). Other crystals appear on some face of the (110) or (101) prism, this late case being the rarest. The crystals (Fig. 2) grow well although the effect of the base (diffusion-less on the slide layer) is pronounced, producing defects or even cracks in the growing crystals. Due to the competitive effect that appears at the end of the growth processes the growth velocity is altered (Fig. 1b, c) and high index faces appear in the growing crystals. Accordingly the final morphology of the crystals grown by the drop technique is not the expected from the theory of equilibrium form. This neighboring effect is also shown in the different velocity of growth of equivalent pairs of faces, as shown in Fig. 1c. The two curves correspond to pairs of faces of (110) prism of the same crystal. The result is an assymmetric crystal. A–A marks a change in slope, the moment when the high indices faces appear.

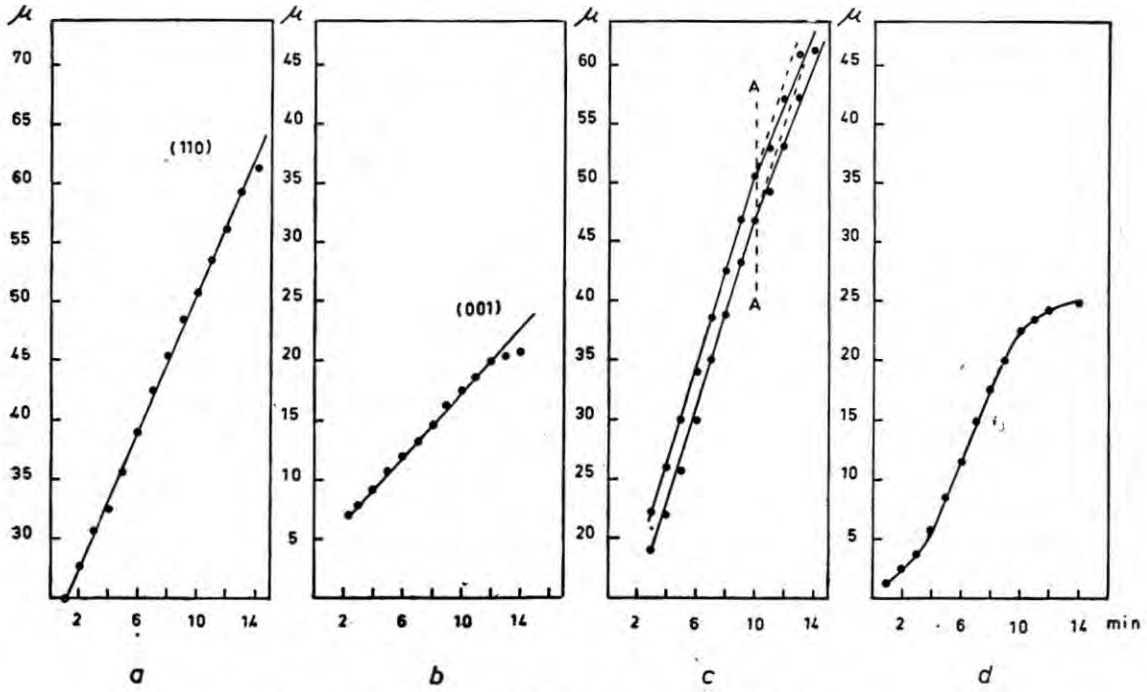

Fig. 1. Velocities of growth of different faces of TGS.

(a) face (110),
(b) face (001),
(c) effect of neighbors,
(d) curve corresponding to long, odd shaped crystals.

Besides the common crystals of " diamond " habit, here and there also appear long, pin like crystals, due to an assymmetric development of the faces (110) and ($1\bar{1}0$). Fig. 2 shows both

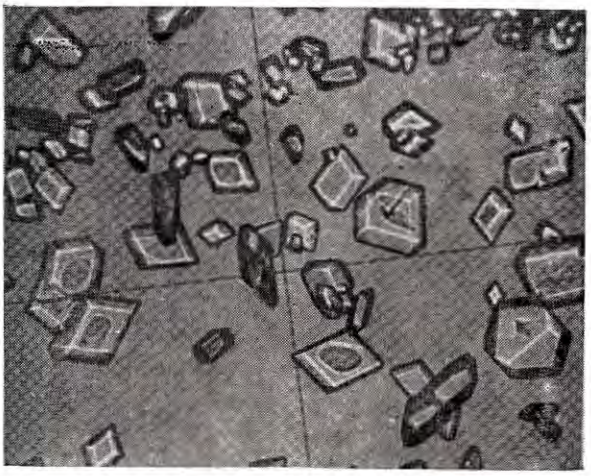

(a)

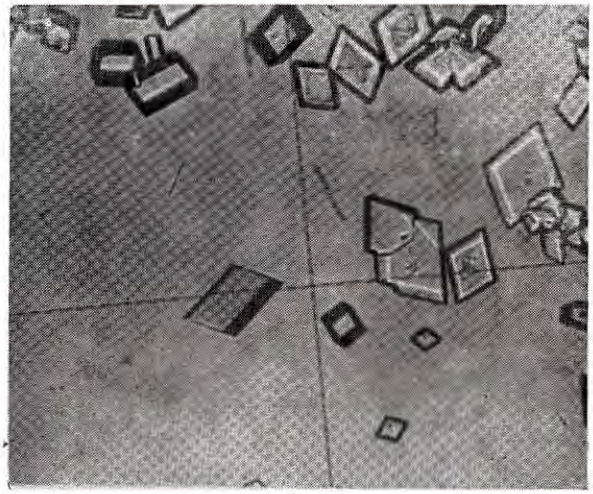

(b)

Fig. 2. Growth of TGS crystals in a drop.
In *a* the crystals develop faces of high indices.
In *b* some anomalous crystals appear.
All photographs, same magnification, (x400).

kinds of crystals. The growth of the long crystals is anomalously large along a given direction. This growth is characterized by a long hysteresis, up to the moment in which a critical supersaturation is attained. In this movement the curve changes drastically its slope. Once started, the growth proceeds rapidly stopping shortly afterward. This anomalous behavior is only shown by a few crystals that will show in its morphology the non presence of the mirror plane. Perhaps the extreme case of this kind of growth should be the formation of whiskers, but we have not yet observed them in crystallization from water solutions.

SOLUTION PITS

Toyoda (1960) showed that a slow etching with alcohol-water produces etch pits that correspond to the emergence points of dislocations. The pits on (010) faces are dove-shaped and those on (001) and (110) faces have trapezoidal bases. We have observed the same things. Besides this when a fresh (010) cleaved surface is allowed to slowly dissolve, there appears pits with a flat bottom (Fig. 3), showing always a prominence in one side, around which solution proceeds. The aspect of such formations is very similar, but the reverse, of the growth step produced by a Frank-Read generator. As the solution proceeds the flat bottom extends and eventually a new pit developes. Therefore, the dissolution of a TGS crystal proceeds layer by layer instead of deeping along dislocations. A similar mechanism has been found in hematites by Sunagawa (1962). Some of these pits have the appearance of the first step of helix. A helix was observed inside the crystal in a starvation surface, suggesting a similar process where the growth was modified by producing a starvation surface (Fig. 4).

MOSAIC AND DOMAIN STRUCTURES

A weak attack shows up structures than can be seen in Fig. 5, and that can be attributed to the delineation of a mosaic structure. Each domain shows a bright peak that probably corresponds to the emergency of a dislocation. Some time ago similar structures were observed in zink single crystals by Rutter and Chalmers (1953).

Important structures are shown when the crystal is cleaved, mainly in crystals obtained at temperatures above the Curie point. Fig. 6, shows the results. The crystal in this case is

formed by microdomains whose walls are perpendicular to [201]. The size of such domains varies from the center to the outside of the crystal. A scheme of the observed distribution is given in Fig. 7.

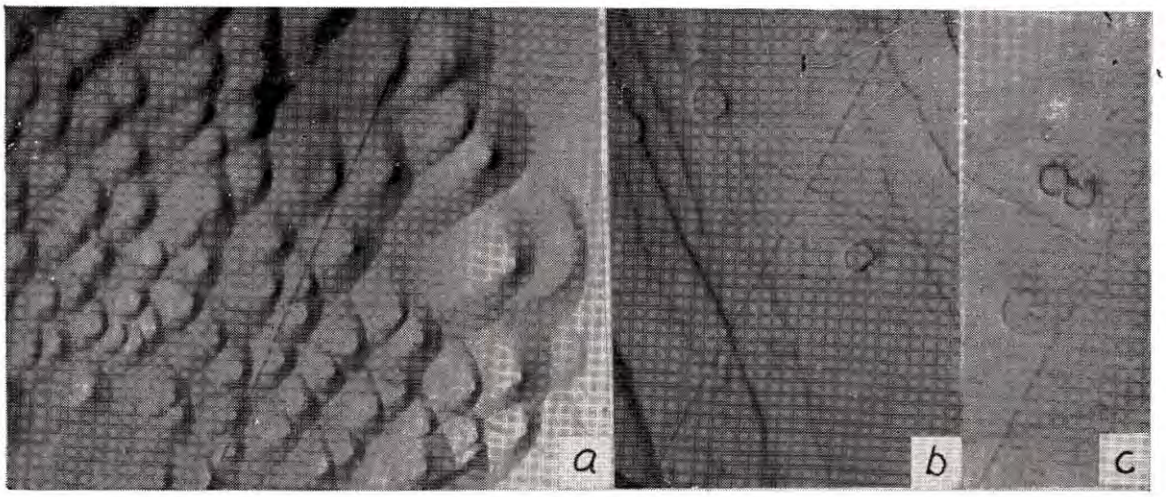

Fig. 3. Effect of etching

(a) Etch pits on (110) (b), (c) Solution pits on (010)

According to this scheme, the crystal presents small domains in the center; the walls of such domains being perfectly to almost perfectly parallel. The domains are long slabs whose ends are wedge shaped, and the thickness is almost constant, of about one μ. This kind of structure is characteristic of the region C. Region A presents domains of a more irregular shape. Although the walls, no longer straight, are still almost perpendicular to [201]. The thickness of the domains is now of 30–50 μ, and they are wedge shaped. The intermediate zone B contains domains of variable but small thickness, the walls of the thin domains being almost parallel. It is curious that the external part of the crystal, namely the region D does not present regular domains (or are not shown by the present technique).

Fig. 4. Helix inside the crystal

Fig. 5. Delineation of domains by weak attack

Some features similar to those just described are also found in single crystals obtained below the Curie temperature. In this case, the presence of domains is sporadic and never show the crystals a structure similar to the Fig. 6. Chynoweth and Feldmann (1960).

If the described structures represent ferroelectric domains they should be sensitive to an electric field. Experiments have shown conclusively that the formation disappears when the crystal is cleaved after being subject to a sufficiently strong electric field (~300 volts cm^{-1}). Therefore the simple technique of cleavage of a crystal can show so important a detail as the presence of ferroelectric domains.

FRACTURE EFFECTS

The cleaved surfaces show many features, besides the delineation of domains as previously said, that can be of interest in a study of fracture effects. When the crystal is cleaved, a

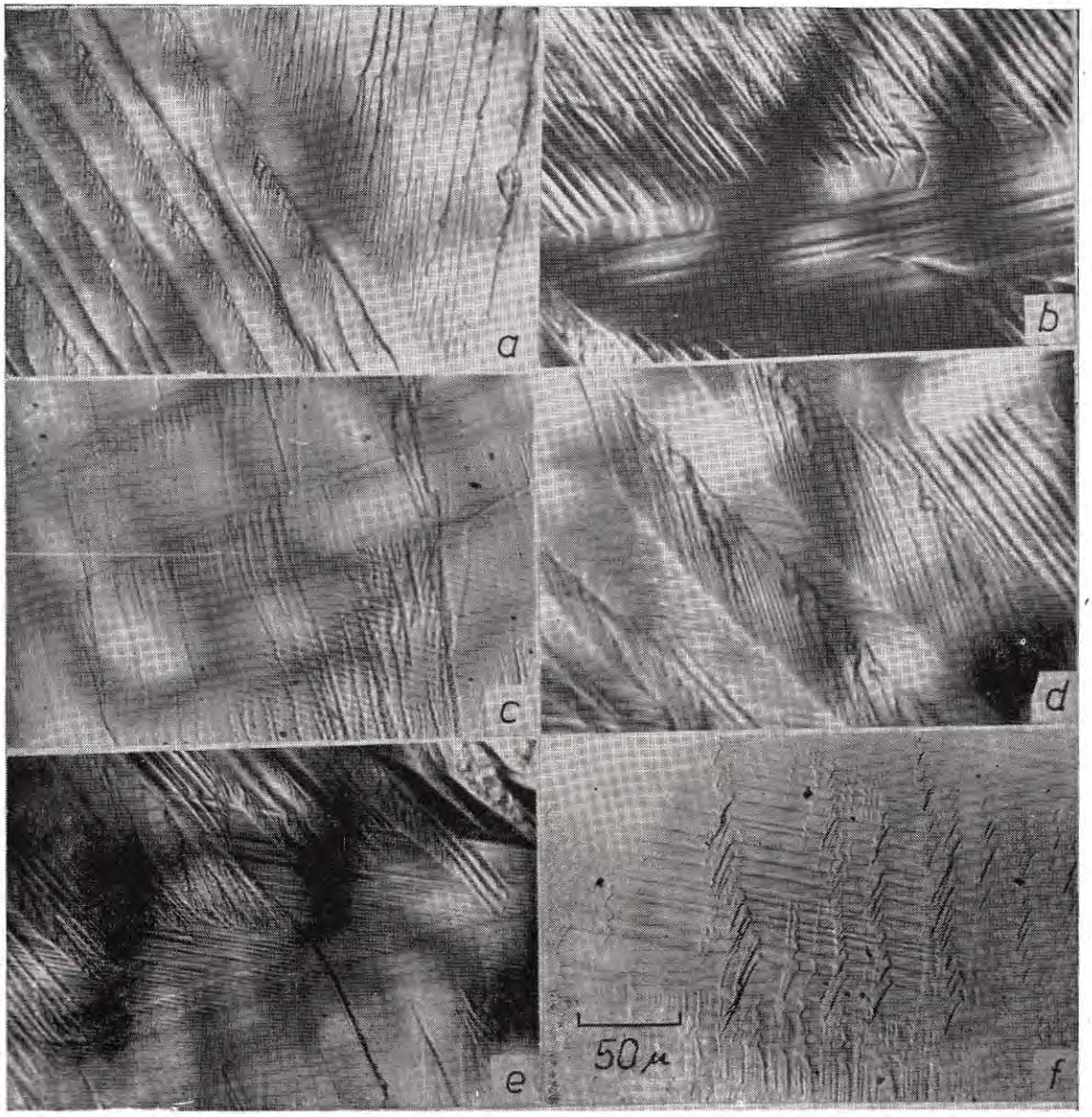

Fig. 6. Delineation of microdomains by plastic deformation due to cleavage along (010).

strong mechanical deformation is propagated along the crystal producing its break along a crystallographic plane. Many secondary effects are expected: plastic deformation, slip and microcracks nucleation, etc. The cleaved surfaces of TGS show many interesting details.

Microcrack nucleation is rare in TGS. However, Fig. 6 f shows a set of such microcracks combined with a domain substructure. Here can be easily seen the anisotropic microcrack extension along 001. The most detailed investigation of the growth of surface microcracks is given in a series of papers by Clarke and co-workers (1960), and by Stokes and Li (1962). The experiments have shown unequivocally that microcracks are extended by plastic flow. Therefore in TGS a similar behavior is expected and the main factor responsible for extending the crack is the local plastic constraint that each microcrack exerts. The constraints is a maximum in the surface experiencing the greatest translational offset due to slip. It is expected that slip is to be produced inside the domains, and accordingly microcracks nucleate almost at right angles with such walls. The extension occurs anisotropically because it is much easier for a crack to propagate parallel to a slip band than to cut across it. Further study of this point can be of interest for the knowledge of the elastic and plastic behaviours of such important crystals as ferroelectrics.

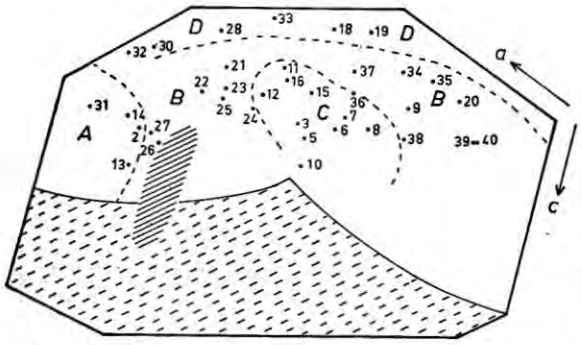

Fig. 7. Domain structure in a crystal grown above the Curie point. The points refer to the positions studied. Shadowed region: seed. Broken lined: broken part of the crystal.
(a) subparallel domains of big, variable thickness,
(b) parallel domains of variable thickness,
(c) parallel domains of constant thickness,
(d) no domains.

The fractographic study of the cleavage surface is of interest because it gives information related to the "secondary" structure of the crystal. Zapffe and Worden (1949) have shown that the technique is very useful. We have modified the technique in the sense that an almost flat beam is allowed to light the surface and the small accidents in it are in this way easily seen. A series of such photographs in Fig. 8. A1 correspond to a fresh (010) cleavage and belong to the "hackle" structures, following Zapffe's terminology, that is patterns determined by the nature of the stress. However, the "hackle" structures are not free of the influence of the presence of substructured details within the crystal. In fact are the results of the interaction stress-crystal substructure.

Fig. 8 shows typical "hackle" structures. No pronounced directional weaknesses within the crystal have played a role in determining the cleavage path (besides the (010) face). The radial distribution of fracture lines are according with the direction of propagation of the fracture from the percussion center.

The cleavage in TGS is good, and the (010) surface is neat far from the percussion center. However, in some cases small portions of the upper layer of the crystal remain sticked to the lower part. This reflects the idea of strong bonding across [010] in the ferroelectric phase.

The breaking of a layer can be a conspicous work and the marks of such work is often left on the cleavage surface. Fig. 8 shows a series of steps, in which after sliding across, the stress breaks the upper layer. The structure reveals the presence of other slip system in TGS crystals. Sometimes the pattern is more complicated due to the existence of some domains as revealed by the twisting of the stress lines across the surface.

DENDRITIC STRUCTURES

In Fig. 9, structures appear that are no relationship to stress conformations. These are

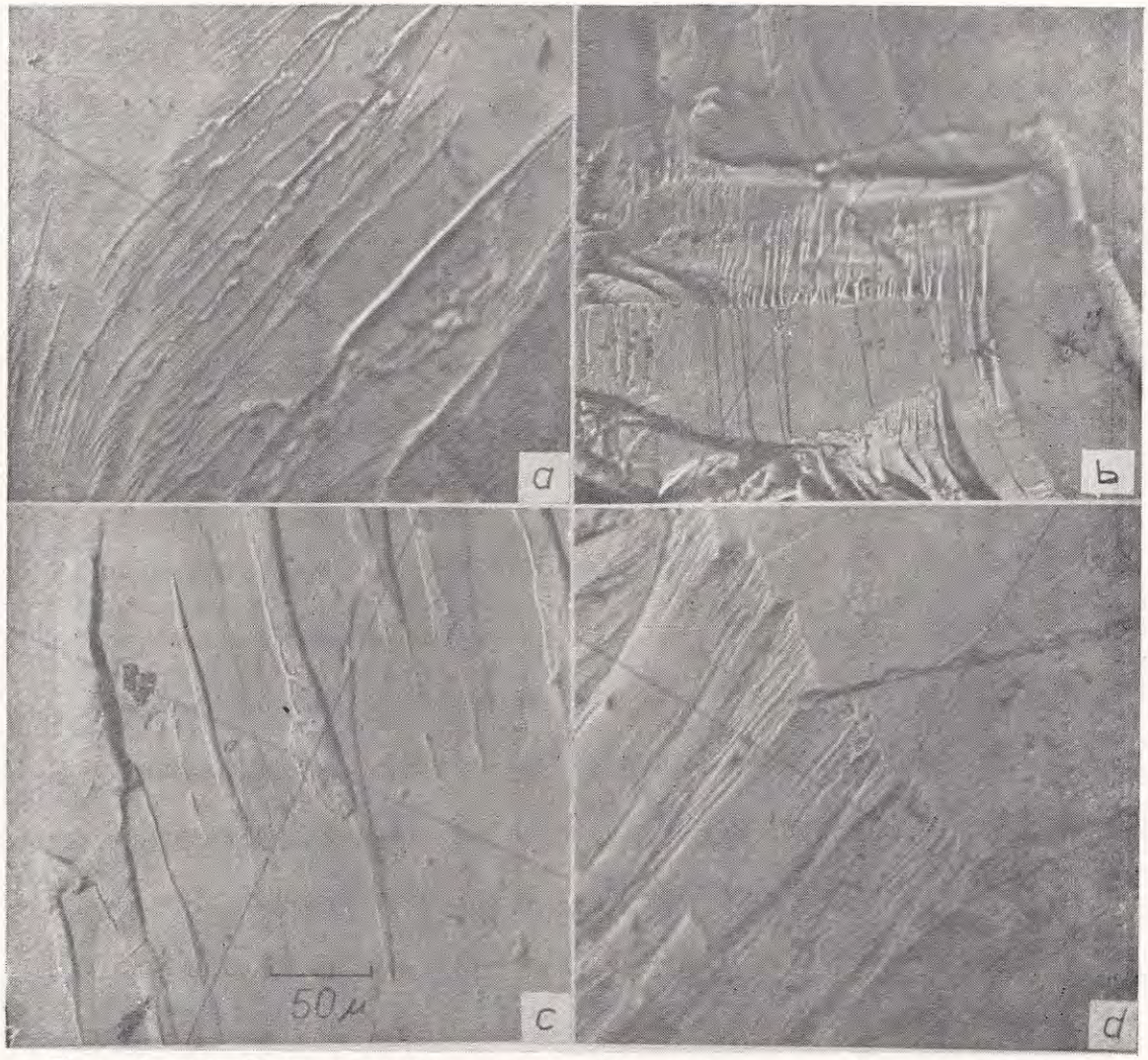

Fig. 8. Fractographic features of TGS crystal grown below the Curie point. Cleavage surface (010). (All photographs, same magnification).

pronounced dendritic forms occuring either in clear area between rows of hackle markings or in areas with very clear microdomains. Such structures might express growth imperfection and were first found in crystals of ammonium dihydrogen phosphate by Zapffe and Worden (1949).

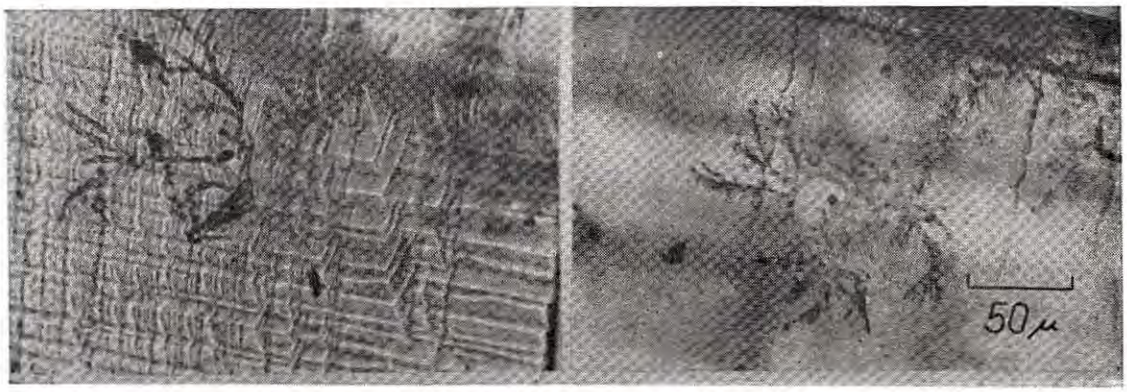

Fig. 9. Fractograph revealing a dendritic structure on the cleavage facet.

We believe that the dendritic formation existed before cleavage. The actual origin of such structure is not clear and further work will be needed.

ACKNOWLEDGMENTS

Thanks are due to Prof. Ray Pepinsky for his kind invitation to work in his laboratory at the Pennsylvania State University. In his Crystal Laboratory, the crystals were obtained and most of the photographic work was done. Thanks also are given to J. Garcia Alonso who checked the influence of the applied electric field in the domain structure, and to E. Martin and P. Tavira who helped in the study of growth in the Departmento de Cristalografia Fisica, Madrid.

REFERENCES

AMOROS, J. L., MARTIN, E. AND TAVIRA, P. (1963) *Bol. R. Soc. Esp. Hist. Nat.*, (G) Vol. 61.

BUTTER, I. W. AND CHALMERS, B. (1953) *Canad. Jour. Phys.*, Vol. 31, p. 15.

CHYNOWETH, A. G. AND FELDMANN, W. L. (1960) *Phys. Chem. Solids*, Vol. 15, p. 225.

CLARKE, F. J. P. AND SAMBELL, R. A. J. (1960) *Phil. Mag.*, Vol. 5, p. 679.

CLARKE, F. J. P., SAMBELL, R. A. J. AND TATTERSALL, H. G. (1962) *Phil. Mag.*, Vol. 7, p. 393.

ENHKOVA, Z. I., Zhdanov, G. S. AND UMANSKII, H. M. (1960) *Soviet Phys. Crystallography*, Vol. 5, p. 63.

HARTMAN, P. (1953) Relations between structure and morphology of crystal, *Thesis*, University of Groningen.

HOSHINO, S., MITSUI, T., JONA, F. AND PEPINSKY, R. (1957), *Phys. Rev.*, Vol. 107, p. 1255.

HOSHINO, S., OKAYA, Y. AND PEPINSKY R. (1959) *Phys. Rev.*, Vol. 115, p. 323.

IKEDA, T., TANAKA, Y. AND TOYODA, H. (1962) *Jap. Jour. App. Phys.*, Vol. 1, p. 13.

MATHIAS, B. T., MULLER, C. E. AND REMEIKA, J. P. (1957) *Phys. Rev.*, Vol. 104, p. 849.

STOKES, R. J. AND LI, C. H. (1962) *In Fracture of Solids*, Interscience, p. 289.

SUNAGAWA, I. (1962) *Am. Mineral*, Vol. 47, p. 1332.

TOYODA, H. (1960) *Jour. Phys. Soc. Japan*, Vol. 15, p. 1539.

WOOD, E. A. AND HOLDEN, A. N. (1957) *Acta Cryst.* Vol. 10, p. 145.

ZAPFFE, C. A. AND WOEDEN, C. O. (1949) *Acta Cryst.*, Vol. 2, p. 377.

———(1949) *Acta Cryst.*, Vol. 2, p. 383.

———(1949) *Acta Cryst.*, Vol. 2, p. 386.

MINERALOGICAL SOCIETY OF INDIA, IMA VOLUME, 1966
INTERNATIONAL MINERALOGICAL ASSOCIATION, PAPERS, FOURTH GENERAL MEETING

ORE MICROSCOPY AND ELECTRON PROBE MICROANALYSIS OF SOME MANGANESE MINERALS WITH VREDENBURGITE-TYPE INTERGROWTH

TAKEO WATANABE AND AKIRA KATO
Geological Institute, Faculty of Science, University of Tokyo
and Department of Geology, National Science Museum, Ueno, Tokyo

ABSTRACT

The mineral vredenburgite found in some Indian manganese ores usually shows a characteristic unmixing intergrowth of hausmannite and jacobsite.

In the course of ore microscopic study of manganese oxide minerals in Japan, the vredenburgite-like textures have often been observed. The intergrowths in manganese oxide ores from one of the manganese deposits in Japan, called Noda-Tamagawa mine, were studied with the aid of electron probe microanalysis and x-ray powder methods. These intergrowths are shown to be hausmannite and galaxite, a new association not hitherto reported. They may be the unmixing products of a manganese oxide mineral formed under higher temperature condition during the contact metamorphic stage.

Comparative studies of these manganese oxide minerals with Indian and the other Japanese vredenburgites were also made.

OCCURRENCE

The ore deposits of the Noda-Tamagawa mine, Iwate prefecture, are found in thermally metamorphosed geosynclinal sediments of unknown age. The ore zone of this mine including some large ore bodies is well developed in the roof pendants of a granodiorite batholith and mainly in the siliceous hornfels of chert origin. The manganese content of the ores is very high in the central part of the ore bodies. The pyrochroite ore (with or without hausmannite) occurs in the center, followed successively outside by hausmannite, tephroite, and rhodonite in the outermost part (Watanabe, 1959). The "vredenburgite" here described was found in the hausmannite ore usually surrounded by pyrochroite and tephroite ores.

ORE MICROSCOPY

Under the ore microscope, the typical Widmanstätten texture of vredenburgite was observed in polished sections of rich manganese oxide ores. The name "vredenburgite" was tentatively given to an intergrowth of a spinel mineral and hausmannite. However, ore-microscopic characters of the spinel mineral occurring as matrix of the intergrowth were not similar to those of jacobsite constituting the original vredenburgite from India.

The spinel mineral in the intergrowth is dark brownish gray in colour. Its internal reflection is very strong and reddish brown. It is isotropic between crossed nicols. The optical properties of this spinel mineral resemble those of galaxite. On the other hand, the lamellar mineral of the intergrowth is strongly anisotropic and has been identified as hausmannite.

In contrast to the strong magnetism of the original vredenburgite, the vredenburgite-like mineral from Noda-Tamagawa mine is weakly magnetic. Therefore, it was considered that this vredenburgite-like mineral might be an intergrowth of galaxite and hausmannite which had not been reported hitherto.

The occurrence of another vredenburgite-like mineral was found by Hirowatari from the Taguchi manganese mine, Aichi prefecture, in 1960. The present authors also examined the specimens containing vredenburgite under the ore microscope. The optical properties of the jacobsite constituting vredenburgite are more similar to those of the jacobsite in the original vredenburgite than the Noda-Tamagawa material.

X-RAY POWDER STUDY

The X-ray powder diffraction study was made on the separated material. The most strongly magnetic fraction under the isodynamic separator was examined by X-ray powder method, but in this fraction were included some other minerals. The diffraction pattern obtained was interpreted as a mixture of hausmannite, galaxite, tephroite, and rhodochrosite. The hausmannite and galaxite are undoubtedly the members forming the vredenburgite-like intergrowth and the diffraction lines corresponding to those of two minerals are indexed in terms of tetragonal and cubic system giving a_0=5.75$_5$Å and c_0=9.43$_0$Å to the hausmannite and a_0=8.258Å to the galaxite respectively. In order to compare the results, Japanese and Indian vredenburgites were also examined by X-ray diffractometer in the same way. The cell constants of the two minerals of the intergrowth from the Taguchi mine calculated by the present authors are a_0=5.77Å and c_0=9.42Å for the hausmannite and a_0=8.408Å for the jacobsite respectively. The Indian vredenburgite from Vizagapatam, India, described by Fermor (1909) was also the intergrowth of hausmannite and jacobsite as already confirmed by Schneiderhöhn and Ramdohr (1931) and Dunn (1936). The cell constants of the hausmannite are a_0=5.771Å and c_0=9.428Å and that of jacobsite is 8.484Å respectively. In Table 1, the X-ray powder data for these three intergrowths are tabulated and compared with those for synthetic $MnFe_2O_4$, synthetic $MnAl_2O_4$, and hausmannite from Ilmenau, Germany given in the Peacock Atlas (1962).

As indicated by the result of electron probe microanalysis, the hausmannite from the Noda-Tamagawa mine has a peculiar composition with Ti and Al, both probably substituting trivalent manganese in the structure.

The cell constants of Indian jacobsite is close to that of synthetic $MnFe_2O_4$, but that of Japanese jacobsite from the Taguchi mine is smaller, and this contraction was explained by Hirowatari (1964) as the substitution of ferric ion by aluminium. In the present case, the cell constant of this galaxite is incidentally equal to that of synthetic $MnAl_2O_4$. This is interpreted by the authors as due to the entrance of smaller ion (Fe^{+2}) in place of larger (Mn^{+2}), and at the same time larger (Mn^{+3}) in place of smaller ones (Al^{+3}) as far as estimated from the result of chemical analysis.

CHEMICAL COMPOSITION

The chemical compositions of the intergrowth-forming galaxite and hausmannite, and associated homogeneous hausmannite grains were estimated by electron microprobe analysis, using the instrument of JXA-3A, Japan Electron Optics Co. Ltd. (Fig. 1) From the observed intensities of respective characteristic lines of MnKα, FeKα, TiKα, and AlKα were estimated the weight percentages of metallic ingredients after the correction and re-calculation, using standard materials. The results are shown in Table 2.

According to the results, it is evident that the host galaxite contains more manganese than ideal $MnAl_2O_4$ and has an intermediate composition between $MnAl_2O_4$ and $MnMn_2O_4$ with minor substitutions, hence a considerable amount of manganese in this galaxite may be in trivalent state. Fig. 2 is the tentative diagram showing the presence of immiscible region between this galaxite and hausmannite.

DISCUSSION

The occurrence of galaxite is reported from several thermally metamorphosed manganese deposits of bedded type. It is a characteristic contact mineral formed in aluminous impure layers of manganese carbonate ores as in case of formation of spinel formed in such layers in contact metamorphosed dolomite-marble. The mineral assemblages of galaxites from such occurrences are ;

(1) galaxite-rhodochrosite-tephroite (or alleghanyite series minerals)

(2) galaxite-manganosite-tephroite (or alleghanyite series minerals) and

(3) galaxite–hausmannite–tephroite – rhodochrosite.

TABLE 1

X-ray powder data for vredenburgites, " vredenburgite ", synthetic $MnFe_2O_4$, synthetic $MnAl_2O_4$, and hausmannite.

1				2				3				4		5			6		
d(Å)	I	Jb	Hs	d(Å)	I	Jb	Hs	d(Å)	I	Gx	Hs	d(Å)	I	d(Å)	I	"Gx" "Jb"	d(Å)	I	Hs
4.92	20	111	101	4.92	20	111	101	4.90	10	111		4.906	20			111	4.94	30	011
3.08	10		112	3.09	30		112	3.08	30		112						3.09	50	112
3.00	40	220		2.98	30	220		2.92	30	220		3.005	35	2.921	60	220			
2.89	5		200														2.89	30	200
2.76	20		103	2.75	40		103	2.75	30		103						2.77	90	103
2.56	100	311		2.55	100	311		2.493	100	311		2.563	100	2.492	100	311			
2.50	20		211	2.49	50		211	2.483	100		211						2.49	100	211
												2.450	11	2.383	10	222	2.36	40	004
2.13	30	400		2.10	20	400		2.07	20	400		2.124	25	2.065	25	400			
2.04	10		220	2.04	20		220	2.03	10	220							2.04	40	220
																	1.825	20	204
																	1.795	50	105
1.735	10	422						1.689	10	422		1.7342	20	1.6862	20	422			
																	1.706	30	312
																	1.642	20	303
1.635	30	511		1.617	10	511		1.593	20	511		1.6355	35	1.5896	40	511			
1.582	5		321					1.579	10		321						1.579	50	321
1.543	10		224	1.539	60		224	1.541	10		224						1.544	80	224
1.500	30	440		1.489	20	440		1.460	30	440		1.5031	40	1.4600	45	440			
																	1.468	10	116
Jb a_o=8.484 Å				Jb a_o=8.408 Å				Gx a_o=8.258 Å				a_o=8.499 Å		a_o=8.258 Å					
Hs a_o=5.77$_1$ Å				Hs a_o=5.77 Å				Hs a_o=5.75$_5$ Å									a_o=5.76 Å		
c_o=9.42$_8$ Å				c_o=9.42 Å				c_o=9.43$_0$ Å									c_o=9.44 Å		

1. Vredenburgite. Devada, Vizagapatam, near Madras. Cu/Ni radiation.
2. Vredenburgite. Taguchi mine, Aichi prefecture, Japan. Cu/Ni radiation.
3. " Vredenburgite ". Noda-Tamagawa mine, Iwate prefecture, Japan. Cu/Ni radiation.
4. Synthetic $MnFe_2O_4$. After NBS Circular 539 *9*, 35-36 (1960), Fe radiation.
5. Synthetic $MnAl_2O_4$. After NBS Circular 539 *9*, 36-37 (1960. Cu radiation.
6. Hausmannite. Ilmenau, Thuringia, Germany. After the Peacock Atlas (1962). Fe/Mn radiation.

(Jb=indices of jacobsite. Hs=indices of hausmannite. Gx=indices of galaxite.
" Jb "=indices of synthetic $MnFe_2O_4$. " Gx "=indices of synthetic $MnAl_2O_4$).

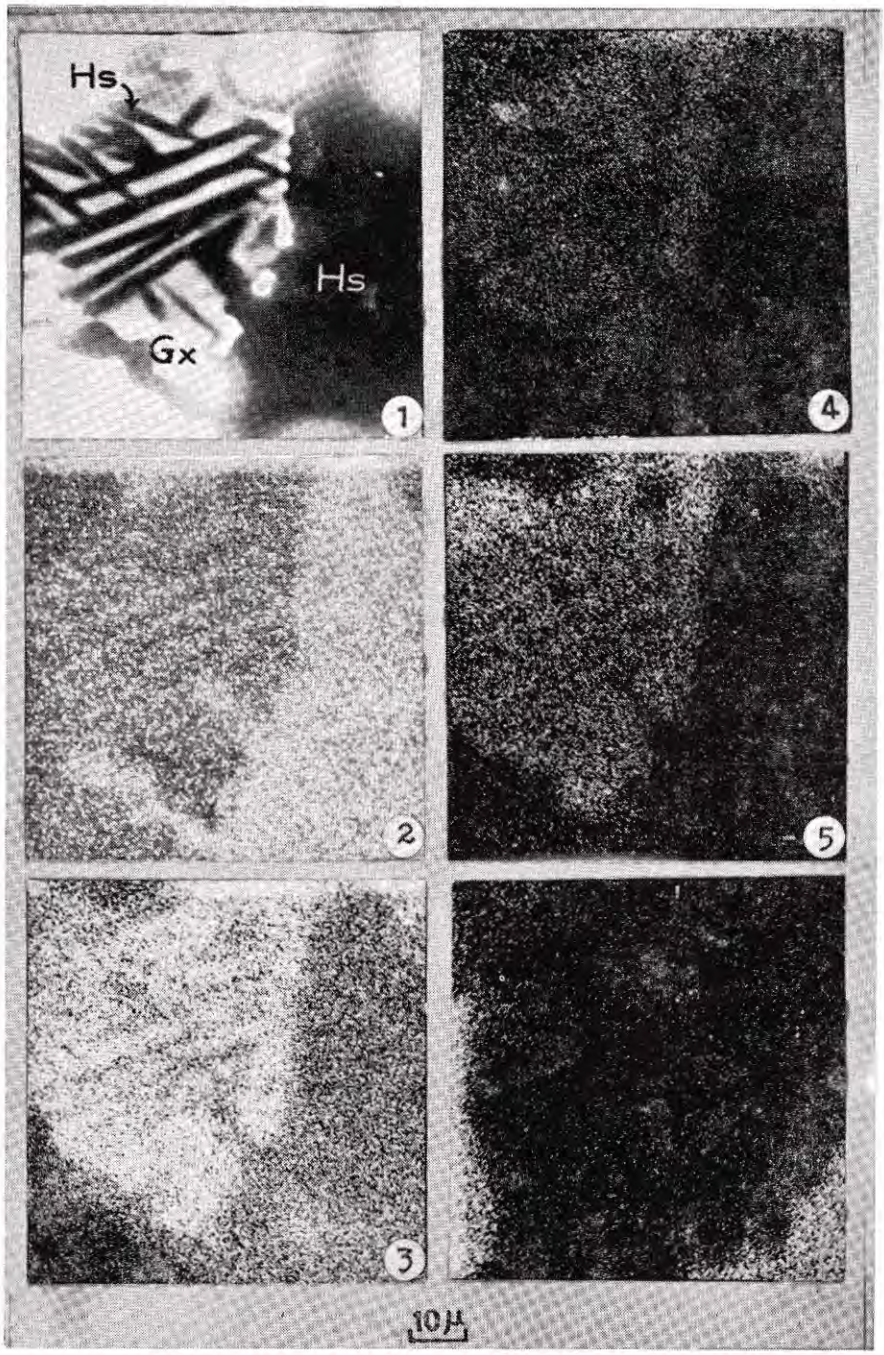

Fig. 1. Display pictures of electron absorption, MnKα, FeKα, TiKα, AlKα, and SiKα of "vredenburgite" bearing manganese oxide ore from the Noda-Tamagawa Mine, Iwate prefecture.

(1) Electron absorption : Hs (white letter) ; hausmannite without intergrowth texture. Hs(black letter) ; hausmannite with lamellae texture in galaxite. Gx ; galaxite.
(2) MnKα : Analyser ; quartz. Vacuum system.
(3) FeKα : Analyser ; quartz. Vacuum system. Note the least Fe content in tephroite (left under).
(4) TiKα : Analyser ; quartz. Vacuum system.
(5) AlKα : Analyser ; muscovite. Vacuum system.
(6) SiKα : Analyser : muscovite. Vacuum system.

TABLE 2

Chemical composition of galaxite (host), hausmannite (guest), and hausmannite (without intergrown body)

	Galaxite (host)		Hausmannite I (guest)		Hausmannite II (without intergrown body)	
	Wt. %	Mole %	Wt. %	Mole %	Wt. %	Mole %
Mn	45±5	0.8	55±5	1.0	71±7	1.3
Fe	6±1	0.1	3±1	0.05	1	0.02
Ti	6±2	0.1	3±1	0.06	—	—
Al	12±3	0.4	5±1	0.2	—	—
Mg	—	—	—	—	—	—

— ; below the limit of detection

Galaxite : $(Mn_{0.8}Fe_{0.2})_{1.0}(Al_{0.9}Mn_{0.9}Ti_{0.2})_{2.0}O_{4.0}$

Hausmannite I : $(Mn_{0.9}Fe_{0.1})_{1.0}(Mn_{1.4}Al_{0.5}Ti_{0.1})_{2.0}O_{4.0}$

Hausmannite II : $(Mn_{1.0}Fe_{0.0})_{1.0}Mn_{2.0}O_{4.0}$

(calculated as total of mole % of Mn, Fe, Ti, and Al as 3)

The occurrence of galaxite-hausmannite intergrowth in restricted to some bands in the galaxite–hausmannite– tephroite – rhodochrosite ore. This means that the galaxite was exclusively formed in aluminum layers as just stated.

In conclusion, the galaxite–hausmannite intergrowth is the product of unmixing of a solid solution having composition between hausmannite and galaxite. The solid solution was probably formed by thermal effect of granitic intrusion and the exsolution was due to subsequent slow cooling.

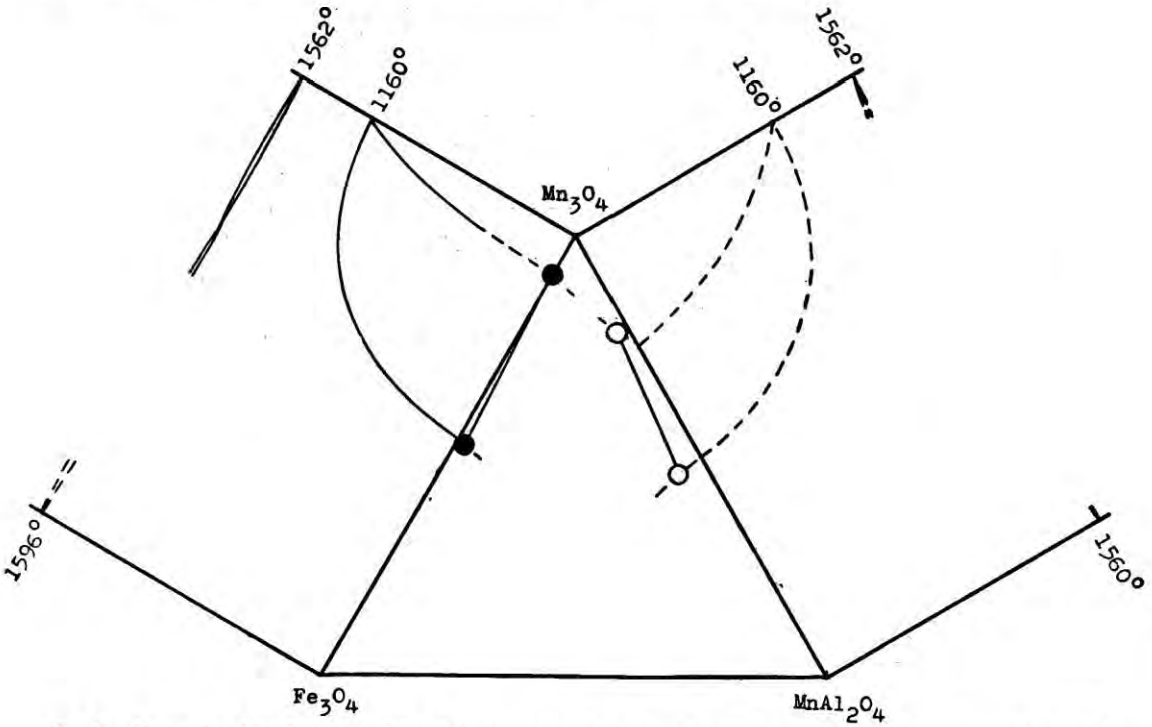

Fig. 2. Tentative Mn_3O_4–Fe_3O_4–$MnAl_2O_4$ triangular diagram showing the chemical compositions of vredenburgite and " vredenburgite "-forming members.

Solid circles : Vizagapatam, near Madras, India. Open circles : Noda-Tamagawa mine, Iwate prefecture, Japan.

ACKNOWLEDGEMENTS

The authors are indebted to Mr. K. Saida, General Manager of the Noda-Tamagawa mine, Shinkonatsu Mining Company, and to Dr. S. Yui, Institute of Mining, Akita University for their help in collecting the specimens studied. Thanks are also due to the late Dr. W. F. Foshag for donation of the specimen of Indian vredenburgite and to Dr. F. Hirowatari of Geological Survey, Japan, for his useful discussions throughout the investigation.

REFERENCES

BERRY, L. G. AND THOMPSON, R. M. (1962) X-ray powder data for ore minerals: The Peacokck Atlas. *Geol. Soc. Amer.* Memoir, 85, pp. 195-196.

DEB, S. (1943) Optical, X-ray and magnetic studies of the mineralogical constituents of vredenburgite from different occurrences in India: *Quart. Jour. Geol. Min. and Metall. Soc. India*, Vol. 15, pp. 137-141.

———(1943) Recent advances in ore-microscopic studies of opaque minerals in India: *Proc. Nat. Inst. Soc. India*, Vol. 26(A), pp. 219-231.

DUNN, J. A. (1936) A study of some microscopical aspects of Indian manganese-ores *Trans. Nat. Sci. India*, Vol. 1, pp. 103-124.

FERMOR, L. L. (1909) Three new manganese bearing minerals: Vredenburgite, sitaparite and juddite. *Rec. Geol. Surv. India*, Vol. 37, pp. 199-212.

———(1938) Notes on vredenburgite (with devadite) and on sitaparite: *Proc. Nat. Inst. Sci. India*, Vol. 4, pp. 253-286.

HIROWATARI, F. (1964) Re-examination of vredenburgite by using X-ray microanalyser (Abstr.): *Jour. Min. and Metall. Inst. Japan*, Vol. 80, pp. 755-756.

MASON, B. (1943) Mineralogical aspects of the system FeO-Fe_2O_3-MnO-Mn_2O_3: *Geo. Fören. Förh.*, Vol. 65, pp. 97-180.

ORCEL, J. et ST. PAVLOVITCH (1931) Les caractères microscopiques des oxydes de manganites naturels: *Bull. Soc. franc. minér. crist.*, Vol. 54, pp. 108-179.

ROY, S. (1958) Mineragraphic study of the manganese ores of Tirodi, Balgaghat District, Madhya Pradesh, India: *Proc. Nat. Inst. Sci. India*, Vol. 24, pp. 89-99.

———(1959) Variation in etch behaviour of jacobsite with different cell dimensions: *Nature*, Vol. 183, pp. 1256-1257.

———(1959) Mineralogy, and texture of the manganese ore bodies of Dongri Buzurg, Bhandara District, Bombay State, India, with a note on their genesis: *Econ. Geol.*, Vol. 54, pp. 1556-1574.

———(1960) Mineralogy and texture of the manganese ores of Kodur, Srikakulam District, Andhra Pradesh, India: *Can. Mineral.*, Vol. 6, pp. 491-503.

SCHNEIDERHOHN, H. AND RAMDOHR, P. (1931) Lehrbuch der Erzmikroskopie. Bd. II, Berlin.

SWANSON, H. E., COOK, M. I., Isaacs, T. AND EVANS, E. H. (1960) Standard X-ray diffraction powder patterns: *National Bureau of Standards*. Circular No. 539, Vol. 9, pp. 35-36.

———(1960) Ibid., pp. 36-37.

WATANABE, T. (1959) The minerals of the Noda-Tamagawa mine, Iwate prefecture, Japan. I. Notes on geology and parageneses of minerals: *Miner. Jour. (Japan)*, Vol. 2, pp. 408-421.

MINERALOGICAL SOCIETY OF INDIA, IMA VOLUME, 1966
INTERNATIONAL MINERALOGICAL ASSOCIATION, PAPERS, FOURTH GENERAL MEETING

NOUVELLES DONNEES SUR LA LOCALISATION DES ELEMENTS EN TRACES DANS LES MINERAUX ET DANS LES ROCHES

J. GONI et C. GUILLEMIN
Bureau de Recherches Géologiques et Minières, Paris

RESUME

Dans cette communication, les auteurs exposent les résultats de leurs recherches sur la répartition du plomb, du zinc et du cuivre dans un granite monzonitique, du cérium et du gadolinium dans un zircon de leptynite, etc.... Ils montrent que ces éléments en traces sont localisés préférentiellement dans les discontinuités des minéraux ou de leurs agrégats. Ces résultats confirment ceux d'un travail antérieur (Goni-Guillemin, 1964) portant sur la localisation du nickel dans l'antigorite, des lanthanides dans le sphène et de différents métaux (cuivre, chrome, vanadium et tungstène) dans des biotites.

En outre, il a été possible de mettre en évidence une hétérogénéité de répartition de certains éléments considérés comme diadochiques, même à l'échelle du monocristal, notamment pour le chrome dans le diopside et pour le titane dans certaines augites titanifères.

Le lessivage à l'aide de solutions aqueuses d'acides organiques permet d'extraire la majeure partie des éléments en traces contenus dans des granites calco-alcalins sans attaquer les silicates constitutifs de la roche.

Ces dernières expériences suggèrent que les éléments en traces sont retenus dans les discontinuités par un mécanisme mettant en jeu de faibles énergies de liaison.

L'utilisation systématique de la lixiviation par des acides faibles, et surtout les possibilités d'analyse ponctuelle offertes par la microsonde électronique, sont un appoint considérable dans le problème de la localisation des éléments en traces dans les minéraux et les roches; les remplacements diadochiques n'en sont pas toujours responsables, et de nombreux éléments sont concentrés, sans former de minéraux, dans les discontinuités des cristaux ou des agrégats cristallins: clivages, faces cristallines, films intergranuliares, micro-fissures et dislocations.

Dans une publication antérieure (Goni-Guillemin, 1964) nous avons présenté quelques examples de la répartition de Ni, Ce, La, Cu, Cr, V, As, W, dans certaines roches et silicates constitutifs de ces roches. Nous exposerons ici les résultats récemment obtenus sur les points suivants:

- La localisation des éléments en traces dans les fissures des minéraux et à l'interface cristal-mésostase des roches.
- La répartition hétérogène des remplacements diadochiques dans certains silicates.
- La mobilité géochimique des éléments en traces dans les roches.

LOCALISATION DES ELEMENTS EN TRACES DANS LES FISSURES DES MINERAUX ET A L'INTERFACE CRISTAL-MESOSTASE

(*a*) *Répartition du plomb et du zinc dans un granite monzonitique:* Il s'agit du granite métasomatique de Gien-Sur-Cure situé sur la bordure nord du synclinal du Morvan; l'analyse globale donne 1500 ppm de plomb et 300 p.p.m. de zinc. Microscopiquement l'échantillon présente de très nombreuses fissures de 10 à 15 μ de largeur recoupant indistinctement tous les minéraux. La Fig. 1* est une microphotographie du granite fissuré et la Fig. 2 présente les images X de la répartition du fer et du zinc, qui montrent la localisation de ces éléments dans les fissures; par exemple la concentration en zinc dans une fissure est de 0,2% sans qu'il soit possible de déceler un anion associé. Dans ce

* Dans les microphotos no. 1, 4, 6 et 8, les surfaces balayées par le faisceau électronique sont encadrées par un trait noir.

même granite, le plomb est aussi concentré dans les fissures, avec des teneurs atteignant 2,5%.

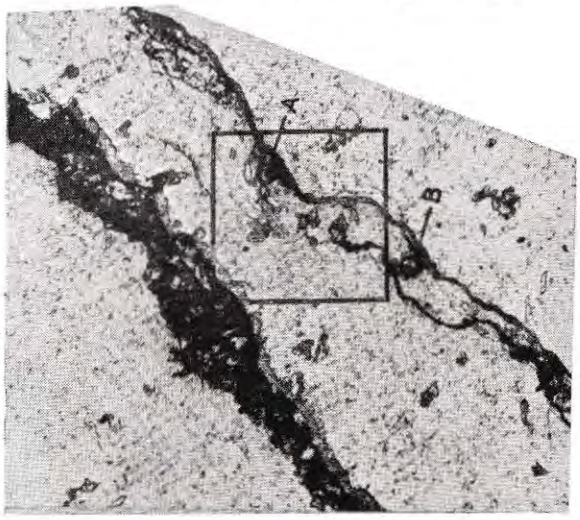

Fig. 1. Microphotographie-Lame mince-L. N-X 300 Champ fissural dans le granite métasomatique de Gien-Sur-Cure.

(*b*) *Répartition du zinc et du cuivre dans une tourmaline lithique de Naïpa Alto Ligonha, Mozambique* : La Fig. 3 met en évidence, dans la répartition du silicium, une discontinuité qui correspond à des fissures, où se trouvent concentrés le zinc et le cuivre (1,5% de zinc et 0,7% de cuivre). Un tel résultat pose la question de l'existence des variétés cuprifères et zincifères de tourmaline.

(*c*) *Localisation du cérium et du gadolinium dans un zircon :* Le zircon provient d'une leptynite de Jakobshavn, Groenland. Dans la Fig. 4 nous observons que le cristal idiomorphe de zircon est bordé par une zone opaque noirâtre,

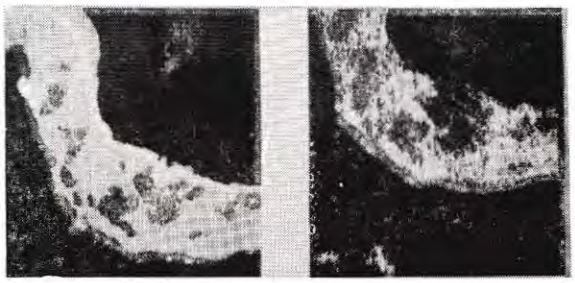

Fe Zn

Fig. 2. Images X de la répartition du fer et du zinc (chanque carré : 300 x 300μ)

dans laquelle l'enregistrement qualitatif, à la microsonde, a mis en évidence la présence de

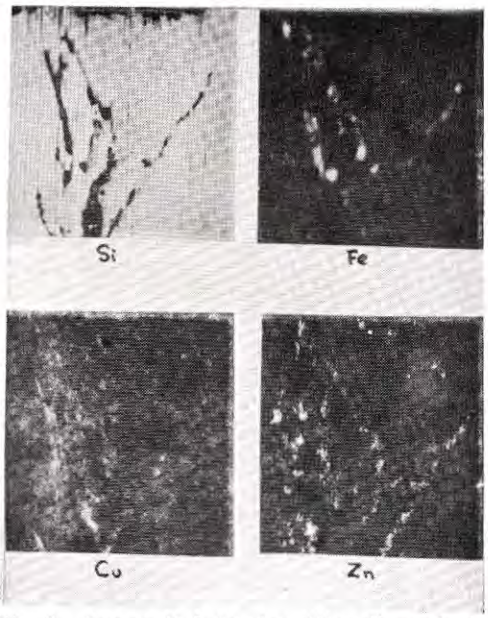

Fig. 3. Images X de la répartition fissurale du fer, du cuivre et du zinc dans des défauts d'un monocristal de tourmaline (chaque carré : 300 x 300μ).

terres rares et en particulier cérium et gadolinium. La Fig. 5 montre la répartition du cérium et du silicium : nous remarquons un déficit en silicium sur la bordure et dans une fissure transversale du zircon, déficit correspondant à l'accumulation du cérium (2,4% de

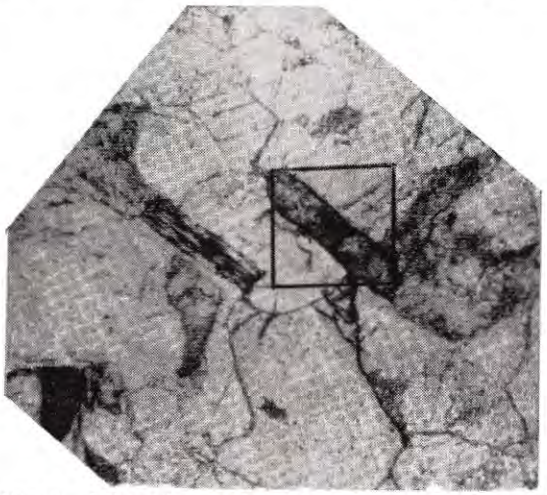

Fig. 4. Microphotographie-lame mince-L. N-X 300, Leptynite, renfermant un cristal idiomorphe de zircon.

cérium) et du gadolinium. A la lueur de ces données, il nous paraît donc nécessaire de reconsidérer le problème des variétés de zircon

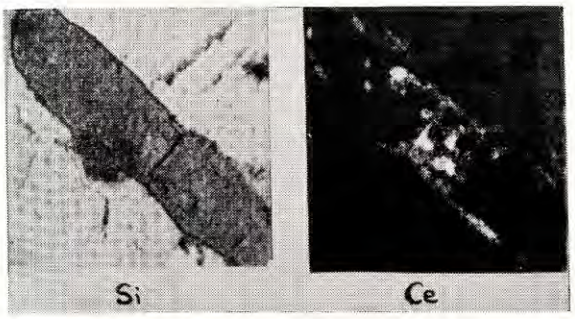

Fig. 5. Répartition du cérium et du silicium dans l'interface zircon-mésostase (chaque carré : 300 x 300μ).

riches en terres rares et en phosphore comme l'oyamalite et la yamaguchilite.

REPARTITION HETEROGENE DES REMPLACEMENTS DIADOCHIQUES

(*a*) *Répartition du titane dans des augites titanifères :* L'augite étudiée provient d'une luscladite doléritique à olivine de Crawfordjohn, Ecosse, de paramètre C. I. P. W. Lacroix : III . 6′ . ′3 . 4.

La Fig. 6 représente un monocristal d'augite violacé en lame mince, homogène du point de vue optique (coloration, angle d'extinction, clivages, etc....). Sur la même figure sont indiquées les deux surfaces balayées par le faisceau électronique. Les images X (Fig. 7) obtenues, montrent une zonalité de répartition du titane, la teneur au centre étant de 3%, celle de l'extrémité de 1,8%. Par contre le calcium, le magnésium et le fer sont répartis d'une facon homogène dans le cristal.

Ces résultats montrent qu'une augite diadochiquement substituée peut-être homogène optiquement et hétérogène chimiquement.

(*b*) *Répartition du chrome dans un diopside :* Ce diopside chromifère provient d'Outokumpu, Finlande. Le minéral a été étudié par Eskola (1933) qui cite des teneurs en chrome atteignant 0,44%. La Fig. 8 représente un agrégat de cristaux de diopside chromifère reconnaissables par leur couleur et le clivage prismatique. On a indiqué sur cette figure la mosaïque des différentes images X étudiées. La Fig. 9 montre la répartition du chrome dans les surfaces III, IV

Fig. 6. Microphotographie-lame mince-L. N-X 300
Monocristal d'augite titanifère dans luscladite à olivine.

et V. Là encore on trouve une structure zonée avec des teneurs en chrome allant de 0,09 à 0,3% sans que ces différences de teneurs se traduisent par des variations optiques.

MOBILITE DES ELEMENTS DANS LES ROCHES

Les résultats obtenus sur la localisation des éléments en traces nous ont amené a penser qu'il devait être possible d'en extraire une grande partie sans détruire le réseau des silicates. Il nous a paru intéressant d'établir ainsi un bilan de ce qui est facilement mobilisable par rapport à ce qui reste fixé dans le minéral. Tous nos essais ont porté sur la granodiorite saine constituant le massif de Flamanville (Manche).

Principe de la méthode : Dans les microfissures, les éléments en trace sont presque toujours accompagnés d'une *quantité importante de fer.* Nous avons donc choisi des réactifs (solution

d'acide oxalique et citrique M/10) ayant une grande affinité pour le fer et susceptibles de former avec le fer et les autres éléments métalliques des composés chelatés stables et solubles.

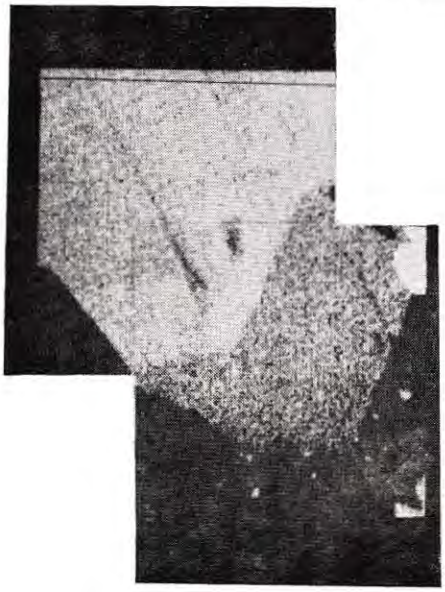

Fig. 7. Distribution zonaire du titane dans le monocristal d'augite (montage de 2 balayages imbriqué's de 300 x 300μ).

Nous avons opéré par percolation et par agitation ; cette dernière méthode s'étant révélée la plus intéressante.

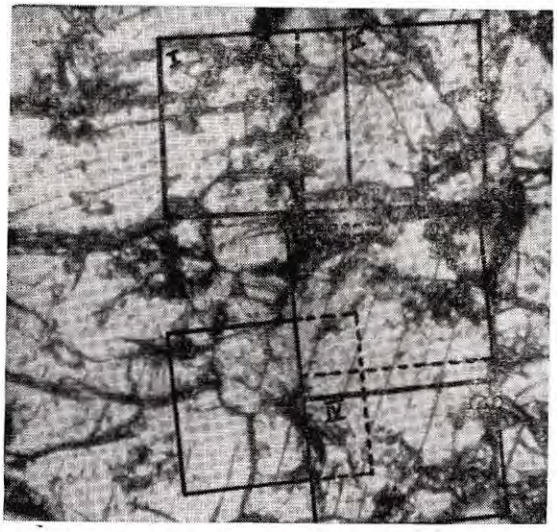

Fig. 8. Microphotographie-lame mince-L. N-X 300. Agrégat de cristaux idiomorphes de diopside chromifère.

La granulométrie jouant un rôle important dans cette étude, nous avons choisi après essais celle de 80 mesh (0,24mm) qui représentait la moyenne de grosseur des grains de la roche. Les

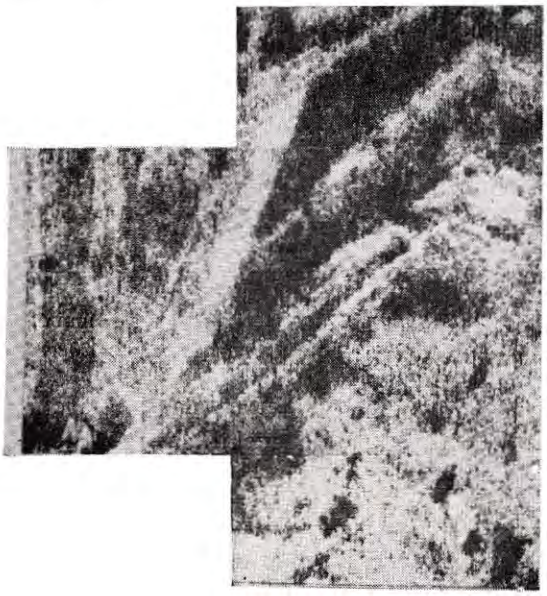

Fig. 9. Mosaique des images X du chrome dans les balayages III-IV-V ci-dessus (chaque carré 300 x 300μ).

échantillons (50 g) étudiés ont été préalablement débarrassés des fines par lavage, puis brassés en présence de 200 cc du réactif.

La Fig. 10 montre l'évolution du poids des résidus d'extraction en fonction du nombre de

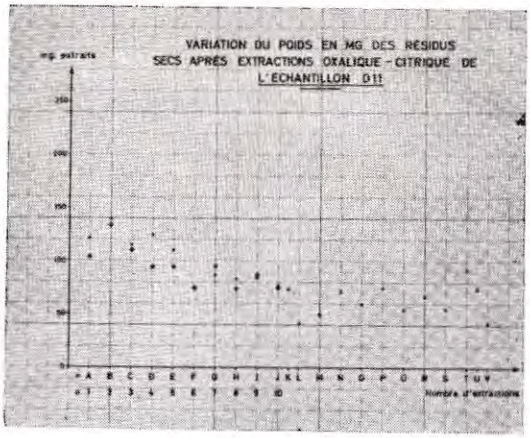

Fig. 10

celles-ci. Nous voyons qu'aprés un maximum correspondant aux quatre premieres extractions, le poids diminue pour finalement se stabiliser

à ce qui doit correspondre à la solubilité des silicates de la roche dans les conditions de l'expérience.

Par example nous trouvons qu'après quatre extractions, nous avons solubilisé 36% du plomb, 53% du cuivre, 31% du chrome, 18% de l'ètain, 27% du vanadium pour des teneurs en roche totale de 18 ppm de plomb, 13 ppm de cuivre, 39 ppm de chrome, 18 ppm d'étain, 75 ppm de vanadium, tous ces résultats étant donnés à ± 10%. Or, au cours de ces quatre extractions, la quantité totale de résidu sec, donc la quantité maximale de silicates ayant pu être détruits est de 0,500 g, 0,351 g, 0,275 g, 0,255 g, soit environ 1 à 0,5% de la prise de départ (dont déjà 44% de Fe_2O_3 dès la première extraction). *Il n'y a donc aucune commune mesure entre le solubilisation des éléments en traces et la solubilisation des silicates,* ce qui montre bien que la majeure partie de ces éléments est en dehors du réseau, et mobilisable sans destruction de celui-ci. On pourraît objecter qu'il s'agit là d'une attaque sélective des minéraux ferromagnésiens, mais d'une part nous avons montré, Goni-Guillemin (op. cit.) que dans la biotite du granite de Flamanville, cuivre, chrome, vanadium, arsenic et tungstène étaient hors du réseau et d'autre part, l'examen microscopique de l'échantillon après les attaques ne montre pas une corrosion nettement visible dans les constituants du granite.

Les pourcentages d'extraction citrique-oxalique pour le plomb, le chrome, l'étain, le molybdène et le nickel ont été exprimés sous forme d'histogrammes sur la Fig. 11, avec en comparaison les teneurs dans la roche globale.

Pour nous reneseigner enfin, sur la nature du fer fissural auquel sont associés les éléments en traces, nous avons soumis à l'extraction différents minéraux de fer (hématite, goethite, lépidocrocite, et stilpnosidérite). Nous avons pu constater que les résidus secs correspondants oscillaient entre 0,9% pour l'hématite et 10% pour la stilpnosidérite ; il est donc très probable que le fer fissural est sous une forme peu cristalline.

CONCLUSIONS

Par ces études, très brièvement esquissées ici, nous avons mis en évidence que :

– la distribution des éléments en traces dans les minéraux et les roches est hétérogène, même dans le cas de remplacements considérés comme typiquement diadochiques, au sein de monocristaux.

– les éléments en traces sont rarement incorporés dans le réseau cristallin, et très fréquemment dans les discontinuités naturelles ou

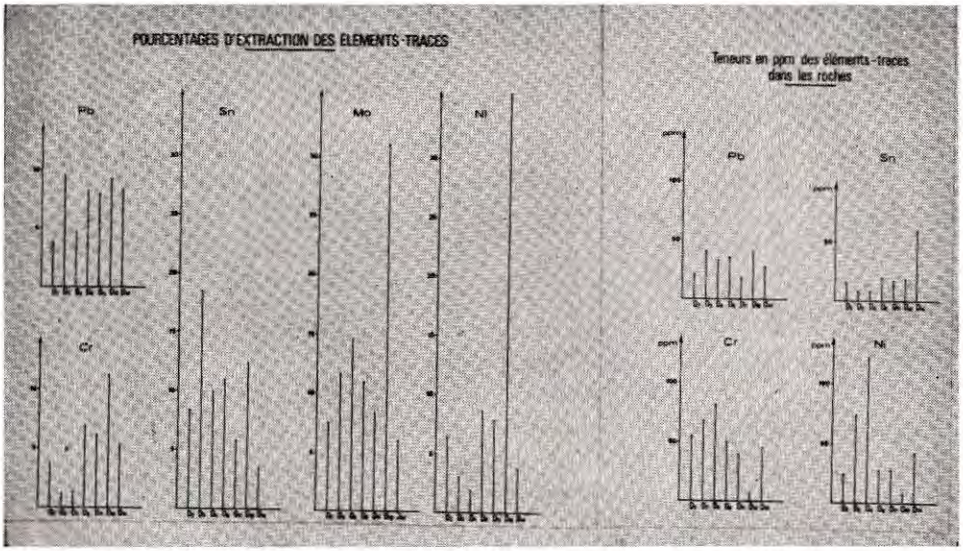

Fig. 11

accidentelles du milieu : clivages, joints, fissures et dislocations renferment la plupart des traces, et c'est leur géométrie qui en conditionne la distribution.

– le plus souvent ces éléments ne sont pas engagés dans des combinaisons minérales ; ils font preuve d'une grande mobilité géochimique, et ne sont liés au support que par une énergie très faible ; ils sont aisément entrainés par lessivage avec des acides organiques.

REFERENCES

ESKOLA, P. (1933) *Comptes-Rendus Soc. Géol. Finlande* (Bull. Comm. Geol. Finnlande) No. 103, pp. 26–44.

GONI, J. et GUILLEMIN, C. (1964) *Bull. Soc. franc. Minér. Crist.*, Vol. 87, pp. 149–56.

MINERALOGICAL SOCIETY OF INDIA, IMA VOLUME, 1966
INTERNATIONAL MINERALOGICAL ASSOCIATION, PAPERS, FOURTH GENERAL MEETING

ILLUSTRATIONS OF HETEROGENEITY IN PHLOGOPITE, FELDSPAR, EUXENITE AND ASSOCIATED MINERALS

J. RIMSAITE AND G. R. LACHANCE
Geological Survey of Canada, Ottawa, Canada

ABSTRACT

Heterogeneity in natural minerals is a very common phenomenon as a result of changes in physical-chemical conditions during mineral growth and/or subsequent alteration.

Several examples of heterogeneity are described on the basis of microscopic, x-ray diffraction and electron microprobe analyses. These consist of :

(1) zoned phlogopite ; and mica containing oriented inclusions and crusts ;
(2) " antiperthitic " and lamellar plagioclases ; and associated biotite and opaque minerals ;
(3) fresh and altered euxenite ; and inclusions in associated feldspar.

The purpose of this study is to determine the differences in chemical composition between various mineral varieties in zoned phlogopites, in " antiperthitic " and lamellar plagioclases, in ilmenite-hematite grains, and multicoloured euxenite.

The concentration of iron in zoned phlogopites may increase by a factor of four from the beginning (centre) to the end of crystallization (rim), and in some phlogopites potassium is absent in the outermost portion of the rim. " Antiperthitic " plagioclase is relatively homogeneous labradorite-andesine (An_{45-52}) with inclusions of potassium feldspar, while lamellar plagioclase consist of lamellae ranging in composition from An_5 to An_{70}, and of alkali feldspars.

The concentrations of uranium and lead show erratic variations in the altered euxenite.

INTRODUCTION

Microscopic studies (by J. R.) of several hundred thin sections of magmatic rocks submitted for age determination indicated that none of these rocks contain homogeneous minerals. The primary minerals are either zoned, filled with inclusions, partly altered to secondary minerals, or exhibit secondary growths. Secondary minerals commonly occur in fine-grained intergrowths, with one another and with the host.

Zoned phlogopites *5*, *9*, *35*, " antiperthite " KA–846, lamellar plagioclase KA–930, euxenite and associated minerals, described by Rimsaite (1964) and by Robinson *et al.* (1963), were selected for the present study of heterogeneity.

Phlogopite 5 is from a metamorphosed limestone. The phlogopite occurs in euhedral crystals reaching several inches in diameter and exhibits an apparent zoning as a result of an inclusion-rich core surrounded by alternating clear and inclusion-rich bands.

Phlogopite 9 is from lamprophyre *9* that is composed of a few zoned phenocrysts of pyroxene and phlogopite in a groundmass of feathery albite and fine-grained pyroxene. Biotite, epidote, sphene, chlorite and serpentine are present in fractures of the lamprophyre, and locally replace phlogopite and pyroxene phenocrysts.

Phlogopite 35 is the major constituent of lamprophyre *35*. The phlogopite occurs as subhedral to euhedral rimmed crystals ranging in size from 50 to 2000 microns and contains inclusions surrounded by dark haloes. The interstices are filled with anhedral plagioclase, fine-grained pyroxene and amphibole. A few phlogopite crystals are replaced by fine-grained serpentine-chlorite aggregates.

" Antiperthite " KA–846 is the major constituent of an anorthosite from Quebec. The plagioclase contains oriented inclusions of alkali feldspar that is associated with muscovite, biotite and opaque grains. Other minerals are : pyroxene with numerous specks of biotite and opaque crusts ; biotite ; anhedral interstitial patches of potassium feldspar ; and ilmenite-hematite intergrowths that consist of wide

(50 microns) and narrow (1 to 5 microns) hematite and ilmenite lamellae.

Lamellar plagioclase KA–930 is from a diabase that is composed of plagioclase, olivine, pyroxene, serpentine, accessory opaque grains, biotite, and numerous apatite needles. Plagioclase grains are clouded by inclusions of apatite and locally altered to fine-grained sericite-chlorite aggregates.

Euxenite is from a feldspar pegmatite. The euxenite is fractured and varies in colour from deep red to almost colourless. The associated feldspar is fractured and stained with iron oxides.

The purpose of the present study is to illustrate several types of heterogeneity, such as: those arising from variations in physical-chemical environment during crystallization and subsquent alterations (zoned phlogopites, multicoloured euxenite); and those formed as a result of inclusions and fine-grained intergrowths (lamellar and "antiperthitic" plagioclases, ilmenite-hematite grains, micas and feldspars with crusts and inclusions). The following are of petrological and geochemical interest: differences in chemical composition between various mineral varieties in zoned phlogopites, in "antiperthitic" and lamellar plagioclases, and in hematite-ilmenite intergrowths; and relative abundance and distribution of selected elements in altered and recrystallized minerals. Furthermore, heterogeneity is one of the most disturbing factors in correlating physical properties with chemical composition and in calculating the structural formulas of minerals, unless the appropriate corrections can be made (Rimsaite 1962, 1964). Several examples of heterogeneity, illustrated in the present study, can be useful in evaluating chemical analyses of similar heterogeneous minerals.

METHODS

Optical studies included examination of specimens in thin and polished sections, and in oil immersion mounts for the determination of the refractive indices. A universal stage was used for determination of optic angles and the shape and orientation of inclusions.

Mineral identifications were made by Mr. R. N. Delabio using conventional 57.3 mm and 114.6 mm diameter Debye-Scherrer x-ray cameras. Metamict minerals were recrystallized by heating in vacuum. An x-ray diffractometer was used to check the efficiency of mineral concentration, particularly where different mineral varieties were selected for chemical analyses. Structural studies on single crystals were made by means of a Weissenberg camera.

Fine-grained radioactive minerals in fractures of feldspar were traced by means of autoradiographs following the procedure described by Robinson (1952).

The heterogeneous minerals were selected in thin or polished sections, or in oil immersion mounts, for further study by means of an electron microanalyser. Depending on the nature of the mineral and the problem, electron microprobe analyses were performed on polished sections,

PLATE I

I–1. Phenocrysts of early phlogopite (grey, left edge and upper field) and small crystals of late biotite (dark grey, centre). The phlogopite is associated with pyroxene that contains fine-grained inclusions of mica (light grey, high relief, left). A fracture traversing the rock is filled with serpentine. Minerals along the fracture are altered. Porphyritic basalt *36*, x 100.

I–2. Distribution of iron in a small phenocryst of phlogopite from lamprophyre *35*:

(a) Photomicrograph of the phlogopite with dark rims and a few inclusions, x 120.

(b) X-ray scanning image, iron K-alpha radiation, x 120.

I–3. Distribution of iron, potassium, titanium and chromium in a double rimmed coarse phlogopite phenocryst from lamprophyre *35*:

(a) Photomicrograph of pale buff phlogopite with black outer and brown-grey inner rims. Inclusions are also surrounded by double rims (upper field left), x 100.

(b) Element concentration obtained from a line scan across the dark border of the phlogopite, x 200.

PLATE I

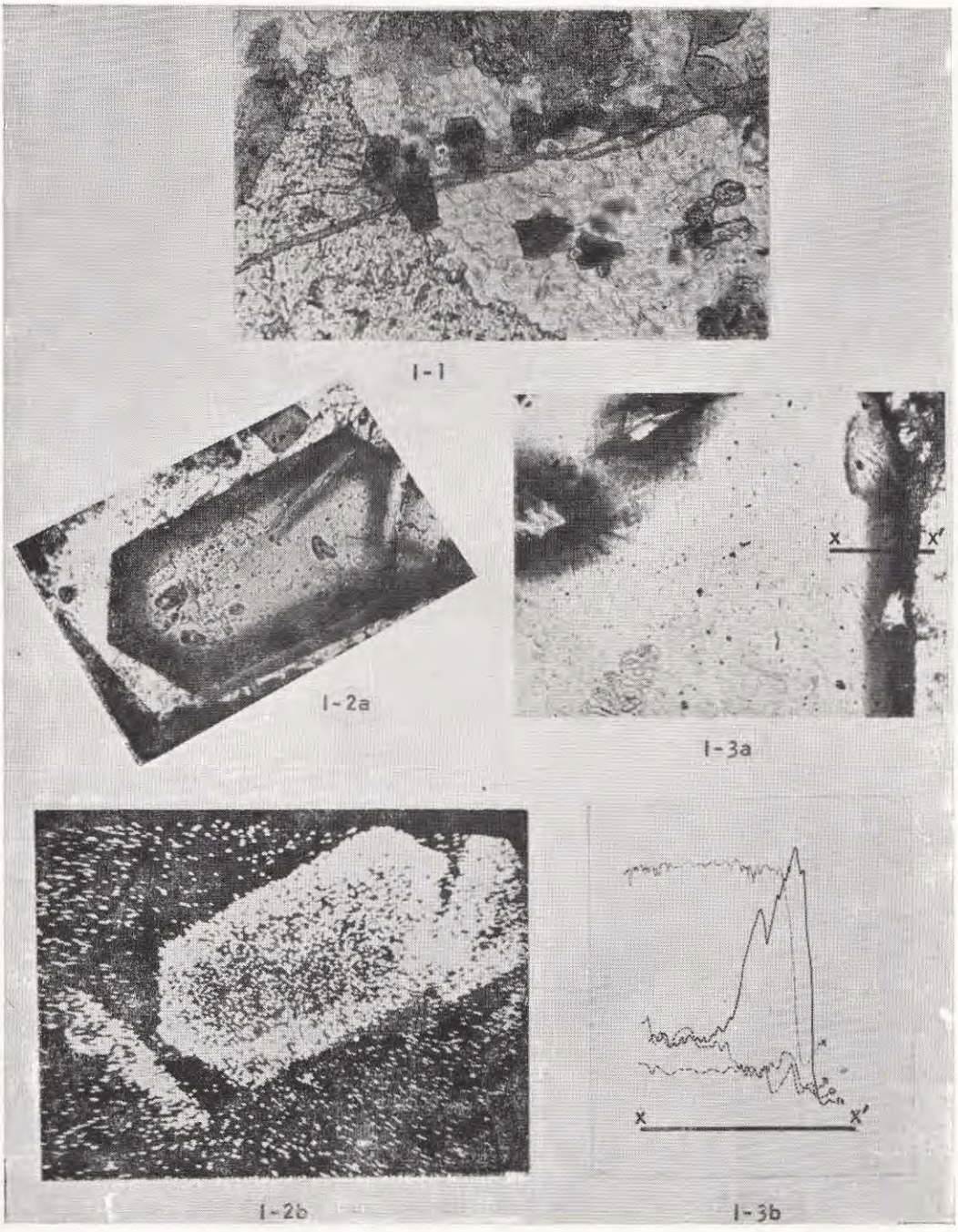

I-1

I-2a

I-3a

I-2b

I-3b

thin-polished sections or on powder mounts. Canada balsam, "Lakeside" cement and cold set mounting medium consisting of three ingredients: plastic polylite TT9-147, catalyst lupersol DDM, and accelerator A were used in sample preparation. Mr. H. Hay prepared most of the mounts.

The minerals that were studied in powder mounts were concentrated in heavy liquids. Separation of different mineral varieties and of grains containing inclusions from relatively clean grains was also accomplished in closely controlled heavy liquids which approached the required grains in specific gravity.

The concentrates (−100+150 mesh fraction) were mounted in a drop of a cold set medium on the glass slide and four standards of similar size fraction were mounted in separate drops on the same slide at each corner for comparsion. After being allowed to harden, the mounts were ground and polished until the selected grains were exposed at the surface of the mount and well polished. The method was satisfactory for blocky minerals but not too good for flaky micaceous minerals and for thin crusts and cleavage-coatings, because in the thin-polished section, and in a powder mount one can not be sure that the desired object is definitely exposed at the surface. To ensure that a selected inclusion or a crust is at the surface, the tiny object itself, such as a crust approximately 1–2 microns thick (Plate II, Fig. II-2) was glued to the surface of the mount and analysed after coating the glass with an aluminium or copper film.

Variations in the concentration of elements were studied using an Elion electron probe microanalyser. Two air path spectrometers and one vacuum path spectrometer permitted simultaneous detection of three elements. The relative intensities of the elements were determined by scanning the electron beam along a line and recording the detector outputs as a function of time. Because it was desired to study the distribution of more than three elements, and in order to relate successive line scans, the element iron was selected as a scanning standard, (i.e. one spectrometer was set to detect iron and remained in this position for all scans). Maximum differences in intensities (Plate IV, Fig. IV-4) were determined by spotting the electron beam on the highest and lowest intensity regions of the line scans, taking two "100 seconds" counts and subtracting normal background. Although chemical analyses were available for

PLATE II

II-1. Basal intergrowths of phlogopite (pale grey) and biotite (dark grey). Some of the basal fractures are coated with opaque crusts. Mica from lamprophyre *9*, x 500.

II-2. Crusts and needle-like aggregates on the basal face of mica, x 500.

II-3. Oriented inclusions in the core of phlogopite *5*. Most of the needles and the platy inclusions are less than one micron in thickness, x 100,+Nicols.

II-4. Braided rows of orthoclase rods concentrated predominantly in one twin lamella of plagioclase, An_{45} from anorthosite, Quebec. x 500,+Nicols.

II-5. Small inclusions of potassium feldspar densely concentrated in one area of plagioclase crystal (most of the microscope field to the right). Small area at left contains only a few rows of potassium-bearing inclusions and a fracture. Black specks in potassium-rich area is mainly hematite. The heterogeneous distribution of potassium feldspar in the plagioclase crystal is illustrated in Fig. III-1. Plagioclase from anorthosite, Quebec, x 500.

II-6. Replacement of plagioclase by potassium-bearing minerals : potassium feldspar and mica. One of the twin lamellae is more affected than the other. Plagioclase from diabase, Ontario, x 500.

II-7. Partly fused inclusions of potassium feldspar in plagioclase An_{45}; 150 mesh fraction of sample illustrated in Figs. II-4 and II-5, heated 21 hours at 1200°C. Left edge of the grain is almost entirely fused.

II-8. Striated (lamellar) appearence of plagioclase that is partly altered to sericite and chlorite, and carries inclusions of apatite. The c-axis of apatite lies roughly parallel to striations of the plagioclase. The plagioclase lamellae differ in refractive index, and thus in chemical composition. An enlarged portion (x 500) of such a striated plagioclase is illustrated in the upper left corner and in Fig. III-3. Plagioclase from diabase, x 100.

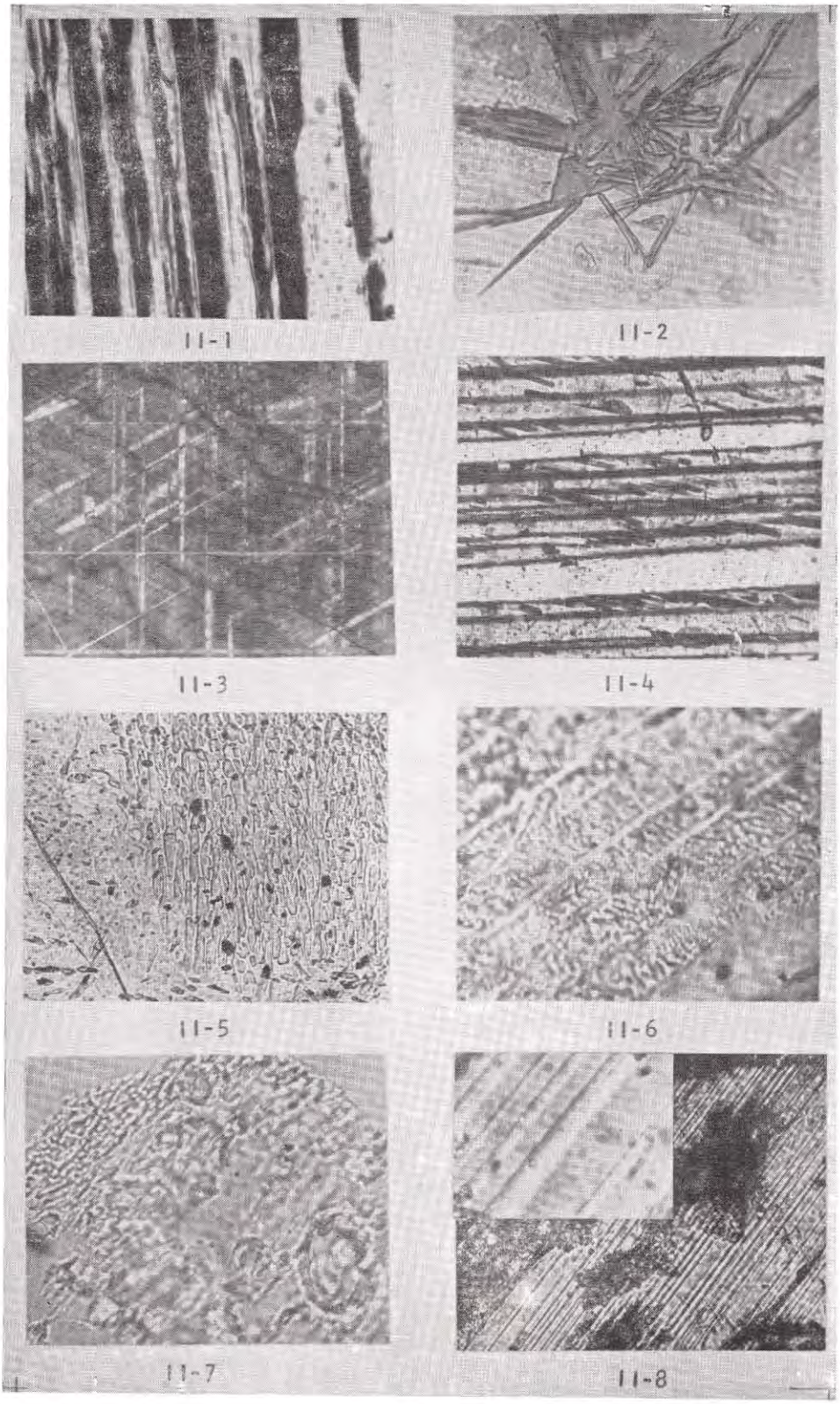

II-1

II-2

II-3

II-4

II-5

II-6

II-7

II-8

comparison on some minerals, the electron probe results are considered semi-quantitative.

ZONED PHLOGOPITES AND OTHER MICAS

The relationship between the chemical composition of micas and their sequence of crystallization in lamprophyres has been discussed by Rimsaite (1964). In rocks containing more than one generation of micas, two modes of occurrence were observed. In the first, the early phlogopite phenocrysts and late biotite in the groundmass occur as distinctly separate crystals (Plate I, Fig. 1–1). In the second, in addition to early phlogopite and late biotite some crystals are zoned, consisting of phlogopite in the cores and biotite towards the margins. Patches of enclosed groundmass and foreign grains in the phenocrysts are also surrounded by dark rims (Plate I, Figs. 1–2a & 3a). Some lamprophyres are composed predominantly of rimmed phlogopites (lamprophyre *35*), while others contain phlogopite and biotite in separate grains, with less distinct zoned crystals and basal intergrowths of the two phases (Plate II, Fig. II–1. phlogopite *9Ph* and biotite *9B*).

Practically all rocks are affected by alteration, resulting in partly altered heterogeneous minerals. Micas are affected by two main types of alteration : hydration which is accompanied by the loss of alkalies, and dehydration (Rimsaite, 1964). Partly altered micas are most affected along the basal cleavage planes and along the margins. The leached elements usually crystallize at the surface of the altered mica forming new minerals, such as chlorite, sphene, anatase, potassium feldspar, iron oxides, or crusts consisting of fine-grained aggregates, including clay minerals (Rimsaite, 1957).

Average chemical composition, unit cell contents and constants, and some other properties of phlogopites *5*, *9ph* and *35*, and of biotite *9B* are presented in Table 1. An x-ray scanning image of the iron distribution in a small phlogopite phenocryst in lamprophyre *35* and some pen recorder traces across the border of a double rimmed coarse phlogopite showing the distribution of iron, potassium, chromium and titanium are illustrated in Figs. I-2b and I-3b, respectively. Traverses along the basal planes of a large and small mica crystals from lamprophyre *9* showed that most of the small dark brown and green biotite crystals contain less iron in the core than at the margin. However, the difference in iron content in the core and at the margins is less striking in small biotite crystals than in large phlogopite phenocrysts.

PLATE III

III-1. Heterogeneous distribution of potassium in andesine An_{45} from anorthosite. Parallel rows of potassium feldspar rods (right) and potassium-rich patch (centre).
(a) Photomicrograph, x 35.
(b) X-ray scanning image, potassium K-alpha radiation, x 100.

III-2. Heterogeneous distribution of potassium in andesine An_{45} from anorthosite. Oriented rod-like inclusions of potassium feldspar, and minor mica, in parallel rows. The directions of the rows intersect at angles of 50°, 53°, 66°, 80° and 134°, respectively. A bundle of densely packed roughly parallel rods can be seen in the upper right field.
(a) Photomicrograph, x 35.
(b) X-ray scanning image, potassium K-alpha radiation, x 100.

III-3. Distribution of calcium, potassium and iron in striated (lamellar) plagioclase from diabase.
(a) Photomicrograph, x 500, right ; x 100, left.
(b) Element concentration obtained from a line scan across apatite inclusion and the feldspar lamellae, x 150.

III-4. Distribution of titanium and iron in ilmenite-hematite intergrowths from anorthosite.
(a) Photomicrograph. Ilmenite dark grey, hematite light grey. Wide, intermediate and thin lamellae are illustrated, x 500.
(b) Element concentration obtained from a line scan across thin and intermediate lamellae of hematite in ilmenite, x 1000.

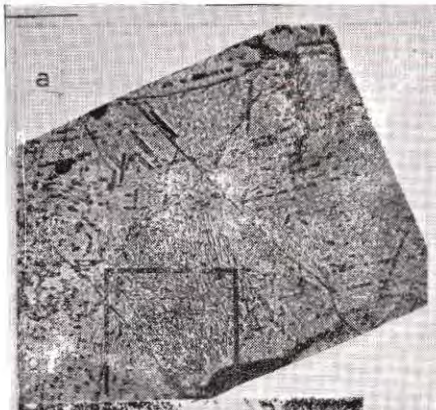

III-1

III-2

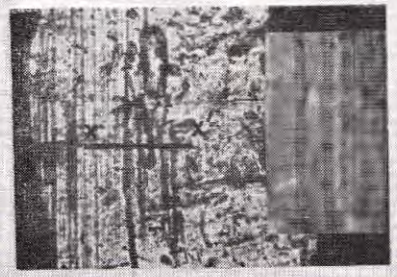

III-3a

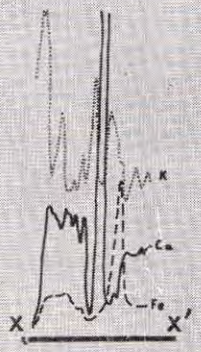

III-3b

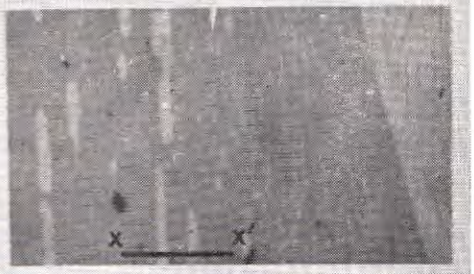

III-4a

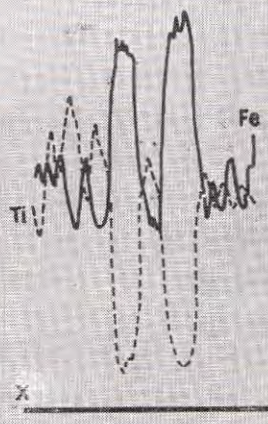

III-4b

Electron probe line scans perpendicular to the basal cleavage of phlogopite *9* showed considerable variation in the concentrations of iron, calcium and potassium, particularly in partly altered phenocrysts. The intensities of iron and titanium increased slightly across dark grey, uniform pleochroic haloes.

The bulk chemical analyses (Table I) of the two phlogopites from lamprophyres are very similar, but phlogopite *35* which is the principal constituent of its rock, contains more water, fluorine and barium than phlogopite *9*.

The difference in chemical composition between the core and the rim in a single phlogopite phenocryst (Plate I, Figs. 2 and 3) is even more striking than the differences obtained on bulk specimens of early phlogopite and late biotite (Table 1). The contents of iron in octahedral sites in light buff phlogopite *9* and in dark brown biotite *9* are 15 and 55 per cent, respectively, determined from the optical and x-ray diffraction properties using available curves (Rimsaite, 1962). This difference in iron content between the early and late micas *9Ph* and *9B* compares well with the differences between the core and the rim in phlogopite *35* obtained by means of the microprobe analysis (Plate I, Fig. 1–3b). Similar differences in chemical composition between the core and the rim were obtained on rimmed phlogopites from lamprophyres be Métais and associates (Métais *et al*, 1962). It is interesting to point out that the outermost part of the opaque rim apparently does not contain any potassium, and thus is not mica. At approximately two microns from the edge, the potassium content increases, and remains relatively uniform along the traverse towards the centre. The outermost dark border may be similar to "opacite" which Tröger (1955) describes as magnetite and pyroxene formed as a result of dehydration during extrusion. Chromium and titanium show similar behaviour to that of potassium, increasing slightly further from the edge than iron. The concentration of titanium is somewhat higher between the opaque and dark rims. Chromium shows an inverse variation to that of iron and increases in the core of the phlogopite. Since chromium does not show any erratic variation, but rather a gradual increase, it appears to be present in the mica lattice, not in inclusions. Calcium, and to some extent, titanium, show erratic variations, especially in partly altered grains that contain inclusions. Calcium is present predominantly in inclusions, while titanium is present in inclusions as well as in the phlogopite lattice. The bright reddish colour of phlogopite is related to the titanium content. In dull greenish, and pale discoloured patches, the intensity of the titanium line decreases to less than one half of that in the unaltered portion of the phlogopite.

There is no direct means of checking the distribution of water in the mica flakes. However, the variation in potassium content and differences in colour in different portions of the mica flake, strongly suggest variations in water content and also in the oxidation state of iron.

The presence of chlorite and serpentine in fractures in the lamprophyres, and the formation

PLATE IV

IV-1. Euxenite that shows variations in colour from deep red (black) to almost colourless (white veins in the lower part of the photograph), x 100.

IV-2. Inclusion of colourless mica in a fracture of euxenite. At the mica-euxenite contact there is a double rim : deep red (black) adjacent to mica and colourless euxenite band adjacent to a normal, brownish euxenite, x 500.

IV-3. A fragment of a crust from the surface of the euxenite. The crust is reddish-brown and contains minute blisters, anisotropic flakes and specks, x 500.

IV-4. Relative abundance of euxenite components in fresh, leached and secondary euxenite and in the crusts obtained directly from intensities of selected elements. Average concentrations of the elements, determined on bulk sample, are given for comparison.

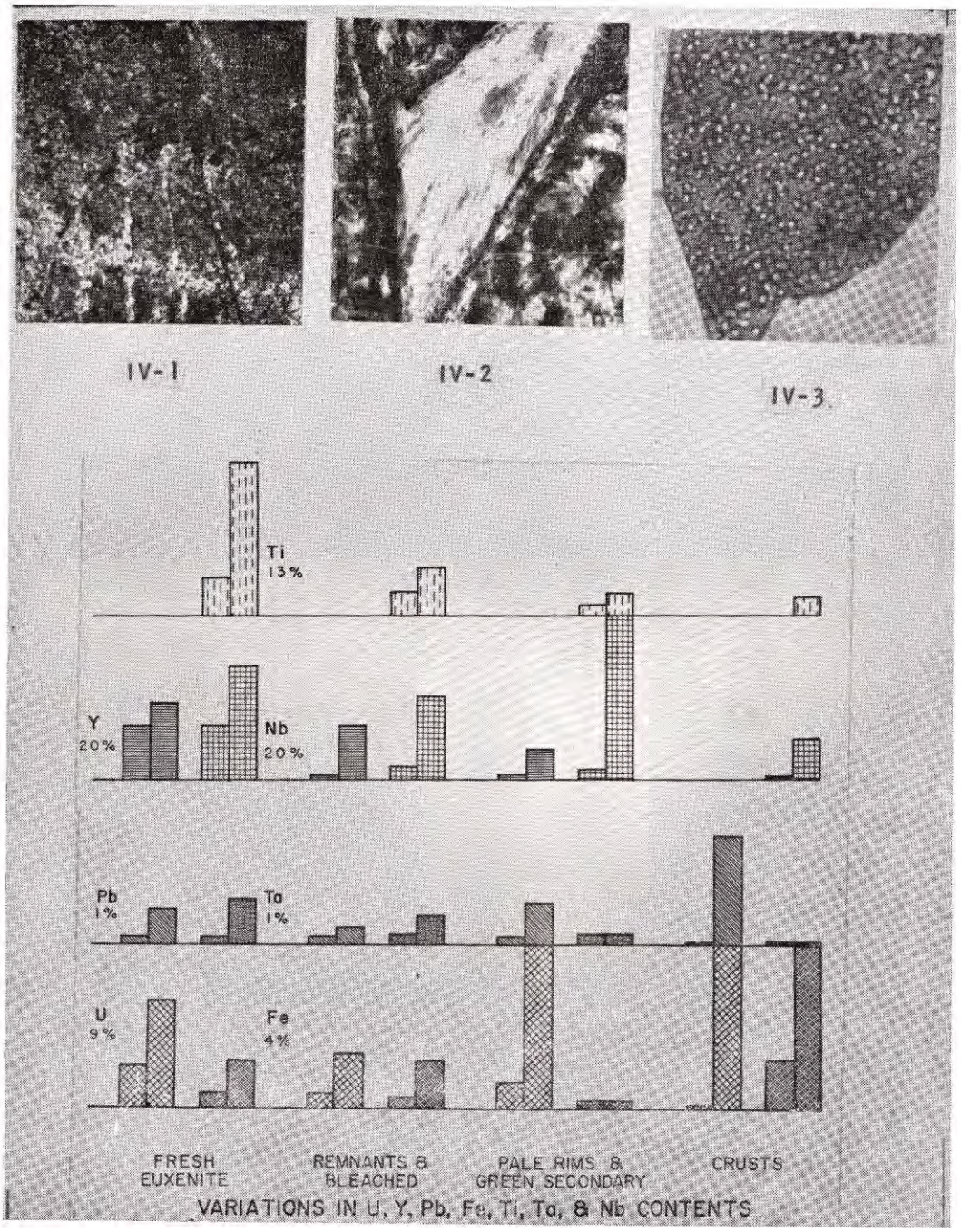
IV-1
IV-2
IV-3
Ti
13%
Y
20%
Nb
20%
Pb
1%
Ta
1%
U
9%
Fe
4%
FRESH EUXENITE
REMNANTS & BLEACHED
PALE RIMS & GREEN SECONDARY
CRUSTS
VARIATIONS IN U, Y, Pb, Fe, Ti, Ta, & Nb CONTENTS

TABLE 1

Bulk chemical composition and some physical properties of micas

% (p.p.m.)	Phlogopite *5*		Micas *9*		Phlogopite *35** some flakes rimmed
	clear rim	core with inclusions	phlogopite	biotite	
X-Ray Spectrographic Analysis					
Total Fe as FeO	2.6	3.0	9.8	16.0	7.0
TiO_2	0.36	0.9	1.7	3.1	2.2
Cr_2O_3	0.05	0.05	0.7	0.1	0.65
NiO (ppm)	70.	100.	450.	100.	1000.
K_2O	9.5	10.4	8.8	7.6	9.4
CaO	0.2	0.4	1.3	2.5	0.75
SrO (ppm)	50.	70.	250.	420.	210.
Rb_2O (ppm)	450.	570.	700.	570.	625.
Classical Chemical Analysis					
SiO_2	39.12		41.34		38.70
Al_2O_3	18.24		14.94		12.56
TiO_2	0.54	0.83	1.43		2.16
Fe_2O_3	0.96		1.82		1.66
FeO	1.27		6.15		5.95
MgO	24.47		18.11		21.17
MnO	0.03		0.07		0.13
Cr_2O_3	0.02		0.93		0.80
NiO	—		0.03		0.07
K_2O	9.46		9.12		9.20
Na_2O	0.34		0.55		0.27
CaO	0.26		0.68		0.52
BaO	0.25		0.54		1.31
H_2O+	2.88		2.94		3.20
H_2O^-	0.32		0.08		—
F	2.28		0.74		1.82
P_2O_5	0.06		0.05		—
Total	100.5		99.52		99.52
Less O=F	0.96		0.31		0.76
Net Total	99.54		99.21		98.76
Optical Properties					
γ	1.580	1.580	1.606–1.608	1.628–1.642	1.602–1.646
α	1.544	1.544	1.564–1.570	1.564–1.590	1.566–1.596
2V°	4–6	6	4–17	4–9	2–20
S. G.	2.745	2.800 (var)	2.956 (var)	3.030 (var)	2.948–2.985
Age in m.y.			1720		1395

* Chemical analysis of phlogopite *35* by J. A. Maxwell, S. Abbey, J. L. Bouvier and J. G. Sen Gupta. Other data from Rimsaite (1964).

Layer Contents	Phlogopite *5*		Micas *9*		Phlogopite *35* some flakes rimmed
	clear rim	core with inclusions	phlogopite	biotite	
Unit Cell Contents, Occupancy and Layer Charge					
Si	5.5		5.74		5.72
IV Al	2.5		2.26		2.18
Ti	—		—		0.10
Occupancy	8		8		8
Charge (–)	2.5		2.26		2.18
Al	0.52		0.27		—
Ti	0.06		0.17		0.13
Fe^{3+}	0.10		0.20		0.18
Fe^{2+}	0.14		0.77		0.73
VI Mg	5.12		4.08		4.64
Mn	0.004		0.004		0.02
Cr	—		0.12		0.09
Ni	—		0.003		0.01
Occupancy	5.94		5.61		5.80
Charge (+)	0.62		0.15		0.13
Na	0.10		0.08		0.08
Ca	0.04		0.09		0.08
K	1.70		1.78		1.73
Ba	0.02		0.03		0.08
Rb	—		0.01		—
Occupancy	1.86		1.99		1.97
Charge (+)	1.90		2.12		2.13
O number	20.14		20.41		20.01
0–20	0.14		0.41		0.01
Anions OH	2.70		2.82		3.13
F	1.02		0.36		0.85
OH+F	3.72		3.18		3.98
4-(OH+F)	0.28		0.82		0.02
Impurities**	clean	apatite calcite rutile	chlorite 2% quartz 2% albite 3%	chlorite epidote apatite	clean dark rims apatite tr
Unit Cell Constants (in Å)					
a (± 0.01)	5.30	5.32	5.34	5.34	5.33
b (± 0.01)	9.20	9.20	9.26	9.22	9.25
c (± 0.02)	10.12	10.12	10.24	10.24	10.22
β (± 30′)	99°48′	100°34′	100°6′	100°10′	100°7′
Structure: Single layer monoclinic hemihedral					
Space group	C_m	C_m	C_m	C_m	C_m

** Structural formulas calculated after correcting for the impurities.

of biotite and serpentine after crystallization of the feldspar in lamprophyre *9*, suggest that a high vapour pressure existed in such rocks during the late stages of crystallization. Phlogopite phenocrysts are locally altered along basal cleavage planes to chlorite, and small brown biotite crystals are overgrown by green biotite and chlorite. Bulk chemical analyses of the early phlogopite *9* indicates a considerable deficiency of the (OH,F) group. The dehydrated phlogopite *9* therefore was not rehydrated at the time of formation of the later hydrated minerals. It is important to point out that chemical analyses of dehydrated and subsequently chloritized phlogopites and biotites can be mistaken for those of normal micas because the deficiency of water in dehydrated portions can be balanced by water in the chloritized portion.

The most reliable test for detection of chlorite in intergrowths with mica is x-ray diffraction analysis of representative oriented samples (not just of one or a few selected flakes) by means of a diffractometer or by means of the Debye–Scherrer camera specially designed for the analysis of flaky minerals by Jasmund (1950). X-ray beam scans across mica flakes indicate variations in potassium content which in many cases are the result of alteration to chlorite.

No structural differences were observed between zoned phlogopites and late biotites on x-ray diffraction Weissenberg photographs. The [100] and [010] patterns of selected mica flakes showed streaky and diffuse reflections, and indicated a single layer monoclinic hemihedral structure, found to be most common among biotites by Hendricks and Jefferson (1939).

Another type of heterogeneity, in phlogopite *5* consists of apparent zoning caused by a clear rim and a heterogeneous core, crowded with oriented inclusions (Plate II, Fig. II–3). The inclusion-rich core contains about twice as much titanium and calcium as the clear rim (Table 1). Coarse prismatic inclusions in phlogopite *5* were identified optically as rutile. Some strongly birefringent platy inclusions that could be separated from mica, gave a calcite x-ray powder pattern and dissolved with effervescence in hydrochloric acid. However, thin, roughly hexagonal plates (1 micron thick), resembling micas could not be positively identified. They did not give any x-ray diffraction pattern and apparently were destroyed during electron probe microanalysis.

Opaque and yellow transparent crusts that coat fractures in minerals are very common in micas. The crusts were studied in phlogopite *9*, (Plate II, Fig. II–1) and in unrelated muscovites and biotites. Electron probe microanalyses of thin (1 to 3 micron) alteration crusts on cleavage planes of micas showed that the intensity of the iron K-alpha line increased by a factor of more than 10 in traverses from the mica into the crust while the intensity of the potassium K-alpha line decreased by 20 to 30 per cent. Most of the crusts that coat fracture surfaces of micas were found to contain high iron and low calcium, nickel and titanium. One black, opaque crust removed from muscovite contained high sulphur in addition to iron, and by means of x-ray diffraction analysis it was identified as pyrrhotite. It is interesting to point out that the pyrrhotite crusts did not give any extra reflections on the x-ray diffraction patterns of the host mica.

The optical method still remains the most sensitive for the detection of zoning, intergrowths, acicular inclusions and very thin crusts along the fractures of micas. Although the detection of inclusions is possible in oriented x-ray diffraction photographs, in most cases the pattern is only that of the host mica.

"ANTIPERTHITIC" AND LAMELLAR FELDSPARS, AND ASSOCIATED MINERALS

Two types of heterogeneous feldspar, "antiperthitic" plagioclase (Plate II, Figs. II–4 & 5) and lamellar feldspar (Plate II, Fig. II–8) were studied in order to determine the differences in chemical composition between the intergrown minerals. "Antiperthitic" plagioclases, with the host ranging in composition from oligoclase to labradorite, were observed in diverse rocks

from across Canada. The striking examples were found in anorthosites and gneisses of Quebec.

The "antiperthitic plagioclase, KA-846, selected for the present study contains inclusions of pyroxene, biotite, muscovite, ilmenite-hematite and other opaque grains, in addition to potassium feldspar. Ferromagnesian inclusions, and muscovite associated with oriented inclusions of potassium feldspar, in plagioclase have been illustrated by Rimsaite (1964, Fig. 2). Analytical results obtained on the feldspars are presented in Table 2 and in Plate III, Figs. 1 to 3.

TABLE 2

Calcium and alkali contents, and some physical properties of feldspars

	"Antiperthitic" Feldspar KA-846		Lamellar Feldspar KA-930		
Sp. G.	$<2.677 \overset{=}{>} 2.665$	$\overset{=}{<} 2.665$*	>2.652	2.652†	<2.652
Highest Refractive Indices on (010) Fragments					
Most fragments	1.556	1.554	1.560	1.550	1.540
Few extremely high	1.560	1.560	1.570	1.560	1.552
Lowest (inclusions)	1.518	1.518	1.520	1.520	1.520
An content (opt)	45-52	44-52	48-70	27-52	5-42
Chemical Analysis §					
CaO	9.61	9.21	8.11	5.04	2.80
Na_2O	5.47	5.02	5.89	6.83	7.40
K_2O	0.74	1.11	1.16	2.10	3.39
Composition of Feldspars Calculated from Chemical Analyses					
An	48	46	40	25	14
Ab	46	43	49	58	63
Or	4.5	7	7	12.5	20
Ratios					
An/Ab	1.03	1.08	0.82	0.44	0.22
An/Or	10.1	7.1	5.9	2.0	0.7
Ab/Or	11.2	6.4	7.1	4.7	3.1

* Plagioclase and potassium feldspar patterns were obtained on x-ray diffraction charts and in oriented crystal photographs. Refractive indices of plagioclase did not change after heating 21 hrs. at 1200°C, while potassium feldspar partly fused (Plate II, Fig. II-7).

† Fine-grained suspension of secondary sericite and chlorite identified by means of the x-ray diffraction analysis was separated from the feldspar before the chemical analysis was performed.

§ By S. Abbey.

Plagioclase KA-846 contains parallel oriented inclusions and some irregular patches of alkali feldspar. The oriented inclusions are elongated rods with rounded to almost square cross sections and plates, some of which resemble blebs and spindles. The inclusions lie on straight, roughly parallel lines; or in slightly curved rows, particularly in strained plagioclase. The directions of the rows of inclusions intersect one another at 50°, 53°, 66°, 80° and 134° on the (010) face of the host. Most of the inclusions extinguish almost simultaneously with the host, but some, particularly in strained crystals, show considerable deviations, *i.e.* extinction angles between coarse blebs and the host reach 1.2°, between long rods and the host 13°, and between different types of inclusions 12°. Irregular patches are composed of densely concentrated irregular blebs, or of roughly parallel bundles of rod-like inclusions (Plate II, Fig. II–5 and Plate III, Figs. III–1 and 2).

It is interesting to point out that some coarse, slightly strained plagioclase crystals contain both types of parallel oriented inclusions and, in addition, potassium rich patches resembling relics of alkali-rich inclusions (Fig. III–1 a & b). The patches contain over 50 per cent potash feldspar. Such a concentration of potassium by the diffusion process from the host plagioclase seems improbable. It also does not resemble replacement, but appears to be a partly digested former potassium feldspar, recrystallized into small irregular blebs.

An attempt was made to concentrate inclusion-rich and inclusion-poor fractions of plagioclase for chemical analysis. Heavy liquid separation of fragments containing only a few inclusions of alkali feldspar from those containing abundant inclusions was only partly successful because of a high concentration of heavy opaque inclusions associated with the alkali feldspar inclusions. However, the results in Table II indicate that the lighter, inclusion-rich fraction contains more potassium and less calcium than the heavy fraction. The anorthite/albite ratio is almost the same in the heavy and light fractions, in agreement with the observation that the inclusions consist mainly of potassium feldspar and some micas. Semi-quantitative electron microprobe analysis showed that the alkali feldspar is more than ninety percent potash feldspar, and that potassium is virtually absent in the plagioclase host. It is interesting to point out that a staining test for potassium described by Dawson and Crawley (1963), applied to "antiperthite" KA-846 by Mr. W. D. Crawley in powder mounts and in thin sections was unsuccessful. The potassium feldspar did not stain.

In addition to "antiperthitic" plagioclase, anorthosite contains minor quantities of feldspar grains that are composed of different feldspar varieties in parallel intergrowths, resembling lamellar twinning, the latter type being far more common in diabase dykes.

Lamellar feldspar KA–930 selected for the present study is from a diabase dyke, Sudbury district, Ontario. The feldspar is locally altered to fine-grained chlorite and sericite aggregates, and contains numerous apatite inclusions. Although the chemical analyses (Table II) indicate considerable differences in composition of the three fractions of specimen KA–930, the actual differences in composition are much greater. As shown by the optical measurements (Table II), the anorthosite content varies from 5 to 70 per cent. These values were confirmed by electron probe micro-analyses. A line scan for potassium, calcium and iron across the lamellae is reproduced in Plate III, Fig. III–3b.

It is interesting to note that iron-rich and calcium-rich inclusions in the plagioclase are surrounded by envelopes of potassium feldspar. Similar envelopes have been observed around disintegrating biotite (Rimsaite, 1964, Fig. 4).

Associated Minerals

Plagioclase KA–846 contains inclusions of hematite-ilmenite which are composed of irregular lamellæ of hematite and ilmenite, 50–70 microns in width. Furthermore, hematite lame-

llæ contain rods and streaks of ilmenite, and the ilmenite contains oriented inclusions of hematite (Plate III, Fig. III–4), resembling in appearance the "antiperthitic" plagioclase. The hematite with inclusions of ilmenite (Fig. III–4a, light grey portion with dark grey inclusions in the right field) shows only the hematite x-ray diffraction powder pattern. Electron probe line scans across the ilmenite lamella with inclusions of hematite are illustrated in Plate III, Fig. III-4b. The concentration of titanium shows inverse variation to that of iron, and the difference in concentration of these two elements is more prominent in coarse hematite inclusions than in very narrow ones.

Lamellar plagioclase KA-930 is associated with biotite and an opaque mineral which occur in finger-like intergrowths. Electron probe line scans showed that the ore mineral consists of high iron and titanium, and only a trace of nickel. The ore mineral is probably titaniferous magnetite, containing a fairly uniform distribution of iron and titanium.

EUXENITE AND ASSOCIATED FELDSPAR

The present study is an extension of previous mineralogical studies (Robinson *et al*, 1963). A pegmatite, located near St. Pierre de Wakefield, Quebec, *ca* 30 miles NE of Ottawa, consists mainly of pale blue-green amazonite, pink stained microcline, and albite, with accessory euxenite, tourmaline, hornblende, purple fluorite, mica, native bismuth and bismuthinite. Most of the minerals are fractured and locally coated with the secondary minerals: hematite, goethite, micaceous clay and chlorite. The feldspar that surrounds euxenite contains numerous fractures coated with red crusts, and at the euxenite contact it is altered to micaceous clay.

The euxenite is transparent in thin fragments and varies in colour from deep red, through brownish, orange and yellow to almost colourless. The variation in colour is partly a result of the variation in chemical composition during crystallization, and partly the result of alteration. In reflected light the euxenite exhibits a mottled appearance as a result of variations in the reflectivity power of these different varieties. The euxenite is traversed by fractures which are usually coated with iron oxide crusts and filled with other minerals, such as feldspar, mica and fluorite (Plates IV and V). The heterogeneous and fractured character of euxenite and related mineral lyndochite from other localities was observed by Ellsworth (1926, 1927), who was unable to obtain entirely clean fragments for chemical analysis. Ellsworth also found that the silica content of euxenite increased with increasing alteration.

In the previous work by Robinson *et al* (1963) an attempt was made to seperate fresh-looking euxenite from altered, bleached material that occurs along grain boundaries and fractures. The separation was poor because the variations in the appearance and alteration state are on too small a scale for any of the tools available for mineral-separating; in some areas the changes take place within a few microns. A narrow rim of colourless euxentie that exhibits low reflectivity is illustrated in Plate IV, Fig. IV–2, and a small area of heterogeneous euxenite is shown in Plate IV, Fig. IV–1. The presence of iron-rich, lead-bearing crusts along fractures in euxenite and at the euxenite-feldspar contact, and differential loss of uranium and lead were observed in the previous study.

The present study is concerned with the determination of variations in the chemical composition of euxenite in fresh and altered areas, with special emphasis on intergranular reactions and leaching and re-deposition of leached elements within the euxenite and along fractures in the host feldspar. Semi-quantitative electron microprobe analyses were performed on euxenite in thin and polished sections and on selected euxenite fragments and crusts mounted directly on glass slides.

The generalized composition of euxenite is given by $AB_2(O,OH)_6$. As can be seen from Table III, component "A" of euxenite consists predominantly of yttrium with minor uranium, calcium and lead, as well as of rare earths.

V-1a

V-2a

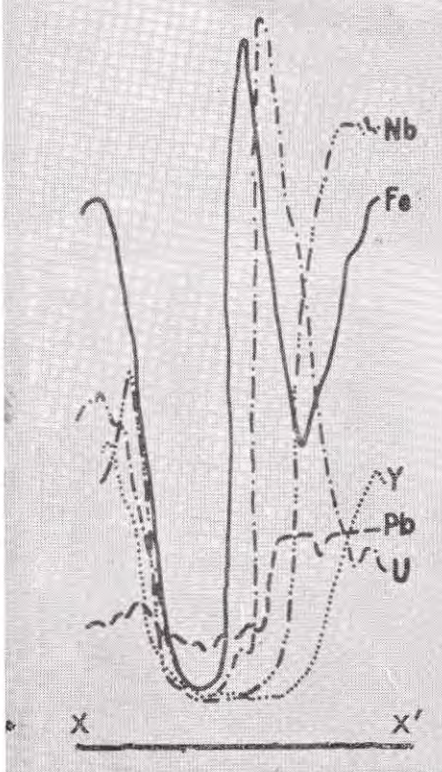

V-1b

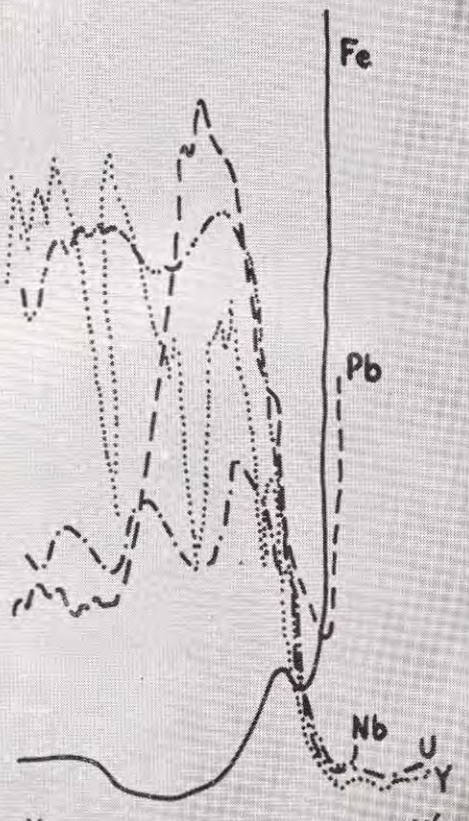

V-2b

Component "B" contains almost equal proportions of niobium and titanium, some ferric iron and tantalum, and traces of manganese and ferrous iron. Traces of silica, alumina and copper found by emission spectrographic analysis are probably due to impurities.

The cations composing euxenite have predominantly an oxyphile character, with the exception of iron and lead, which have also strong siderophile and chalcophile properties. All these elements are soluble in the form of bicarbonates or hydroxides. They could thus be removed from the euxenite lattice, transported in solution or in colloidal suspension and precipitated as hydrolysates, which through dehydration could form secondary oxides and niobate-titanates.

In order to trace a geochemical cycle of the euxenite cations and interpret their distribution in altered euxenite and in newly-formed products, it is important to know the magnitude of their variations in apparently fresh euxenite. These variations are illustrated in the first four columns of Fig. IV-4, Plate IV. The cations of group "B" (iron, titanium, niobium, etc.) exhibit the most prominent variations. The red variety of euxenite contains more titanium, uranium and lead, and less niobium and yttrium than the pale yellow variety. X-ray diffraction powder patterns of ignited yellow and red euxenite are similar. The strongest lines and bands compare reasonably well with those published by Arnott (1950).

Secondary pale yellow to colourless rims that surround fractures filled with colloform greenish crusts, mica and other minerals, were found to be low in iron, titanium and yttrium, whereas niobium and uranium showed erratic variations. The intensity of the uranium line in one fracture approached that of pure uraninite; and small irregular grains of columbite that appears to be secondary were observed in other fractures. Mottled purple-white fluorite, cyrtolite and thorite were found near the euxenite-feldspar contact. They do not seem to be alteration products of the euxenite.

Crusts surrounding the euxenite grains and coatings in fractures consist predominantly of iron oxides. Some brown speckled crusts containing tiny mica-like birefringent crystals, contain small quantities of yttrium and titanium, and erratically distributed uranium and lead. Greenish colloform crusts are also locally enriched in uranium and lead. X-ray diffraction powder patterns of unheated and ignited crusts, showed reflections only of hematite, goethite and mica. Uranium and lead apparently adsorbed on iron-rich crusts, did not cause any additional lines on the x-ray diffraction powder pattern, probably as a result of small grain size and low concentration of the secondary compounds.

The distribution of uranium, lead, yttrium, niobium and iron in relatively fresh and in remnant euxenite, and the concentration of these elements along euxenite-fluorite and

PLATE V

V-1. Distribution of U, Pb, Y, Nb and Fe in reasonably fresh euxenite, at the euxenite-fluorite contact, in mottled purple-white fluorite, and in a small euxenite remnant enclosed in fluorite.

(a) Photomicrograph showing euxenite host (right, grey, high relief) with inclusion of purple fluorite (white with black patches, from centre towards left), and a small slightly elongated inclusion of euxenite in the fluorite veinlet. A white double rim can be seen at the contact of fluorite and the euxenite, x 200.

(b) Element concentration obtained from a line scan. This scan started in host euxenite (right), across fluorite to small euxenite remnant in fluorite, left, x 500 (A higher magnification, x 1000, was used across the edge in order to show the resolution between iron and uranium peaks).

V-2. Distribution of U, Pb, Y, Nb and Fe at the euxenite-feldspar contact.

(a) Photomicrograph showing dark mottled euxenite crystals in fractured feldspar, x 80.

(b) Element concentration obtained from a line scan across the euxenite-feldspar contact, (from euxenite, left, to feldspar, right). Lead shows two peaks: one in euxenite approaching the edge, the other in iron-rich crust. The scans for Fe, Pb and Nb end in the crust; x 200.

euxenite-feldspar contacts, is illustrated in Plate V, Figs. 1 and 2. In Plate V, Figs. V-la and b, the electron probe line scans show that uranium is enriched in a rim adjacent to the host euxenite, and is depleted in an outer iron-rich crust adjacent to fluorite; lead remains reasonably constant in the euxenite and in uranium-rich rim, but sharply decreases in the iron-rich crust; niobium and yttrium are virtually absent in the uranium-rich rim, adjacent to the euxenite; and iron and yttrium show progressive decrease in euxenite as the edge of the grain is approached. The edge-effects are less noticeable in the small remnant of euxenite enclosed in fluorite than in the main euxenite host, and the concentration of lead in relation

TABLE 3

Bulk chemical composition of euxenite and ionic proportions $[AB_2(O,OH)_6]$

X-Ray Fluorescence Analysis*		Ionic Proportions					Ionic and Atomic Radii §			
Oxide	%				Occupancy %	Charge		Radius kX		Radius kX
U_3O_8	11.	A	U	0.1	9	0.27	U^{4+}	1.05 (0.89)	U	1.38
ThO_2	3.		Th	0.04	3	0.16	Th^{4+}	1.10	Th	1.80
PbO	1.		Pb	0.02	2	0.04	Pb^{2+}	1.32	Pb	1.75
Y_2O_3	26.		Y	0.84	80	1.32	Y^{3+}	1.06	Y	1.81
Ca	2.		Ca	0.12	6	0.24	Ca^{2+}	1.06	Ca	1.96
				1.12	100	(+) 2.03				
Nb_2O_5	29.	B	Nb	0.74	38	3.70	Nb^{5+}	0.69	Nb	1.43
Ta_2O_5	1.		Ta	0.02	1	0.10	Ta^{5+}	0.68	Ta	1.43
TiO_2	22.		Ti	0.96	48	4.80	Ti^{4+}	0.64	Ti	1.46
FeO†	0.1						Fe^{2+}	0.83		
Fe_2O_3†	5.4		$Fe^{3\pm}$	0.24	12	0.72	Fe^{3+}	0.67	Fe	1.24
MnO	0.5		Mn	0.02	1	0.04	Mn^{2+}	0.68	Mn	1.36
				1.98	100	(+) 9.36				
H_2O†	2.18		OH	0.43	7	0.43				
F†	0.13		F	0.02	1	0.02				
			O	5.48	92	10.96				
				5.93	100	(—) 11.41				
			Total (—) charge			11.41				
			Total (+) charge			11.39				

* By Mrs. M. E. Bartlett and G. R. Lachance. In addition, semiquantitative emission spectrographic analysis reported by W. F. White indicated traces of Si, Al, Mg, Nd, La, Sc, Yb, and Cu.

† Chemical determination by J. L. Bouvier and S. Abbey.

§ Taken from Rankama and Sahama (1949).

to uranium is lower in the remnant euxenite than in the host euxenite. In Plate V, Fig. V-2a and b, lead exhibits two peaks at the contact of the euxenite and feldspar: one in euxenite, approaching the edge, and the second within the iron-rich crust at the grain boundary. Uranium, niobium and yttrium show no enrichment in either the euxenite border or iron-rich crust.

Some examples of the heterogeneity of the albite feldspar that is associated closely with euxenite are illustrated in Plate VI. Iron-rich crusts and stains along twin lamellæ and fractures of the host feldspar (Plate VI, Figs. VI-la & b) are composed predominantly of minute specks of hematite and goethite. Some red transparent fracture fillings and red-brown crusts containing minute anisotropic plates were found to have an erratic distribution of lead in addition to high iron (Plate VI, Fig. VI-3a and b). Iron-rich colloform crusts that are associated with inclusions of colourless mica in the feldspar (Plate VI, Figs. VI–2a and b) are seen to contain relatively high lead and uranium near the contact of the iron-rich crust and mica. Minor amounts of yttrium and traces of niobium in the iron-rich crust possibly indicate the presence of small euxenite remnants.

The observed high concentrations of uranium and lead along grain boundaries of mica and feldspar, and in contact with these same minerals in iron-rich crusts filling fractures in feldspar, suggest that an alkalic environment is favourable for re-deposition of uranium and lead believed to have been leached from the euxenite. The high concentration of uranium approaching the fluorite boundary indicates that the presence of fluorine may be favourable for re-deposition of uranium, but may not have any effect on re-deposition of lead. Autoradiographs of fractured minerals that did not contain any visible euxenite grains indicated that some fractures in feldspar, particularly those filled with micaceous clay, contain radioactive traces. Small radioactive areas were observed at the contact between stained microcline and albite, and between feldspar and fluorite. It is believed that these radioactive minerals in the fractures and along grain boundaries are secondary.

SUMMARY

An electron microprobe has been used to study the distribution of selected elements in fresh and altered zoned phlogopite phenocrysts; in "antiperthite" and lamellar feldspars; in fresh and altered euxenite, and in inclusions and red crusts in its host feldspar. The results may be summarized as follows:

Mica

Dark zoned rims in phlogopite form as a result of increasing iron and probably of partial dehydration during emplacement of the lamprophyre. The outermost, darkest rim is rich in iron but does not contain any potassium, and thus it is not mica. The concentration of iron in the phlogopite increases by a factor of approximately four from beginning to the end of crystallization. Small fresh biotite crystals in the groundmass of the lamprophyre also exhibit compositional zoning; the differences between the zones being less prominent than in the phlogopite phenocrysts.

Altered mica crystals show greater variations in chemical composition than unaltered ones. Potassium, in particular, shows considerable variation in traverses along and across the basal cleavage planes. Potassium decreases near the edges of the mica flakes, where alteration to chlorite and to iron oxides has taken place.

Feldspar

Two examples are presented; in one, the "antiperthitic" plagioclase (KA–846) varies in composition from An_{45} to An_{52} and contains inclusions of pure or almost pure potassium feldspar; in the second, lamellar plagioclase KA–930 consists of parallel lamellae ranging in composition from An_5 to An_{70}.

Andesines and labradorites from anorthosites contain oriented and random inclusions of potassium feldspar. The inclusions are in the form of rods, tablets and coarse patches. Densely packed blebs of potassium feldspar in some areas constitute more than 50% of total

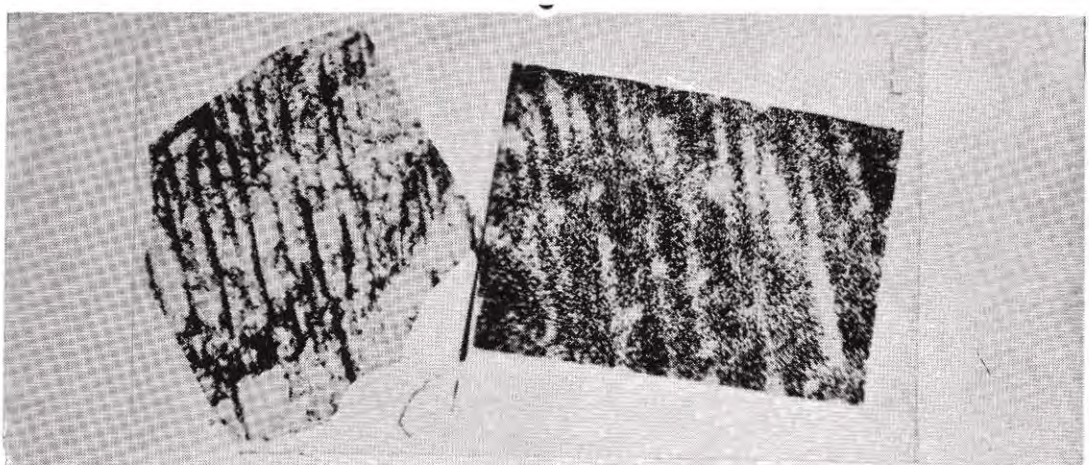

VI-1a

VI-1b

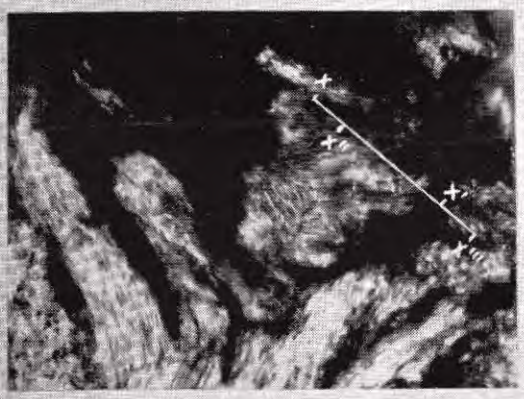

VI-2a

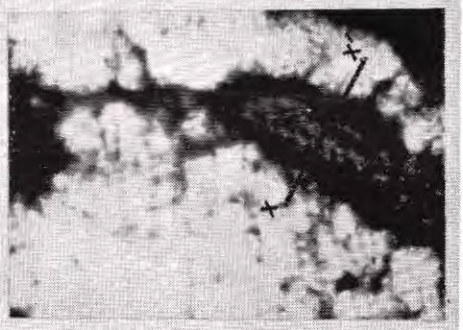

VI-3a

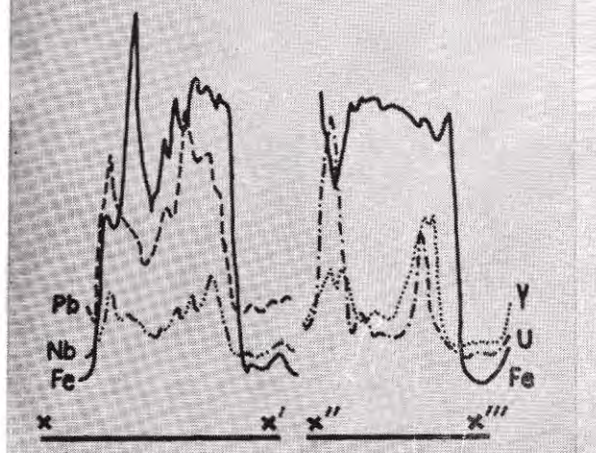

VI-2b

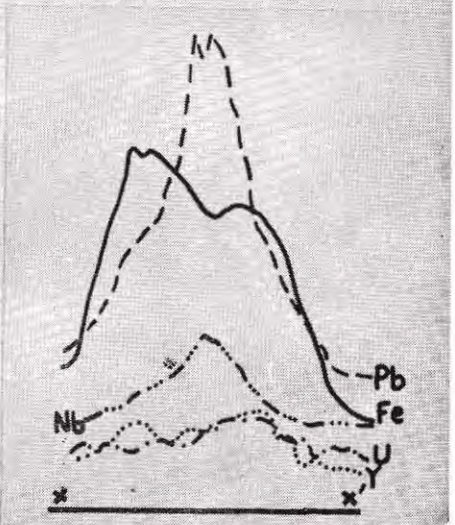

VI-3b

feldspar. Such potassium-rich patches resemble relics of partly digested potassium-bearing inclusions.

Lamellar plagioclase KA-930 from a diabase in addition to plagioclase lamellae An_{5-70}, contains potassium feldspar that surrounds inclusions of mica, apatite and iron oxides.

Euxenite

Euxenite from Wakefield, Quebec, is mosaic in appearance and shows considerable differences in chemical composition. It is locally impoverished in lead, uranium and iron. Enrichment of uranium and lead bordering the euxenite is closely associated with iron-rich crusts : uranium concentrates along the borders of fluorite and mica inclusions, and lead is enriched at the contact between the euxenite and albite, and around mica.

Crusts in red-stained, fractured feldspar that surrounds euxenite, are composed of hematite, goethite, or micaceous clay and locally contain erratic concentrations of uranium and lead.

ACKNOWLEDGMENTS

The authors wish to thank Dr. R. J. Traill for his advice during the electron microprobe analysis, Miss C. M. Hunt for her assistance in x-ray diffraction studies and in preparation of drawings, and Mr. R. Lake of the Mines Branch for heating the feldspar. Dr. J. E. Reesor and Dr. R. J. Traill read the manuscript. Their suggestions are gratefully acknowledged.

REFERENCES

DAWSON, K. R. AND CRAWLEY, W. D. (1963) An improved technique for staining potash feldspars : *Can. Mineral*, Vol. 7, pt. 5, pp. 805-808.

ELLSWORTH, H. V. (1926) Euxenite-polycrase from Mattawan Township Nipissing District, Ontario : *Am. Mineral*, Vol. 11, pp. 329-331.

ELLSWORTH, H. V. (1927) Lyndochite-a new mineral of the euxenite group from Lyndoch Township, Renfrew County, Ontario : *Am. Mineral*, Vol. 12, pp. 212-218.

HENDRICKS, S. B. AND JEFFERSON, M. E. (1939) Polymorphism of the micas : *Am. Mineral*, Vol. 24, pp. 729-771.

JASMUND, K. (1950) Texturaufnahmen von blättchenförmigen Mineralen submikroskopischer Grössenordnung in einer Debye-Scherrer-Kamera : *Neues Jb. Mineralog., Geolog. und Paläont.* Mh. H. 3, pp. 63-72.

METAIS, D., RAVIER, J. et PHAN-KIEN-DUONG (1962) Nature et composition chimique des micas des deux lamprophyres : *Bull. Soc. francs. minéral. et crist.*, Vol. 85, No. 4, pp. 321-328.

RANKAMA, K. AND SAHAMA, Th. G. (1949) *Geochemistry*. The University of Chicago Press.

RIMSAITE, J. (1957) über die Eigenschaften der Glimmer in den Sanden und Sandsteinen : *Beitr. zur Mineral. u. Petrogr.*, Vol. 6, pp. 1-51.

———(1962) Studies of rock-forming micas (Abstract) : *Am. Mineral*, Vol. 47, p. 201.

———(1964) On micas from magmatic and metamorphic rocks : *Beitr. zur. Mineral. u. Petrogr.*, Vol. 10, pp. 152-183.

ROBINSON, S. C., LOVERIDGE, W. D., RIMSAITE, J. AND von PETEGHEM, J. (1963) Factors involved in discordant ages of euxenite from a Grenville pegmatite : *Can. Mineral*, Vol. 7, pt. 3, pp. 533-546.

TROGER, W. E. (1955) Optische Eigenschaften und Bestimmung der wichtigsten gesteins-bildenden Minerale (pp. 150-151, 214). In : Freund, Hugo : Handbuch der Mikroskopie in der Technik, Vol. 4, pt. 1. Umschau Verlag-Frankfurt am Mein.

PLATE VI

VI-1. Distribution of iron along fractures of albite which is host of euxenite.
(a) Photomicrograph, x 35 (Hematite, dark streaks).
(b) X-ray scanning image, iron K-alpha radiation, x 100.

VI-2. Distribution of U, Pb, Y, Nb and Fe in iron-rich crusts coating a mica inclusion in albite.
(a) Photomicrograph showing mica with iron-rich crusts and intergrowths, x 500.
(b) Element concentration obtained from a line scan across the iron-rich crust and the contacts between the mica and the crust, x 500.

VI-3. Distribution of U, Pb, Y, Nb and Fe in red transparent fracture filling in feldspar.
(a) Photomicrograph showing hematite veinlets (black), and bright red transparent fracture filling in the centre of the veinlet (right, dark grey), x 250.
(b) Element concentration obtained from a line scan across the red transparent veinlet. Lead increases in ihe centre of the veinlet, x 500.

MINERALOGICAL SOCIETY OF INDIA, IMA VOLUME, 1966
INTERNATIONAL MINERALOGICAL ASSOCIATION, PAPERS, FOURTH GENERAL MEETING

OBSERVATIONS ON HYDROTHERMAL GROWTH OF QUARTZ

TARUN BANDOPADHYAYA AND P. SAHA
Calcutta, India

ABSTRACT

Experiments for hydrothermal growth of quartz on basal seed plates, etched in 30% ammonium bifluoride solution for different periods have been carried out in stainless steel autoclave designed at the Institute. In a series of runs varying in time from 1 to 7 days, with carbonate solution of lithium and sodium as medium of growth, in the range of temperature 320°C—350°C and pressure 2000 psi.—4000 psi., successful growth was recorded only in one case. Further experiments are being carried on.

Growth of isolated hillocks of circular, hexagonal and other different shapes, around centrally located triangular pits, have been recorded on the successfully grown seed plate. A microscopic examination of those pits indicates that the walls grow more rapidly than the centre, though innumerable etch pits of similar orientation are found to occur on the growth hillocks (can be seen only in high magnification). Furthermore, growth has also taken place inside the pits, being more prominent at the corners in the form of steps, sometimes resembling discontinuous spires. It also appears that the number of growth centres are far less than the number of etch centres.

UNIT CELL AND SPACE GROUP OF ARTIFICIAL COBALTOMENITE

WILLIAM G. R. de CAMARGO
S. Paulo, Brazil

ABSTRACT

Artificial cobaltomenite crystals, of composition $CoSeO_3 . 2H_2O$, have been synthesized by A. M. Giesbrecht, at the Pharmacology Department of the Medical School, University of S. Paulo, Brazil. The rose-red cobaltomenite crystals of the monoclinic system display a prismatic habit, with the forms : c(001) and m(110).

Morphological data : m(110) : m′(110) = 82° ;
$\beta = 81° 30'$
Unit cell dimensions : a = 7.58 Å ; b_c = 8.73 Å ;
c_c = 6.59 Å ; $\beta = 81° 30'$
Observed specific gravity : 3.50 g./cm.^{3}
Number of formulas per unit cell : 4
Space group : P $2_1/n$
Main lines of the powder diagram : (in Å) : 5.76 (10)—3.81 (8)—3.47 (9)—3.02 (8)—2.75 (8)
—2.39 (8)

The unit cell dimensions and the space group were obtained with rotation and precession photographs, and the Debye-Scherrer diagram was taken in a 114.6 mm. Buerger powder camera of Philips manufacture.

METAMORPHIC ECLOGITES FROM CO. DONEGAL, EIRE

W. R. CHURCH
London (Ont.), Canada

ABSTRACT

Garnet-coronite metagabbro with tectonically deformed rims composed of feldspar-eclogite are present in the Moine Series of Co. Donegal, Eire. The metagabbro grades into eclogite concomitant with increasing garnet and decreasing feldspar content, conclusively proving their metamorphic origin. The amount of primary feldspar in the eclogites is a function of their bulk composition, in particular the proportions of normative albite and magnetite. The pyroxenes of both the metagabbro and the eclogite are jadeite bearing but those from the eclogite have a significantly higher jadeite content, and jadeite : acmite ratio, than those from the metagabbro.

The variation in the iron-magnesium partition coefficient for the mineral pairs clinopyroxene and garnet, and clinopyroxene and orthopyroxene from eclogitic rocks, is compared with the variation in jadeite : acmite ratio of the clinopyroxenes.

PHASE TRANSFORMATIONS IN A NATURAL BERYL

DIBYENDU GANGULY AND PRASENJIT SAHA
Calcutta, India

ABSTRACT

High-temperature studies have been carried out with finely ground, acid-leached samples of natural beryl in vertical tube quench furnace and in a strip furnace.

The heating runs indicate an incongruent melting temperature of 1507°C±2°C for the beryl, the transition being :

Beryl→phenacite+chrysoberyl+liquid. Phenacite does not persist for more than about 20°C above the reaction point. The primary phase is chrysoberyl, which melts completely at 1627°C±5°C.

The natural beryl, heated to complete melting and then slowly cooled to 1460°C, produces well-developed crystals of chrysoberyl and phenacite (?) in a glassy matrix. Quenched glass of natural beryl shows development of very fine grains of chrysoberyl and phenacite in a glassy matrix at 1475°C ; when seeded with beryl crystals, however, it shows profuse development of beryl at the same temperature indicating that chrysoberyl and phenacite exist below the reaction point as metastable phases.

THE APPLICATION OF NUCLEAR MAGNETIC RESONANCE TECHNIQUE IN THE STUDY OF CATION ORDER-DISORDER AND PHASE TRANSITIONS IN SOLIDS

SUBRATA GHOSE
Zurich, Switzerland

ABSTRACT

Nuclei like ^{11}B, ^{23}Na, ^{27}Al, etc., possessing electric quadrupole moments and occupying sites with a non-cubic symmetry in a crystal, split the nuclear magnetic resonance line into 2I (I=spin) components. This splitting of the NMR line provides information about the number and symmetry of sites, occupied by the nuclei in a crystal. Recently, this technique has been applied to determine the structural state in feldspar, *namely*, albite, microcline, orthoclase and sanidine

(Brun, Hafner, Hartmann, Laves and Satub, 1960 ; Hafner, Hafner, Hartmann and Laves, 1962 ; Hafner and Laves, 1963), Mg—Al and Zn—Al spinels (Brun and Hafner, 1962 ; Ghose, 1963) and danburite, $CaB_2 Si_2 O_8$ (Brun and Ghose, 1964). After prolonged heating, Al—Si disordering in albite and microcline has been confirmed using this technique. The B—Si order in danburite, however, persists upto the decomposition temperature.

Second order phase transitions in solids, *e.g.*, ferroelectric phase transition of colemanite, CaB_3O_4 $(OH)_3.H_2O$ at—2°C (Holuj and Petch, 1960), antiferromagnetic phase transitions in $CuCl_2.2H_2O$ at 4.3°K (Poulis and Herdeman, 1952) and in azurite, Cu_3 $(OH)_2$ $(CO_3)_2$m at 1.86°K (van der Lugt, Poulis, van Agt and Gorter, 1962) have been studied by the proton magnetic resonance technique.

CRYSTAL CHEMISTRY OF BASIC COPPER PHOSPHATE AND ARSENATE MINERALS

SUBRATA GHOSE
Zurich, Switzerland

ABSTRACT

The structures of libethenite, $Cu_2PO_4(OH)$ and olivenite, Cu_2AsO_4 (OH), which are isostructural with andalusite, Al_2SiO_5, have been known for a long time. The recent determination of the structures of pseudomalachite, $Cu_5(PO_4)_2(OH)_4$ (Ghose, 1963), cornetite, $Cu_3PO_4(OH)_3$ (Fehlmann, Ghose and Finney, 1964), clinoclase, Cu_3AsO_4 $(OH)_3$ (Ghose, Fehlmann and Sundaralingam, 1964) and euchroite, $Cu_2AsO_4(OH)$. $3H_2O$ (Guiseppetti, 1963) reveals new structural principles in this group of basic oxy-hydroxy copper (II) complexes.

Among the chemically analogous phosphates and arsenates, only cornetite and clinoclase are not isostructural and there is no known Panalog of euchroite. Libethenite, pseudomalachite and cornetite on the one hand, and olivenite erinite and clinoclase on the other, build two series with increasing Cu : P and Cu : As ratios, namely, 4 : 2, 5 : 2 and 6 : 2. With increasing Cu : P (or As) ratio, the co-ordination of copper (II) becomes irregular, changing from a distorted octahedral to tetragonal pyramidal ; at the same time, the copper co-ordination polyhedra tend to form dimeric ($Cu_2(OH)_4O_4$) groups, by two tetragonal pyramids sharing an edge.

The structures of libethenite and olivenite can be described as three dimensional networks, composed of simple copper octahedral chains, bonded through PO_4/AsO_4 groups and ($Cu_2(OH)_2$ O_6) dimers, formed of two trigonal bipyramids sharing an edge. In pseudomalachite and erinite, $Cu_5(AsO_4)_2(OH)_4$, slightly wavy sheets are formed by two different types of octahedral chains : the first is composed of alternating single and dimeric octahedral groups sharing edges and the second, by single octahedra, sharing opposite edges of the copper co-ordination plane and is similar to the chain found in libethenite. These sheets are held to each other through isolated PO_4/AsO_4 groups. In the structures of cornetite and euchroite, the dimeric ($Cu_2(OH)_4O_2$) groups are stacked upon each other in a zigzag fashion, so that each dimer has two (OH) groups common with two other dimers above and below it, thus giving rise to a dimeric chain. In euchroite, these chains are bonded to each other through AsO_4 groups and O—H.....O bonds, while in cornetite, they are held together in a three dimensional network through isolated ($Cu_2(OH)_4O_4$) dimers, PO_4 groups and O—H.....O bonds. A different type of a dimeric chain is found in clinoclase, which is formed of ($Cu_2(OH)_4O_4$) dimers, sharing one (OH) corner each with two adjacent dimers in a plane. These chains, lying zigzag with respect to each other in the unit cell, sandwich between them isolated AsO_4 groups and ($Cu_2(OH)_4O_4$) dimers, thus giving rise to a complex sheet structure. These sheets are held to each other through long Cu—O and O—H.....O bonds. In all of these

structures, the (OH) groups are almost invariably involved in hydrogen bonding. These hydrogen bonds provide additional support to the structure, made up of non-hydrogen atoms.

A CHEMICAL STUDY OF SOME AMPHIBOLES FROM ALKALINE IGNEOUS ROCKS

R. A. HOWIE
Department of Geology, King's College, London

ABSTRACT

Chemical analyses are reported for several amphiboles from alkaline rocks, including amphiboles from a jacupirangite from Slada, Alnö, and from a syenitic pegmatite from Ula, Larvik. A new analysis of eckermannite is also reported.

A SYSTEM OF NOMENCLATURE FOR RARE-EARTH MINERALS

A. A. LEVINSON
The Dow Chemical Company, Freeport, Texas

ABSTRACT

Numerous rare-earth element analogues have been found for well-established rare-earth minerals. In order to prevent a multitude of impractical names a system of nomenclature is proposed.

A group name, *e.g.*, monazite, is suggested for rare-earth minerals for which the rare-earth element distribution has not been determined. A species name, *e.g.*, monazite—(Ce), monazite—(La), etc., is suggested for rare-earth minerals for which the rare-earth element distribution has been determined ; the species name is obtained by appending the chemical symbol of the predominant rare-earth element to the group name.

INFLUENCE OF GASES ON THE FORMATION AND DESTRUCTION OF "COLOUR CENTERS" IN QUARTZ BY ELECTROLYSIS

JOACHIM LIETZ AND BENOD B. MEHROTRA
Hamburg, Germany

ABSTRACT

The general conditions of the smoky coloration in quartz by electrolysis in air have been studied by Lietz and Haenisch (IMS Report 1960). The decoloration which follows the coloration is dependent on the electrode geometry. In order to examine the mechanism of the decoloration, a systematic search has been done by electrolysis of quartz in vacuum and in the atmosphere of different pure gases (Ar, N_2, O_2, H_2). It is found that in vacuum there is a complete coloration, independent of the anode form and the orientation of the samples as well as the same smoky color even at 300°C. The typical decoloration can also be obtained in vacuum by using high electric fields. Thus the above mentioned results rule out the necessity of the proton ($H+$) diffusion, which have been examined in the IR—measurements in the region of 3μ. All the processes of the coloration and decoloration were studied after documenting in a film.

THE DISTRIBUTION OF TRACE ELEMENTS AND SILICATES IN MEDITERRANEAN MARBLES

H. U. NISSEN
Zurich, Switzerland

ABSTRACT

Trace element distribution in marbles is related to problems of petrology (differences in marbles formed under different conditions), crystallography (substitution of metal atoms in the calcite structure) and archeology (recognition of sculpture and building materials worked, for example, by the ancient Greeks and Romans). The distribution of Na, Mg, K, Fe, Sr and Pb in relatively pure white marbles has been investigated. In view of the archeological application of the results, specimens have mainly been collected from the ancient marble quarries in Attika and the Kykladic Islands (Greece) and Western Anatolia (Turkey). From each quarry a number of specimens were investigated.

Na and Mn have been investigated by neutron activation, treating small slices of the rock for 40 hours with 3.6. 10^{12} slow neutrons/cm^2 and measuring the gamma-spectra of the activated ^{24}Na and ^{56}Mn. The other trace elements except Mg and including check data for Mn were determined by x-ray flourescence spectroscopy in powdered samples. Mg was determined complexometrically from the same powders.

The trace element contents, though mostly low show less variation within a hand specimen or a quarry than is found for whole petrologically different marble bodies, which can therefore be characterized by their trace element constitution. The differences are interpreted as being inherited from the parent limestones metamorphosed later on. The analyses are compared with trace element contents of carbonate sediments.

The optical and x-ray determination of silicates in the residues of the marbles insoluble in HCl shows much quantitative and qualitative variation. The characteristic mineral associations class the marbles as belonging to the quartz-albite-muscovite-chlorite subfacies of the greenschist facies, with chlorite-epidote (or piemontite)—calcite as common mineral association.

CALCIUM SILICATE AND HYDROGARNET FORMATION IN THE SYSTEM $CaO–Al_2O_3–SiO_2–H_2O$

DELLA M. ROY
University Park (Penn.), U.S.A.

ABSTRACT

Conditions for synthesis of a number of calcium silicate hydrates have been determined at elevated temperatures and pressures, and information on their stabilities obtained, . Two of these phases, first synthesized in the laboratory, and now found as natural minerals (kilchoanite-phase Z; $9CaO.6SiO_2.O—1H_2O$; and phase Y—$6CaO.3SiO_2.H_2O$) are stable to above 800°C, an unusually high temperature for hydrous minerals. Information on stabilities of hillebrandite, calciochondrodite ($5CaO.2SiO_2.H_2O$), foshagite and tobermorite was obtained. Substitution of Al^{3+} in the tobermorite structure raises its stability limit from 285°C to about 325°C in the pressure range 2—3 kilobars (H_2O pressure). Above this temperature hydrogarnets and other phases are stable. Hydrogarnet crystalline solutions ranging in composition from $3CaO.\ 1Al_2O_3$.

$6H_2O$ to $3CaO.1Al_2O_3.2SiO_2.2H_2O$ are stable at maximum temperatures ranging from 300° to 360°C, respectively. Silica-rich "hydro-grossular" type phases are formed, perhaps metastably, at higher temperatures.

APPLICATION OF VARIATIONS IN CRYSTAL FIELD SPLITTING OF ENERGY LEVELS OF IONS TO INDICATE STRUCTURAL CHANGES IN VARIOUS MINERALS INCLUDING DEHYDRATING ZEOLITES AND CLAYS

RUSTUM ROY
University Park (Penn.), U.S.A.

ABSTRACT

X-ray methods at present provide the only well-developed way to study the nearest-neighbour environment of a cation, and they are lengthy and require single crystals. By using 3d ions in selected sites, it is possible to determine, in certain cases, changes in packing of the nearest-neighbour oxygen ions or water molecules in minerals.

Ni^{2+}, Co^{2+}, Mn^{2+}, and to a lesser extent : Fe^{2+}, Fe^{+3}, Co^{+3}, have been used either in partial or total replacement. Energy-level diagrams for the first four ions are well known for 4 and 6 co-ordination. Simply calculated values for 8 co-ordination or the higher valence states are presented.

The dehydration process in a clay or zeolite is accompanied by rearrangements of the water molecules around the exchangable cation. Montmorillonites and vermiculites, the P (phillipsite—harmotome) zeolite, analcite, faujasite and chabazite families have been studied. Changes in the absorption or reflection spectrum (and hence, of course, color) are shown to indicate the pH_2O—t conditions under which stepwise co-ordination changes occur, and these pH_2O—t conditions are correlated with the high temperature X-ray data on the same changes.

Other illustrations are chosen from phases such as akermanite, olivine, $12CaO.7Al_2O_3$, garnets, etc., where the co-ordination of certain ions has been in doubt.

PRESSURE-TEMPERATURE RELATIONS FOR THE DEHYDRATION OF METASTABLE SERPENTINE AT PRESSURES FROM 15 TO 20,000 psi.

RUSTUM ROY AND JON N. WEBER
University Park (Penn.), U.S.A.

ABSTRACT

Extrapolation of the reaction curve for serpentine→talc+fosterite+water to low water vapor pressures indicates that serpentine is an unstable phase above about 500°C. Published DTA curves, however, show that dehydration of serpentine may not take place until temperatures of 750°C. or more are attained. Using high pressure DTA apparatus, and a modified Herold-Planje thermocouple arrangement, the decomposition curve of metastable serpentine has been determined for two specimens, and the catalytic effect of water above 10,000 psi has been demonstrated. Contrary to some earlier work, particle size appears to have a negligible effect on the dehydration temperature. Heats of reaction have been measured using the area under the DTA curve and have also been calculated from the Clausius-Clapeyron equation. The concentration of ferrous iron in the specimen greatly influences the value of $\triangle H$; 55 and 84 cal/gm were obtained from specimens with 3.6 and 2.3% FeO respectively. At atmospheric pressure, the order of reaction

and activation energy for the lower Fe^{++} specimen are 1.0 and 37 K cal, while for the higher Fe^{++} sample, measurements of 1.1 and 93 K cal were obtained. The thermodynamic and kinetic parameters for the dehydration of metastable serpentine are of utmost importance in designing water extraction systems for future lunar bases.

HIGH-PRESSURE AUTOCLAVE FOR HYDROTHERMAL CRYSTAL GROWTH

PRASENJIT SAHA
Calcutta, India

ABSTRACT

Stainless steel autoclaves of monoblock construction have been designed for the study of hydrothermal growth of single crystals, which, in the absence of thermal shocks and hidden defects in the material from which the autoclaves are fabricated, can withstand pressures upto 15,000 psi. at 400°C indefinitely. The design of the autoclave is based on a careful evaluation of the different theories for stress analysis in thick cylinders, and high temperature rupture stress data for stainless steel. Salient features of the design are that deformable gaskets, O-seal rings, delta-seal rings etc. are not required, and re-machining of some of the component parts can be avoided altogether, or can be kept at a minimum. Provision has been made to record the internal pressure by means of a Bourdon gauge and to record the temperature differential between the nutrient and growth zones by means of external thermocouples.

Preliminary experiments on growth of single crystals of quartz are being conducted with these autoclaves. Because of poor corrosion resistance of stainless steel in alkali media as compared to other materials like stellite, inconel X, udiment 500 etc., carbon steel and silver liners have been designed.

POLYGONAL TEXTURE IN BERYL

Th. G. SAHAMA
Helsinki

ABSTRACT

Relatively thick (say, 0.3—0.5 mm) sections of clear beryl cut perpendicular to the c-axis of the crystal exhibit often a kind of polygonal texture with the polygon boundaries parallel to the traces of $(11\bar{2}0)$ and $(10\bar{1}0)$. The margin surrounding this polygonal core looks "zoned" *i.e.*, shows successive layers of growth with varying birefrigence. Such crystals are invariably optically biaxial with 2V ranging up to some 18°—20° with the acute bisectrix parallel to the crystallographic c-axis. The traces of the optic axial plane on different spots of the section do not obey hexagonal symmetry.

It will be demonstrated that the optical anomaly mentioned is caused by strain in the structure. It seems that, on rapid crystallization, the beryl structure exceedingly easily becomes strained. The nature of this strain varies with the conditions of growth. On the basal plane (0001) of beryl, flat haxagonal growth pyramids are commonly seen. By using suitable optical techniques, similar growth pyramids can be detected also inside the crystal. The entire crystal consists of a mosaic of such growth pyramids each pyramid slightly differing in strain from its neighbour pyramids. On a horizontal section, the net result is a polygonal texture the boundaries just representing traces of pyramidal plans that separate domains of different strain conditions. Single crystal precession photographs show a uniform reciprocal pattern throughout the crystal.

STRUCTURAL CHANGES IN SYNTHETIC AND NATURAL Al-HYDROXIDES (BAUXITE FROM FRANCE)

I. VALETON AND B. B. MEHROTRA
Geologisches Staatsinstitut, Hamburg, Germany

ABSTRACT

The systematic geochemical and petrological work on the bauxite of the South France, in which the hydrargillite, boehmite and diaspore predominate, has been done by I. Valeton and co-workers (1962, 1963). As some structural changes could not be interpreted, fundamental work on synthetic bayerite, hydrargillite (gibbsite), boehmite, diaspore, norstrandit, to compare with the Al-Hydroxide in the bauxite on dehydration and H—D exchange has been performed using Infrared, X-ray diffraction, Electronmicroscope and NPR. The experiments show that in the bauxite there is also a systematic transformation from one Al-hydroxide to another.

PROCEEDINGS OF THE INTERNATIONAL MINERALOGICAL ASSOCIATION

Fourth General Business Meeting of Delegates

New Delhi, December 15 and 22, 1964

FIRST SESSION

The first session of the IV General Business Meeting of Delegates of the 23 Member Societies of the International Mineralogical Association was held in the Auditorium of the National Museum in New Delhi, India on December 15, 1964, at 2–30 p.m. Of the possible 46 voting delegates, 40 were present, representing the National Mineralogical Societies of Austria, Canada, Czechoslovakia, Egypt, Finland, France, Germany, India, Italy, Japan, Netherlands, Norway, Spain, Sweden, Switzerland, United Kingdom, U.S.A., and U.S.S.R. The Member Societies of Belgium, Brazil, Bulgaria, Denmark and New Zealand were not represented. After identification of the voting delegates by the Secretary, the Session proceeded according to the following agenda :

1. Opening Remarks
2. Reports of the Officers
3. Appointment of the Auditors
4. Affiliation with the International Union of Geological Sciences
5. Amendments to the Constitution
6. New Commission on Correlation of Petrographic Nomenclature
7. Next Meeting
8. Other Business

The President, D. Jerome Fisher, and Prof. P. R. J. Naidu, Chairman of the Local Committee, welcomed the Delegates and other attendants at the meeting organized by the I.M.A.

REPORTS OF THE OFFICERS

Secretary's Report

The Secretary, J. L. Amorōs, reported that no important business was handled by him except that related to the preparation of the business of the present Meeting, and already reported in the published Proceedings of the III General Business Meeting that were approved by the Assembly. Only one new member, Brazil, has been accepted in the I.M.A., and the Secretary stressed the need of co-ordinated efforts for bringing new National Societies into the Association.

Report of the Treasurer

The Treasurer, L. G. Berry, submitted the following reports covering (1) receipts and disbursements from April 1, 1962 to October 31, 1964, and (2) status of the World Directory of Mineralogists. (refer Pages 239 & 240)

APPOINTMENT OF THE AUDITORS

The Delegates nominated Drs., A. P. Sandrea and J. R. Butler as auditors and scrutineers for this meeting of the Association.

AFFILIATION WITH THE INTERNATIONAL UNION OF GEOLOGICAL SCIENCES

After brief remarks by the President who explained that it was advantageous for the I.M.A. to vote for the proposed affiliation with I.U.G.S., the affiliation was approved by the unanimous vote of the Assembly. The Assembly, upon request of the President, asked Prof. Berry to contact the International Union of Geological Sciences in order to consummate the affiliation.

AMENDMENTS TO THE CONSTITUTION

For the acceptance of the I.M.A. in the I.U.G.S., the following amendment was required, as requested by the I.U.G.S. Secretary :

Article 3 (a) to be re-written (the proposed modification is in italics) :

" The members of the Association shall be Mineralogical Societies *recognized as Societies representing mineralogists of individual countries or other bodies of mineralogists representing individual countries.* In what follows the word Member Society shall be deemed to include such a representative body. " etc.

REPORT OF THE TREASURER

Receipts

Cash on hand April 1, 1962, Bank		2,293.64	
Cheque on hand (Egypt, 1961–62)		30.40	
Refund of cheque incorrectly endorsed, on hand		200.00	
Dues for July 1, 1961 – Dec. 31, 1962			
Mineralogical Societies of Bulgaria (15), Canada (60), Finland (30), Norway (30), Spain (30), Sweden (60)	225.00		
Dues for 1963			
Mineralogical Societies of Beligum (30), Bulgaria (14.17), Canada (64.80) Czechoslovakia (30), Denmark (30), Finland (30), France (90), Japan (60), Netherlands (15), New Zealand (15), Norway (30), Sweden (96.69), Switzerland (60), U.S.S.R. (150), United Kingdom (90), U.S.A. (150)	1,165.66		
Dues for 1964			
Mineralogical Societies of Austria (30), Belgium (30), Brazil (30), Bulgaria (14.17), Canada (60), Czechoslovakia (30), Denmark (30) Finland (30), France (120), Germany (120), Italy (90), Japan (90), Netherlands (15), Norway (15), New Zealand (15), Sweden (60), Switzerland (60), U.S.S.R. (150), United Kingdom (90), U.S.A. (150)	1,229.17		
Dues for 1965			
Mineralogical Society of Netherlands (15)	15.00		
Interest on savings account	152.07		
Sales of directories	552.40		
Total receipts April 1, 1962 to October 31, 1964	3,339.30	3,339.30	
Grand Total		5,863.34	5,863.34

Disbursements

President's office, 1962 and 1963		
D. J. Fisher – postage, telephone, telegraph	67.57	
Secretary's office, 1962, 1963 and 1964		
J. L. Amorōs – postage, duplicating	496.28	
Publication of World Directory		
Balance of publication cost	680.00	
Postage and shipping	30.25	
Commission on Cosmic Mineralogy		
Postage and duplicating (Roy S. Clarke)	19.82	
Program Committee, 1964 meeting		
C.E. Tilley–postage	10.00	
Bank charges on cheques	10.02	
Reprints from Geotimes for April 1961 – Am. Geol. Inst.	7.00	
Reprints of Proceedings April 1962 meeting from Special Paper I...	62.74	
Total Disbursements	1,383.68	1383.68

Outstanding cheque from March, 1962	59.49	59.49	
Bank balance a c 51–90819–E	1,768.10		
Bank balance a c 1966584	2,652.07		
Total cash on hand	4,420.17	4,420.17	
		5,863.34	5,863.34

Report on World Directory of Mineralogists

Distribution of stock		
Washington, U.S.A.	620 copies	
Kingston, Canada	30	
India (Popular Book Depot)	25	
London (Dr. Butler)	70	
Belgium (Dr. van Tassel)	5	
Germany (Prof. Winkler)	25	
Barcelona	225	
	1,000	
Sales		
Washington	376 copies	$564.40
Kingston	11	16.50
India	25	37.50
Barcelona	101	151.50
Total	513	769.90
Unsold		
Washington	227	
Kingston	19	
Barcelona	124	
London	70	
Belgium	5	
Germany	25	
Total	470	
Expenses		
Printing		880.00
Shipping (from Barcelona)		153.50
Shipping (from Washington)		30.25
		1,063.75

The amendment was unanimously adopted by the Delegates.

Two versions were proposed to amend Article 4 B. (c). One proposed by the Council: "The members of the Council shall normally hold office for four years (but until their successors have been duly elected). *The President and Vice-Presidents are not eligible for re-election to the same office. Other officers are immediately eligible for re-election.* (The additions are in italics.) And another by the French Mineralogical Society: "The President and Vice-Presidents are not eligible for re-election to the same office. The President is to be chosen from the Vice-Presidents. Other officers are immediately eligible for re-election." President Fisher

stressed the point that the amendment proposed by the Council was more general and included the French proposal as a particular case. Prof. Wyart pointed out that the French Delegation favored the second text as more automatic. Prof. Font-Altaba noted the differences of opinion between the French Mineralogical Society and the I.M.A. Council. Prof. Curien stressed the idea that the French proposal would show the willingness of the person to be elected President avoiding unnecessary written acceptance. After a few words of President Fisher, and after a consultation with their own Delegates, the French delegation withdrew its proposal.

By unanimous vote, the Assembly approved the amendment of the Article 4 B. (c) as proposed by the Council.

NEW COMMISSION ON CORRELATION OF PETROGRAPHIC NOMENCLATURE

President Fisher read a letter from the German Mineralogical Society in which the proposal for a New Commission on Correlation of Petrographic Nomenclature was made. Prof. Guillemin opposed the creation of the new commission based on the fact that the existing commissions were already a heavy load for the I.M.A. Prof. Mehnert explained the scope and need of the commission. President Fisher referred to the work of the previously existing liaison committee of Petrographic Nomenclature chaired by Prof. Burri. Prof. Neumann opposed extending the activities of the I.M.A. to petrography, and suggested that the I.U.G.S. be asked to establish such a commission with broader scope. This was accepted by the Assembly.

NEXT MEETING

President Fisher called the attention of the Delegates to the fact that no invitation had been extended for the holding of the next meeting, and stressed the need of receiving such an invitation in the very near future if we were to meet in 1966.

OTHER BUSINESS

President Fisher referred next to the election for the Council and Commission officers. Secretary Amorōs noted that proposals for new nominations could be sent to his office up to 30 hours before the election, provided that at least three Delegates signed each of the proposals (Art. II).

President Fisher emphasized that authors of scientific papers presented at the meeting should submit the manuscripts in final form by March 31, 1965, in order to obtain publication in a special issue of the Indian Mineralogist. He also announced that the Local Committee had arranged for a banquet on Monday evening, December 21, at Wenger's Restaurant in Connaught Circle.*

A statutory vote was taken to define the value of the contribution unit for the next period. The present value of U.S. $15.00 was approved.

Prof. Guillemin asked that the nominations for chairman and secretary of each Commission be made by the members of the Commission, based on the fact of a better knowledge of the persons concerned. However, as this would imply a change in the constitution, this proposal was not accepted.

With no further business to be transacted, the first Session of the IV General Meeting was adjourned by the President at 4.30 p.m.

SECOND SESSION

The second session of the Business Meeting of the Delegates was held on December 22, at 9.00 a.m. at the same place. The President opened the session by calling the roll of the Delegates. The session proceeded according to the following agenda :

1. Reports from Commissions
2. Report of the Auditors
3. Other Business
4. Elections

* More than 100 mineralogists and allied scientists registered at the meetings, and about 70 attended the banquet. This was a most successful finale, marred only by the enforced absence of Professor P.R.J. Naidu.

1. REPORTS FROM COMMISSIONS

(A) Commission on Abstracts

Professor Fornaseri, Chairman of the Commission presented the following report :

" The commission on Abstracts, notes with satisfaction that thanks to the co-operation of the various countries now adhering to the I.M.A. the abstracting work for Mineralogical Abstracts is going on satisfactorily, although a more extensive co-operation and a wider coverage would be desirable.

The commission expresses the thanks to all organizers of abstracting work in different countries for their valuable and disinterested co-operation.

The commission is also pleased to note that more countries are joining in co-operating in the preparation of mineralogical abstracts. This is the case of Portugal, whose national Geological Society agreed to appoint four members to co-operate in various branches of mineralogical science.

Having investigated the opinions of the various members and of the British and American Societies, present owners of the Mineralogical Abstracts, about the possibility of further internationalization of the abstracting service in line with our efforts since 1959, the Commission came to the following conclusion : the British and American Societies being well disposed towards the suggestion that the Mineralogical Abstracts be made more International in character than it now is, the Commission recommends to the Council of the I.M.A. that a plan be formulated to allow Mineralogical Abstracts to become an I.M.A. sponsored Journal with an International Board of Control.

A plan involving business and financial arrangements could be developed in the next two to four years and the Commission suggests the possibility be explored of obtaining substantial support from UNESCO after the I.M.A. is affiliated with the I.U.G.S.

The commission is strongly in favor of making efforts and of continuing a policy towards the aims of further international co-operation in the abstracting service.

The commission on abstracts has considered the advisability of broadening the distribution of the mineralogical section of Bulletin Signaletique of the C.N.R.S. It suggests that collective orders of the National Mineralogical Societies may be obtained at reduced rates for the corresponding section of the Bulletin Signaletique. "

A discussion followed showing some differences of opinion among the members of the commission. Dr. Butler, Prof. Font-Altaba, and Prof. Fornaseri participated in the discussion.

(B) Commission on Cosmic Mineralogy

Dr. Sandrea of France reported that he was the only member of the Commission on hand, and thus no business could be transacted.

(C) Commission on Mineral Data

Prof. Strunz reported the following to the Assembly :

" The Mineral Data Commission met in New Delhi on Tuesday, Dec. 15., and on Wednesday, Dec. 16. Seventeen societies were represented.

1. Thanks to Dr. Fleischer :

It was agreed to send a note of thanks to Dr. Fleischer (Washington) for sending regularly his memoranda on New Minerals and Mineral Names to the Mineral Data Commission.

2. Use of the recommended symbols in periodicals :

The Chairman read a letter from Dr. El-Hinnawi (Egypt) pointing out that a number of periodicals do not follow the recommendations made by the I.M.A. in Copenhagen and Washington. It was agreed that the Chairman send a memorandum about the recommended symbols to the Editors of crystallographical and mineralogical periodicals.

3. Misuse of the symbol of the sixfold inversion axis :

It was further agreed that the Chairman send a memorandum to the Editor of International Tables for X-ray Crystallography–of which new

edition is in preparation–concerning the proper use of the symbol for the sixfold inversion axis.

4. Crystal drawings:

There was a discussion on the drawings of crystals dealing with structure and morphology. Not the clinographic, but the *orthographic* projection should be used for both structure and morphology, with the same degree of Rotation and Inclination in each.

5. New Data and Classification of Minerals 1962–64:

As in Copenhagen and Washington a Classification of the New Minerals (with authors, formulae and x-ray data) was distributed to the members of the commission and the delegates. Those absent received the list in late December 1964 by postage.—There was an active discussion of nearly two hours with unanimous agreement. Further proposals were not made and none were received to the end of February 1965.

6. International Mineral Data File:

There was agreement that the International Mineral Data File should be started now beginning with the year 1960. Strunz was proposed as the Editor, with Curien to collect the data for the elements and sulfides, Tennyson for the phosphates, arsenates and vanadates, Gallitelli shall be asked for these on the clay minerals, and Howie and Zussman for those on all the other silicates. More help is necessary.

Prof. W. P. van Leckwijck (Antwerp), General Secretary of the International Union of Geological Sciences (IUGS), wrote to the Chairman of the Mineral Data Commission (February 18th, 1965) stating that " a possible help towards the printing and publishing of this File could be envisaged by the IUGS if a request to this effect was sent to it by the President of the International Mineralogical Association which became affiliated with the IUGS in December 1964 at New Delhi. "

After his report, Prof. Strunz asked the council to provide the commission with funds for its work. President Fisher pointed out that the final resolution of this matter depends on the Next Council.

(D) Commission on Museums

The following statement was read by Secretary Amorōs :

" Dr. Caillere (France), Prof. Fagnani (Italy), Dr. Meen (Canada) and Dr. Sunagawa (Japan) met as representatives of the Museum Commission of the I.M.A. at the time fixed for the meeting, and found that neither the Chairman Prof. Frondel, nor the Secretary, Dr. Leutwein was present. Dr. Amorōs stated that the Chairman was going to publish the list of Museums of the World. However, no information has been received about the activities of the Museum Commission since the last meeting at Washington in 1962. After an exchange of views, the members present decided to transmit this short report to the General Secretary of the I.M.A. "

Prof. Hurlbut reported that he was working closely with Prof. Frondel, and he knew that Prof. Frondel had already finished the collection of data, and that the report is ready to be printed. After some remarks by President Fisher, Secretary Amorōs moved to nominate Prof. Frondel as a candidate for Chairman of the Commission.

(E) Commission on New Minerals and Mineral Names

Prof. Hey reported the following to the Assembly :

" Mr. Hey, Président par intérim à la demande de Mr. Fleischer, ouver la sèance.

La première question soulevée concerne l'élection du Président et du Secrétaire de la Commission pour le prochain terme de l'I. M.A. Mr. Hey propose que Mrs Fleischer et Guillemin soient respectivement proposés comme Président et Secrétaire. Cette recommendation est approuvée par les membres présents (un certain nombre de sociétés membres avaient exprimé par correspondance le même désir : Canada, Finlande, Italie, Nouvelle-Zélande, Norvège, Tchecoslovaquie, USA).

Mr. Hey propose de soumettre à l'approbation du Conseil de l'IMA la possibilité pour notre Commission de créer des sous-commissions chargées de mettre au point la nomenclature de certains groupes complexes de minéraux (par exemple les amphiboles). Ces sous commission devraient être composées de quatre spécialistes au plus, qui auront latitude de demander des conseils à d'autres scientifiques. Les sous commissions feront des propositions concernant la nomenclature, propositions qui seront soumises á l'approbation de la Commission.

Les membres prèsents proposent que deux sous commissions soient créées pour étudier :

a) la nomenclature des amphiboles
b) la nomenclature des mineraux du groupe du pyrochlore.

Une discussion s'engage alors sur la facon de choisir les membres de ces sous commissions. Sur proposition de Mr. Gottardi, il est convenu que le Président de la Commission demandera à chaque membre de proposer un certain nombre de noms (quatre au plus pour chague sous commission). Après collationnement des réponses, une liste des différents noms proposés sera envoyée à chaque membre de la Commission pour vote, les spécialistes ayant recueilli le plus grand nombre de suffrages formeront la sous commission jusqu' à concurrence de quatre membres.

M. Guillemin soumet à la commission, une proposition du Groupe français des argiles, concernant la classification des minéraux des argiles. Ilest décidé que cette proposition sera envoyée aux différents membres de la Commission pour examen.

Avant de clore sa séance, la Commission dècide de demander à nouveau aux Sociétès membres d'examiner avec la plus grande attention toutes les publications pouvant conduire á une modification de la nomenclature minèralogique. Ilest en particulier necéssaire que les secretaires des périodiques traitant des Sciences de la Terre, demandent aux auteure de soumettre à la Commission des Nouveaux Noms et des Noms de Minéraux leurs propositions concernant des changements de nomenclature et en particulier la création de nouvelles espèces. "

He pointed out also the suggestion of the Commission to appoint small sub-commissions inside its own Commission and asked the Council for its advice. President Fisher pointed out that the Constitution established the freedom of the commissions to pursue their own activities in any manner which they desired.

(F) Commission on Ore Microscopy

Prof. Uytenbogaardt presented the following report :

" The Commission on Ore Microscopy (COM) was formed during the I.M.A. Meeting in Washington April, 1962.

The objectives of the COM are :

a) To discuss methods of standardizing quantitative techniqes of ore microscopy.
b) To provide for the accumulation and distribution of standard data on the above and on other properties of ore minerals.

The first business of the COM was to obtain the names of officially appointed members from the various national societies of the I.M.A. By November 1962, the members of 11 nations had been appointed. The list of all 21 members was not complete until July 1963, and was distributed soon thereafter.

In the meantime discussions took place as regards the suitable form of tables of quantitative data for ore minerals.

From June 23rd till July 2nd, 1963, on International Summer School on Ore Mineralogy was held in Cambridge, England. Since 15 member countries were represented there, the opportunity was taken of holding an informal meeting of the COM. On June 28th, 1963, in St. John's College, Cambridge. The following subjects were discussed.

Standards for reflectivity measurement
Polishing standards
Standard wavelength for monochro
-matic light
Determinative tables
Supply of type material to COM

The minutes of this meeting together with a draft scheme of tables were distributed to all members on July 4th, 1963.

A number of replies were received and, as a result, modifications were made in the draft. A definite proposal was prepared for discussion at the meeting of the COM in New Delhi.

On the 12th November 1963, a questionnaire was sent out to all members. The object of this was to get information about the workers in this field as well as about the equipment used. It was also hoped that the infomation obtained would facilitate the exchange of specimen material, and the choice of suitable standards for measurement of reflectivity.

The response to this was rather disappointing although the information obtained from those three countries which up to August 1964 had made returns, was very useful. A new invitation to complete and return the questionnaires before November 12, 1964, was sent to the other members.

Every opportunity has been taken of discussing problems of interest to the COM with individual mineralogists, such as at the combined meeting of the Mineralogical Society and the Institution of Mining and Metallurgy held in London on April 23rd, 1964, and at a meeting in Cambridge held immediately after.

Progress has been made on the selection of standards. The spectral reflectivities of the provisional standards *carborundum* and *pyrite* have been measured by Dr. Piller (Germany) and by the National Physical Laboratory (London).

Extensive work has been done on metals and metal mirrors, and a choice of the most practical available standards was made at the Commission meeting on Monday, December 14th, 1964, the minutes of which will be distributed to the members of the commission as soon as possible after the congress.

The commission agreed upon the following definite standards: *black glass* of known refractive index for the reflectivity range 0–15%, and *carborundum* for the range 15–25%.

As provisional standards were chosen:

Silicon for the range 25–45%,
pyrite for the range 45–65%,
and a glass-covered silver-backed mirror for 65–100%.

Without diminishing the value of the work done by many of the members of our commission, I should like to stress here the stimulating activity shown by our Secretary, Dr. Bowie, during the past two and a half years."

(G) Commission on Teaching

Prof. Orcel reported the following:

(Not yet received)

All the reports of the Commissions were discussed and approved by the Assembly.

2. REPORTS OF THE AUDITORS

The Auditors, Drs. Butler and Sandrea presented the following report:

"We have examined the treasurer's books and records and the bank statements of the International Mineralogical Association for the period April 1, 1962 to October 31, 1964, and find them to be in order and in agreement with the financial statement presented by the treasurer."

The report was approved by the Assembly by unanimous vote.

3. OTHER BUSINESS

Prof. Hurlbut moved the following:

"That the Delegates to the IV General Meeting of the International Mineralogical Association, New Delhi, December 1964, unanimously vote to express their sincere thanks to the Local Committee under the Chairmanship of Prof. P.R.J. Naidu for the excellent organization of the scientific meetings and social functions, and to the Secretary General of the International Geological Congress, Dr. B. C. Roy for the cooperation given to the International Mineralogical Association."

The motion was seconded and approved by unanimous vote of the Assembly.

Prof. Amorōs also thanked the student personnel of the Local Committee for the

constant help that he received in his secretarial work.

President Fisher read the following letter from Prof. Naidu :

" Dear Professor Fisher.

I am sorry I have not been able to attend to you and the other delegates the way I intended to. I am ill and I am leaving for Chandigarh. I wish you and the delegates a Merry X'mas and a Happy New Year.'

Sincerely
P. R. J. NAIDU "

The Academy of Sciences of Rumania asked for membership in the I.M.A. Secretary Amorōs pointed out the need for a group of mineralogists or of a Mineralogical Society of national standing to exist in order for the approval of such membership according to the constitution.

Following a suggestion of Secretary Amorōs, President Fisher halted the session for 10 minutes in order to allow discussion of and preparation for the elections.

4. ELECTIONS

Called again to business by President Fisher, the Assembly continued its work.

The elections proceeded, first for the Officials of the Commissions. The following were the recorded results :

Abstracts :
Chairman : Hugi (No contest), elected.
Secretary : Howie, 31 votes : van Tassel, 9 votes.

Cosmic Mineralogy : No changes proposed.

Mineral Data :
Chairman : No change proposed.
Secretary : Faust, 8 votes ; Butler 31 votes.

Museums :
Chairman : Switzer, 16 votes : Frondel 24 votes.
Secretary : Zwaan (No contest) elected.

New Minerals and Mineral Names :
No changes proposed.

Ore Microscopy : No changes proposed.

Teaching :
Chairman : Hurlbut, 28 votes ; Orcel 12 votes.
Secretary : den Tex, 22 votes ; Vincent 18 votes.

Those nominees with a majority of the votes were announced by the Secretary as the new officers of the Commissions.

Before the voting for the members of the new Council, President Fisher made several remarks explaining the efforts of the council in finding a desirable slate. He also called attention to the recommendation of the I.U.G.S. on avoiding re-elections of officers. In addition to the slate presented by the out-going Council, there was another slate proposed by French, Spanish, Italian and Japanese Delegates ; also P.R.J. Naidu as Second Vice President, was proposed by Indian, Swedish, and Dutch Delegates.

The vote took place. The following results were recorded :

President : C.E. Tilley, 24 votes (elected) ; J. Wyart, 17 votes.
1st Vice-President : H. Strunz, 22 votes (elected) ; D. S. Korshinski, 19 votes.
2nd Vice-President : D. S. Korshinski, 18 votes (elected) ; H. Strunz, votes not valid as he was already elected 1st Vice President. (Art. 4 B (a)).
Secretary : A. Preisinger, 23 votes (elected) ; J. L. Amorōs, 18 votes.
Treasurer : L. G. Berry, (No contest) elected
Councillors : T. F. W. Barth, 36 votes (elected)
J. Kutina, 39 votes (elected)
T. Watanabe, 26 votes (elected)
F. den Tex, 19 votes.

Professor J. H. Taylor moved that a hearty vote of thanks be given to the members of the retiring Council ; this was seconded and unanimously approved.

President Fisher introduced the New Council, and asked its members to take the forum. The New President, Professor C. E. Tilley addressed the assembly briefly and then adjourned the IV General Meeting of the I.M.A. at 11 : 00 a.m.

INDEX

The names of **authors** of complete articles are set in **bold-face type**

A system of nomenclature for rare-earth minerals. Levinson, A. A. 233
Abundance and significance of some minor elements in carbonatitic calcites and dolomites. **Quon, Shi H.**, and **Heinrich, E. Wm.** 29
Acadialite 152, 153
Alaskite 46
Al-hydroxides
——structural changes in 237
Alkalic intrusive complexes 38, 39
Alkaline undersaturated rocks,
——genesis of 179
Alnö 106, 126, 140
Alnöite, 112, 114
——breccia 112
Alumino fluorides 42
Alvikite 148
——dykes 55
Ambs, H., with **Paulitsch, P.**, Carbonatites, their fabric, chemistry and their genesis 140
Amigo, J. M., with **Font-Altaba, M.**, and **Montoriol-Pous**, Study of the temperature of crystallization of some Spanish fluorites by decrepitation method 172
Amoros, J. L., Clevage fractures in a Domain (twin) crystal 189
Analcime from sedimentary and burial metamorphic rocks. Whetten, J. T., and Coombs, D. S. 169
Analcime
——cell dimensions of 169
Analcite 152, 153
Ankerite 19, 29, 31
Apatite
——segregations in carbonatites 103
Apophyllite 152, 153
Application of nuclear magnetic resonance technique in the study of cation order-disorder and phase transitions in solids. Ghose, Subrata 231
Application of variations in crystal field splitting of energy levels of 3d ions to indicate structural changes in various minerals including dehydrating zeolites and clays. Roy, Rustum 235
Arkansas river area 37
Assam
——Makum basin 170
Auerbach marble 140
Augites, titaniferes-repartition du titane 205
Aumento, F., and **Friedlaender, C.**, Zeolites from North Mountains, Nova Scotia 149
Autoclave 236
Average and typical composition of carbonatites. **Gold, D. P.** 83
Bailey, D. K., Potash felspar and phlogopite as indices of temperature and partial pressure of CO_2 in carbonatites and kimberlites 5
Balgrod, W., with Roy, Rustum and Taylor, A. M., Structural changes in zeolites caused by cation exchange at room temperature and dehydration under controlled pH_2O 168
Bandopadhyaya, Tarun and Saha, P., Observations on hydrothermal growth of quartz 230
Barium
——in carbonatites 29, 31, 106
——in metamorphic and sedimentary carbonate 32, 35
Bastnasite 29
Bauxite, of Southern France 237
Beforsites 106
Bergalite 55
Beryl, phase transformations in 231
——polygonal texture in 236
Betafite 51
Biggar, G. M., with **Wyllie, P. J.**, Fractional crystallization in the " Carbonatite Systems " $CaO-MgO-CO_2-H_2O$ & $CaO-CaF_2-P_2O_5-CO_2-H_2O$ 92
Biotite, relationship with phlogopite 214
——chemical composition of 218
——unit cell data of 219
Britholite 123

Calciochondrodite 234
Calcite axes, orientation of 142
Calcite grain fabric 140
Calcite veins 49
Calcium silicate and hydrogarnet formation in the system $CaO-Al_2O_3-SiO_2-H_2O$. Roy, M. Della 234
Carbonate rocks,
——Sr^{87}/Sr^{86} ratio of 60
Carbonatites
——average and typical composition of 84
——fabric of 140
——origin of 68
——relationship with kimberlites 1
——Sr^{87}/Sr^{86} ratio of 59
Carbonatitic complexes of
——Alnö, Sweden 106, 126
——Arkansas river area, Colorado 37
——Ice river area, Southern Canadian Rocky Mountains 9
——Kaiserstuhl, W. Germany 54, 140, 148
——Luesche, Congo 148
——Meach Lake area, Ottawa 45
——Oka complex, Quebec 109
——Rufunsa, Zambia 5
Carbonatitic dikes 41

Carbonatite magmas 67
Carbonatites and alkalic rocks of the Arkansas river area, Fremont County, Colorado. **Heinrich, E. Wm.**, and **Dahlem, D. H.** 37
Carbonatites in the alkaline complex of the Ice river area, Southern Canadian Rocky Mountains. **Rapson, June, E.** 9
Carbonatites, their fabric, chemistry and their genesis. **Paulitsch, P.**, and **Ambs, H.** 140
Carbonatites of the Kaiserstuhl (W. Germany) and their magmatic environment. **Wimmenauer, W.** 54
Chabazite 152, 153
Chemical composition of Analcime from the low grade metamorphic rocks in Japan. Nakajima, Waitsu and Koizumi, Mitsue. 167
Chemical study of some amphiboles from alkaline igneous rocks. Howie, R. A. 233
Chilwa 7
Church, W. R., Metamorphic eclogites from Co. Donegal, Eire 231
Clevage features in a Domain (twin) crystal. **Amoros, J. L.** 189
Clinoptilolite
——cell parameters of 156
——chemical composition of 156
——thermal behaviour of 157
——potassium rich 167
Cobaltomenite, unit cell data of 230
Commission's reports 242, 243
Composition of some garnets from African kimberlites. **Grattan-Bellew, P. E.** 23
Coombs, D. S., with Whetten, J.A., Analcime from sedimentary and burial metamorphic rocks. 169
Cryolite 37, 42
Crystal chemistry of basic copper phosphate and arsenate minerals. Ghose, Subrata 232

Dahlem, D. H., with **Heinrich, E. Wm.**, Carbonatites and alkalic rocks of the Arkansas river area, Fremont County, Colorado 37
Dawson, J. B., Kimberlite-Carbonatite relationship 1
de Camargo, William, G. R. Unit cell and space group of artificial cobaltomenite 230
Decrepitation technique in fluorite crystallization 172
Dehydration and chemical composition of Laumontite. **Pipping, Frederick** 159
Dendritic structures in crystals 194
Diadochiques dans silicates 203
Diopside-repartition du chrome 205
Distribution of trace elements and silicates in Mediterranean marbles. Nissen, H. U. 234
Ditroite 12

Edgar, A. D., and **Nolan, J.**, Phase relations in the System $NaAlSi_3O_8$ (Albite)-$NaAlSiO_4$ (Nepheline)-$NaFeSi_2O_6$ (Acmite)-$CaMgSi_2O_6$ (Diopside)-H_2O and its importance in the genesis of alkaline undersaturated rocks 176
Edgar, A. D., (Discussion) 105
Effects of exchanged cations on the thermal behaviour of heulandite and clinoptilolite. **Shepard, Anna, O.**, and **Starkey, Harry, C.** 155
Elections-New Council Members 246
Elements en traces-localisation les fissures 203
——mobilite dans les roches 205
Experimental data bearing on the petrogenetic links between kimberlites and carbonatites. **Wyllie, Peter, J.** 67
Euxenite 210, 223
——distribution of U, Yt, Ni, Fe in 225
——chemical composition of 226

Faure and Harley
——Sr^{87}/Sr^{86} ratios in carbonatites and granites 58
Fenite 15, 110
Fenitization in Meach Lake area 50, 51
Fetid gas in carbonatite dikes 42
Fluorite 37, 173, 174
Fisher, Jerome, D. 238
Font-Altaba, M., Montoriol-Pous and **Amigo, J. M.**, Study of the temperature of crystallization of some Spanish fluorites by decrepitation method 172
Foshagite 234
Foyaite 12
Fractional crystallization in the "Carbonatite Systems" $CaO-MgO-CO_2-H_2O$ & $CaO-CaF_2-P_2O_5-CO_2-H_2O$. **Wyllie, P. J.**, and **Biggar, G. H.** 92
Fracture effects in crystals 193
Freidlaender, C. with **Aumento, F.**, Zeolites from North Mountains, Nova Scotia 149

Galaxite
——chemical composition of 201
——genesis of 198, 199
——hausmannite intergrowths 201
——x-ray powder data 199
Ganguly, Dibyendu and Saha, Prasenjit. Phase transformations in a natural beryl 231
Garnets, from African kimberlites 23
——chemical composition of 25, 26
——lattice constants of 24
Geochemistry of the Oka Complex 114
Ghose, Subrata, Application of nuclear magnetic resonance technique in the study of cation order-disorder and phase transitions in solids 231
Ghose, Subrata, Crystal chemistry of basic copper phospate and arsenate minerals 232

Gittins, J., (Discussion) 8, 64
Gold, D. P., Average and typical composition of carbonatites 83
Goswami, D. N. D., Melanterite from the Makum coal basin, Assam 170
Granites,
——Sr^{87}/Sr^{86} ratio 62
Grattan-Bellew, P. E., Composition of some garnets from African kimberlites 23
Guillemin, J. Goni et C., Nouvelles donnees sur la localisation des elements en traces dans les mineraux et dans les roches 203

Hausmannite 197
——chemical composition of 201
——x-ray powder data 199
Heinrich, E. Wm., (Discussion) 22, 108
Heinrich, E. Wm., and **Dahlem, D. H.**, Carbonatites and alkalic rocks of the Arkansas river area, Fremont County, Colorado 37
Heinrich, E. Wm., with **Quon Shi H.**, Abundance and significance of some minor elements in carbonatitic calcites and dolomites 29
Heterogeneity in minerals 209
——examples of 209
——methods of study 210
Heulandite 152, 168
——cell parameters of 155
——chemical composition of 155
——thermal behaviour of 155
High pressure autoclave for hydrothermal crystal growth. Saha, Prasenjit 236
Hogarth, D. D., Intrusive carbonate rocks near Ottawa, Canada 45
Howie, R. A., Chemical study of some amphiboles from alkaline igneous rocks 233
Hydrogen bonding site distribution on layer silicate surfaces. **Johns, W. D.**, and **Sen Gupta, P. K.** 182
Hydrothermal synthesis of pollucite and its iron analogue. Kume, Shoichi and Koizumi, Mitsue 167

Ice river valley 9
Illustrations of heterogeneity in phlogopite, felspar, euxenite and associated minerals. **Rimsaite, J., and Lachance, G. R.** 209
Influence of gases on the formation and destruction of " color centres " in quartz by electrolysis. Lietz, Joachim and Mehrotra, Benod, B. 233
Intrusive carbonate rock near Ottawa, Canada. **Hogarth, D. D.** 45
Intrusive dolomite-calcite rock 46
Isotopic composition of strontium in carbonatites and kimberlites. **Powell, J. L.** 58

Jacobsite 197
Jacupirangite 111, 114
Jadeite-acmite ratio in eclogites 231
Johns, W. D., and **Sen Gupta, P. K.**, Hydrogen bonding site distribution on layer silicate surfaces 182

Kaiserstuhl 140, 148
——Schelingen 140
Kato, Akira with **Nakajima, Waitsu,** Synthesis and electron probe microanalysis of some manganese minerals with vredenburgite type intergrowth 197
Koizumi, Mitsue, with Nakajima, Waitsu, Synthesis and stability of zeolites in the system $(Na_2, Ca)O$-Al_2O_3-$7SiO_2$-H_2O 168
Koizumi, Mitsue with Kume, Shoichi. Hydrothermal synthesis of pollucite and its iron analogue 167
Kimberlite-Carbonatite relationship. **Dawson, J. B.** 1
Kimberlite
——chemistry of 2
——genesis of 3
——relationship with undersaturated rock types 1
——Rb/Sr ratio of 63
——Sr^{87}/Sr^{86} ratio of 62
——world occurrences of 1
Kimberlite Province 27
Kume Shoichi and Koizumi Mitsue, Hydrothermal synthesis of pollucite and its iron analogue 167

Lachance, G. R. with **Rimsaite, J.**, Illustrations of heterogeneity in phlogopite, felspar, euxenite and associated minerals 209
Laumontite 152
——cell dimensions of 161
——chemical analysis of 162
——D.T.A., T.G.A. data on 164
Leonhardite 152
——cell dimensions of 161
——chemical analysis of 162
——D.T.A., T.G.A. data on 164
Levinson, A. A., A system of nomenclature for rare earth minerals 233
Lietz, Joachim and Mehrotra, Benod, B. Influence of gases on the formation and destruction of " color centres " in quartz by electrolysis 233
Lueshe carbonatite deposit, Congo 148

Makum coal basin, Assam 170
Marble-Sr^{87}/Sr^{86} ratio of 60
Marble pegmatite 12
Mediterranean marbles
——distribution of trace elements in 234
Mehrotra, Benod, B., with Leitz, Joachim, Influence of gases on the formation and destruction of " color centres " in quartz by electrolysis. 233

Mehrotra, B. B. with Valeton, I. Structural changes in synthetic and natural Al-hydroxides 237
Melanterite from the Makum coal basin, Assam, **Goswami, D. N. D.** 170
Melanterite 171
Melilite ankaratrites 55
Mesolite 152
Metamorphic eclogites from Co. Donegal, Eire. Church, W. R. 231
Metastable serpentine 235
———importance of in lunar bases 236
Minato, Hideo. Two zeolites in zeolitic rocks in Japan. (potassium clinoptilolite and powdery mordenite). 167
Minerals of the Oka carbonatite and alkaline complex, Oka, Quebec. **Gold, D. P.** 109
Mineralogical and geochemical evolution of the carbonatites of the Kaiserstuhl, Germany. van Wambeke, L. 148
Monteregian petrographic province 109
Montoriol-Pous with **Font-Altaba, M.**, and **Amigo, J. M.**, Study of the temperature of crystallization of some Spanish fluorites by decrepitation method 172
Mordenite 168
———powdery 167
Mosaic and Domain structures in crystals 192
Mukherjee, Bibuti, (Discussion) 139

Nakajima, Waitsu and Koizumi, Mitsue, Synthesis and stability of zeolites in the system (Na_2, Ca)O.Al_2O_3.7SiO_2–H_2O 168
Natrolite 152, 153
Nepheline melilite-basalt magma 55
Ngurumanite 56
Niocalite 111, 123
Nissen, H. U., Distribution of trace elements and silicates in Mediterranean marbles 234
Nolan, J., with **Edgar, A. D.**, Phase relations in the system $NaAlSi_3O_8$ (Albite) –$NaAlSiO_4$ (Nepheline) –$NaFeSi_2O_6$ (Acmite) –$CaMgSi_2O_6$ (Diopside) –H_2O and its importance in the genesis of alkaline undersaturated rocks 176
North Mountain basalts 149
Nouvelles donnees sur la localisation des elements en traces dans les mineraux et dans les roches. **Guillemin, J. Goni et C.,** 203
Nova Scotia 149
Nuclear magnetic resonance technique 231

Observations on hydrothermal growth of quartz. Bandopadhyaya, Tarun and Saha, P. 230
Oka complex
———geochemistry of 114
———structure of 112
———origin of 123
Okaite 111
Ore microscopy and electron probe micro-analysis of some manganese minerals with vredenburgite type intergrowth. **Watanabe, Takeo** and **Kato, Akira** 197
Orthoclase 5, 6, 7
Ottawa-Meach lake area 45

Paulitsch, P., and **Ambs, H.**, Carbonatites, their fabric, chemistry and their genesis 140
Perovskite 123
———Niobium rich 148
Phase relations in the system $NaAlSi_3O_8$ (Albite) –$NaAlSiO_4$ (Nepheline) –$NaFeSi_2O_6$ (Acmite)–$CaMgSi_2O_6$ (Diopside) and its importance in the genesis of alkaline undersaturated rocks. **Edgar, A. D.**, and **Nolan, J.** 176
Phase transformations in a natural beryl. Ganguly, Dibyendu and Saha, Prasenjit 237
Phlogopite 5
Phlogopite zoned 209
———chemical composition of 218
———distribution of Fe, K, Ti, Cr, H_2O in 211, 214
———unit cell data of 219
Pipping, Frederick, Dehydration and chemical composition of Laumontite 159
Plagioclase, antiperthetic, 209
———heterogeneity in 221, 222
———lamellar 209
Pollucite 167
Polygonal texture in beryl. Sahama, Th. G. 236
Porphyritic carbonatite 34
Potash felspar and phlogopite as indices of temperature and partial pressure of CO_2 in carbonatites and kimberlites. **Bailey, D.K.** 5
Potash felspar 5
Powell, James, L., Isotopic composition of strontium in carbonatites and kimberlites 58
Powell, James. L., (Discussion) 3
Proceedings of the International Mineralogical Association 238
Pressure, temperature relations for the dehydration of metastable serpentine at 15 to 20,000 psi. Roy, Rustum and Weber, Jon, N. 235
Pyroxenes of the Alnö carbonatite (Sövite) and of the surrounding fenites. von **Eckermann, Harry.** 126
Pyroxenes of the Alnö carbonatites 127
———chemical data 128
———optical data 135
Pyrochroite 197

Quartz
——— hydrothermal growth of 230
———formation and destruction of "color centres" in 233

Quon Shi H. and **Heinrich, E. Wm.**, Abundance and significance of some minor elements in carbonatitic calcites and dolomites 29

Rapson, June, E., Carbonatite in the alkaline complex of the Ice river area, Southern Canadian Rocky Mountains 9
Rare earth minerals nomenclature of 233
Recrystallization texture in calcites 142
Rhodonite 197
Rhodochrosite 198
Rimsaite, J., and **Lachance, G. R.**, Illustrations of heterogeneity in phlogopite, feldspar, euxenite and associated minerals 209
Roy, M. Della, Calcium silicate and hydrogarnet formation in the system $CaO-Al_2O_3-SiO_2-H_2O$. 234
Roy, Rustum, Taylor, A. M., and Balgrod, W., Structural changes in zeolites caused by cation exchange at room temperature and dehydration under controlled pH_2O 168
Roy, Rustum, Application of variations in crystal field splitting of energy levels of 3d ions to indicate structural changes in various minerals including dehydrating zeolites and clays 235
Roy, Rustum and Weber, Jon, N., Pressure-temperature relations for the dehydration of metastable serpentine at 15 to 20,000 psi. 235
Rufunsa volcanic province 5

Saha, Prasenjit, High pressure autoclave for hydrothermal crystal growth 236
Saha, P. with Bandopadhyaya, Tarun, Observations on hydrothermal growth of quartz 230
Saha, Prasenjit with Ganguly, Dibyendu, Phase transformations in a natural beryl 231
Sahama, Th. G., Polygonal texture in beryl 236
Secretary's report. Amoros, J. L. 238
Sedimentary carbonates and limestones
——Isotopic composition of 87
Sengupta, P. K. with **Johns, W. D.**, Hydrogen bonding site distribution on layer silicate surfaces 182
Shephard, Anna, O., and **Starkey, Harry, C.**, Effects of exchanged cations on the thermal behaviour of heulandite and clinoptilolite 155
Si–O covalent bonding in silicates
——importance of 182
Solution pits in crystals 191
Sōve 140
Sōvites 106, 126, 148
——Badberg 54
——Schelingen 55
Spinel 197
Starkey, Harry, C., with **Shephard, Anna, O.**, Effects of exchanged cations on the thermal behaviour of heulandite and clinoptilolite. 155
Stilbite 152
Strontium
——in carbonatites 29, 31, 52, 58, 106
——tracer technique 58
Strontium and barium contents of the Alnö carbonatites. **von Eckermann, Harry** 106
Structures of alkyl-ammonium vermiculites 185
Structures of 232
——clinoclase 232
——erinite 232
——euchroite 232
——libethenite 232
——olivenite 232
——pseudomalachite 232
Structural changes in zeolites caused by cation exchange at room temperature and dehydration under controlled pH_2O. Roy, Rustum, Taylor, A. M., and Balgrod, W. 168
Structural changes in synthetic and natural Al-hydroxides. Valeton, I., and Mehrotra, B. B. 237
Study of the temperature of crystallization of some Spanish fluorites by decrepitation method. **Font-Altaba, M., Montoriol-Pous, J.**, and **Amigo, J. M.** 172
Study of the pyrochlores, the columbite and fersmite from the Leusche carbonatite deposit (Republic of Congo). van Wambeke, L. 148
Synclinal du Morvan 203
Systems
——$CaO-SiO_2-CO_2-H_2O$ 69
——$CaO-MgO-SiO_2-CO_2-H_2O$ 73
——Albite–nepheline–$CaCO_3$–$Ca(OH)_2$–H_2O 76
——$CaO-Na_2O-Al_2O_3-SiO_2-CO_2-H_2O$ 77
——$Na_2O-Al_2O_3-SiO_2-CO_2$ 79
——Plagioclase felspar–Na_2CO_3–H_2O 79
——$CaO-CO_2-H_2O$ 92
——$CaO-MgO-CO_2-H_2O$ 93
——$CaO-CaF_2-P_2O_5-CO_2-H_2O$ 101
——$(Na_2, Ca)\ O-Al_2O_3-7SiO_2-H_2O$ 168
——$NaAlSi_3O_8-NaAlSiO_4-NaFeSi_2O_6-CaMgSi_2O_6-H_2O$ 176, 178
——$NaAlSi_3O_8-NaAlSiO_4-CaMgSi_2O_6-H_2O$ 177
——$NaAlSi_3O_8-NaAlSiO_4-NaFeSi_2O_6-H_2O$ 177
——$CaO-Al_2O_3-SiO_2-H_2O$ 234

Tephroite 197
Thomsonite 152, 153
Tobermarite 234
Tourmaline lithique 204
Travertines 43
Treasurer's report. Berry, L. G. 239

Triglycine-sulfate crystals
——velocities of growth in 189

Upper Rhein graben 54
Urtite ijolite 114

Valeton, I., and Mehrotra, B. B. Structural changes in synthetic and natural Al-hydroxides 237
van Wambeke, L., Mineralogical and geochemical evolution of the carbonatites of the Kaiserstuhl, Germany 148
van Wambeke, L., A study of the pyrochlores, the columbite and fersmite from the Leusche carbonatite deposit (Republic of Congo) 148
von Eckermann, Harry, Strontium and barium contents of the Alnö carbonatites 106
von Eckermann, Harry, Pyroxenes of the Alnö carbonatites of the surrounding fenites 126
Vredenburgite,
——chemical composition of 201
——Windmanstatten texture in 197
——x-ray powder data 199

Wairakite 123
Watanabe, Takeo and **Kato, Akira,** Ore microscopy and electron probe microanalysis of some manganese minerals with vredenburgite type intergrowth 197
Weber, Jon, N., with Roy, Rustum, Pressure, temperature relations for dehydration of metastable serpentine at 15 to 20,000 psi. 235
Whetten, J. T., and Coombs, D. S., Analcime from sedimentary and burial metamorphic rocks 169
Wimmenauer, W., Carbonatites of the Kaiserstuhl, (W. Germany) and their magmatic environment 54
Wyllie, Peter, J. (Discussion) 8
Wyllie, Peter, J., Experimental data bearing on the petrogenetic links between kimberlites and carbonatites 67
Wyllie, Peter, J., and **Biggar, G. M.,** Fractional crystallization in the "carbonatite system" (CaO–MgO–CO_2–H_2O) & (CaO–CaF_2–P_2O_5–CO_2–H_2O) 92

Zeolites from North Mountains, Nova Scotia. **Aumento, F.,** and **Freidlaender, C.** 149
Zeolites from North Mountains
——cell parameters of 152
——chemical analysis of 153
Zeolites in system (Na_2, Ca)$O.Al_2O_3.7SiO_2.H_2O$ 168
Zeolites
——dehydration process in 235
——structural changes in 169
Zeolites from Nova Scotia 149
——from Japan 167, 168
Zircon
——cerium, gadolinium-localisation 204